UNIVERSIDAD POLITÉCNICA DE MADRID
Escuela Técnica Superior de Ingenieros Industriales

SAFETY ANALYSIS OF VVER-1000 REACTORS WITH CONVENTIONAL AND PASSIVE SAFETY SYSTEMS

DOCTORAL THESIS

Submitted for the degree of Doctor by:

Elena Redondo Valero
Master in Nuclear Science and Technology

Madrid, 2025

UNIVERSIDAD POLITÉCNICA DE MADRID
Escuela Técnica Superior de Ingenieros Industriales

Doctoral Degree in Sustainable, Nuclear and Renewable Energy

SAFETY ANALYSIS OF VVER-1000 REACTORS WITH CONVENTIONAL AND PASSIVE SAFETY SYSTEMS

DOCTORAL THESIS

Submitted for the degree of Doctor by:

Elena Redondo Valero
Master in Nuclear Science and Technology

Under the supervision of:
Dr. Cesar Queral Salazar

Madrid, 2025

Title: Safety Analysis of VVER-1000 Reactors with Conventional and Passive Safety Systems

Author: Elena Redondo Valero

Doctoral Programme: Sustainable, Nuclear and Renewable Energy

Thesis Supervision:

Dr. Cesar Queral Salazar, Professor, Universidad Politécnica de Madrid

External Reviewers:

Thesis Defense Committee:

Thesis Defense Date:

Mire vuestra merced -respondió Sancho- que aquellos que allí se parecen no son gigantes, sino molinos de viento, y lo que en ellos parecen brazos son las aspas, que, volteadas del viento, hacen andar la piedra del molino.

El ingenioso hidalgo Don Quijote de la Mancha (1605), Miguel de Cervantes

Acknowledgement

I would like to express my deep gratitude to my PhD thesis supervisor, César Queral, for his guidance and mentorship. His insightful comments and active participation have been instrumental in shaping the research. The knowledge I have gained under his supervision has been invaluable and his expertise has greatly enriched this experience.

I wish also to express my sincere gratitude to Victor Hugo Sánchez-Espinoza. His generosity in allowing me to work with the esteemed professionals at the INR institute has greatly enhanced this research.

A special thank you goes to Kevin Fernández-Cosials. His extensive knowledge of VVER reactors has been invaluable and his involvement in the studies conducted throughout this PhD thesis has been essential. I am also deeply grateful to Javier Gómez-Magán, whose expertise with the TRACE code has been crucial in the development of a VVER-1000/V320 reactor model, and whose presence throughout the PhD thesis has been greatly appreciated.

I don't want to forget the incredible colleagues who have become friends over the years in office 722: Jaime Valverde, Sergio Courtin, Yago Martínez, Alejandro Taboada, Jorge Sánchez-Torrijos, Jorge Arrabal, Julia Herrero, Alberto García... I cherish the countless coffees we have shared, the conferences, and the courses we have taken together. These experiences have made this journey unforgettable.

Quiero expresar mi más profundo agradecimiento a mis padres, Rosa y Adrián, y a mis hermanas, Rosa y María. Su aliento incondicional me ha acompañado desde que decidí realizar esta tesis doctoral. Sin su cariño y respaldo, este logro no habría sido posible.

Finalmente, a ti, Víctor, quiero dedicarte un agradecimiento muy especial. Tu apoyo constante, tus palabras de ánimo en los momentos difíciles, y tu firme creencia en mi capacidad han sido fundamentales para que pudiera llegar hasta aquí. No encuentro palabras suficientes para expresar toda mi gratitud.

¡A todos vosotros, gracias de corazón!

Thesis Outcomes

Journal Papers related to the thesis:

1. **Redondo-Valero, E.**, Queral, C., Fernandez-Cosials, K., Sanchez-Espinoza, V. Safety margins improvement by means of the Passive Heat Removal System and the HA-2 in VVER-1000/V320 reactors. Progress in Nuclear Energy (preprint). http://dx.doi.org/10.2139/ssrn.4942879

   JCR: NUCLEAR SCIENCE & TECHNOLOGY, 2023, 4/40 (Q1).

2. **Redondo-Valero, E.**, Queral, C., Fernandez-Cosials, K., Sanchez-Espinoza, V., Sanchez-Perea, M., Groudev, P., 2024. Management of the SBLOCA sequences with HPIS failure in VVER-1000/V320 reactors; comparison with Westinghouse PWR strategies. Progress in Nuclear Energy, 177, 105414. https://doi.org/10.1016/j.pnucene.2024.105414

   JCR: NUCLEAR SCIENCE & TECHNOLOGY, 2023, 4/40 (Q1).

3. **Redondo-Valero, E.**, Queral, C., Fernandez-Cosials, K., Sanchez-Espinoza, V, 2023. Safety margins improvement by means of the passive second stage hydroaccumulators in a VVER-1000/V320 reactor. Nuclear Engineering and Design 414, 112644. https://doi.org/10.1016/j.nucengdes.2023.112644.

   JCR: NUCLEAR SCIENCE & TECHNOLOGY, 2023, 10/40 (Q1).

4. **Redondo-Valero, E**, Queral, C., Fernandez-Cosials, K., Sanchez-Espinoza, V., 2023. Analysis of MBLOCA and LBLOCA success criteria in VVER-1000/V320 reactors: New proposals for PSA Level 1. Nuclear engineering and technology 55, 623–639. https://doi.org/10.1016/j.net.2022.10.006.

   JCR: NUCLEAR SCIENCE & TECHNOLOGY, 2023, 7/40 (Q1).

5. Queral, C., Sánchez-Espinoza, V., Egelkraut, D., Fernández-Cosials, K., **Redondo-Valero, E.**, García-Morillo, A., 2021. Safety Systems of Gen-III/Gen-III+ VVER reactors. Nuclear España (October). https://www.revistanuclear.es/wp-content/uploads/2021/10/Art.seguridad-reactores.pdf.

   Review not included in the JRC.

Conferences and meetings related to the thesis:

1. **Redondo-Valero, E.**, Queral, C., Fernandez-Cosials, K., 2024. Analysis of the impact of passive safety systems on accidental sequences of VVER-1000 reactors, in: 7th International Conference on Nuclear and Renewable Energy Resources (NURER 2024). Ankara, Turkey.
2. **Redondo-Valero, E.**, Queral, C., Sanchez-Torrijos, J., Castro-Gonzalez, E., 2024. Comparative analysis of accidental sequences with conventional and Advanced Tolerant Fuels (ATF) in VVER-1000 reactors, in: 7th International Conference on Nuclear and Renewable Energy Resources (NURER 2024). Ankara, Turkey.
3. **Redondo-Valero**, E., Queral, C., Fernandez-Cosials, K. Sanchez-Espinoza, V., 2024. Analysis of the passive safety systems impact in VVER-1000 reactors, in: 50th Annual Meeting of the Spanish Nuclear Society (RASNE 2024). Cordoba, Spain.
4. Queral, C., Fernandez-Cosials, K., **Redondo-Valero, E.**, Canal, D., Castro-Gonzalez, E., Sanchez-Torrijos, J., Martinez-Gonzalez, Y., Arrabal de Haro, J., Taboada-Asensio, A, Perez, M., 2024. Activities of the UPM oriented DEC-A sequences (in Spanish), in: 10ª CAMP-España meeting. Madrid, Spain.
5. **Redondo-Valero, E.**, Queral, C., Gomez-Magan, J., Sanchez-Espinoza, V., 2023. SBLOCA with HPIS failure sequences management in VVER-1000/V320 reactors (in Spanish), in: 48th Annual Meeting of the Spanish Nuclear Society (RASNE 2023). Toledo, Spain.
6. **Redondo-Valero, E.**, Queral, C., Gomez-Magan, J., Fernandez-Cosials, K., Sanchez-Espinoza, V., 2023. Thermal-Hydraulic analysis of the SBLOCA sequences with HPIS failure and secondary side depressurization in VVER-1000/V-320 reactors, in: Spring CAMP Meeting Budapest 2023. Budapest, Hungary.
7. **Redondo- Valero, E.**, Queral, C., Gomez-Magan, J., Fernandez-Cosials, K., Sanchez-Espinoza, V., 2023. Thermal-hydraulic analysis of SBLOCA sequences with HPIS failure and secondary side depressurization in VVER-1000/V320 reactors, in: 30th International Conference on Nuclear Engineering (ICONE30). Kyoto, Japan. https://doi.org/10.1299/jsmeicone.2023.30.1957.

8. Queral, C., **Redondo-Valero, E**., Canal, D., Castro, E., Sanchez-Torrijos, J., Soler, A., Sanchez-Espinoza, V., 2023. Transient analysis in PWR, VVER, SMRs and experimental facilities, in: Fall CAMP Meeting 2023. Washington, EEUU.
9. **Redondo-Valero, E.**, Queral, C., Sanchez-Espinoza, V., Fernandez-Cosials, K., 2022. Thermal-hydraulic analysis of the 2nd stage hydroaccumulators impact in LOCA sequences with SBO, in: International Youth Nuclear Congress (IYNC 2022). Koriyama, Japan.
10. Gomez-Magan, J., Queral, C., Sanchez-Torrijos, J, Fernandez-Cosials, K., **Redondo-Valero, E**., Campos, D., 2022. BEPU analysis of SBLOCA sequences in PWRs (in Spanish), in: 9ª CAMP-España meeting. Valencia, Spain.
11. **Redondo-Valero, E.**, Queral, C., Sanchez-Espinoza, V., Fernandez-Cosials, K, 2022. Analysis of the impact of second stage hydro-accumulators in VVER-1000 reactors on MB/LBLOCA sequences with SBO (in Spanish), in: 9ª CAMP-España meeting. Valencia, Spain.
12. **Redondo-Valero, E.**, Queral, C., Sanchez-Espinoza, V., Fernandez-Cosials, K., 2022. Thermal-hydraulic analysis of the 2nd stage hydroaccumulators impact in MB/LBLOCA sequences along with SBO, in: 31st International Conference Nuclear Energy for New Europe (NENE). Portoroz, Slovenia.
13. Queral, C., Fernandez-Cosials, K., Magan, J., Courtin, S., Sanchez-Torrijos, J., **Redondo-Valero, E**., 2022. Experience in DEC-A sequences analysis, in: WGFS/WGAMA Kick-off Meeting of the task "Status Report on Good Practices for Analyses of DEC-A for Operating Nuclear Power Plants". Madrid, Spain.
14. Queral, C., Magan, J., Sanchez, J., **Redondo-Valero, E**., Perez, M., 2021. Analyses of accidental sequences in PWR, VVER and SMR. Problems found in TRACE5 patch6, in: Virtual Fall CAMP Meeting 2021.
15. **Redondo-Valero, E.**, Queral, C., Sanchez-Espinoza, V., 2021. Thermal-hydraulic analysis of accidental sequences in a VVER-1000/V320 reactor with TRACEv5p5 code (in Spanish), in: 46th Annual Meeting of the Spanish Nuclear Society (RASNE 2021). Granada, Spain.

16. **Redondo-Valero, E.**, Queral, C., Sanchez-Espinoza, V., 2021. Thermal-hydraulic analysis of a VVER-1000/V320 reactor with TRACE5p5 code, in: Proceedings of the European Nuclear Young Generation Forum (ENYGF21). Tarragona, Spain.

Journal Paper unrelated to the thesis:

1. Campos-Muñoz, A., Sanchez-Espinoza, V., **Redondo-Valero, E.**, Queral, C., 2024. Verification of the coupled code PARCS/ TWOPORFLOW with Rod Ejection Accident calculations for Small Modular Reactors. Nuclear Science and Engineering. https://doi.org/10.1080/00295639.2024.2357953.

   JCR: NUCLEAR SCIENCE & TECHNOLOGY, 2023, 25/40 (Q3)

2. Queral, C., **Redondo-Valero, E.**, Sanchez-Torrijos, J., Canal, D., Jimenez, G., Larriba, S., Cuervo, D., Cabellos, O., Duran-Vinuesa, L.F., Herranz, L.E., Garcia, M., Martinez-Quiroga, V., Freixa, J., Barrachina, T., Miro, R., Perez-Rodriguez, E., Dominguez-Bautista, M.T., Larrosa, O., Hueso-Ordonez, C., Gonzalez-Sevillano, I., Ruiz-Martin, J.A., 2024. Spanish research related to SMRs projects. Nuclear Engineering and Design 417, 112818. https://doi.org/https://doi.org/10.1016/j.nucengdes.2023.112818

   JCR: NUCLEAR SCIENCE & TECHNOLOGY, 2023, 10/40 (Q1)

Conferences and meeting unrelated to the thesis:

1. Martinez-Gonzalez, Y., Queral, C., **Redondo-Valero, E**., Sanchez-Torrijos, J., 2024. Simulation of MOTEL experimental tests MS-SG01 and MS-SG02 using TRACE code, in: 7th International Conference on Nuclear and Renewable Energy Resources (NURER 2024). Antalya, Türkiye.

2. Campos-Muñoz, A., Sanchez-Espinoza, V., **Redondo-Valero, E.**, Queral, C., 2023. Verification of Neutronic and Thermal-hydraulic Multi-physics Calculations for SMRs Rod Ejection Accident with PARCS/TWOPORFLOW, in: The International Conference on Mathematics and Computational Methods Applied to Nuclear Science and Engineering (M&C 2023). Niagara Falls, Ontario, Canada.

3. Sanchez-Torrijos, J., **Redondo-Valero, E.**, Queral, C., Cabellos, O., Meca, R., Diaz-Pesador, E., Kliem, S., Sanchez-Espinoza, V., 2023. On the Application of Advanced Modeling Tools to the SLB Analysis in NuScale. Part I: TRACE/PARCS, TRACE/PANTHER and ATHLET/DYN3D, in: International Conference on Mathematics and Computational Methods Applied to Nuclear Science and Engineering (M&C 2023). Niagara Falls, Ontario, Canada.
4. **Redondo-Valero, E.**, Queral, C., Sanchez-Torrijos, J., Gomez-Magan, J., 2023. Thermal-hydraulic analysis of accidental sequences in NuScale and SMR experimental facilities, in: Spring CAMP Meeting 2023. Budapest, Hungary.
5. **Redondo-Valero, E.**, Sanchez-Torrijos, J., Queral, C., Cabellos, O., 2022. Analysis of a Main Steam Line Break accident in the NuScale reactor by means of the coupled code TRACE/PARCS, in: International Young Nuclear Conference (IYNC 2022). Koriyama, Japan.
6. Queral, C., **Redondo-Valero, E.**, Sanchez-Torrijos, J., Cabellos, O., 2022. SLB analysis in NuScale using TRACE/PARCS, in: 47th Annual Meeting of the Spanish Nuclear Society (RASNE 2022). Cartagena, Spain.
7. Casas, V., **Redondo-Valero, E.**, 2022. Simulation SMR-NuScale with PARCS code, in: 4th Workshop of Spanish Users on Nuclear Data on"Neutronic Design of Small Modular Reactors". Online.
8. Larriba, S., Krpan, R., Jiménez, G., **Redondo-Valero, E.**, Queral, C., Kljenak, I., 2022. Scaling down of PWR nuclear power plant secondary side conditions for SIRIO experimental facility and verification using system thermal-hydraulic codes, in: 31st International Conference Nuclear Energy for New Europe (NENE). Portoroz, Slovenia.
9. **Redondo-Valero, E.**, de la Fuente-Garcia, E., Queral, C., Jimenez, G., 2020. Thermohydraulic analysis of an Isolation Condenser self-regulating by non-condensable gases (SIRIO facility), in: Virtual Meeting of the Spanish Nuclear Society (RASNE 2020).
10. de la Fuente-Garcia, E., **Redondo-Valero, E.**, Jimenez, G., Queral, C., 2020. Evaluation and scaling of an innovative passive Isolation Condenser to BWR technology, in: Virtual Meeting of the Spanish Nuclear Society (RASNE 2020).

Awards:

- Best presentation on Nuclear Safety and Licensing at the 48th Annual Meeting of the Spanish Nuclear Society.
- Best presentation on Nuclear Safety and Licensing at the 50th Annual Meeting of the Spanish Nuclear Society.

Abstract

The VVER are one of the most common reactor types in the world. In addition, many of the Gen-III/III+ reactors under construction or recently commissioned are VVER designs. On other hand, passive safety systems are attracting increasing interest for several reasons: their simplicity and reliability, reduced need for human intervention, lower maintenance requirements and long-term cost effectiveness.

To address these two main concerns, a detailed VVER-1000/V320 model has been developed for system code TRACEV5P5, including the conventional safety systems from this design. In addition, two passive safety systems found in Gen-III/III+ VVER designs have been included in the VVER-1000/V320 model. These passive safety systems are the Second Stage Hydro-accumulators (HA-2) of the VVER-1200/V392M and the air-cooled Passive Heat Removal System (PHRS) of the VVER-1000/V412 (Kudankulam Nuclear Power Plant).

Several safety analyses have been carried out using the developed full plant model of a VVER-1000/V320 reactor. The first two have been performed considering the conventional safety systems. First, the success criteria for the Loss of Coolant Accident (LOCA) event trees have been verified. Then, the different strategies presented in the emergency operating procedures for the management of small LOCAs have been studied. Hereafter, two further analyses have been conducted with the aim of gain more in-depth knowledge of the passive safety systems incorporated in Gen-III/III+ VVER reactors. Thus, Small and Large LOCA have been simulated under Station Blackout (SBO) conditions, considering the performance of the HA-2 and the air-cooled PHRS.

It is important to emphasize the use of the Integrated Safety Assessment (ISA) methodology throughout the analyses conducted in the PhD thesis, especially for the verification of the success criteria of the conventional safety systems, the identification of the success criteria for the passive safety systems incorporated in the VVER-1000/V320 model and the determination of available times required for human actions.

Several conclusions have been drawn from this doctoral thesis. Firstly, a certain conservatism has been observed in the public event trees for the LOCAs, as the simulations show that a relaxation of the success criteria is possible. Therefore, a new proposal for the event trees has been made, including a new extended event

tree approach. It has also been found that human actions are necessary when the break sizes are smaller than 2 inches and the high pressure injection system is not available. The simulations show that the human action related to controlled SG depressurisation at a reactor coolant system cooling rate of 60 K/h in VVER-1000/V320 provides a large safety margin, similar to that obtained in the Westinghouse PWR for the cooling rate of 55 K/h.

On the other hand, it has been obtained that for the LOCA sequences under SBO conditions, the single actuation of the four HA-2 trains along with the injection of the First Stage Hydroaccumulators (HA-1) would be enough to avoid core damage for medium/large break sizes. In addition, the simulations of both SBLOCA and LBLOCA under SBO conditions, considering the performance of the HA-2 and the air-cooled PHRS, show that, given the availability of success criterion for LOCA of these safety systems in Gen-III/III+ VVER reactors (3 out of 4 trains), the performance of active safety systems is not necessary to avoid core damage during the first 24 hours of the sequence.

On the basis of all the knowledge gained from hundreds of simulations, it has been possible to propose new event trees for LOCA and for the LOOP sequences, incorporating headers relating to the advanced passive safety systems studied, the HA-2 and the air-cooled PHRS.

Resumen

Los reactores VVER son uno de los diseños de reactores nucleares más comunes. Tal es así que muchos de los reactores Gen-III/III+ que se están construyendo o que han entrado recientemente en operación son diseños VVER. Asimismo, los sistemas de seguridad pasivos están despertando un interés creciente por varias razones: su simplicidad, fiabilidad, menor intervención humana, bajo mantenimiento y rentabilidad a largo plazo.

Para abordar estas dos cuestiones, se ha desarrollado un modelo detallado para el código de sistemas TRACEV5P5 de un reactor VVER-1000/V320. Este modelo incorpora los principales sistemas de seguridad convencionales, así como dos sistemas de seguridad pasivos presentes en los diseños de reactores VVER Gen-III/III+: los acumuladores de segunda etapa (HA-2), del diseño VVER-1200/V392M, y el sistema de eliminación de calor residual por aire (PHRS), del diseño VVER-1000/V412 (Central Nuclear de Kudankulam).

Se han llevado a cabo varios análisis utilizando el modelo de planta desarrollado. En los dos primeros se ha considerado únicamente la disponibilidad de los sistemas de seguridad convencionales. En primer lugar, se han verificado los criterios de éxito para los árboles de sucesos de las secuencias de perdida de refrigerante (LOCA). Posteriormente, se han estudiado las diferentes estrategias presentadas en los procedimientos de operación de emergencia para la gestión de secuencias de roturas pequeñas de LOCA. A continuación, se han realizado otros dos análisis con el objetivo de profundizar en el conocimiento de los sistemas de seguridad pasivos incorporados en los reactores VVER avanzados. Así, se han simulado secuencias de LOCA en condiciones de pérdida total de la corriente alterna (SBO).

Es importante destacar el empleo de la metodología "Integrated Safety Assessment (ISA)" a lo largo de los análisis realizados en la tesis, especialmente para la verificación de los criterios de éxito de los sistemas de seguridad convencionales, la identificación de los criterios de éxito para los sistemas de seguridad pasivos incorporados al modelo de VVER-1000/V320 y la determinación de los tiempos disponibles para realizar acciones humanas.

Se han obtenido importantes conclusiones a partir estos análisis. En primer lugar, se ha observado cierto conservadurismo en los árboles de sucesos de las secuencias de LOCA. Ello ha llevado a proponer nuevos árboles de sucesos, entre los que destacan los árboles de sucesos expandidos. Por otro lado, se ha encontrado que las

acciones humanas son necesarias cuando el tamaño de la rotura en las secuencias de LOCA es más pequeño de 2 pulgadas y el sistema de inyección de alta presión está indisponible. Las simulaciones indican que, en los reactores VVER-1000/V320, la despresurización controlada de los generadores de vapor a 60 K/h ofrece un margen de seguridad similar al de los reactores Westinghouse con una velocidad de enfriamiento de 55 K/h.

Por otro parte, se ha visto que, para las secuencias de LOCA en condiciones de SBO, la inyección de los cuatro trenes del HA-2 junto con la inyección de los acumuladores de primera etapa (HA-1) podría ser suficiente para evitar el daño al núcleo en roturas medianas y grandes. Además, las simulaciones tanto de SBLOCA como de LBLOCA en condiciones SBO, considerando la actuación del HA-2 y del PHRS, muestran que, dada la disponibilidad del criterio de éxito para LOCA de estos sistemas de seguridad (3 de 4 trenes), la actuación de los sistemas de seguridad activa no es necesaria para evitar el daño al núcleo en las primeras 24 horas de la secuencia.

En base al conocimiento obtenido a través de cientos de simulaciones realizadas, ha sido posible proponer nuevos árboles de sucesos para secuencias de LOCA y secuencias de perdida de la corriente externa (LOOP), incorporando cabeceros relacionados con los sistemas de seguridad pasivos analizados en la tesis doctoral, el HA-2 y el PHRS.

Table of Contents

List of Figures

List of Tables

Abbreviations and Acronyms

ACC	Accumulator
AFW	Auxiliary Feedwater
AKZ	Alfanumericheskaya Kodovaya Znakovaya
ASVAD	Automatic Safety Valve for Accumulator Depressurization
ATLAS	Advanced Thermal-Hydraulic Test Loop for Accident Simulation
ATWS	Anticipated Transient Without SCRAM
B&W	Babcock & Wilcox
BDBAMG	Beyond Design Accident Management Guidance
BRU-A	Steam Dump Valves to the Containment
BRU-K	Steam Dump Valves to the Condenser
BRU-SN	Steam Dump Valves to the Atmosphere
BZOK	Fast Acting Isolating Vales
BWR	Boling Water Reactor
CC	Core Catcher
CE	Combustion Engineering
CET	Core Exit Thermocouples
CD	Core Damage
CL	Cold Leg
CMT	Core Make-up Tank
CR	Control Rod
CSF	Critical Safety Function
CSS	Containment Spray System
CVCS	Control Volume and Chemical System
DBA	Design Basis Accident

DC	Downcomer
DCC	Degraded Core Cooling
DD	Damage Domain
DEGB	Double Ended Guillotine Break
DVI	Direct Vessel Injection
EBIS	Emergency Boron Injection System
ECCS	Emergency Core Cooling System
ECS	Emergency SG Cooldown System
EDG	Emergency Diesel Generator
EET	Expanded Event Tree
EFW	Emergency Feed Water
EGRS	Emergency Gas Removal System
EHRT	Emergency Heat Removal Tanks
EMT	Emergency Makeup Tank
EOP	Emergency Operating Procedure
ET	Event Tree
ETHARINUS	Experimental Thermal Hydraulics for Analysis, Research and Innovations in Nuclear Safety
FA	Fuel Assembly
GT	Generic Transient
HA-1	First Stage Hydro-accumulator
HA-2	Second Stage Hydro-accumulator
HA-3	Third Stage Hydro-accumulator
HA-DC	Hydro-accumulator connected to the vessel Downcomer
HA-UP	Hydro-Accumulator connected to the vessel Upper Plenum
HHSI	High Head Safety Injection
HL	Hot Leg
HPIS	High Pressure Injection System

HHPIS	High Head Pressure Injection System
HPSI	High Pressure Safety Injection
HX	Heat Exchanger
IAEA	International Atomic Energy Agency
IC	Isolation Condenser
ICC	Inadequate Core Cooling
IE	Initiating Event
IPPE	Leipunskii Institute of Physics and Power Engineering
IRWST	In-containment Refuelling Water Storage Tank
ISA	Integrated Safety Assessment
ISASMORE	Integrated Safety Analysis of Modular and Evolutive Reactors
JSC	Joint-Stock Company
KIT	Karlsruhe Institute of Technology
KKS	Kraftwerk-Kennzeichensystem
LBLOCA	Large Break Loss of-Coolant Accident
LOCA	Loss Of Coolant Accidents
LOOP	Loss of Offsite Power
LPIS	Low Pressure Injection System
LPSI	Low Pressure Safety Injection
LWR	Light Water Reactor
LW-SMR	Light Water Small Modular Reactor
MBLOCA	Medium Break Loss of Coolant Accident
MCP	Main Coolant Pump
MCR	Main Control Room
MDP	Motor Driven Pumps
MFW	Main Feed Water
MOV	Motor Operated Valves

MSH	Main Steam Header
MSIV	Main Steam Isolation Valve
NFMC	Neutron Flux Measuring Channels
NPP	Nuclear Power Plant
PAR	Passive Autocatalytic Recombines
PCT	Peak Cladding Temperature
PD	Previous Damage
PHRS	Passive Heat Removal System
PHRS-C	Passive Containment Cooling System
PKL	Primary Coolant Loop Test Facility
PORV	Pilot Operated Relief Valve
PSA	Probabilistic Safety Analysis
PSD	Pulse Safety Devices
PSS	Passive Safety System
PWR	Pressurizer Water Reactor
PWR-W	Pressurized Water Reactor Westinghouse
PZR	Pressurizer
QBIS	Quick Boron Injection System
RCP	Reactor Coolant Pump
RCS	Reactor Coolant System
PHRS	Residual Heat Removal System
RPV	Reactor Pressure Vessel
RVLIS	Reactor Vessel Level Indicator System
RWST	Refuelling Water Storage Tank
SBLOCA	Small Break Loss-of-Coolant Accident
SBO	Station Blackout
SC	Success Criterion

SFP	Spent Fuel Pool
SFR	Sodium Fast Reactor
SG	Steam Generator
SGTR	Steam Generators Tube Rupture
SL	Steam Line
SLB	Steam Line Break
SLOCA	Seal Loss Of Coolant
SMR	Small Modular Reactor
SS	Steady State
SWS	Service Water System
TH	Thermal-hydraulic
TT	Turbine Trip
TLFW	Total Loss of Feed Water
UP	Upper Plenum
VVER	Water Water Energetic Reactor

Chapter 1.
Introduction

The present doctoral thesis has been developed within the project "Integrated Safety Analysis of Modular and Evolutive Reactors" (ISASMORE), conducted by the Universidad Politécnica de Madrid (UPM) in collaboration with the Karlsruhe Institute of Technology (KIT). The project and, consequently, this doctoral thesis are driven by two main motivations:

- On the one hand, interest in studying the VVER reactors has grown considerably, as they are one of the most widely operated nuclear reactors in the world, particularly in countries such as Russia, China, India and several Eastern European countries. Among the different VVER reactors, the VVER-1000/V320, a Gen-II design, is the most widely deployed, with a total of 25 units in operation worldwide. This design has served as an important precursor to the more Gen-III/III+ VVER reactors. The transition from Gen-II VVER to Gen-III/III+ VVER is driving further interest in understanding the performance and safety aspects of these reactors.
- On the other hand, there is a renewed and growing interest in the Passive Safety Systems (PSS) that ensure the core integrity during accidental sequences with a total loss of AC power. These PSSs, which could operate without the need for active human intervention or external power sources, could be useful to ensure reactor safety under extreme conditions. This focus is particularly relevant following accidents such as that at Fukushima Daiichi, which have highlighted the vulnerability of conventional active safety systems.

It should be noted that the majority of the Gen-III/III+ VVER reactors incorporate advanced PSSs, which are found in the Emergency Core Cooling System (ECCS), in the heat removal systems and in the containment.

Based on this, the primary objective of this doctoral thesis is to assess the enhancement of safety margins provided by the new advanced PSSs in the VVER reactors. To achieve this, safety analyses have first been conducted on a VVER-1000/V320 reactor with conventional safety systems. Subsequently, a series of

safety analyses have been carried out on a VVER-1000/V320 reactor equipped with the Second Stage Hydro-accumulators (HA-2), of the VVER-1200/V392M, and the air-cooled Passive Heat Removal System (PHRS), of the VVER-1000/V412 at the Kudankulam Nuclear Power Plant (KKNPP).

As a result of this effort, it has been possible to acquire a comprehensive understanding of the VVER-1000/V320 technology, with particular emphasis on nuclear safety. The various safety systems incorporated in this reactor design, including their configurations and their ability to cope with different accident sequences, have been explored in depth. A key aspect of this research has been to identify and analyse the main differences between the safety systems of VVER reactors and those of Western Pressurizer Water Reactors (PWR).

In parallel, extensive knowledge has also been gained about new safety systems incorporated into Gen-III/III+ VVER reactors. Some of the main aspects explored have been: what are the strengths and weaknesses of these Gen-III/III+ VVER safety systems; what types of accident sequences are they specifically designed for; how do they differ from the PSSs used in Western PWR; and for how long can these systems maintain the integrity of the nuclear fuel without human intervention or dependence on external AC power.

The document is structured as follows: Chapter 2 presents a comprehensive review of the state of the art covering the main topics of the doctoral thesis. It begins with an introduction to the PSSs found in Light Water Reactors (LWR). This is followed by an overview of the evolution of VVER reactors, providing a historical context for this technology, a detailed description of the VVER-1000/V320 reactor and the various Gen-III/III+ VVER designs, with particular emphasis on their safety systems. Finally, the VVER-1000/V320 standard Event Trees (ET) for Generic Transient (GT), Loss Of Off-site Power (LOOP), Small Break Loss Of Coolant Accident (SBLOCA), Medium Break Loss Of Coolant Accident (MBLOCA) and Large Loss Of Coolant Accident (LBLOCA) are presented.

Then, in Chapter 3 the model developed for the TRACEV5P5 system code of a VVER-1000/V320 reactor is detailed in depth. Thereafter, Chapter 4 presents a series of transients conducted by means of the VVER-1000/V320 model to verify the correct performance of the implemented controls, safety systems, and their respective actuation signals. The analyses include a SCRAM, a Main Coolant Pump (MCP) trip, a Station Blackout (SBO) and two LOCA sequences.

Next, Chapter 5 presents two analyses carried out with the VVER-1000/V320 reactor model, considering only the conventional safety systems of this technology. In the first analysis, the MBLOCA and LBLOCA ETs are assessed, re-evaluating the Success Criterion (SC) of each safety system involved in the accident, and developing new ETs for sequences where the old SCs are updated. In the second analysis, a study is made of the different strategies for managing the SBLOCA sequences along with High Pressure Injection System (HPIS) failure in VVER-1000/V320 reactors. A comparison is also made with the strategies implemented for this accidental sequence in the Pressurized Water Reactor Westinghouse (PWR-W). In this analysis, a previous review of the Emergency Operating Procedures (EOP), the SBLOCA ETs and the experimental tests has been conducted.

Subsequently, Chapter 6 presents two further analyses based on the performance of two PSSs incorporated in the Gen-III/III+ VVER reactors, the HA-2 and the air-cooled PHRS. For this purpose, the VVER-1000/V320 reactor model for the TRACEV5P5 system code has been used, implementing the new PSSs. The first analysis of the chapter aims at studying the impact of the HA-2 on the event of a LOCA sequence, with and without SBO conditions. The second analysis focuses on the performance of the air-cooled PHRS in SBO sequences with and without LOCA, also considering the actuation of the HA-2. Furthermore, at the end of Chapter 6, based on all the knowledge gained through the realisation of the analyses involved in this doctoral thesis, proposed ETs for the LOOP, SBLOCA and LBLOCA Initiating Events (IE), including headers related to the PSS analyzed, are presented.

Finally, Chapter 7 summarises the findings and presents the concluding remarks of the doctoral thesis.

Chapter 2.
State of the art

This chapter deals with the latest advances and developments in the field of nuclear reactor technology, with particular emphasis on VVER designs. It is divided into three main sections. First, in Section 2.1, the PSSs included in Gen-III/III+ reactors are presented. Next, in Section 2.2, the evolution of VVER reactors is shown followed by a comprehensive description of the VVER-1000/V320 design and the Gen-III/III+ VVER. Finally, Section 2.3 gives the standard ET of the VVER-1000/V320 for different accidental sequences.

2.1. Passive Safety Systems

The International Atomic Energy Agency (IAEA) defines a PSS as "a System which is composed entirely of passive components and structures or a system which uses active components in a very limited way to initiate subsequent passive operation", (IAEA, 1994, 1991). Based on this definition, the IAEA establishes a classification to determine the passiveness level of a system based on whether it moves fluids or mechanical parts and whether it requires external power or signal inputs, see Table 2-1 and (Burgazzi, 2012; Fil et al., 1999; IAEA, 2009). In fact, PSSs cannot be classified exclusively as "passive" or "active", as both passive and active means can be found in the single safety system, e.g. a system could be driven by natural forces, such as gravity, but need a valve opening to initiate the operation.

Furthermore, a PSSs can also be classified according to the safety function they perform into three groups that are commonly found in the literature (Bryk et al., 2019; Buchholz et al., 2015; Heung Chang et al., 2013; IAEA, 2019, 2016; Kaliatka, 2017; Yamada and Tuniz, 2011): passive ECCS, PHRS and passive containment cooling safety systems, see Table 2-2.

Among the advantages of the PSS, it is worth highlighting the following (Burgazzi, 2012; Fil et al., 1999; Prosek et al., 2022):

- Independence from AC power
- Simplified configuration and a reduced number of devices
- Reduced probability of human error

- Less sensitive to equipment failure
- Economically competitive

However, the PSS have some disadvantages compared to active safety systems: lack of knowledge of certain phenomena, lack of operational experience or lack of data, (Burgazzi, 2012; Fil et al., 1999; Prosek et al., 2022). Moreover, the PSSs present some Thermal-hydraulic (TH) challenges, such as the effect of the non-condensable gases, which degrade the heat transfer process, and the temperature stratification in the water pools, (Kaliatka, 2017). The driving mechanism associated with the PSSs are the following (Prosek et al., 2022):

- Gravity, including density difference (e.g. elevated tanks)
- Pressure difference (e.g. ACCs)
- Thermal exchanges (e.g. HXs, ICs)
- Internal heating phenomena (e.g. nuclear decay heat)
- Internal chemical phenomena (e.g. passive autocatalytic recombiners)
- Phase change (e.g. from steam to liquid water or from liquid water to steam)
- Any combination of the above forces

There are several NEA/CSNI/WGAMA activities, see (NEA, 2020), and European projects that have studied the behaviour of the PSSs: McSafer (Sanchez-Espinoza et al., 2021), PASTELS (Montotut, 2021), sCO2-4-NPP (Prosek et al., 2022), PIACE (De Grandis et al., 2019), PERSEO Benchmark (Mascari et al., 2023), ISP-51 experiment in ACME (in progress), OECD/NEA Advanced Thermal-Hydraulic Test Loop for Accident Simulation (ATLAS) projects (NEA, 2022), or the OECD/NEA ETHARINUS project involving the Primary Coolant Loop Test Facility (PKL) (NEA, 2004).

The different types of PSS that can be found in the large and small LWR are presented below: the Passive ECCSs in Section 2.1.1, the PHRSs in Section 2.1.2 and the Passive Cooling Containment Safety Systems in Section 2.1.3.

Table 2-1 Passive Safety Systems IAEA classification

	Cat.	Criteria						Examples
		Moving fluids	Moving parts	Signal Inputs	Extern. Power	Human initiation	Human interact.	
Passive	A	No	No	No	No	No	No	Cooling radiation, concrete building
	B	Yes	No	No	No	No	No	Cooling based on natural circulation
	C	Yes	Yes	No	No	No	No	Accumulators, check valves
	D	Yes	Yes	Yes	No/Yes*	No	No	Passive heat removal systems, elevated gravity drain tank
Active	E	Yes	Yes	Yes	Yes	No	No	ECCS of GEN-II LWRs
	F	Yes	Yes	Yes	Yes	Yes	No	Boron injection
	G	Yes	Yes	Yes	Yes	Yes	Yes	Fire protection system

Table 2-2 Passive Safety Systems classified by safety functions

Passive Emergency Core Cooling Systems	Accumulators	
	Make-up tanks	
	Elevated Gravity Drain Tanks (inside/outside containment)	
	Long Term Core Cooling	
Passive Heat Removal Systems	Through the SGs	Cooled by a water pool
		Cooled by air flow
	Through the RCS	Cooled by a water pool
		Cooled by a closed extra loop
Passive Cooling Containment Safety Systems	Suppression Pool	
	Containment Condenser (cooled by water or air)	
	Condensation in Containment inner wall	

2.1.1. Passive Emergency Core Cooling Systems

The following is an overview of the passive ECCSs implemented in different reactor designs included in Table 2-2:

- Accumulators (ACC): Tanks containing borated water and pressurized with non-condensable gases. All Gen-II and Gen-III PWR include this PSS, see Table 2-3 and (AREVA, 2007; Bajorek, 2007; Ebrahimgol et al., 2021; Gavrilas et al., 1995; Hosseini et al., 2020; Queral et al., 2021; Shoushtari et al., 2016; USNRC

HRTD, 2011). Moreover, ACCs can also be found in almost all the Light Water Small Modular Reactor (LW-SMR). The name given to the ACCs can be different depending on the design, so that for Babcock & Wilcox (B&W) reactors they are known as Core Flood Tanks, for Combustion Engineering (CE) reactors as Safety Injection Tanks and for the VVER reactors as First Stage Hydro-accumulators (HA-1). The main characteristics of ACCs are:

- ACCs are isolated from the Reactor Coolant System (RCS) by implementing check valves that open when the pressure in the RCS drops below the pressure of the non-condensable gases. It is noteworthy that the ACC pressure in VVER reactors is higher than in the other PWR reactors, see fourth column in Table 2-3.
- According to the reactor design, different connections to the RCS can be found, see fifth column of Table 2-3. Some ACC designs are directly connected to the Reactor Pressure Vessel (RPV) and not to the Cold Legs (CL) or Hot Legs (HL), ensuring that in the event of a CL/HL LOCA the ACC inventory is not lost through the break instead of reaching the core.
- Some reactors designs are equipped with a valve downstream of the ACCs, which isolates them automatically when the borated water level dropped below a certain level, thus preventing non-condensable gases from entering the RCS and being deposit on the SG tubes, deteriorating the heat exchange in them (D. C. Cacuci (ed.), 2010). In VVER-1000 reactors, these valves are AC motorised, but they are powered by first category of secured power supply, which implies that there is a DC/AC inverter at the battery output capable of powering the isolation valves for at least 12 hours, so that in the event of an SBO sequence, isolation of the HA-1 is guaranteed (ČEZ, 2012). Previous VVER-440 reactors are equipped with floating valves inside the ACCs that have a similar function (Kral et al., 2011; Queral et al., 2021). Other PWR designs, e.g. Westinghouse, include in the EOPs a manual action of isolating the ACCs or venting the nitrogen valves. In addition, new venting valves have been proposed, e.g. the Automatic Safety Valve for Accumulator Depressurization (ASVAD), which have been developed to passively vent ACCs when they reach 1.5 MPa (Freixa et al., 2021).

- Finally, it can be highlighted that the design incorporated in the APR1400/APR+ reactors, which include a Fluidic Device that allows for the injection of the borated water in two stages. This enables a more efficient use of ACCs inventory during the refill phase of the LOCA and therefore extends injection to the end of the reflood phase, so that the Low Pressure Injection System (LPIS) can be excluded from the reactor design (Korea Hydro & Nuclear Power Co., 2012). An application to a VVER-1000/V446, Bushehr NPP, has shown they could improve the safety margins in LBLOCA sequences (Pouresgandar et al., 2022).

Table 2-3 Accumulator designs comparison

Reactor Design	Number ACC/HA-1	Total Capacity (m^3)	Pressure (MPa)	Injection Connection
Westinghouse (3/4loop)	3/4	41 (x3) / 34 (x4)	4.4 / 4.5	CL
Siemens (Konvoi)	8	34 (x4)	2.5	4 to CL and 4 to HL
Framatome (P4)	4	47 (x4)	4.0	CL
B&W	2	51 (x2)	4.13	DVI to DC
CE	4	46.5 (x4)	4.11	CL
CPR1000	3	33.2 (x 3)	4.93	CL
VVER-1000 and VVER-1200	4	60 (x4)	6.0	2 UP and 2 DC
VVER-1000/V446	4 + 8 KWU-ACCs	60(x4) + 45 (x8)	6.0 2.5	HA-1:2UP and 2DC KWU ACCs: 4 CL and 4 HL
EPR	4	150 (x4)	5.5	CL
AP1000 and CAP1400	2	56.6 (x2) / 65(x2)	4.9	DVI to DC
APR1400	4	68 (x4)	4.2	DVI to DC
Hualong	3	50 (x 3)	5.5	CL

- Make-up Tanks: Tanks that are completely full of borated water. In VVER reactors this system is usually referred to as HA-2, while for the other reactors is usually known as Core Make-up Tank (CMT). A comparison of the make-up tanks included in different designs can be seen in Table 2-4 and (Deng et al., 2020; Kim et al., 2020; Shi et al., 2021; Yang et al., 2024; Yeh and Xie, 2024; Yusheng et al., 2024). Some proposals have been made to include also this system in the secondary side of the CPR1000 and Hualong reactors, where it is known as the Emergency Makeup Tank (EMT), (Li et al., 2021; Sun et al., 2018; Zhang et al., 2011). The main characteristics of the make-up tanks are the following:
    - They are connected upstream by a line to the RCS, either to the CL in the large reactors or to the RPV in the LW-SMR (Kim et al., 2020; Qiu et al., 2023). In the AP1000, CAP1400, ACP100 and SMART reactors this upper line is open, i.e. in stand-by mode the CMTs are at the RCS pressure, however in the VVER reactors this line is initially closed but contains a special dual check valve that opens when the pressure in the RCS is below 1.5 MPa (IAEA, 2017).
    - On the bottom, both the CMTs and the HA-2 are usually connected to the ACCs and HA-1 injection lines to the vessel. Under normal operation this line is isolated from the RCS with check or isolation valves which open when the system is required to fulfil its safety function allowing the inventory flows into the RCS by the effect of the hydrostatic pressure (Veselov and Tishin, 2017).
    - It should be noted that in the case of the VVER reactors, the pressure setpoint of the HA-2 (1.5 MPa) is lower than that of the ACCs (labelled HA-1 in VVER reactors), so they actuate as a low pressure injection system, while in other designs the pressure setpoint of the CMT (11.7 MPa) is higher than that of the ACCs, and then actuate as a high pressure injection system, see fourth column in Table 2-4.

Table 2-4 Make-up tank designs comparison

Reactor Design	Number of trains	Total volume (m^3)	Pressure setpoint (MPa)	Injection connection	Stages
VVER-1200/V392M & VVER-1300/V510 (VVER-TOI)	4	120 x 2 (x4)	1.5	Accumulator Injection Line UP/DC	4
VVER-1000/V412	4	120 x 2 (x4)	1.5	Accumulator Injection Line UP/DC	6
AP1000 / CAP1400	2	70.8 (x2) / 85 (x2)	11.7	DVI	1
ACP100	2	18 (x2)	N/A	DVI	1
SMART	4	N/A	~11	DVI	1
SMR-160	2	N/A	N/A	DVI	1

- Elevated Gravity Tanks: Tanks with large volumes, that can be placed outside or inside the containment at atmospheric conditions. They are located at higher elevation and have the capability of supply water to the RCS by gravity during several days at low pressure conditions (Buchholz et al., 2015; IAEA, 2019; Yamada and Tuniz, 2011). An example is the In-containment Refuelling Water Storage Tank (IRWST) of the AP1000 reactors, which is connected to the Direct Vessel Injection (DVI) lines and has a total volume of 2070 m^3 (Queral et al., 2015). Furthermore, there are Gen-II reactors that have tanks at a higher level than their injection point to the RPV, so that it is possible to inject borated water to the RCS from this tank passively, (Gavrilas et al., 1995), mainly at reduced inventory or mid-loop conditions.
- Long Term Core Cooling: this PSS consists of the containment sump or the RPV cavity connected to the RPV by a recirculation line, like in the AP1000. Its function is to passively return the inventory lost during a LOCA sequence to the RCS (Buchholz et al., 2015).

All the PSSs described are designed to inject water into the RCS in the event of a LOCA sequence. In this sense, it can be highlighted how the ACCs/HA-1 and the

CMTs are mostly intended to replenish the RCS inventory during the initial stages of the accidental sequence. However, in order to ensure core cooling for several hours or days, the make-up tank included in the VVER, i.e., the HA-2, the Elevated Gravity Tanks and the Long Term Core Cooling PSSs have been mainly conceived, (Buchholz et al., 2020). An overview of the large Gen-III PWR and LW-SMR that includes the passive ECCS can be found in Table 2-5 and (Buchholz et al., 2020, 2015; ROSATOM, 2019a; Zeliang et al., 2020).

Following this review a clear distinction can be made between the passive ECCS at the AP1000/CAP1400 and the VVER reactors, see Figure 2-1. Both designs are the only large nuclear reactors to include both high/medium and low pressure passive ECCS.

On the one hand, the AP1000/CAP1400 incorporates the CMTs as a passive high pressure ECCS, the ACCs and the IRWST, which is able to replenish water into the RCS at low pressure. On the other hand, there is no passive high pressure ECCS for VVER reactors whose function is equivalent to that of the CMTs in the AP1000/CAP1400 reactors, however, their ACCs have a higher pressure than that of the AP1000/CAP1400 ACCs. The HA-2 of the VVER is a make-up tank, however its function is not similar to that of the CMT, since it is designed to replenish water in the RCS at low pressure for 24 hours, which justifies that its volume is greater than that of the CMTs.

Table 2-5 Reactor designs with passive ECCS

ECCS	IAEA Category	Reactor Designs
Accumulator	C	ACP100, SMART, CAREM, SMR-160, NUWARD, RITM-200, VVER-1200, EPR, AP1000/CAP1400, APR1400, Hualong and Gen-II PWR
Make-up Tank	D	ACP100, SMART, AP1000/CAP1400, VVER-1200/V-392M, VVER-1000/V-412
Elevated Gravity Tanks	D	ACP100, SMR-160, AP1000/CAP1400
Long Term core cooling	D	ACP100, CAREM, RITM-200, SMART, SMR-160, NuScale, NUWARD, AP1000/CAP1400

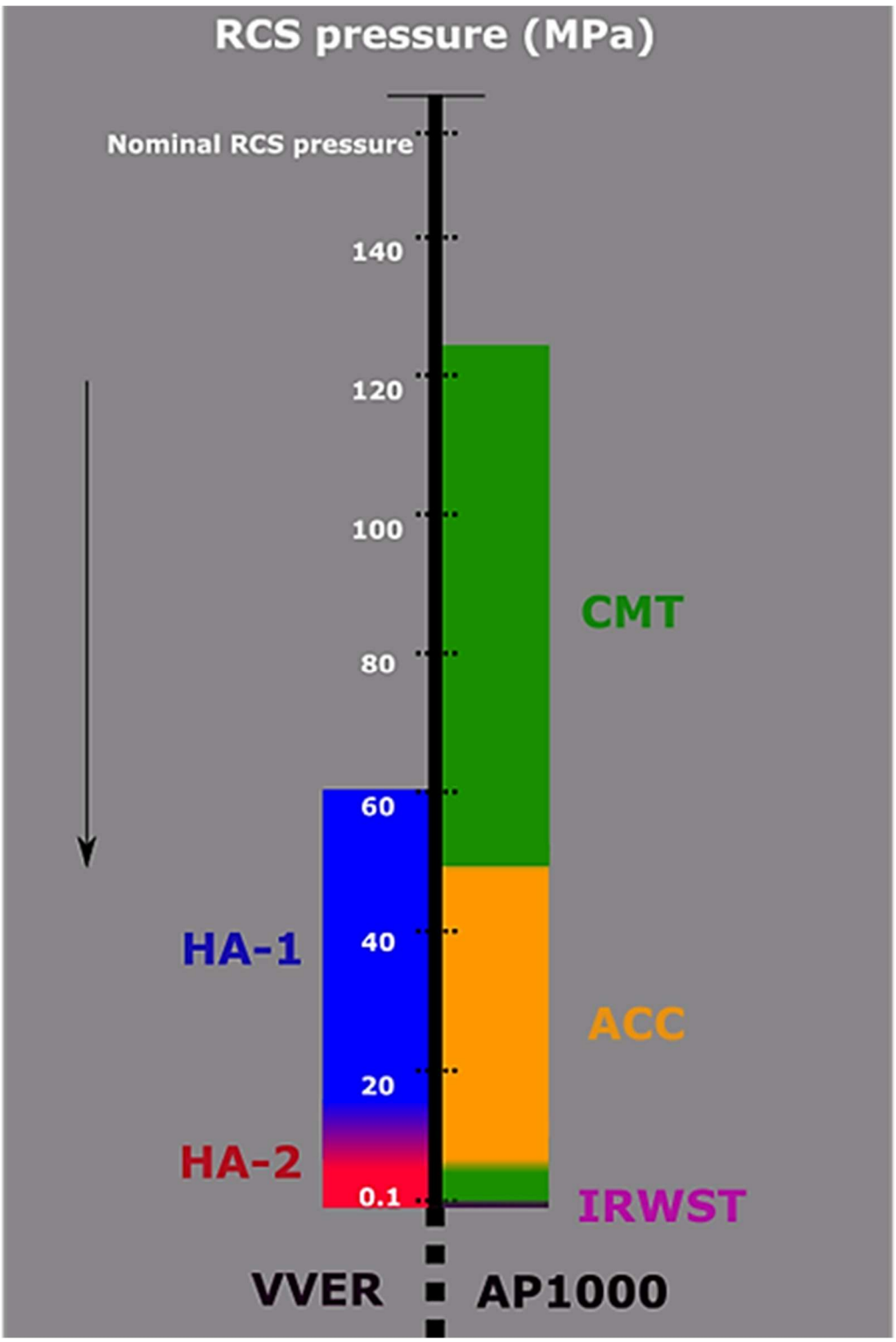

Figure 2-1 VVER and AP1000 Passive ECCS comparison

2.1.2. Passive Heat Removal Systems

The PHRSs are designed to remove decay heat from the core over extended periods of time without the need for AC power or human intervention, (Surip et al., 2022). The following section provides an overview of the different types of PHRS designs.

There are different PHRS designs, which are incorporated into several Gen-III/III+ LWR designs. The PHRS can be divided into two groups, those that are connected to the secondary side of the SG and those that are connected to the RCS or the RPV. That PSS can also be distinguished according to the heat sink: a pool or the atmospheric air:

- PHRS in the secondary side of the SGs: The PHRSs in the SGs are typically found in a large number of Gen-III/III+ PWR designs, both small and large, with some exceptions such as the AP1000 and the CAREM reactors. In this PHRS configuration, the decay heat is removed via a two-phase natural circulation loop connecting the elevated Heat Exchanger (HX) to the SGs, (IAEA, 2009). The number of PHRS trains is usually equal to the number of RCS loops. The PHRS in the SGs can be water or air cooled:
    - Cooled by a water pool: The HXs are located in a large pool of water at atmospheric conditions. When the PSS comes into operation, the steam energy from the SGs is transferred to the water pool, which heats up and evaporates. This design is found in the HPR-1000 (Xing et al., 2016) and the VVER-1200/V491 (Bezlepkin et al., 2014), where the water pool is located in an elevated position between two containment structures. It is also found in small reactors; ACP-100, SMART, RITM-200 (Ekariansyah et al., 2021) and in the NuScale, where the tube bundle is located in the external pool where the NuScale power modules are inserted, (NuScale Power LLC, 2019).
    - Cooled by air flow: The HXs are cooled by external atmospheric air. When the PSS is operating, the air passes through the HX tube bundle by natural circulation, increasing its temperature. This design is found in the VVER-1000/V412 (Agrawal et al., 2006) and in the VVER-1200/V392M (Galiev et al., 2017), V509 and V523. The HXs are housed in a shell in the outer part of the containments and are connected to air ducts through which the air flow passes.

- PHRS in the RCS or RPV: The PHRS connected to the RCS can be found in the AP1000 (Westinghouse, 2011) and the CAREM PWRs, and in the classical and advance Boiling Water Reactors (BWR) such as the ESBWR (GE Hitachi Nuclear Energy, 2014), the BWRX-300 (Rassame et al., 2017) or the conceptual design KERENA (IAEA, 2011a). In this PHRS configuration, the decay heat is removed via a HX loop, which can be either a two-phase or a single-phase liquid natural circulation. The HX can be connected directly to the RPV or the RCS, or to another HX within the RPV:
    - Cooled by a water pool: The HXs, which are placed in a water pool, are connected to the RPV or the RCS. When this PSS comes into operation, the inventory from the core passes into the HX tubes where it causes the water pool to evaporate. In the AP1000 reactor, the HX loop is a liquid single-phase natural circulation loop, but in CAREM and in BWR, the HX loop is a two-phase natural circulation loop.

      Besides, in the BWR the water-cooled PHRS is referred to as Isolation Condenser (IC). On the other hand, it should be noted that not only the Gen-III/III+ reactors such as the BWRX-300 and the ESBWR have this PSS, but also the Gen-II BWR/3 such as the Fukushima Daiichi (unit 1) (Dolganov, 2024). However, this design in the BWR/3 were not developed to withstand an SBO event, so the water pool is considered to be smaller than that of the Gen-III/III+ LWRs (Grant et al., 1996).
    - Cooled by a closed extra loop: The decay heat is removed from the core through a loop containing two HXs, one inside the RPV and one introduced into a pool of water. The main purpose of this design is that the coolant passing through the core does not leave the RPV. This structure is included in some conceptual designs, but no LWR reactor has currently been built with this type of PHRS (Buchholz et al., 2015).

Table 2-6 PHRS designs comparison

Reactor Design	Reactor Thermal Power (MW)	Number of PHRS trains (HXs/train)	Heat removal / train (MW)	Cooled by (HX location)	IAEA PSS category
AP1000	3000	1 (1 HX/trains)	60	Water pool (RCS)	D
BWR/3	1400	1-2 (1-2 HX/trains)	40	Water pool (primary)	D
BWRX-300	870	3 (2 HX/trains)	33	Water pool (primary)	D
ESBWR	4500	4 (2 HX/trains)	33	Water pool (primary)	D
HPR-1000 (CGN, CNNC)	3000	3 (1 HX/trains)	20	Water pool (SGs)	D
NuScale	160	2 (1 HX/trains)	4	Water pool (SGs)	D
VVER-1000/V412	3000	4 (3 HX/trains)	20	Air (SGs)	D
VVER-1200/V392M	3200	4 (2 HX/trains)	30	Air (SGs)	D
VVER-1200/V491	3200	4 (16 HX/trains)	30	Water pool (SGs)	D
KERENA	3370	4 (1 HX/train)	N/A	Water pool (primary)	B

As previously discussed, the IAEA establishes a classification to determine how passive a safety system is based on the moving fluids, the moving parts, the signal input, the external power and the human actions, see Table 2-1. Most PHRSs are classified by the IAEA as Category D PSS because they require an input signal to open the isolation valves or the gates that allow the PSS to begin removing decay heat.

In particular, the PHRS in the KERENA reactor design (never built) does not have isolation valves. Heat transfer during normal reactor operation is prevented by an anti-circulation loop, which blocks the flow between the RPV and the PHRS tubes in stand-by conditions. Therefore, the PHRS for the KERENA reactor does not require signal inputs to start operation and hence is classified as Category B.

It is important to note that not only are some LWRs equipped with PHRS, but other designs, such as liquid metal cooled reactors (IAEA, 1999) and high temperature reactors, also incorporate these PHRS (U.S. Nuclear Regulatory Commission, 2021). In Sodium Fast Reactors (SFRs), several designs, including PFR, PFBR, CFBR, BN-1200, JSFR, Kalimer, SPX-1, EFR and ESFR, see (Chetal, 2011; Choi, 2009; Kurisaka, 2012), incorporate air-cooled PHRS, consisting of a closed loop that transfers the decay heat from the reactor pool to the atmosphere. Moreover, the ALMR, PFBR, BN-500, Phenix and Astrid SFRs have air-cooled PHRS, and the Astrid SFR has water-cooled PHRS connected to the SGs. Furthermore, there are some SFRs, such as the ALMR and the PFR, where the PHRS consists of air flowing around the vessel walls, see (Gluekler, 1997; Jensen and Ølgaard, 1995). On the other hand, it is worth mentioning the HTR-PM, a high-temperature reactor in which the decay heat is transferred from the vessel to the water-filled PHRS tubes by radiation, see (China Nuclear Engineering Group Corporation (CNEC), 2019; Takeda and Inagaki, 2021).

2.1.3. Passive Containment Cooling Safety Systems

In order to manage the RCS or secondary side inventory discharges into the containment, several PSS can be found which are capable of cooling and depressurising the containment. Most Gen-II LWRs utilize active safety systems that spray water droplets from the upper part of the containment, condensing the steam and thereby lowering the pressure and temperature to maintain containment integrity.

In contrast, some Gen-III/III+ large and small LWRs are equipped with PSSs designed to maintain the temperature and pressure within design limits for a long time during an accidental sequence without the need for AC power or human intervention, see Table 2-7 and (Buchholz et al., 2020, 2015; IAEA, 2016; Kaliatka, 2017). The main passive containment cooling safety systems are:

- Suppression pool: High pressure and temperature steam from the RPV and the containment is conducted to the suppression pool in the wet well to mitigate the pressure increase. This system is common in BWR but is also implemented in PWR-SMR such as CAREM, where it is considered as category D due to the need for external signals.
- Containment Condenser: Found in both BWRs and PWRs, the IC is located in the upper part of the containment. In most reactor designs with this PSS, it requires external signals and is therefore considered as category D. In the BWR, the steam in the containment condenses inside the IC tubes, which are immersed in a large water pool. In these reactors, the effect of the non-condensable gases present in the containment must be considered, (Buchholz et al., 2020). In the ESBWR, the steam-gas mixture in the dry-well passes through the inner part of the IC tubes, condenses, and returns to a pool connected to the RPV, while the non-condensable gases are sent to the suppression pool. In contrast, in the ABWR, the condensate from the IC is sent to the suppression pool in the wet-well, (Burgazzi, 2012).

  In the PWR designs, the IC is connected to an elevated water pool rather than immersed in it. The IC tubes are angled slight angle to allow natural circulation within the tubes so that the steam in the containment condenses on the outer wall of the IC tubes and the water inside evaporates. In stand-by mode, this system is filled with water that is at a temperature similar to that of the containment, and when a LOCA occurs, the heat transfer takes place due to the pressure and temperature difference between the IC tubes and the containment. This design is found in the VVER-1200/V491, Hualong and ACP100 PWRs, and is also present in the KERENA BWR design, (Bryk et al., 2019).
- Condensation on Containment inner Wall. This facilitates both steam condensation on the inner containment wall and the decay heat release by convention or conduction mechanisms, (IAEA, 2016). There are two variants of this system:

- In Small Modular Reactors (SMR), as in the NuScale reactor, the metal containment is immersed in a pool of water, which is possible due to the reduced dimensions of the RPV. In the SMR, the condensation on the inner wall of the containment is considered as category B, as external signals are not required (NuScale Power LLC, 2020).
- The large LWRs containment cannot be fully immersed in a water pool. Instead, they use a large water of pool at the top of the containment. In an accidental sequence, the metallic containment is cooled by air flowing through the annulus between the metallic and the concrete containments, driven by a chimney effect, and by water bubbles from the upper water pool. This configuration is found in the AP1000 (Westinghouse, 2011) and the CAP-1400 reactors, where it is classified as category D.

It should be noted that most of the Gen-III/III+ LWR have other safety systems designed for severe accidents, such as the in-vessel retention system, developed to retain the corium inside the RPV, the Core Catcher (CC), designed to contain the corium if it escapes from the RPV and the Passive Autocatalytic Recombines (PAR), to reduce the H_2 concentration in the containment.

Table 2-7 Reactor designs with passive containment cooling safety systems

Passive containment cooling safety system	IAEA Category	Reactor design
Suppression Pool	D	CAREM
Containment Condenser	D	ACP100, VVER-1200/V491, Hualong, ACP100, ESBWR, ABWR
Condensation on containment inner wall	B or D	ACP100, NuScale, AP1000/CAP1400

2.2. VVER reactors

The aim of this section is to present the state of the art concerning VVER reactors. To this end, the historical development of VVER models is first discussed in Section 2.2.1. Subsequently, in Section 2.2.2, the VVER-1000/V320 reactor is described in detail, both in terms of its components and its auxiliary and safety systems. Section 2.2.3 then outlines the different designs of Gen-III/III+ VVER reactors, with particular emphasis on their safety systems. Finally, Section 2.2.4 gives a detailed description of the two PSSs analyzed in this PhD thesis, the HA-2 and the air-cooled PHRS.

2.2.1. Evolution of the VVER reactors

The acronym VVER stands for "Vodo-Vodyanoi Energeticheskii Reactor" that in English means "Water-Water Energetic Reactor", so it is also typical to find them referred to as WWER. These nuclear reactor designs represent a remarkable path of technological advancement from the first VVER designs to the Gen-III + VVER-1200, see Figure 2-2.

VVER reactors emerged in the 1950s, around the same time as Western PWRs. Both types of reactors use UO_2 as fuel and operate on a Rankine steam cycle on the secondary side of the SGs, achieving efficiencies close to 33%. The similarities in their basic operating principles are so that VVERs and Western PWRs are often considered to be variations of the same reactor type, (ROSATOM, 2019b). Although the design of VVER reactors has changed significantly over the decades, the first models had features that later became common to all VVERs:

- The dimensions of the RCS components and SGs allow them to be transported by rail, which was one of the key conditions for the design of the first VVERs, (Ryzhov et al., 2010). These requirements determine not only the maximum diameter of the reactor, but also the configuration of some of its elements (angles between loops, nozzles characteristics, etc.).
- VVERs are characterised by hexagonal Fuel Assemblies (FA), as well as tighter triangular FA lattices and fuel rods with a smaller pitch, (Luciano et al., 2016). As a result, VVERs have a high specific energy density. The VVER typically used 9.1 mm diameter fuel pellets with a lattice pitch from 12.2 mm to 12.75 mm.

- VVER reactors have consistently utilized horizontal SGs, unlike the vertical SGs found in Western PWRs, (Egorov et al., 2020). This horizontal configuration offers greater compactness and a larger heat transfer area, (Ghazanfari et al., 2014; Rabiee et al., 2016). However, it complicates the containment layout.
- There are no penetrations in the RPV below the top of the core. This removes the probability of a LOCA in the lower part of the RPV. It should be noted that almost all western Gen-III PWR designs have this feature.
- The Pressurizer (PZR) volume in VVER reactors is typically larger, providing a greater safety margin during operational transients, (ROSATOM, 2019b).
- In VVERs RPV, two characteristic internal structures are highlighted: the core barrel and the core baffle. The core baffle, which acts as a neutron reflector (Georgieva et al., 2015), is located inside the core barrel. Both structures protect the RPV from the neutron flux. It is emphasised that the modern Western PWR designs include structures similar to the core baffle, with the aim of reducing the impact of the neutron flux in the RPV.

The VVER designs development was started by OKB "GIDROPRESS" and the RRC "Kurchatov Institute" in 1955, (Mokhov, 2010). The evolution of these reactors consists of several generations, each characterised by technological advances, safety features and operational efficiency. The first VVER to be developed were the VVER-210 and the VVER-70, in the late 1950s and early 1960s, which pioneered the use of light water as a moderator and coolant in the Russian design reactors. These early models laid the basis for subsequent VVER reactors, see Table 2-8.

In the 1960s, the VVER-365 design emerged with the Novovoronezh I NPP (unit 2), which went into operation in 1969. It was the forerunner of the VVER-440 series, which marked the Gen-I VVER reactors. With an electrical capacity of 440 MWe, these reactors were designed to meet the energy needs of the time, providing a compact and reliable solution. The VVER-440 series is characterised by six RCS loops, see Figure 2-3. The first VVER-440 in operation were the VVER-440/V179 at Novovoronezh I NPP (units 3 and 4) and the VVER-440/V270 at Armenia NPP (units 1 and 2). However, unit 1 of the Armenia NPP was shut down after the 1995 earthquake.

The VVER-440/V230, a more advanced version, was introduced in the late 1960s and early 1970s in several countries, including Russia, Bulgaria, Slovakia and Germany. The NPPs with these designs are Kola NPP (units 1 and 2), Kozloduy NPP (units 1 to 4), Greifswald NPP (units 1 to 4) and Bohunice I NPP (units 1 and 2).

The evolution of the VVER continued with the VVER-440/V213 design in the 1970s. This design was widely used in Eastern Europe, with significant projects such as the Dukovany NPP in the Czech Republic, which was commissioned to the grid in 1988. Other notable NPPs of this design are Mochovce in Slovakia and Paks in Hungary.

It is worth noting that after German reunification in 1990, the four VVER-440/V230 units at Greifswald NPP were shut down for safety reasons. In addition, Greifswald unit 5, a VVER-440/V213 under construction, and the VVER-70 reactor at Rheinsberg NPP were also shut down. In addition, the closure of the four VVER-440/V230 units at the Kozloduy NPP in Bulgaria and the two VVER-440/230 units at the Bohunice I NPP in Slovakia was required as part of the entry of these countries into the European Union (World Nuclear Association, 2024). Nevertheless, many VVER-440/213 reactors remain in operation after undergoing extensive upgrades to improve safety and efficiency (Kovacs, 2014). More detailed information about the VVER-440 reactors can be found in (Kovacs. Z, 2014; Slugen, 2011).

The transition to the 1000 MWe VVER-1000 series in the 1970s and the 1980s represented a significant advance in reactor technology, such as a larger core size and improved safety systems. Although the VVER-1000 reactors have a higher thermal power than the VVER-440, it is important to note that the VVER-1000 has four RCS loops instead of six, see Figure 2-4. The VVER-1000 series, started with the Novovoronezh I NPP (unit 5), a VVER-1000/V187, which was connected to the grid in 1971. The VVER-1000 design was further refined with the introduction of the VVER-1000/V320. This variant became particularly prominent, with a total of 25 reactors in operation in Russia, Ukraine, Bulgaria and other countries. In particular, the Zaporizhzhia NPP in Ukraine, where six VVER-1000/V320 reactors were built between 1977 and 1986, became the largest NPP in Europe. It should be noted that some VVER-1000 NPP, as the Temelin NPP in the Czech Republic, has been upgraded with Western FAs, instrumentation and equipment (Tusheva, 2012).

The XXI century saw the emergence of the Gen-III/III+ VVER-1000 and VVER-1200 designs, see Table 2-8. Most of these reactors incorporated PSSs to meet the evolving challenges of the nuclear industry. The emphasis was on increasing both the operating life and the economic viability of these reactors to make them more competitive in the global economy. Two design families can be distinguished for Gen-III/III+ VVER reactors, that of the Joint Design Institute Atomproekt (in Saint Petersburg) and that of the Joint Design Institute Atomenergoproekt (in Moscow). In the following text, the former is referred to as the Saint Petersburg Institute and the latter as the Moscow Institute. The two main designs of the VVER-1000 Gen-III are the VVER-1000/V428 and the VVER-1000/V412:

- VVER-1000/V428, also known as AES-91, developed by the Saint Petersburg institute (ROSATOM, 2021). This design was deployed at the Tianwan NPP (units 1 to 4), in China.
- VVER-1000/V412, also known as AES-92, developed by the Moscow institute (ROSATOM, 2021). It is a modification of an earlier Gen-III design, the VVER-1000/V392, which was never built. The six units at the KKNPP in India are VVER-1000/V412.

Table 2-8 VVER reactors in operation and under construction (World Nuclear Association, 2024)

NPP	Country	VVER design	Beginning of construction	Grid connection
Novovoronezh I 1	Russia	VVER-210	1957	1964
Rheinsberg	Germany	VVER-70	1956	1966
Novovoronezh I 2	Russia	VVER-365	1963	1969
Novovoronezh I 3, 4	Russia	VVER-440/V179	1966	1971
Kola 1, 2	Russia	VVER-440/V230	1967	1972
Kozloduy 1-4	Bulgaria	VVER-440/V230	1970/70/73/73	1974/75/80/82
Bohunice I 1, 2	Slovakia	VVER-440/V230	1972	1978/80

Greifswald 1- 4	Germany	VVER-440/V230	1967/68/72/73	1973/74/77/79
Greifswald 5	Germany	VVER-440/V213	1974	-
Loviisa 1, 2	Finland	VVER440/V213	1971/72	1977/80
Kola 3, 4	Russia	VVER-440/V213	1975/77	1981/84
Mochovce 1, 2	Slovakia	VVER-440/V213	1982/85	1998/99
Bohunice II 1, 2	Slovakia	VVER-440/V213	1982/84	1998/99
Dukovany 1-4	Czech Republic	VVER-440/V213	1974/76/79/80	1985/86/87/88
Parks I 1-4	Hungary	VVER-440/V213	1972/74/81/82	1982/84/87/92
Rivne 1,2	Ukraine	VVER-440/V213	1973/81	1980/86
Armenian 1, 2	Armenia	VVER-440/V270	1972/75	1976/80
Novovoronezh I 5	Russia	VVER-1000/V187	1968	1971
South Ukraine 1	Ukraine	VVER-1000/V302	1973	1983
South Ukraine 2	Ukraine	VVER-1000/V338	1977	1985
Kalinin 1,2	Russia	VVER-1000/V338	1976/81	1984/86
Balakovo 1-4	Russia	VVER-1000/V320	1977/79/84/86	1985/86/93/95

Kozloduy 5, 6	Bulgaria	VVER-1000/V320	1980/81	1987/91
Kalinin 3, 4	Russia	VVER-1000/V320	1985/86	2004/11
Rostov 1-4	Russia	VVER-1000/V320	1977/83/09/10	2001/10/14/18
Zaporizhzhia 1-6	Ukraine	VVER-1000/V320	1977/80/83/84/85/86	1984/85/86/87/89/95
South Ukrainian 3	Ukraine	VVER-1000/V320	1983	1989
Rivne 3, 4	Ukraine	VVER-1000/V320	1981/83	1986/93
Khmelnytskyi 1, 2	Ukraine	VVER-1000/V320	1981/83	1987/94
Temelin 1,2	Czech Republic	VVER-1000/V320	1981	2000/02
Bushehr 1	Iran	VVER-1000/V446	1995	2011
Tianwan 1, 2 / 3, 4	China	VVER-1000/V428 (AES-91) VVER-1000/V428M (AES-91)	1999-2000 2012-13	2006-07 2017-18
Kudankulam 1-6	India	VVER-1000/V412 (AES-92)	2002/02/17/17/21/21	2013/16/-/-/-/-
Novovoronezh II 1,2	Russia	VVER-1200/V392M (AES-2006)	2008/09	2018/21

Akkuyu 1-4	Turkey	VVER-1200/V509 (AES-2006)	2018/20/21/22	2025/26/27/28
Rooppur 1, 2	Bangladesh	VVER-1200/V523 (AES-2006M)	2017/18	2025
Leningrad II 1 -3	Russia	VVER-1200/V491 (AES-2006)	2008/10/24	2018/21/-
Ostrovets 1, 2	Belarus	VVER-1200/V491 (AES-2006E)	2013/14	2020/23
Kursk II 1, 2	Russia	VVER-1300/V510K (VVER-TOI)	2018/19	2025
Bushehr 2	Iran	VVER-1000/V466B	2019	2028
El Dabaa 1-4	Egypt	VVER-1200/V529 (AES-2006E)	2022/22/23/24	-
Tianwan 7, 8	China	VVER-1200/V491 (AES-2006E)	2021	2026/27
Xudabao 3, 4	China	VVER-1200/V491 (AES-2006E)	2021/22	2027/28

Table 2-9 VVER reactors planned in a near term (World Nuclear Association, 2024)

NPP	Country	VVER design
Leningrad II-4	Russia	VVER-1200/V491 (AES-2006)
Smolensk II 1, 2	Russia	VVER-1300/V510 (VVER-TOI)
Paks II 1, 2	Hungary	VVER-1200/V527 (AES-2006E)
Kursk II 3, 4	Russia	VVER-1300/V510K (VVER-TOI)
Kola II 1, 2	Russia	VVER-600/V498

The latest stage in this evolution is the VVER-1200, considered as Gen-III+ reactors. There are two families of VVER-1200 reactors, derived from the two main VVER-1000 Gen-III design (Queral et al., 2021):

- Evolution from the VVER-1000/V428 (Tianwan NPP): The first VVER-1200 reactor design developed from the VVER-1000/V428 is the VVER-1200/V491, see Figure 2-5, which is in operation in Russia, Belarus and China, and a new one is planned at the Leningrad II NPP in Russia. Subsequently, new models of this reactor family are under construction as the VVER-1200/V527 (Paks II 1 and 2) and the VVER-1200/V529 (Dabaa NPP, units 1 to 4) in Hungary and Egypt respectively.
- Evolution from the VVER-1000/V412 (KKNPP): The VVER-1200/V392M, see Figure 2-6, deployed at the Novovoronezh II NPP (units 1 and 2), is the successor of the VVER-1000/V412. This reactor family also includes the VVER-1200/V509 (Akkuyu NPP, units 1 to 4) and the VVER-1200/V527 (Rooppur NPP, units 1 and 2), in Turkey and Bangladesh respectively.

The Bushehr NPP (unit 1) in Iran is a special case as it is a VVER-1000 NPP with a spherical containment of KWU design, (Noori-Kalkhoran et al., 2014). This is because this NPP was originally intended to be a German-designed KWU reactor. An agreement between Iran and Russia in 1995 stabilised that ROSATOM would

complete unit 1 of the Bushehr NPP using the infrastructure already in the place, (ROSATOM, 2019b).

Most recently, the VVER-1300/V510, known as the VVER-TOI, has been developed from the VVER-1200/V392M/V509/V527. It is being built for the Kursk II NPP in Russia. There are also plans to build two VVER-1300/V510 (VVER-TOI) at the Smolensk II NPP and two more at the Kursk II NPP, see Table 2-9. It should be noted that the Akkuyu NPP (VVER-1200/V509) incorporates several features and standards of the VVER-1300/V510 (VVER-TOI), (Queral et al., 2021). On the other hand, a new design of VVER, the VVER-600/V498, has been developed and is planned for construction at the Kola II NPP.

It is highlighted that the first VVER design to receive a certificate of compliance with the European Utility Requirements was the AES-92 in 2007. Later, in 2019, the same certificate was issued for the VVER-1300/V510K (VVER-TOI) design.

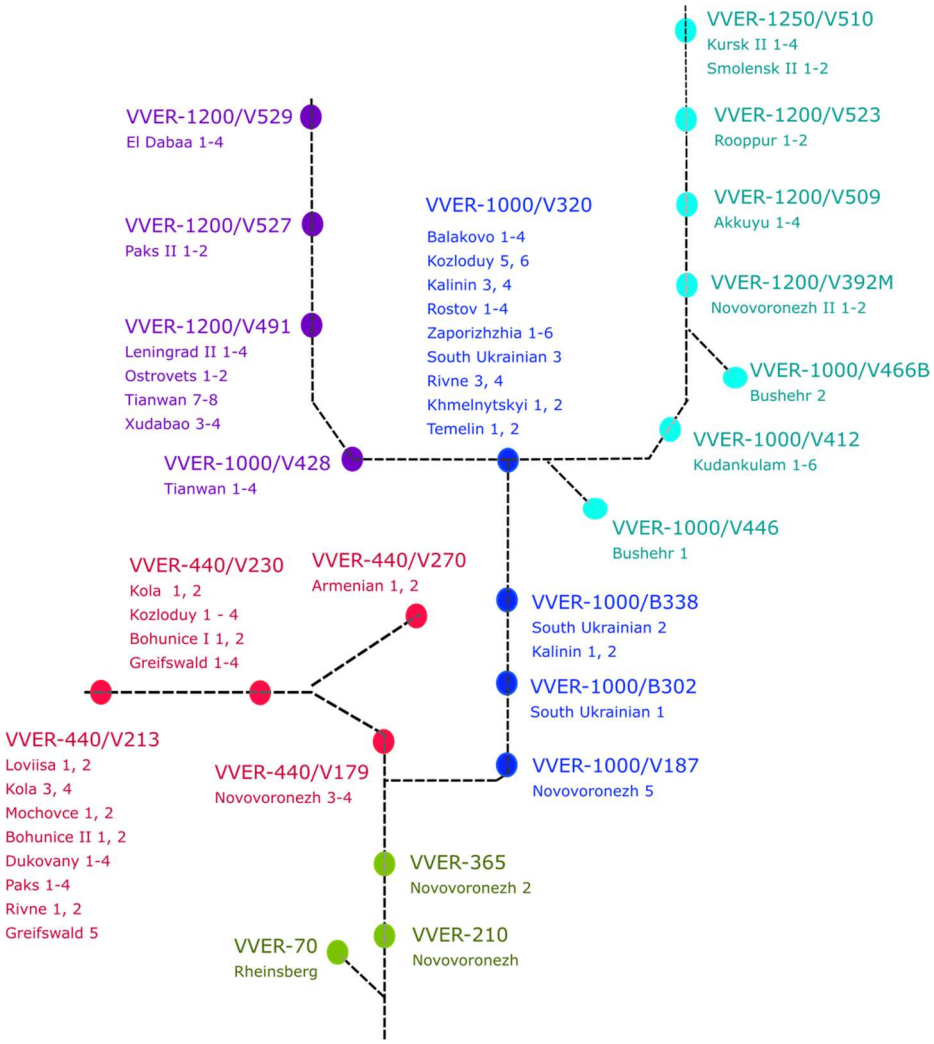

Figure 2-2 VVER reactors designs evolution (modified from (ROSATOM, 2019b)

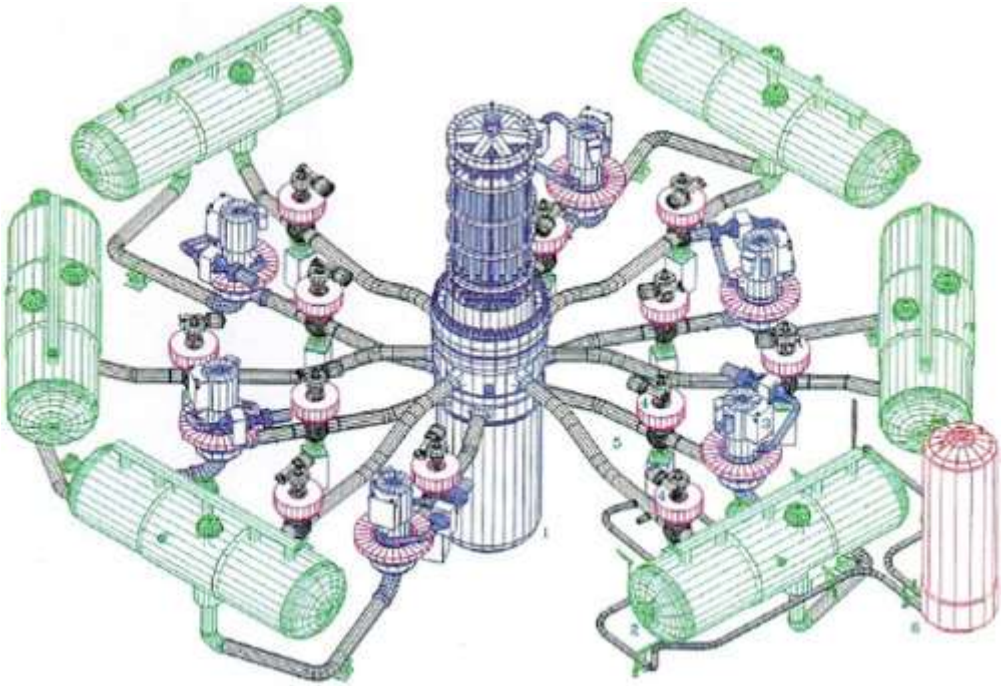

Figure 2-3 VVER-440 RCS (Misak, 2024)

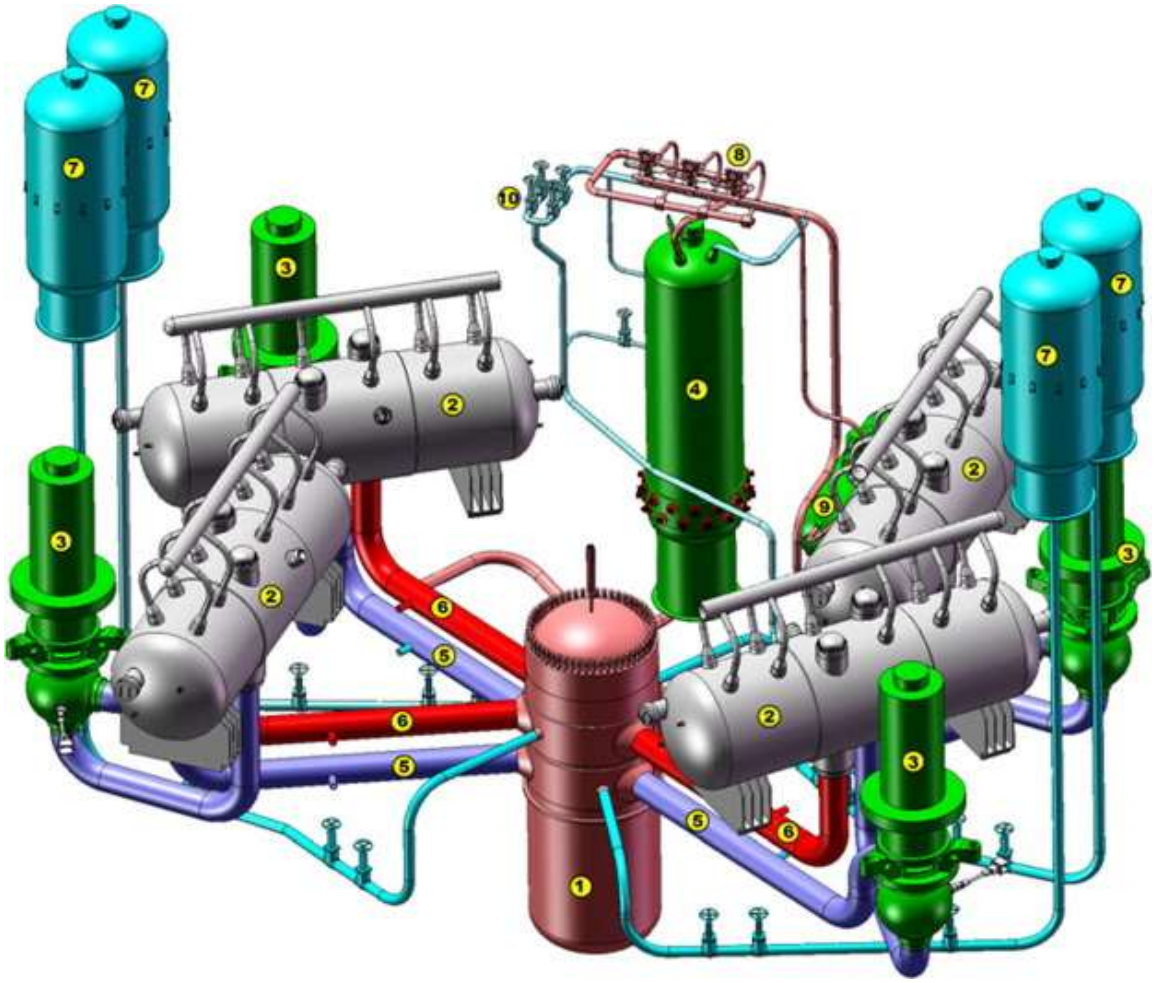

Figure 2-4 VVER-1000/V320 RCS (Tabadar et al., 2019)

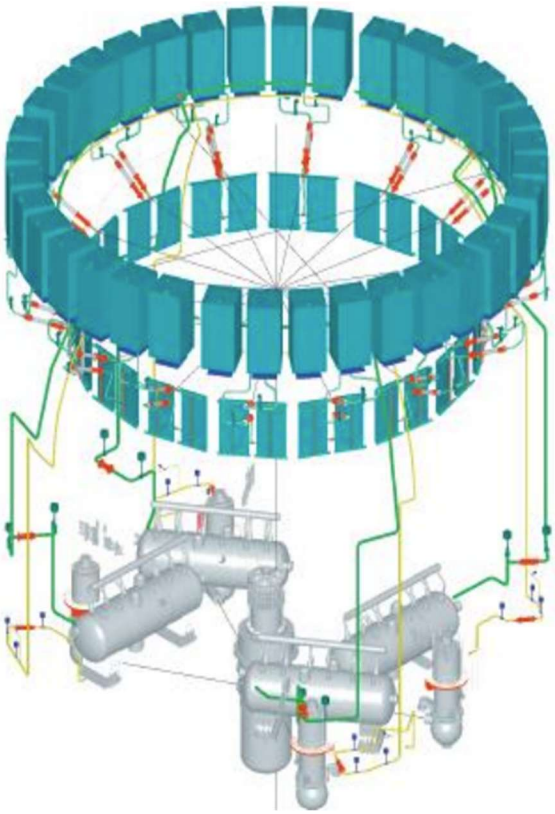

Figure 2-5 VVER-1200/V491 with water-cooled PHRSs (Svetlov, 2017)

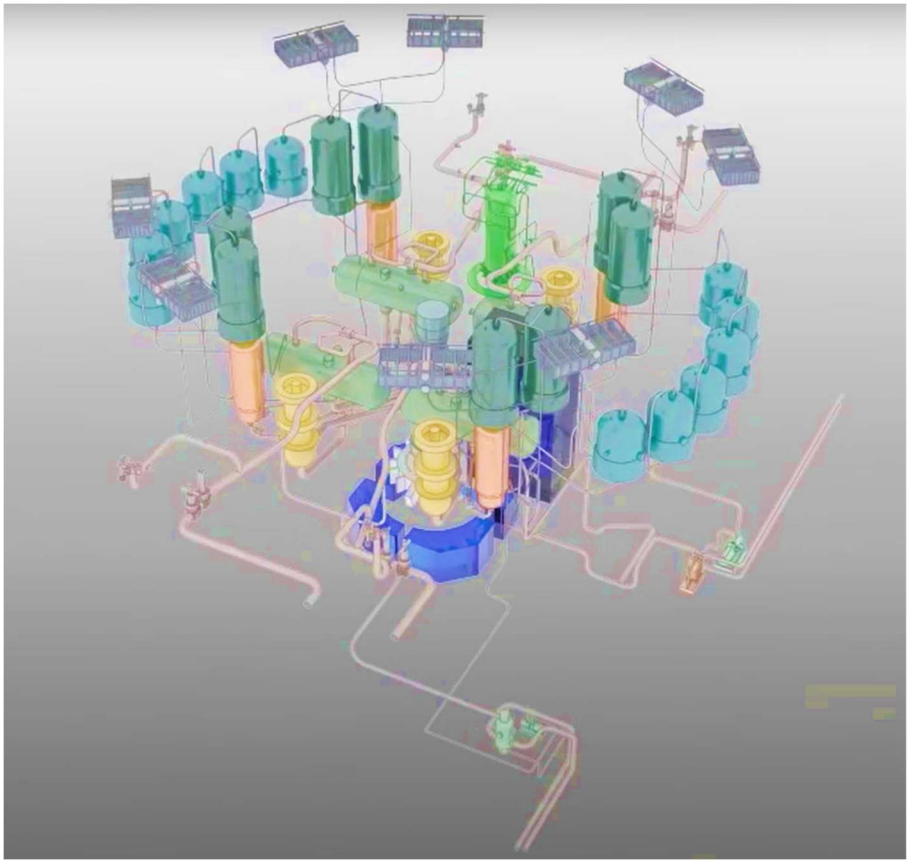

Figure 2-6 VVER-1200/V509/V527 with air-cooled PHRS (Rosenergoatom, 2017)

2.2.2. VVER-1000/V320 reactors

The VVER-1000/V320 is the most widely used Russian-designed Gen-II PWR. This reactor operates on a thermal neutron spectrum, using borated water as both coolant and moderator, and utilizes lightly enriched UO_2 as fuel, (IAEA, 2011b). It has a thermal power of 3000 MW and generates 1000 MWe. Several features distinguish the VVER-1000/V320 from the VVER-440 models (IAEA, 2011b; VVER working group, 2019):

- The containment is designated to withstand the conditions of a LBLOCA.
- Four RCS loops instead of six, see Figure 2-7.
- The RCS loops have no isolation valves.
- The safety systems have 100% capacity per train.
- The SFP is placed in the containment.

Section 2.2.2 is structured as follows: first, Sections 2.2.2.1 to 2.2.2.4 describe the RCS, followed by the reactor core, the balance of plant and the containment. Subsequently, Section 2.2.2.5 deals with the electrical power supply. Section 2.2.2.6 then presents the auxiliary systems. Finally, Section 2.2.2.7 describes the safety systems connected to the RCS, the secondary circuit and the containment.

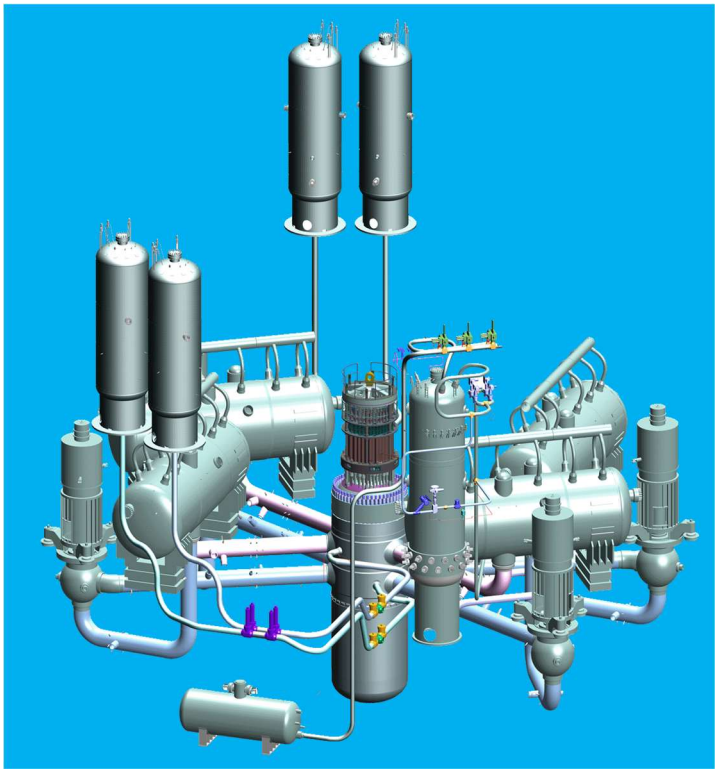

Figure 2-7 VVER-1000/V320 plant layout

2.2.2.1. Reactor Coolant System

The RCS of the VVER-1000/V320 consists of four loops, each with CL and HL of 0.85 m diameter and no isolation valves. The HLs are connected to the RPV at the same angular position as the CLs, with the HLs positioned 1.8 m above the CLs, (Kolev et al., 2006). The connection of the CLs and the HLs to the RPV is not symmetrical in the azimuthal direction; loops 1 and 4 are separated by an azimuthal angle of 55°. In addition, the HLs connect directly to the SGs collectors with a 90° elbow. The total primary side water volume is 337 m^3 while the total volume is 361 m^3, (Ivanov et al., 2004).

A layout of the RCS is shown in Figure 2-8 and Figure 2-9. This is followed by a detailed description of the Reactor Pressure Vessel (RPV), the MCP, the Pressurizer (PZR) and the Steam Generators (SGs).

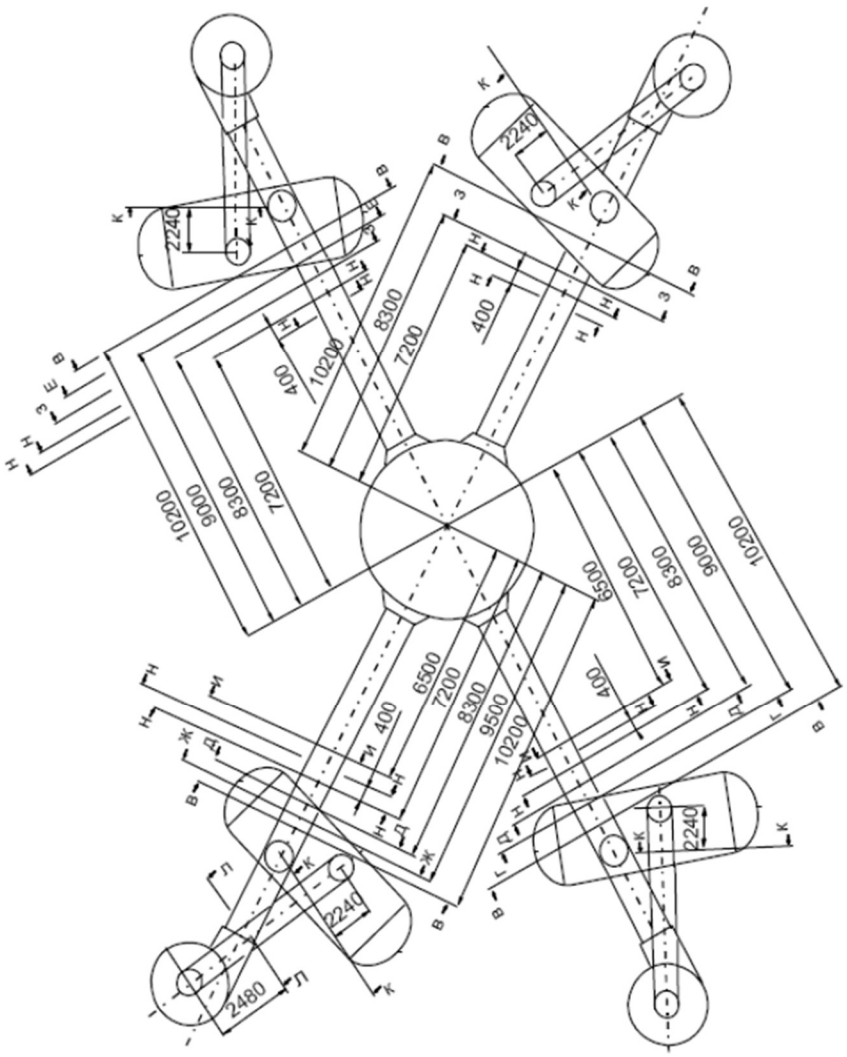

Figure 2-8 VVER-1000/V320 RCS floor plan

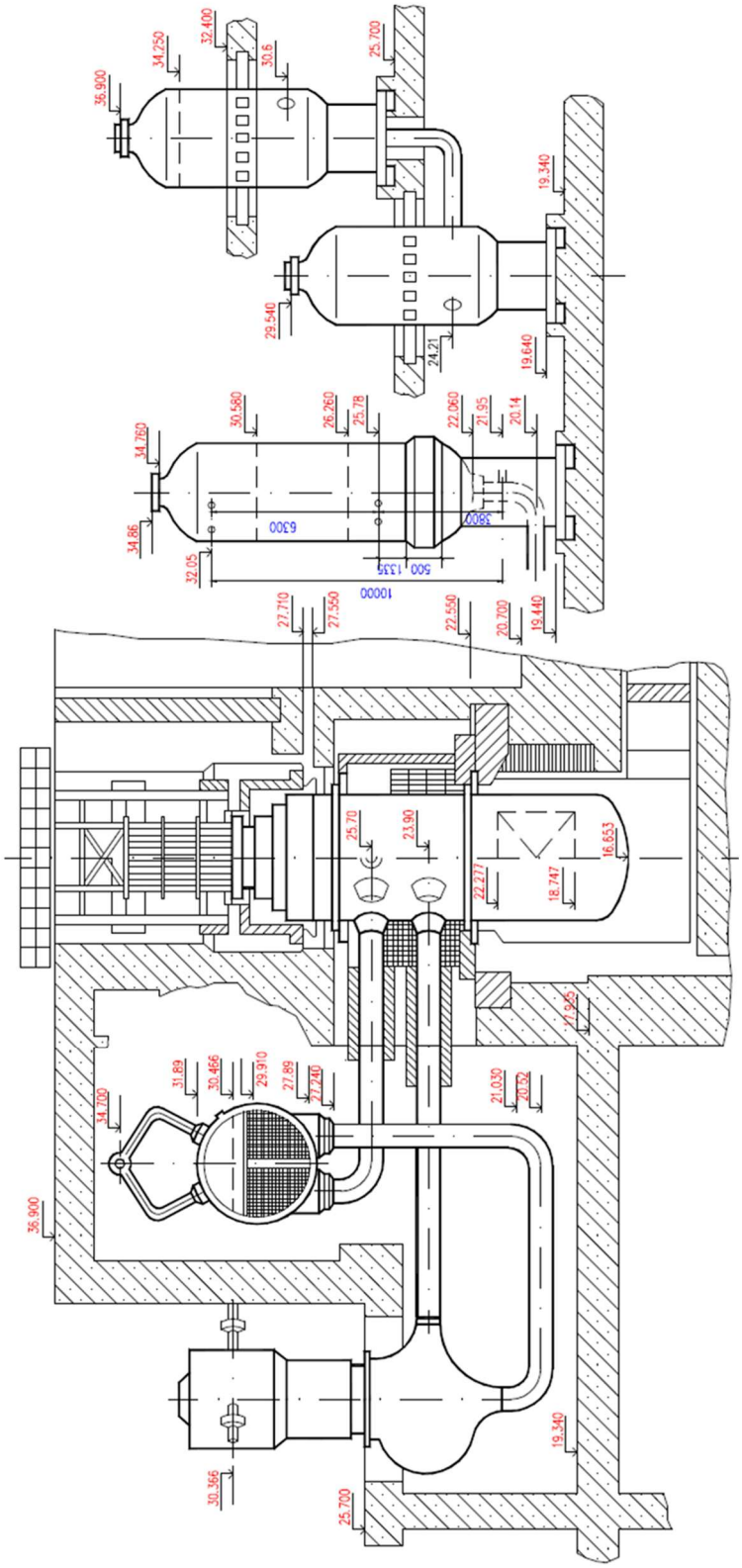

Figure 2-9 VVER-1000/V320 RCS components elevation (State nuclear regulatory inspectorate of Ukraine, 2011)

The RPV has an overall height of 19.1 m, an external diameter of approximately 4.5 m and an internal free volume of 110 m^3. Inside the RPV, three different structures can be identified: the core barrel, the core baffle and the protective tube unit, see Figure 2-10:

- The core barrel is a structure that encloses the core baffle and the protective tubes units. Its upper section is perforated with cylindrical holes to allow coolant to flow from the Upper Plenum (UP) to the HLs. Meanwhile, coolant enters the RPV through the CLs, which are below the HLs, and flows through the annular space between the RPV wall and the core barrel. An annular ring separates the CL and the HL connections to the RPV, ensuring that the coolant from the CLs does not mix with the coolant flowing through the upper core barrel holes to the HLs. The core barrel is supported by a ledge recessed in the upper part of the RPV, positioned just below the level where the RPV head is bolted on, see Figure 2-11 and (Iegan et al., 2018; Ivanov et al., 2004).

  The lower section of the core barrel is perforated with 1344 holes, each 44 mm in diameter, to allow coolant from the Downcomer (DC) to enter the lower plenum, (Ivanov et al., 2004). This lower section is elliptical and has a greater curvature than that of the elliptical RPV bottom, see Figure 2-11.

  Fuel support columns are welded to the lower part of the core barrel, i.e., in the lower plenum. The upper part of each column has a hexagonal shape with a central circular opening of 194 mm, designed to hold the FAs. There are a total of 163 fuel support columns, one for each FA. These columns are perforated with slots to distribute the flow and allow the coolant to flow upward into the FA. These openings are designed to prevent debris from entering and potentially blocking the active part of the FA in the event of a severe accident, (Ivanov et al., 2004).

- Protective tubes unit is positioned immediately above the top of the FA. It includes top, middle and bottom plates.

- The core baffle is a structure that surrounds the core. It is perforated longitudinally so that some of the coolant from the lower plenum passes through these holes, with the aim of cool the core baffle structure.

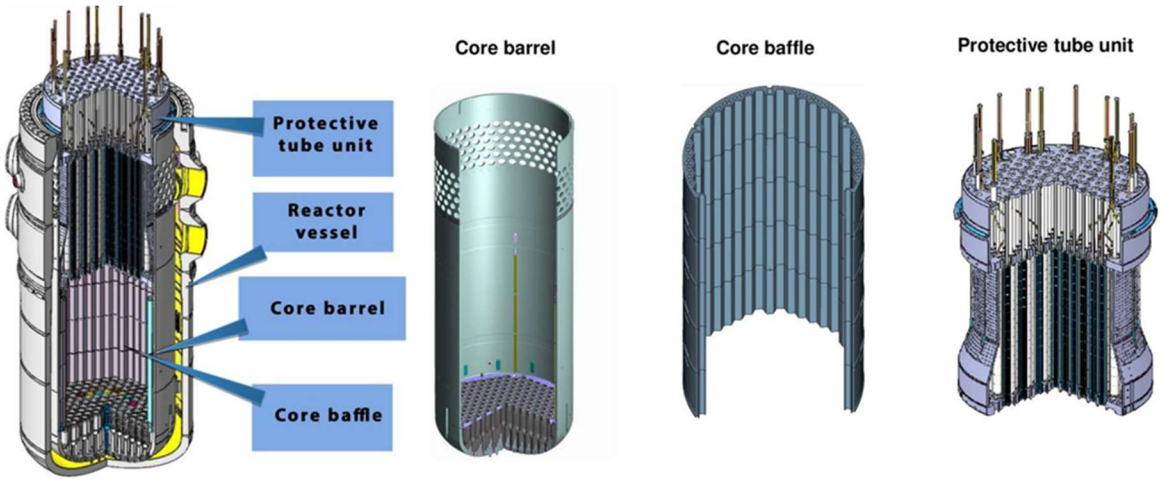

Figure 2-10 VVER-1000/V320 Reactor RPV inner components (Komolov et al., 2019)

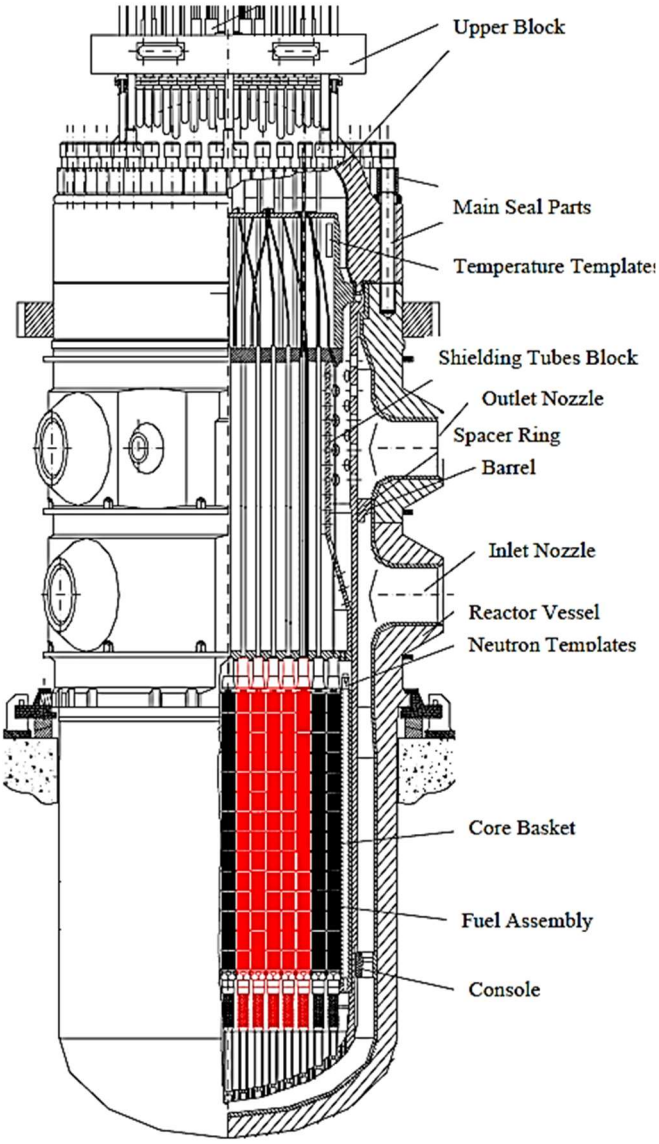

Figure 2-11 VVER-1000/V320 RPV coolant flow paths (Ivanov et al., 2004)

The MCP, or Reactor Coolant Pump (RCP), are GCN-195M vertical centrifugal type pump driven by 6kV AC motors, see Figure 2-12 and (Muellner, 2010). At 50 Hz, the nominal flow rate of each MCP is 5.9 m^3/s with a nominal head of 0.66 MPa. The pumping capacity varies depending on the number of MCPs in operation: 6.76 m^3/s with 3 MCPs available, 7.33 m^3/s with 2 MCPs available and 7.50 m^3/s with a single MCP available (Ivanov et al., 2004). The principal characteristics of the MCPs are shown in Table 2-10

The MCPs are controlled leakage pumps with seals maintained by the Control Volume and Chemical System (CVCS) make-up pumps. Part of the seal injection flow goes to the RCS and the remainder is returned to the CVCS via a seal return line, (Ryzhov et al., 2010). The desired MCP coast-down is achieved by a specific flywheel. The MCP coast-down time in the event of a power loss is 55 s for 1 out of 4 MCPs and 210 s for 4 out of 4 MCPs, (Tusheva, 2012).

Table 2-10 VVER-1000/V320 MCP characteristics (Ivanov et al., 2004)

Parameter	Value	Unit
Coolant volume per MCP	3	m^3
Nominal flow at 50Hz per MCP	5.9	m^3/s
Nominal speed of the rotor	104.2	rad/s
Rated torque	47500	Nm

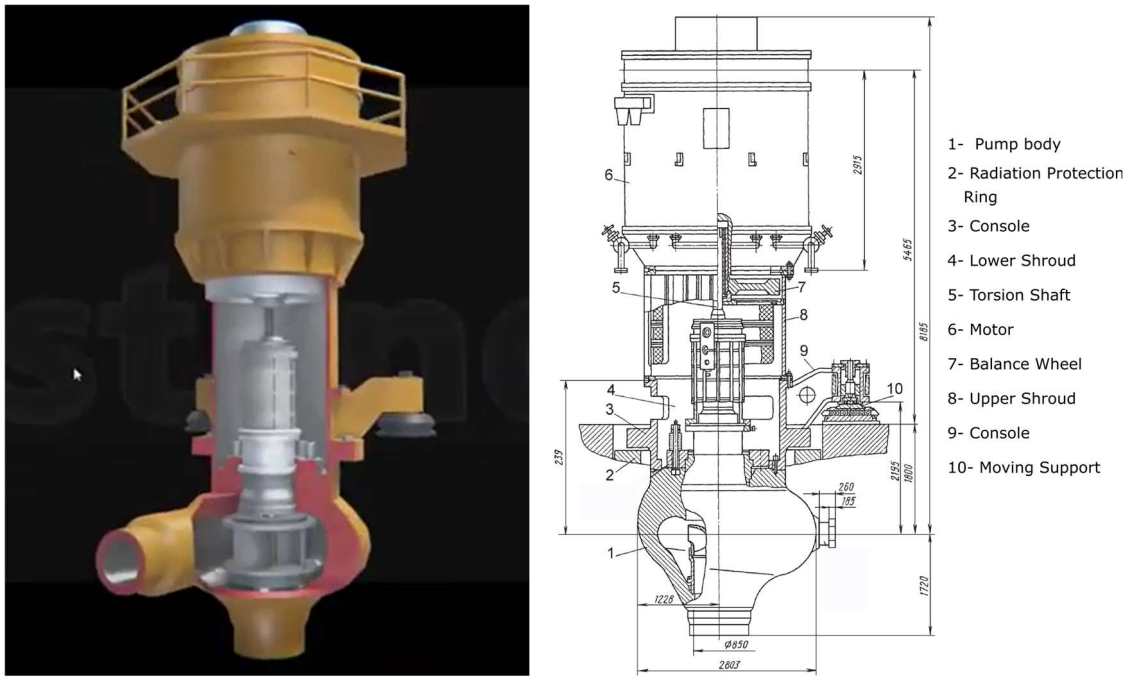

Figure 2-12 VVER-1000/V320 MCP (Ivanov et al., 2004; Kuzmanov, 2021)

The PZR is a vertical tank that has a saturated vapour/liquid interface at nominal operation, see Figure 2-13 and Figure 2-14. The PZR is designed to maintain the RCS coolant in the liquid phase. It also performs other functions such as increasing the RCS pressure during reactor start-up and decreasing the RCS pressure during reactor shutdown, (IAEA, 2011b). It is connected to the rest of the RCS in the lower part by the HL 4 through the surge line (Fortava, 2018). The main features of the PZR are listed in Table 2-11. The PZR is supplied by two systems that allow the RCS pressure to be controlled:

- The sprays: This system sprays water in the upper part of the PZR to condense the steam and allow the pressure drop. These sprays take water from one of the CLs, downstream of the MCP.
- Heaters: In the lower part of the PZR there are 28 heaters in four groups with the following power: 360 kW in the group 1; 180 kW in the group 2; 720 kW in the group 3 and 1260 kW in the group 4 (Ivanov et al., 2004). They are designed to boil water in order to increase pressure. During nominal operation, one group of the heaters is switched on to compensate heat losses.

The PZR relief and safety valves are connected to a horizontal tank known as a bubbler condenser, see Figure 2-15. The main function of this tank is to condense the steam inventory released from the PZR relief and safety valves. If the pressure in the relief tank rises above the limit, a disc ruptures and coolant is released to the containment, (Iegan et al., 2018).

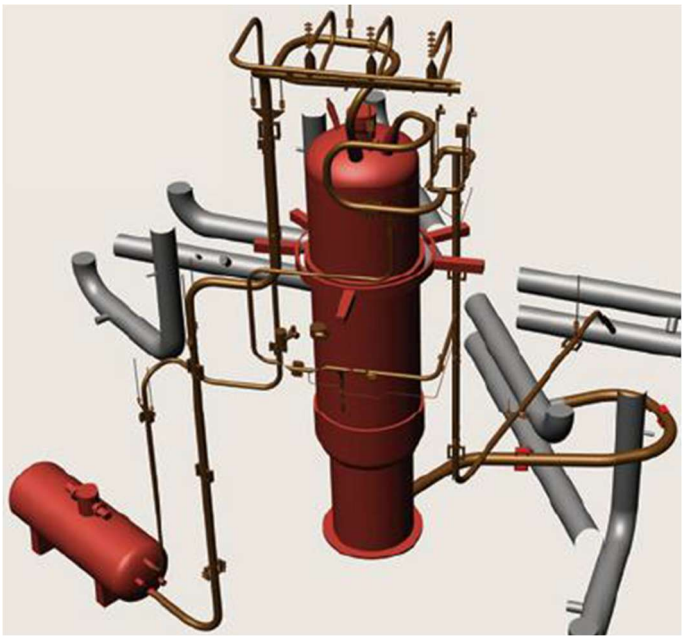

Figure 2-13 VVER-1000/V320 PZR and bubbler condenser (ROSATOM, 2022)

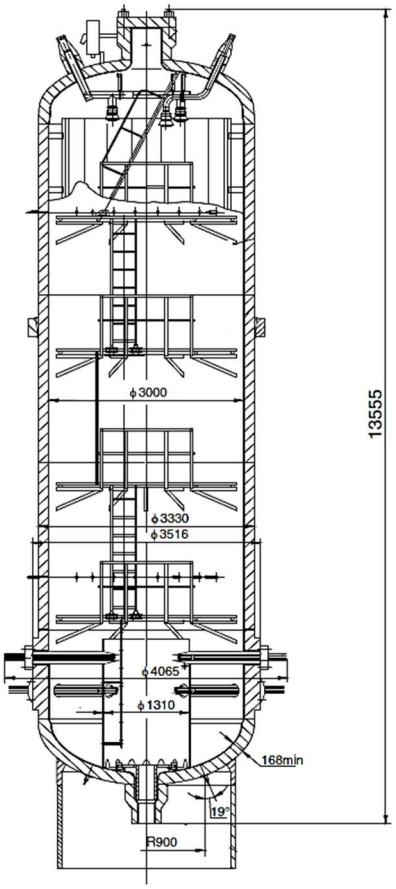

Figure 2-14 VVER-1000/V320 PZR dimensions (Ryzhov et al., 2010)

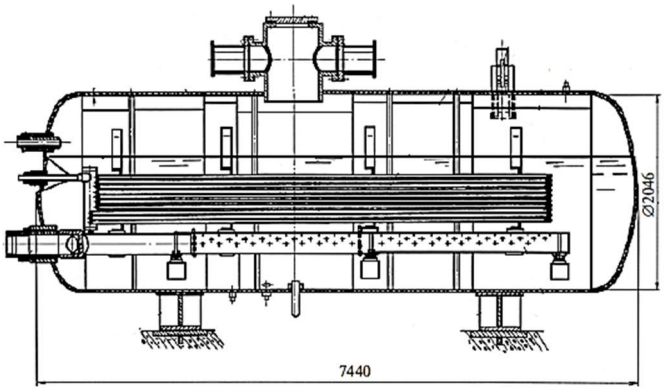

Figure 2-15 VVER-1000/V320 PZR bubbler condenser dimensions (Ryzhov et al., 2010)

Table 2-11 VVER-1000/V320 PZR characteristics (Ivanov et al., 2004)

Parameter	Value	Unit
Volume	79	m^3
Water volume in nominal conditions	55	m^3
Steam volume in nominal conditions	24	m^3
Heaters maximum power	2.5	MW

The SGs of the VVER-1000/V320 reactors are SG PGV-1000M type (Tusheva, 2012), see Figure 2-16. They are horizontal HXs designed to produce dry saturated steam on the secondary side. The heat from the RCS coolant, which passes through a submerged bundle of horizontal U-shaped tubes, see Figure 2-17, is transferred to water on the secondary side to produce steam. On the primary side they contain a total RCS inventory volume of 23.4 m^3, while on the secondary side the total volume is 66 m^3 (Muellner, 2010; Tusheva, 2012). The main dimensions of the SGs are given in Figure 2-18. The SGs contain the following components:

- Hot and cold collectors. The RCS inventory from the HLs enters in the hot collector where it is distributed through the horizontal U-shape tubes. Once the inventory has passed through the U-shape tubes, it enters the cold collector and from there to the CLs. The height of both collectors is 5 m and the volume is 2.4 m^3.
- U-shape horizontal tube bundle. There are a total of 11000 U-shaped tubes per SG, with an internal diameter of 13 cm and an average length of 11.1 m (Tusheva, 2012). The vertical step between tubes is 19 mm and the horizontal step is and 23 mm. On the secondary side, there are submerged perforated plates between the tube bundles to provide structure between them. The total volume of the 11000 U-shape tubes is approximately 16.2 m^3.
- Main Feedwater (MFW)/Auxiliary Feedwater (AFW) manifold. The water from the MFW and the AFW enters the SGs through a 0.42 m diameter pipe. From this pipe the water is distributed to 16 collectors of 80 mm diameter, to which 38 pipes are connected (Ivanov et al., 2004).
- Emergency Feed Water (EFW) manifold and distribution pipes.
- Steam separators in the upper part.
- Steam Collector. Above the SGs is a steam collector where the steam is directed to the SLs.

The volume of water in the horizontal SGs is greater than that in the vertical SGs of the Western type, and therefore the water mass and water surface area are greater. This means that the transient response of horizontal SGs can be very different from that of vertical SGs. The main dimensions of the VVER-1000/V320 reactor SGs is shown in Table 2-12.

Table 2-12 VVER-1000/V320 SGs dimensions (Muellner, 2010)

Parameter	Value	Unit
Average tube length	11.1	m
No of tubes	11000	-
Tube ID/OD	0.013/0.016	mm
SG collector volume	2.4	m^3
SG collector height	5	m
Primary side volume	23.4	m^3
Primary side tubes volume	16.2	m^3
Secondary side volume	66	m^3

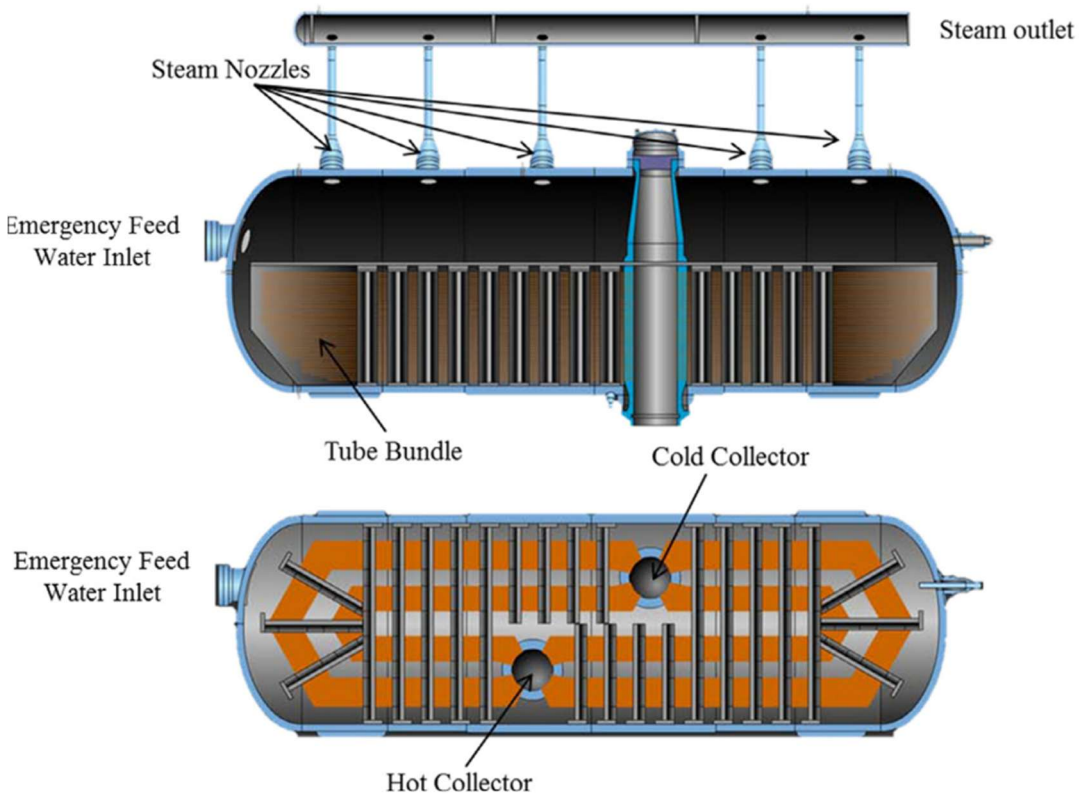

Figure 2-16 VVER-1000/V320 SGs layout (Rabiee et al., 2016)

Figure 2-17 VVER-1000/V320 SGs U-shaped tubes

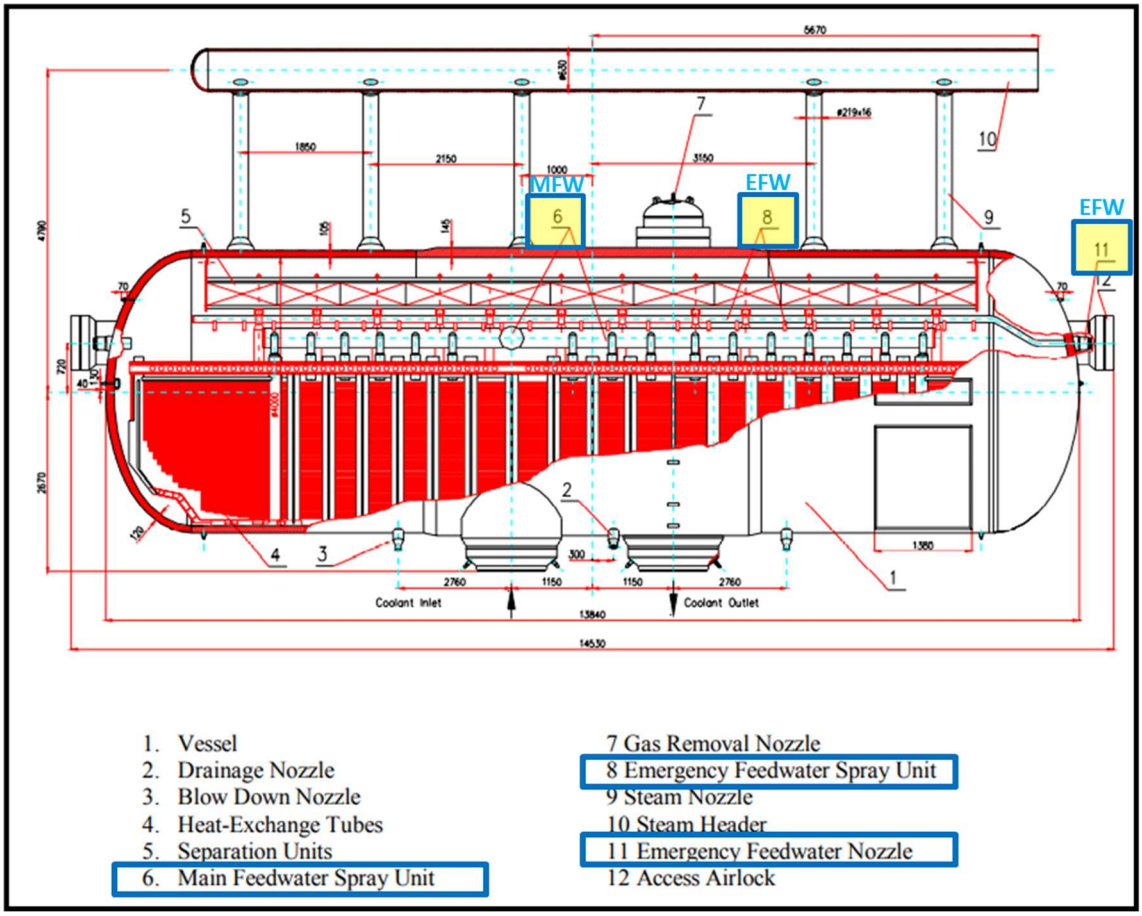

Figure 2-18 VVER-1000/V320 SGs dimensions (Ryzhov et al., 2010)

2.2.2.2. Reactor core

The core consists of 163 hexagonal FA (Lee and Cho, 2006) with a regular triangular grid of 312 fuel rods, see Figure 2-19. The active part of the core is approximately 3.53 m long, and the equivalent diameter is 3.16 m, see Table 2-13. During normal operation, the pressure drops across the core is approximately 0.18 MPa, (Tusheva, 2012)

The fuel rod pitch is 12.75 cm, see Table 2-14 and Figure 2-20. Among the FAs, 61 have 18 positions where the fuel rods are replaced by tubes for control rod. In addition, some FAs contain tubes for in-core instrumentation and rods with burnable absorber. The FA type for the VVER-1000/V320 reactors, such as the Balakovo NPP, is the TVS-2M, (VVER working group, 2019), and the cladding material is Zircaloy E110.

Besides, the core is equipped with Neutron Flux Measuring Channels (NFMC) to monitor the radial and axial neutron flux. These NFMCs are located in the central tube of 64 FA and in the guide channel of the protective tube block. In addition, 91 FAs are fitted with Core Exit Thermocouples (CET) at the outlet to measure the temperature, (IAEA, 2011b).

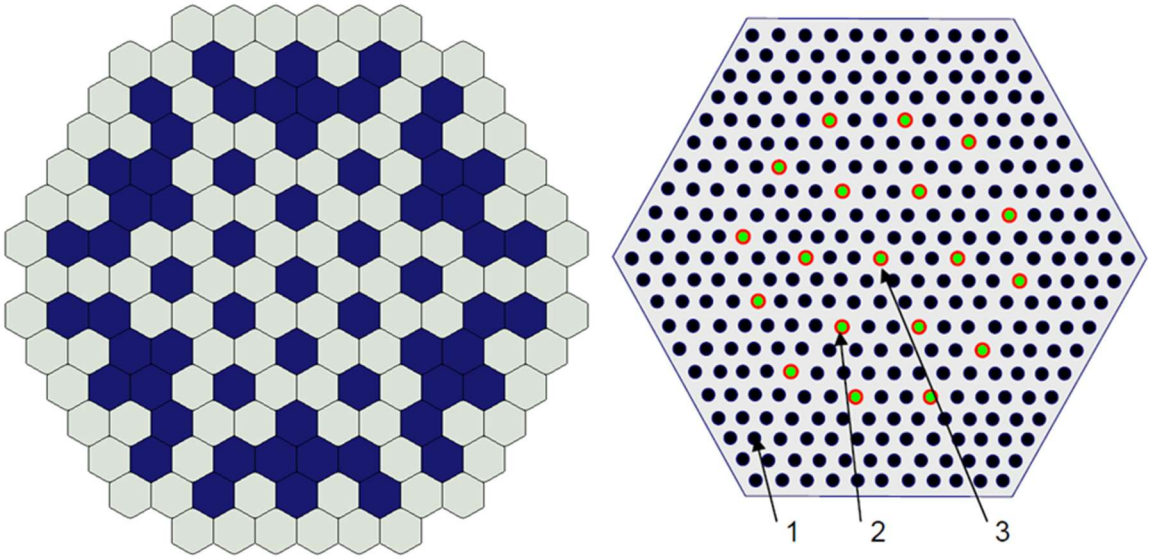

Figure 2-19 VVER-1000/V320 core (in blue FA with CRA) and FA designs; 1. Fuel rod, 2. Tube for CRs, 3. Central tube for in-core instrumentation (IAEA, 2011b)

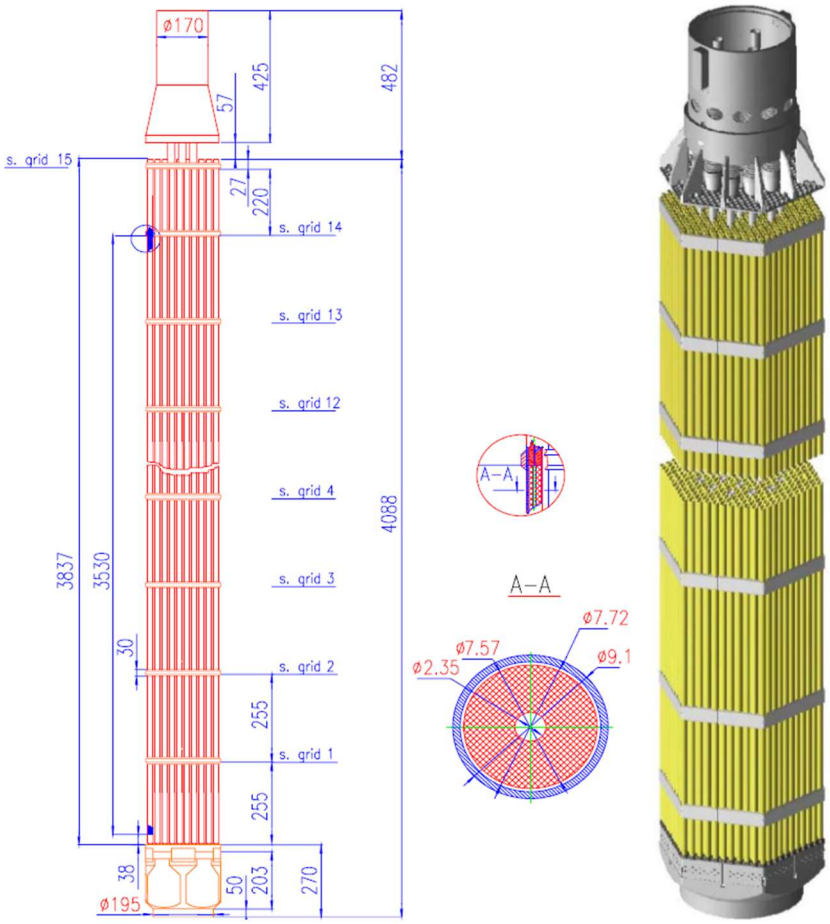

Figure 2-20 VVER-1000/V320 FA geometry (Asmolov, 2009; Kolev et al., 2006)

Table 2-13 VVER-1000/V320 core geometrical data (Ivanov et al., 2004)

Parameter	Value	Unit
Number of FA	163	-
Number of FA with CRA	61	-
Heating length of the FA	3.53	m
FA pitch	0.236	m
Heating core flow area	4.17	m^2
Equivalent Diameter	3.16	m

Table 2-14 VVER-1000/V320 FA characteristics (Ivanov et al., 2004)

Parameter	Value	Unit
Number of fuel rods	312	-
Fuel rods pitch	0.1275	m
Number of tubes per CRA	18	-
Number of axial support plates	14	-
FA height	4.57	m

The fission chain reactor is controlled by means of two reactor control and protection systems which are based on different principles: the control rods and the CVCS. On the one hand, the CVCS regulates the boron RCS concentration. This system is used to achieve small changes in reactivity throughout the fuel cycle. On the other hand, the Control Rod Assemblies (CRA) are used to control reactivity and axial power shape during operation, (IAEA, 2011b). They are also used during normal reactor shutdown and emergency shutdown to interrupt fission reactions.

The CRAs are organized in 10 banks, (IAEA, 2011b), see Figure 2-21. They are made from two different materials, the upper 90% axial length consists of B_4C, while the remaining 10%, located at the bottom, is made of DyTi, (Fadaei and Setayeshi, 2009).

All CRA are of full length, except for bank V, which contains partial length control rods designed to manage the axial power profile, see Figure 2-21. The CRA banks are connected at the top to electromagnets, which are responsible for adjusting their position. In case of activation of the protection system or loss of the AC power, the electromagnets release the CRAs, which enter the core passively by gravity within a maximum of 4 s.

When the reactor is operating at nominal conditions, all CRA banks are out except bank X. It is normally positioned at a height of 70-90% from the bottom and is used to compensate for small changes in reactivity due to variations in temperature, boron concentration, etc, (IAEA, 2011b).

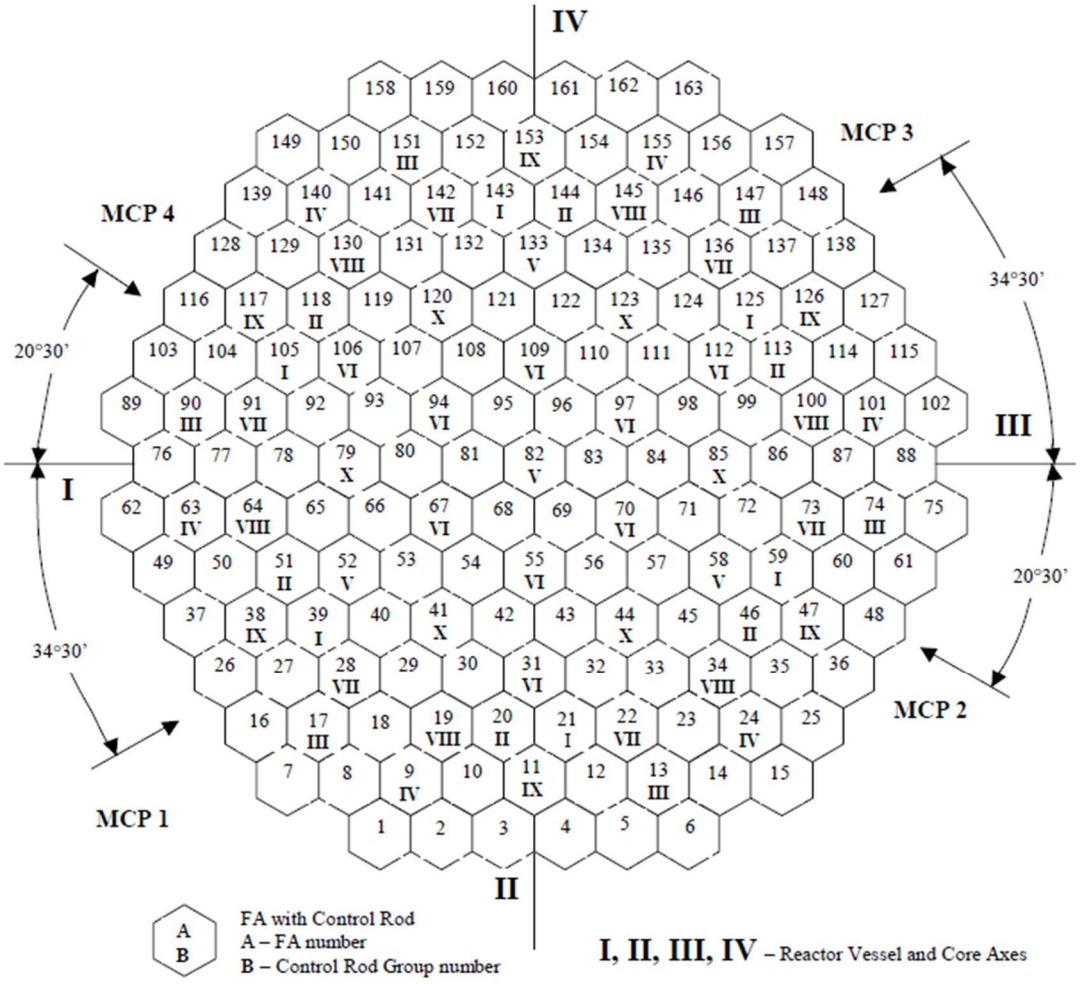

Bank	No. of rods	Purpose
I	6	Safety
II	6	Safety
III	6	Safety
IV	6	Safety
V	4	APSR
VI	9	Safety
VII	6	Safety
VIII	6	Safety
IX	6	Safety
X	6	Control

Figure 2-21 VVER-1000/V320 Control Rod Assemblies banks (Kolev et al., 2006)

2.2.2.3. Secondary circuit and Balance of plant

The SGs are HXs in which the thermal power of the core is transferred to the secondary circuit to produce electricity. Therefore, these components have a part below the RCS and a part below the secondary circuit. The other components in the secondary circuit are the SLs, the Main Steam Header (MSH) and the balance of plant consisting of the high and low pressure turbines, the condenser, the condenser pumps, the low pressure heater, the aerators, the MFW pumps and the high pressure heaters, see Figure 2-22 (Nuclear Regulatory Agency, 2011).

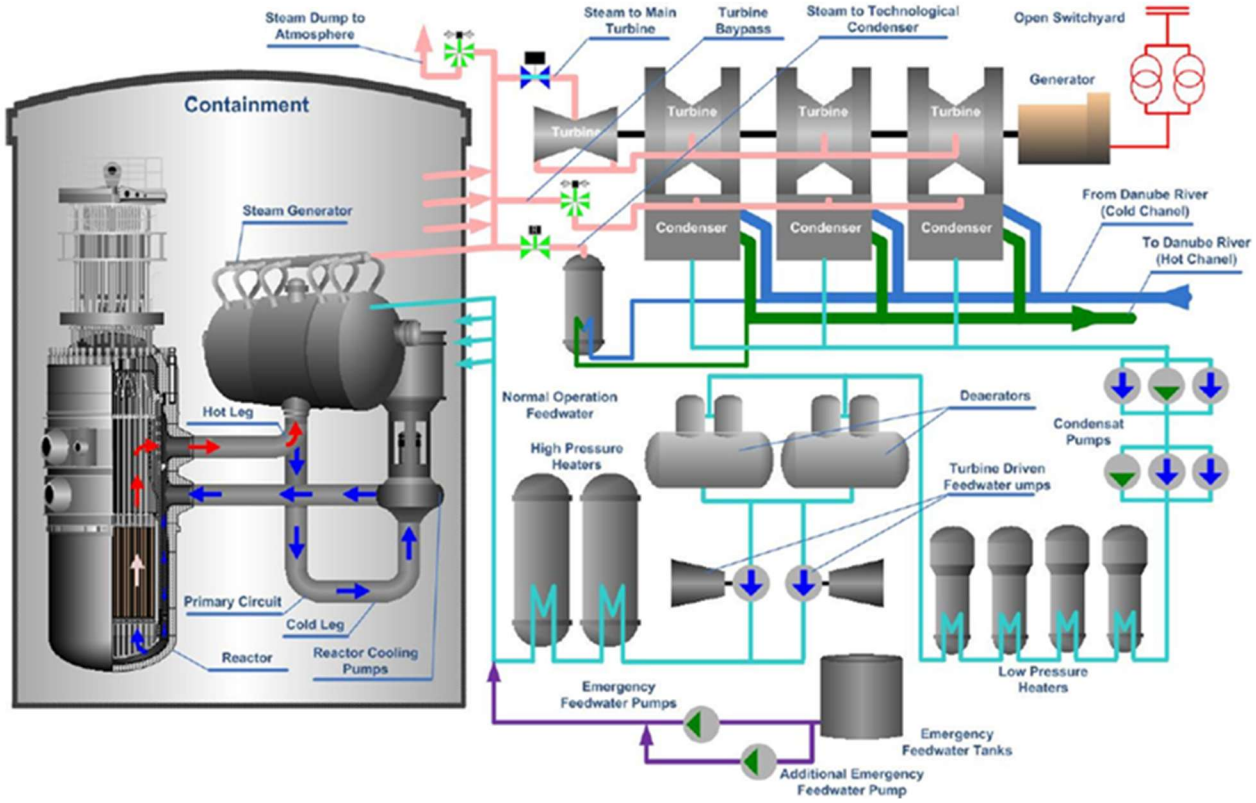

Figure 2-22 VVER-1000/V320 balance of plant (Nuclear Regulatory Agency, 2011)

The steam produced in the SGs is transported through the four SLs to the MSH where the pressure is equalizes before entering into the balance of plant (Ryzhov et al., 2010). During normal reactor operation, most of the steam is sent to the high pressure turbine, (IAEA, 2011b). After leaving the high pressure turbine, the steam enters to a separator to remove the moisture before passing through a HX, where it is reheated and then sent to the low pressure turbine. Then, steam from both the high and low pressure turbines enters the condenser. It should be noted that the high and low pressure turbines are connected to the separate condensers

(IAEA, 2011b). From the condenser, the water is pumped by the condenser pumps to the low pressure heaters and then to the deaerator to remove non-condensable gases. The deaerated water is then pumped by the MFW pumps to the high pressure heaters before returning to the SGs.

The MFW system consists of two turbine-driven feedwater pumps designed to operate when the reactor power exceeds 6-7% (Nuclear Regulatory Agency, 2011), see Figure 2-23. Feedwater is taken from the deaerator, which has a total capacity of 400 m^3, and delivered to the high pressure heater through 0.5 m diameter pipes. After passing through the high pressure heater, the feed water flows into a collector and is then distributed to the SGs through 0.4 m diameter pipes. Each turbine-driven pump has a capacity of approximately 1650 m^3/h (Ryzhov et al., 2010).

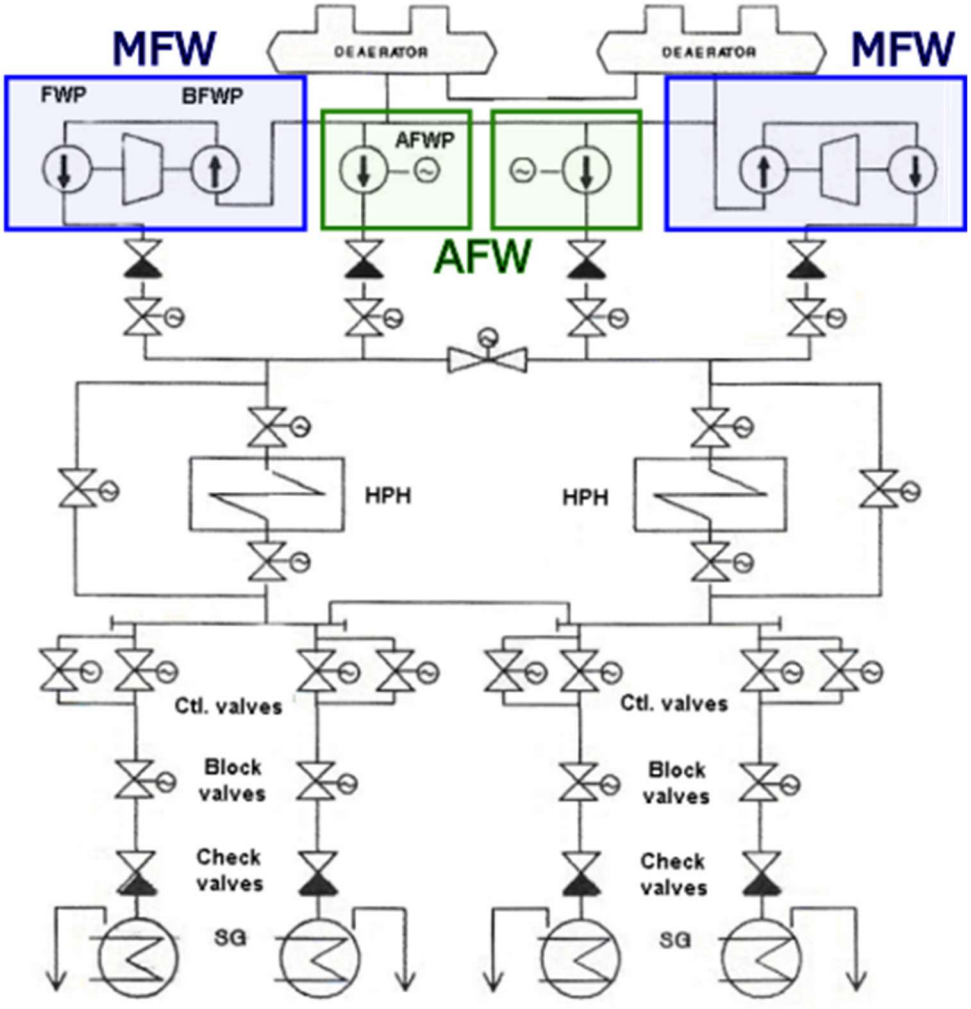

Figure 2-23 VVER-1000/V320 MFW and the AFW diagram (Kolev et al., 2006)

2.2.2.4. Containment

All elements of the primary side are housed in a single-wall cylindrical containment made of pre-stressed reinforced concrete lined with steel on the inside (Tusheva et al., 2009; VVER working group, 2019). The building consists of a cylinder 66 m high and 45 m in diameter, topped by a dome. The base of the containment is at 7 m above ground level. The lower part of the reactor building houses the ECCS pumps and the containment sump, see Figure 2-24.

Inside the containment is a spent fuel pool with a total volume of 585 m^3 (Nuclear Regulatory Agency, 2011). The pool is maintained at a subcritical state of at least 5% by ensuring a reliable distance between the stainless steel cells containing the FAs and by using borated water at a concentration of 16 g/kg. The spent fuel pool cleaning system is responsible for maintaining the water level at +28.8 m and ensuring the correct water chemistry (Nuclear Regulatory Agency, 2011).

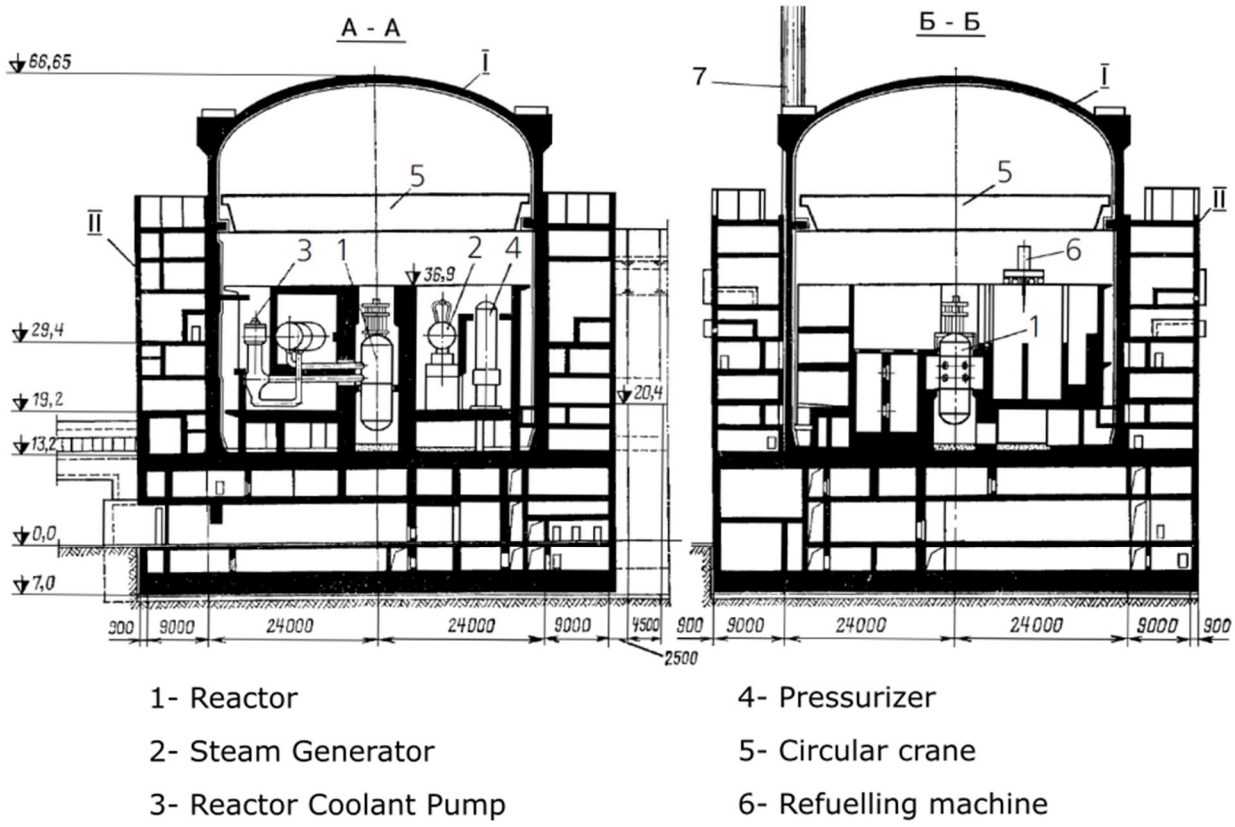

Figure 2-24 VVER-1000/V320 containment (Environment Agency Austria, 2019)

2.2.2.5. Electric Power Supply System

An example of the electrical power supply of the Kozloduy NPP (units 5 and 6) and the Temelin NPP (units 1 and 2) is shown in Figure 2-25 and Figure 2-26. As illustrated, various electrical loads are present in the VVER-1000/V320 reactors for electric power supply (ČEZ, 2012), including:

- Main sources: Supplied by transformers connected to the generator driven by the NPP turbines.
- Auxiliary sources: Supplied by auxiliary transformers connected to the off-site electrical grid.
- Emergency sources: Consists of independent emergency diesel generators (EDG) installed separately as far as possible from each other on site. There are three EDGs in the VVER-1000/V320 reactors, each with a capacity of about 6 kV (ČEZ, 2012). Each EDG is connected to one of the three safety trains. In the event of a power failure from the main and auxiliary sources, the EDGs start up automatically within 15 seconds (VVER working group, 2019). These EDGs are equipped with storage tanks that provide fuel for at least 48 hours.

In addition, some VVER-1000/V320 NPPs have backup EDGs connected either to all three safety trains or to only one of them. Moreover, after Fukushima, some NPPs have implemented mobile EDGs to supply power to mobile EFW pumps (Nuclear Regulatory Agency, 2011).

On the other hand, the safety systems components in VVER-1000/V320 reactors are divided into three electrical supply categories, depending on the sources of supply (Nuclear Regulatory Agency, 2011):

- Category I components are battery powered, allowing them to operate under SBO conditions for long as battery life permits.
- Category II components are connected to the EDG, enabling them to operate in Loss of Offsite Power (LOOP) conditions, but not during an SBO,(Nuclear Regulatory Agency, 2011).
- Category III components are not connected to battery or EDG, so are not available in the case of LOOP.

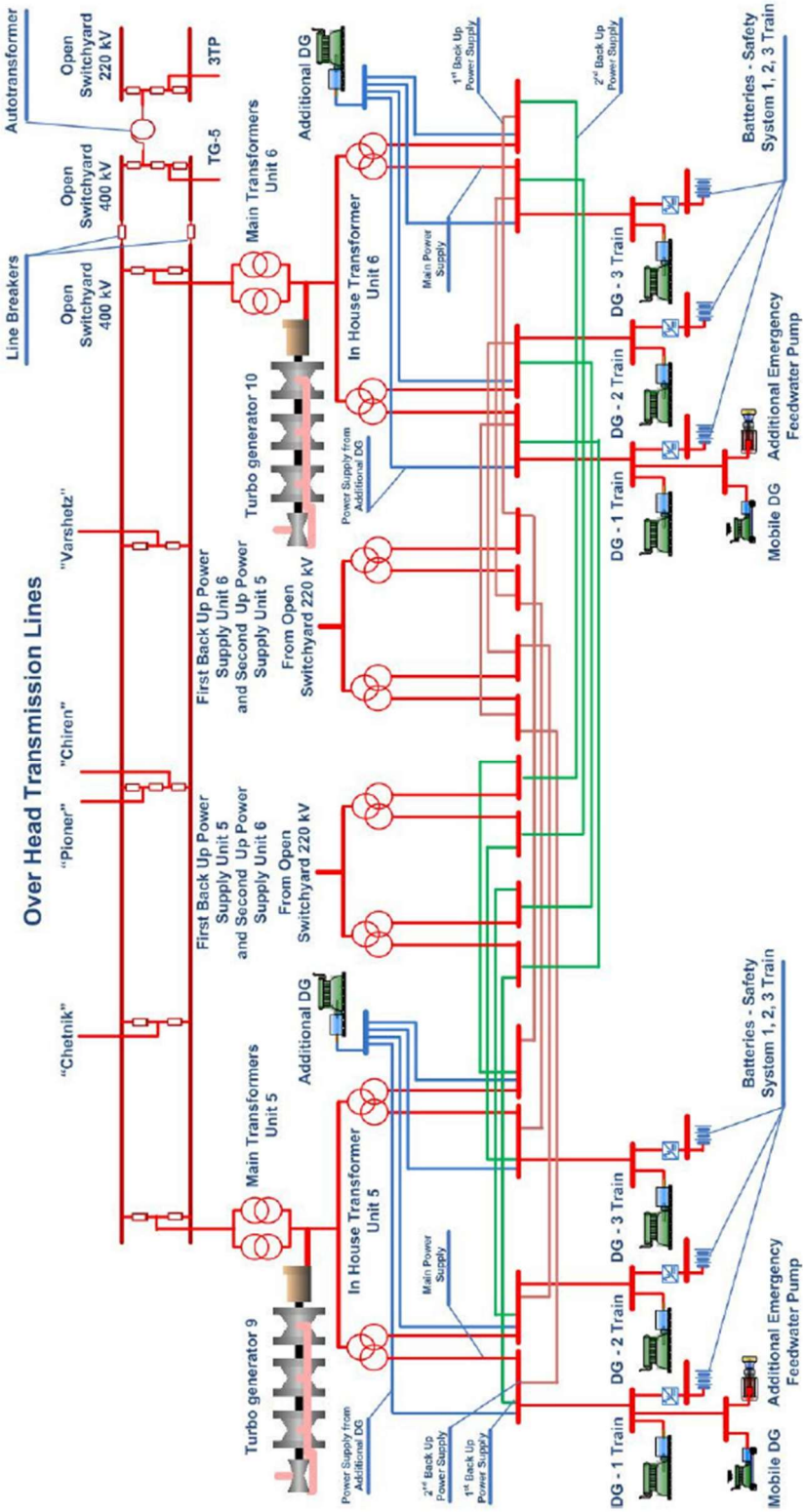

Figure 2-25 Single-line diagram for Kozloduy NPP (units 5 and 6) (Nuclear Regulatory Agency, 2011)

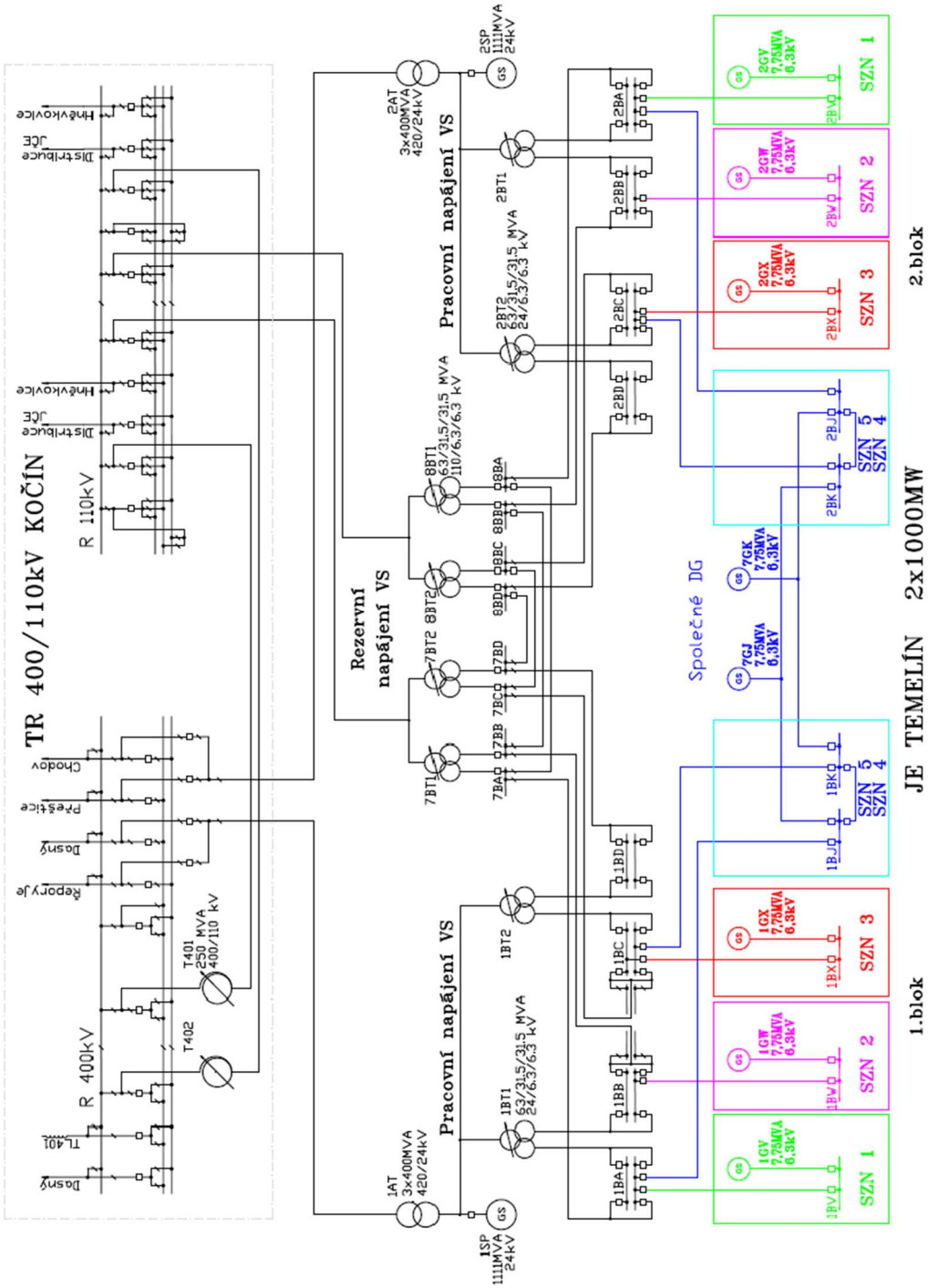

Figure 2-26 Single-Line diagram for Temelin NPP (units 1 and 2) (ČEZ, 2012)

2.2.2.6. Auxiliary systems

The main auxiliary systems found in VVER-1000/V320 reactors are presented below. These auxiliary systems are the CVCS, the Service Water System (SWS), the Residual Heat Removal System (PHRS) and the AFW.

The CVCS consists of three independent trains, each located at separate sites to prevent the simultaneous loss of both in the event of flooding, fire, or other hazards. During normal reactor operation only one train is active, and performs several functions, including (Iegan et al., 2018; Ryzhov et al., 2010): controlling the RCS inventory, controlling the boron concentration in the RCS, compensating for minor leaks in the RCS equipment, purifying the RCS inventory and supplying water to the MCPs seals (2 m^3/h for each MCP).

In addition, the CVCS is also designed to release a boron solution in the RCS to bring the reactor to a subcritical state in the event of an accidental scenarios, as well as to replenish the water in the RCS during SBLOCA of small break sizes. For this purpose, the CVCS has two tanks with a capacity of 200 m^3 of boric acid. Moreover, the CVCS is involved in the start-up and shutdown of the reactor (Iegan et al., 2018).

The CVCS consists of the make-up system, which takes the water from the RCS, and the let-down system, which discharges the treated water to the RCS. The make-up system supplies water to the four CLs at a nominal flow rate of 8.19 kg/s (Ivanov et al., 2004).

The water from the RCS sucked through the let-down lines passes through the HXs, where it transfers heat to the water supplied to the RCS through the make-up lines. The let-down inventory then passes through the low pressure water purification system and then the degassing system to remove non-condensable gases (IAEA, 2011b). Finally, the purified water is ready to be injected into the RCS by the three pumps of the system, i.e., TK21-23D01,02 see Figure 2-27.

The SWS consists of two parts, one for cooling the components of the auxiliary and operating systems and the other for cooling the components of the safety systems. The one responsible for the safety system components is composed of 3 x 100% trains.

The SWS cool the components of the following systems: the HPIS, the LPIS, the CSS, the containment ventilation system, the EFW and the EDGs. In addition, the SWS also provide cooling to the MCPs.

The RHRS is the system responsible for the removal of core decay heat during planned reactor shutdown or a reactor SCRAM scenario. This auxiliary system is part of the LPIS. The RHRS consists of three trains.

The RHRS takes the RCS inventory from the connection of train 1 to HL 1. Thereafter, the inventory is directed to the HXs of the system, one per train, and finally fed to the injection points of the three trains. These injection points are the CL1 and the four injection lines of the HA-1. A diagram of the LPIS when operating in RHR mode is shown in Figure 2-28.

The AFW is an auxiliary system used during reactor start-up, shutdown or in the event of MFW pump malfunction. The AFW system consists of two auxiliary electric pumps designed to operate in transient mode at power levels below 6-7%, sharing the loading lines with the MFW system (Nuclear Regulatory Agency, 2011). A detailed diagram of the MFW and AFW is shown in Figure 2-29.

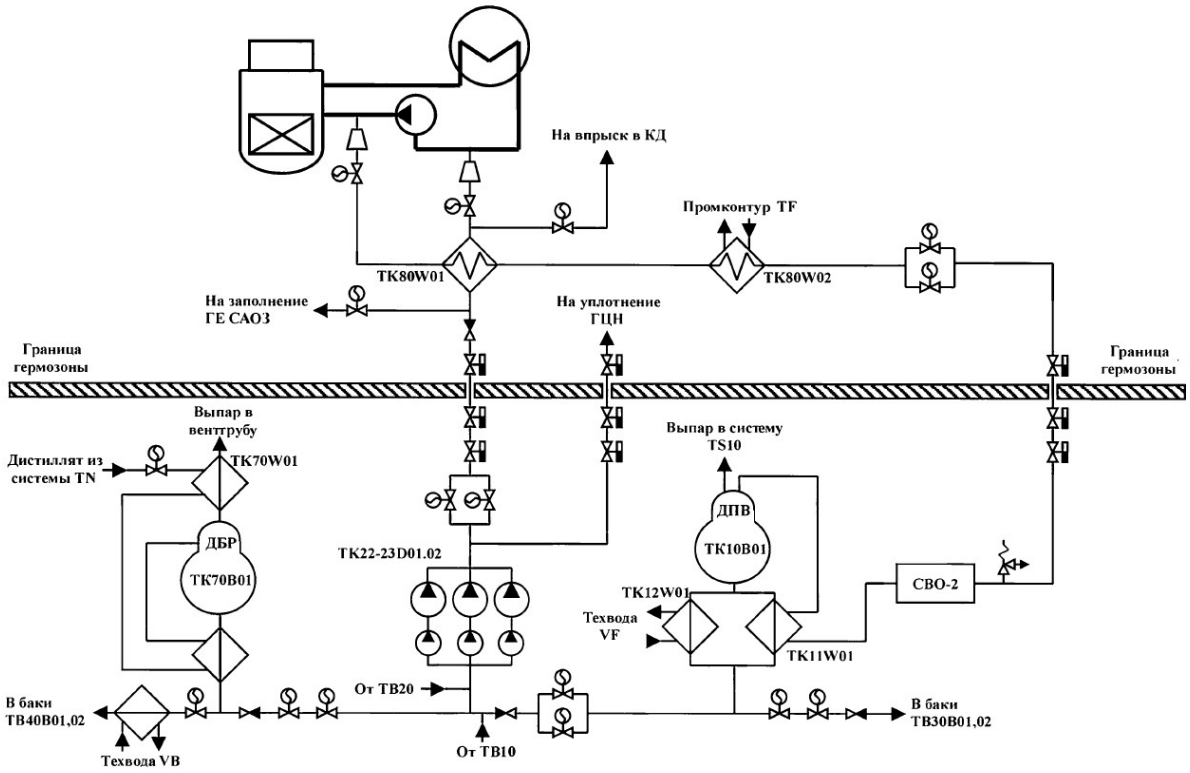

Figure 2-27 VVER-1000/V320 diagram of the CVCS (Andruschenko et al., 2010)

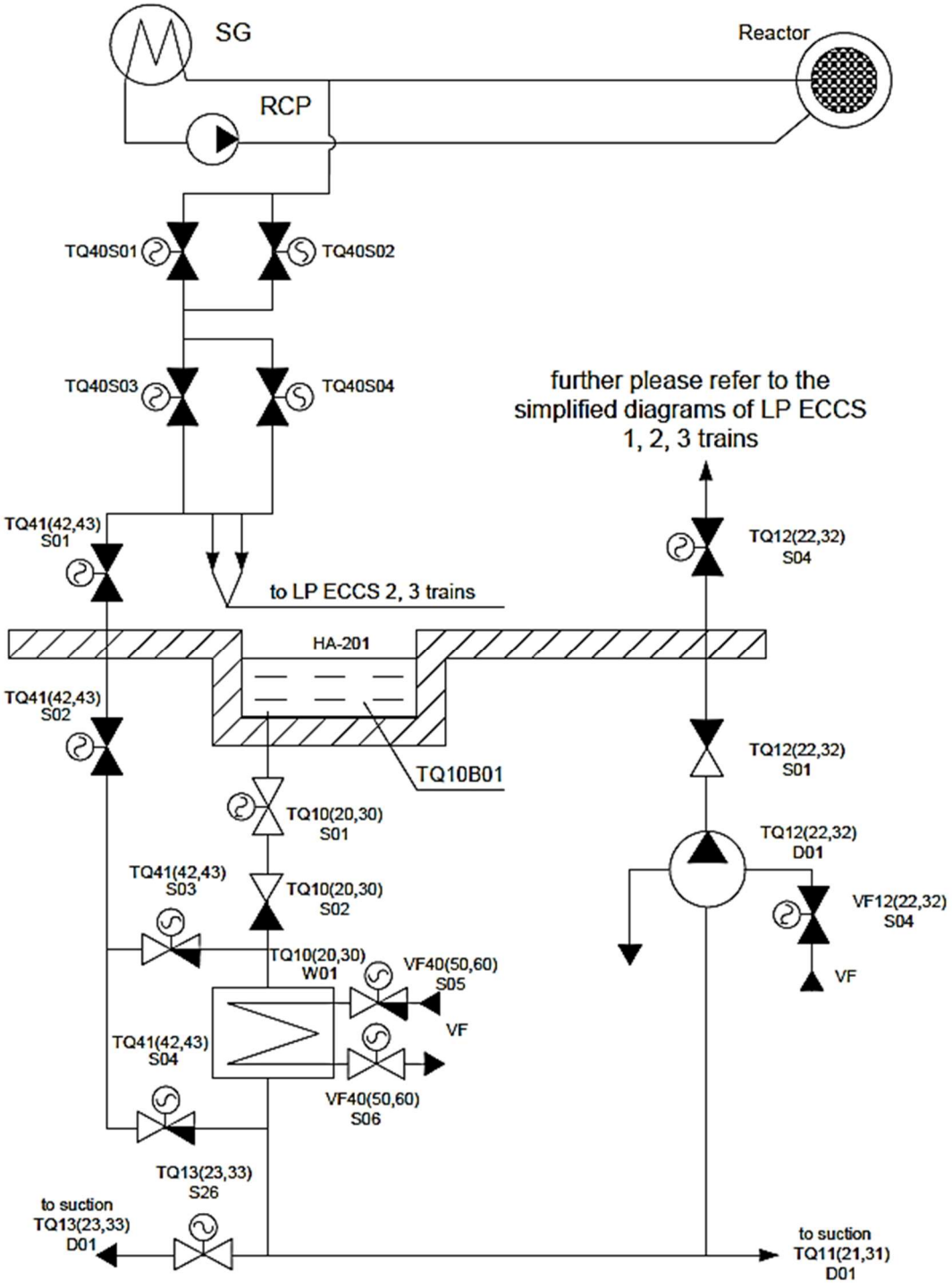

Figure 2-28 VVER-1000/V320 diagram of the LPIS in the RHR mode

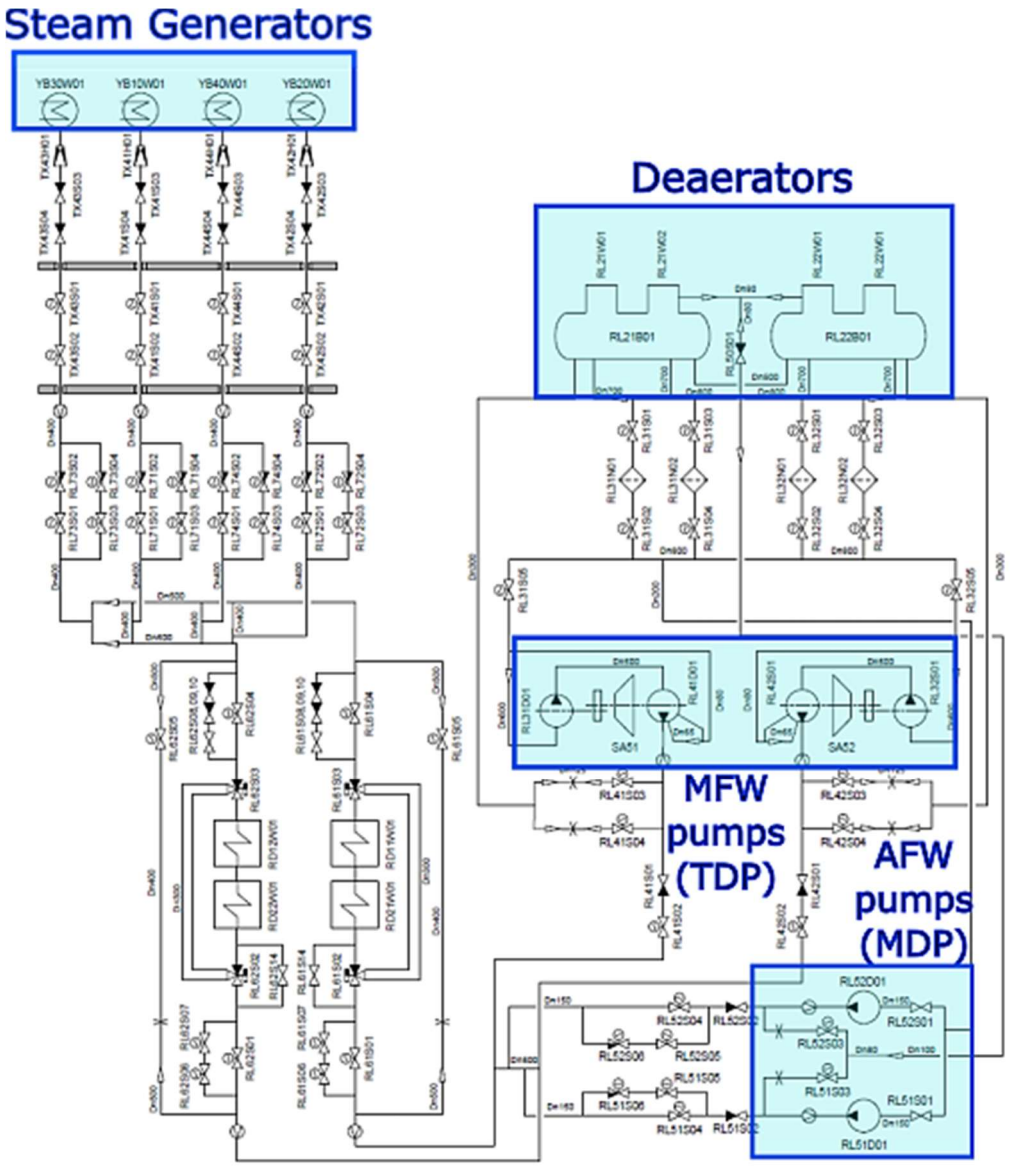

Figure 2-29 VVER-1000/V320 MFW and the AFW layout (Iegan et al., 2018)

2.2.2.7. Safety systems

The safety systems present in the VVER-1000/V320 reactors are described below. Therefore, the safety systems connected to the RCS are described in Section 2.2.2.7.1, the safety systems connected to the secondary circuit are given in Section 2.2.2.7.2 and the safety systems in the containment are referred to in Section 2.2.2.7.3.

2.2.2.7.1. Safety systems connected to the RCS

The safety systems connected to the RCS are the Emergency Core Coolant System (ECCS), the EBIS, the RCS overpressure protection system, and the EGRG. In turn the ECCS includes the HA-1, the HPIS and the LPIS, (Rijova and Steinborn, 2008). A general scheme of the ECCS is shown in the Figure 2-30.

There are four HA-1 with a design criteria of 2 out of 4 trains and a total volume of 60 m^3 per HA-1 (Kovacs, 2014), partially filled with borated water, 50 m^3, and pressurized with N_2 to 6 MPa, (State nuclear regulatory inspectorate of Ukraine, 2011). The HA-1 are located in two pairs in the containment at levels 27.0 m and 36.0 m. They are arranged in diagonally opposite positions close to the inner surface of the containment wall. The HA-1 situated at the higher level discharge into the RPV downcomer (HA-DC) and the HA-1 at the lower level discharge into the RPV upper plenum (HA-UP), see Figure 2-31 (Tusheva, 2012). Moreover, the HA-1 are equipped with automatic isolation valves to isolate them when the water level drops below 1.2 m (Queral et al., 2021).

The HPIS consists of 3 identical trains (TQ13, TQ23 and TQ33) connected to the CL 1, CL 3 and CL 4, with a design criterion of 1 out of 3 trains, (D. C. Cacuci (ed.), 2010). Initially, the HPIS pumps take suction from HPIS storage tanks (TQ13B01, TQ23B01 and TQ33B019) with a boron concentration of 16 g/kg. When these storage tanks are empty, the pumps start to take suction from the containment sump tank (TQ10), which is shared with the LPIS (Iegan et al., 2018). A diagram of the HPIS is shown in Figure 2-32.

The LPIS consists of three identical trains (TQ12, TQ22 and TQ32). All three trains take suction from the containment sump and include HXs to cool the water prior to injection into the RCS. The system is designed with a 1 out of 3 trains design criteria. One of the trains is connected to CL 1 and HL 1, see Figure 2-33, while trains 2 and 3 are each connected to the HA-DC and HA-UP discharge lines to the RPV, see Figure 2-34.

VVER-1000 reactors have also implemented mobile equipment, e.g. Balakovo NPP has installed pumps with the capacity to inject water into LPIS trains 2 and 3 with the mass flow of up to 150 m^3/h at the pressure of up to 8.8 MPa, (VVER working group, 2019).

A comparison of the number of trains, volumes, cut-off pressures and capacity per pump of the LPIS, HPIS of various PWR reactor designs is given in the Table 2-15, (AREVA, n.d.; Bui and Tran, 2015; Chul-Hwa and Jong-Kyun, 2004; Gavrilas et al., 1995; General Nuclear System, 2021; Huang et al., 2020; ROSATOM, 2022; Sang-Won et al., 2014).

Table 2-15 ECCS active comparison in different PWR designs

		Westinghouse (3-loop)	Siemens (Konvoi)	Framatome (P4)	VVER-1000 V-320	VVER-1200 V392M	EPR	APR1400	Hualong
Themal Power		3000	3600	3800	3000	3600	5000	4000	3600
HPIS	Number of trains	2	4	2	3	2	4	4	2 or 3
	Shutoff head (MPa)	18	11	12.0-10.2	10.6	8.6	9.8	11-14.5	~9
	Capacity per pump (kg/s)	30-40	62	68-136	78	83	40	50	~30
LPIS	Number of trains	2	4	2	3	2	4	-	2 or 3
	Shutoff head (MPa)	~1.5	0.9	2.3-2.0	2.5	~2.5	2.35	-	N/A
	Capacity per pump (kg/s)	300	306	120-280	207	250	140	-	~130

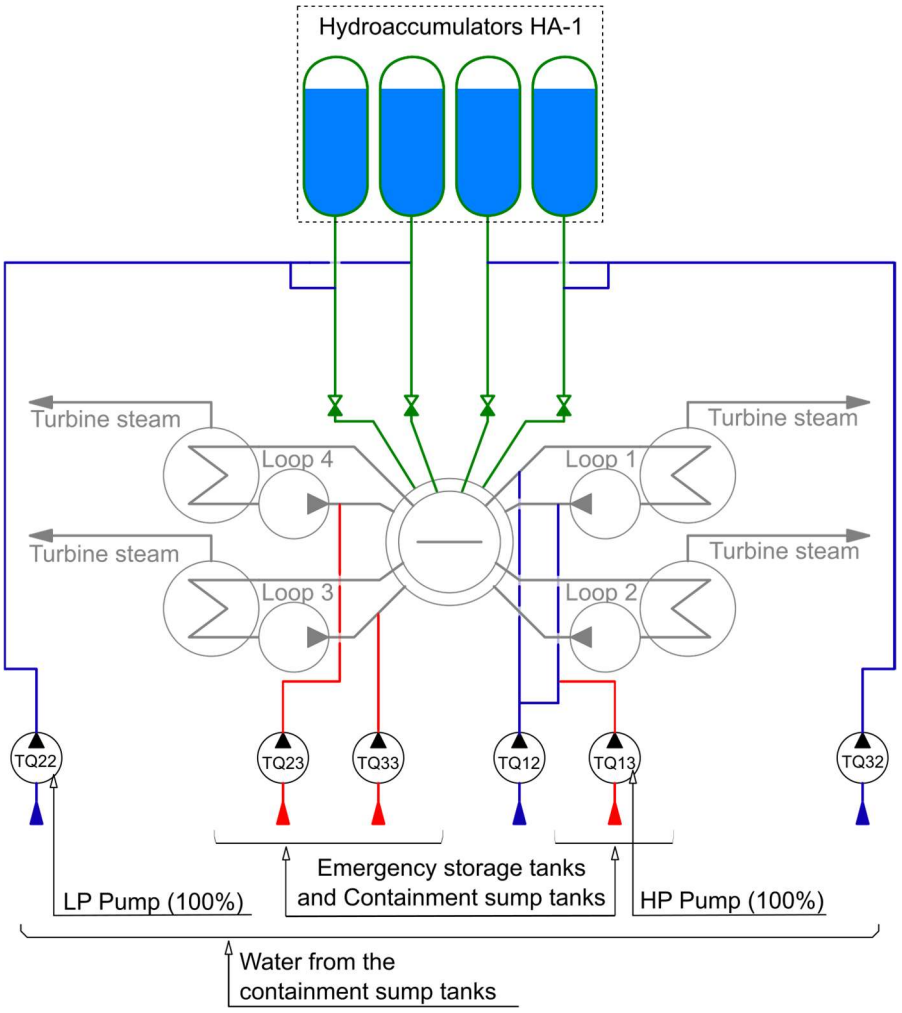

Figure 2-30 VVER-1000/V320 ECCS configuration. Modified from (WWER-1200 Nucleopedia, 2021)

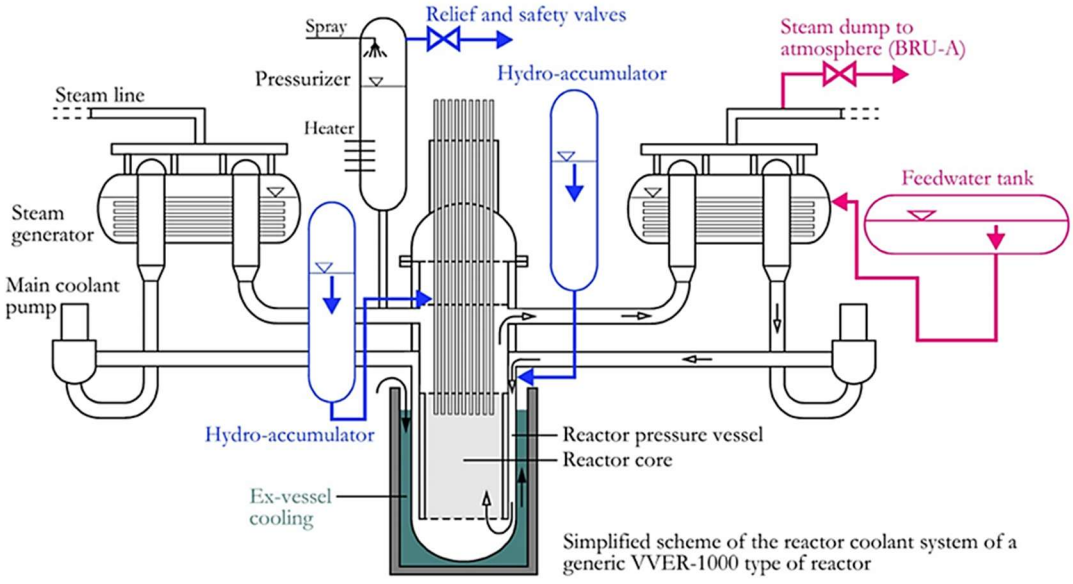

Figure 2-31 VVER-1000/V320 HA-1 connections to the RPV (Tusheva, 2012)

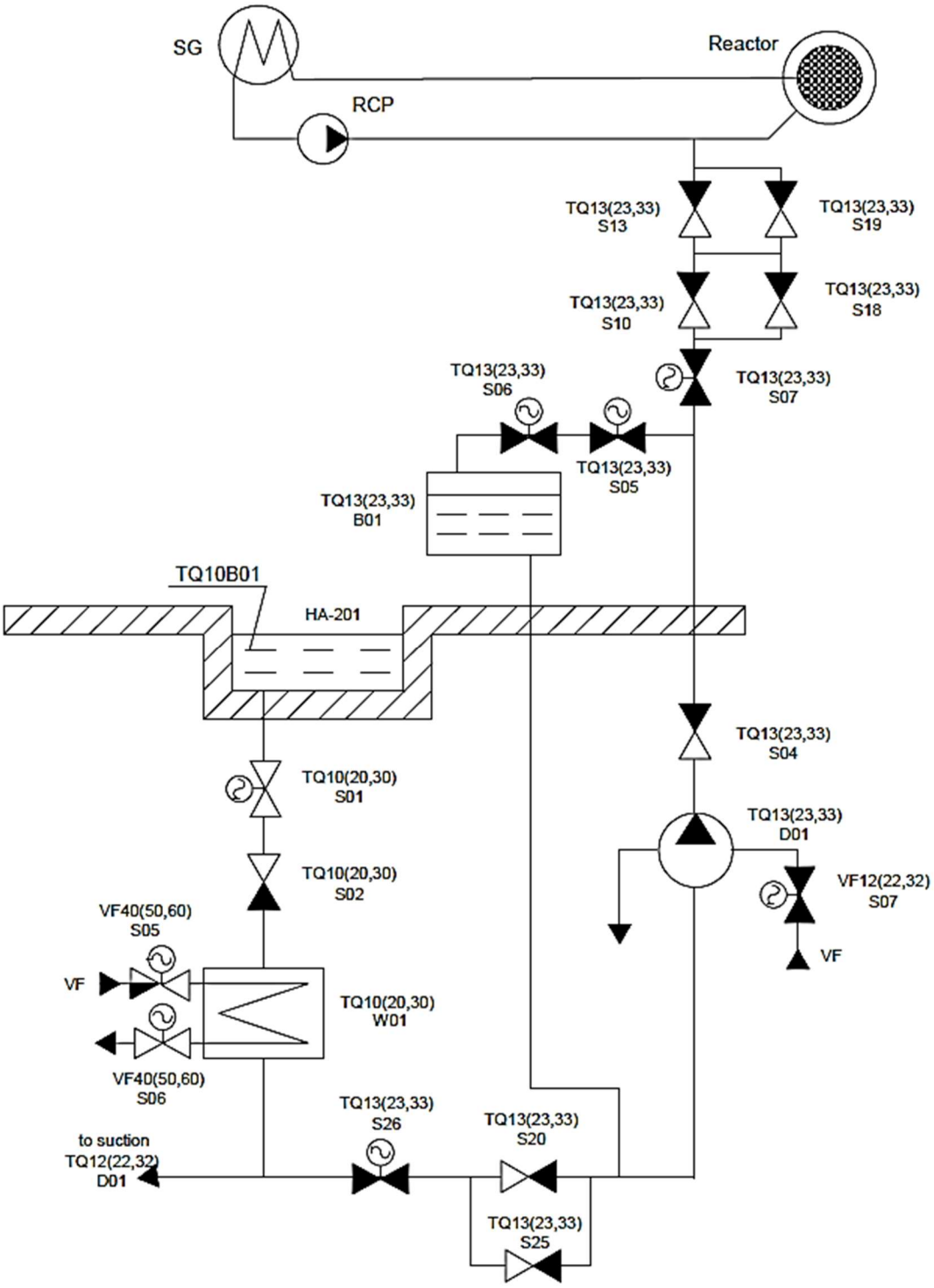

Figure 2-32 VVER-1000/V320 diagram of the HPIS

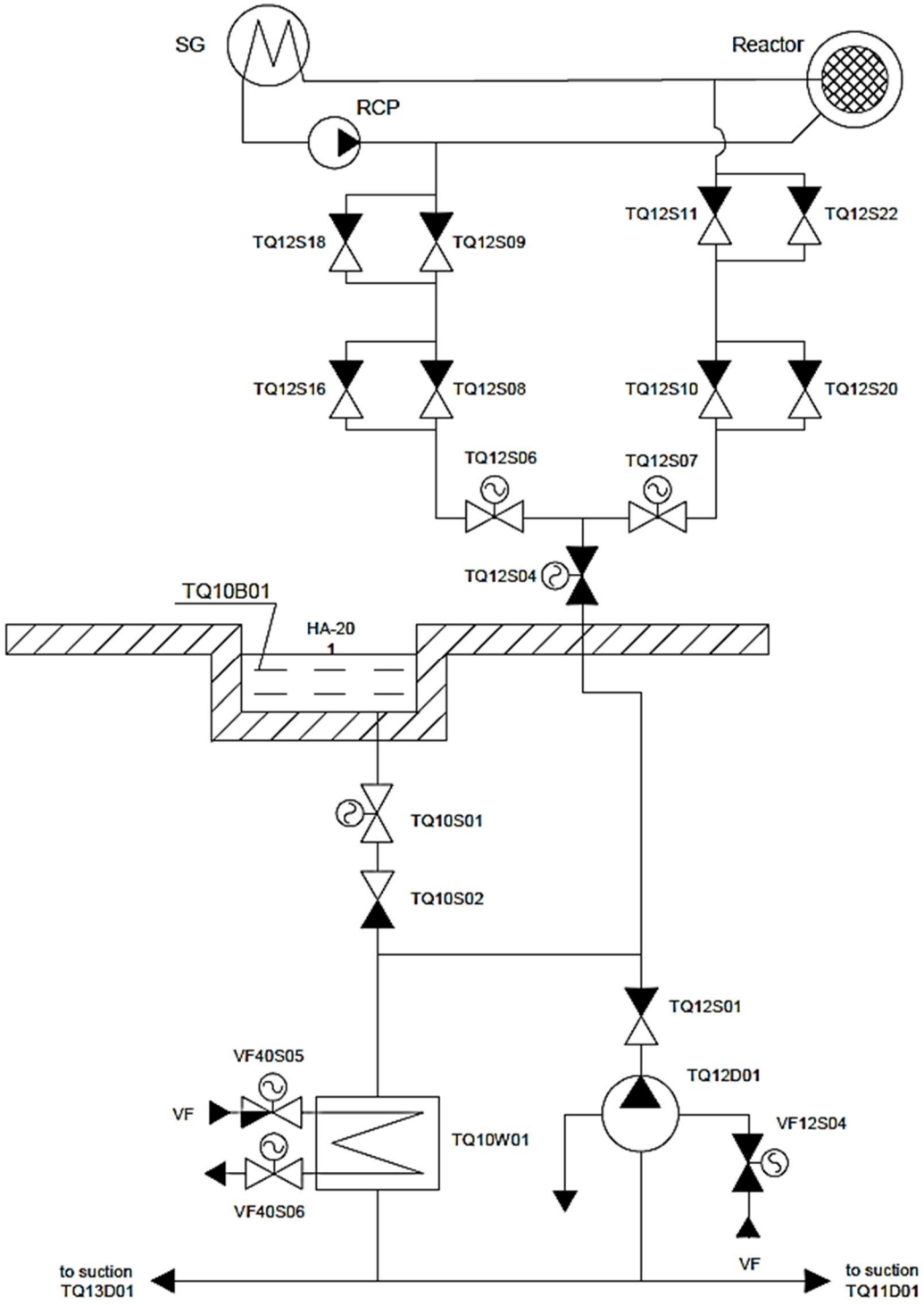

Figure 2-33 VVER-1000/V320 diagram of the LPIS train 1

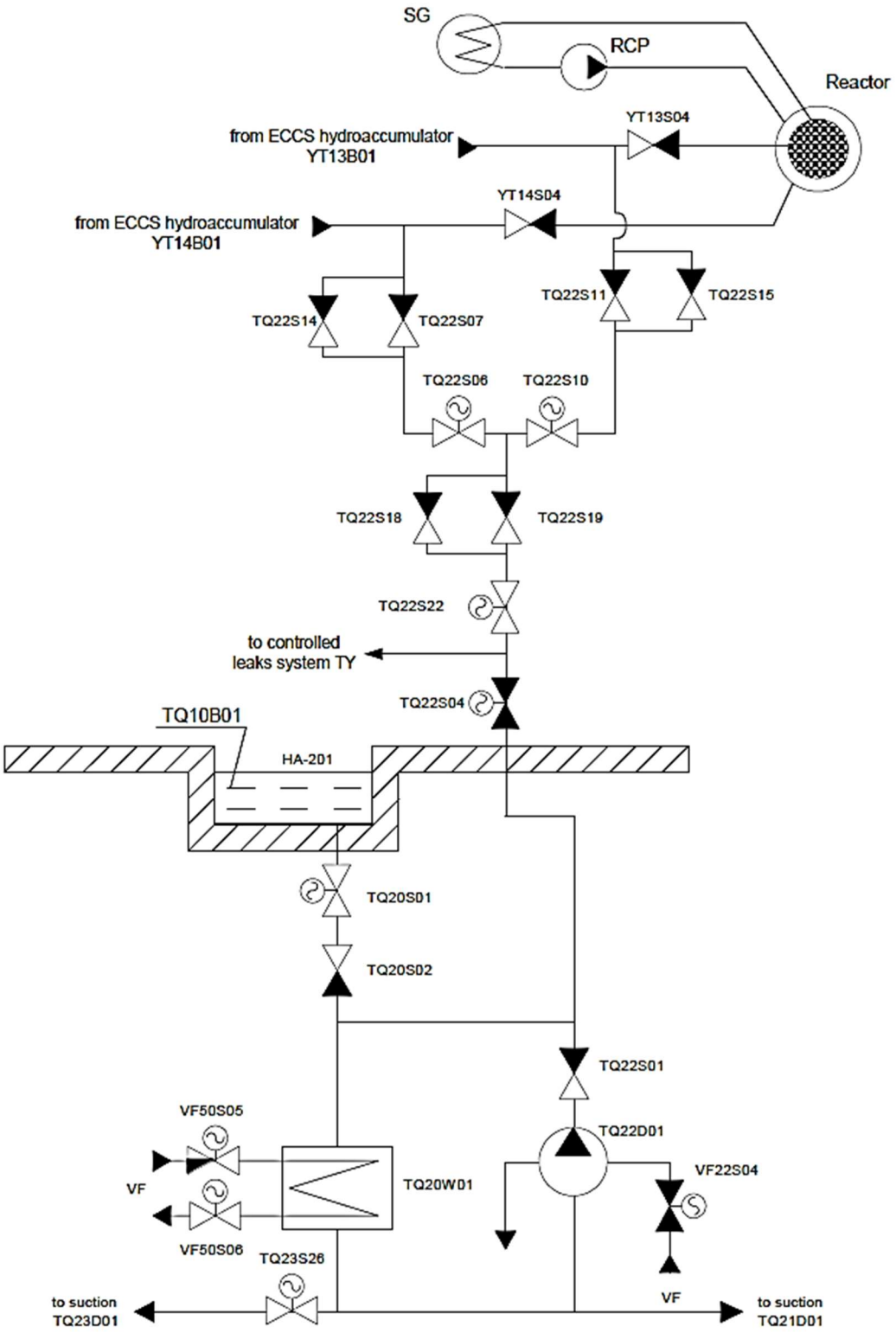

Figure 2-34 VVER-1000/V320 diagram of the LPIS trains 2 and 3

The EBIS, also known as the High Head Pressure Injection System (HHPIS), is designed to discharge a boric acid solution into the RCS to bring the reactor to a subcritical state. This safety system consists of 3 identical trains (TQ14, TQ24, TQ34) with a design criterion of 1 out of 3 trains. The EBIS share the connection points with the HPIS, i.e., the CL 1, the CL 2 and the CL 3, see Figure 2-35.

This system takes suction from a storage tank with a high boron concentration of 40 g/kg, with a volume of 15 m^3 each. The system pumps are capable of injecting 6.3 m^3/h of borated water at an RCS pressure of up to 20.0 MPa (Iegan et al., 2018). A diagram of the EBIS is shown in Figure 2-36.

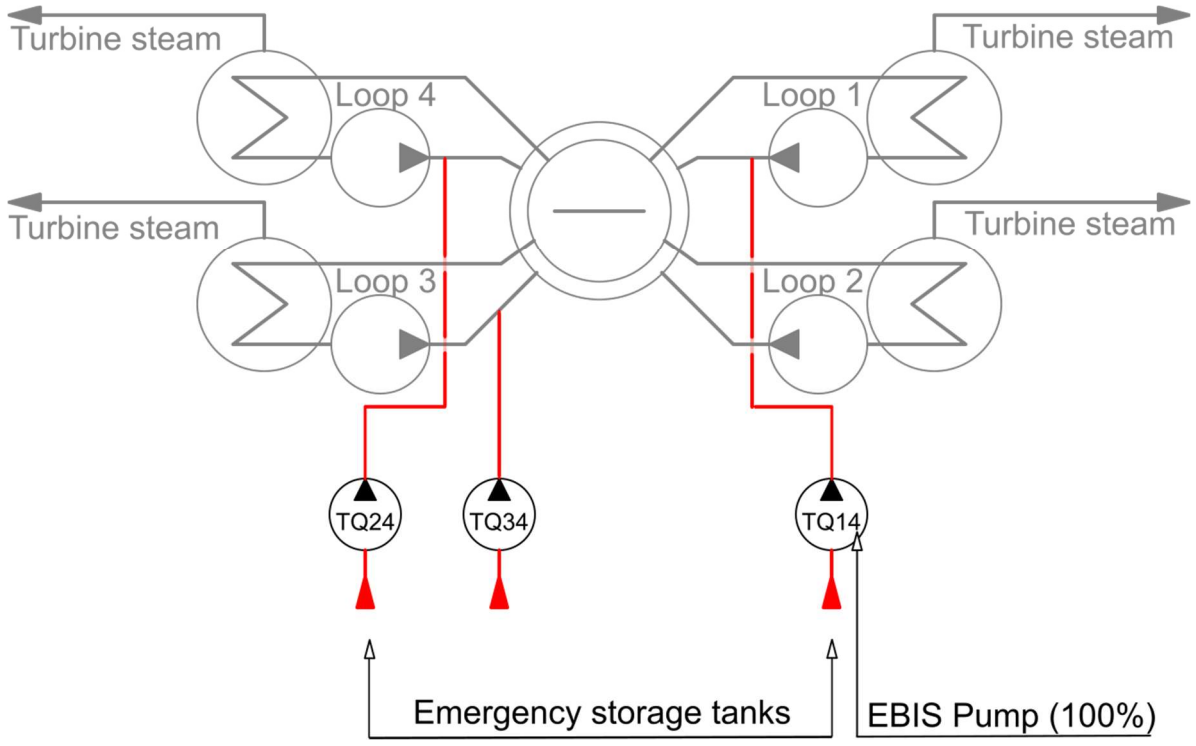

Figure 2-35 VVER-1000/V320 EBIS configuration. Modified from (WWER-1200 Nucleopedia, 2021)

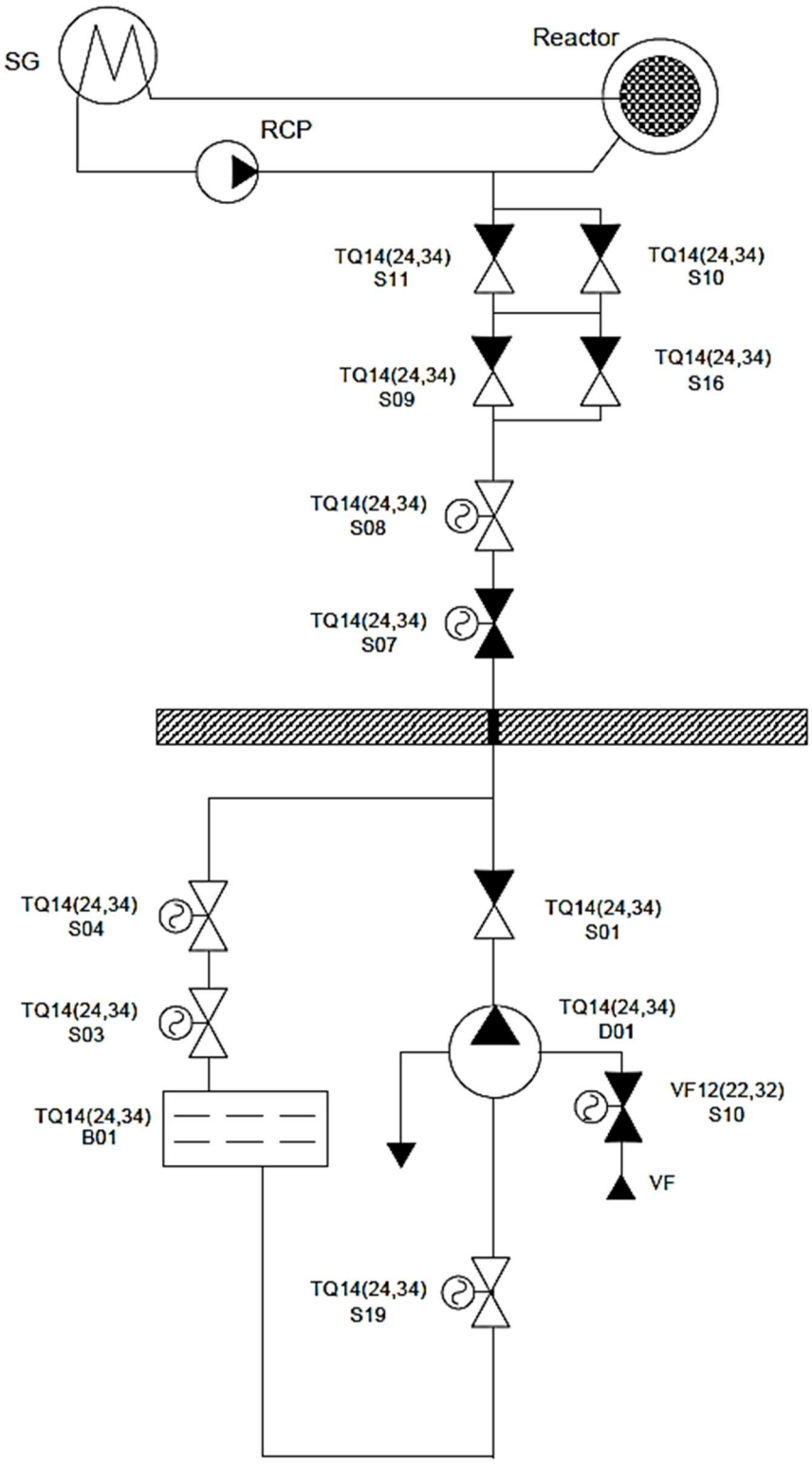

Figure 2-36 VVER-1000/V320 diagram of the EBIS

The RCS overpressure protection system is designed to protect the RCS structures from pressure exceeding design limits, (IAEA, 2011b). The safety system consists of three relief and safety valves located in the upper part of the PZR (Chatterjee et al., 2009). In the references it has been found that one valve opens at a setpoint around 18 MPa, while the second and the third valves open at a setpoint around 18.6 MPa (Gencheva et al., 2005; Ivanov et al., 2004; Tusheva, 2012), see Table 2-16.

These valves can also be manually operated to depressurize the RCS and implement the feed and bleed strategy, (Muellner, 2010). The RCS overpressure protection system is composed of Category I components, which means that they are battery powered. Therefore, the safety system is capable of operating in an accidental sequence under SBO conditions, (Tusheva, 2012). A diagram of the RCS overpressure protection system is shown in Figure 2-37.

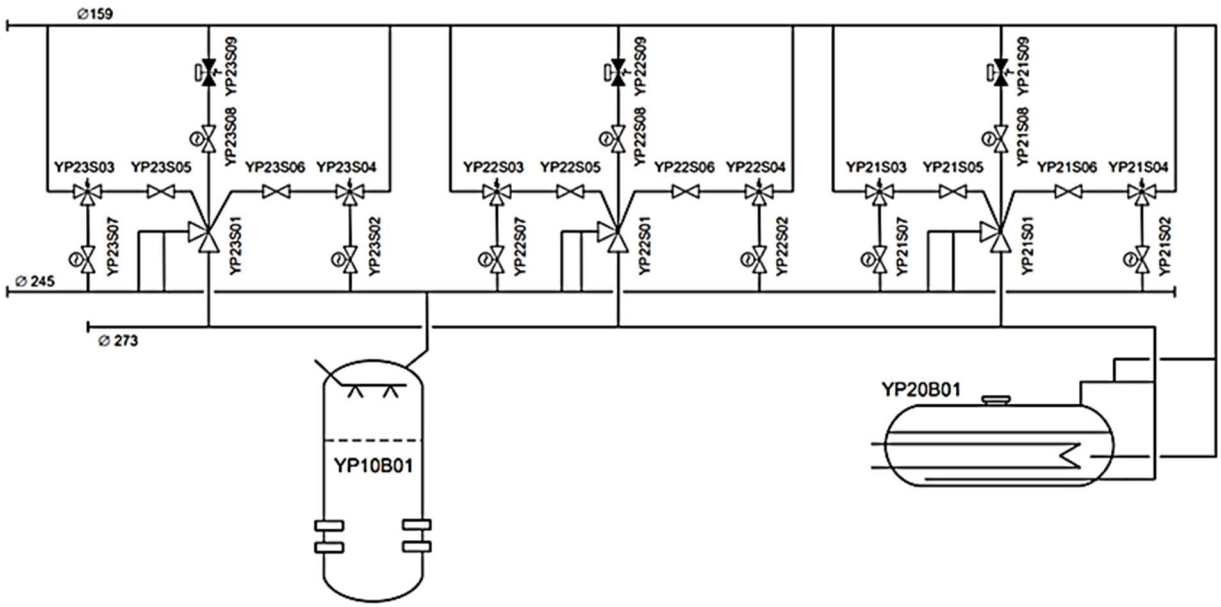

Figure 2-37 VVER-1000/V320 diagram of the RCS overpressure protection system (Iegan et al., 2018)

Table 2-16 VVER-1000/V320 PZR relief and safety valves (Ivanov et al., 2004)

PZR relief and safety valves	Value	Unit
#1	17.7	MPa
#2	18.6	MPa
#3	18.6	MPa

The EGRS is a safety system designed to ensure emergency depressurisation by venting the steam-gas mixture formed at the uppermost points of the RCS in the event of an accident (Gencheva et al., 2005).

The EGRS consists of a series of valves in the upper head of the RPV, in the SG collectors and in the upper part of the PZR (Iegan et al., 2018), see Figure 2-38. The system is manually operated from the Main Control Room (MCR). The valves of the EGRS are Category II electrical power supply. Therefore, under SBO conditions, these valves cannot be used for RCS depressurisation (Tusheva, 2012).

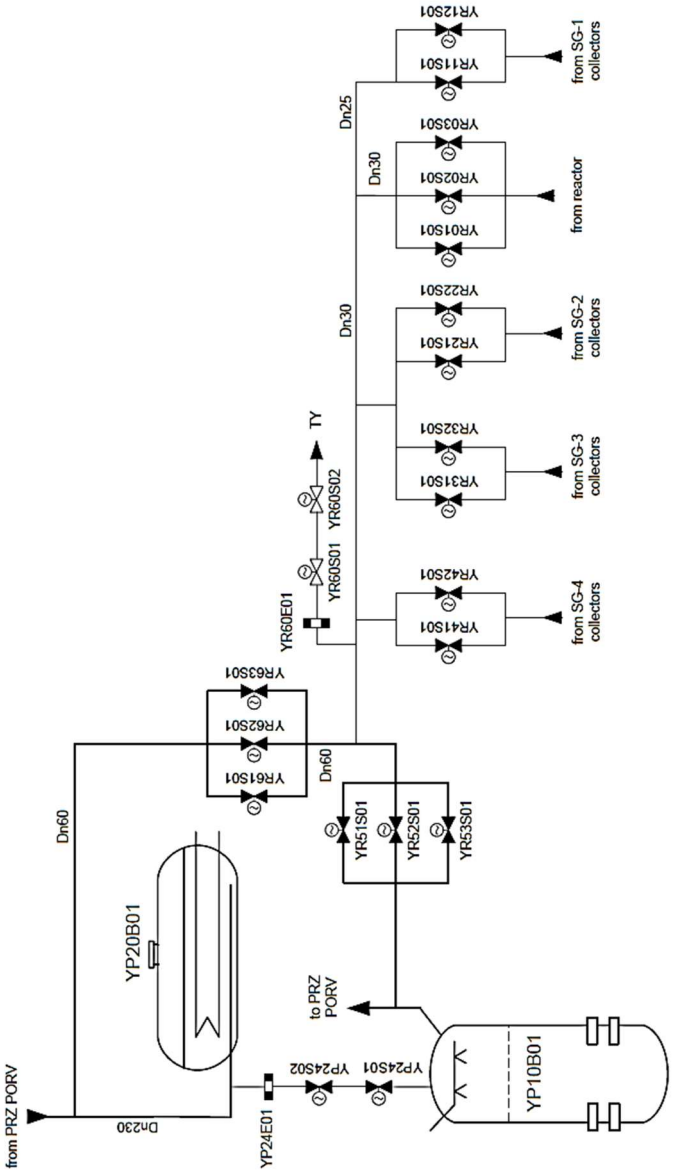

Figure 2-38 VVER-1000/V320 diagram of the EGRS (Iegan et al., 2018)

2.2.2.7.2. Safety systems connected to the secondary circuit

The VVER-1000/V320 reactors have two safety systems on the secondary circuit: the secondary pressure relief system and the EFW system. In addition, SL are equipped with Main Steam Isolation Valves (MSIV), also known as Fast Acting Isolation Valves (BZOK), and check valves. The secondary pressure relief system, see Figure 2-39, includes the following valves:

- Relief valves to the atmosphere (BRU-A). Each SL upstream of the MSIV is equipped with a BRU-A valve. They are designed to relieve steam to the atmosphere to prevent pressure increase in the SGs. The BRU-A valves open when the SL pressure exceeds 7.3 MPa and maintain the pressure between 6.8 and 7.3 MPa, (IAEA, 2011b; Iegan et al., 2018).

  In addition to maintaining SG pressure during emergency scenarios, the BRU-A valves can also be used as part of an emergency strategy to cool and depressurize the RCS via the SGs, (Groudev, 1998). This approach is only employed if the Steam Dump Valves to the Condenser (BRU-K) valves are unavailable and either the AFW or EFW systems are operational, (Iegan et al., 2018). This strategy provides controlled RCS cooling rates of either 30 K/h or 60 K/h. Alternatively, the BRU-A valves can be fully opened to achieve maximum RCS cooling rates.

- Safety Valves. Each SL is equipped with two safety valves located between the MSIV and the BRU-A valve. These valves are designed to prevent the SG pressure from exceeding 15% of the design value during emergency scenarios, (Ivanov et al., 2004). The safety valves on each SL have different setpoints: one valve opens when the pressure exceeds 8.4 MPa, and the other opens at 8.6 MPa. Both valves close when the pressure drops below 7 MPa. Additionally, the valves can be manually operated from either the main or reserve MCR, (Tusheva, 2012).

- BRU-K. There are 4 BRU-K valves located in the MSH. These valves have a total turbine bypass capacity of 60 % (VVER working group, 2019). They are designed to keep the pressure in the steam header below 6.8 MPa, (Muellner, 2010). The valves open automatically when the pressure rises above 6.8 MPa and maintain the pressure between 6.4 and 6.8 MPa.

The BRU-K valves are also used for the RCS cooling and depressurization management strategy through the SGs, when the AFW or the EFW are available. The RCS cooling rates provided by these valves are those of the BRU-A, 30 K/h or 60 K/h, (Iegan et al., 2018).

- Relief valves to the atmosphere (BRU-SN). In the MSH there are to BRU-SN intended to relief steam to the atmosphere. This type of valves has been removed from the VVER Gen-III/III+ designs, (Queral et al., 2021).

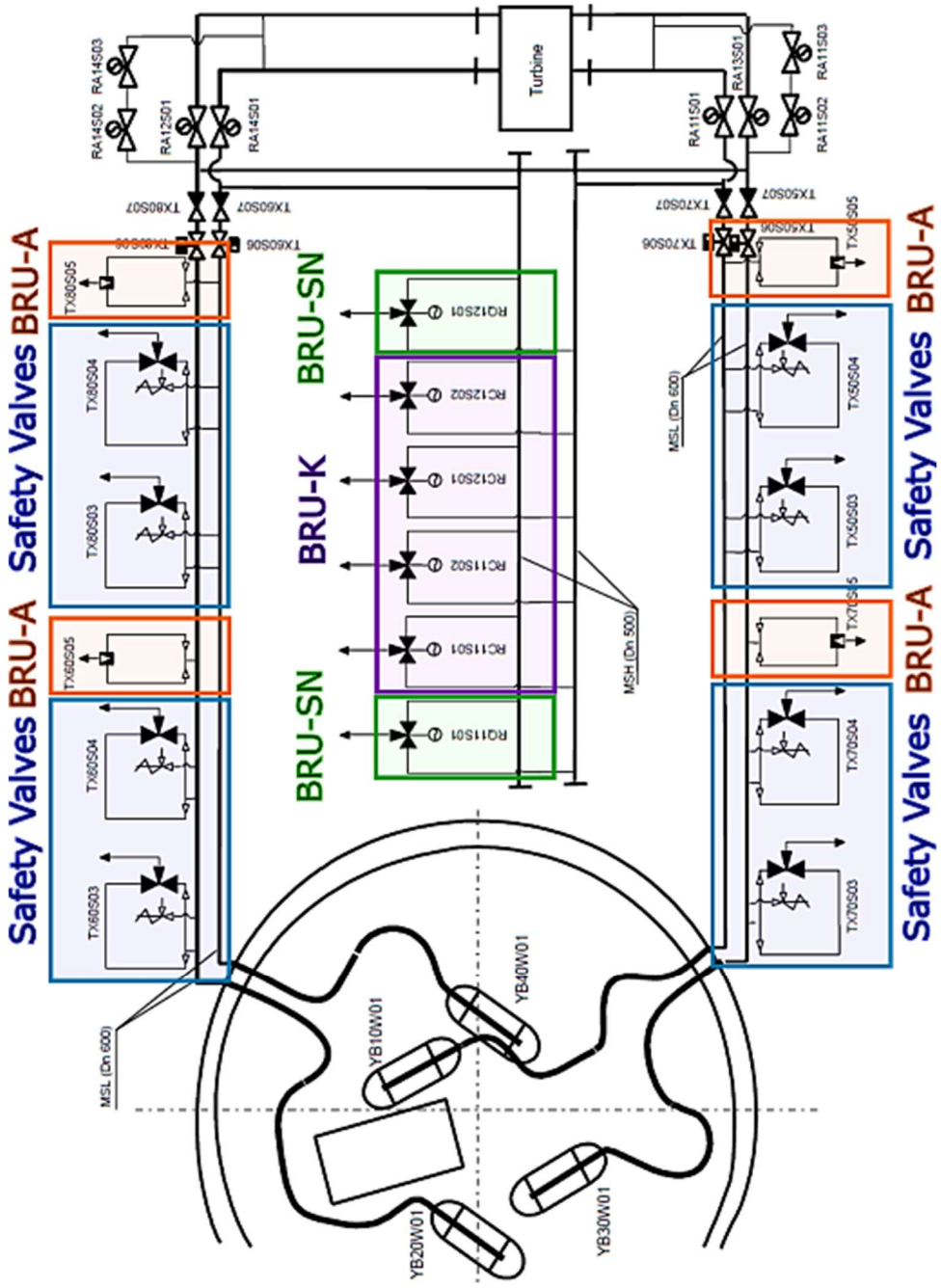

Figure 2-39 VVER-1000/V320 SL valves (Iegan et al., 2018)

The EFW is designed to provide feed water to the SG during accident sequences with loss of MFW and AFW. The EFW is an open circuit consisting of 3 x 100% trains, see Figure 2-40. One train supplies water to SG 1 and SG 4, another train supplies water to SG 2 and SG 3 and a third train supplies water to the fourth SG, (Iegan et al., 2018). Each train draws water from a tank with a volume of 500 m^3. A diagram of the HPIS is shown in Figure 2-41.

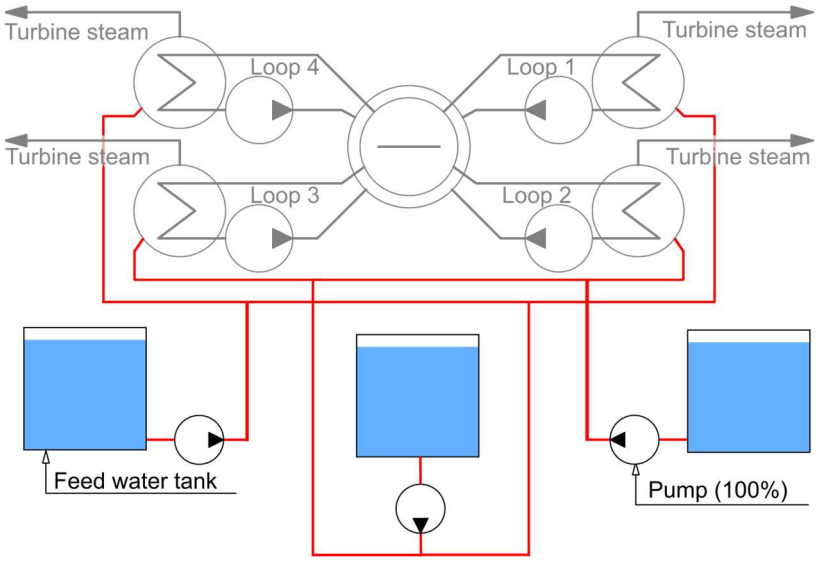

Figure 2-40 VVER-1000/V320 EFW connections to the SGs. Modified from (WWER-1200 Nucleopedia, 2021)

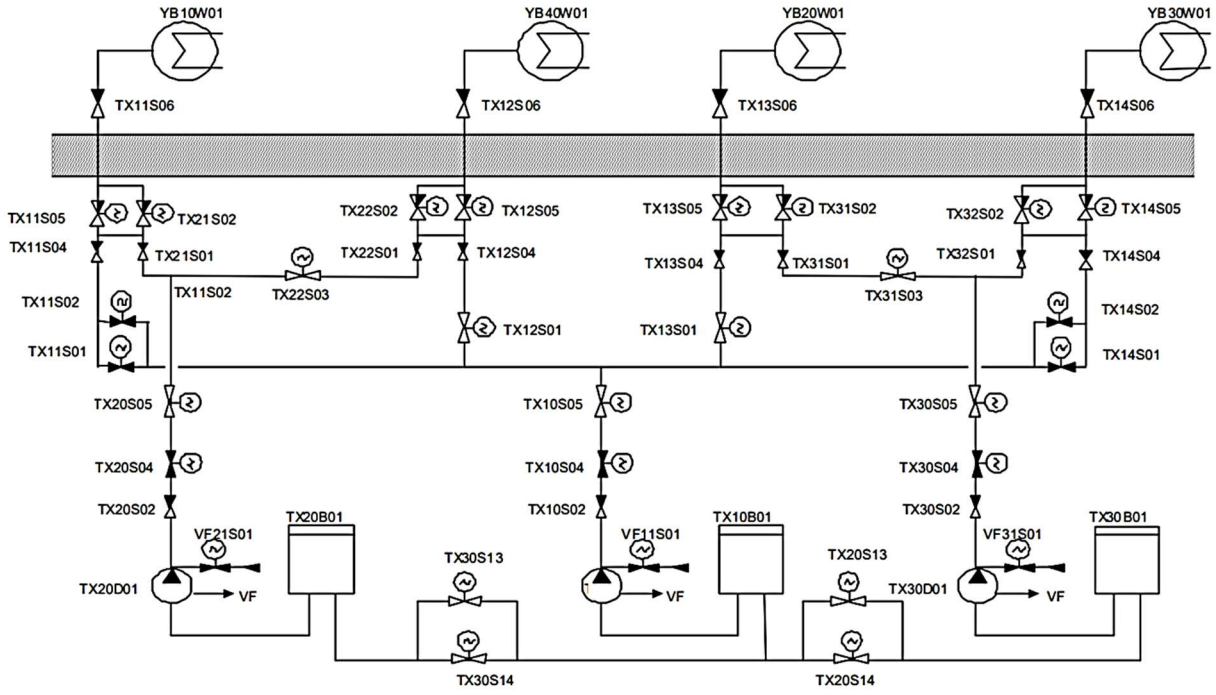

Figure 2-41 VVER-1000/V320 diagram of the EFW

2.2.2.7.3. Safety systems in the containment

The containment is equipped with the Containment Spray System (CSS), the Containment Isolation System (CIS), the Containment Ventilation System (CVS) and in some VVER-1000/V320 NPPs also with PARs. A short description of these systems is given below.

The CSS consists of 3 x 100% trains (TQ11, TQ21 and TQ31) (Rijova and Steinborn, 2008). This safety system is designed to reduce the pressure and temperature in the containment, to minimise the radioisotopes and to condensate the inventory release during a LOCA or a Steam Line Break (SLB) accident.

The CSS is provided with three rings of 20 spray nozzles each at the top of the dome, see Figure 2-42. They are connected by vertical pipes to the pumps and the HXs of the system located below the containment. The pumps take suction from the containment sump, which is common to all three systems and is shared with the HPIS and LPIS. The CSS start to operate when the pressure in the containment reaches 0.03 MPa (relative value) (VVER working group, 2019). It should be noted that during normal operation the containment is at subatmospheric pressure.

The CIS, on the other hand, is a safety system designed to seal the containment in the event of a LOCA. This system is triggered by two activation signals: a high pressure condition and a temperature rise. Isolation valves are installed in various systems with components both inside and outside the containment.

Moreover, the CVS aims to remove heat from the containment during normal operation and to prevent activation of the CSS in the event of an accidental sequence. The system consists of three trains, of which only one operates under normal conditions. If the containment temperature rises above 50°C, the operators activate a second train. Each train contains a motorised air fan and is connected to an SWS HX.

In addition, a significant number of VVER-1000 NPPs are equipped with PARs, type RVK-500 or RVK-1000 (Tarasov et al., 2017), see Figure 2-43. This PAR contains fourteen γ-Al_2O_3 ceramic cylinders and impregnated with Pt catalyst (Malakhov et al., 2024).

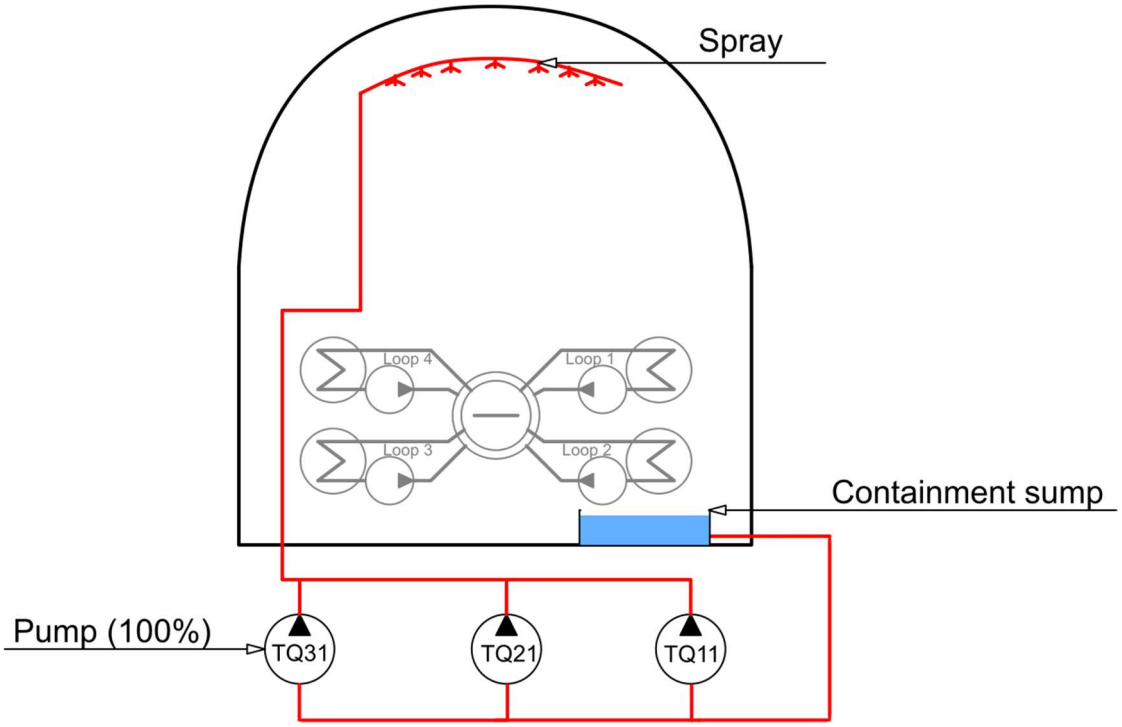

Figure 2-42 VVER-1000/V320 CSS configuration. Modified from (WWER-1200 Nucleopedia, 2021)

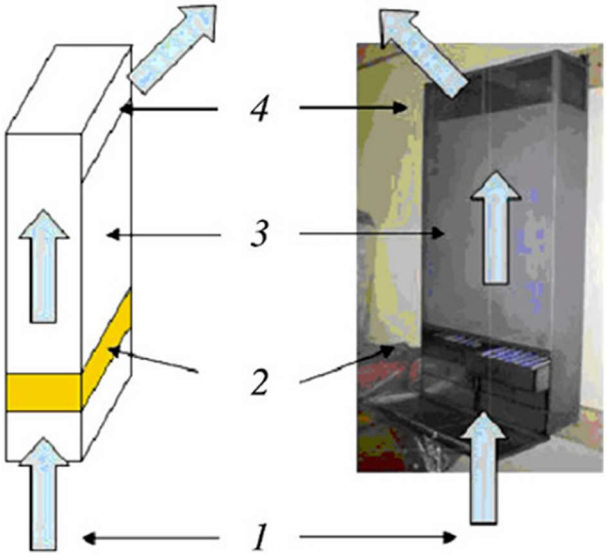

Figure 2-43 RVK-1000 PAR. 1. Gas inlet, 2. Hydrogen recombination in the catalytic block, 3. Draft section, 4. Gas outlet (Tarasov et al., 2017)

2.2.3. Gen-III/III+ VVER reactors

Two different families of Gen-III/III+ VVER reactors have been developed by two separate Russian institutes, one in Saint Petersburg and the other one in Moscow. Initially, both institutes developed Gen-III VVER-1000 designs based on the earlier Gen-II VVER-1000/V320 reactor. The Saint Petersburg institute developed the VVER-1000/V428, while the Moscow institute developed the VVER-1000/V412 in Moscow. Later, each institute independently has designed Gen-III+ VVER-1200 models, see Figure 2-44. Some of the main differences between these two families can be found in their safety systems, which also affect the shape and geometry of the containment structures, (World Nuclear Association, 2024; WWER-1200 Nucleopedia, 2021).

A detailed overview of the main characteristics, capabilities and layout of the active and PSS found in the Gen-III/III+ VVER designs is given below. Besides, three tables at the end of this section summarize the safety systems, both passive and active, found in the Gen-II, Gen-III and Gen-III+ reactors in the RCS, the secondary circuit and the containment, see Table 2-17, Table 2-18 and

Table 2-19, using the nomenclature specified in the Kraftwerk-Kennzeichensystem (KKS) and the Alfanumericheskaya Kodovaya Znakovaya (AKZ) coding system.

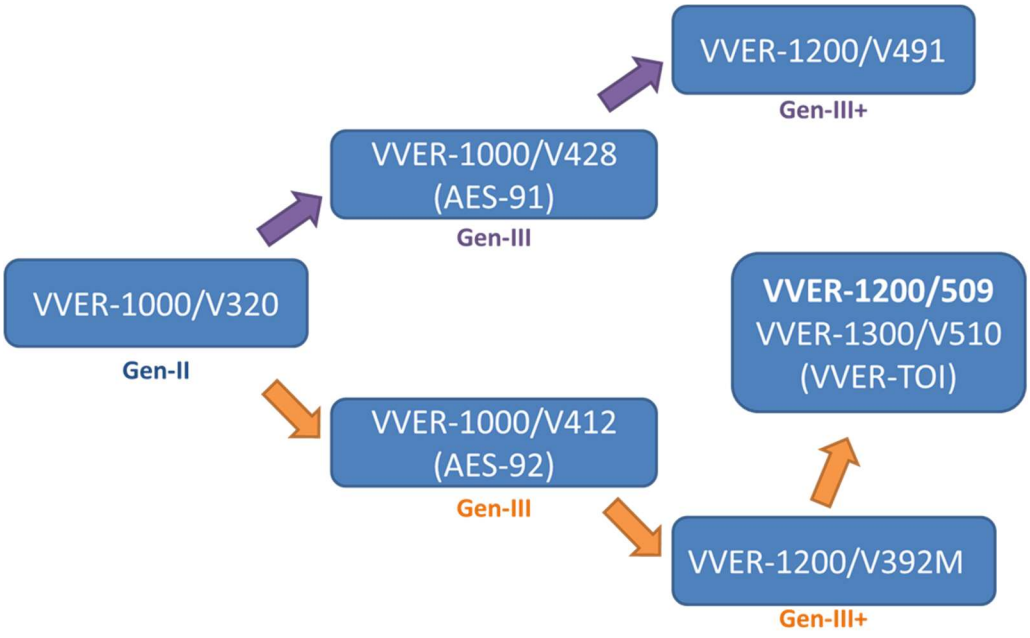

Figure 2-44 Main Gen-III/III+ VVER reactor designs

2.2.3.1. Gen-III/III+ VVER from the Saint Petersburg institute

The safety systems of the Saint-Petersburg institute VVER designs are shown below, with particular emphasis on to the VVER-1000/V428 (Tianwan NPP) and the VVER-1200/V491.

This family of reactors has a characteristic cylindrical containment. The VVER-1200/V491 has a double containment, consisting of an inner containment made of pre-stressed reinforced concrete lined with carbon steel in the inner part, and an outer containment made of monolithic reinforced concrete designed to provide protection against external impacts, see Figure 2-45 and (WWER-1200 Nucleopedia, 2021).

In the upper part of the outer containment, in the VVER-1200/V491 there is a water pool, known as Emergency Heat Removal Tanks (EHRT), belonging to the water-cooled PHRS connected to the SGs and the PHRS-C in the containment.

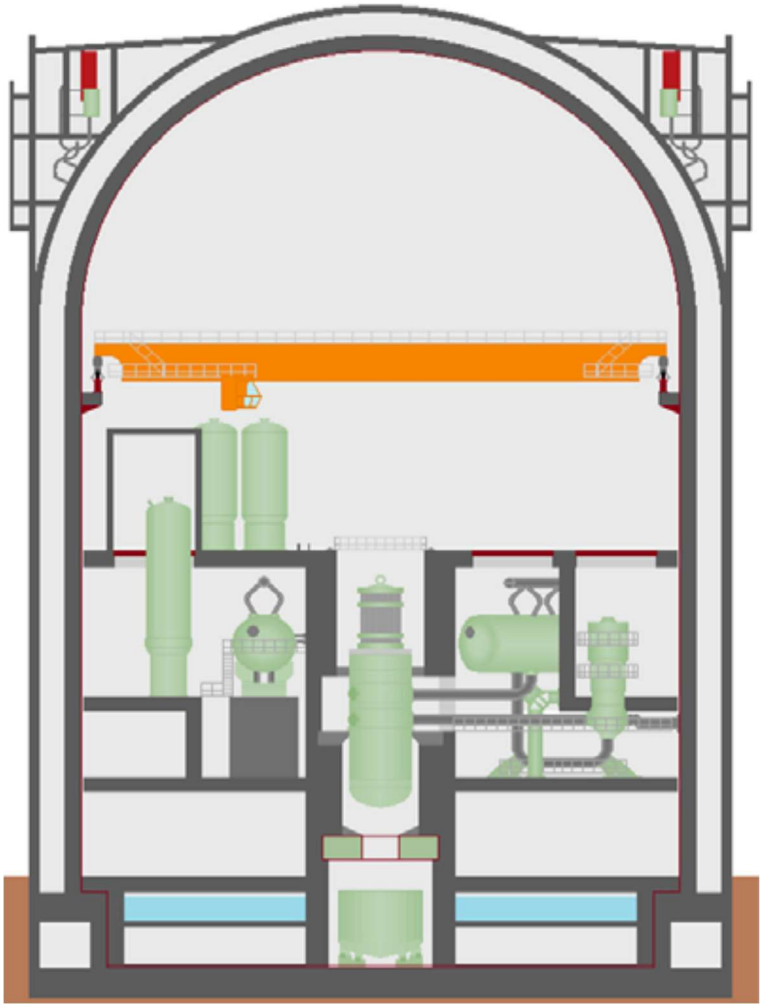

Figure 2-45 VVER-1200/V491 containment building (WWER-1200 Nucleopedia, 2021)

Safety systems connected to RCS

The RCS safety systems include the ECCS, the EBIS, the RCS pressure relief system and the EGRS. With regard to the ECCS, there are two active injection systems, the LPIS and the HPIS, and one passive injection system, the HA-1:

- The HPIS (JND) in the VVER-1000/V428 consists of 4 trains injecting into the CLs, with a 100% capacity each (4 x 100%). The VVER-1200/V491 design, also includes 4 x100% trains, but with a different configuration: 2 trains inject into the 4 HA-1 discharge lines, while the other 2 inject into the CLs and HLs of 2 loops of the RCS (Belarus nuclear regulatory authority, 2017; Bykov, 2013; WWER-1200 Nucleopedia, 2021), see Figure 2-46.
- The LPIS (JNG) consists of 4 x 100% trains, of which 2 inject into the HA-1 discharge lines and 2 inject into the CLs and HLs of two RCS loops, see Figure 2-46. In the VVER-1200/V491, the water source for both the HPIS and the LPIS is the containment sump tank, (Bykov, 2013; D. C. Cacuci (ed.), 2010).
- The HA-1 (JNG 2) are the only passive ECCS in the Saint-Petersburg Gen-III/III+ VVER reactors. They consist of 4 x 33% trains. The HA-1 tanks are filled with 50 m^3 of borated water and 10 m^3 of N_2 at 6 MPa, (Belarus nuclear regulatory authority, 2017; Veselov and Tishin, 2017). They are attached to the RPV, with two connections to the UP and two others to the DC, see Figure 2-46.

With regard to the EBIS (JDH), the VVER-1200/V491 and the VVER-1000/V428 employ 4 x 50% trains each (Belarus nuclear regulatory authority, 2017), see Figure 2-47. On the other hand, the RCS pressure relief system comprises three Pilot Operated Safety/Relief valves (PORV/JEF) which are activated by solenoid or spring (Belarus nuclear regulatory authority, 2017). This system is designed to handle anticipated transients and accidental sequences without Core Damage (CD). Additionally, the EGRS (KTP) in the VVER-1200/V491, is designed for severe accident sequences and consists of 2 trains, each with 2 Motor Operated Valves (MOV), which allow the RCS pressure to be reduced to values below 1 MPa (Belarus nuclear regulatory authority, 2017).

Safety systems connected to the secondary circuit

The VVER designs of the Saint Petersburg institute include two heat removal systems (the EFW and the water-cooled PHRS) and the secondary pressure relief system.

The EFW in the VVER-1000/V428 and the VVER-1200/V491 is an open circuit similar to the that in the VVER-1000/V320. Both reactor designs feature 4 x 100% trains, supplying water from two storage tanks (Bykov, 2013; D. C. Cacuci (ed.), 2010), see Figure 2-48. Additionally, these reactors are also equipped with the AFW (LAR/LAS), which is mainly used during startup, shutdown and planned cooldown.

The water-cooled PHRS (JNB) is only present in the VVER-1200 reactors, not in the VVER-1000/V428. It is activated if the EFW is unavailable. The water-cooled PHRS consists of 4 x 33 % trains, see Figure 2-49. Each train includes 18 HX located inside the EHRT, see Figure 2-50 and Figure 2-51, which are maintained at atmospheric conditions in the upper part of the containment, situated above the double containment containments structure, (Belarus nuclear regulatory authority, 2017; Bykov, 2013; Fennovioma, 2015; Laaksonen, 2015). These tanks are shared with the Passive Containment Cooling System (PHRS-C) and are designed to remove the heat from the SGs and the containment for up to 72 hours. When the water-cooled PHRS is activated, steam from the SLs flows to the HX, where it condenses and return to the SGs through natural circulation.

With respect to the secondary pressure relief system, three types of valves can be found in the Gen-III/III+ Saint-Petersburg VVER designs (WWER-1200 Nucleopedia, 2021):

- BRU-A: MOV which discharge steam into the atmosphere. They are equipped with battery power, allowing the operation from the control room during LOOP and SBO sequences. In both the VVER-1000/V428 and the VVER-1200/V491, there is one BRU-A per SL, see Figure 2-52.
- Safety valves: The VVER-1000/V428 comprises two per SL while the VVER-1200/V491 contains one per SL, see Figure 2-52.
- The BRU-K: They consists of 8 valves that discharge into the condenser. They are not equipped with a battery, so they are not available in the event of an AC power loss.

Containment safety systems

The VVER-1200/V491 reactors also have a passive heat removal system in the containment, the PHRS-C, mainly relevant in SBO sequences.

Moreover, the CSS of the VVER-1000/V428 and VVER-1200/V491 is similar to that of the VVER-1000/V320 reactor. It consists of 4 x 100% trains in the VVER-1000/V428 and 4 x 50% trains in the VVER-1200/V491. The pumps of this system take suction from the same water sources as the HPIS and the LPIS, the containment sump tank, see Figure 2-53.

The PHRS-C consists of 4 x 33% trains, see Figure 2-54. Each train contains an open circuit which takes suction from the EHRT, see Figure 2-55. Condensation of the steam from the containment on the outer walls of the HX tubes causes evaporation of the water inside the tubes, which returns to the pool by natural circulation, see Figure 2-56 and (Belarus nuclear regulatory authority, 2017; Bykov, 2013; Laaksonen, 2015). A similar PSS, albeit in a closed circuit, is found in the Hualong One CNNC design. Other Gen-III/III+ reactors, such as the AP1000 and CAP1400, also feature PHRS in the containment, but the design is significantly different.

In addition to the active and passive heat removal systems, VVER designs from the Saint Petersburg institute also includes a CC which aims to protect the containment structures from the corium in the event of severe accidents, (Udalov et al., 2014). It contains sacrificial oxides, such as alumina, which can be melted by the corium to reduce hydrogen generation.

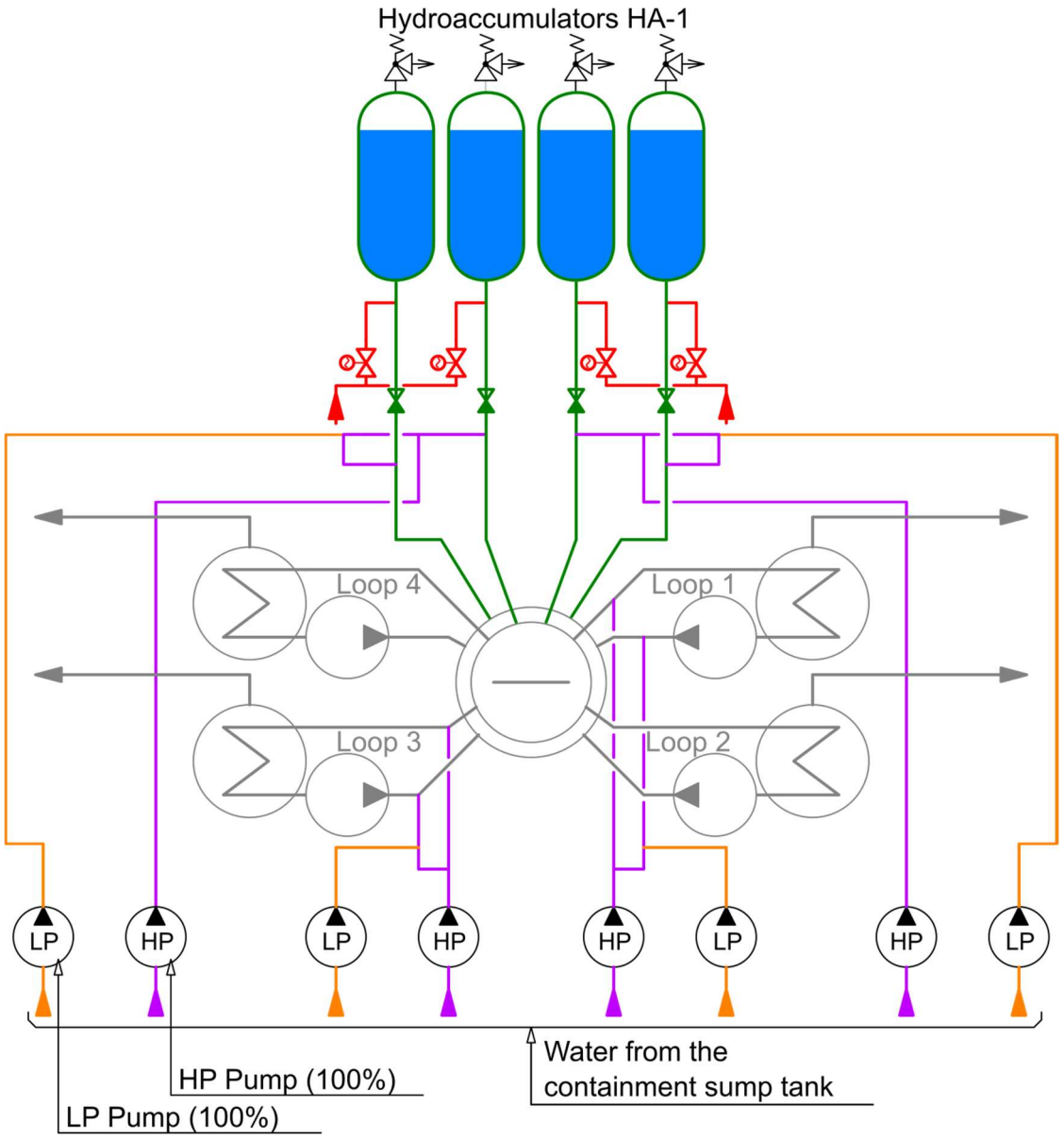

Figure 2-46 VVER-1200/V491 active and passive ECCS. Modified from (WWER-1200 Nucleopedia, 2021)

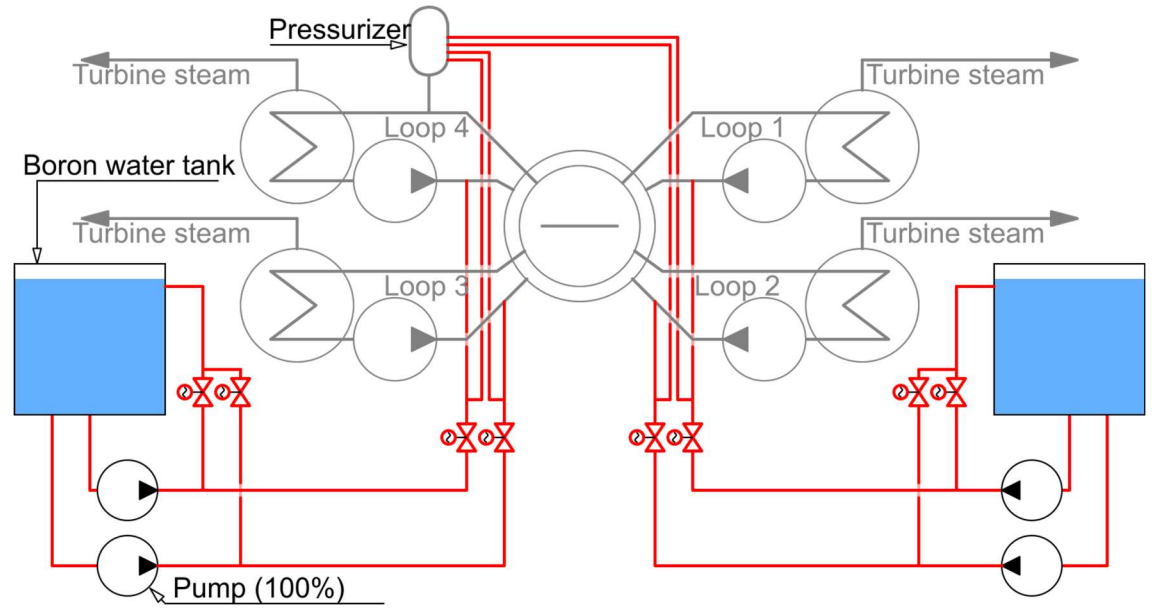

Figure 2-47 VVER-1200/V491 EBIS. Modified from (WWER-1200 Nucleopedia, 2021)

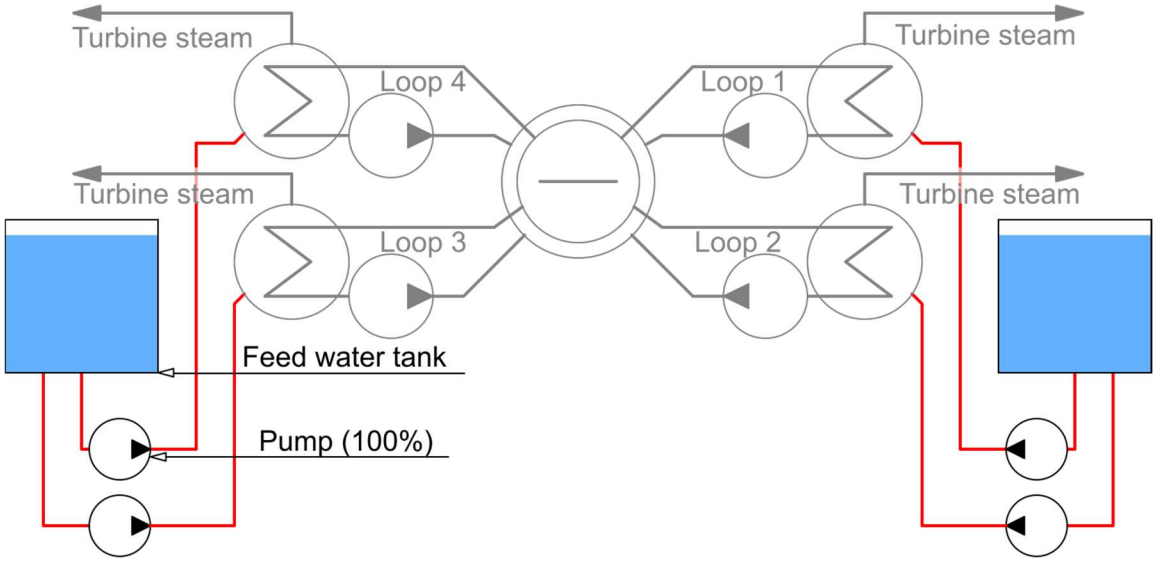

Figure 2-48 VVER-1200/V491 EFW. Modified from (WWER-1200 Nucleopedia, 2021)

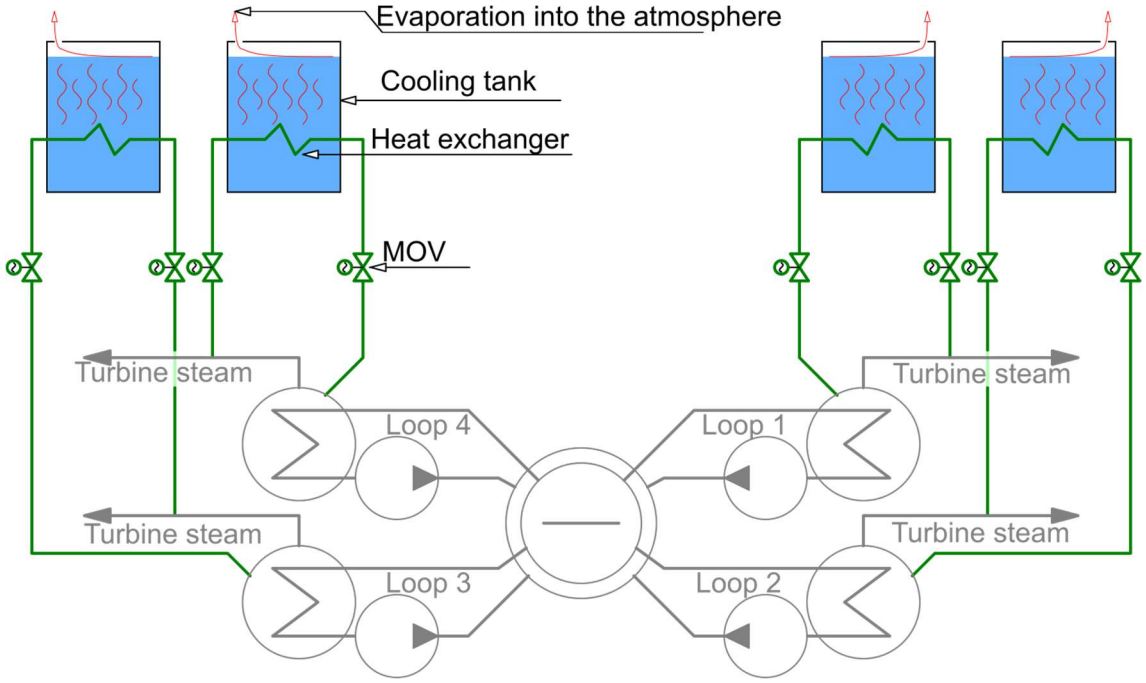

Figure 2-49 VVER-1200/V491 water-cooled PHRS. Modified from (WWER-1200 Nucleopedia, 2021)

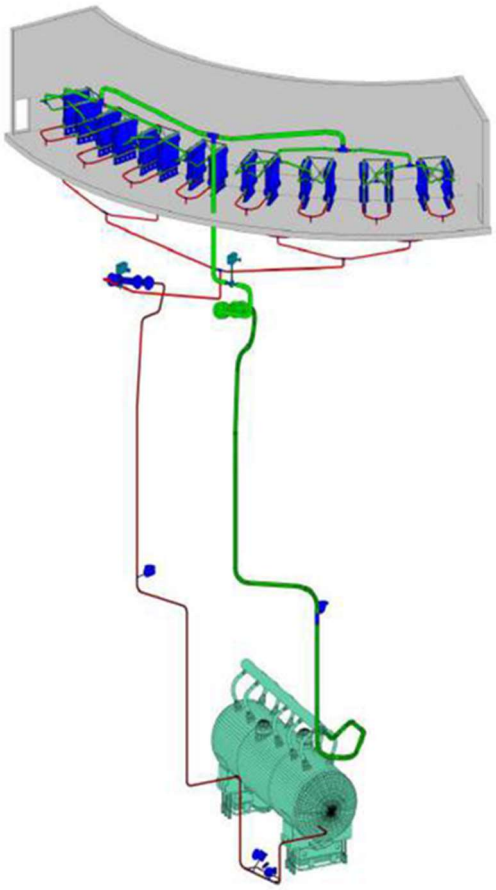

Figure 2-50 PHRS heat exchanger connection to the SGs (Bezlepkin et al., 2014)

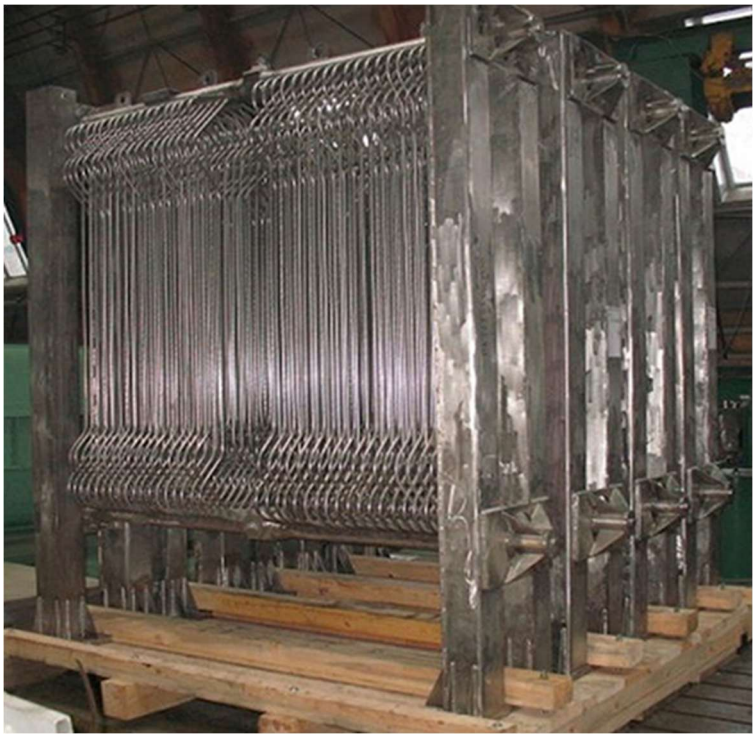

Figure 2-51 PHRS heat exchanger imagen (ROSATOM, 2022)

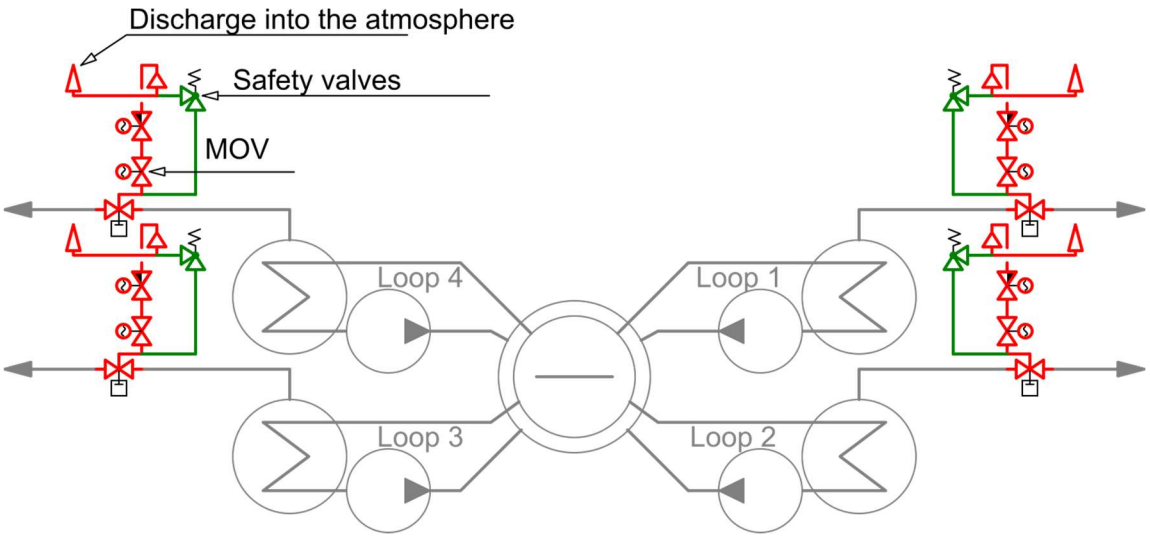

Figure 2-52 VVER-1200/V491 secondary circuit relief pressure system. Modified from (WWER-1200 Nucleopedia, 2021)

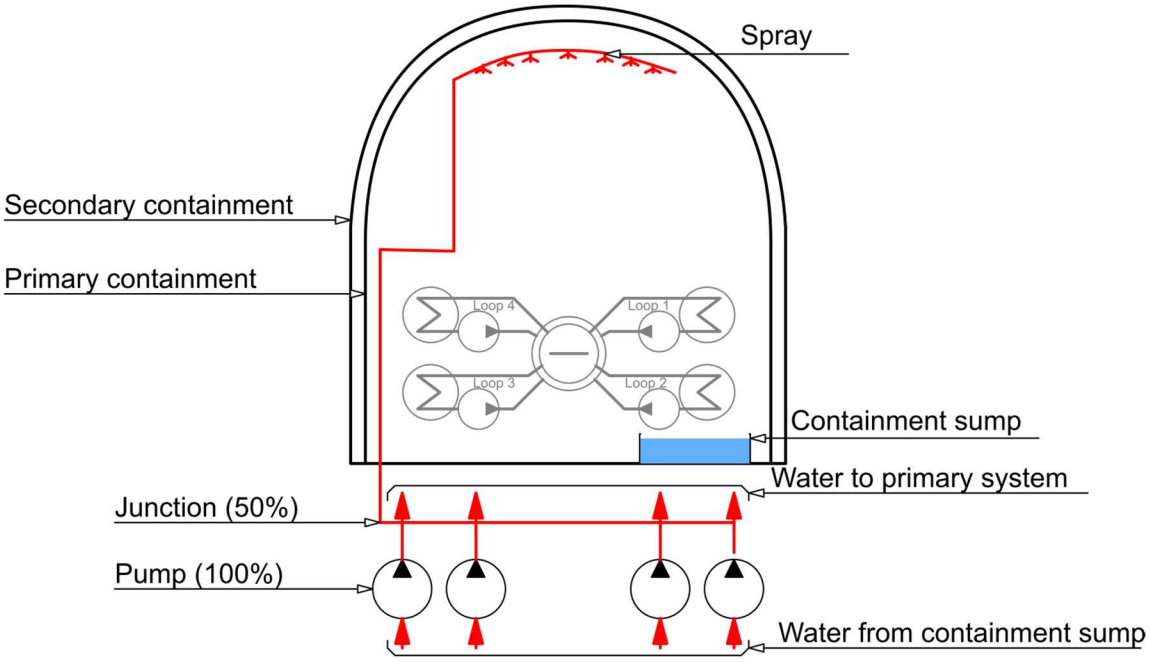

Figure 2-53 VVER-1200/V491 CSS. Modified from (WWER-1200 Nucleopedia, 2021)

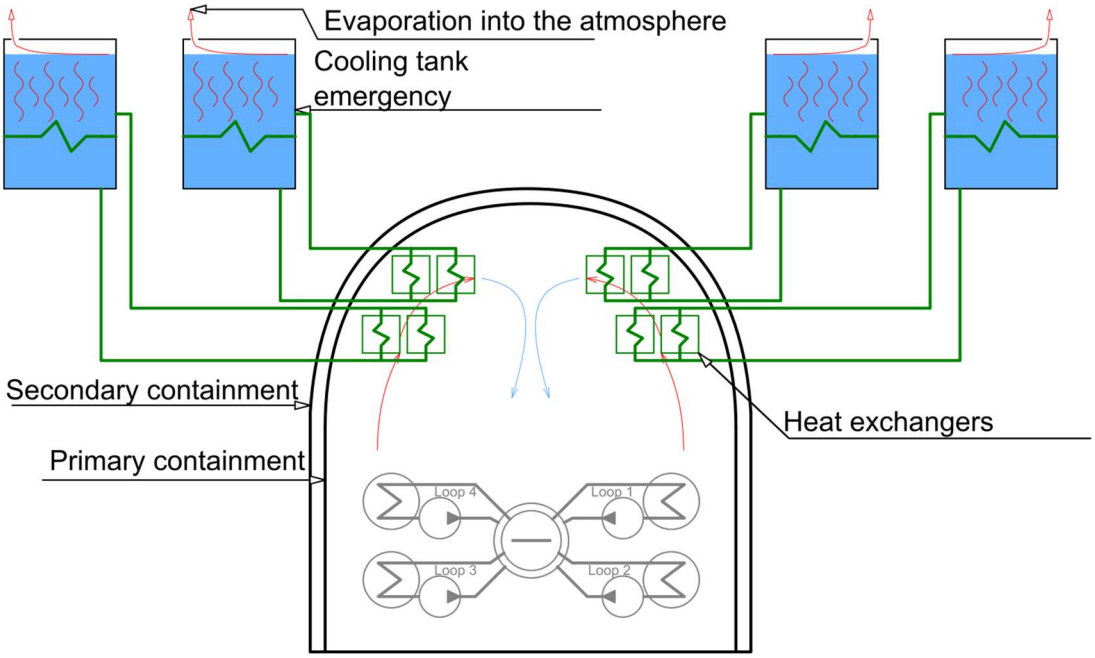

Figure 2-54 VVER-1200/V491 PHRS-C. Modified from (WWER-1200 Nucleopedia, 2021)

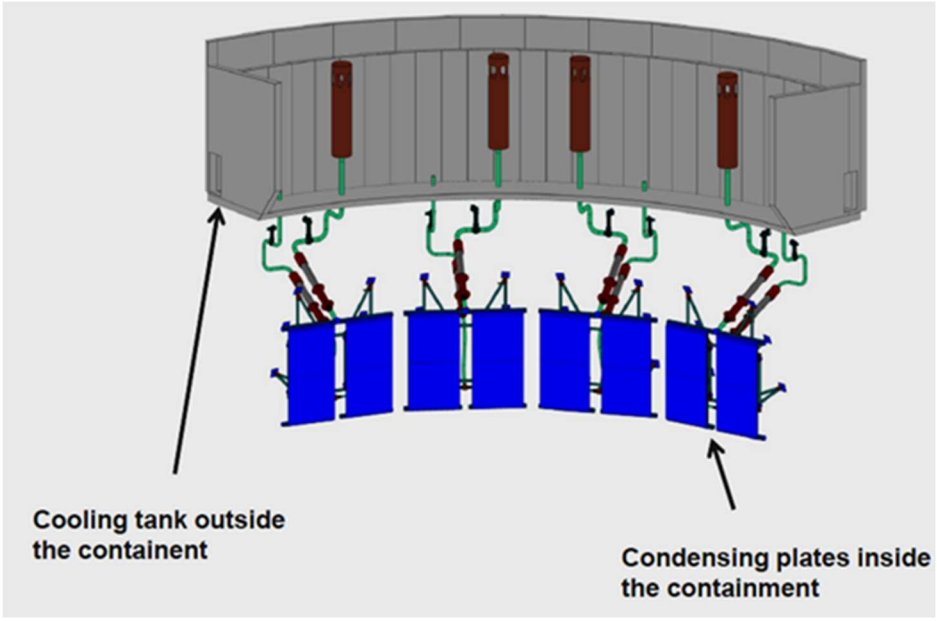

Figure 2-55 PHRS-C heat exchanger connection to the EHRT

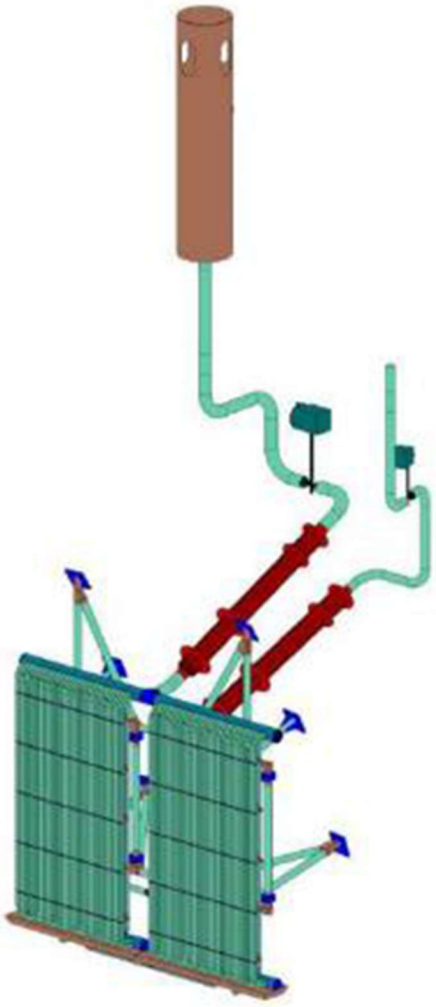

Figure 2-56 PHRS-C heat exchanger scheme

2.2.3.2. Gen-III/III+ VVER from the Moscow institute

The Gen-III/III+ VVER from the Moscow institute incorporates a dual containment structure, with a primary containment of pre-stressed reinforced concrete and an outer non-stressed reinforced concrete (VVER working group, 2019). Reactors of this series have a unique containment design that integrates the air ducts and the HXs of the air-cooled PHRS, see Figure 2-57.

A detailed analysis of the VVER-1000/V412 and VVER-1200/V392M designs is given below, together with some comments on the VVER-1200/V509 reactor. Also include are specific details on Bushehr NPP (unit 1), a VVER-1000/V446, which is a special version of the VVER-1000 derived from the VVER-1000/V392 and the KWU reactor designs.

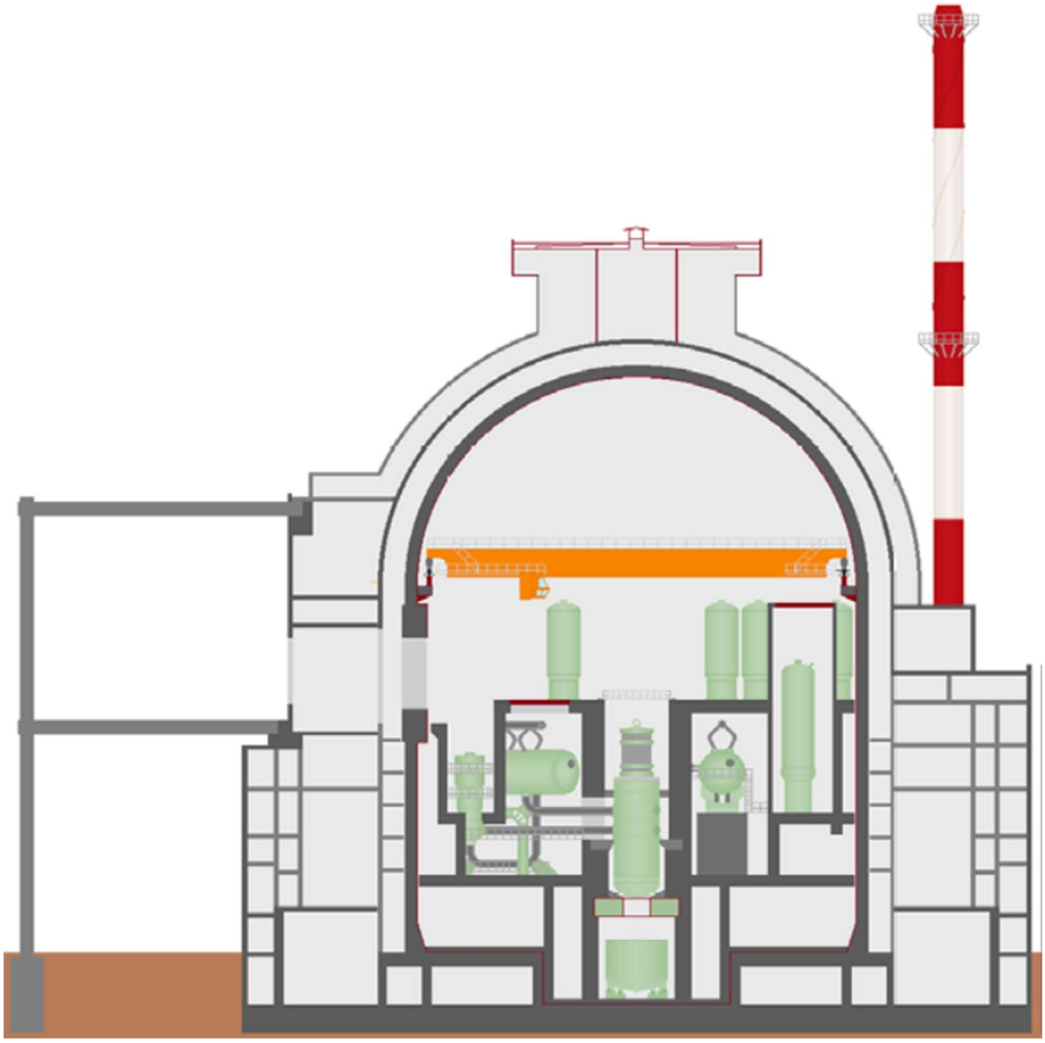

Figure 2-57 VVER-1200/V392M containment building (WWER-1200 Nucleopedia, 2021)

Safety systems connected to the RCS

The RCS safety systems include the ECCS, the EBIS, the RCS relief system and the EGRS. The ECCS consist of two active injection systems, i.e., the LPIS and the HPIS, and three passive injection systems, i.e., the first, second and third hydro-accumulators.

- The HPIS (JND) varies according to the VVER reactor version. In the VVER-1000/V412 (KKNPP), it consists of 4 x 100% trains injecting into the CLs, (Agrawal et al., 2006). While, in the VVER-1200/V392M, it consists of 2 x 100% trains injecting into both the CLs and the HLs of two separate RCS loops (Statsura et al., 2017), see Figure 2-58. In the VVER-1200/V509, the HPIS also has 2 x 100% trains: one injects into the HA-UP discharge lines, while the other injects into two CLs, see Figure 2-59. On the other hand, in the VVER-1000/V446 (Bushehr NPP), the HPIS consists of 4 x 100% trains connected to the four CLs and HLs.
- The LPIS (JNG) in the VVER-1000/V412 (KKNPP) consists of 4 x 100% trains, two of which inject into the HA-1 discharge lines and two into the CLs and HLs of two RCS loops (Agrawal et al., 2006). In the VVER-1200/V392M design, the LPIS (JNA) consists of 2 x 100% trains injecting directly into the RPV through the HA-1 discharge lines (IAEA, 2013; Turkish Atomic Energy Authority, 2018; Veselov and Tishin, 2017), see Figure 2-58. On the other hand, in the VVER-1300/V509 reactor, the system also has 2 x 100% trains connected to the CLs and HLs of two RCS loops, see Figure 2-59. The water source for both, the HPIS and the LPIS is the Spent Fuel Pool (SFP). In addition, the LPIS in the VVER-1000/V446 (Bushehr NPP), has the same injection points as the HPIS.
- The HA-1: It consists of 4 x 33% trains. Each HA-1 is filled with 50 m^3 of borated water and 10 m^3 of N_2 pressurized to 6 MPa. They are similar to those of the Gen-II VVER-1000/V320 and the Gen-III/III+ Saint Peterburg institute VVER reactor. It is worth mentioning that in the VVER-1200/509 the heigh of the HA-1 has been optimized (Atomenergoproekt, 2021; Maltsev, 2015).
- The HA-2: This PSS is incorporated in all the VVER designs from the Moscow institute, see Figure 2-58 and Figure 2-59. The HA-2 was used for the first time at the KKNPP (IAEA, 2017). It consists of 4 x 33% trains with two make-up tanks per train. The HA-2 tanks are connected to the HA-1 discharge lines and have the capacity to inject borated water into the RCS for 24 hours when the pressure is below 1.5 MPa (Turkish Atomic Energy Authority, 2018; Veselov

and Tishin, 2017). The long discharge period is achieved by the internal geometry of the tanks, which consists of several pipes of different heights through which the water flows into the injection line. At the beginning of the operation, the tanks are full, so water flows out of all the pipes. Later, as the level of the tanks drops, the pipes are gradually uncovered, so that no more water flows out of them and therefore the flow rate is reduced, (Maltsev, 2015; ROSATOM, 2022). In the VVER 1200 of the Moscow Institute, the HA-2 consists of four injection stages (ROSATOM, 2022), whereas in the VVER 1000/V412 (KKNPP), the HA-2 consists of six injection stages (Agrawal et al., 2006). A detailed description of the HA-2 is given in Section 2.2.4. as it is one of the PSS analyzed in this PhD thesis.

The VVER-1000/V446, also incorporates a second ACC design, consisting of 4 trains with 2 tanks per train. The tanks are known as KWU-ACC and are connected to the HLs and CLs of the four RCS loops, (Hosseini et al., 2024). It should also be noted that the HA-2 has some similarities to the CMTs of the AP1000 and the ACCs of the Korean designs APR-1400 reactors, as commented on in Section 2.1 above.

- The HA-3 are also a type of make-up tank which is found in the VVER-1200/V509 and the VVER-1300/V510 (VVER-TOI) reactors, see Figure 2-59. The HA-3 start injecting into the HA-1 discharge lines when the HA-2 tanks are depleted. It consists of 4 x 33% trains. Each train consists of three tanks located outside the containment. With a total water capacity of 720 m^3, the HA-3 can inject for up to 48 hours, (Turkish Atomic Energy Authority, 2018).

Regarding the EBIS, it can be noted that the VVER-1200/V392M has 2 x 100% trains, each train with two Motor Driven Pumps (MDP) (ROSATOM, 2022; Turkish Atomic Energy Authority, 2018), see Figure 2-60. On the other hand, the VVER-1000/V412 (KKNPP) has a different design with a passive four-channel system with 4 x 33% trains, called the Quick Boron Injection System (QBIS) (Agrawal et al., 2006; Veselov and Tishin, 2017). The RCS pressure relief and safety valves, and the EGR are similar to those in the Gen-III/III+ VVER designs of the Saint Petersburg institute.

Safety systems connected to the secondary circuit

In the Gen-III/III+ VVER from the Moscow institute, it can be found two heat removal systems, the air-cooled PHRS and the Emergency Cooldown System (ECS). The ECS is incorporated in both the VVER-1000/V412 and the VVER-1200/V392M. It consists of a closed circuit with MDP and HX, which takes the steam from the SLs and condenses it in the HX when the pressure in the SL is higher than 7.35 MPa. The system in the VVER-1000/V412 has 4 x 100% trains, in the VVER-1200/392M has 2 x 100% trains with two MDPs per train, see Figure 2-61, and in the VVER-1200/V509 has 2 x 100% trains but with one MDP per train, (Agrawal et al., 2006; Asmolov et al., 2017; ROSATOM, 2022).

The air-cooled PHRS consists of 4 x 33 % trains, with 3 HXs per train for the VVER-1000/V412 and 2 HXs per train for the VVER-1200/V392M, see Figure 2-62. Each HX is located in an air duct outside the two containments. The air-cooled PHRS is designed to remove residual heat when the ECS is not available, (Agrawal et al., 2006; Asmolov et al., 2017; Galiev et al., 2017; IAEA, 2013; Khubchandani et al., 2013a; Veselov and Tishin, 2017). A detailed description of the air-cooled PHRS is given in Section 2.2.4, as it is one of the PSS analyzed in this PhD thesis.

Regarding the secondary pressure relief system, three types of valves are found (WWER-1200 Nucleopedia, 2021):

- BRU-A: similar to those installed in other VVER Gen-III/III+ designs. In both the VVER-1000/V412 and the VVER-1200/V392M there is one BRU-A per SL, see Figure 2-63.
- Safety valves: in the VVER-1000/V412 there are four per SL. Whereas, on the VVER-1200/V392M, there are two per SL, see Figure 2-63.
- The BRU-K: similar to the other incorporated in the other VVER Gen-III/III+ designs.

Containment safety systems

The Gen-III/III+ VVER design from the Moscow institute do not incorporate PHRS-C. However, they feature a CSS similar to that in the VVER-1000/V320. In the VVER-1000/V412, the CSS consists of 4 x 100 % trains while in the VVER-1200/V392M it consists of 2 x 100 % trains, see Figure 2-64.

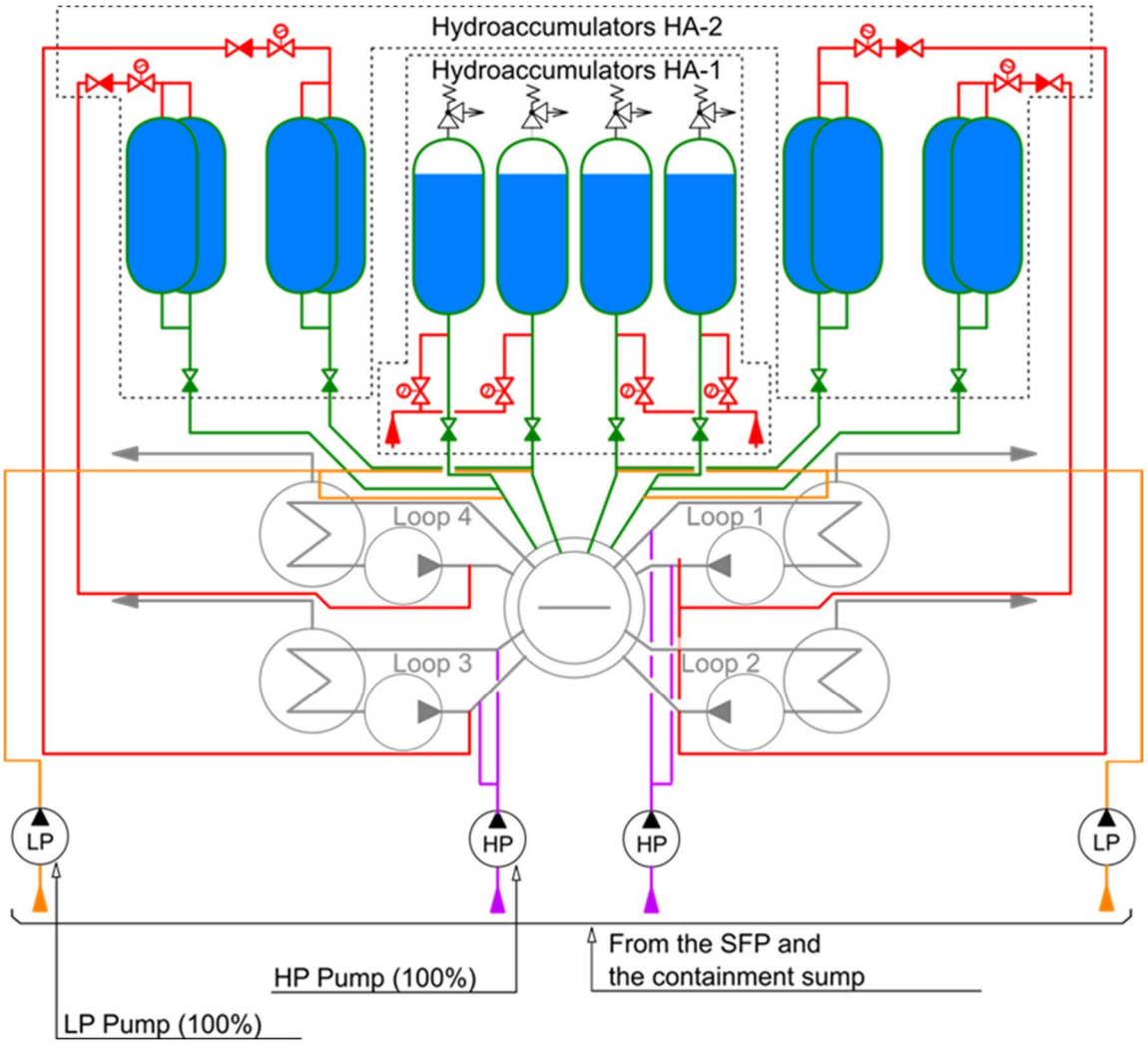

Figure 2-58 VVER-1200/V392M; active and passive ECCS. Modified from (WWER-1200 Nucleopedia, 2021)

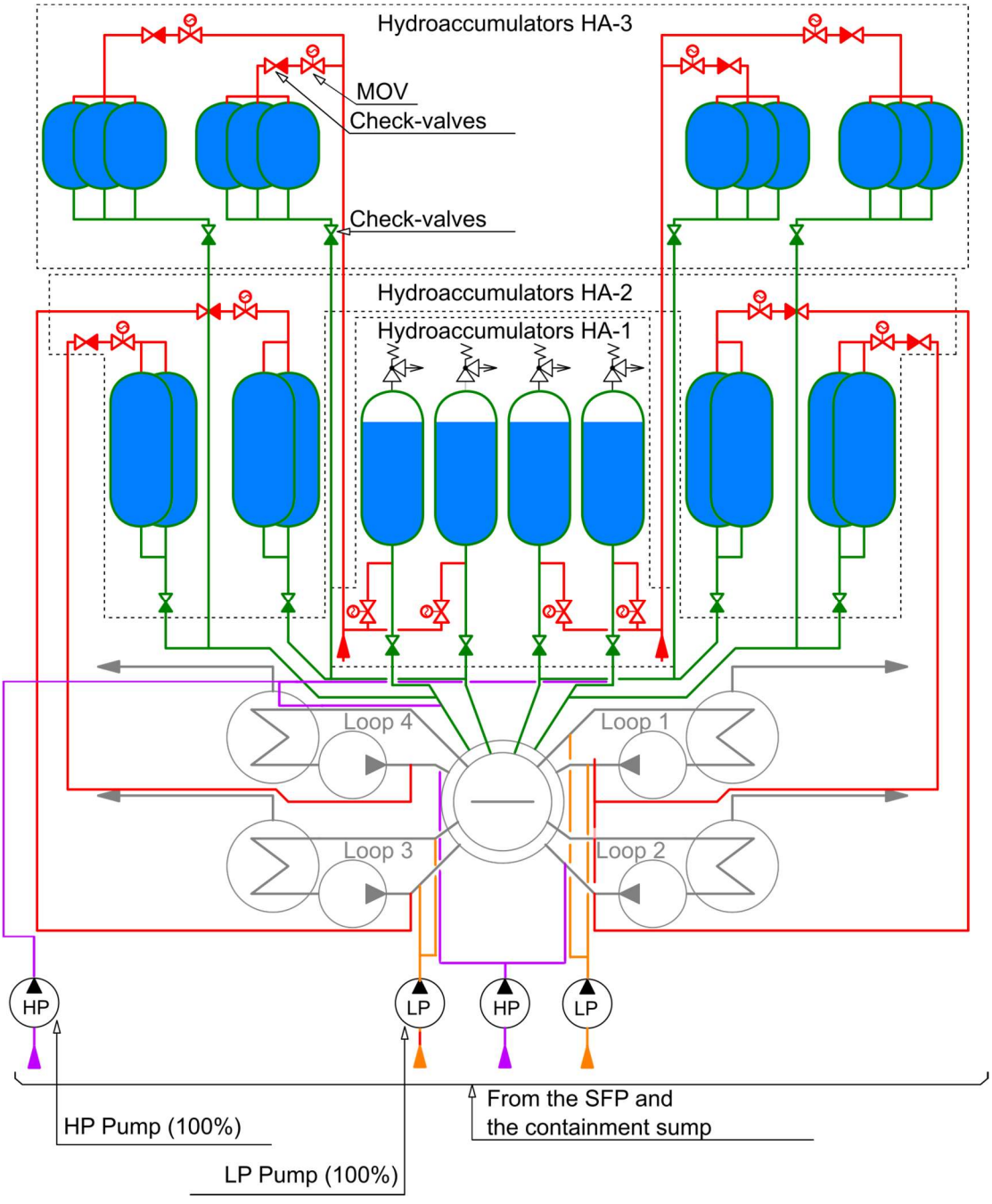

Figure 2-59 VVER-1200/V509 active and passive ECCS. Modified from (WWER-1200 Nucleopedia, 2021)

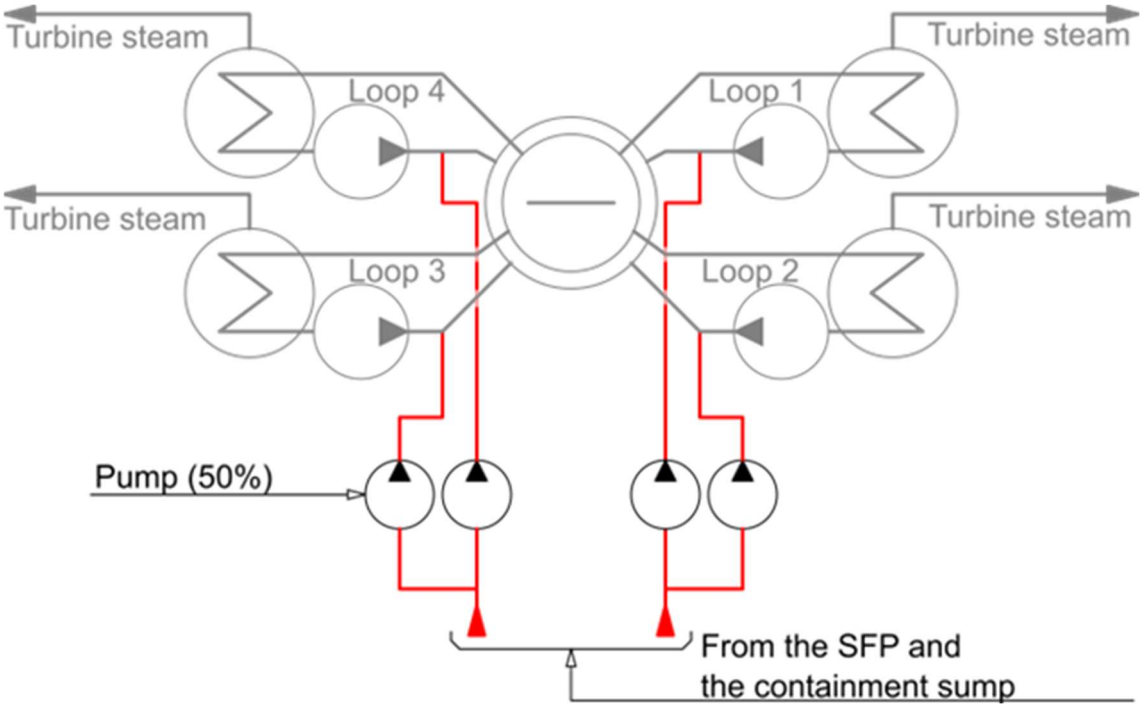

Figure 2-60 VVER-1200/V392M; EBIS. Modified from (WWER-1200 Nucleopedia, 2021)

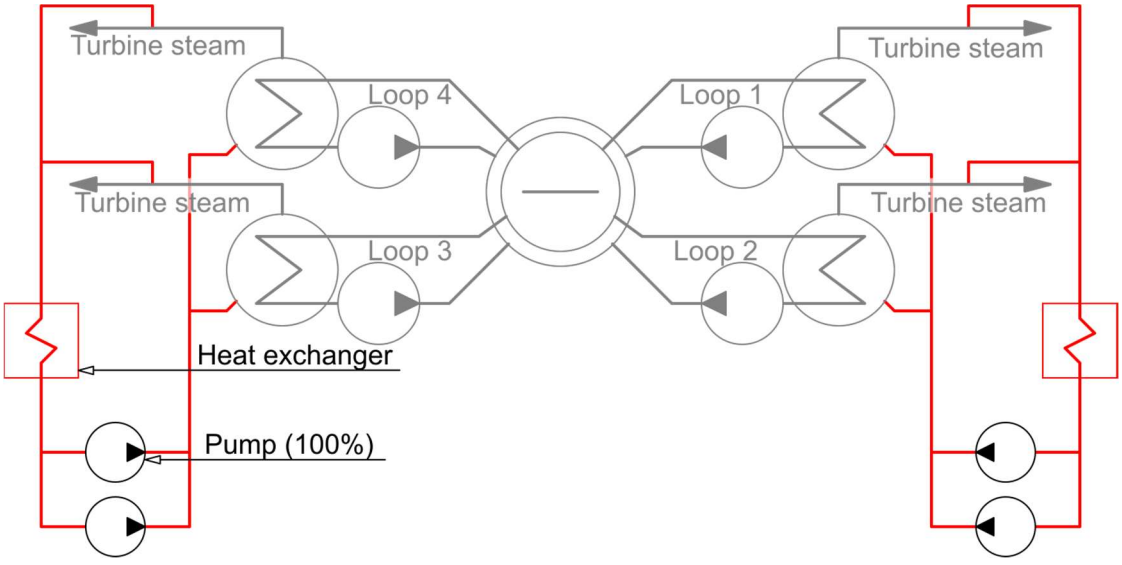

Figure 2-61 VVER-1200/V392M ECS. Modified from (WWER-1200 Nucleopedia, 2021)

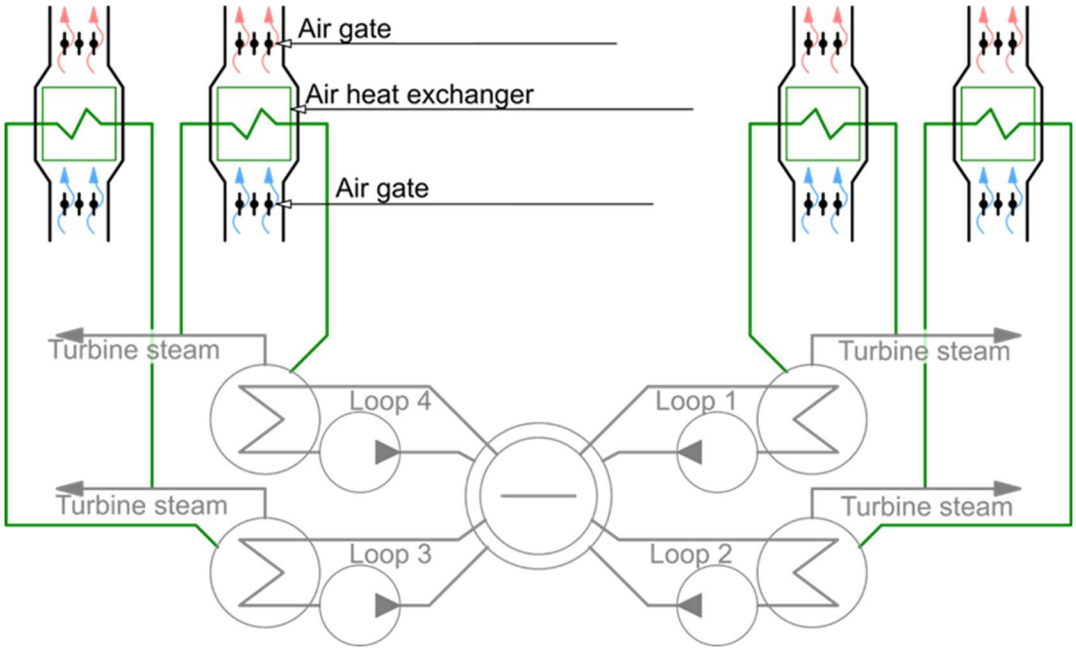

Figure 2-62 VVER-1200/V392M air-cooled PHRS. Modified from (WWER-1200 Nucleopedia, 2021)

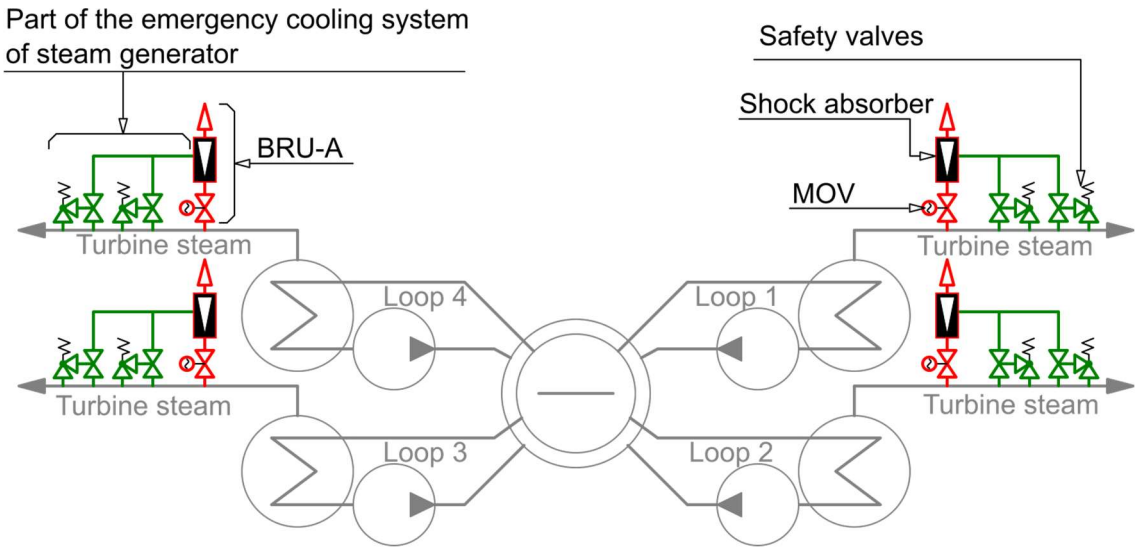

Figure 2-63 VVER 1200/V392M secondary circuit relief pressure system. Modified from (WWER-1200 Nucleopedia, 2021)

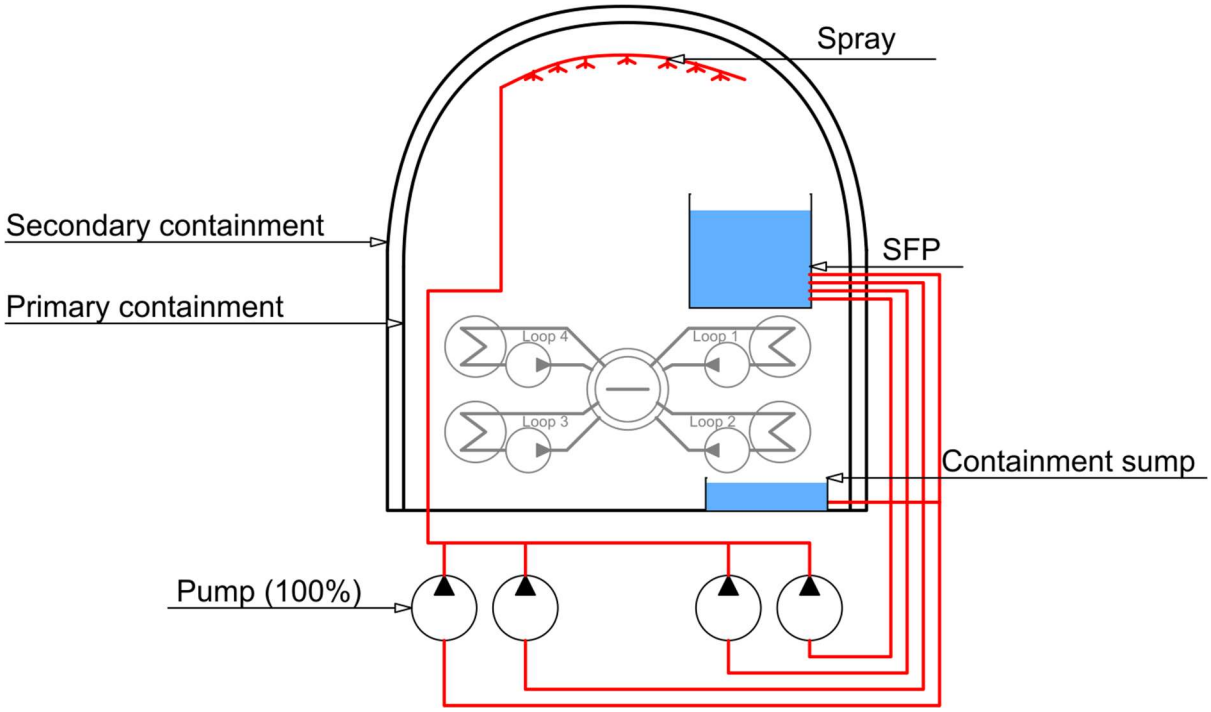

Figure 2-64 VVER-1200/V392M CSS. Modified from (WWER-1200 Nucleopedia, 2021)

Table 2-17 Safety systems related to the RCS (KKS/AKZ Coding System)

	VVER-1200		VVER-1000			
System	392M/ V509/V510	V491	V412 (AES-92) KKNPP	V428 (AES-91) Tianwan NPP	V446 Bushehr NPP	V320
	Gen-III+		Gen-III		Gen-II+	Gen-II
ECCS Active	JNA: JNA30/60 (HPIS) 2TX100% + JNA20/50 (LPIS) 2Tx100%	JND (HPIS) 4Tx100% JNG1 (LPIS) 4Tx100% JNA (PHRS) 4Tx100% MDP and HX from JNG1	JND10-40 (HPIS) 4Tx100% JNG (LPIS) 4Tx100%	JND (HPIS) 4Tx100% JNG (LPIS) 4Tx100%	HPIS 4Tx100% LPIS 4Tx100%	TQ (HPIS) 3Tx100% TQ LPIS 3Tx100%
HA-1	JNG50-80 (GE-1) 4Tx33%	JNG2 JNG50-80 4Tx33%	JNG JNG10-40 4Tx33%	JNG2 JNG50-80 4Tx33%	ACC 4Tx33%	YT 4Tx50%
HA-2	JNG10 (GE-2) 4Tx33%		JNG50-80 4Tx33%		KWU-ACC 8 HA	
HA-3	JNG10 (GE-3) 4Tx33% (only V509 and V510)					
EBIS	JND 2Tx (2x50%)	JDH 4Tx50%	JND50-80 (EBIS) 4Tx50% JDJ 4Tx33% (QBIS)	JDH 4Tx50%	TW 4Tx50%	TQ 3Tx100%
RCS relief system	PORV (3)	JEF (3)	JEF (3)	PORV (3)	PSD (3)	YP PORV (3)
EGRS	KTP	KTP	KTP	EGRS	EGRS	YR

Table 2-18 Safety systems related to the secondary circuit (KKS/AKZ Coding System)

	VVER-1200		VVER-1000			
System	392M/V509/ V510	V491	V412 (AES-92) KKNPP	V428 (AES-91) Tianwan NPP	V446 Bushehr NPP	V320
	Gen-III+		Gen-III		Gen-II+	Gen-II
EFW		LAR/LAS 4Tx100%	EFW 4Tx100%	EFW 4Tx100%	TX 3Tx100%	EFW 3Tx100%
ECS	JNB10 V392 2Tx100% V509/V510 2Tx100%		JNB10-40 4Tx100%			
PHRS-SG	JNB50-80 4Tx33% Air-cooled HXs	JNB 4Tx33% Water-cooled HXs	JNB50-80 4Tx33% Air-cooled HXs			
SGs pressure relief system	BRU-A 4x1 PORV 4x2 BRU-K	LBU (BRU-A) 4x1 PORV 4x1 BRU-K	LBK (BRU-A) 4x1 SGPD 4x4 BRU-K	BRU-A 4x1 SV 4x2 BRU-K	BRU-A 4x1 PSD 4x2 BRU-K (6)	BRU-A 4x1 SV 4x2 BRU-K (4) BRU-SN (2)

Table 2-19 Safety systems related to containment (KKS/AKZ Coding System)

	VVER-1200		VVER-1000			
System	392M/V509/ V510	V491	V412 (AES-92) KKNPP	V428 (AES-91) Tianwan NPP	V446 Bushehr NPP	V320
	Gen-III+		Gen-III		Gen-II+	Gen-II
PHRS-C		JMP 4Tx33%				
CSS	JMN 2Tx100%	JMN 4Tx50%	JMN 4T	CSS 4T	TJ 2Tx100%	TQ 3Tx100%
CC	JMN	JMR	JKM	CC		

2.2.4. Passive safety systems relevant to the PhD thesis

As mentioned in the introduction, this doctoral thesis analyses the impact of two of the passive safety systems incorporated in the Gen-III/III+ VVER reactors. These safety systems are the second stage hydro-accumulators (HA-2) and the passive heat removal systems, the air-cooled PHRS.

The two PSS selected are from the VVER designs of the Moscow Institute. They have been selected because the combined performance of both allows to fulfil two CSF, the core decay heat removal and the RCS inventory replenishment. This makes it possible to analyse LOCA sequences under SBO conditions without reaching CD conditions. The HA-2 selected to analyse is from the VVER-1200/392M, as there is no publicly available information for the HA-2 in the VVER-1000/V412 (KKNPP). Similarly, the air-cooled PHRS design selected is that of the VVER-1000/V412 (KKNPP) reactor.

The aim of this section is to describe the HA-2 and the air-cooled PHRS in more detail and to get to know their geometries, layouts, design criteria, setpoints and operating modes.

2.2.4.1. Secondary State Hydro-accumulators (HA-2)

The HA-2, included in the VVER-1200 reactors, consists of 4 x 33 % trains, each containing two borated water tanks. These tanks are connected at the top to a common head, which is connected to the CLs through a line with a special check valve. At the bottom they are connected to the HA-1 injection lines so that this system also provides top and bottom core flooding, see Figure 2-65.

The total volume of water is 960 m^3 with each tank containing 120 m^3. The total height of a tank is 10.4 m and the diameter is 4 m, see Figure 2-66. The RCS pressure below 1.5 MPa, with a delay of 100 s, is the actuation signal for the HA-2 (ROSATOM, 2022).

The HA-2 has been designed taking into account the mass flow rate required to compensate for the decay heat, see Table 2-20. It is noteworthy that the HA-2 discharges in four stages, which is achieved by means of four discharge pipes located inside the HA-2 at different heights (Maltsev, 2015). Figure 2-67 shows the scheme of an experimental facility for the HA-2, along with some results showing that as the water level drops, the different pipes are uncovered and therefore the mass flow through the HA-2 is reduced (Maltsev, 2015).

Table 2-20 HA-2 mass flow rate (per train)

Stage interval (s)	100 - 4000	4000 - 10000	10000 - 30000	30000 - 86400
Flow rate from one HA-2 train (kg/s)	10	5	3.3	1.78

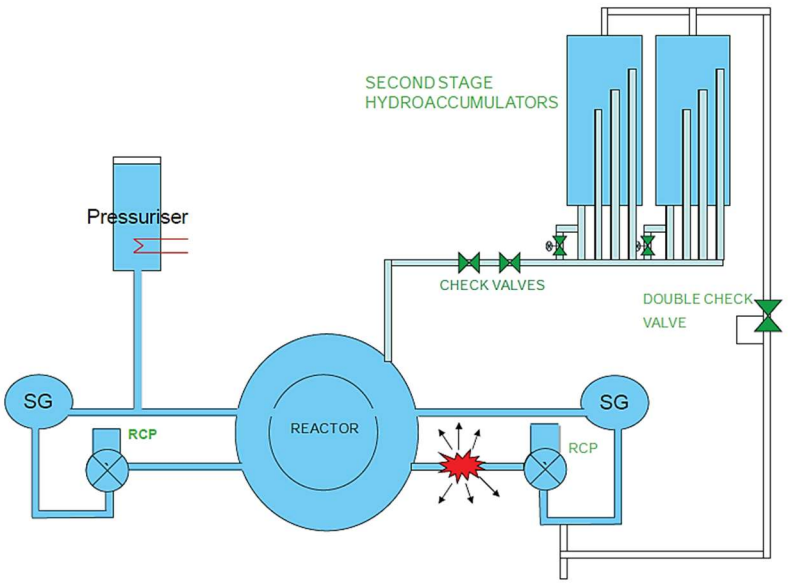

Figure 2-65 Connection to the RCS of the Second Stage Hydro-accumulators (HA-2) (Nu-Power, 2015)

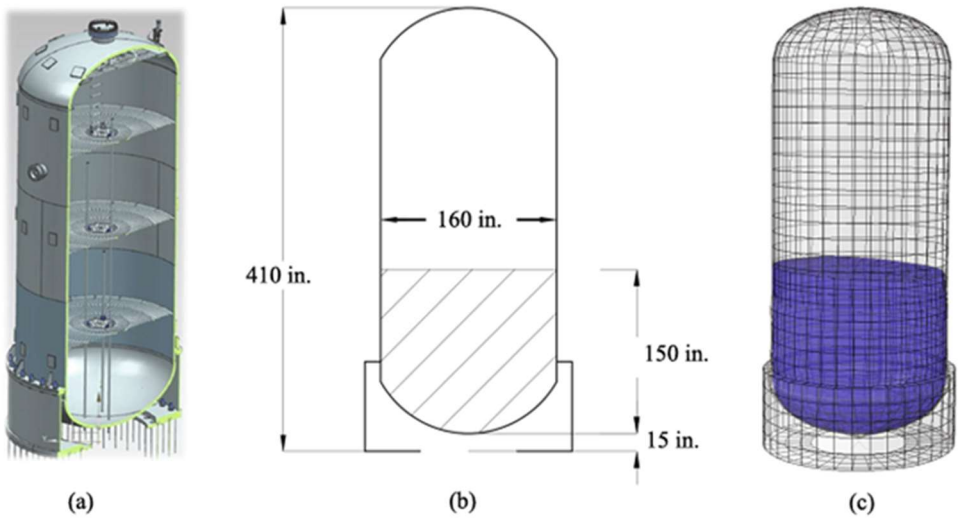

Figure 2-66 HA-2 layout (Kasapoglu et al., 2024)

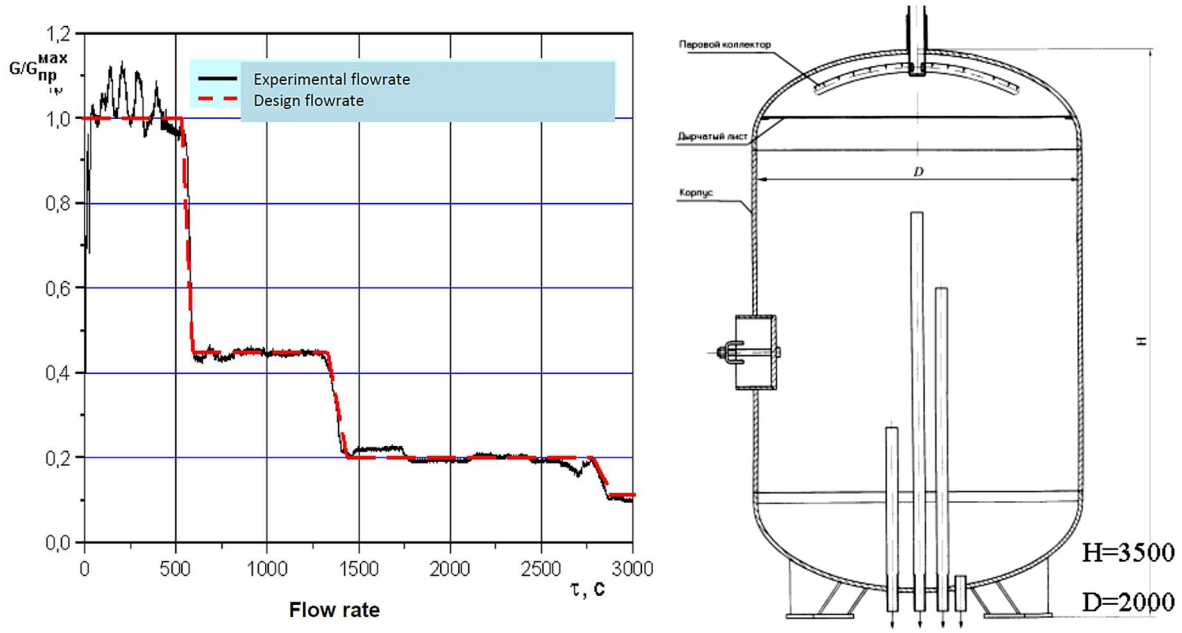

Figure 2-67 HA-2 experimental facility results (Maltsev, 2015)

2.2.4.2. Air-cooled Passive Heat Removal System (PHRS)

The air-cooled PHRS incorporated in the VVER-1000/V412 (KKNPP) consists of four trains, one per SG, see Figure 2-62. Each of the PHRS trains contains three HXs, which are located in an elevated position, right where the containment dome begins (Khubchandani et al., 2013a), see Figure 2-68. It is important to note that in the VVER-1200/V392M, V509, V523 and the VVER-1300/V510 (VVER-TOI), the air-cooled PHRS also consists of four trains, but each has two HXs instead of three (Galiev et al., 2017), see Figure 2-69. The design criterion for the air-cooled PHRS in all these reactor designs is that a minimum of 3 out of 4 trains are required to fulfil their safety function, (Ayhan and Sokmen, 2016a).

Each HX is placed in a shell inside an air duct. In the air duct, upstream and downstream of the HXs, there are air gates with the capacity to isolate the HXs from the atmosphere (Agrawal et al., 2006), see Figure 2-70. These air gates have only two positions, closed and open, with no intermediate positions. They remain in the closed position during reactor operation by means of electromagnetic actuators which are de-energized in the event of a loss of AC power, allowing the air gates to open (Agrawal et al., 2006).

Moreover, between the HX and the upstream air gates, there is a regulator consisting of flaps, see Figure 2-70 and (Polunichev et al., 2007). This regulator is equipped with two actuators, a passive actuator and an active actuator which is powered by the safety class 1 emergency power system (battery powered).

Each HX contains a steam collector and a condensate collector; the steam collector is located above the condensate collector, see Figure 2-71 and Figure 2-72. On the one hand, the steam collector is connected to the condensate collector by a total of 630 horizontal U-shaped tubes with a slight slope, (Chaudhary et al., 2017). Moreover, the steam collectors and condensate collectors are connected to the SGs thought the steam lines and the condensate lines.

In order to know the geometry of this system, an extensive review of references has been necessary (Ahmed Pirouzmand and Shahabinejad, 2021; Bharat Heavy Electricals Limited, n.d.; Chaudhary et al., 2017; IAEA, 2009; Khubchandani et al., 2013a; ROSATOM, 2023; Sri Krishna College of Engineering and Technology (SKCET), 2019). For some parameters, different values have been found, so it has been decided to take approximate values in some cases. Table 2-21 summarizes the values adopted for the model of the air-cooled PHRS developed for the TRACEV5P5 system code.

The air-cooled PHRS is designed to remove decay heat for extended periods of time in the event of unavailability of the active heat removal system through the SGs or total loss of AC power, i.e. SBO conditions, (Agrawal et al., 2006; Khubchandani et al., 2013b). Therefore, the air-cooled PHRS should start operating due to (ROSATOM, 2022):

- AC power loss, i.e., SBO conditions
- A high SGs pressure signal, i.e., pressure above 8.44 MPa

The electromagnetic actuators of the air gates take 30 s to de-energize, see (Ayhan and Sokmen, 2016a). Moreover, the air gates need 90 s to be fully open, (ROSATOM, 2022).

In addition, the air-cooled PHRS has two operating modes: SGs pressure maintenance mode and RCS cool-down mode, (IAEA, 2012; ROSATOM, 2022):

- SGs pressure maintenance mode: The aim is to remove the decay heat from the core through the SGs by maintaining the pressure of the SGs between 5.35 MPa and 6.05 MPa, (Khubchandani et al., 2013b). This is achieved by controlling the regulator flaps position in the air duct and therefore the air flow through the HX tubes. When the air-cooled PHRS starts to operate, the regulators flaps are fully open. As the pressure in the SGs drops below 6.05 MPa, the regulators flaps begin to close, reducing the power that the PHRS

can remove compared to the power it could remove if the regulators flaps were fully open, see the red line in Figure 2-73.

This operating mode is controlled by the passive actuator of the regulator flaps which operates by means of a spring-operated piston system. The piston is driven both by the steam pressure on the secondary side of the SG and by the spring force. The direction of movement of the piston rod, and therefore whether the regulator flaps open or close, is determined by the balance between the SGs steam pressure and the spring force, (Galiev et al., 2017; Polunichev et al., 2007).

- RCS cool-down mode: If the SBO sequence or the loss of the active heat removal systems is followed by a LOCA, the PHRS operates in RCS cool-down mode. When the subcooling margin in the HL is below 8 ^{o}C, (ROSATOM, 2022), the control that regulates the regulators flaps position is inhibited, forcing them to remain fully open. In this mode, the air-cooled PHRS behavior is characterized by a power vs. SG pressure curve, see blue line in Figure 2-73.

  The active actuator of the regulator flaps is responsible for overriding the passive actuator to keep the regulator flaps fully open (Galiev et al., 2017; Polunichev et al., 2007), without the need for human intervention. In addition, if necessary, the active actuator can also be operated by the operator to switch to RCS cool-down mode (Asmolov, 2011, Turkish Atomic Energy Authority, 2018).

In stand-by mode, the HXs are isolated from the atmosphere by the air gates located both upstream and downstream of the HXs. Otherwise, the regulators flaps are fully open, (ROSATOM, 2022). Moreover, the steam lines and the condensate lines are open, allowing the PHRS tubes to be at SG pressure, (Agrawal et al., 2006; IAEA, 2012).

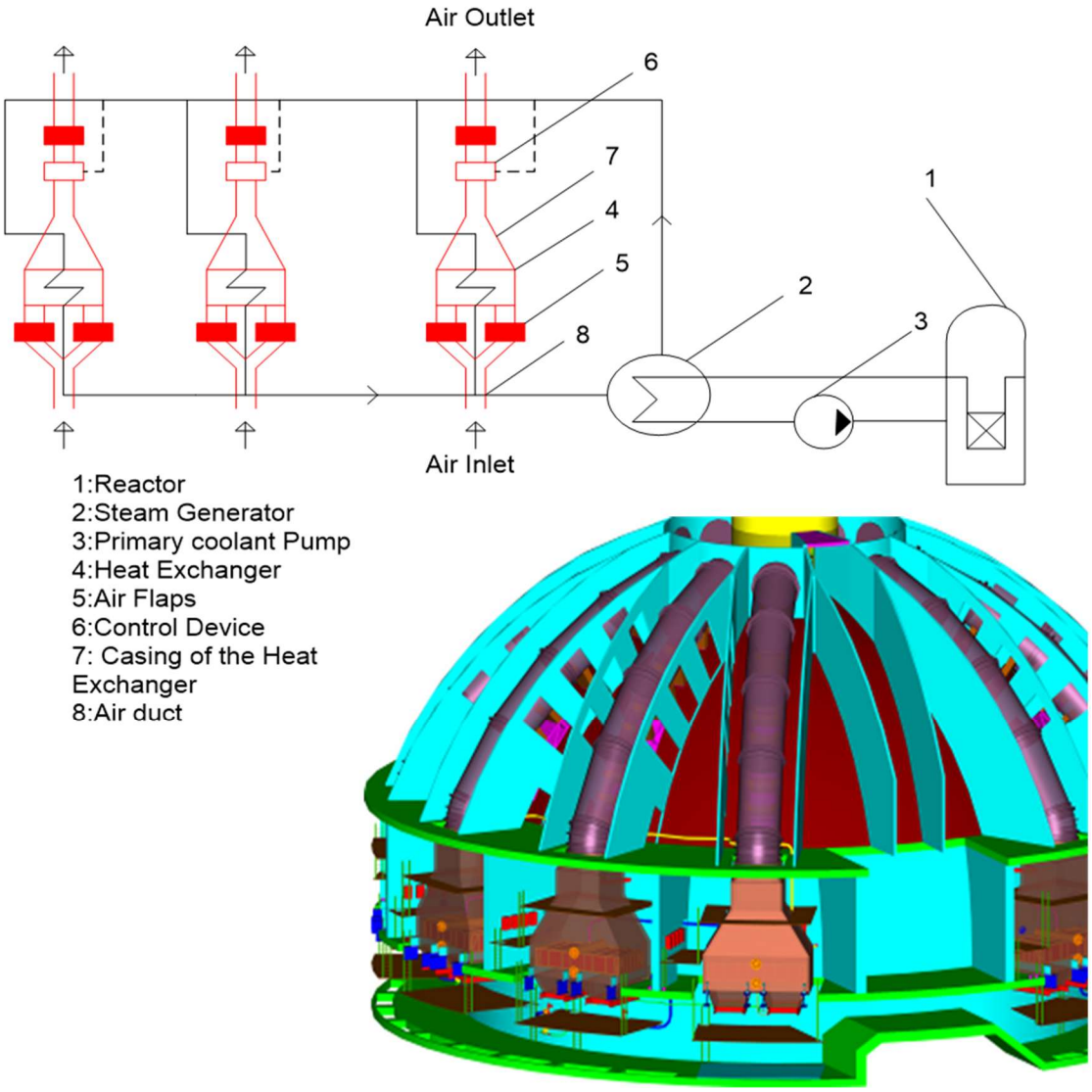

Figure 2-68 VVER-100/V412 air-cooled PHRS with three HX per trains,

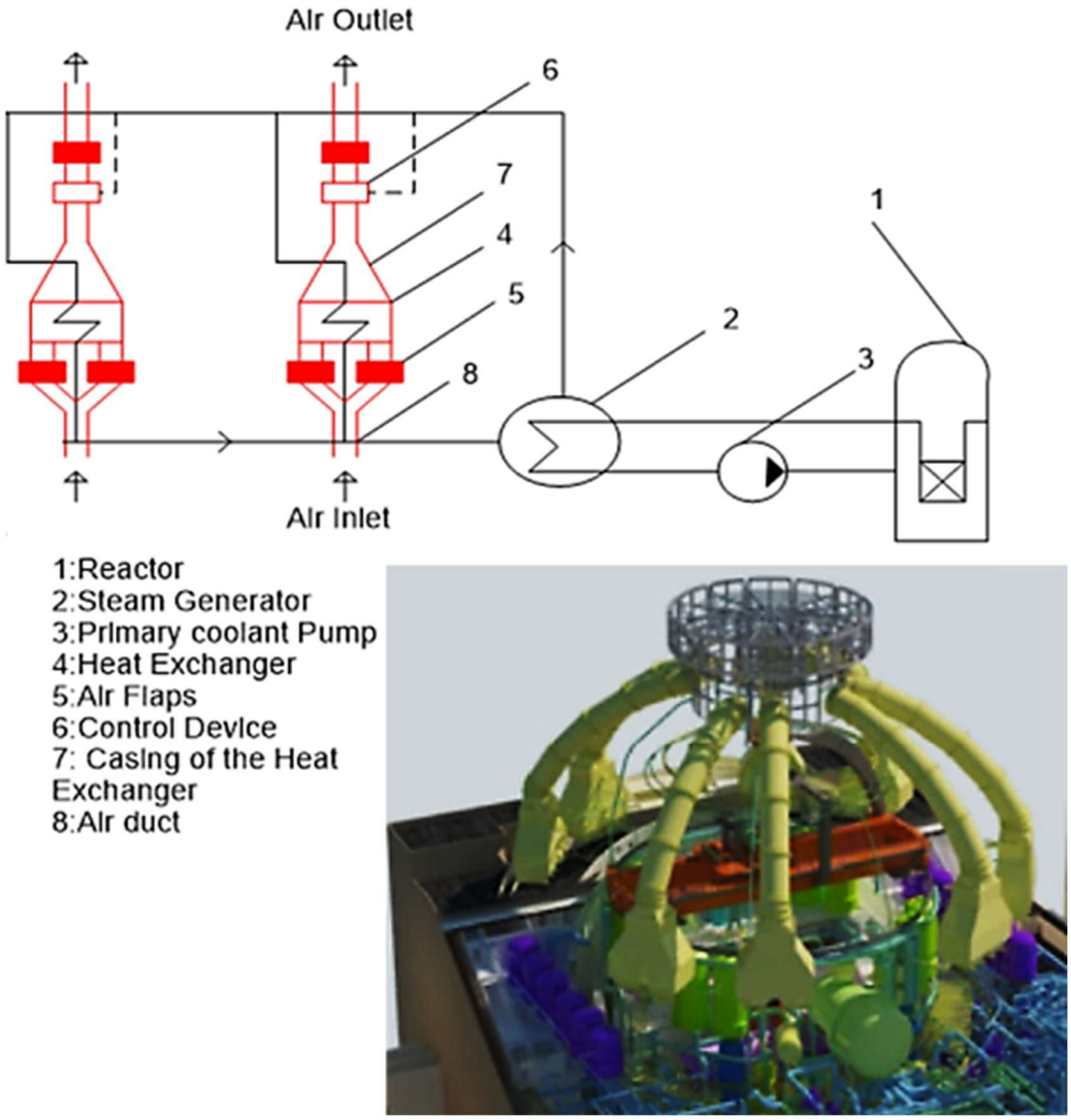

Figure 2-69 VVER-1200/V392M air-cooled PHRS with two HX per train

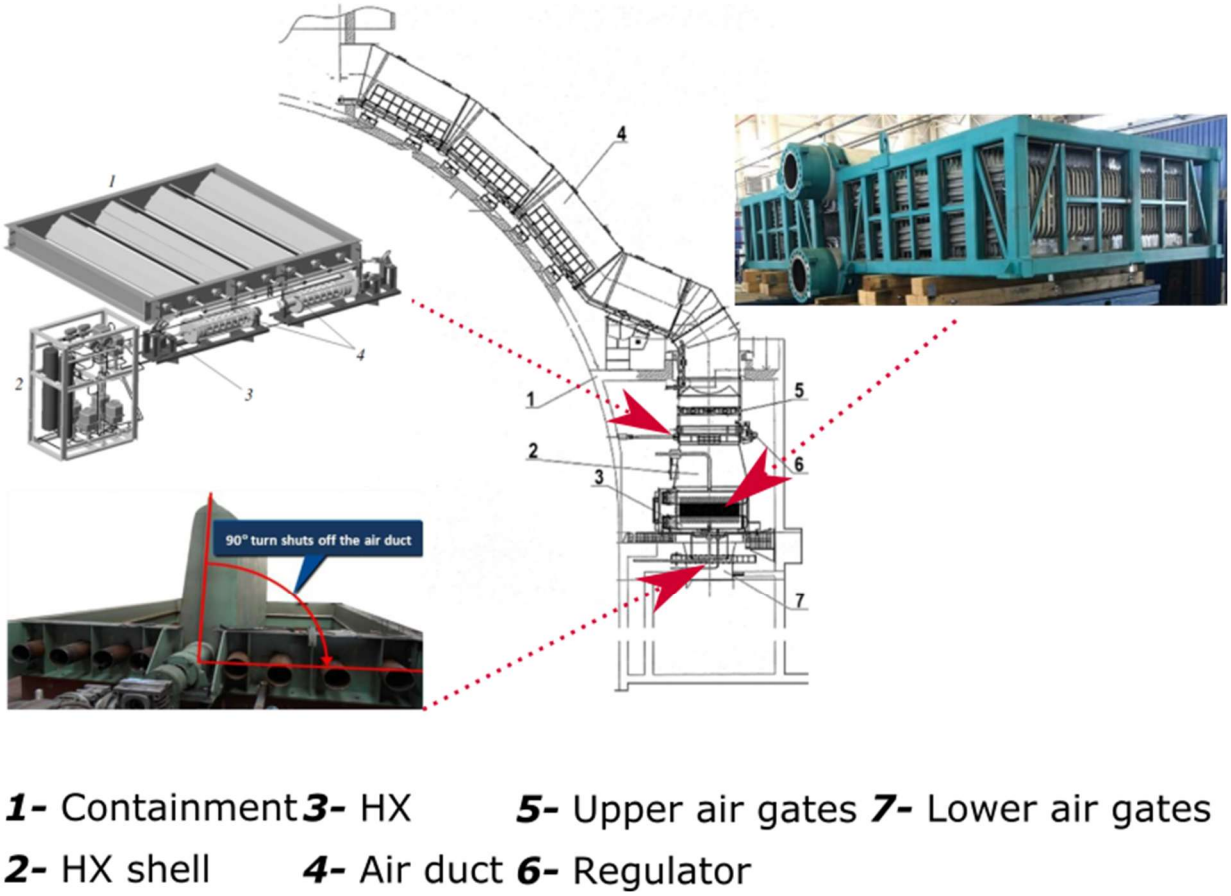

Figure 2-70 Air-cooled PHRS. Modified from (Galiev et al., 2017; Polunichev et al., 2007; ROSATOM, 2023, 2022)

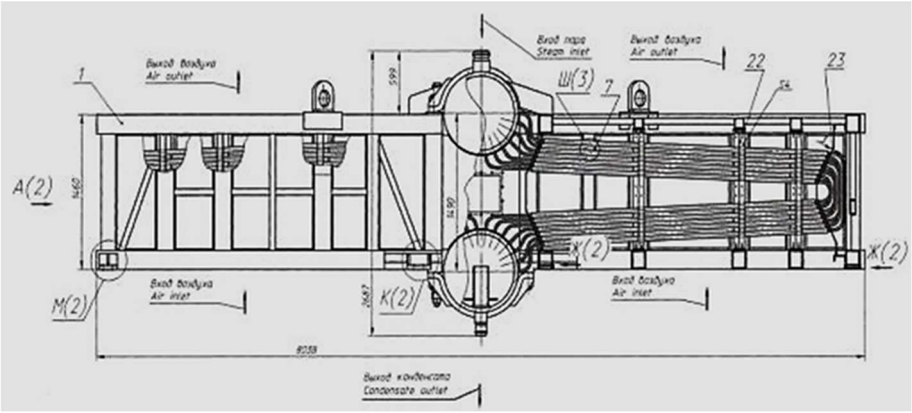

Figure 2-71 Air-cooled PHRS HX bundle of tubes (Ahmed Pirouzmand and Shahabinejad, 2021)

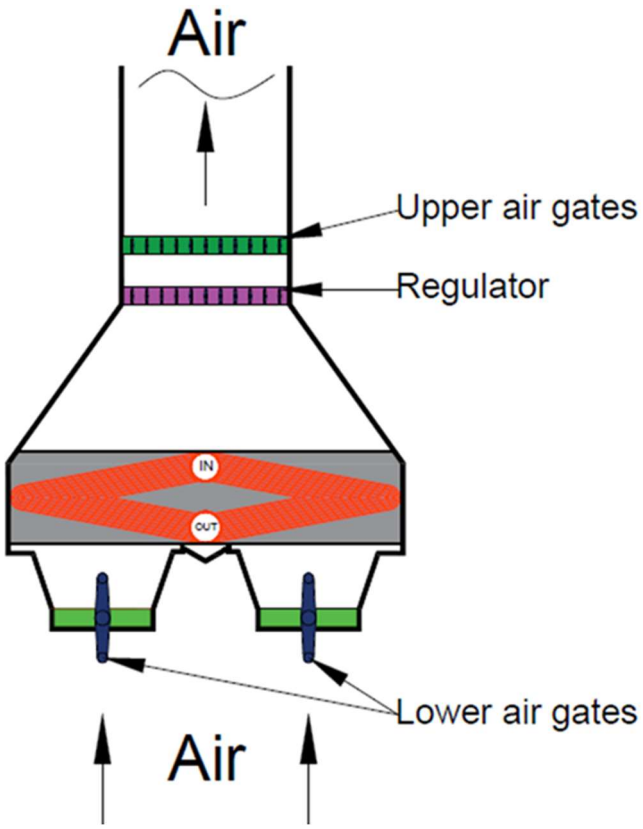

Figure 2-72 air-cooled PHRS HX scheme

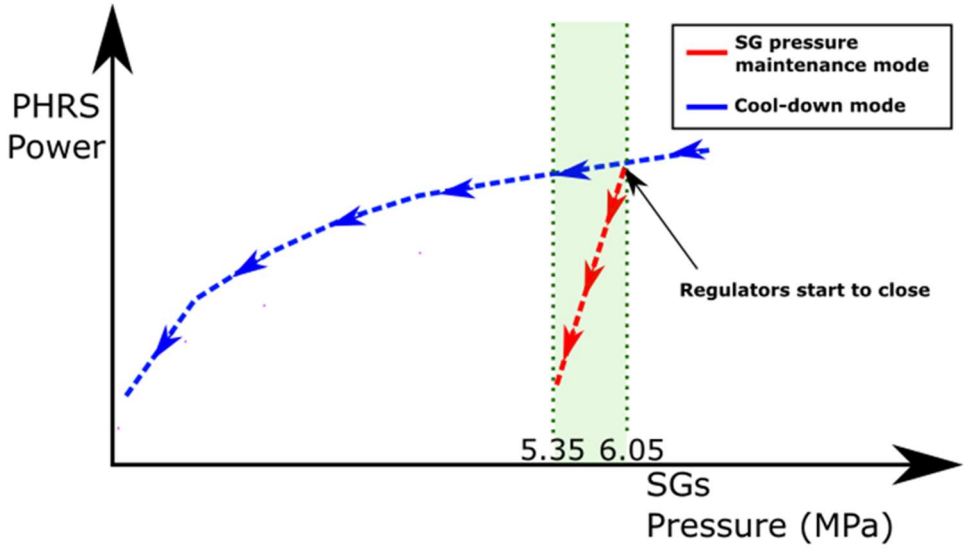

Figure 2-73 PHRS power vs. SGs pressure curves in both operating modes

Table 2-21 Air-cooled PHRS geometry

Parameters		Value	Units	Reference
Steam lines	Diameter	0.2	m	(Ahmed Pirouzmand and Shahabinejad, 2021; Ayhan and Sokmen, 2015; IAEA, 2009)
PHRS tubes	Nº HX	3	-	(Ahmed Pirouzmand and Shahabinejad, 2021; Khubchandani et al., 2013a)
	Nº tubes per HX	630	-	(Chaudhary et al., 2017)
	Length	8	m	(Ahmed Pirouzmand and Shahabinejad, 2021; Bharat Heavy Electricals Limited, n.d.; ROSATOM, 2023)
	Height	1.49	m	
Condensate lines	Diameter	0.1	m	(Ahmed Pirouzmand and Shahabinejad, 2021)
	Height	19.2	m	(Khubchandani et al., 2013a; Kopytov et al., 2011, 2009)
Air ducts	Flow area (Regulator – Air duct outlet)	12	m^2	(Bharat Heavy Electricals Limited, n.d.; ROSATOM, 2022; Sri Krishna College of Engineering and Technology (SKCET), 2019)
	Height (Lower air gates - Regulator)	7.5	m	
	Height (Regulator – air duct outlet)	30	m	(Sri Krishna College of Engineering and Technology (SKCET), 2019)

2.2.4.3. Experimental facilities related to the air-PHRS and the HA-2

The aim of this section is to give an overview of the experimental facilities that have been employed to investigate the joint effect of HA-2 and air-cooled PHRS on the Gen-III/III+ VVER from the Moscow Institute. In particular, two experimental facilities can be highlighted, the PSB-VVER facility, which has been modified to include the HA-2 and the air-cooled PHRS, and the HA2M-SG facility.

In the 1990s, the PSB-VVER facility, a large scale integral test facility modeling the VVER-1000/V320 reactor, was constructed at the Electrogorsk Research and Engineering Centre on NPP Safety (EREC) in Russia. Several international projects have been developed to analyse numerous accidental sequences at the PSB VVER facility, see (Blaha, 2014; Shahedi et al., 2010; Varju et al., 2024). These include the TACE-97 R2.03 project "Development of software for accident analysis of VVER and RBMK reactors" (European commission EuropeAid Co-operation Office, 2006) and the OECD PSB-VVER project (Melikhov et al., 2008).

Between 2017 and 2018, the PSB-VVER facility was upgraded to model a VVER-TOI reactor, including the HA-2 system and the air-cooled PHRS, see Figure 2-74. In (Elkin et al., 2018), it has been noted that LOCA scenarios under SBO conditions have been realised at the upgraded PSB-VVER plant. However, there is limited publicly available information on the modified version of the PSB-VVER plant reflecting the upgrade to a VVER-TOI reactor.

The HA2M-SG, on the other hand, is designed to study the combined performance of the PSS in Gen-III/III+ VVER reactors. It is located at the Leipunskii Institute of Physics and Power Engineering (IPPE) of the Joint-Stock Company (JSC) in Russia, (Kopytov et al., 2009). The HA2M-SG consists of a VVER SG model, a tank accumulator for steam supplied and a PHRS HX, see Figure 2-75 and (Kopytov et al., 2011).

In the HA2M-SG, several experiments have been carried out related to the study of the effect of the non-condensable gases in the SG tubes, (Berkovich et al., 2006). The conclusions of these analyses reflect that in the first 24 hours of operation of the HA-2 and the PHRS, the line connecting the upper part of the HA-2 to the CLs takes the mixture of steam and non-condensable gases from the RCS, reducing the presence of the latter in the SGs tubes. Therefore, the effect of the non-condensable gases in the condensation of the steam in the SGs tubes due to the PHRS operation is not appreciable, (Kopytov et al., 2011, 2009).

The IPPE also has other experimental facilities, such as the GROT facility, which has been used to analyse, among other things, the reduction in heat exchange in the SG tubes due to the presence of different concentrations of non-condensable gases or the effect of boiling boric acid, see (Morozov et al., 2014; Morozov and Sakhipgareev, 2017; Shlepkin et al., 2020).

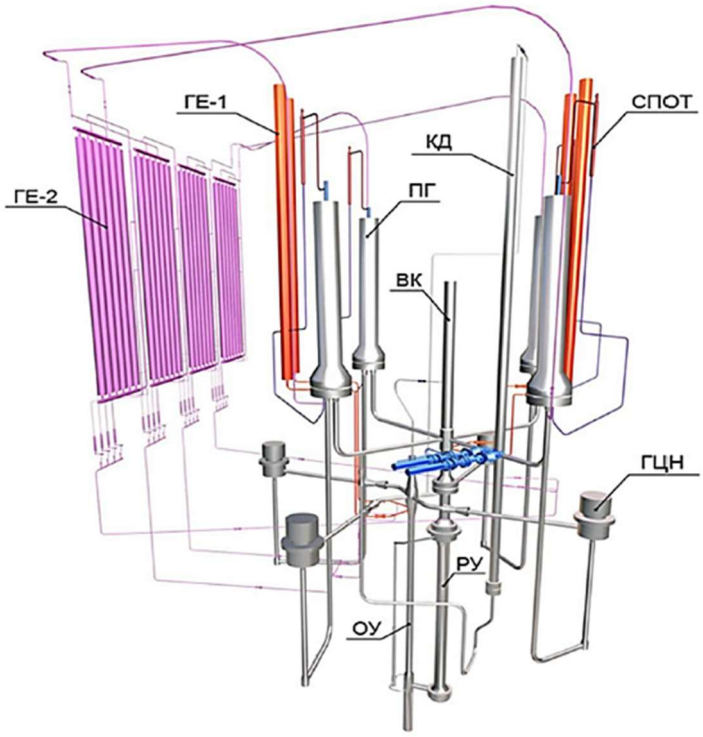

Figure 2-74 PSB-VVER facility including HA-2 and air-cooled PHRS (Elkin et al., 2018)

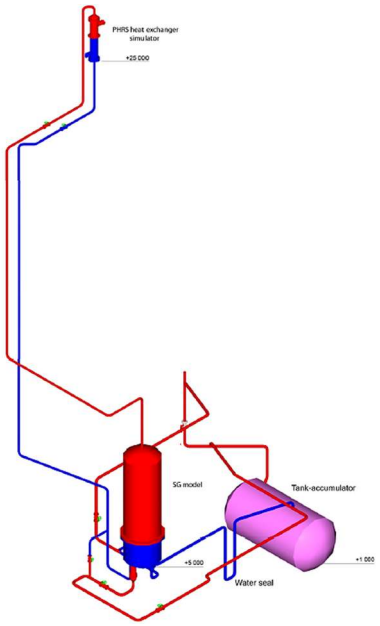

Figure 2-75 HA2M-SG facility (Kopytov et al., 2011)

2.3. Standard Event Trees for the VVER-1000/V320

This section aims to present the VVER-1000/V320 ETs, focusing on those that are particularly relevant to this PhD thesis, as they are the ones considered in Sections 4 to 6. The ETs covered include, on the one hand, the GT and LOOP ETs, based on those found in (Begun et al., 2000; Kovacs, 2014; Science Applications International Corporation (SAIC), 1987), see Figure 2-76 and Figure 2-77. On the other hand, the SBLOCA, MBLOCA and LBLOCA ETs are based on those found in (Skalozubov et al., 2010), see Figure 2-78, Figure 2-79 and Figure 2-80. The headers that appear in these ETs are often repeated from one ET to another. These headers are:

- S Header – SCRAM or reactor protection system actuation

The success of the S header consists of the correct insertion of the CRs in the core at a required speed and without getting stuck in an intermediate position when the trip setpoints of the emergency protection are reached or when the emergency protection is initiated by the operator. Its failure leads to an Anticipated Transient Without SCRAM (ATWS) in all the ETs.

- EF Header – EFW/AFW

The success of the EF header consists of the availability of 1 out of 3 AFW trains or 1 out of 3 EFW trains together with the operation of 1 out of 4 BRU-A or BRU-K valves. Note that this header consists only of EFW availability and not AFW availability for LOOP ET.

- BF Header – Bleed and Feed

This management action consists of opening the PZR relief and safety valves to reduce the pressure in the RCS, thus allowing the HPIS to be injected. The purpose of the strategy is to cool the RCS when this is not possible via the SGs.

- EDG Header – Diesel Generators

The success of the EDG header consists of the availability of 1 of the 3 EDG, with the capacity to supply on-site power to one of the safety trains.

- R-EX Header – Recovery of the external power

The success of the R-EX header consists of the recovery of one of the safety bus.

- H Header – HPIS

This system performs the function of injecting borated water into the RCS when the pressure is high. H header SC is accomplished if 1 out of 3 HPIS trains inject successfully, except for the LBLOCA for which the SC is the availability of 2 out of 3 HPIS.

- A Header – HA-1

The HA-1 re-flood the core with borated water. They can inject at an intermediate pressure (below 6 MPa). A header SC is accomplished if 1 out of 2 HA-UP and 1 out of 2 HA-DC inject successfully.

- L Header – LPIS

As the HPIS, the LPIS mission is to introduce borated water into the RCS at low pressure to compensate for the coolant lost through the break. L header is considered successful if 1 out of 3 LPIS trains inject successfully.

- B Header – EBIS

This header is related to the performance of the EBIS. The mission for this safety system is to inject borated water into the RCS to ensure the subcriticality of the reactor, B header is considered successful if 1 out of 3 EBIS trains is available.

- D Header – RCS cooling and depressurization through the SGs

This header is related to the depressurization of the SGs at a controlled RCS cooling rate, 30 K/h or 60 K/h, or a maximum RCS cooling rate. It should be noted that this header is not related to an automatic action, but to a human action. This management action is achieved by opening the BRU-K valves or the BRU-A valves if the condenser is not available. The success of the D header consists in the operation of 1 out of 2 AFW pumps or 1 out of 3 EFW pumps together with the availability of 1 out of 4 BRU-K or BRU-A valves.

- EG Header – EGRS

This header appears in the SBLOCA ET, with the mission to depressurize the RCS. The SC for the EG header is the opening of one of the EGRS valves.

A summary of the previously described headers is shown in Table 2-22, together with the SC associated with each one.

Table 2-22 Success criteria for VVER-1000/V320 ETs

Header	Success Criteria
S	Forming a signal of SCRAM and the activation of the reactor control and protection system
EF	1 out of 3 EFW pumps or 1 out of 2 AFW pumps + 1 out of 4 BRU-A or BRU-K (SG pressure maintenance mode)
BF	1 out of 3 PZR valves + 1 out of 3 HPIS trains
EDG	1 out of 3 EDG
R-EX	Recovery of 1 safety bus
H	1 out of 3 HPIS trains (2 out of 3 trains in the LBLOCA ET)
A	2 out of 4 HA-1 trains
B	1 out of 3 EBIS trains
L	1 out of 3 LPIS trains
D	1 out of 3 EFW pumps or 1 out of 2 AFW pumps + 1 out of 4 BRU-A or BRU-K (human action) (RCS cool-down mode)
EG	1 EGRS valve in the RCS

The ETs for the GT, LOOP, SBLOCA, MBLOCA and LBLOCA IEs are described below. It should be noted that the sequences that reach a success end state are denoted by "S", while those that reach core damage are denoted by "CD". In addition, there are some sequences that are transferred to other ETs, such as the Generic GT ET or the ATWS ET. Moreover, a specific wording is used to identify the sequences. A sequence is defined by concatenating the letter identifying its headers, written in upper or lower case, so that if it is in upper case it represents a success, while if it is in lower case it represents a failure of the system.

- GT ET

The GT ET consists of four headers: GT, S, EF and BF, see Figure 2-76. When the SCRAM signal occurs, if the S header is not successful the sequence is transferred to the ATWS ET. If on the other hand the S header is successful, the sequence reaches success end state whether the EF header (S-EF-bf) or the BF-header (S-EF-BF) is successful. Otherwise, if neither the EF header nor the BF header is successful (S-ef-bf), the sequence reaches CD end state.

- LOOP ET

The LOOP ET consists of four headers: S, EDG, EF and R-EX, see Figure 2-77. When the SCRAM signal occurs, if the S header is not successful, the sequence is transferred to the ATWS ET. On the other hand, if the S header is successful along with the EDG and the EF headers (S-EDG-EF-r-ex), the sequence reaches a success end state. Furthermore, if the EDG header fails but the R-EX header succeeds (S-edg-ef-R-EX) the sequence is transferred to the GT ET.

Conversely, if the EDG header is successful but the EF header fails (S-EDG-ef-r-ex), the sequence reaches a CD end state. In addition, a CD end state is also reached if neither the EDG nor the R-EX headers are successful (S-edg-ef-r-ex). It is worth noting that those sequences where the EDG failed are SBO sequences.

Furthermore, in the sequence 3 (S-edg-ef-R-EX), if the leakage through the seals of the MCPs is considered and the recovery of the external power is not immediate, the sequence is transferred to the Seal Loss Of Coolant (SLOCA) ET.

- SBLOCA ET

The SBLOCA ET consists of eight headers: S, H, EF, D, B, EG, A, L, see Figure 2-78. The break size range for this LOCA ET is between 0.5 and 2 inches. As in the GT and LOOP ETs if the S header is not successful the sequences is transferred to the ATWS ET. This ET has two successful sequences, one corresponds with the only successful of the S, H and EF headers (S-H-EF-d-b-eg-a-l) and the other one correspond with the successful of all the headers except for the H and EF headers (S-h-ef-D-B-EG-A-L).

This highlights the importance of HPIS performance in SBLOCA. In case HPIS is not available, human actions, reflected in the D and EG headers, are necessary to depressurise the RCS, thus allowing the injection of HA-1 and LPIS. This issue is extensively discussed in Chapter 5, Section 5.2, where the damage domains and the available times for the different management strategies in SBLOCA with HPIS failure are analyzed.

- MBLOCA ET

The MBLOCA ET consists of four headers: S, H, A, L, see Figure 2-79. The break size range for this LOCA ET is between 2 and 8 inches. As for the other ETs with S header, if it is not successful, the sequence is transferred to the ATWS ET. To reach a success end state it is necessary that all headers, i.e. S, H A and L, are successful (S-H-A-L). In fact, if any of the headers associated with the ECCS fail, the sequence leads to a CD end state.

It should be noted that in Chapter 5, Section 5.1, a verification of the SC for the MBLOCA headers is performed and, based on the results obtained, new ETs proposals are made for MBLOCA, taking into account new break size ranges and SC.

- LBLOCA ET

The LBLOCA ETs is the only one present in this section that does not consider the S header. This is due to the fact that reactivity does not play a significant role in this type of transient. Therefore, the LBLOCA ET headers are H, A and L, see Figure 2-80. The LBLOCA ET has a range between 8 inches and the DEGB. The DEGB area corresponds to 1.135 m^2 and an equivalent diameter of 47 inches as the diameter of the CL is 33.5 inches. Moreover, the SC for the H header is more restrictive, going from 1 out of 3 to 2 out of 3 trains successfully injecting.

The LBLOCA ET contains two sequences with a success end state: H-A-l and h-A-L, all other sequences reach a CD end state. Thus, for a success end state, it is mandatory that one HA-1 injects into UP and another one into DC, in addition to the injection of one LPIS or two HPIS trains.

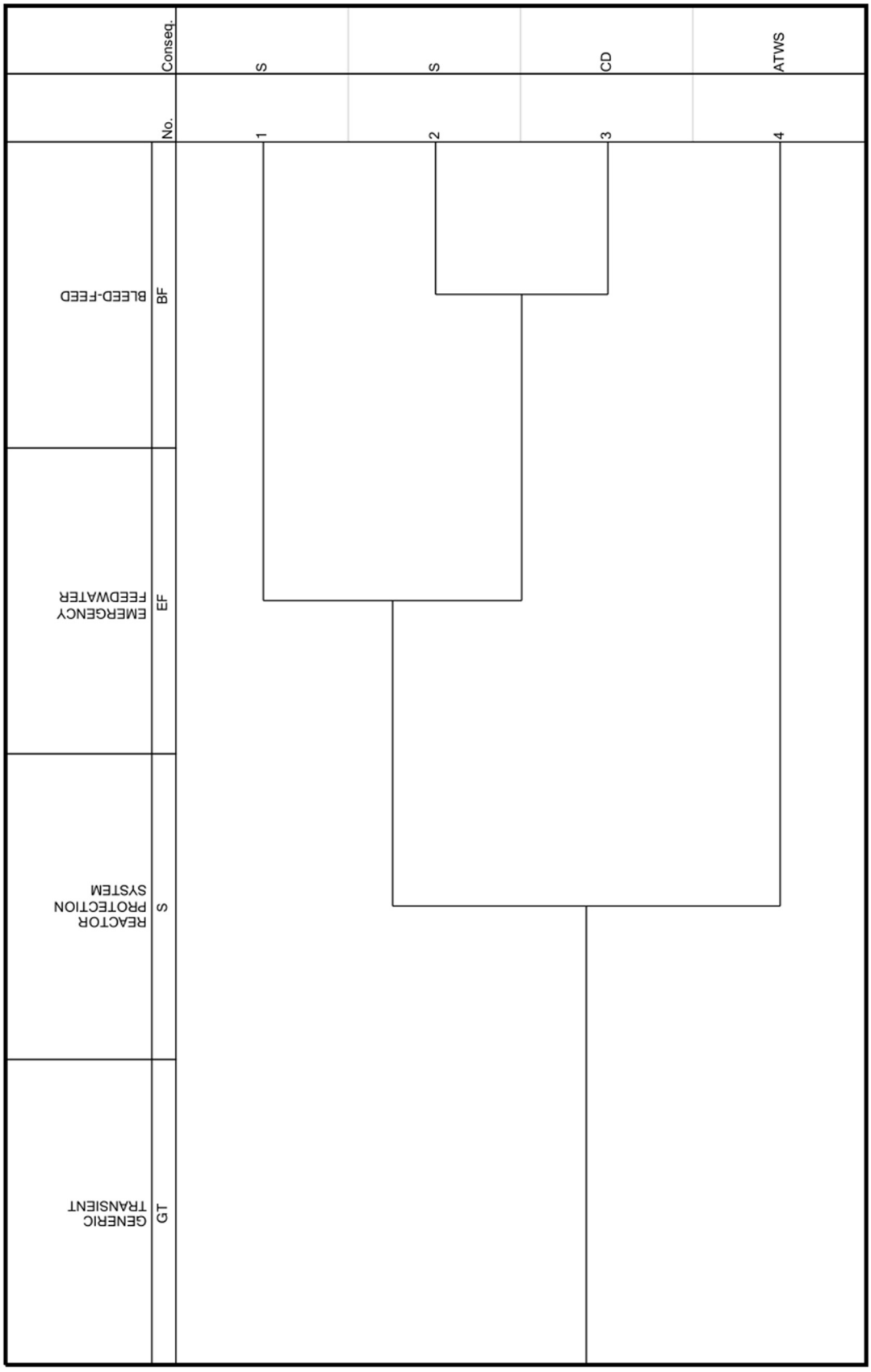

Figure 2-76 GT ET of VVER-1000/V320 reactor

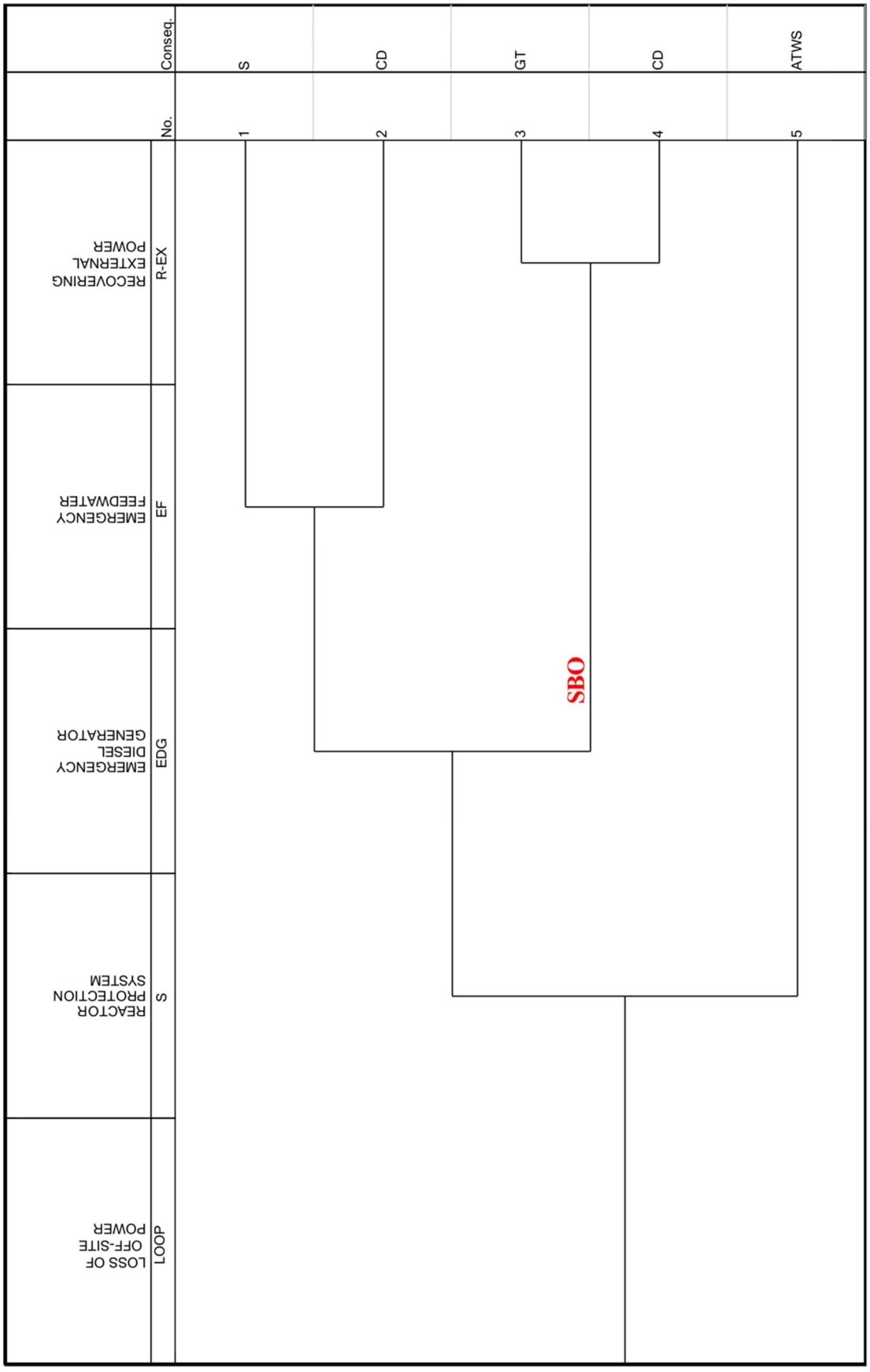

Figure 2-77 LOOP ET of VVER-1000/V320 reactor

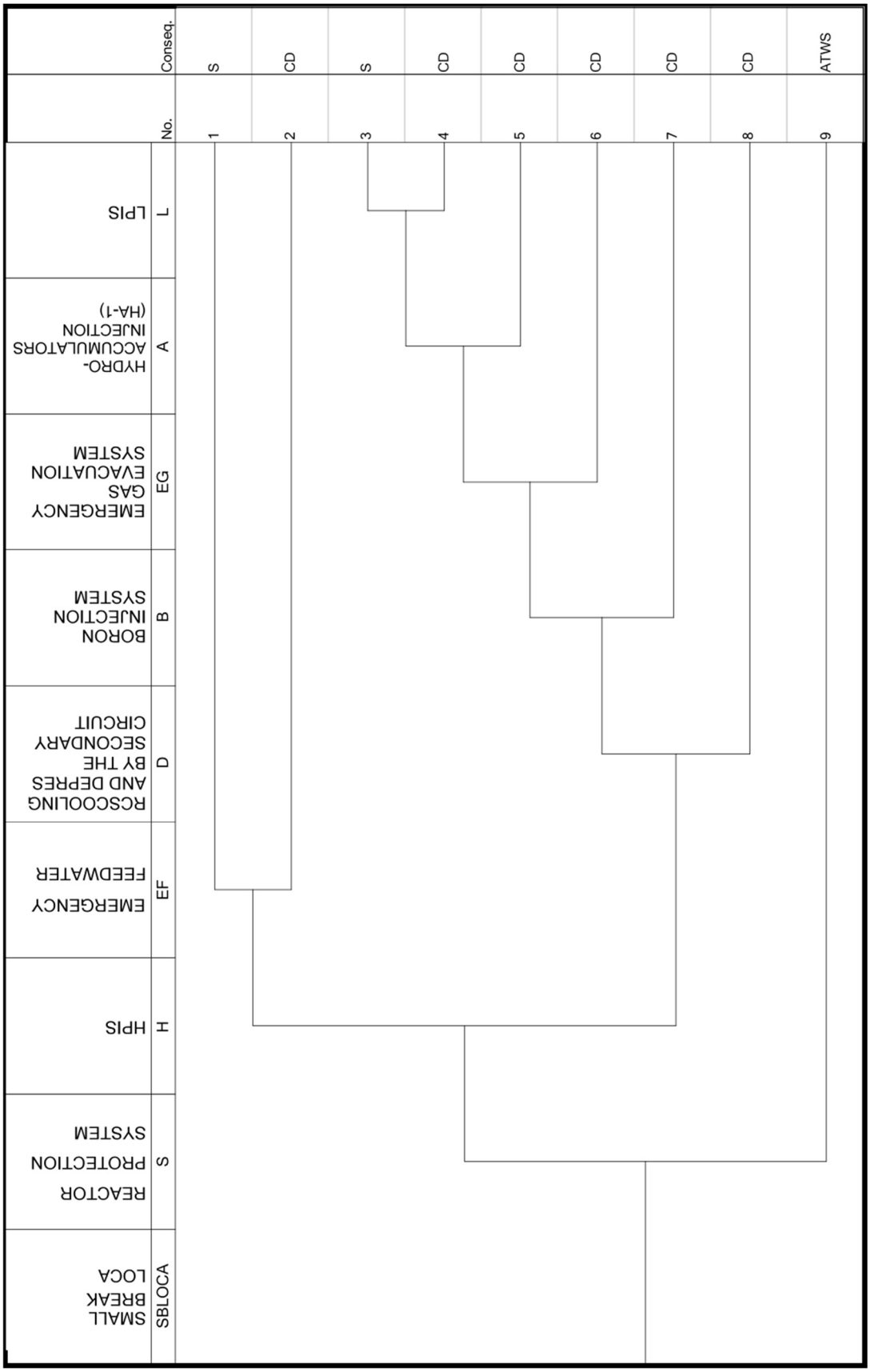

Figure 2-78 SBLOCA ET for VVER-1000/V320 reactor (Skalozubov et al., 2010)

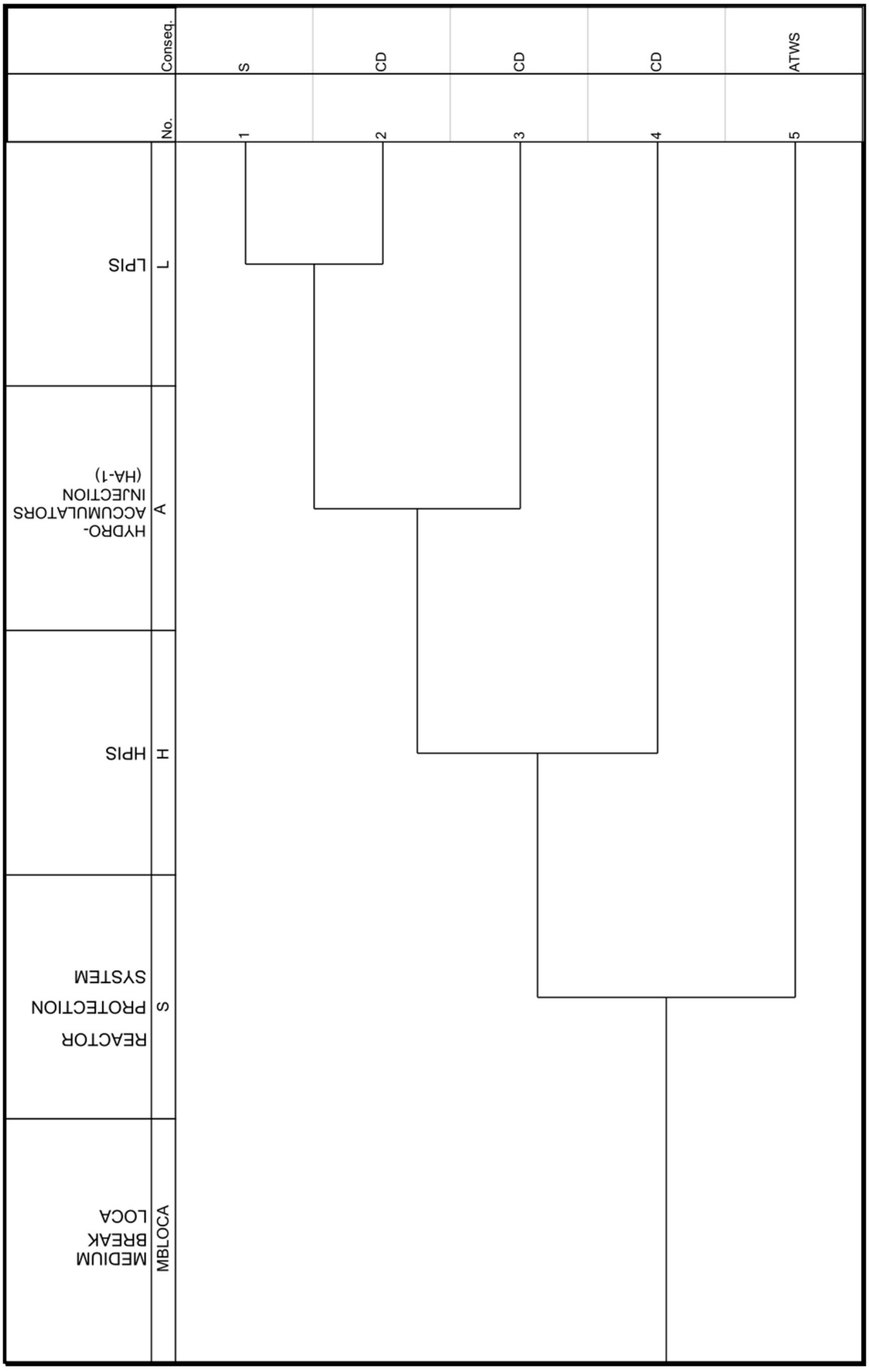

Figure 2-79 MBLOCA ET for VVER-1000/V320 reactor (Skalozubov et al., 2010)

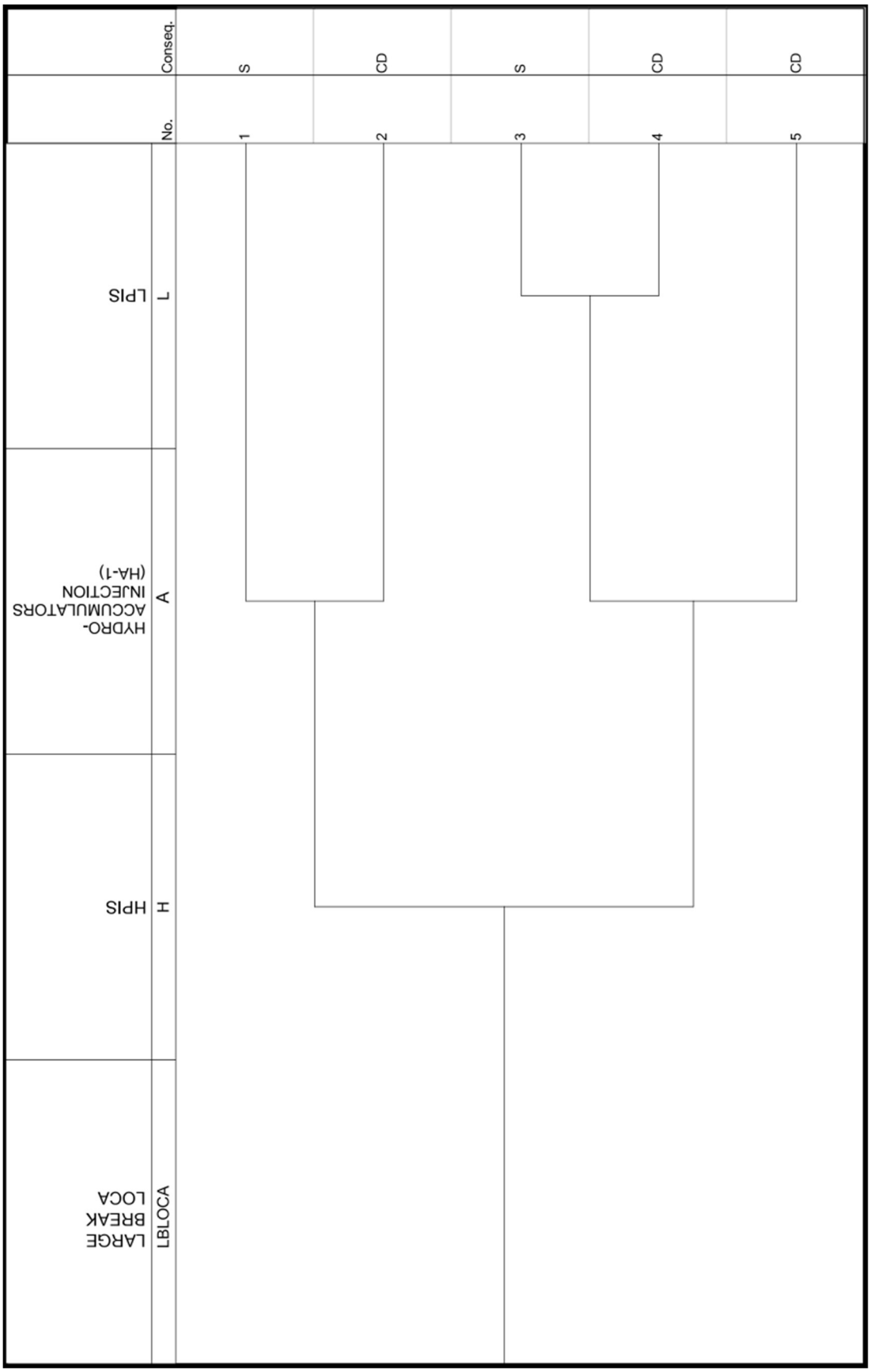

Figure 2-80 LBLOCA ET for VVER-1000/V320 reactor (Skalozubov et al., 2010)

Chapter 3. VVER-1000/V320 reactor model for the TRACEV5P5 code

The following chapter is intended to describe the model of the VVER-1000/V320 reactor developed for the TRACEV5P5 systems code (NRC, 2017) throughout the PhD thesis. Note that this model comes from an earlier RELAP5 model (Sanchez-Espinoza and Bottcher, 2006), which has been completed with controls, actuation signals and safety systems. In addition, the VVER-1000/V320 model has been implemented with human actions and the passive safety systems previously described in Section 2.2.4, as part of the analyses carried out in chapters 5 and 6.

Firstly, Section 3.1 shows the TH model of the RCS and the secondary circuit. Next, the actuation signals for the SCRAM, the MCPs, the MFW and the Turbine Trip (TT) are described in Section 3.2. The conventional safety systems of the VVER-1000/V320 reactor are presented in Section 3.3, the human actions in Section 3.4 and the advanced passive safety systems in Section 3.5. Finally, the Section 3.6 ends with the steady-state values obtained in the final model.

3.1. RCS and secondary circuit model

The TH model for VVER-1000/V320 RCS is shown in Figure 3-1 and the TH model for the VVER-1000/V320 secondary circuit is shown in Figure 3-2. The conversion of the TH model from the RELAP5 to the TRACEV5P5 code has been performed component by component, adjusting the pressure drops for the RCS, the secondary side of the SGs and the SLs. In this approach, the Cell Elevation Change (DELEV) option was selected to specify the elevation and orientation of the TH components due to its equivalence to RELAP5.

The SETS numerical method has been selected to solve the two-phase flow equations in the TH components. With regard to the friction factor correlation option, the homogeneous wall flow friction factor was selected, except for the abrupt area changes which were adjusted to reproduce the RELAP5 model pressure drops.

Moreover, the TH model of the SGs has been modified from modeling the U-shaped tubes in three levels to modeling them in five levels. This has had a great impact on the simulation of the SBO sequence, as the water level of the SGs is very sensitive to the number of cells used to model the heat transfer.

This has resulted in the final VVER-1000/V320 TH model with a total of 16 BREAKs, 29 FILLs, 164 PIPEs, 4 PUMPs, 4 SEPARATORs, 37 VALVEs, 1 VESSEL, 432 hydraulic connections. The main components of the RCS are described below:

- RCS loops: The CLs and HL have been modeled with 1D PIPEs.
- The MCPs: These have been modeled using the specific PUMPs component. In addition, the coast-down has been introduced by means of a time vs. speed table.
- The PZR: Connected to the HL 4 by the Surge Line. The PZR model also includes the spray lines attached to the CL 1, the relief and safety valves and four groups of heaters.
- RPV: Modeled using a 3D VESSEL component divided into 50 axial levels, 6 azimuthal sectors and 6 radial sectors. The three inner rings are dedicated to the modeling of the core, the fourth ring to the modeling of the bypass, the fifth to the modeling of the core barrel and the sixth to the modeling of the DC.
- Core: A total of 18 HEAT STRUCTURE components are used to model the 50856 fuel rods (163 hexagonal fuel assemblies with 312 fuel rods each). The HEAT STRUCTUREs have a height of 4 m and are divided into 12 axial levels (10 corresponding to the active part and 2 to the reflector part). A cosine axial power distribution is assumed and a hot fuel rod peaking factor of 1.74 (Iegan et al., 2016) has been included.
- Primary side of the SGs. The 11000 U-shaped tubes have been modeled with five horizontal PIPEs components. In addition, the cold and hot collectors have also been modeled with six vertical PIPEs components each.

The model also includes the CVCS, consisting of the make-up and the let-down systems with a mass flow rate of 8.19 kg/s. The make-up system has been modeled with four boundary conditions using FILL components connected to the four CLs. Whereas the let-down system has been also modeled with two FILL components connected to CL 2 and CL 3.

The secondary circuit of the VVER-1000/V320 reactor has been modeled up to the turbine stop valve, including the secondary side of the SGs, the SLs and the MSH.

- Secondary side of the SGs. The heat transfer zone is modeled with five vertical PIPE components, each connected each to a horizontal PIPE modeling the U-shaped tubes in the primary side of the SGs. In addition, the downcomer of the SGs has also been modeled with vertical PIPE components, cross connected to the five PIPEs modeling the heat transfer zone. In the upper part the liquid/steam SEPARATOR component is placed.
- SL: including a BRU-A valve, two safety valves, a MSIV valve, and a check valve in each SL.
- MSH: including BRU-K valves and BRU-SN valves.

It should be noted that the MFW is modeled as a boundary condition with a FILLs component. A FILL per SGs introduces water at 409 K with a rated mass flow that is a function of the water level in the secondary side of the SGs.

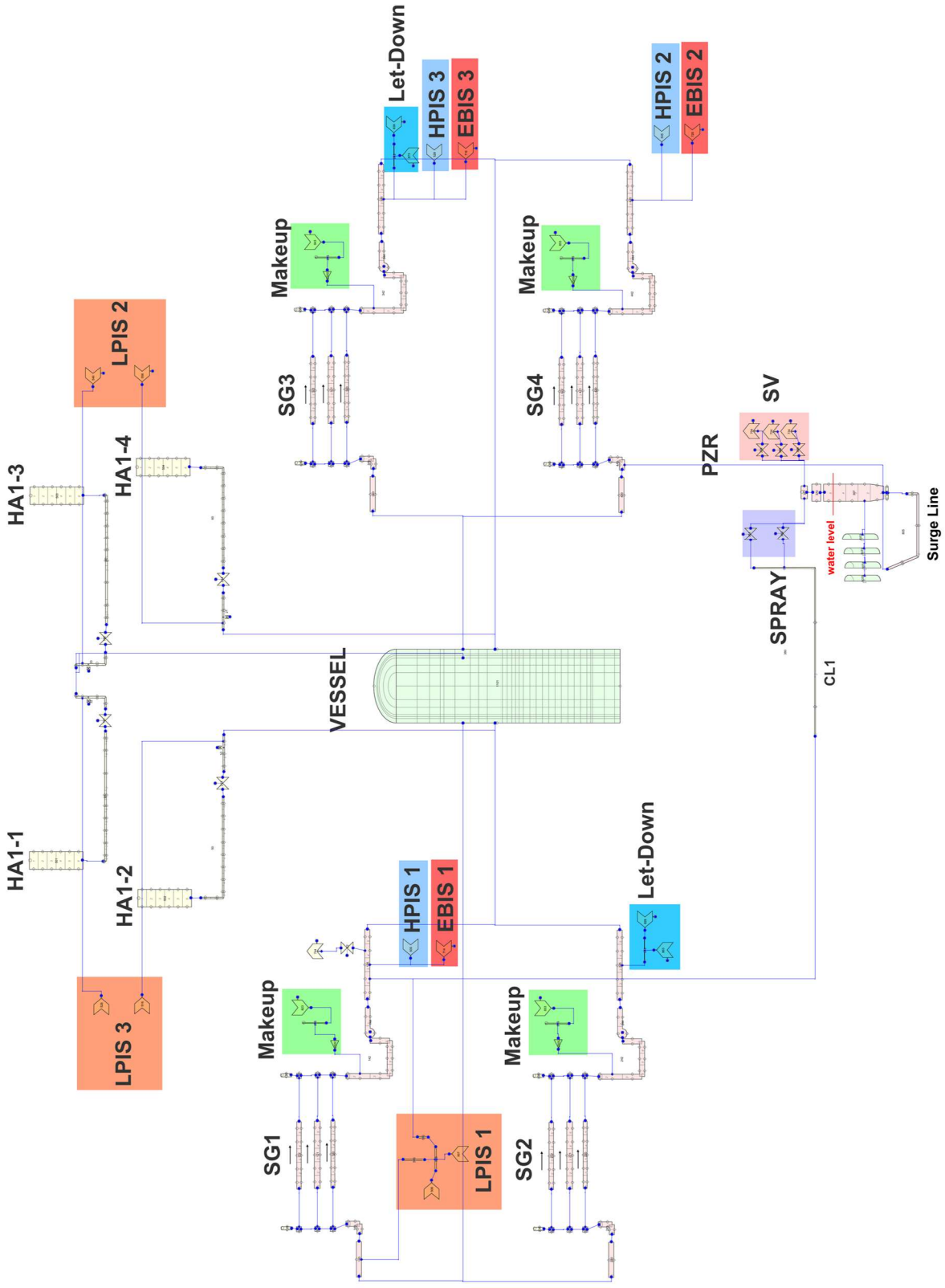

Figure 3-1 VVER-1000/V320 RCS TRACEV5P5 TH model

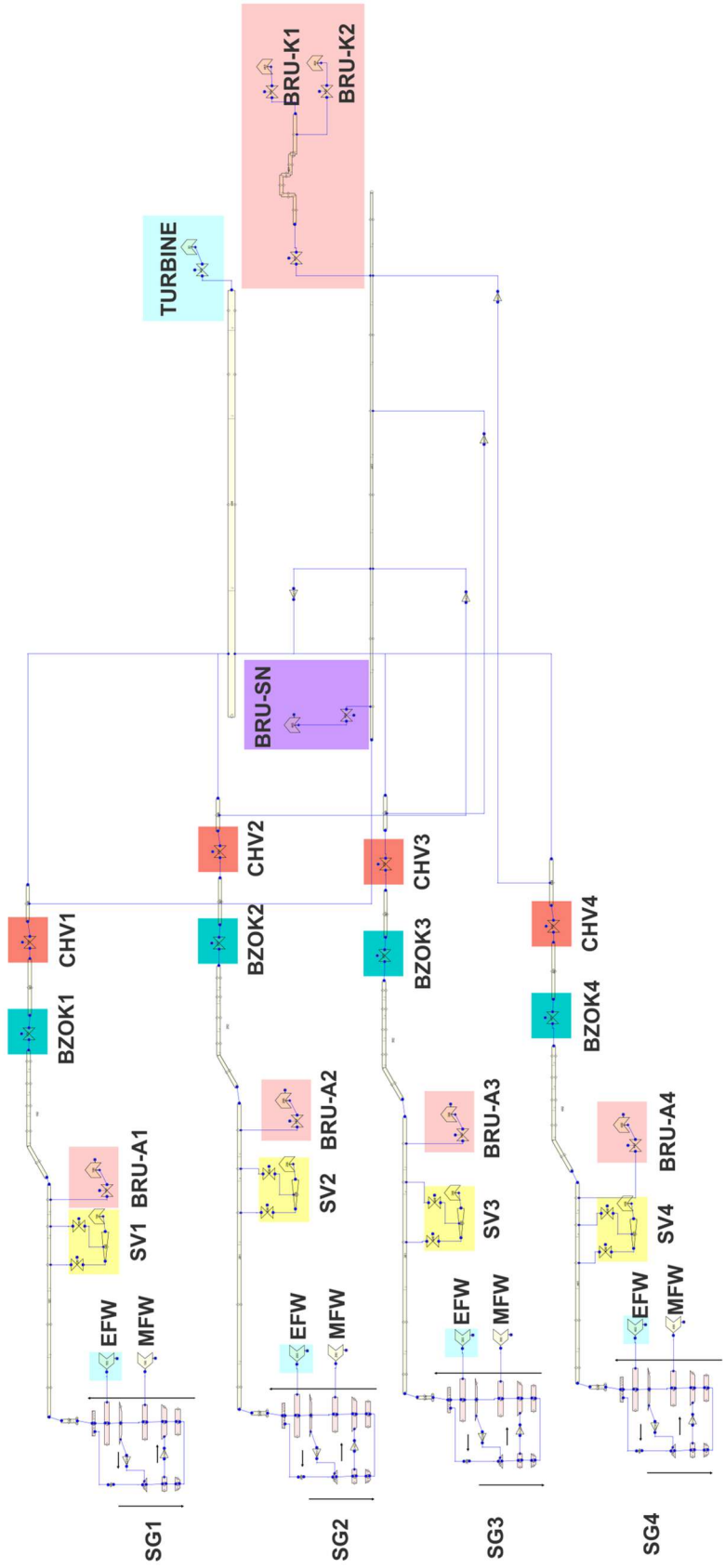

Figure 3-2 VVER-1000/V320 secondary circuit TRACEV5P5 TH model

3.2. Actuation signals for SCRAM, MCPs trip, MFW pumps trip and Turbine trip

The following section describes the signals for the SCRAM, the MCPs trip, the MFW pumps trip and the TT included in the VVER-1000/V320 model. It should be noted that the SCRAM and the MCPs trip signals are taken from (Muellner, 2010). Moreover, a summary of that signals is given in Table 3-1.

The SCRAM can be caused by a large number of signals, see Figure 3-3. On the one hand, the signals related to the RCS consist of high core power, high RCS pressure, low level in the PZR, a subcooling margin in the HLs below 10 K, low pressure drop in the RCS, high HLs temperature. On the other hand, the signals related to the secondary circuit are low level in the SGs and high pressure in the SGs. In addition, there are other combined signals: a low pressure in the SL together with a difference between the saturation core temperature and the SL temperature below 75 K, a low pressure at the core outlet together with a high temperature in the HLs, a core power higher than 75% together with the RCS trip and a core power higher than 75% together with a low core outlet pressure.

The RCSs trip can be activated by four signals. Three of these are low level in the SGs, high level in the SGs and closing of the MSIV valves. The fourth is a combination of signals consisting of low pressure in the SL together with a difference between the core saturation temperature and the SL temperature of 75 K and a HL temperature below 473.15 K, see Figure 3-4.

The MFW can be switched off by five signals: a subcooling margin in the HLs below 10 K, a temperature in the HLs above 599.15 K, a PZR level below 4 m, a pressure in the RPV head above 17.65 MPa and a pressure in the HLs below 14.71 MPa, see and Figure 3-5.

The TT can be caused by the seven signals: a subcooling margin in the HLs below 10 K, a temperature in the HLs above 599.15 K, a PZR level below 4 m, a pressure in the RPV head above 17.65 MPa, a pressure in the HLs below 14.71 MPa, a high SG level and a low pressure in the MSH, see Figure 3-6. All TT signals have a 15 s delay.

Table 3-1 SCRAM, MCPs trip, MFW pumps trip and TT signals, VVER-1000/V320 model

SCRAM	
Power > 107 %	**OR**
SG level < 1.60 m	**OR**
P_{RCS} > 17.65 MPa	**OR**
PZR level < 4.6 m	**OR**
P_{SG} > 7.84 MPa	**OR**
P_{SL} < 4.1 MPa **AND** $T^{sat}_{core\_out} - T_{SL}$ > 75 K	**OR**
$T^{sat}_{HL} - T_{HL}$ < 10 K	**OR**
ΔP_{MCP} < 0.245	**OR**
$P_{core\ out}$ < 13.73 MPa **AND** T_{HL} > 533.15 K	**OR**
T_{HL} > 597.15 K	**OR**
Power > 75 % MPa **AND** MCPs trip	**OR**
Power > 75 % MPa **AND** $P_{core\ out}$ > 14.7 MPa	
MCPs	
ΔSG_{level} < - 0.5 m	**OR**
ΔSG_{level} > 0.25 m	**OR**
MSIV closing signal	**OR**
P_{SL} < 4.1 MPa **AND** $T^{sat}_{core\_out} - T_{SL}$ > 75 K **AND** T_{HL} > 473.15 K	
MFW	
$T^{sat}_{HL} - T_{HL}$ < 10 K	**OR**
T_{HL}> 599.15 K	**OR**
PZR level < 4 m	**OR**
P_{top_RPV} > 17.65 MPa	**OR**
P_{HL} < 14.71 MPa	
TURBINE TRIP	
$T^{sat}_{HL} - T_{HL}$ < 10 K	**OR**
T_{HL} > 599.15 K	**OR**
PZR level < 4 m	**OR**
P_{top_RPV} > 17.65 MPa	**OR**
P_{HL} < 14.71 MPa	**OR**
SG level > 2.65 m	**OR**
P_{MSH} < 5.098 MPa	

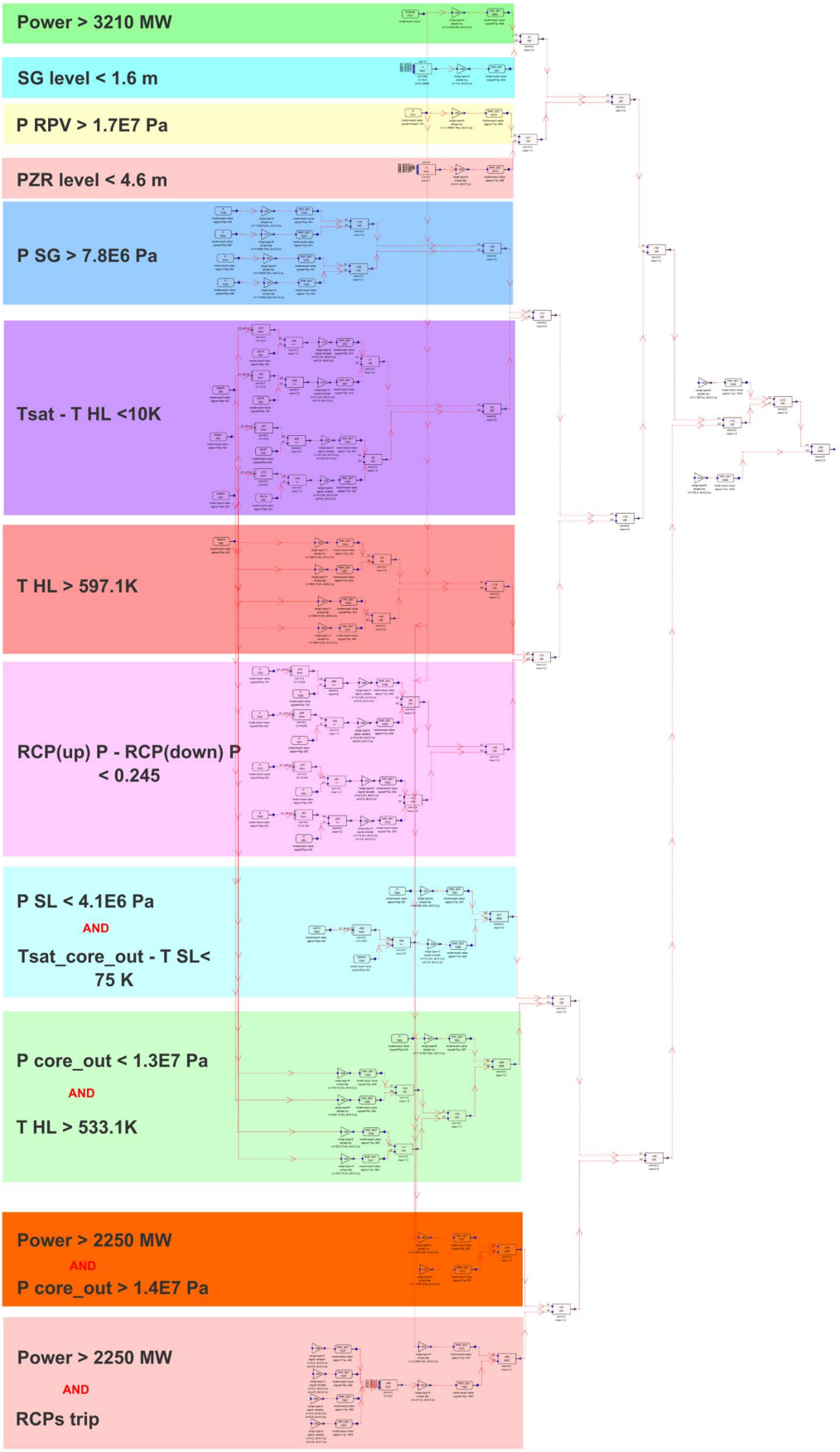

Figure 3-3 SCRAM signals, VVER-1000/V320 model

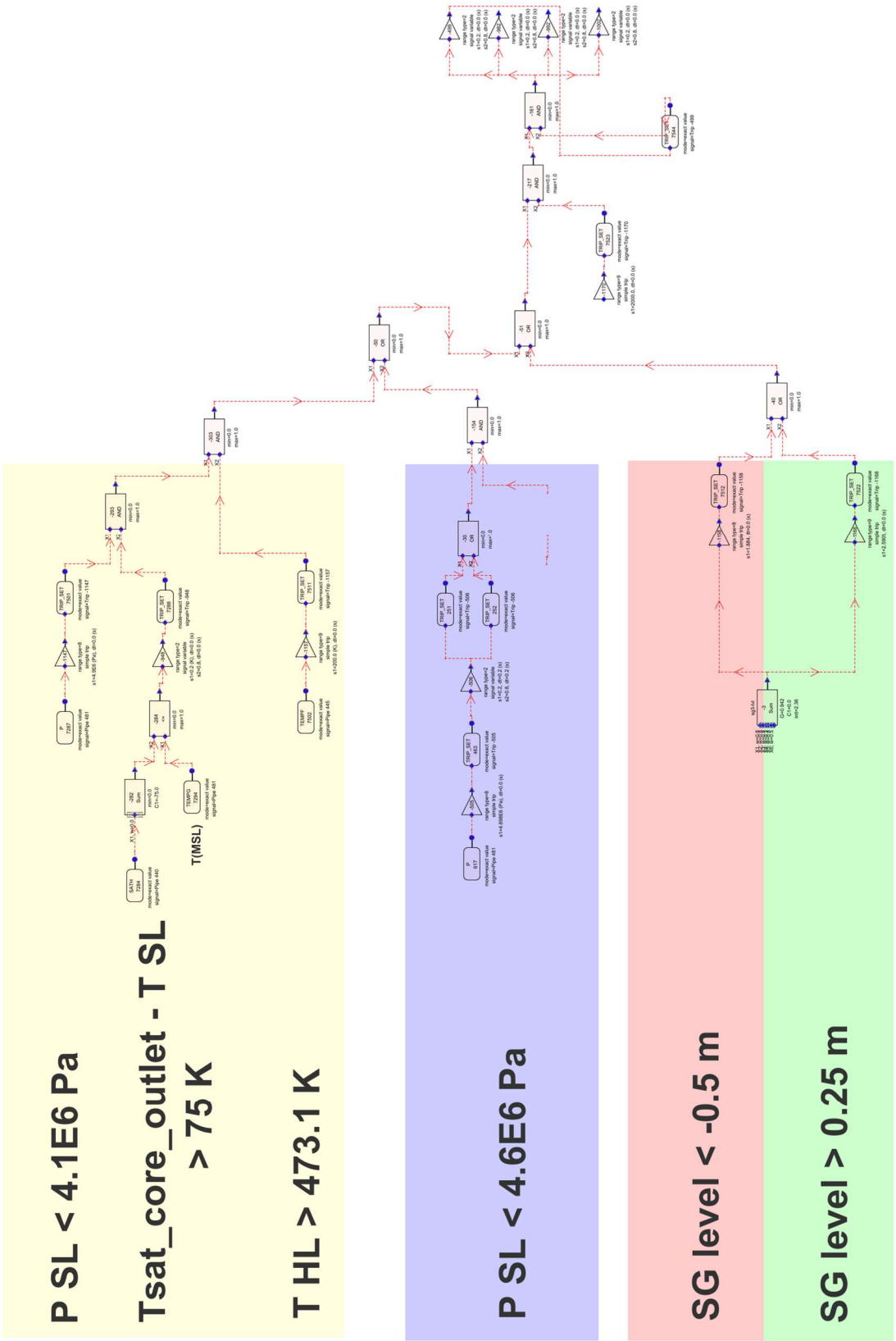

Figure 3-4 MCPs trip signals, VVER-1000/V320 model

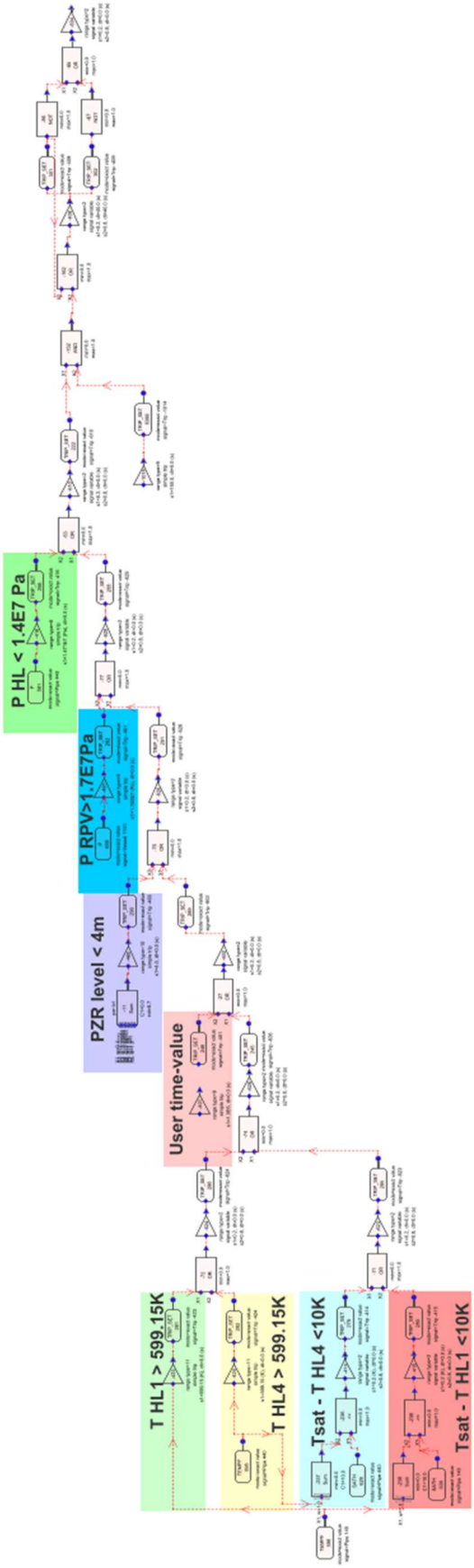

Figure 3-5 MFWs pumps trip signals, VVER-1000/V320 model

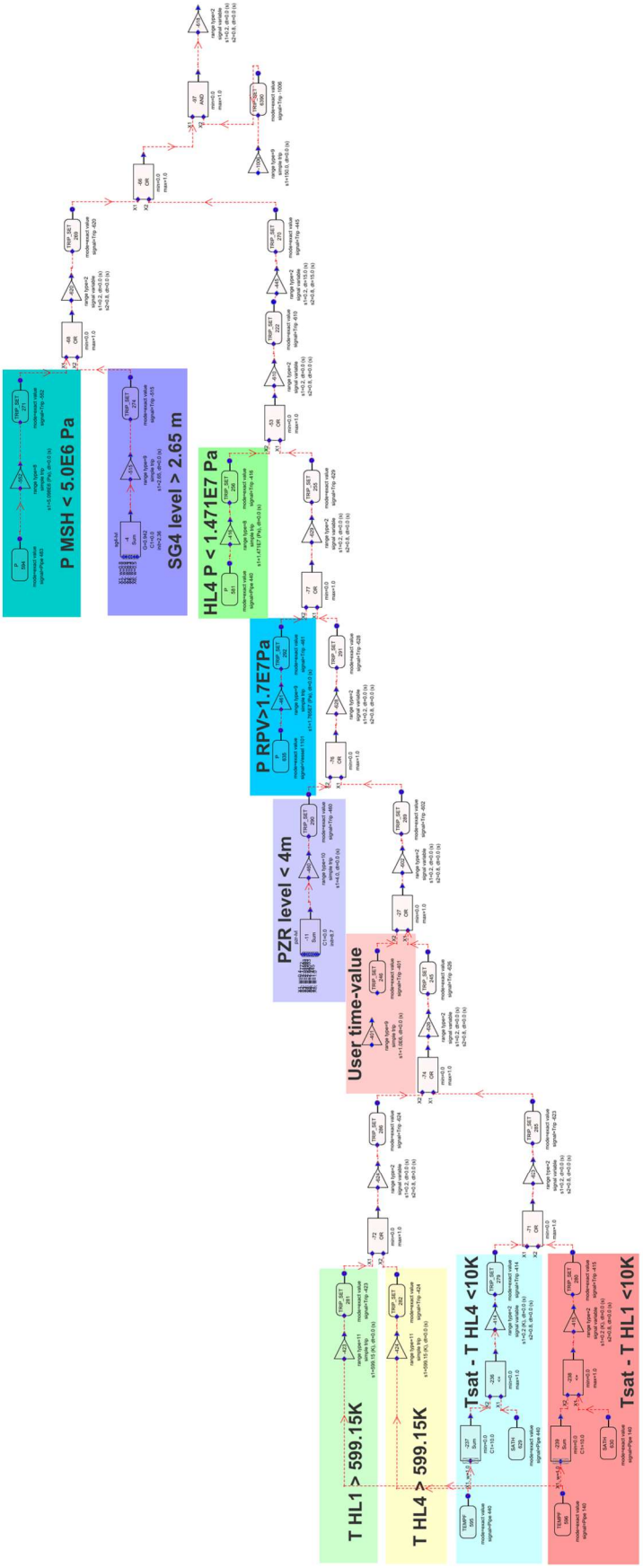

Figure 3-6 Turbine trip signals, VVER-1000/V320 model

3.3. Conventional control and safety systems

The model for the TRACEV5P5 code includes the following safety systems: the ECCS, the EBIS, the RCS and secondary pressure relief systems and the EFW. The following describes how each of these safety systems is modeled in the model for the VVER-1000/V320 reactor.

The active part of the ECCS consists of the HPIS and the LPIS, which are modeled with boundary conditions. The LPIS is connected to the four HA-1 injection lines and to CL 1 and HL1, while the HPIS is connected to the CL 1, CL 3 and CL 4. The injection curves of which are shown in Figure 3-7. The triggering of the actuation signal of both the LPIS and the HPIS requires the fulfilment of two conditions; the first is that the subcooling margin in the HLs falls below 10 K and the second is that the vessel head pressure is less than 10.78 MPa for the HPIS and 2.55 MPa for the LPIS, see Table 3-2 and the Figure 3-8.

The conventional PSS of the ECCS consists of four HA-1, each modeled with a special PIPE component and divided into 6 cells of 10 m^3 each, of which 5 are filled with water and 1 with N_2. They are isolated from the RCS by check valves. This PSS is also equipped with valves that close when the level in HA-1 is below 1.2 m. They are connected to the RCS by means of the HA-1 injection lines, two of which are attached to the RPV UP and the other two to the RPV DC.

The EBIS is modeled by means of FILL components. The connection points to the RCS are those of the HPIS, i.e. the CL 1, the CL 3 and the CL 4. This safety system does not have an automatic actuation signal and can be activated by the user.

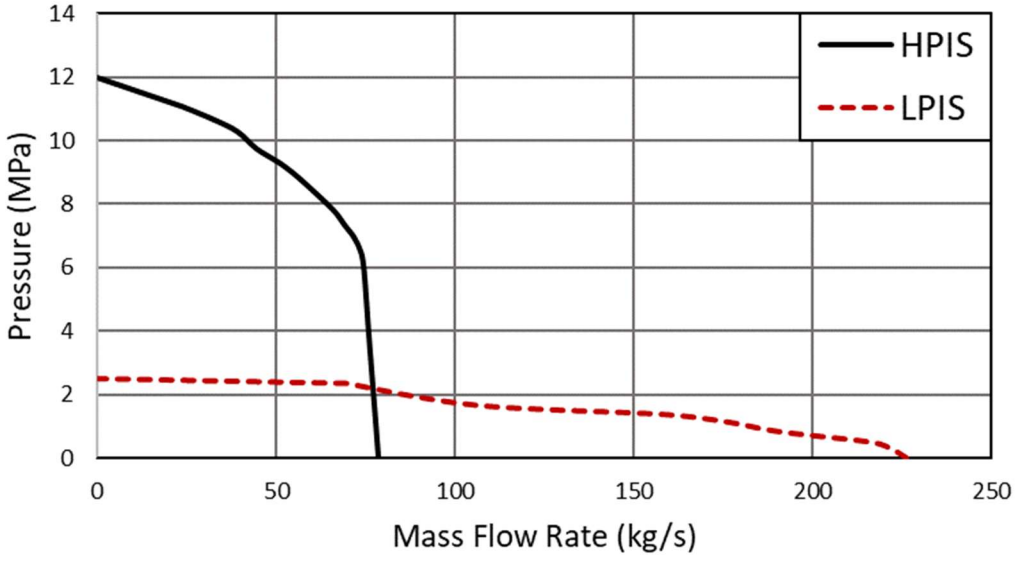

Figure 3-7 HPIS and LPIS injection curves (per pump), VVER-1000/V320 model

Table 3-2 Active ECCS signals, VVER-1000/V320 model

ECCS		
LPIS	$T_{HL}^{sat} - T_{HL} < 10$ K	**AND**
	$P_{RPV} < 2.55$ MPa	
HPIS	$T_{HL}^{sat} - T_{HL} < 10$ K	**AND**
	$P_{RPV} < 10.7$ MPa	

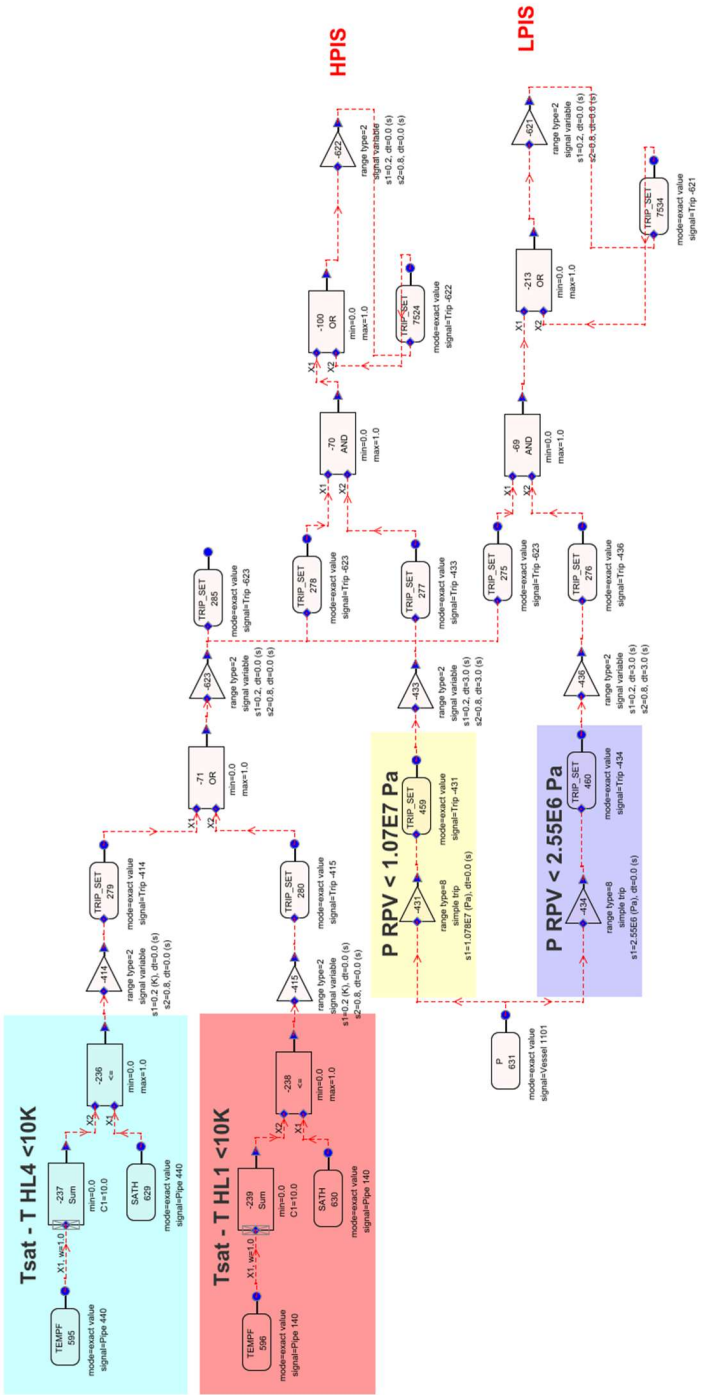

Figure 3-8 LPIS and HPIS actuation signals, VVER-1000/V320 model

The RCS relief system consists of three relief and safety valves located in the upper part of the PZR. Two of them have the same opening setpoint of 18.62 MPa and a closing setpoint of 17.84 MPa, while the third has an opening setpoint of 18.13 MPa and a closing setpoint of 17.25 MPa, see Table 3-3 and Figure 3-9.

Table 3-3 PZR relief and safety valves signals, VVER-1000/V320 model

PZR Valves	
Valve 1 and 2	Open: $P_{top\_PZR} > 18.62$ MPa
	Close: $P_{top\_PZR} < 17.84$ MPa
Valve 3	Open: $P_{top\_PZR} > 18.13$ MPa
	Close: $P_{top\_PZR} < 17.25$ MPa

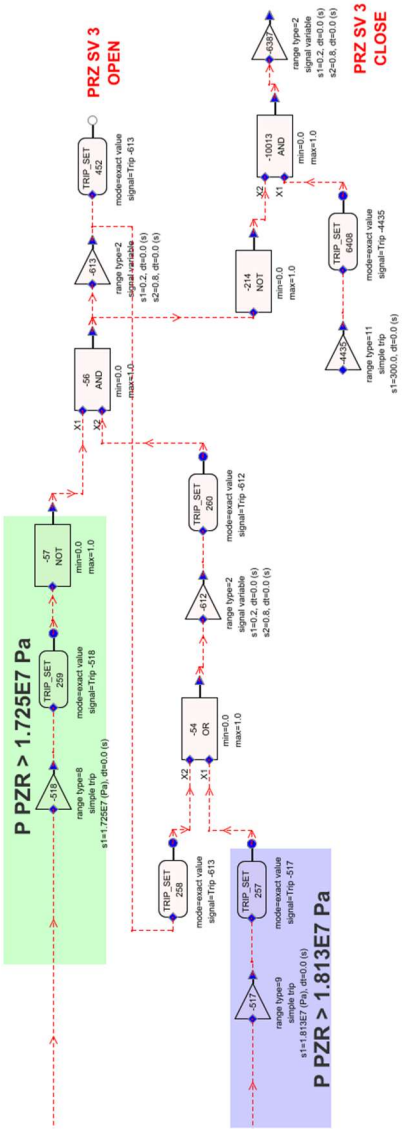

Figure 3-9 PZR valves signals, VVER-1000/V320 model

In addition to the relief and safety valves in, the model includes connected to the PZR two other auxiliary systems, the sprays and the heaters, whose function is to control the RCS pressure. There are a total of 4 heaters groups modeled by 4 HEAT STRUCTURE components, each connected to a POWER component with a power of 360 kW, 180 kW, 720 kW and 1260 kW respectively. The heaters are switched on according to different values of the RPV pressure, see Table 3-4 and Figure 3-10. In addition, for any of the heaters to be switched on, it is a requirement that the PZR level does not drop below 4.2 m. In steady-state conditions, heater 1 is switched on to compensate losses.

Table 3-4 PZR heaters on/off signals, VVER-1000/V320 model

PZR Heaters	
Heater 1	On: P_{top_RPV} < 15.6 MPa **AND** PZR level > 4.2 m
	Off: P_{top_RPV} > 15.78 MPa **OR** PZR level > 4.2 m
Heater 2	On: P_{top_RPV} < 15.6 MPa **AND** PZR level > 4.2 m
	Off: P_{top_RPV} > 15.6 MPa **OR** PZR level > 4.2 m
Heater 3	On: P_{top_RPV} < 15.3 MPa **AND** PZR level > 4.2 m
	Off: P_{top_RPV} > 15.5 MPa **OR** PZR level > 4.2 m
Heater 4	On: P_{top_RPV} < 15.3 MPa **AND** PZR level > 4.2 m
	Off: P_{top_RPV} > 15.5 MPa **OR** PZR level > 4.2 m

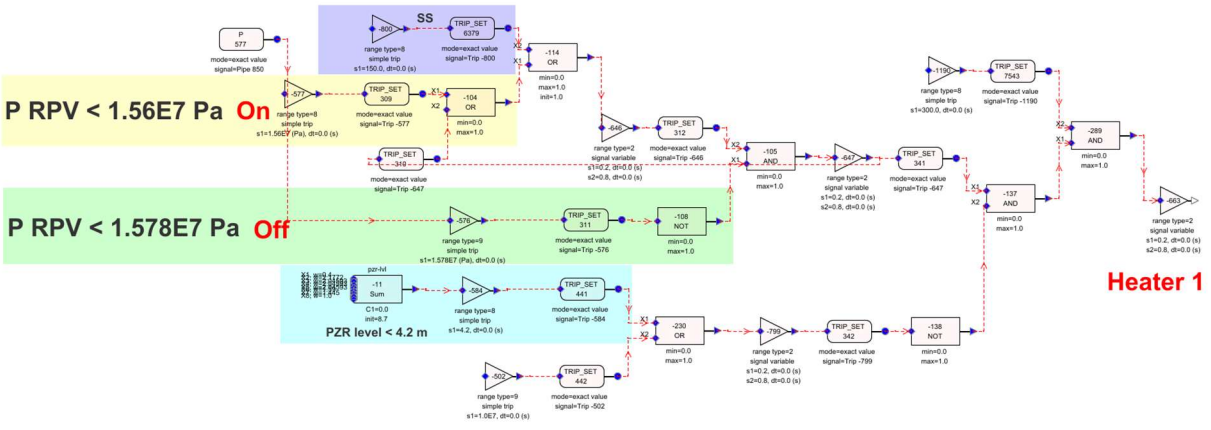

Figure 3-10 PZR heaters on/off signals, VVER-1000/V320 model

Two PZR sprays are modeled with two valves connecting the CL 1 to the upper part of the PZR. This system is designed to reduce the RCS pressure. Therefore, when the pressure in the PZR rises above 16.27 MPa, valve 1 opens and if it continues to rise, valve 2 opens when it reaches 16.46 MPa. Conversely, if the pressure starts to decrease, valve 2 closes at 16.17 MPa and valve 1 closes at 15.97 MPa, see Table 3-5 and Figure 3-11.

Table 3-5 PZR sprays signals, VVER-1000/V320 model

PZR Sprays	
Spray 1	Open: $P_{top\_PZR} > 16.27$ MPa
	Close: $P_{top\_PZR} < 15.97$ MPa
Spray 2	Open: $P_{top\_PZR} > 16.46$ MPa
	Close: $P_{top\_PZR} < 16.17$ MPa

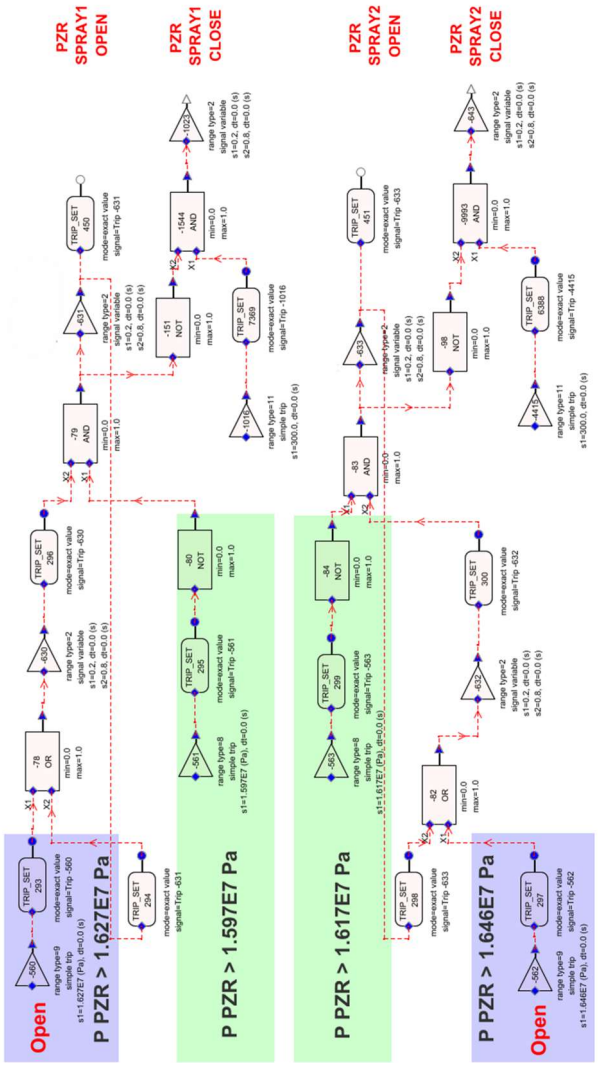

Figure 3-11 PZR spray 1 and 2 actuation signals, VVER-1000/V320 model

The secondary overpressure system included in the model for the VVER-1000/V320 reactor consists of the BRU-A valves and the safety valve located in the SLs and the BRU-K valves located in the MSH. All these valves have opening and closing pressure signals, with the BRU-K setpoint being the lowest and the safety valves setpoint being the highest. This means that if the pressure in the SGs starts to rise, first the BRU-K, then the BRU-A and finally the two safety valves open, see Table 3-6, Figure 3-12, Figure 3-13 and Figure 3-14. It should be noted that the BRU-K valves are not available in SBO conditions, so even if the pressure in the MSH rises above their setpoint, they will not open.

In the model, the BRU-SN valves are also implemented, but no automatic signals are associated with these valves, so they can only be opened by user intervention. On the other hand, there are MSIV in the four SLs downstream of the safety valves. These valves close when the pressure in the SLs falls below 4.9 MPa.

The EFW is modeled as a boundary condition by means of FILL components connected to the secondary side of the four SGs. This safety system begins to inject into the SGs secondary side when the MFW is unavailable. The maximum mass flow rate considered for the EFW system is 41.6 kg/s per SG, with the mass flow rate becoming 0 kg/s when the SG level rises above 2.65 m.

Table 3-6 Secondary overpressure system signals, VVER-1000/V320 model

Secondary overpressure system	
BRU-K	Open: PMSH > 6.667 MPa
	Close: PMSH < 5.786 MPa
BRU-A	Open: P_{SL} > 7.25 MPa
	Close: P_{SL} < 6.27 MPa
Safety Valve 1	Open: P_{SL} > 8.23 MPa
	Close: P_{SL} < 6.86 MPa
Safety Valve 2	Open: P_{SL} > 8.43 MPa
	Close: P_{SL} < 6.86 MPa

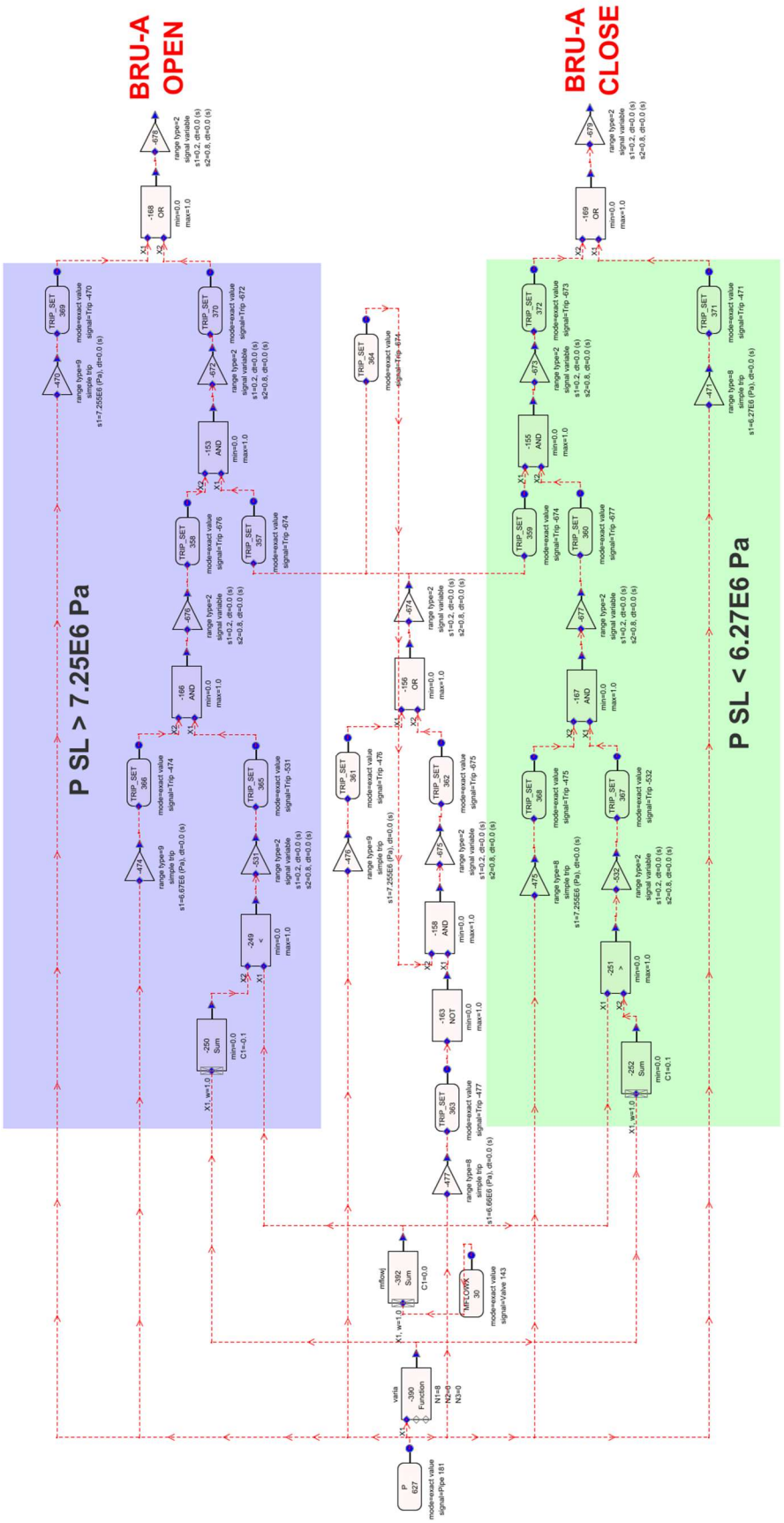

Figure 3-12 BRU-A valves actuation signals, VVER-1000/V320 model

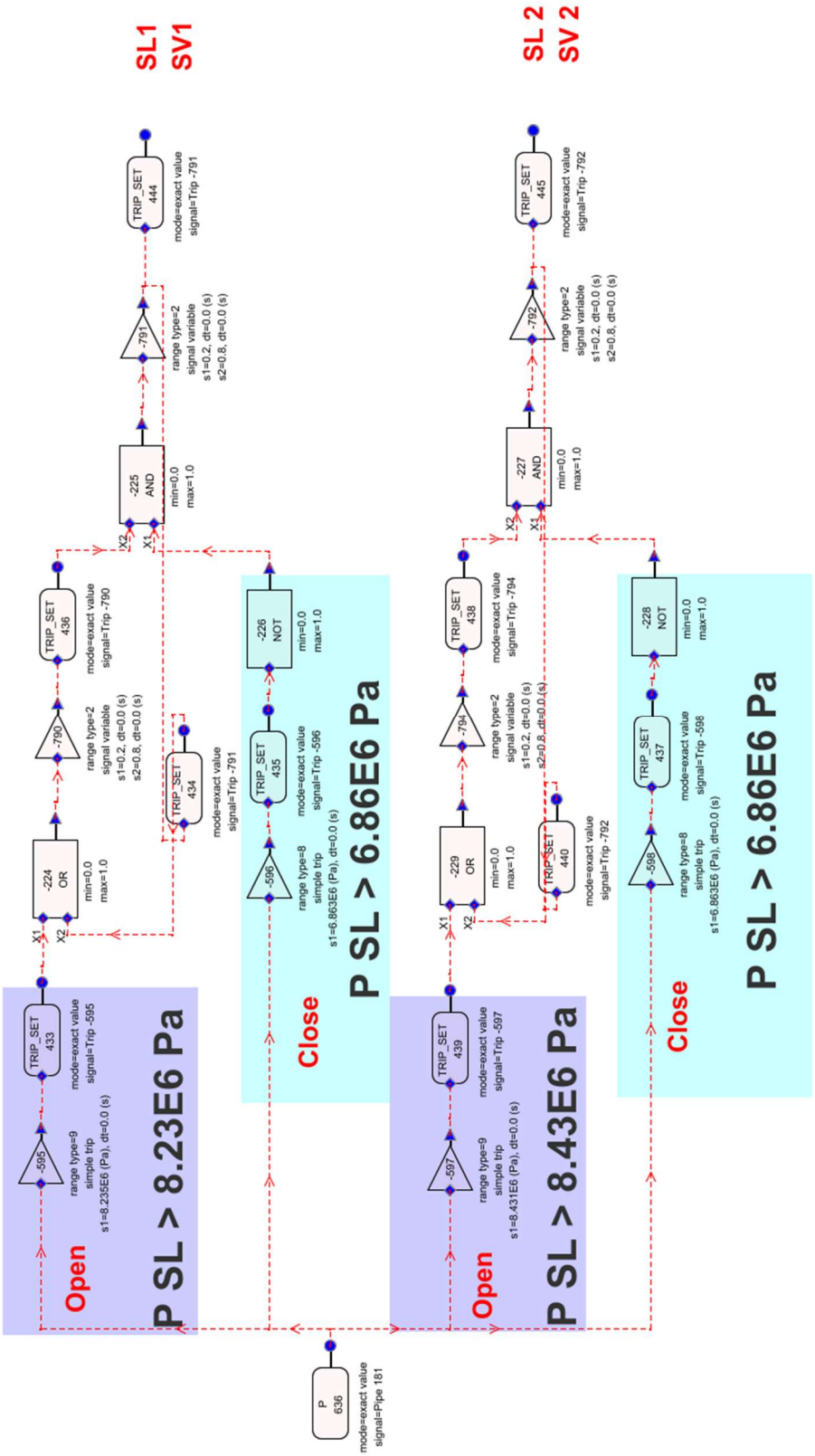

Figure 3-13 SL safety valves 1 and 2 actuation signals, VVER-1000/V320 model

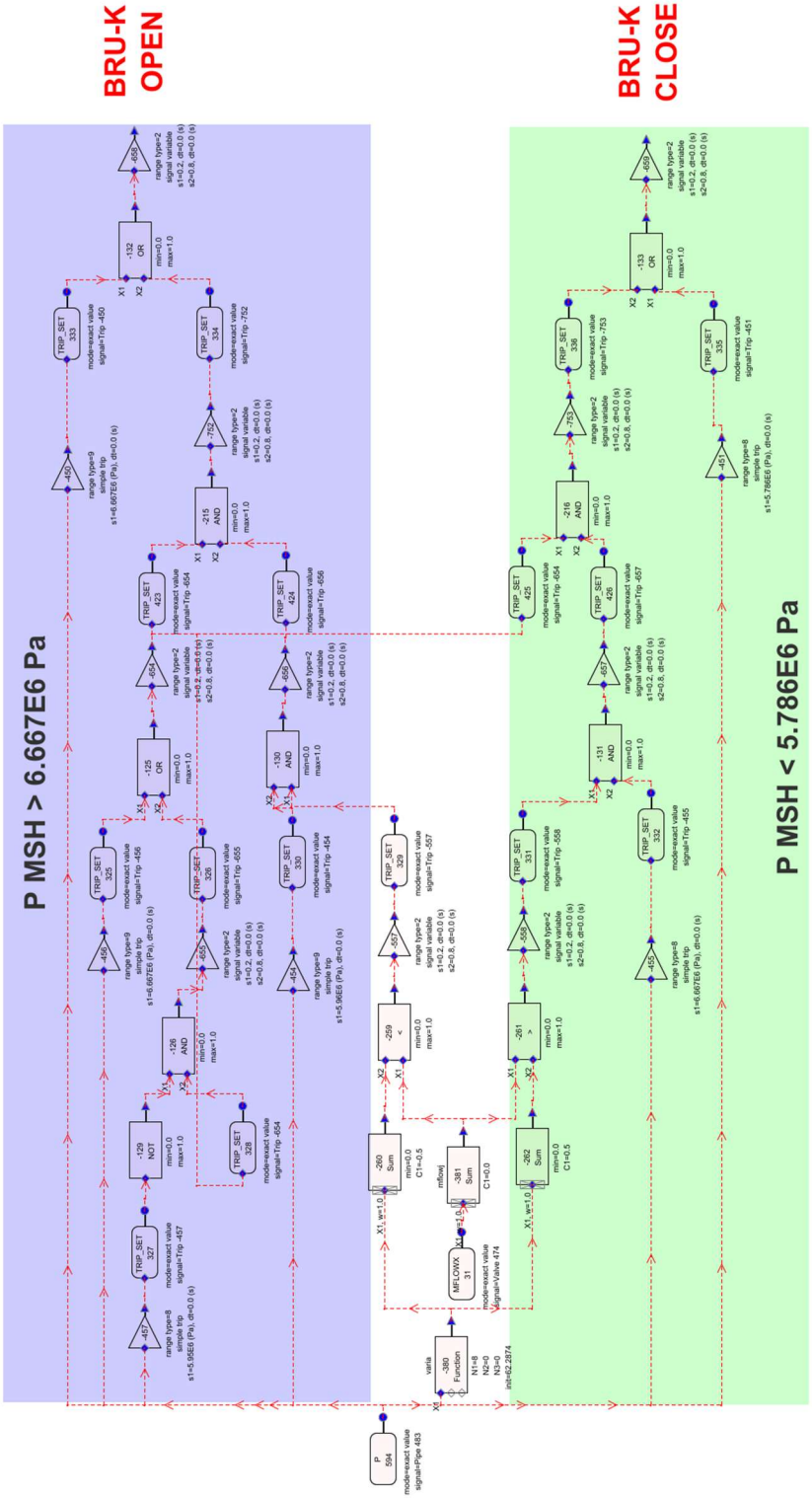

Figure 3-14 BRU-K valves actuation signals, VVER-1000/V320 model

3.4. Human Actions: RCS cooling and depressurization by means of the SGs

The human action consisting of cooling and depressurization of the RCS through the SGs by means of the BRU-A valves has been implemented in the TRACEV5P5 model. This human action is considered in SBLOCA sequences, as the analyzed in Section 5.2. The control implemented calculates the cooling function at 30 K/h or 60 K/h from the average temperature of the RCS at the moment the manual action is started. On the other hand, it measures the average temperature of the four RCS loops and calculates the difference with the value of the cooling curve at 30 K/h or 60 K/h at each time step. This deviation between the average RCS temperature and the control value is then used as input in the control model to give the corresponding opening for the four BRU-A valves at any given time, see Figure 3-15.

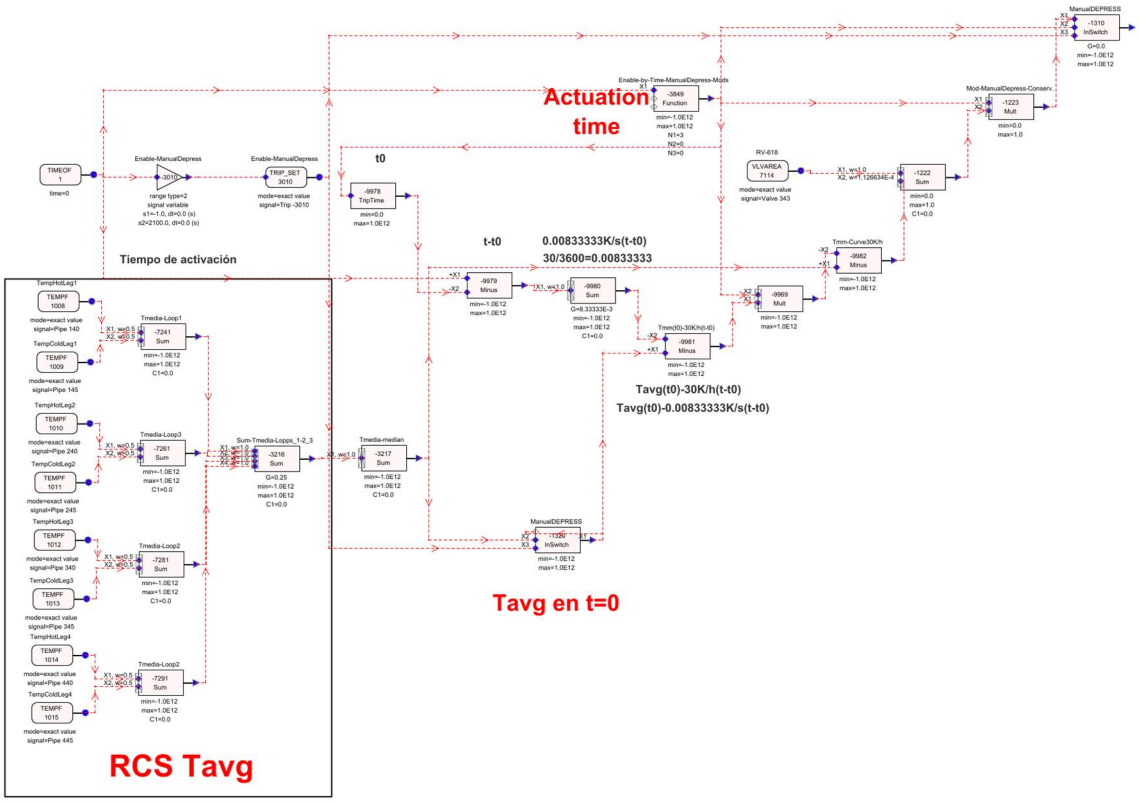

Figure 3-15 RCS cooling and depressurization control, VVER-1000/V320 model

3.5. Advanced passive safety systems

The HA-2 is a PSS included in some Gen-III/III+ VVER designs which, as part of the analysis presented in Chapter 6, has been included in the VVER-1000/V320 model to study its impact on some accident sequences. It should be noted that this PSS is extensively described in Section 2.2.4.

Each of the four HA-2 PSS train has been modeled with a mass flow rate boundary condition by means of FILL components connected to the four HA-1 discharge lines. This approach has been taken because of the lack of sufficient information in public references to accurately model the system using TH components. The four injection stages considered for modeling the HA-2 are those of (ROSATOM, 2022), Figure 3-16. The actuation signal for the HA-2 is activated when the pressure in the RCS is below 1.5 MPa, and this signal also includes a 100 s delay.

In the model, the line connecting the top of the HA-2 to the CLs is also modeled, see Figure 3-17. This line is opened when the HA-2 start to operate, allowing the HA-2 to remain at RCS pressure. This causes some of the inventory from the CLs to be drawn into the HA-2. The inventory sucked in is equal to the volume flow rate being injected by the passive low pressure ECCS. Therefore, the mass flow rate sucked in by the upper lines of the HA-2 is the volumetric flow rate being injected by the HA-2 per the density in the CLs.

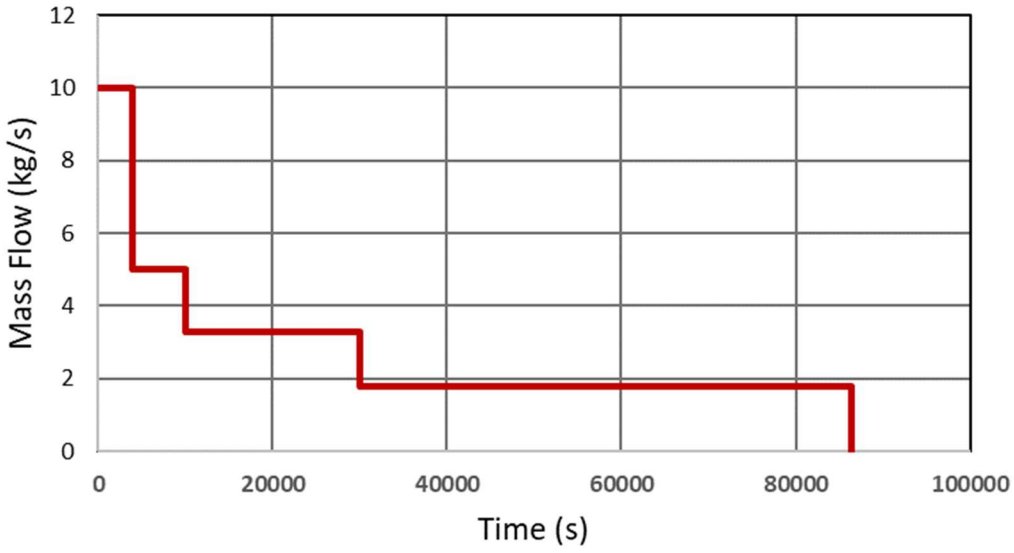

Figure 3-16 HA-2 mass flow rate (per train), VVER-1000/V320 model

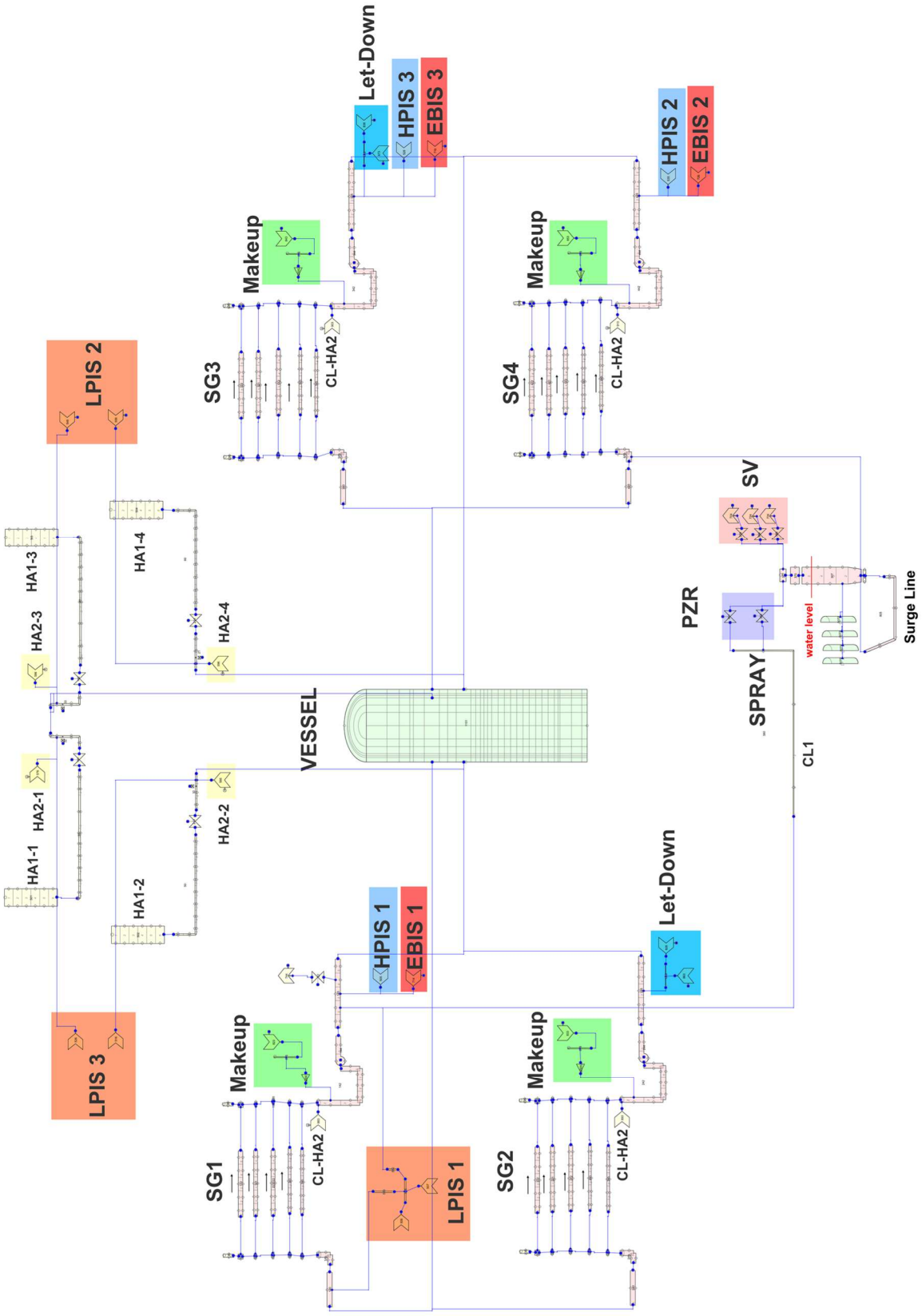

Figure 3-17 VVER-1000/V320 RCS TRACEV5P5 TH model including the HA-2

The air-cooled PHRS is a PSS which has been included in the VVER-1000/V320 model, as part of the analysis presented in Section 6.2. Moreover, it should be noted that the main characteristics, setpoints and operating modes have been defined in Section 2.2.4.

First, an isolated TH model of an air-cooled PHRS train was developed for the TRACEV5P5 system code. This TH model includes the air duct from the air inlet to the outlet, the U-tube of the HXs, the SLs and the condensate lines, see Figure 3-18.

- Air duct: the three air ducts of each train have been modeled in a single one. In the model, the air ducts can be differentiated into three sections modeled with a PIPE component each:
    - Air duct between the upper air gate and the atmosphere.
    - Air duct between the upper air gate and the regulator.
    - Air duct between the regulator and the lower air gates. Here is the HEAT-STRUCTURE coupled to the PIPE where the heat transfer to the SGs takes place.

  The inlet and outlet of the air duct have been modeled using pressure boundary conditions. In a first calculation of the pressure drop, the difference in height between the air duct inlet and outlet and the air density were taken into account. The pressure difference was then further adjusted to avoid generating a non-zero air flow in the absence of a heat source in the PHRS.
- PHRS Tube bundle: The tube bundle has been modeled with a single PIPE component, with three slopes to properly reproduce the U-shape of the pipes. In the available references it has been found that the tubes diameter of the PHRS is around 0.03 m, so this has been chosen as the tubes diameter for the model, see (Ma et al., 2021; Yücehan-Kutlu, 2019).

  The heat transfer between the PHRS tube bundle and the air duct has been modeled using a HEAT STRUCTURE with cylindrical geometry The inner surface is connected to the PIPE component that represents the PHRS tube bundle, while the outlet surface is linked to the first cell of the PIPE modeling the air duct between the regulator and the lower air gates. The HEAT STRUCTURE follows the nodalization of the PIPE representing the PHRS tube bundle, consisting of eight cells with a one-to-one connection.

- Steam lines and Condensate lines: both lines have been modeled using PIPE components, with each PIPE divided into six cells.

To verify the performance of the isolated model of an air-cooled PHRS train, the power that it can remove at different pressures has been determined. The results obtained have been then compared with the results from the FSAR code for an isolated PHRS model of the KKNPP (Khubchandani et al., 2013a) . In order to have a comprehensive view of the behaviour of the PHRS under different outdoor conditions, the PHRS power vs. pressure curves have been obtained for various air temperatures: 10 ºC, 20 ºC, 30 ºC and 40 ºC, see Figure 3-19.

Each curve has been obtained for a total of nine pressure values, from 0.1 MPa to 8 MPa. It is noteworthy that the TRACE model curves are very close to the KKNPP curves from 0.1 MPa to 8 MPa. The value for atmospheric pressure at KKNPP is not available in (Khubchandani et al., 2013a), but it can be found in (Kopytov et al., 2009), that the power for a pressure of 0.15 MPa is about 15 MW for an outside temperature of 38 ºC at the Novovoronezh NPP, which is about 3.75 MW per train, see Figure 3-19.

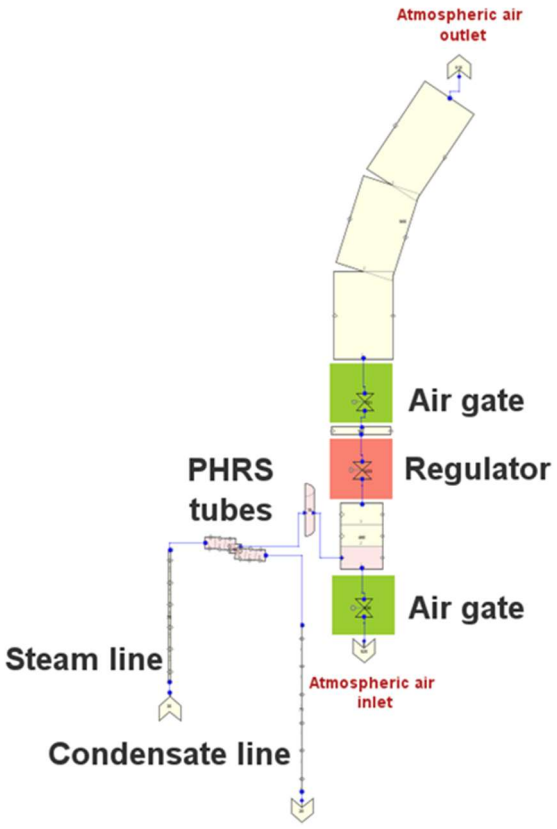

Figure 3-18 air-cooled PHRS (one train) isolated TH model for the TRACEV5P5 code

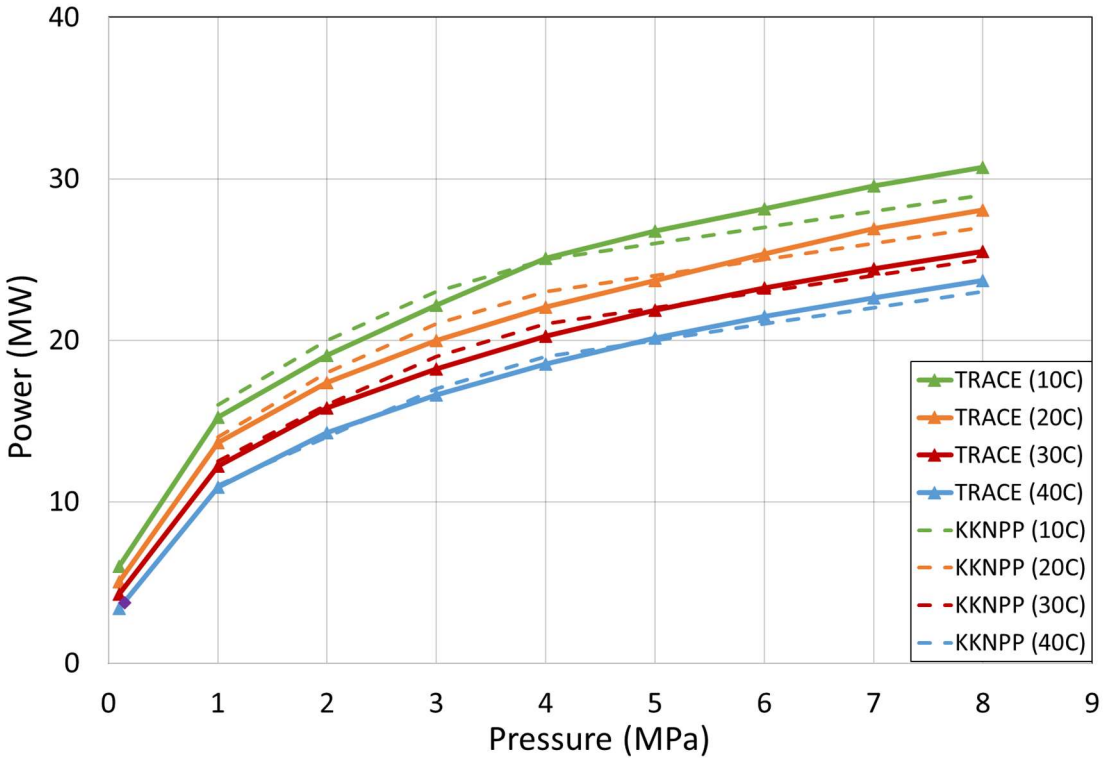

Figure 3-19 TRACEV5P5 air-cooled PHRS model, power vs. SGs pressure curves

Once the performance of the isolated model has been verified, it has been implemented in the VVER-1000/V320 model, see Figure 3-20. This system starts operating when both the upstream and downstream air valves open. In the TRACEV5P5 model, these valves have two opening signals: SBO conditions and SG pressure above 8.44 MPa, see Table 3-7. These signals have a delay of 30 s and the valves take 90 s to be fully open.

The air-cooled PHRS has two operating modes depending on the position of the regulators: SG pressure maintenance mode and RCS cool-down mode. The SG pressure maintenance mode consists of controlling the regulator to maintain the SG pressure within 5.35 and 6.05 MPa. This mode has been incorporated into the TH mode by means of a control that determines the regulators area as a function of the SG pressure in the following way:

- When the SGs pressure is above 6.05 MPa, the regulators are fully open.
- When the SG pressure starts to drop below 6.05 MPa, the regulators start to close.
- When the SGs pressure drops below 5.35 MPa, the regulators close completely.

On the other hand, the RCS cool-down mode consists in keeping the regulator fully open in order to achieve a rapid depressurisation of the SGs and thus of the RCS. This mode has been incorporated into the TH mode by means of an HLs subcooling signal ($T_{sat} - T_{HL} < 8$ °C) which forces the regulators to remain fully open, overriding the regulator area control.

Table 3-7 PHRS actuation signals, VVER-1000/V320 model

air-cooled PHRS	
SBO condition	**OR**
P SGs > 8.44 MPa	

In addition, SNAP tools have been used to create a video mask of the VVER-1000/V320 reactor model for the TRACEV5P5 system code, including the HA-2 and the air-cooled PHRS, see Figure 3-21. This enabled the generation of videos showing various parameters such as void fraction in the hydraulic components. This provided a comprehensive view of the response of the plant model to the sequences analyzed.

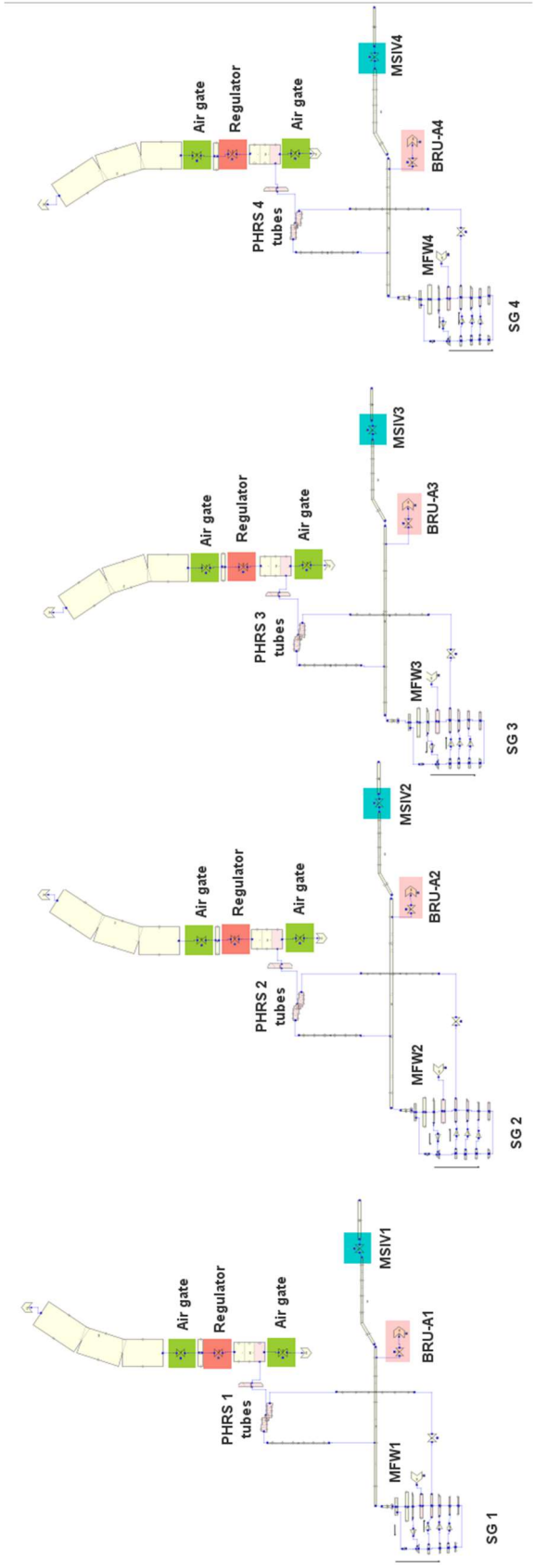

Figure 3-20 VVER-1000/V320 secondary circuit TRACEV5P5 TH model including the PHRS

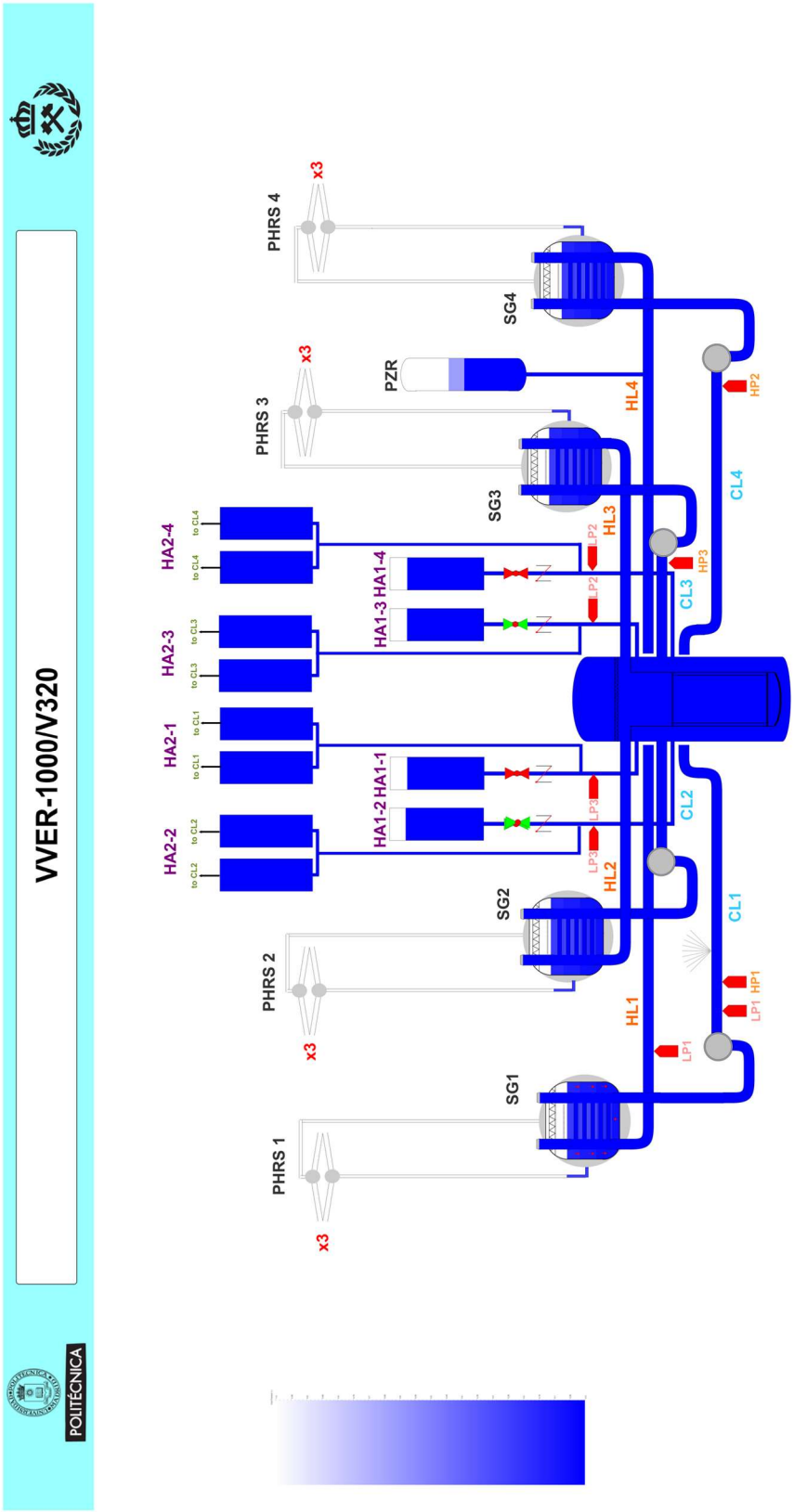

Figure 3-21 SNAP video for VVER-1000/V320 TRACEV5P5 model including HA-2 and air-cooled PHRS

3.6. Steady State model results

In order to demonstrate the proper performance of the VVER-1000/V320 model developed for the TRACEV5P5 code, including both PSS, the HA-2 and the air-cooled PHRS, the SS values of the model are compared with reference data from the VVER-1000/V320 at Kozloduy NPP (Kolev et al., 2006) in Table 3-8. It can be observed that the data from the simulation are close to the data from the real values of the NPP.

Table 3-8 SS values, VVER-1000/V320 model

Parameter	Reference NPP	TRACEV5P5
Core Power (MW)	3010	3010
Core outlet pressure (MPa)	15.70	15.74
PZR level (m)	8.70	8.71
CLs temperature (K)	560.85	560.96
HLs temperature (K)	591.55	591.13
Average RCS loop mass flow rate (kg/s)	4456.00	4457.21
SG outlet pressure (MPa)	6.27	6.27
MFW mass flowrate (kg/s)	409.00	408.09
MFW temperature (K)	493	493
SGs level (m)	2.50	2.50

Chapter 4. Verification sequences of the VVER-1000/V320 TRACEV5P5 model

To validate the TRACEV5P5 model for the VVER-1000/V320 reactor and ensure that all safety system signals and models have been correctly implemented, five sequences have been conducted:

- Reactor SCRAM
- MCPs Trip
- Station Blackout
- Large Loss Of Coolant Accident (LBLOCA)
- Small Loss Of Coolant Accident (SBLOCA).

In order to verify the reliability of the results obtained by the model developed for the TRACEV5P5 system code, it has been necessary to gain insight into the expected behaviour of VVER-1000/V320 reactors during accidental scenarios that are typically studied in nuclear safety.

For this purpose, an extensive literature review of public references on transient analysis in VVER-1000/V320 reactors has been performed, see Table 4-1. The accidental sequences found are SBO, SBLOCA, LBLOCA, Steam Generator Tube Rupture (SGTR), Total Loss of Feed Water (TLFW), MCP Trip, MCP startup, loss of "core cooling" in cold conditions, ATWS, BRU-A opening and SLB.

Table 4-1 VVER-1000/V320 accidental sequences references

Sequence	Reference
SBO	(Chatterjee et al., 2009; Groudev and Kitchev, 1998; Mazzini et al., 2015; Pavlova et al., 2007; Tusheva, 2012; Tusheva et al., 2010, 2009)
LBLOCA	(Chatterjee et al., 2010, 2008a, 2008b; Dina et al., 2019; Khalil Mousavian et al., 2003; Sabotinov and Srivastava, 2008; GadEl-karim et al., 2025)
SBLOCA	(Belozerov et al., 2019; Chatterjee et al., 2010, 2008b; Groudev et al., 1997; Groudev, 1998; Sabotinov et al., 2013)
SGTR	(Gencheva and Groudev, 2000)
TLFW	(Gencheva et al., 2005; Muellner et al., 2005; Pavlova et al., 2004)
One MCP Switching-on	(Groudev and Pavlova, 2004, 2002; Iegan et al., 2018; Petkevich et al., 2011; Skalozubov et al., 2010)
Loss of "Core cooling" in cold condition	(Groudev and Andreeva, 2016; P.P Groudev and Georgieva, 2010)
ATWS	(Velkov et al., 2009)
BRU-A opening	(Macek and Vyskocil, 2013)
SLB	(Stefanova et al., 2002)
Inadvertent MSIV Closure	(Iegan et al., 2018)

4.1. Reactor SCRAM sequence

The SCRAM signal occurs at 2000 s. Due to the delay time, the CRAs start inserting 0.3 s later and take 4 seconds to be fully inserted into the core. The SCRAM causes RCS pressure decrease to 13.30 MPa in the first 35 s and the PZR level drop to 5.38 m, Figure 4-1 and Figure 4-2.

Subsequently, the pressure starts to increase until it reaches the PZR spray setpoint, which cycle three times until close definitely. Because there is no MCPs trip, the forced circulation continues, so the HL temperature is similar to the CL temperature, Figure 4-3.

In the SGs, the pressure decreases until the TT actuates. Subsequently, the pressure increases until the MFW pumps trip and the starts of the EFW pumps. Finally, BRU-K valves start to cycle to maintain the SGs pressure between the opening/closure setpoint of the BRU-K valves, Figure 4-1. The sequence of the SCRAM is shown in Table 4-2.

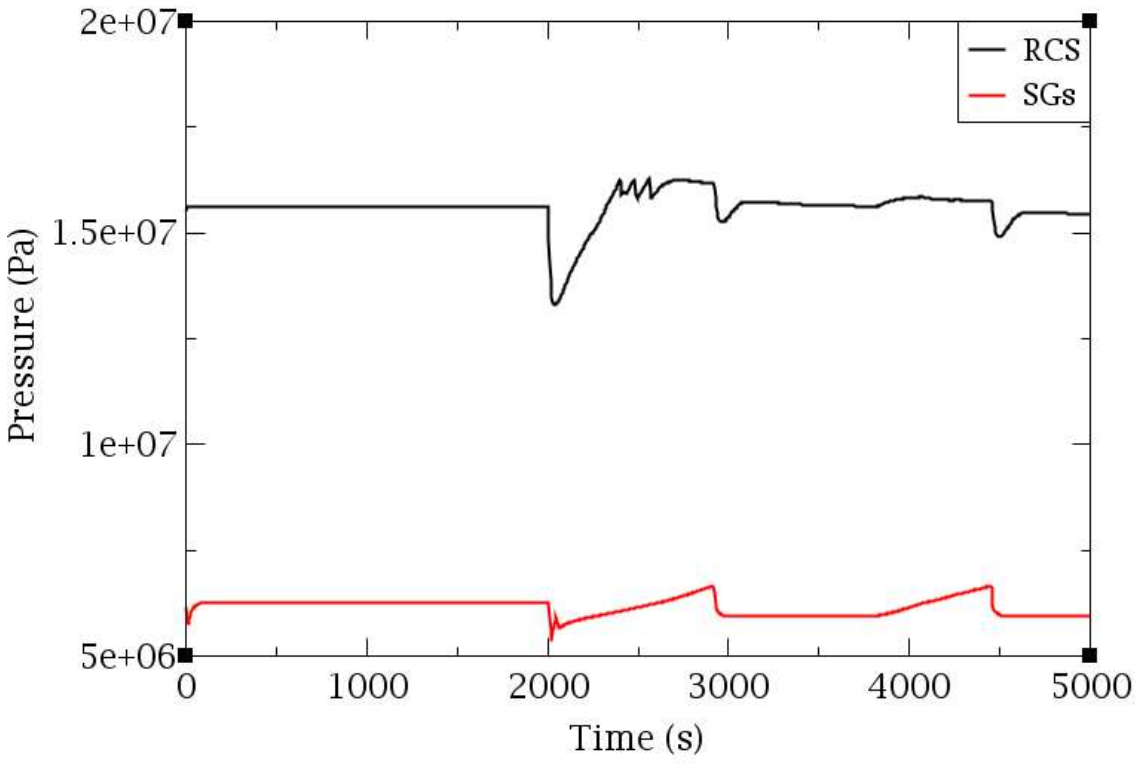

Figure 4-1 RCS and SGs pressure, reactor SCRAM sequence

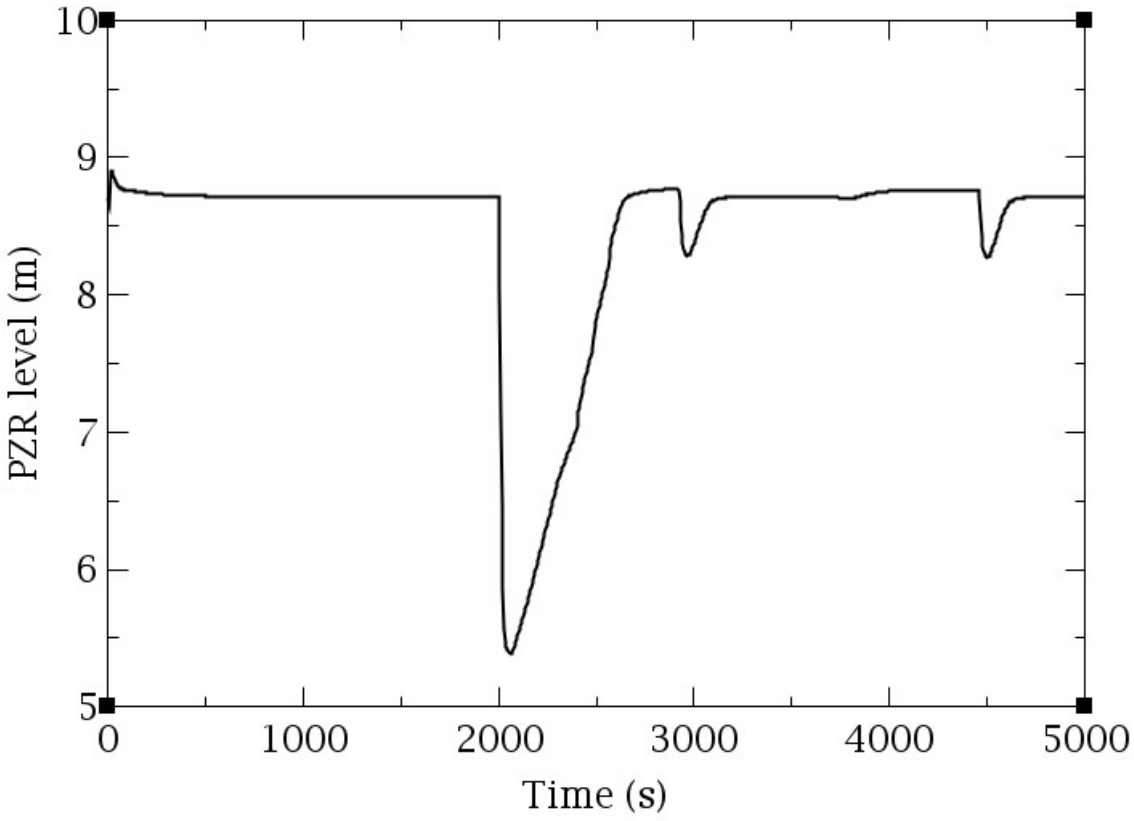

Figure 4-2 PZR level, reactor SCRAM sequence

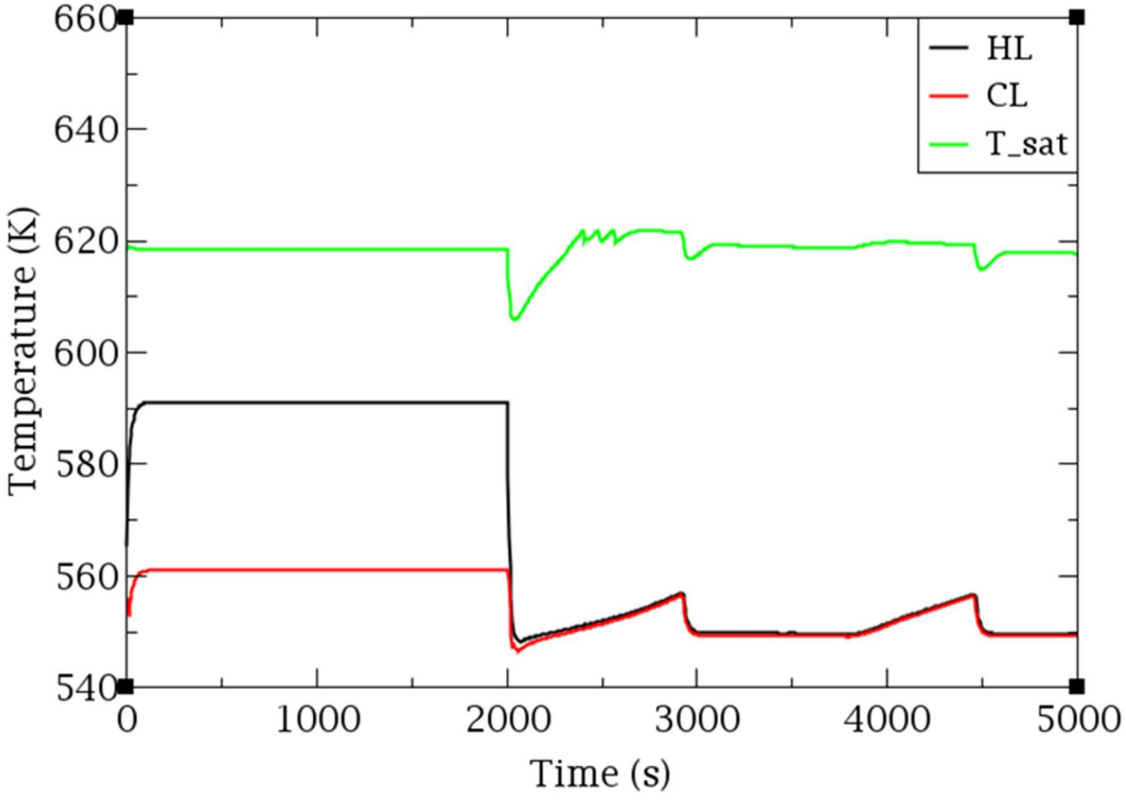

Figure 4-3 RCS temperature, reactor SCRAM sequence

Table 4-2 Reactor SCRAM sequence events

Time (s)	Event
2000	SCRAM signal
2000.3	SCRAM actuation (signal + delay)
2004.3	CRAs fully inserted
2005	PZR heaters 2, 3 and 4 on (P_{top_RPV} < 15.6 MPa)
2006	TT and MFW/EFW trip signal (P_{HL} < 14.71 MPa)
2020	TT (signal + delay)
2045	MFW/EFW trip (signal + delay)
2401	PZR Spray begins to cycle (P_{top_PZR} > 16.27 MPa)
2571	PZR Spray off (P_{top_PZR} < 15.97 MPa)
2916	BRU-K valves open (P_{MSH} > 6.66 MPa)
4588	PZR heaters 3 and 4 off (P_{top_RPV} > 15.5 MPa)
4763	PZR heater 2 off (P_{top_RPV} > 15.78 MPa)

4.2. MCPs trip sequence

The MCP trip occurs at 2000 s from the beginning of the sequence. The SCRAM immediately occurs, because more than two MCPs have started the cost-down with the reactor power level above 75 %.

Thereafter, the RCS pressure decreases to 13.39 MPa, see Figure 4-4, and the PZR level decreases approximately 3 m, Figure 4-5, in the first 39 s. Then, it starts to rise until it reaches the setpoint of the PZR sprays, so the RCS pressure starts to decrease again, Figure 4-4. Due to there is MCPs trip, the temperature difference between the HLs and the CLs increases sharply after RCSs cost-down, Figure 4-6.

In the SGs, the pressure decreases until the TT actuates. Subsequently, the pressure increases until the MFW pumps trip and the start-up of the EFW pumps occurs. Finally, BRU-K valves start to cycle to maintain the SGs pressure between the opening/closure setpoint of the BRU-K valves, Figure 4-4. The sequence of the

MCPs trip transient is shown in Table 4-3

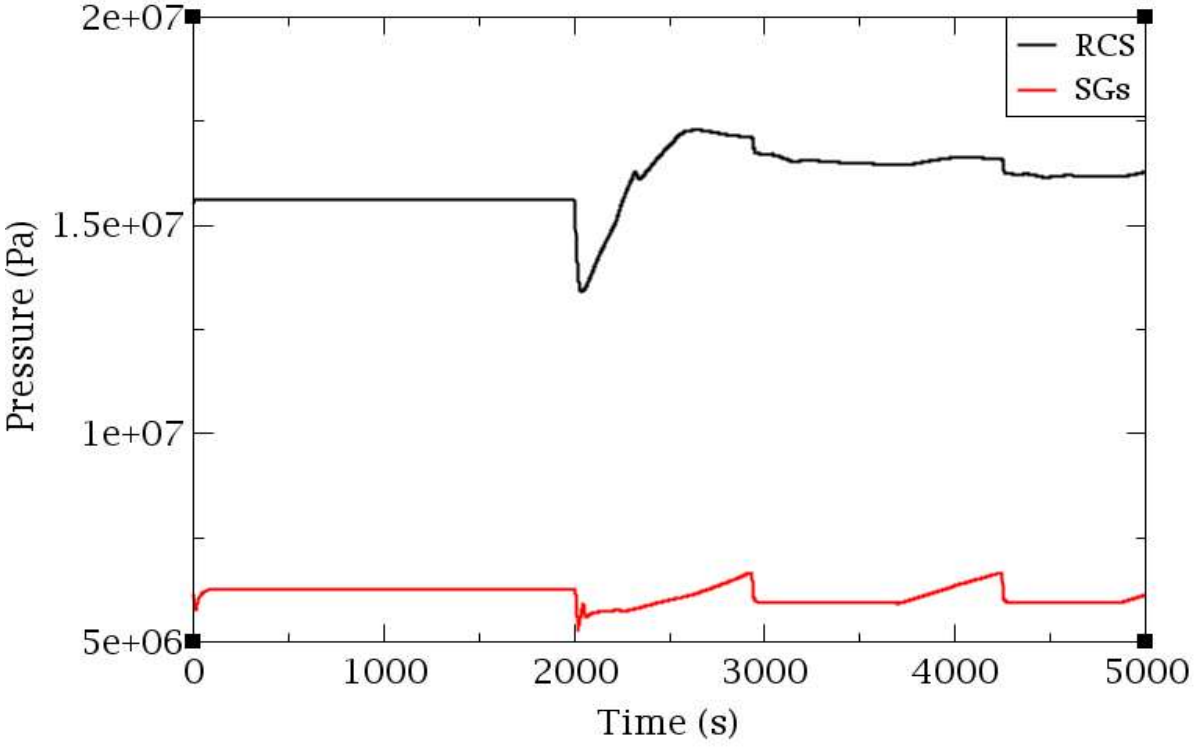

Figure 4-4 RCS and SGs pressure, MCPs trip sequence

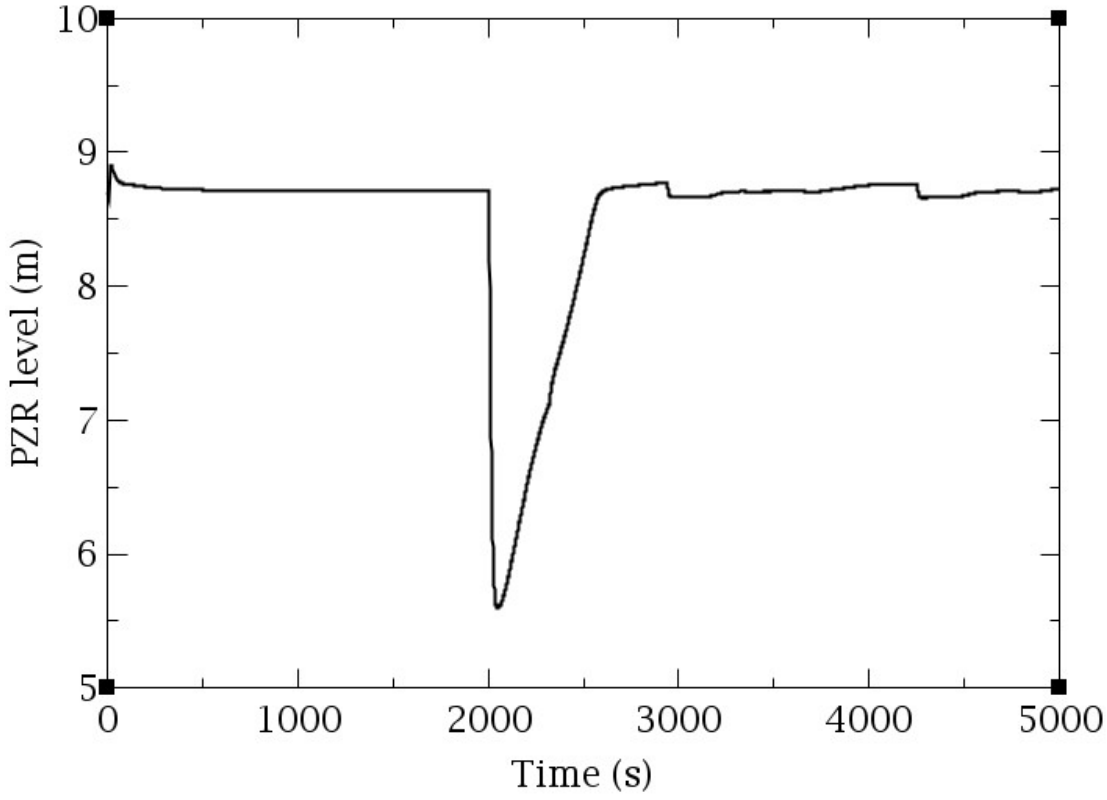

Figure 4-5 PZR level, MCPs trip sequence

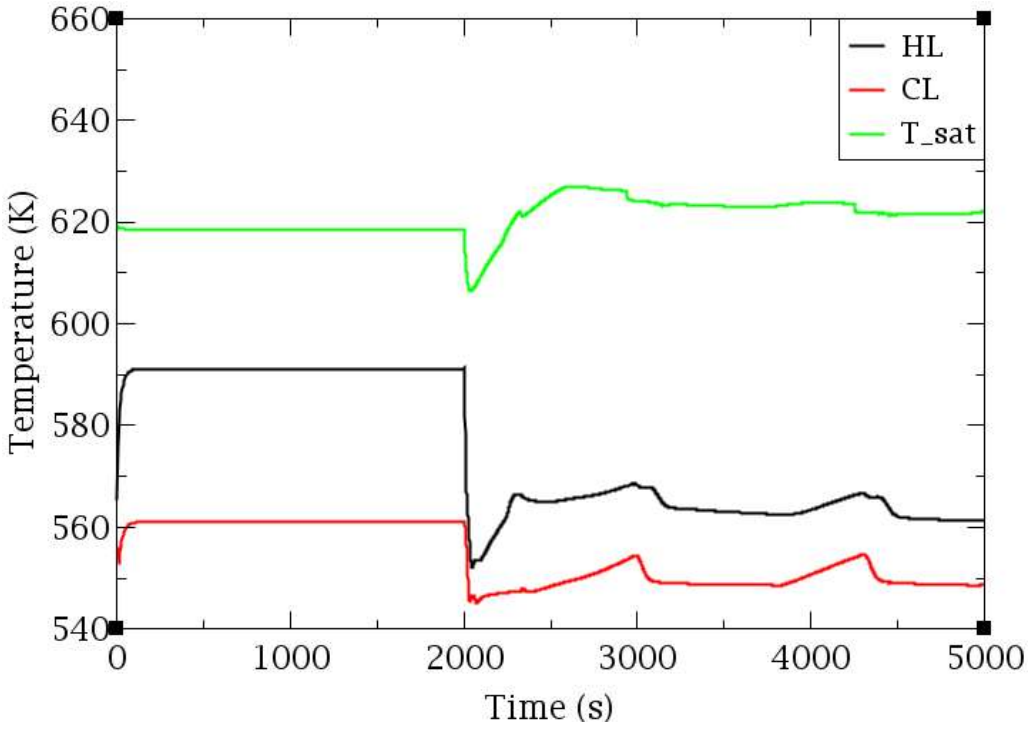

Figure 4-6 RCS temperature, MCPs trip sequence

Table 4-3 MCPs trip sequence events

Time (s)	Event
2000	MCPs cost-down SCRAM signal
2000.3	SCRAM signal + delay
2003	PZR heaters on (P_{top_RPV} < 15.6 MPa)
2004.3	CRAs fully inserted
2007	TT and MFW/EFW trip signal (P_{HL} < 14.71 MPa)
2021	TT (signal + delay)
2047	MFW/EFW trip (signal + delay) PZR level = 5.38 m
2032	MCP angular velocity = 0 rad/s
2243	PZR heaters off (P_{top_RPV} > 15.5 MPa)
2319	PZR Spray on (P_{top_PZR} > 16.27 MPa)
4445	PZR Spray off (P_{top_PZR} < 15.97 MPa)
2927	BRU-K valves open (P_{MSH} > 6.66 MPa)

4.3. Station Blackout (SBO) sequence

The SBO sequence starts 300 s after the beginning of the sequence, see Figure 4-7. While there is water in the SGs, the RCS is cool-down via the secondary side. Once the SGs are emptied, around 8500 s, Figure 4-8, the pressure in the RCS is controlled by the PZR valves, Figure 4-7, which means the loss of the RCS inventory and therefore the uncovering of the core because there is no active ECCS injecting water to the RCS, see Figure 4-9 and Figure 4-10. Finally, it can be seen as the Peak Cladding Temperature (PCT) reaches 1477 K near to the 14400 s. The sequence events of the SBO transient are shown in Table 4-4.

It should be noted that in this sequence the SLOCA has not been considered. If SLOCA is considered, the sequence event could be different as RCS inventory is lost from the beginning of the transients instead of the beginning of the opening of the PZR valves.

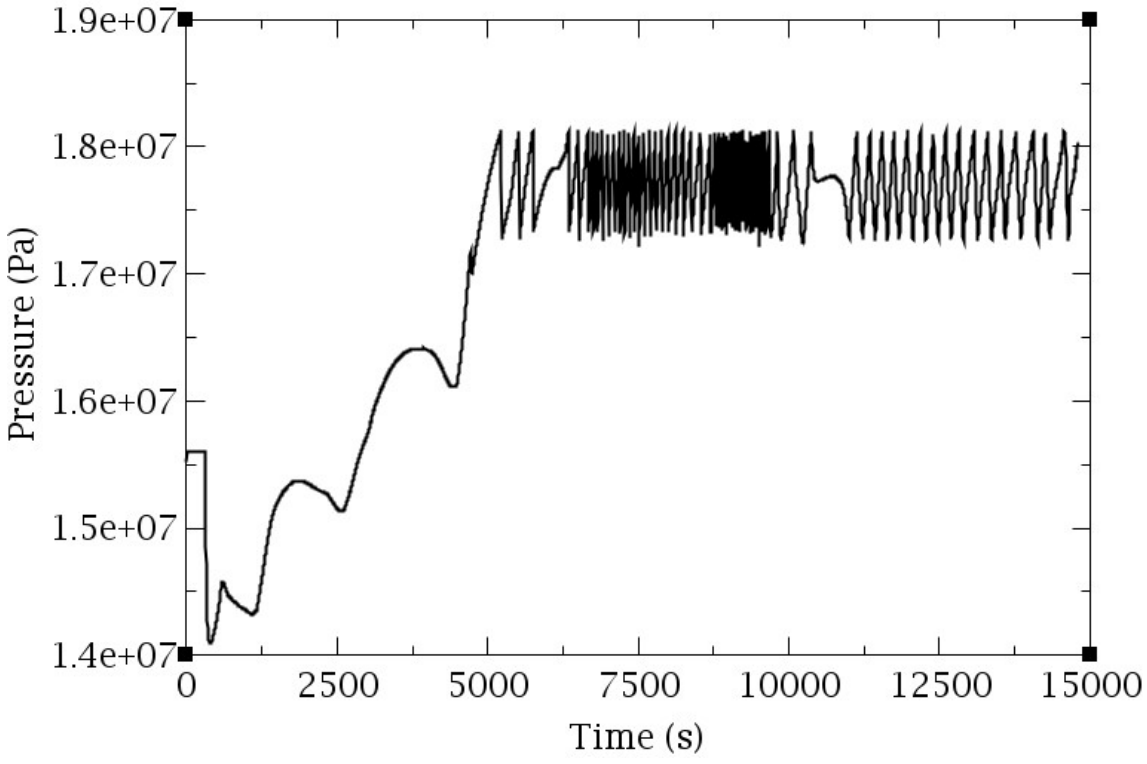

Figure 4-7 RCS pressure, SBO sequence

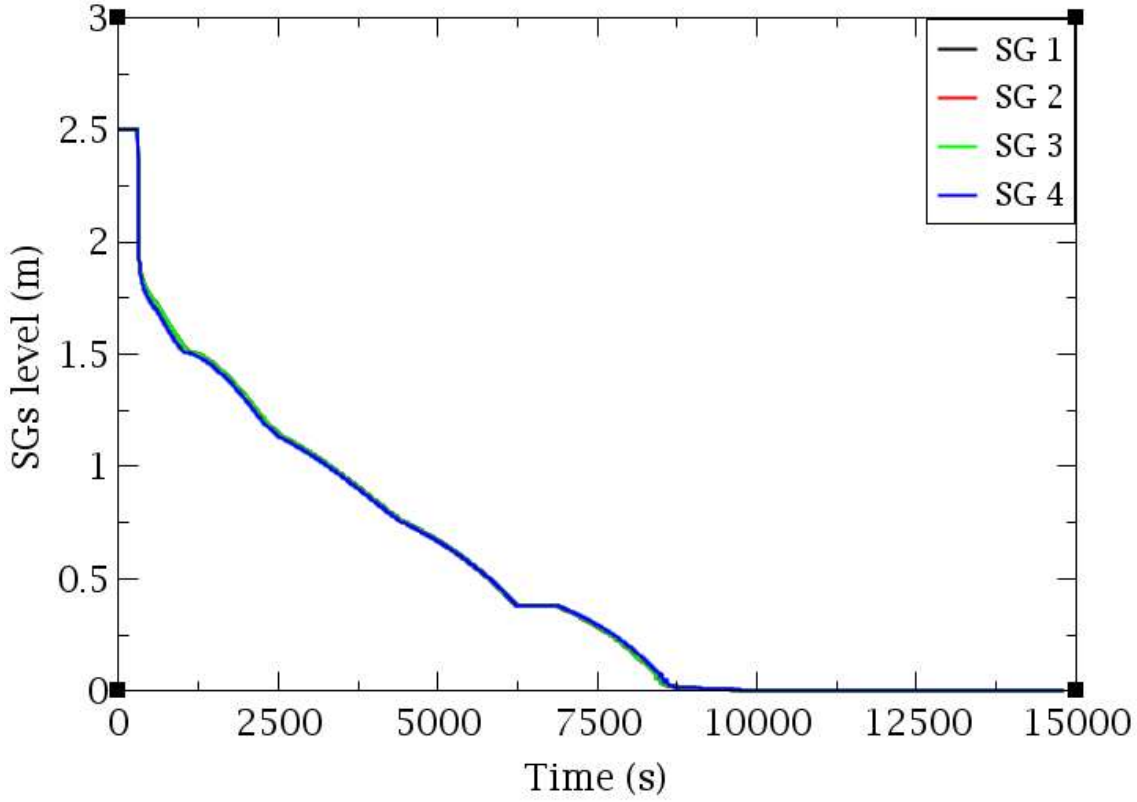

Figure 4-8 SGs level, SBO sequence

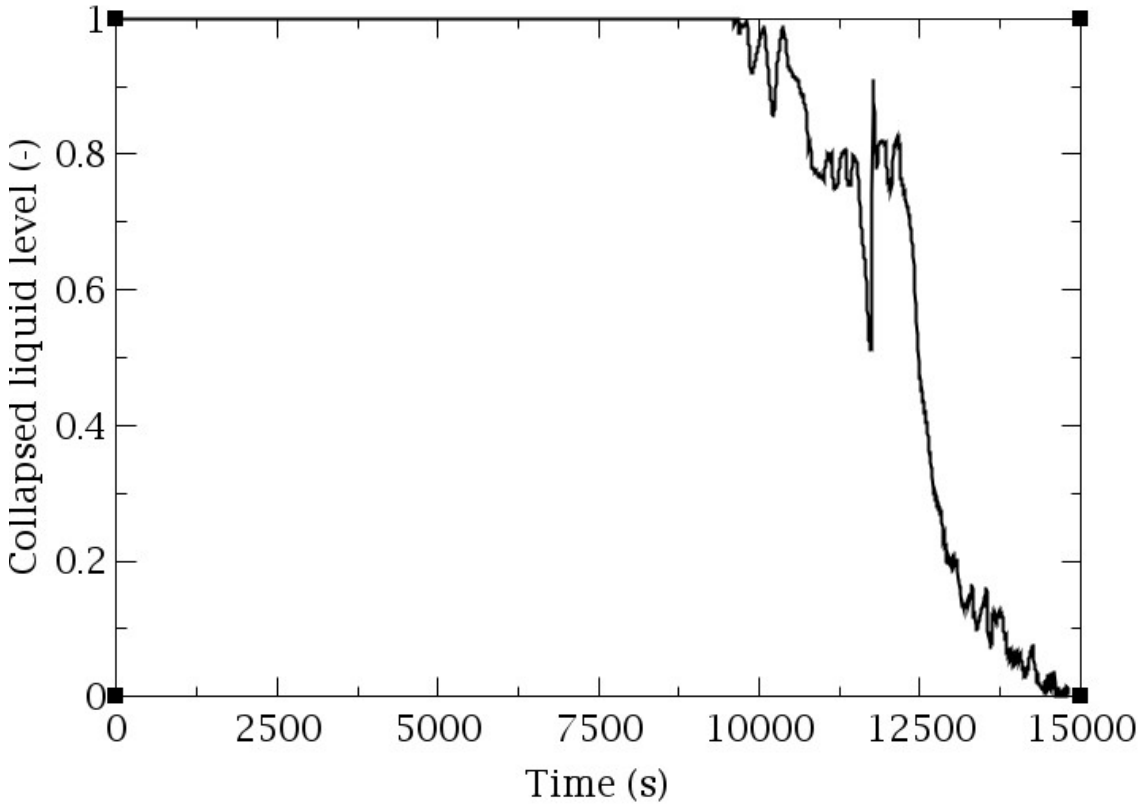

Figure 4-9 Collapsed liquid level, SBO sequence

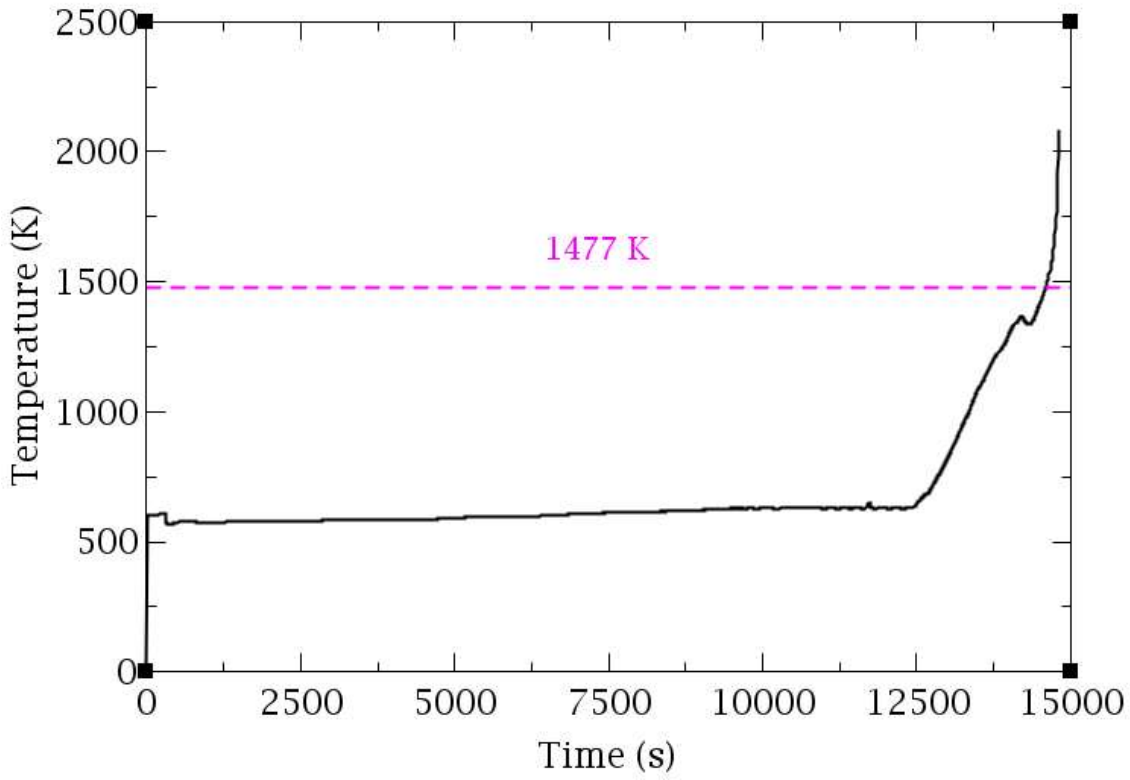

Figure 4-10 PCT, SBO sequence

Table 4-4 SBO sequence events

Time (s)	Event
300	SBO (SCRAM, MFW pumps and MCPs trip, TT, loss of the condenser, CVCS off)
300.3	CRAs fully inserted
308	BRU-A valves open (P_{SL} > 7.25 MPa)
332	MCP angular velocity = 0 rad/s
4498	PZR relief and safety valves begins to cycle (P_{top_PZR} > 18.13 MPa)
9450	Collapsed liquid level in the core starts to decrease
12565	Core uncovered
14400	PCT > 1477 K

4.4. Large Break Loss Of Coolant (LBLOCA) sequence

The Double Ended Guillotine Break (DEGB) LBLOCA, located in the CL 1, occurs at 300 s. The availability systems considered for the sequence are those of the SC of the LBLOCA ET, which has been discussed in Section 2.3:

- 2 out of 4 HA-1
- 1 out of 3 LPIS trains
- 0 out of 3 HPIS trains

During the first seconds of the transient the RCS pressure reaches nearly atmospheric values, see Figure 4-11 while the collapsed liquid level in the core reaches values near to the 10%, see Figure 4-12. Despite the quick actuation of two HA-1 and one LPIS train, core reflooding is not completed until 1620 s. At 2500 s, the LPIS mass flow rate equals the break leakage and the collapsed liquid level in the core is stabilized allowing to reach a pseudo-SS. Then, it can be seen that CD has not occurred, since the PCT does not exceed 1477 K, see Figure 4-13 and the Local Maximum Oxidation did not surpass 6.7%, see Figure 4-14. The sequence events of the LBLOCA transient are shown in Table 4-5.

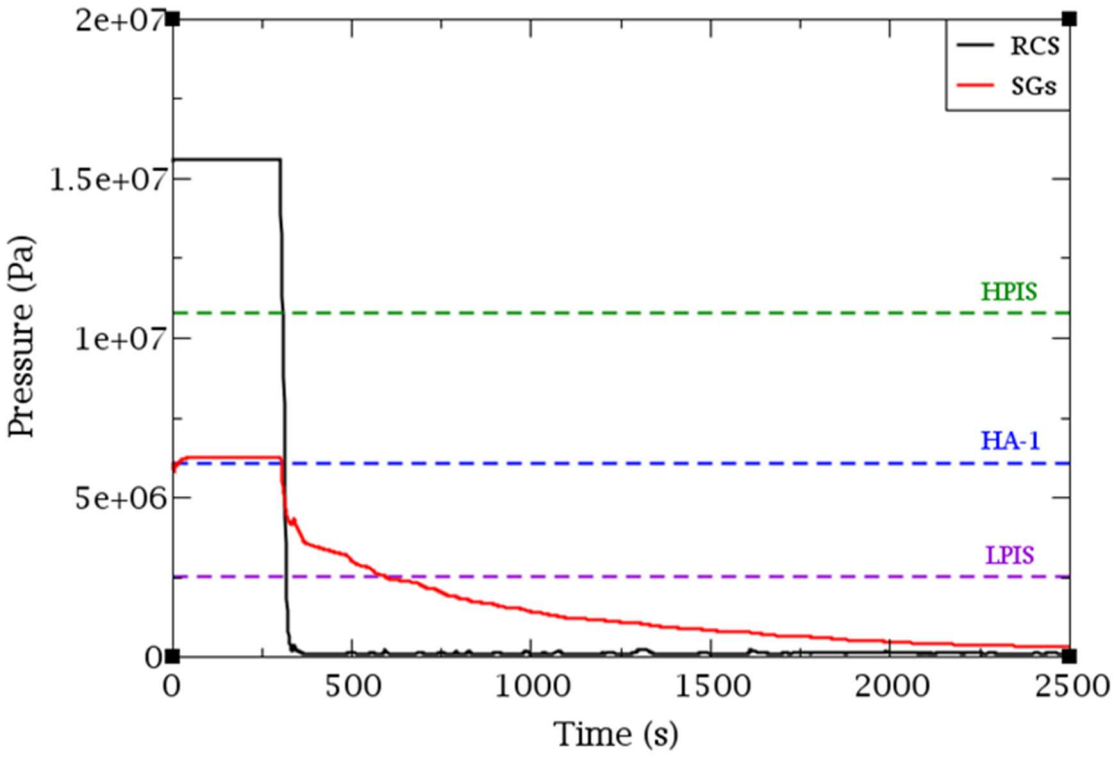

Figure 4-11 RCS and SGs pressure, DEGB LBLOCA sequence

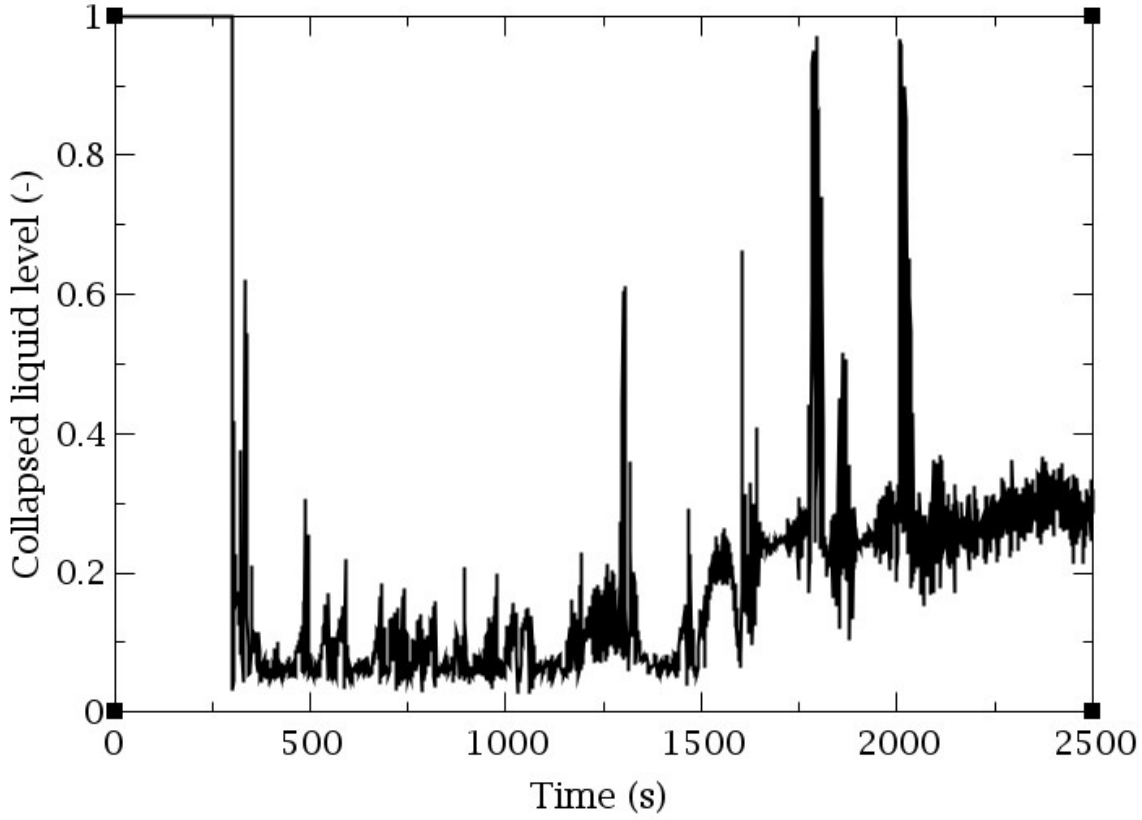

Figure 4-12 Collapsed liquid level, DEGB LBLOCA sequence

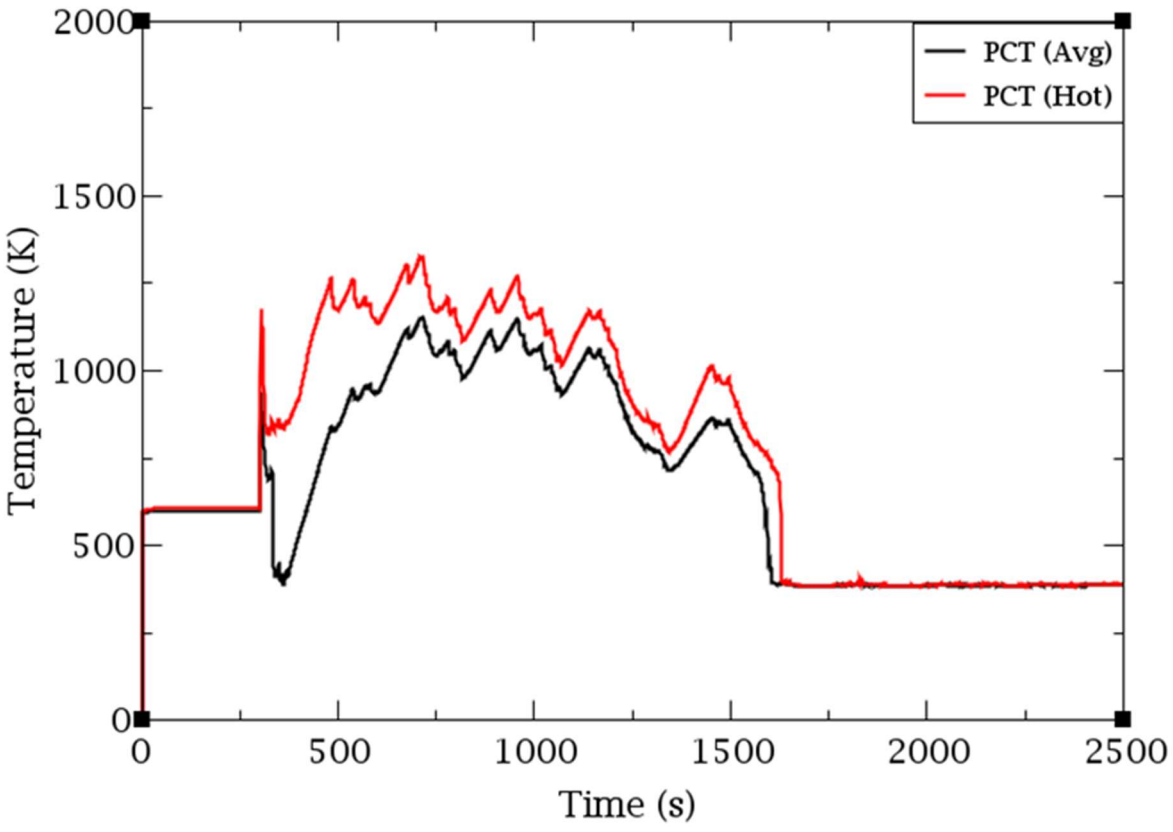

Figure 4-13 PCT, DEGB LBLOCA sequence

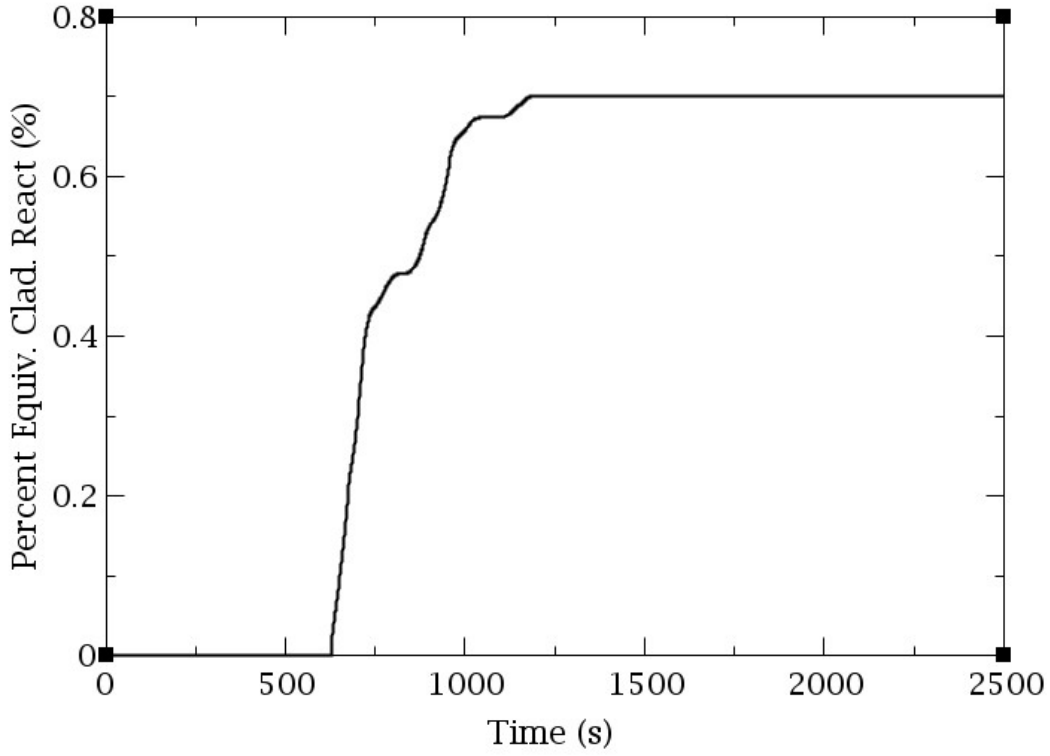

Figure 4-14 Equivalent Cladding Reacted, DEGB LBLOCA sequence

Table 4-5 DEGB LBLOCA sequence events

Time (s)	Event
300	DEGB-LBLOCA
302	SCRAM signal (Power > 2250 MW and $P_{core\ outlet}$ < 14.7 MPa) TT signal and MFW pumps shutdown signal (P_{HL} < 14.7 MPa)
302.3	Start of the CRAs insertion (signal + delay)
310	MCPs coast-down begins (P_{SL}< 4.69E6 Pa and SG level < 2m) Closing of the MSIV (P_{SL} < 4.69 MPa) Start of HA-1 and HA-4 injection ($P_{DC/UP}$ < 6.07 MPa)
315	TT (signal + delay + turbine closing time) Start LPIS injection (P_{DC} < 2.55 MPa and $T_{HL}^{sat} - T_{HL}$ < 10 K)
340	MFW pumps trip (signal + delay)
760	Maximum PCT (1253 K)
1390	Collapsed liquid level starts to increase
1620	Core reflooding ends
2500	Collapsed liquid level in the core is stabilized.

4.5. Small Break Loss Of Coolant (SBLOCA) sequence

The SBLOCA (2 inches), located in the CL 1, occurs at 300 s. The availability systems considered for the sequence are those of the SC for the SBLOCA ET, which has been discussed in Section 2.3:

- 2 out of 4 HA-1
- 1 out of 3 LPIS trains
- 1 out of 3 HPIS trains
- 1 out of 3 EFW pumps

At the beginning of the transient a fast depressurization of the RCS occurs. This causes the triggering of the HPIS signal at 470 s and the injection of the HA-1 at the 760 s. ECCS coolant entering the RPV causes the depressurization rate to decrease, see Figure 4-15, and therefore the LPIS pressure setpoint is not reached until 5000 s.

Nevertheless, the LPIS signal does not trigger because the difference between the HLs temperature and the saturation temperature has to be less than 10 K. Consequently, the LPIS does not start injecting until 8036 s. At 10000 s, the mass flow rate through the break and the ECCS injection equals, allowing a pseudo-SS to be reached, Figure 4-16.

The SGs pressure follows the RCS, Figure 4-15. Finally, it can be concluded that, applying the SC from the core is covered during all periods of the accidental sequence, Figure 4-17 and, therefore, no CD occurs, Figure 4-18. The sequence events of the SBLOCA transient are shown in Table 4-6.

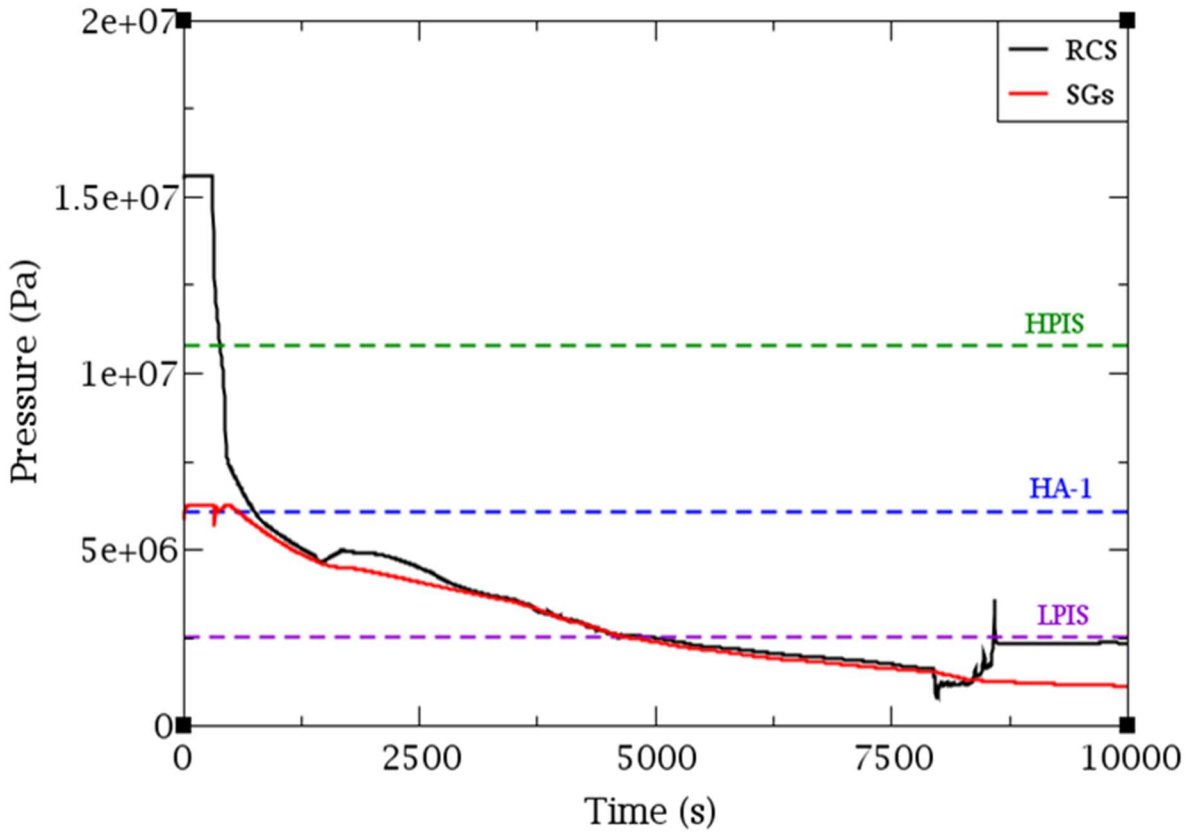

Figure 4-15 RCS and SGs pressure, SBLOCA (2 inches) sequence

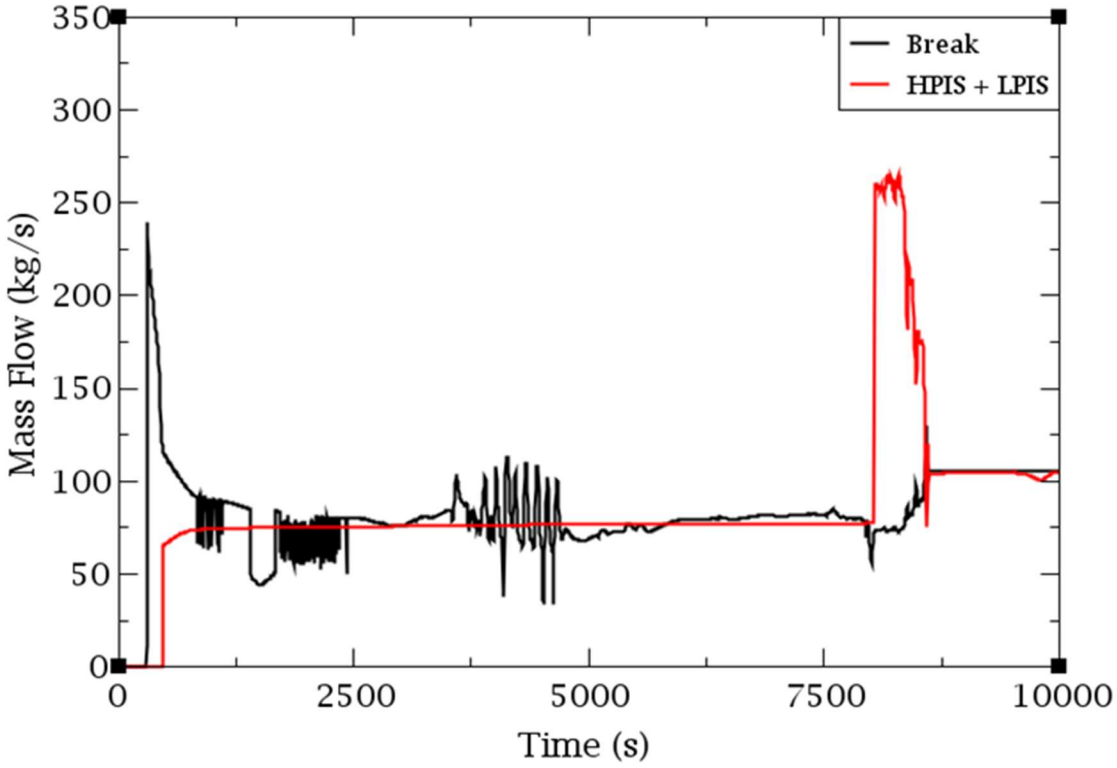

Figure 4-16 RCS inlet/outlet mass flow rate, SBLOCA (2 inches) sequence

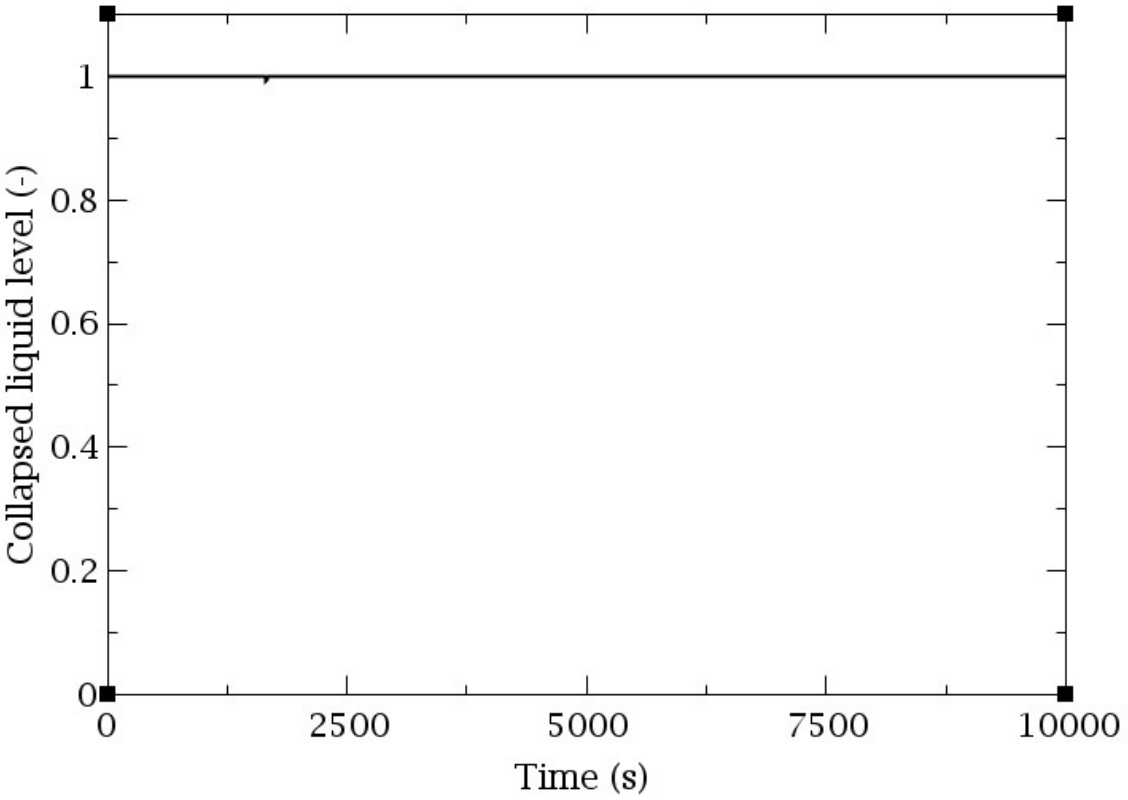

Figure 4-17 Collapsed liquid level, SBLOCA (2 inches) sequence

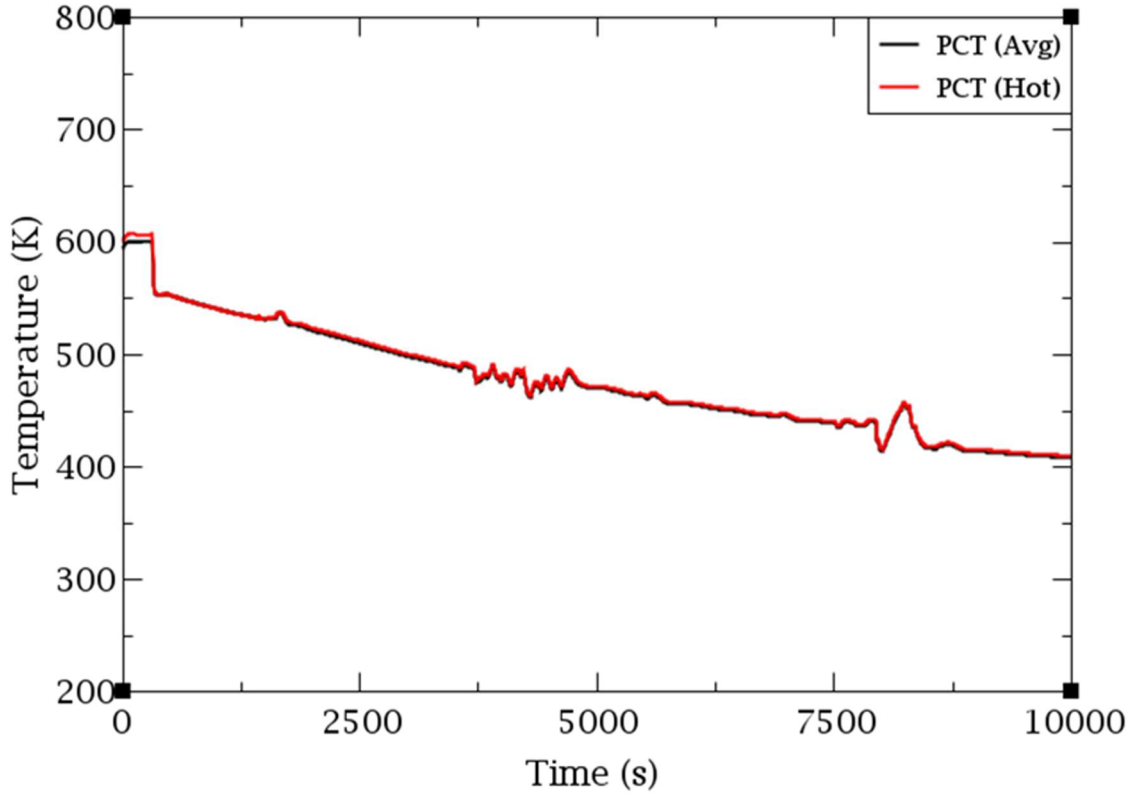

Figure 4-18 PCT, SBLOCA (2 inches) sequence

Table 4-6 SBLOCA (2 inches) sequence events

Time (s)	Event
300	SBLOCA (Ø= 2 inches)
315	SCRAM signal (Power > 2250 MW and $P_{core\text{-}outlet}$ < 1.47 MPa) TT and MFW trip signals (P_{HL} < 14.7 MPa)
330	TT (signal + delay + turbine closing time)
355	MFW pumps trip and EFW pumps start-up (signal + delay)
470	HPIS injection (P_{DC} < 10.78 MPa and $T_{HL}^{sat} - T_{HL}$ < 10 K)
760	HA-1 and HA-4 injection ($P_{DC/UP}$ < 6.07 MPa)
1405	MCPs coast-down and closing of the MSIVs (P_{SL}< 4.69 MPa)
8036	LPIS injection (P_{DC} < 2.55 MPa and T_{sat} -T_{HL} < 10K)

Chapter 5.
Safety analyses considering conventional safety systems

Chapter 5 deals with two analyses related to the VVER-1000/V320 considering the conventional safety systems of the technology. The first one is related to the LBLOCA and MBLOCA sequences, while the second one is related to the SBLOCA sequences without considering the actuation of the HPIS, which implies the need for management strategies.

5.1. Analysis of MBLOCA and LBLOCA Success Criteria in VVER-1000/V320 reactors. New proposals for PSA Level 1

Probabilistic Safety Analysis (PSA) and Deterministic Safety Analysis (DSA) are the methodologies for the overall safety evaluation of NPP. PSA is based on both fault and ET techniques that require reliability data of components/human actions to predict the probability of occurrence of accidental sequences.

In the frame of PSA, ETs are used to identify the different outcomes of an initiating event depending of the availability of safety systems or operator actions, and in this process evaluate the end state according to an acceptance criterion. The usual acceptance criterion is accomplished if the PCT remains below 1477 K during the full transient. This temperature is the one used by many countries but in other countries with LWR the acceptance criterion is PCT below 1473 K, nevertheless this difference has a small impact on PSA results. The compliance or not with the criterion is assessed with system TH codes. Then, the performance of those safety systems or crew human actions is compared against the end state defining the SC of the system, i.e., the minimum performance required to comply with the acceptance criteria of the sequence. This method plays a central role in the PSA of NPPs (Kovacs, 2014).

The principal steps in ET development consists of determining boundaries of the analysis, identifying CSF available to mitigate each IE, determine systems or operator actions available to perform each CSF and determine the SC for each safety system.

Currently, the are new methods associated with ET which are still under development, such as the Expanded ET (EET), (Najafi et al., 2022; Queral. C et al., 2021; Queral et al., 2017; Sanchez-Torrijos et al., 2022). In addition, the computational codes used to simulate the different transients of an ET are upgraded and improved over the years. This makes the verification of ET outcomes with these upgraded codes necessary, as previously unseen phenomenology or combination of phenomenology could be now simulated modifying the outcome of previous ET (Hosseini et al., 2020).

One of the most studied ET of all NPPs is the Loss of Coolant Accident (LOCA), due to its rapid and long-lasting impact on the integrity of the reactor core. The investigations of LOCA simulations in VVER type reactors is relatively extensive (Dina et al., 2019; Federal Environmental, 2005; Gibson-Daud-Thulu et al., 2021; Hossain-Khan et al., 2019; IAEA, 2001; Mousavian et al., 2003; OECD, 2001; Sabotinov et al., 2013; Sabotinov and Srivastava, 2008; Tarantino et al., 2001). However, there are no analyses in the open literature related to the LOCA ETs of this type of NPPs. In the following a verification of the SC of the ETs headers for the Medium and Large Break LOCA sequences is conducted.

This Section 5.1 is organised as follows: Section 5.1.1 reviews the SC proposed in the reference ETs for the MBLOCA and LBLOCA presented in Section 2.3. The possibility of relaxing the SC is then analyzed in Section 5.1.2. With the new SC obtained previously, two new approaches to the LOCA ETs are proposed in Section 5.1.3, one using the classical ET and the other using the EETs. Finally, Section 5.1.4 presents the conclusions of this analysis.

5.1.1. MBLOCA and LBLOCA success criteria verification

A verification of the sequences with a success end state has been performed for all break sizes of both MBLOCA and LBLOCA ETs. The results obtained in the simulations for the MBLOCA sequences with a success end state, S-1/3H-2/4A-1/3L, show a wide safety margin as the PCT values are largely under 1477 K, see Table 5-1. The 8 inches MBLOCA is the only break size where the maximum PCT exceeds the operational value by 56 K. The maximum PCT reached in the LBLOCA

success end state sequences; 2/3H-2/4A-l and h-2/4A-1/3L, also shows a large safety margin, although it decreases as the LBLOCA break size increases, see Table 5-2. Therefore, it can be confirmed that the SC in (Skalozubov et al., 2010) for the MBLOCA and LBLOCA IEs are valid. However, they can be conservative and then, a refined SC are sought below.

Table 5-1 Maximum PCT for the MBLOCA reference success sequence

BREAK SIZE	PCT
	S-1/3H-2/4A-1/3L
2 inches	607 K
3 inches	607 K
4 inches	607 K
6 inches	607 K
8 inches	661 K

Table 5-2 Maximum PCT for the LBLOCA reference success sequences

BREAK SIZE	PCT	
	2/3H-2/4A-l	h-2/4A -1/3 L
8 inches	638 K	607 K
12 inches	607 K	607 K
20 inches	849 K	1005 K
25 inches	1102 K	1155 K
30 inches	1250 K	1302 K
DEGB	1387 K	1305 K

5.1.2. MBLOCA and LBLOCA refined success criteria

In order to carry out a more in-depth study, it has been evaluated whether there are other sequences with different SC from those previously analyzed. Hereby, new simulations have been performed considering all configurations for the HPIS, HA-1 and LPIS systems, applying a similar approach to (Queral et al., 2018), as well as the entire MBLOCA and LBLOCA break size range. For that purpose, a

preliminary generic MB/LBLOCA ET has been considered, see Figure 5-1, on which the following assumptions have been made:

- In the MBLOCA sequences, the SC of the ECCS-related headers have been examined based on the assumption that the reactor SCRAM always occurs, i.e., ATWS sequences have not been analyzed. On other hand, in the LBLOCA sequences the performance of SCRAM has not been considered, since, as mentioned above, SCRAM does not cover any CSF for this IE.
- All sequences in which both the LPIS and HPIS are not available, i.e. S6 and S8 in Figure 5-1, have not been analyzed since it is already known that they cannot reach a success end state due to the fact that the CSF of the RCS coolant supply will not be fulfilled in the long term. Therefore, the sequences considered for both IEs have been: S1, S2, S3, S4, S5 and S7, with the exception that the S-header is only considered in the MBLOCA sequences.

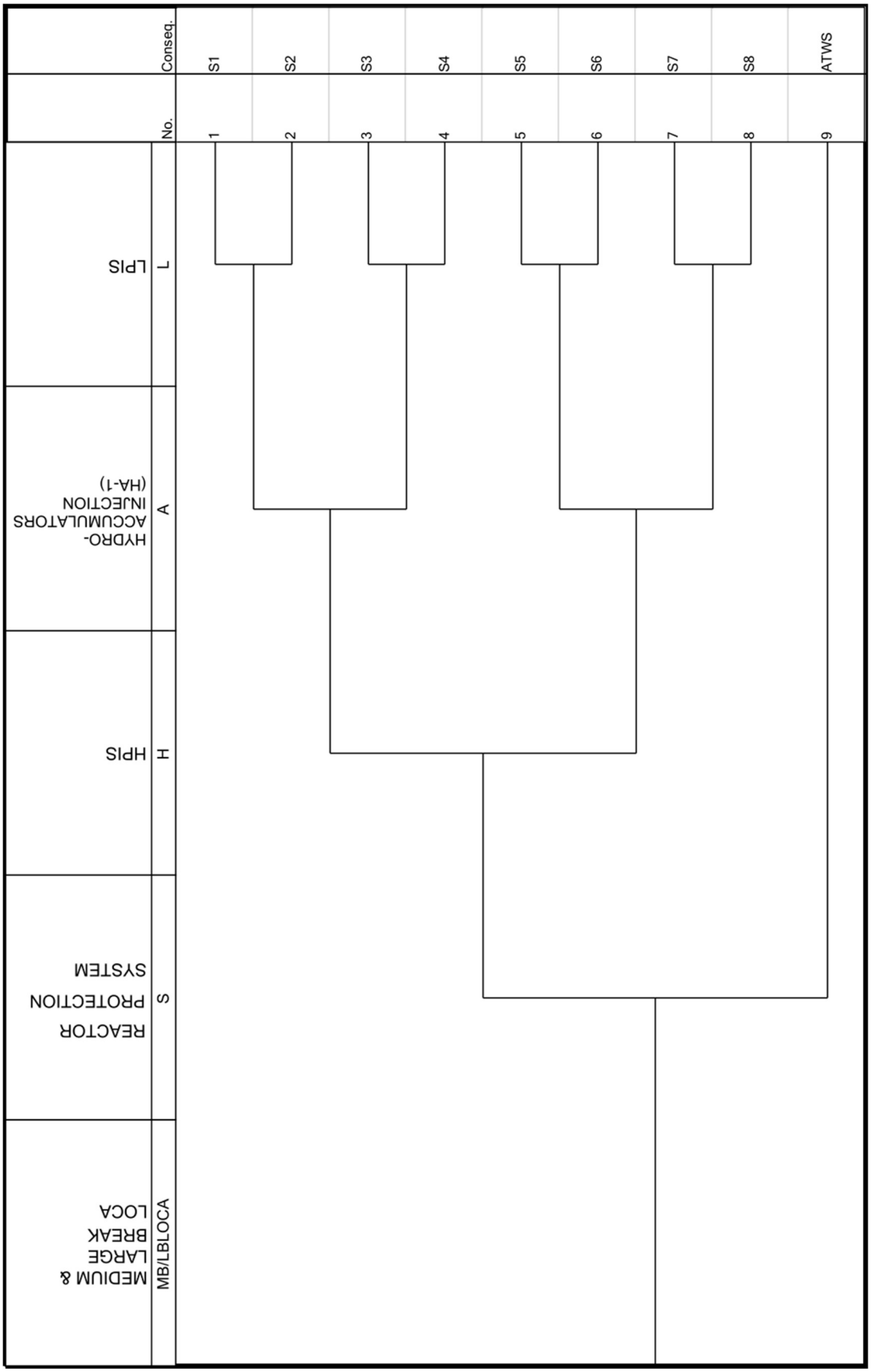

Figure 5-1 MBLOCA and LBLOCA generic ET

5.1.2.1. Review of the MBLOCA success criteria

More than 50 MBLOCA simulations have been performed considering different configurations of HPIS, HA-1 and LPIS systems, as well as various break sizes. The minimum configuration of the ECCS required to avoid the CD, obtained for each of the five break sizes simulated, along with the PCT values are shown in Table 5-3. As an example, Figure 5-2 and Figure 5-3 present the evolution of the RCS pressure and the PCT for the full MBLOCA range of the sequence S-1/3H-a-l. Figure 5-4 and Figure 5-5 show the different cases for a break of 2 inches.

It has been found that 1 out of 3 HPIS trains are enough to reach a success end state for the whole MBLOCA break size range. In addition, 1 out of 3 LPIS trains are also adequate for 3 to 8 inches MBLOCA IE to avoid CD. Nevertheless, for the 2 inches MBLOCA it has been proven that 3 out of 3 LPIS trains plus 4 out of 4 HAs are required if no HPIS train is available, as shown in Figure 5-4 and Figure 5-5. Thus, it can be considered that the MBLOCA ET in (Skalozubov et al., 2010) contains conservatism since it assumes that to have a sequence with a success end state all three ECCS (1 out of 3 HPIS trains plus 1 out of 3 LPIS trains plus one HA-1 of each type (HA-UP + HA-DC)) are needed, but according to the simulations performed, over the whole MBLOCA range, the single actuation of LPIS (1 out of 3 trains) or HPIS (1 out of 3 trains) is enough to prevent reaching a PCT value of 1477 K.

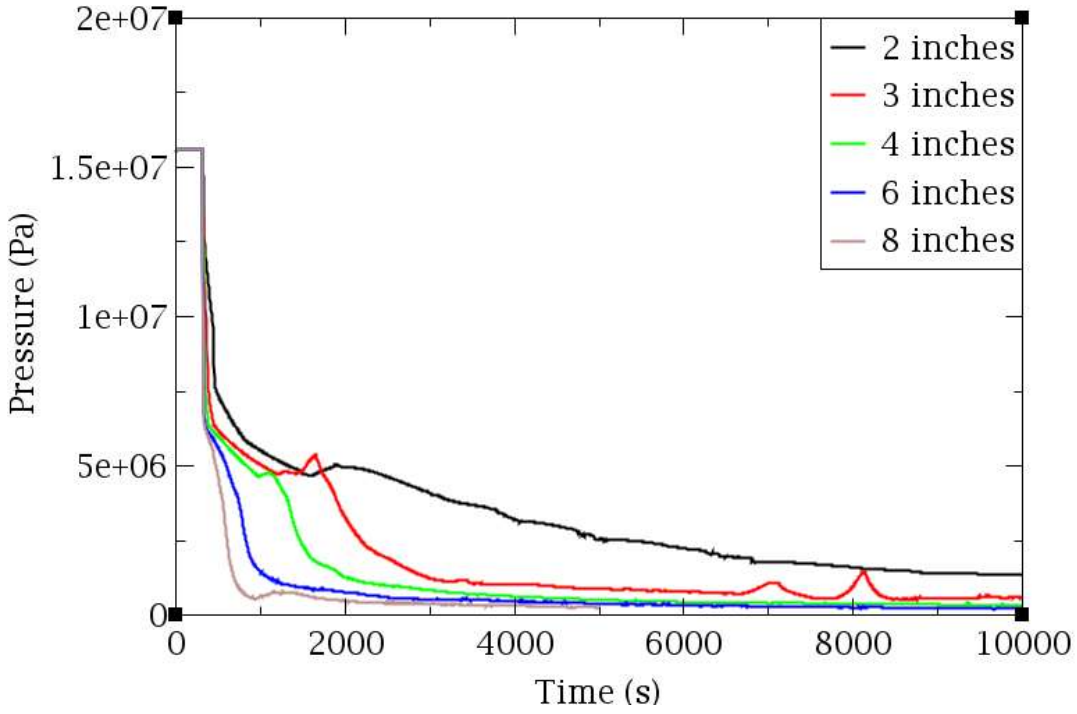

Figure 5-2 RCS pressure, MBLOCA S-1/3H-a-l sequences

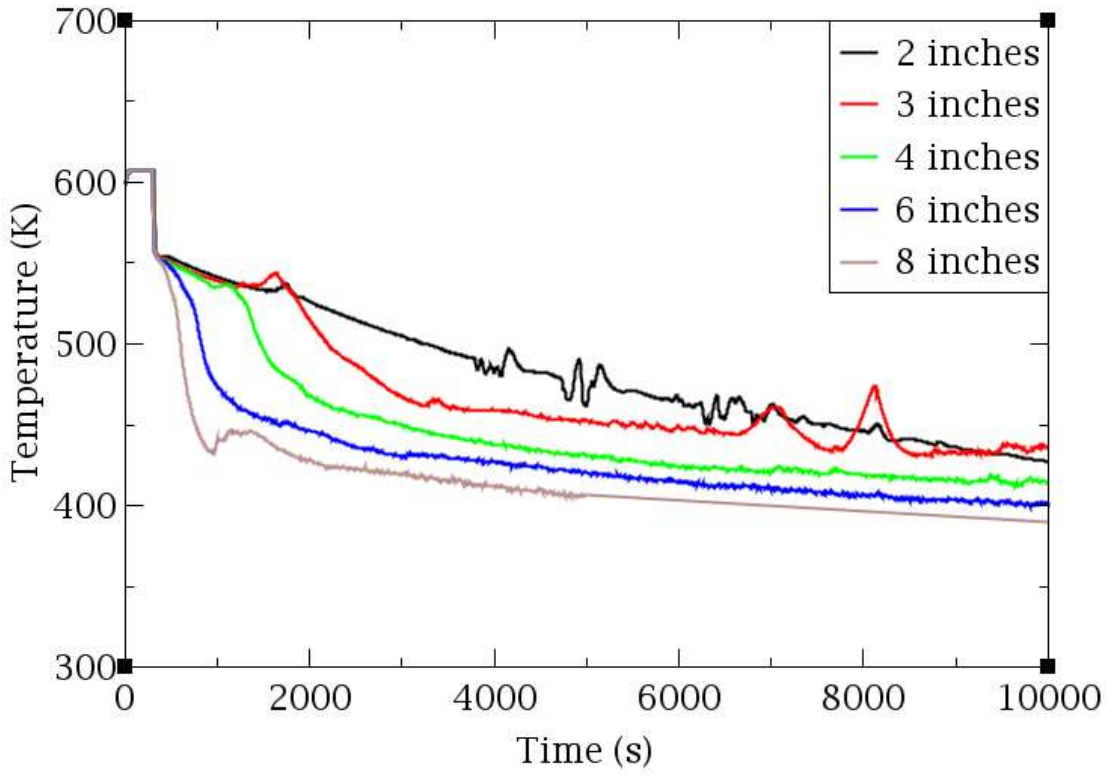

Figure 5-3 PCT, MBLOCA S-1/3H-a-l sequences

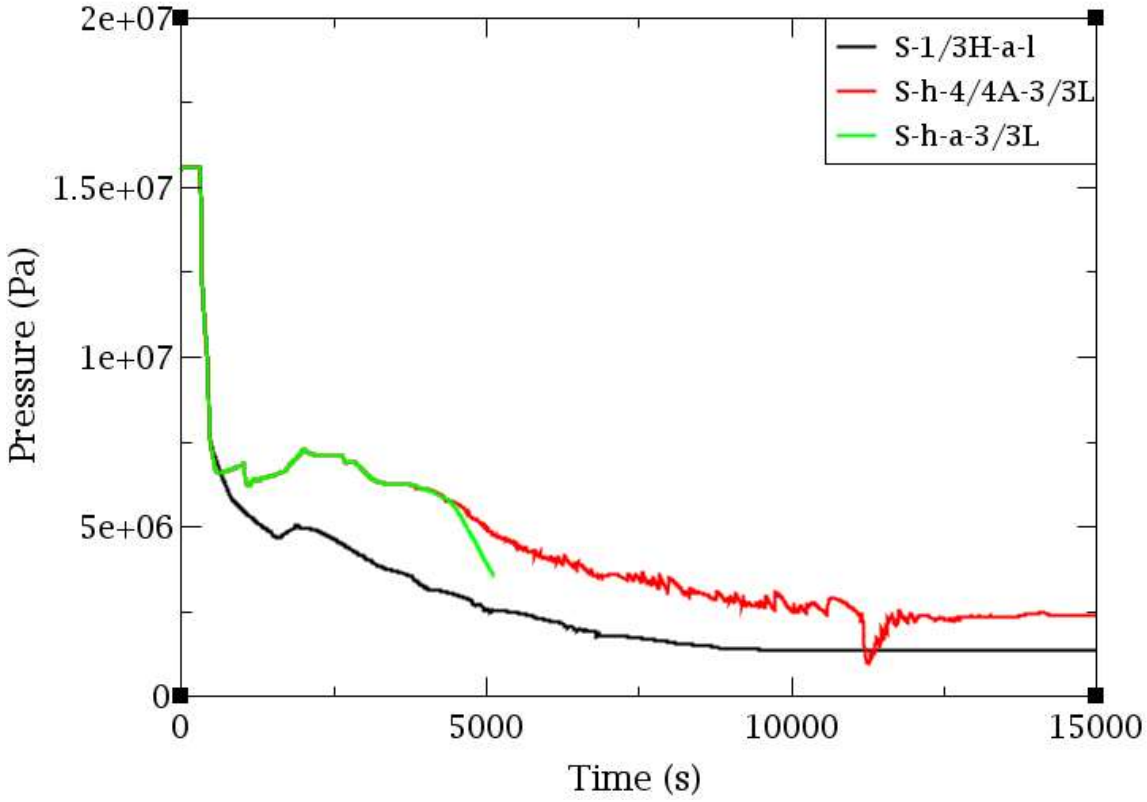

Figure 5-4 RCS pressure, MBLOCA (2 inches) sequences

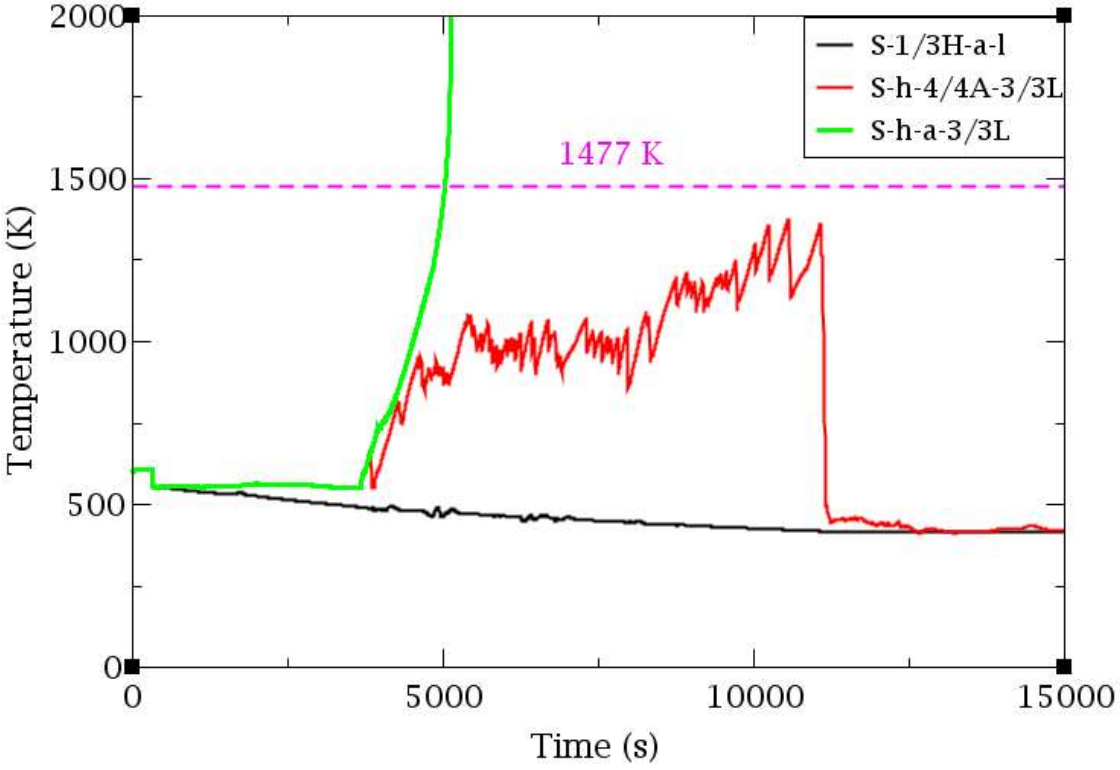

Figure 5-5 PCT, MBLOCA (2 inches) sequences

Table 5-3 Success criteria and maximum PCT, MBLOCA sequences

Sequence	BREAK SIZE				
	2 inches	3 inches	4 inches	6 inches	8 inches
S1: H-A-L	1/3 H (607 K)	1/3 H (607 K)	1/3 H (607 K)	1/3 H (607 K)	1/3 H (607 K)
S2: H-A-l					
S3: H-a-L					
S4: H-a-l					
S5: h-A-L	4/4 A + 3/3 L (1374 K)	1/3 L (1169 K)	1/3 L (923 K)	1/3 L (656 K)	1/3 L (655 K)
S7: h-a-L	CD (>1477 K)				

5.1.2.2. Review of the LBLOCA success criteria

For a similar approach to MBLOCA analysis, about 50 LBLOCA simulations have been performed, considering different HPIS, HA-1 and LPIS systems configurations, as well as multiple break sizes. As an example, Figure 5-6 and Figure 5-7 present the evolution of the RCS pressure and the PCT for all the LBLOCAs analyzed with the only availability of the L header (sequence h-a-1/3L for LBLOCAs from 8 to 25 inches and sequence h-a-2/3L for LBLOCAs from the 30 inches to DEGB).

Table 5-4 shows all the SC obtained for the six LBLOCA break sizes evaluated together with their PCT values. It can be seen how the ECCSs SC gets stringent as the break size increases; from 3 to 12 inches it is enough with a single LPIS or HPIS train to avoid the CD, but as break size get larger, the availability of more safety systems is required.

Furthermore, for 20 inches LBLOCAs onwards, more than one SC appears for some ECCSs. This is because, for larger LBLOCAs, LPIS and HPIS require the availability of more trains if they operate alone than if they perform their safety function in combination with another safety injection system. On other hand, it has been found that from 30 inches LBLOCA onwards, the sole availability of all three HPIS trains is not enough to avoid the CD. However, the sole availability of two LPIS trains is enough to have a success sequence in the DEGB LOCA. Figure 5-8 and Figure 5-9 shows the RCS pressure (left) and the PCT (right) for the DEGB sequences included in the Table 5-4.

It can be highlighted how in none of the LBLOCAs the injection of the HA-1 is a necessary requirement to prevent the PCT from exceeding 1477 K, since the availability of the LPIS and the HPIS, with different configurations, is enough to reach the success end state.

Moreover, the success sequence 1/3H-1/3A-l for the 30 inches LBLOCA follows a non-monotonic trend, as the HA-1 SC is relaxed to a single train relative to the 25 inches LBLOCA where the injection of 2 HAs is required if only one HPIS train and no LPIS trains inject successfully. This is because a larger break has a double effect. In the one hand, the mass flowrate through the break is greater and therefore the RCS inventory is lost in a shorter time, and therefore the core uncovery is reached earlier. On the other hand, the larger the break, the faster the RCS depressurizes and the injection systems can actuate sooner. For all these reasons, the SC are not always monotonic with respect to the break diameter. This

type of behaviour has also been found in other designs such as the Westinghouse PWR (Queral et al., 2018).

Table 5-4 Success criteria and maximum PCT, LBLOCA sequences

<table>
<tr><th rowspan="2">Sequence</th><th colspan="6">BREAK SIZE</th></tr>
<tr><th>8 inches</th><th>12 inches</th><th>20 inches</th><th>25 inches</th><th>30 inches</th><th>DEGB</th></tr>
<tr><td>S1: H-A-L</td><td rowspan="4">1/3 H
(607 K)</td><td rowspan="4">1/3 H
(723 K)</td><td rowspan="2">1/3 H + 1/4 A
(849 K)</td><td rowspan="2">2/3 H + 1/4 A
(1184 K)
1/3H + 2/4 A
(1228 K)</td><td rowspan="2">1/3H + 1/4 A
(1119 K)</td><td>1/3 H+ 1/4 A + 1/3 L
(1305 K)</td></tr>
<tr><td>S2: H-A-l</td><td>2/3 H + 1/4 A
(1428 K)</td></tr>
<tr><td>S3: H-a-L</td><td rowspan="2">2/3 H
(1266 K)</td><td rowspan="2">3/3 H
(1309 K)</td><td>1/3 H + 1/3 L
(1338 K)</td><td>2/3 H + 1/3 L
(1349 K)</td></tr>
<tr><td>S4: H-a-l</td><td>CD
(>1477 K)</td><td>CD
(>1477 K)</td></tr>
<tr><td>S5: h-A-L</td><td rowspan="2">1/3 L
(655 K)</td><td rowspan="2">1/3 L
(1067 K)</td><td rowspan="2">1/3 L
(1314 K)</td><td rowspan="2">1/3 L
(1392 K)</td><td>1/4 A + 1/3 L
(1169 K)</td><td>2/4 A + 1/3 L
(1305 K)</td></tr>
<tr><td>S7: h-a-L</td><td>2/3 L
(1251 K)</td><td>2/3 L
(1275 K)</td></tr>
</table>

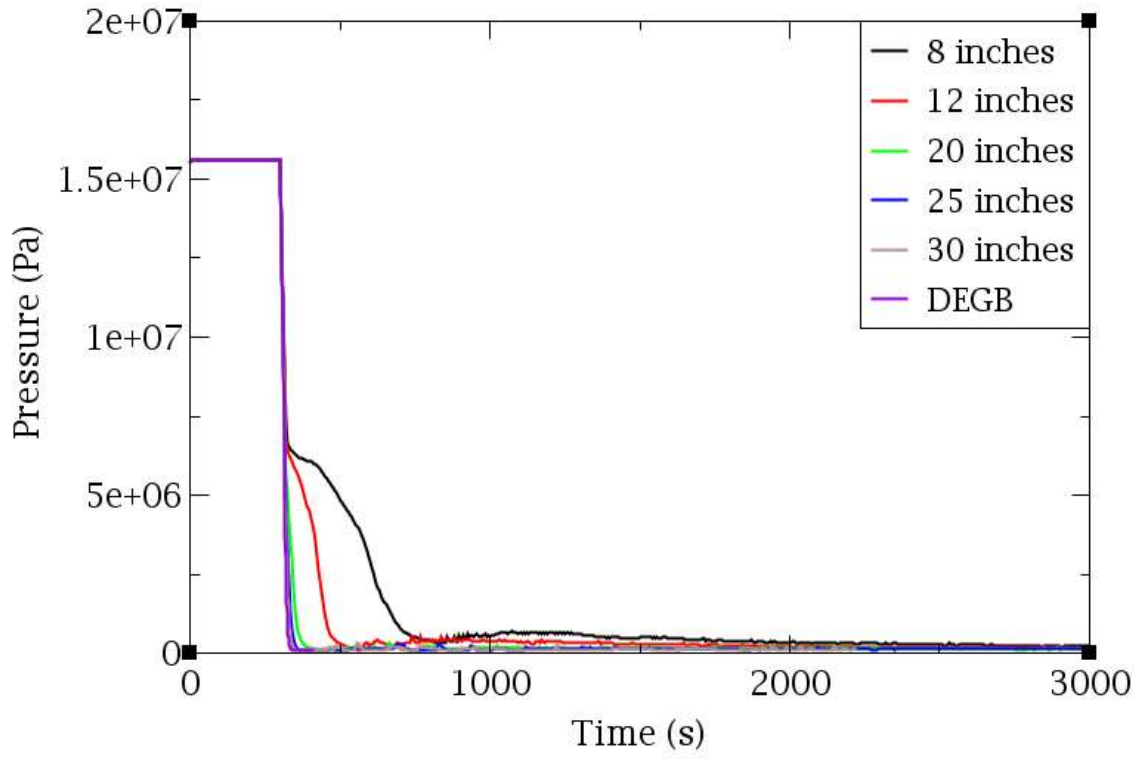

Figure 5-6 RCS pressure, LBLOCA h-a-1/3L (8 - 25 inches) and h-a-2/3L (30 inches-DEGB) sequences

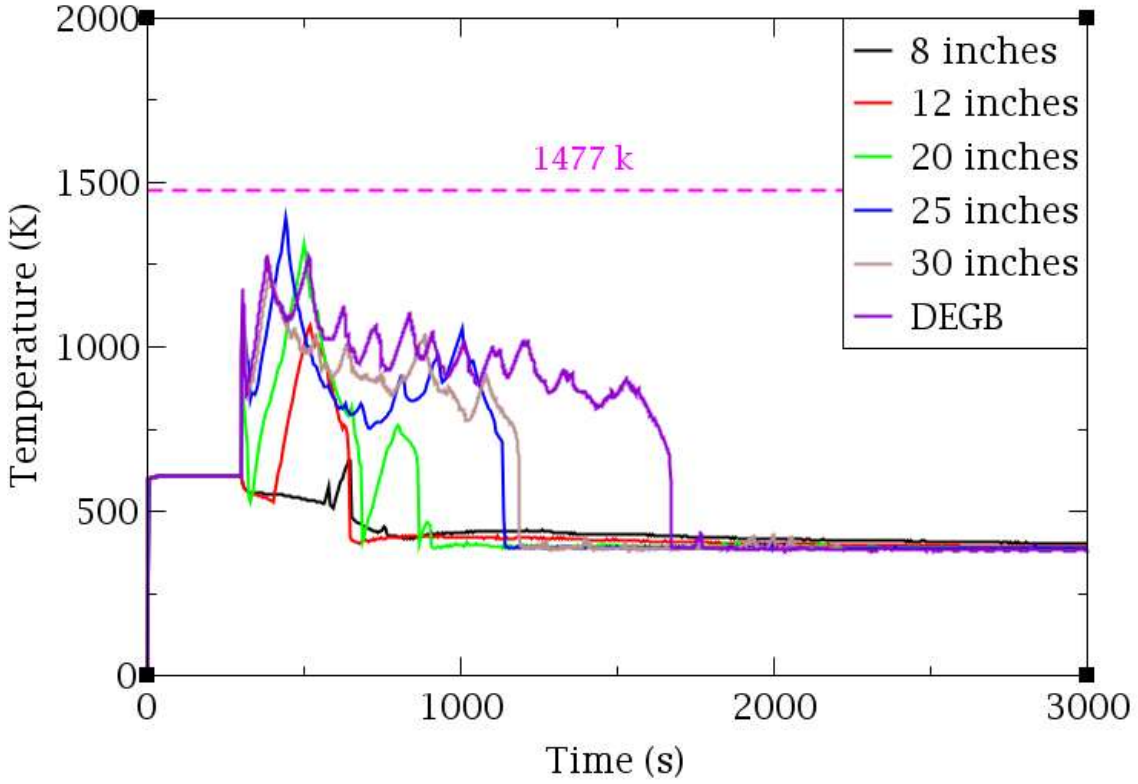

Figure 5-7 PCT, LBLOCA h-a-1/3L (8 - 25 inches) and h-a-2/3L (30 inches-DEGB) sequences

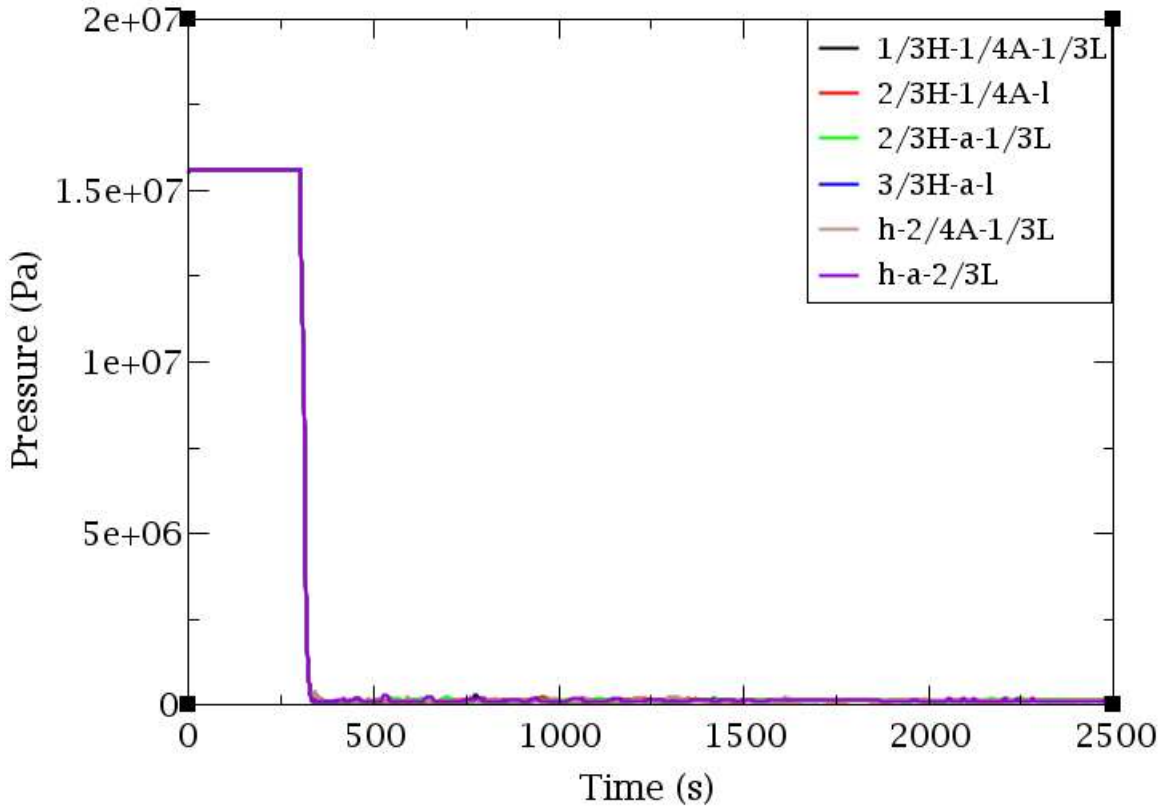

Figure 5-8 RCS pressure, DEGB LBLOCA sequences

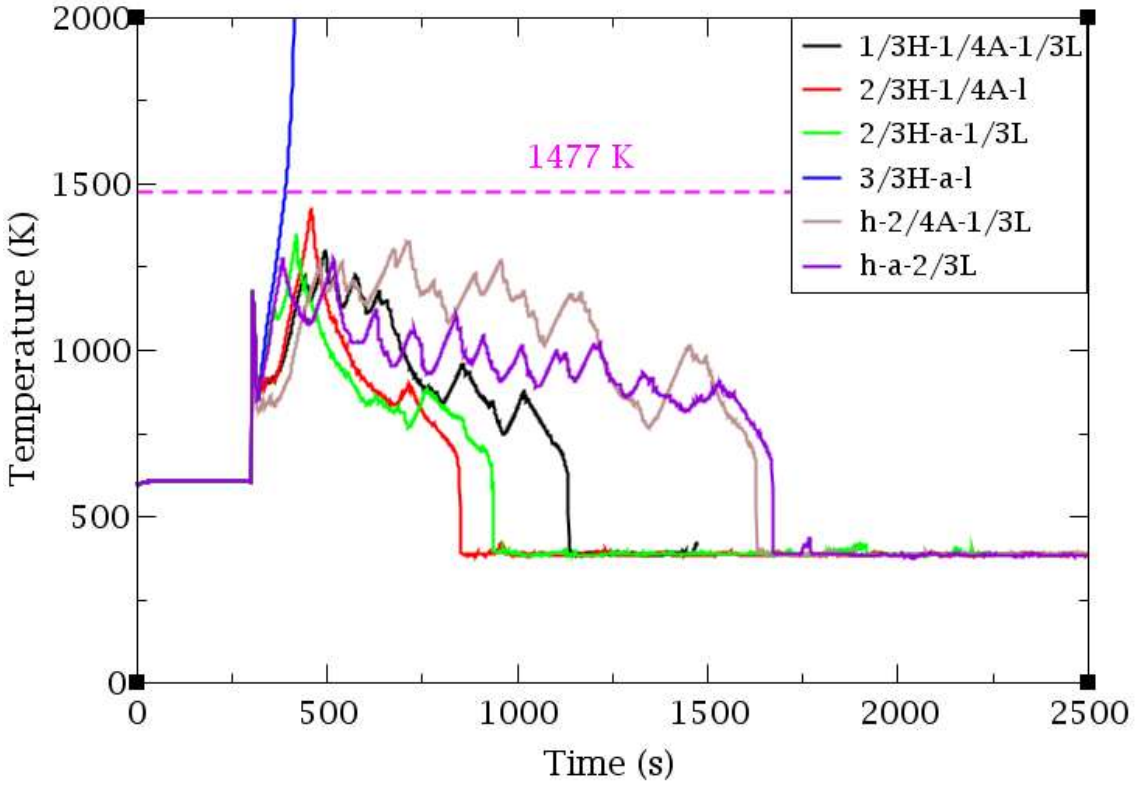

Figure 5-9 PCT, DEGB LBLOCA sequences

5.1.3. Event Tree and success criteria proposals

The SC of the MBLOCA and LBLOCA ETs have been reviewed in Section 5.1.3, the results obtained in both ETs are summarized in Table 5-5. The results show that the SC for MBLOCA from 3 to 8 inches and those for LBLOCA from 8 to 12 inches are identical, since the sole availability of one HPIS train or that of the LPIS is enough to prevent the CD end state. This indicates that it is possible to modify the boundaries between both IEs, by increasing the MBLOCA break size range from [2 – 8] inches to [2 – 12] inches and thereby reducing the LBLOCA break size range from [8 inches – DEGB] to [12 inches – DEGB].

The classic PSA uses a binary state for each header: failure or success, which presents a challenge since, as seen in Table 5-5, for some sequences there is more than one SC. Some different approaches to handle this drawback are available, two of them are proposed below.

In the first approach, a careful selection of the SC has been carried out with the aims of establishing new classic ETs. In a second approach, it is proposed to use EETs that allow to consider all available configurations of the safety injection

systems and not only their minimum requirement to meet the CSF, i.e. they provide the possibility to consider more than one SC for each ECCS.

Table 5-5 New MBLOCA and LBLOCA success criteria

<table>
<tr><th rowspan="2">Sequence</th><th colspan="6">BREAK SIZE</th></tr>
<tr><th>2 inches</th><th>3 - 12 inches</th><th>20 inches</th><th>25 inches</th><th>30 inches</th><th>DEGB</th></tr>
<tr><td>S1: H-A-L</td><td rowspan="4">1/3 H</td><td rowspan="4">1/3 H</td><td rowspan="2">1/3 H + 1/4 A</td><td rowspan="2">2/3 H + 1/4 A or
1/3H + 2/4 A</td><td rowspan="2">1/3 H + 1/4 A</td><td>1/3 H + 1/4 A + 1/3 L</td></tr>
<tr><td>S2: H-A-l</td><td>2/3 H + 1/4 A</td></tr>
<tr><td>S3: H-a-L</td><td rowspan="2">2/3 H</td><td rowspan="2">3/3 H</td><td>1/3 H + 1/3 L</td><td>2/3 H + 1/3 L</td></tr>
<tr><td>S4: H-a-l</td><td colspan="2">CD</td></tr>
<tr><td>S5: h-A-L</td><td>4/4 A + 3/3 L</td><td colspan="3" rowspan="2">1/3 L</td><td>1/4 A + 1/3 L</td><td>2/4 A + 1/3 L</td></tr>
<tr><td>S7: h-a-L</td><td>CD</td><td colspan="2">2/3 L</td></tr>
</table>

5.1.3.1. Event Trees for the classic PSA approach

New classic ETs for MBLOCA and LBLOCA IEs are proposed considering the SC obtained previously. First, a grouping of the break size ranges with the most similarities between them is carried out. Then, the optimal SC for each range is selected.

Thus, the proposed break ranges for the new ETs could be: MBLOCA-I [2 - 3 inches], MBLOCA-II [3 - 12 inches], LBLOCA-I [12 - 25 inches] and LBLOCA-II [25 inches – DEGB]. A difference between the original ETs and these new ETs proposed can be found in the choice of splitting the range of each IE into two, as well as having considered the MBLOCA-II break size range up 12 inches.

The selection of SC for the MBLOCA-I and II ETs is straightforward, as there are no different SC for a single safety injection system. This is not the case for the LBLOCA, which presents several combinations of the SCs. For this second IE, it is proposed to consider the SCs in the following manner:

- For the LBLOCA-I ET, the minimum SC for the HPIS, 1 out of 3 trains, has been chosen at the expense of selecting the more restrictive HA-1 SC, 2 out of 4, since the HA-1 failure probability is lower (passive system) than that

of HPIS (active system). Regarding the number of LPIS trains required, the results show that a single train is enough to avoid CD.

- For the LBLOCA-II ET, it is proposed that the SC for the LPIS and the HPIS is 2 out of 3 trains. The selected SC for the HA-1 is 2 out of 4. This is because the sequences with 1 out of 3 HPIS trains and 1 out of 4 HA-1 configurations succeed by a small margin, less than 50 K (Table 5-6).

Table 5-6 Proposed success criteria for MBLOCA and LBLOCA sequences

<table>
<tr><th rowspan="2">Sequence</th><th colspan="4">BREAK SIZE</th></tr>
<tr><th>MBLOCA-I
(2 - 3 inches)</th><th>MBLOCA-II
(3 - 12 inches)</th><th>LBLOCA-I
(12 - 25 inches)</th><th>LBLOCA-II
(25 inches - DEGB)</th></tr>
<tr><td>S1: H-A-L</td><td>1/3 H or
4/4 A + 3/3L</td><td>1/3 H or
1/3 L</td><td>1/3 H + 2/4 A or
1/3 L</td><td>2/3 H + 2/4 A or
2/3 L</td></tr>
<tr><td>S2: H-A-l</td><td colspan="2">1/3 H</td><td>1/3 H + 2/4 A</td><td>2/3H + 2/4 A</td></tr>
<tr><td>S3: H-a-L</td><td>1/3 H</td><td>1/3 H or
1/3 L</td><td>1/3 L</td><td>2/3 L</td></tr>
<tr><td>S4: H-a-l</td><td colspan="2">1/3 H</td><td colspan="2">CD</td></tr>
<tr><td>S5: h-A-L</td><td>4/4 A + 3/3 L</td><td colspan="2">1/3 L</td><td>2/3 L</td></tr>
<tr><td>S7: h-a-L</td><td>CD</td><td colspan="2">1/3 L</td><td>2/3 L</td></tr>
</table>

Considering the previous findings, the proposed ET for each IE are the following: The ET for the MBLOCA-I, Figure 5-10, consists of the four original headers (S, H, A and L), while the MBLOCA-II ET, Figure 5-11, dispenses with the A header as its actions are not required to avoid the CD. The proposed LBLOCA-I and LBLOCA-II ETs, Figure 5-12, feature the original LBLOCA ET headers (H, A and L), with the success and failure sequences being the same for both, but with different SC, those of the LBLOCA-II being more restrictive than those of the LBLOCA-I.

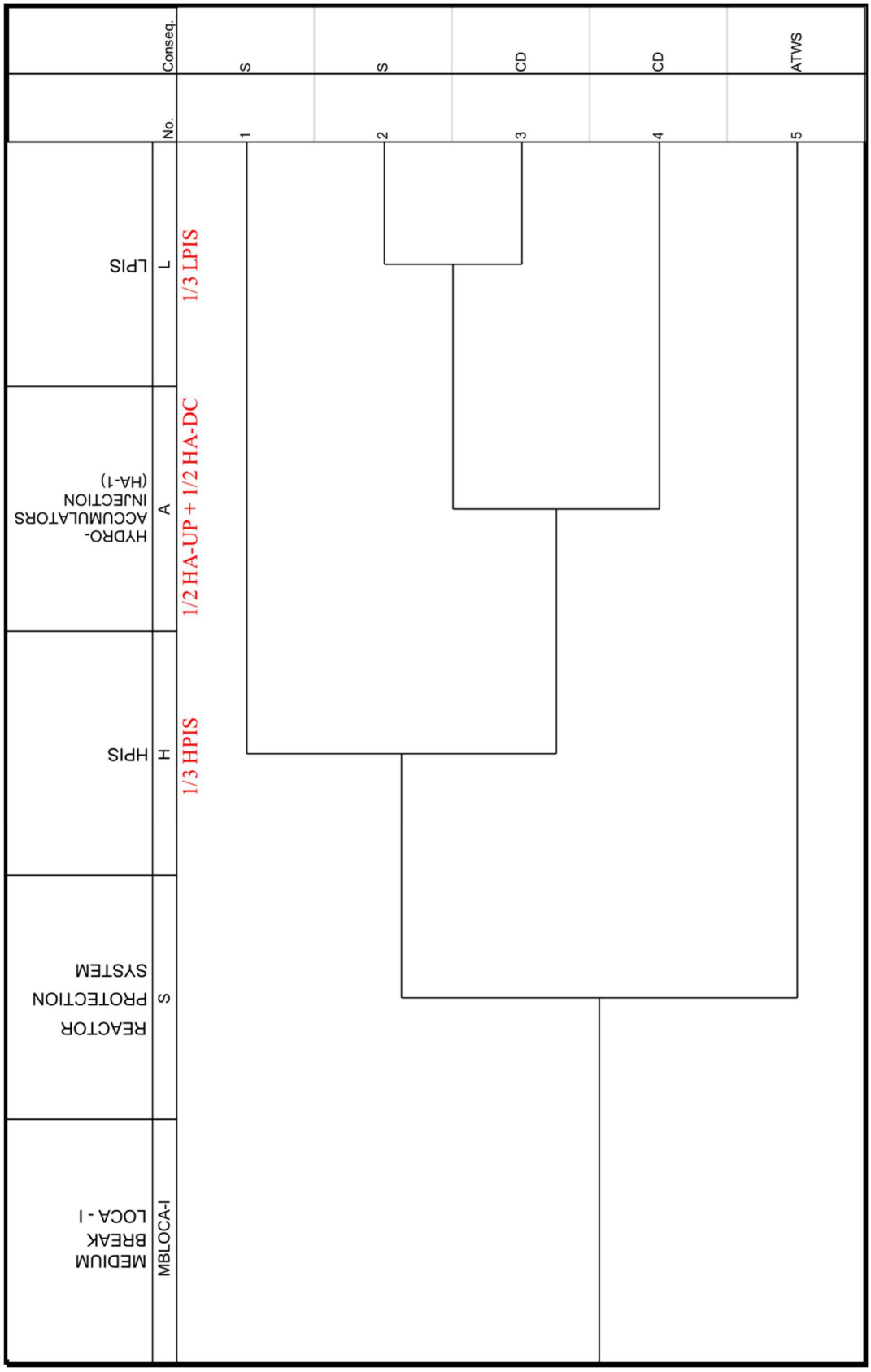

Figure 5-10 Proposed MBLOCA-I ET

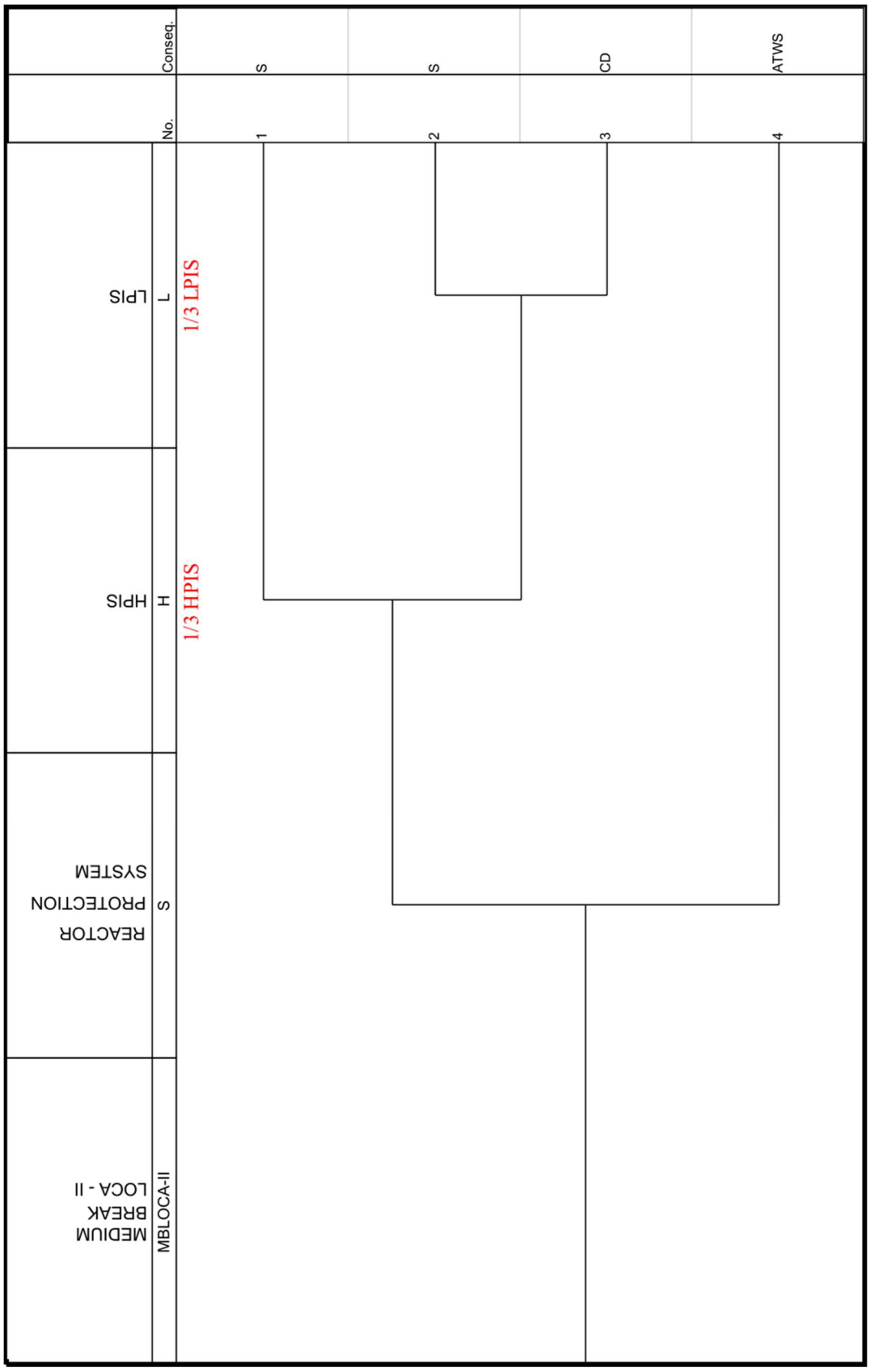

Figure 5-11 Proposed MBLOCA-II ET

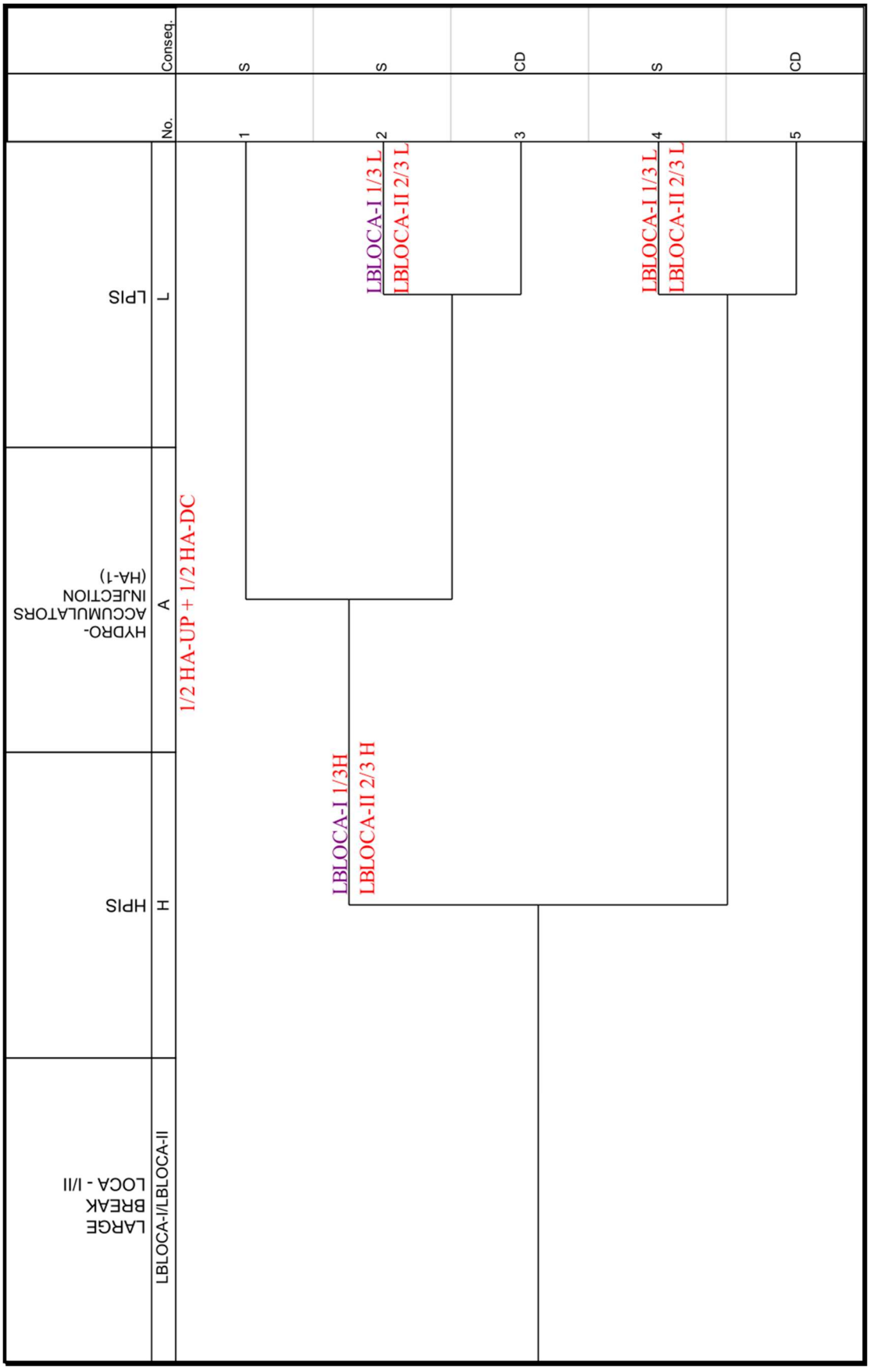

Figure 5-12 Proposed LBLOCA-I and LBLOCA-II ET

5.1.3.2. LBLOCA Expanded Event Trees Approach

The selection of SC for the MBLOCA ETs is relatively straightforward, SC are unique for a single break size range, whereas for the LBLOCA there are several combinations of SC that lead to having to make a selection by choosing the most conservative one to propose new classic ETs. In this second approach, the authors make use of the EETs, (Queral. C et al., 2021; Queral et al., 2017), in order to find a more realistic model for the LBLOCA sequences.

The difference between classic ETs and EETs is that whereas in the first one there are only two possible options for each header, i.e., success or failure (Sanchez-Torrijos et al., 2022), in the second one it is feasible to have more than one success configurations, which allow considering a wide range of sequences. In addition, a relaxation of the grouping of the LBLOCA range could be done, so that four EETs are proposed:

- LBLOCA-A EET (12 to 20 inches). The H header is the only one that needs to be expanded in three possible configurations: zero trains, one train and more than two trains, Figure 5-13.
- LBLOCA-B EET (20 to 25 inches). Again, the only header expanded is the HPIS header, but in this case in four configurations: zero, one, two or three trains. All other headers are not expanded, Figure 5-14. The only configuration that does not need the availability of other ECCS is 3 out of 3 HPIS trains the other configurations require the HA-1 or the LPIS to inject successfully.
- LBLOCA-C EET (25 to 30 inches). This break size range that does not require the expansion of any of its headers, Figure 5-15. With HPIS alone, it is not possible to avoid the CD, but with 1 out of 4 HA-1 or 1 out of 3 LPIS trains successfully injecting all that is required is to successfully inject with one HPIS train.
- LBLOCA-D EET (30 inches to DEGB). In the EET it is again found that the H header must be expanded in three configurations: failure, one train and two or more trains, Figure 5-16. For the configuration of two or more trains the injection of one HA-1 is enough to achieve a successful end state, however, when the configuration is relaxed to 1 out of 3 HPIS trains, the successful injection of 1 out of 4 HA-1 and 1 out of 3 LPIS trains or 2 out of 3 LPIS trains is required.

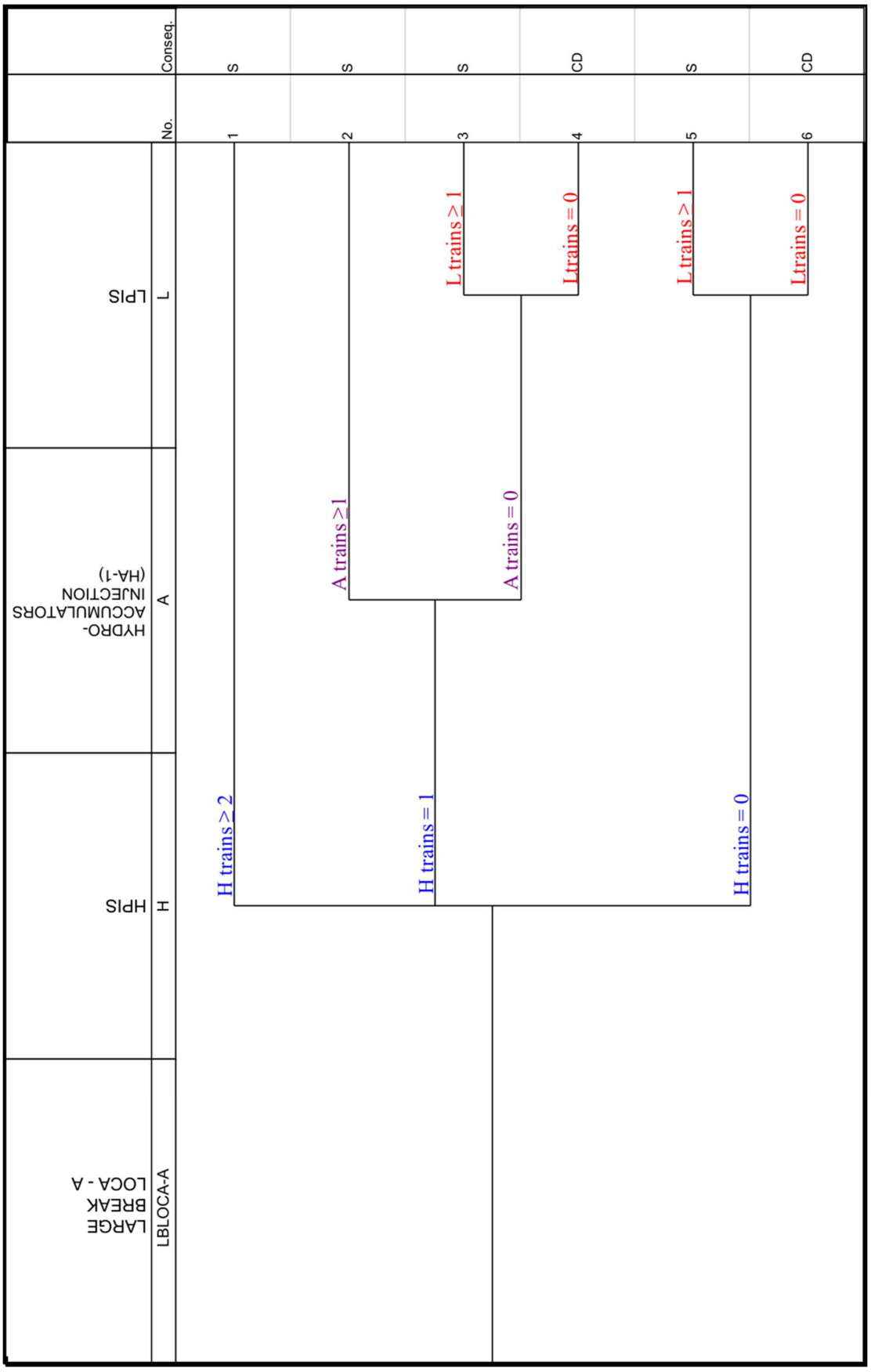

Figure 5-13 LBLOCA-A Expanded ET

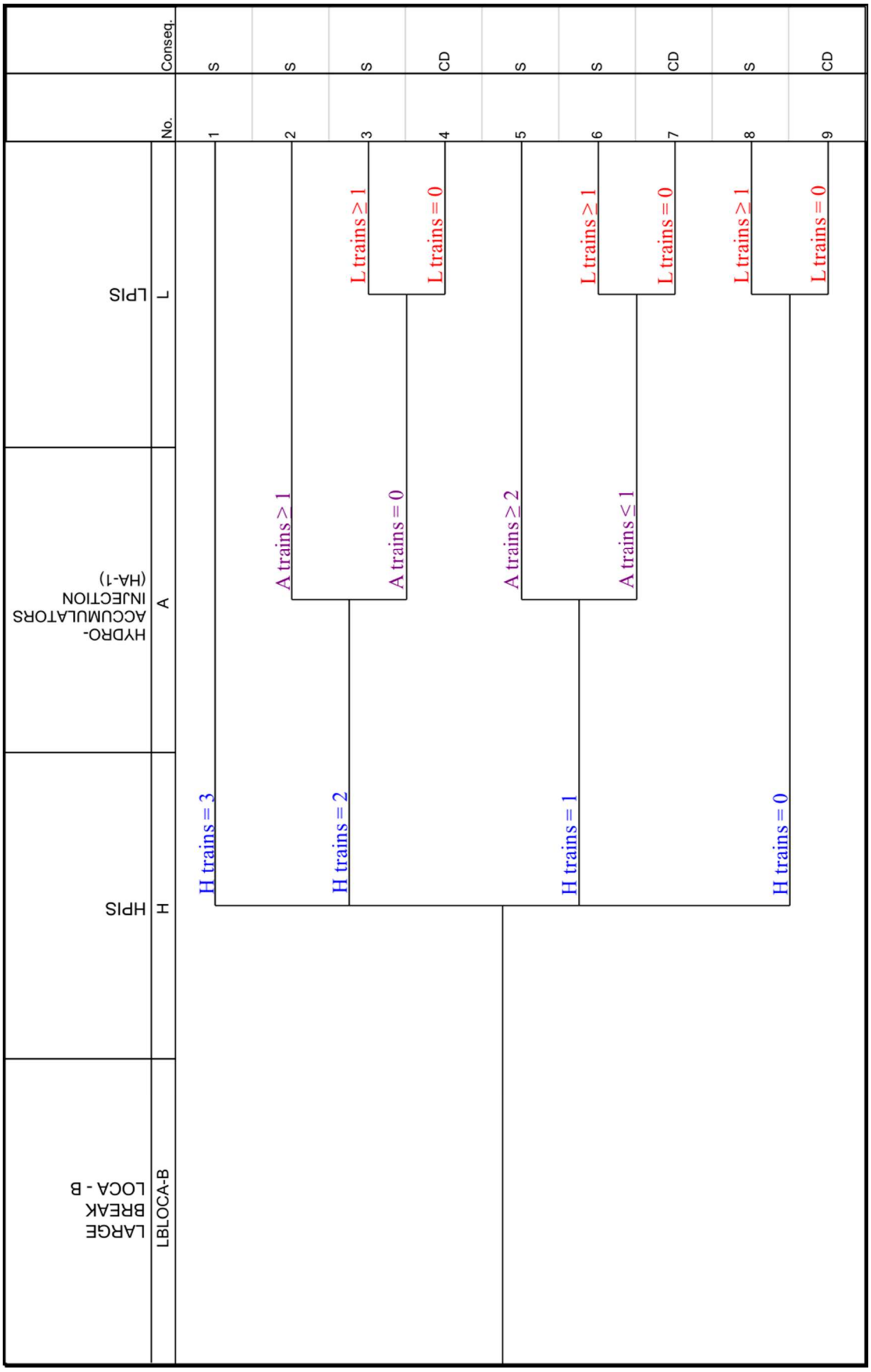

Figure 5-14 LBLOCA-B Expanded ET

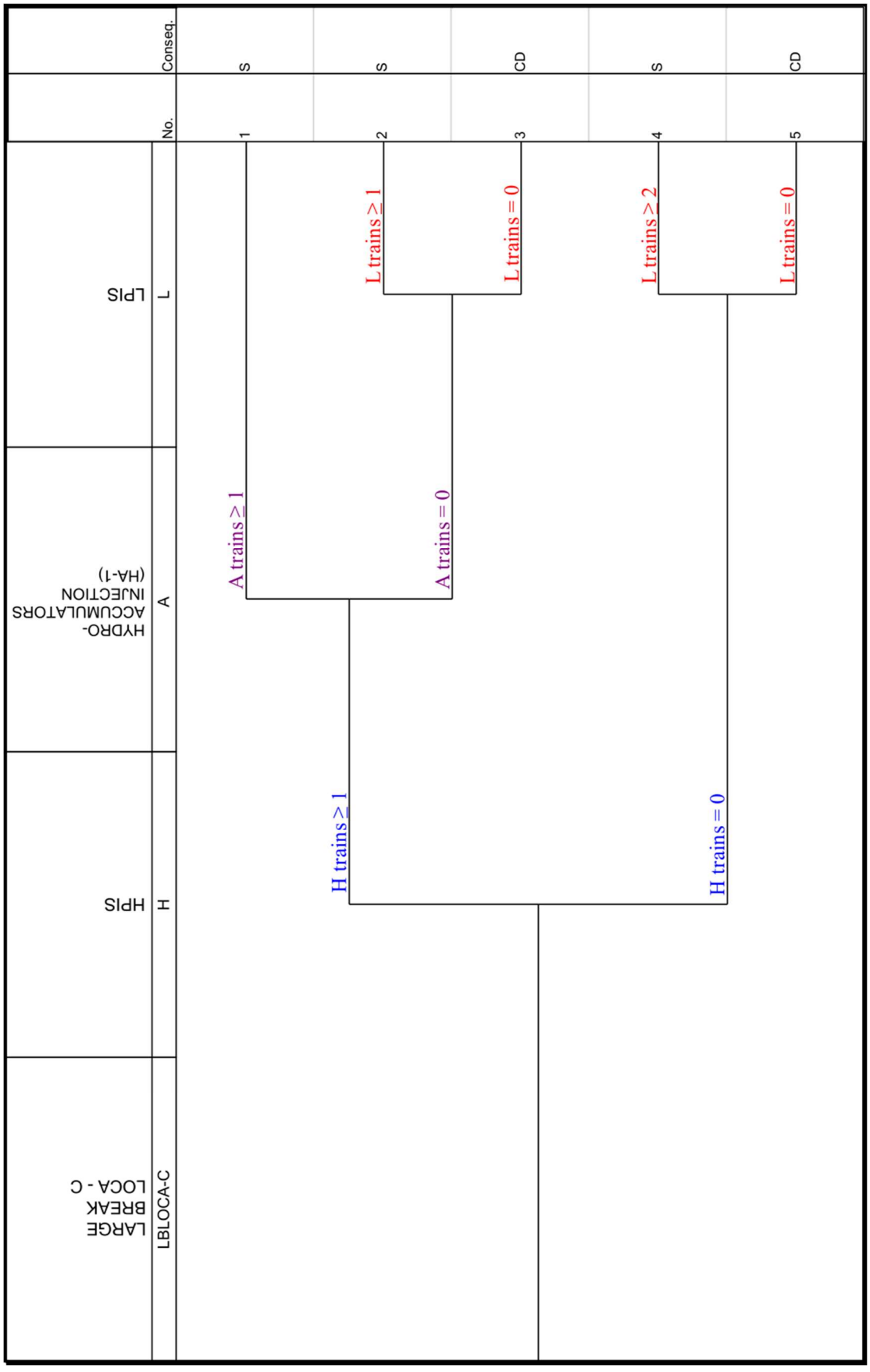

Figure 5-15 LBLOCA-C Expanded ET

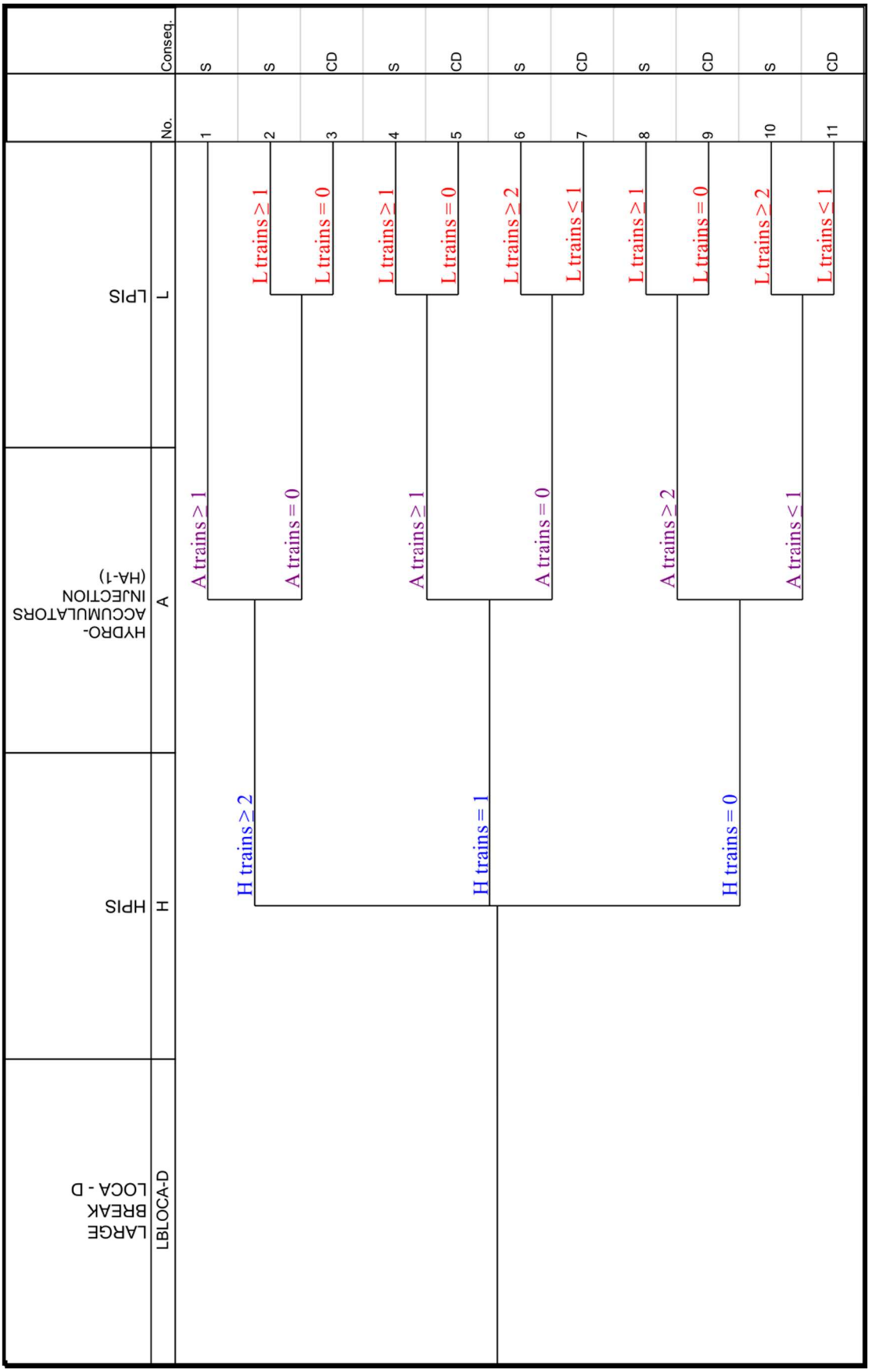

Figure 5-16 LBLOCA-D Expanded ET

5.1.4. Conclusions regarding MB/LBLOCA ET verifications and new proposals

In this section a reassessment of the MBLOCA and LBLOCA ETs of the VVER-1000/V320 reactor has been performed. The SC of HPIS, LPIS and HA-1 have been assessed and confirmed; and to deepen into the sequence, all availability configurations have been simulated, which has provided the following insights:

- For LOCA break range between 2 and 12 inches the sole actuation of 1 out of 3 HPIS trains is enough to prevent core damage. But above 12 inches, 1 HPIS train is not enough and would need either HA-1 actuation or more HPIS/LPIS trains.
- LOCA break sizes above 3 inches and below 25 inches can avoid core damage with the successful actuation of one LPIS train.
- For LOCA break sizes over 20 inches, more than one success criterion appears for some headers.

Taking these findings into account, new proposals for the MB/LBLOCA ETs study have been developed:

- First, a reconfiguration of break sizes into four ranges allows using classic ETs and then four new ET are proposed.
- Second, if an EET approach is used, four EETs are proposed for the range from 20 inches to DEGB. Each of those EET have different SC for the different ECCS headers, supporting the aim of this work.

These new proposals could be considered in the PSA of current and future NPPs, helping to develop a more comprehensive and efficient evaluation of LOCA sequences.

5.2. Management of the SBLOCA sequences with HPIS failure in VVER-1000/V320 reactors; comparison with Westinghouse PWR strategies

In a VVER-1000/V320 reactor, if a MBLOCA sequence occurs with HPIS failure, the RCS depressurization is fast enough to allow first the HA-1 and then the LPIS to act in time preventing CD. However, in SBLOCA sequences with HPIS failure, the RCS pressure may stagnate above the HA-1 pressure, preventing the HA-1 and LPIS from replenishing the RCS inventory before reaching CD.

This behaviour can be also observed in Western PWR designs, such as the PWR-W, but the range of break sizes in which it appears depends on several factors. Among the most important are: the thermal power of the core, the total RCS water inventory and the ECCS designs. These types of sequences are some of the most risk-important design extension condition sequences and it is highly desirable that they be mapped in detail.

Therefore, in SBLOCA sequences with HPIS failure the operators must perform manual actions, following the appropriate EOPs, to cool and depressurize the RCS allowing the injection of the HA-1 and the LPIS. The EOPs provide guidance to the operator to bring the plant to a safe and stable condition in the event of this accidental sequence.

In the present section, the Integrated Safety Assessment (ISA) methodology (Ibánez et al., 2016) has been applied to study different operator actions for managing SBLOCA sequences with HPIS failure in VVER-1000/V320 reactors and 3 loops PWR-W. The Previous Damage (PD) curve and the different Damage Domains (DD) of the possible manual actions or strategies have been obtained by using the ISA methodology.

The Section 5.2 is structured as follows: Section 5.2.1 reviews strategies related to the SBLOCA sequence management in VVER-1000/V320 and PWR-W. Subsequently, the SBLOCA sequences with HPIS failure without human actions and considering three different strategies in VVER-1000/V320 reactors are analyzed in Sections 5.2.2 to 5.2.5, respectively. This is followed by a comparison of the previously discussed manual actions in Section 5.2.6. Afterwards, in Section 5.2.7, the SBLOCA with HPIS failure in 3 loops PWR-W is analyzed and the results are compared with those of the VVER-1000/V320 reactors in Section 5.2.8. Finally, conclusions are given in Section 5.2.9.

5.2.1. Strategies related with SBLOCA sequences with HPIS failure in VVER-1000/V320 and Westinghouse PWR

The different strategies for managing SBLOCA with HPIS failure sequences in VVER-1000/V320 and 3 loops PWR-W are discussed below. A review of the literature on EOPs, ET related to SBLOCA sequences, and experimental tests has been performed to provide a global overview.

It is important to note that, although both reactor designs have similar thermal power, ~3000 MWth, there are differences in the liquid volumes in both the RCS and SG, see Table 5-8, and also in their ECCSs characteristics, see Table 5-7. The ECCSs are labelled differently in the VVER-1000/V320 and in the 3 loops PWR-W; the high pressure system is named HPIS in the VVER-1000/V320 and High Pressure Safety Injection (HPSI) or High Head Safety Injection (HHSI) in the 3 loops PWR-W. The low pressure system is named LPIS in the VVER-1000/V320 and Low Pressure Safety Injection (LPSI) in the 3 loops PWR-W. The Hydro-Accumulators are named HA-1 in the VVER-1000/V320 and ACC in the PWR-W.

Table 5-7 HA-1/ACC and LPIS/LPSI characteristics

	Parameters	VVER-1000/V320	3 loops PWR-W
HA-1/ACC	Nº of trains	4	3
	Total Volume (m^3)	60 (x4)	41 (x3)
	Liquid Volume (m^3)	50 (x4)	36 (x3)
	Discharge pressure (MPa)	6	4.4
LPIS/LPSI	Nº of trains	3	2
	Shutoff head (MPa)	1.5	2.5
	Max mass flow rate per pump (kg/s)	406.8	207.2

Table 5-8 VVER1000/V320 and PWR-W approximate liquid volumes

Reactor	VVER-1000/V320	3 loops PWR-W
RCS (m^3)	340	260
SGs (m^3)	220	160

5.2.1.1. Management of Westinghouse PWR SBLOCA sequences with HPIS failure

In the PWR-W, the EOPs aim to provide symptom-based recovery strategies to guide the Main Control Room (MCR) crew in the management of accident scenarios (Westinghouse owners group, 1983). They are divided into two different groups: The Optimal Recovery Guidelines (ORGs) and the Function Restoration Guidelines (FRGs), see Figure 5-17. In an SBLOCA with HPSI failure sequence, the EOPs involved are as follows:

- When a reactor SCRAM occurs, the MCR crew begins to follow the ORG, specifically the EOP E-0 "reactor trip or safety injection". In EOP E-0, the RCS integrity is checked. If it is not preserved, there is a transition to EOP E-1 "loss of reactor or secondary coolant". Following the EOP E-1, the operator checks the RCS pressure. If it is higher than 1.5 MPa, there is a transition to the EOP ES-1.2 "post LOCA cooling and depressurization". The action indicated in EOP ES-1.2 to depressurize and cool the RCS is the controlled depressurization of the SGs at a cooling rate of 55 K/h through the SGs (TECNATOM, 1999), see Figure 5-18.
- From the EOP E-0, the CSF start to be monitored. There are six CSF status trees: F.0.1 "subcriticality", F.0.2 "core cooling", F.0.3 "heat sink", F.0.4 "RCS integrity", F.0.5 "containment integrity", F.0.6 "RCS coolant inventory", see (EPRI, 2011). The following criteria are used to determine the degree of threat for the CSF status tree: satisfied (green), not satisfied (yellow), severe challenge (orange) and extreme challenge (red). In those cases, where the status of the CSF status tree becomes severe challenge or extreme challenge, there is a transfer from the ORGs to the corresponding FRGs. In SBLOCA with HPSI failure sequences, the F.0.2 status tree plays an important role. Three FRGs can be distinguished in the F.0.2 status tree (EPRI, 2011), see Figure 5-19:
    - The EOP FR-C.3: Response to saturated core cooling (yellow).
    - The EOP FR-C.2: Response to Degraded Core Cooling (DCC) (orange).
    - The EOP FR-C.1: Response to Inadequate Core Cooling (ICC) (red).

The DCC condition is reached when the temperature of the CET exceeds 376 ^{o}C (649 K), see(Eisenhut, 1982; IEEE, 2002; Lutz, 2004; NRC, 2006, 1983). If this occurs, the FR-C.2 indicates that the SGs have to be depressurized at an RCS cooling rate of 55 K/h, similar to EOP ES-1.2. However, if the ICC condition is

reached, i.e., the CET exceeds 650 ºC (923 K), the EOP FR-C.1 indicates that the RCS shall be cooled through the SGs at the maximum RCS cooling rate (full opening of secondary circuit relief valves). It should be noted that there are F.0.2 status trees that consider the Reactor Vessel Level Indicator System (RVLIS) and the number of MCP running in addition to the CET temperature, to indicate which FRG must be followed FR-C.1, FR-C.2 or FR-C.3, see (EPRI, 2011; Montero-Mayorga et al., 2014).

To understand the management of the SBLOCA sequence in the 3 loops PWR-W in case of HPSI failure, it is also useful to study the SBLOCA ET in addition to the EOPs, see Figure 5-20. The SBLOCA ET indicates that in case of HPSI failure, to reach a successful end state, the success of the following headers is required, see red path (sequence 10) in Figure 5-20:

- [S] SCRAM.
- [AF] AFW.
- [D] RCS cooling and depressurization via the SGs.
- [A] Effective injection of the ACCs.
- [A-IS] Manual ACCs isolation or venting in order to avoid N2 injection in the RCS.
- [L] LPSI, in its two actuation modes, first the injection from the Refuelling Water Storage Tank (RWST) and
- [LR] the recirculation from the containment sump.

In most of the PSA of the PWR-W, the ETs header "RCS cooling via the SGs" considers the controlled SGs depressurization (ES-1.2 or FR C.2). However, some of them consider the fast SGs depressurization at the maximum RCS cooling rate (FR C.1). In summary, the main management strategies of SBLOCA with HPSI failure sequences in the PWR-W are:

- Controlled SGs depressurization through the relief valves in the SLs at an RCS cooling rate of 55 K/h (in ES-1.2 or FR-C.2).
- Fast SGs depressurization through full opening of the relief valves in the SLs when the ICC condition is reached, i.e., when CET temperature exceeds 650 ºC (923 K) (in FR C.1).

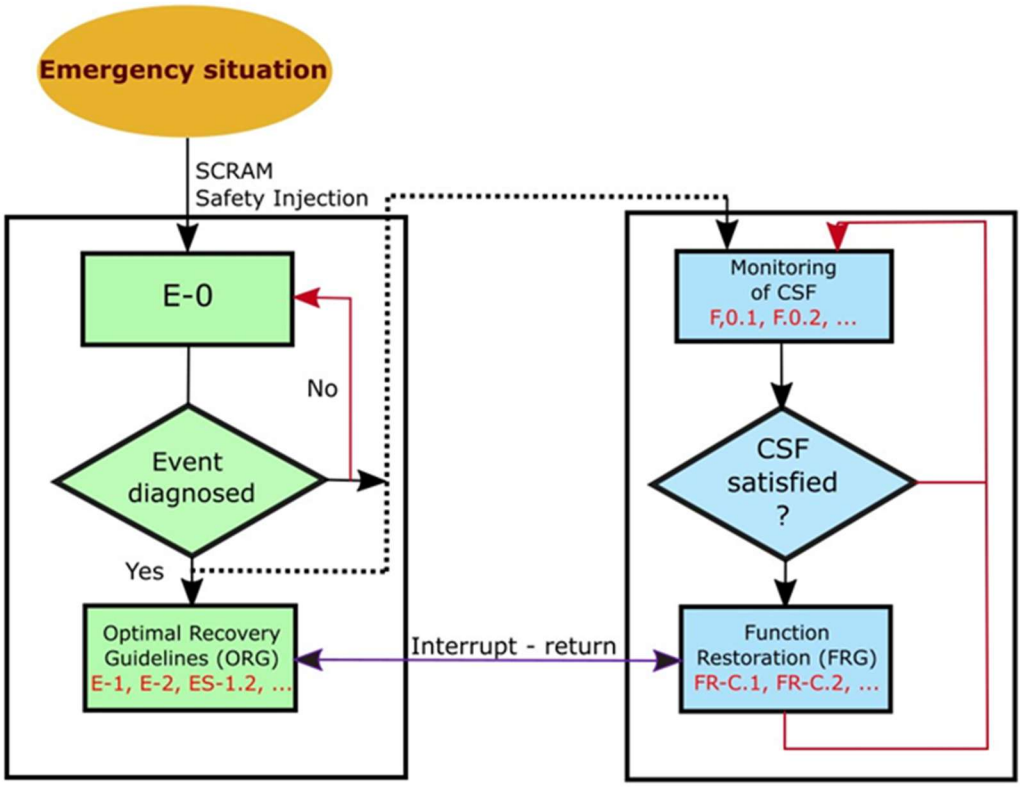

Figure 5-17 Emergency Operating Procedures scheme

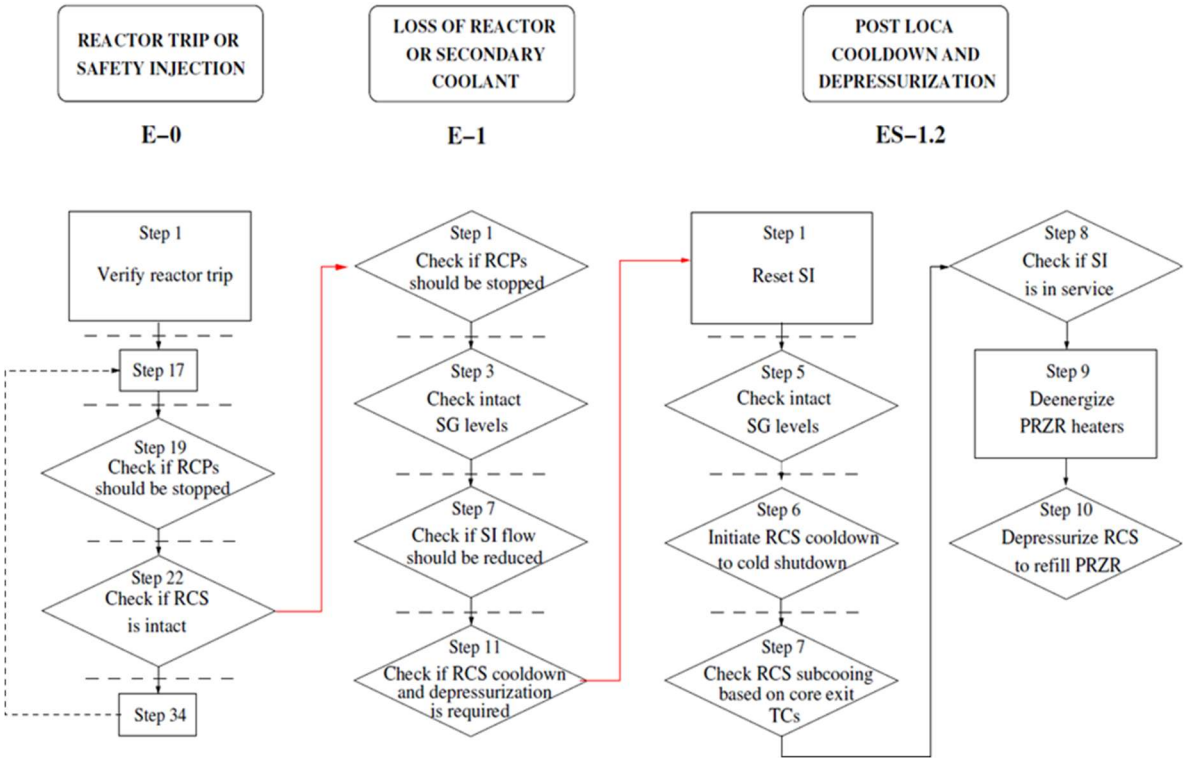

Figure 5-18 Westinghouse PWR EOP related with SBLOCA sequences (E-0, E-1, ES-1.2)

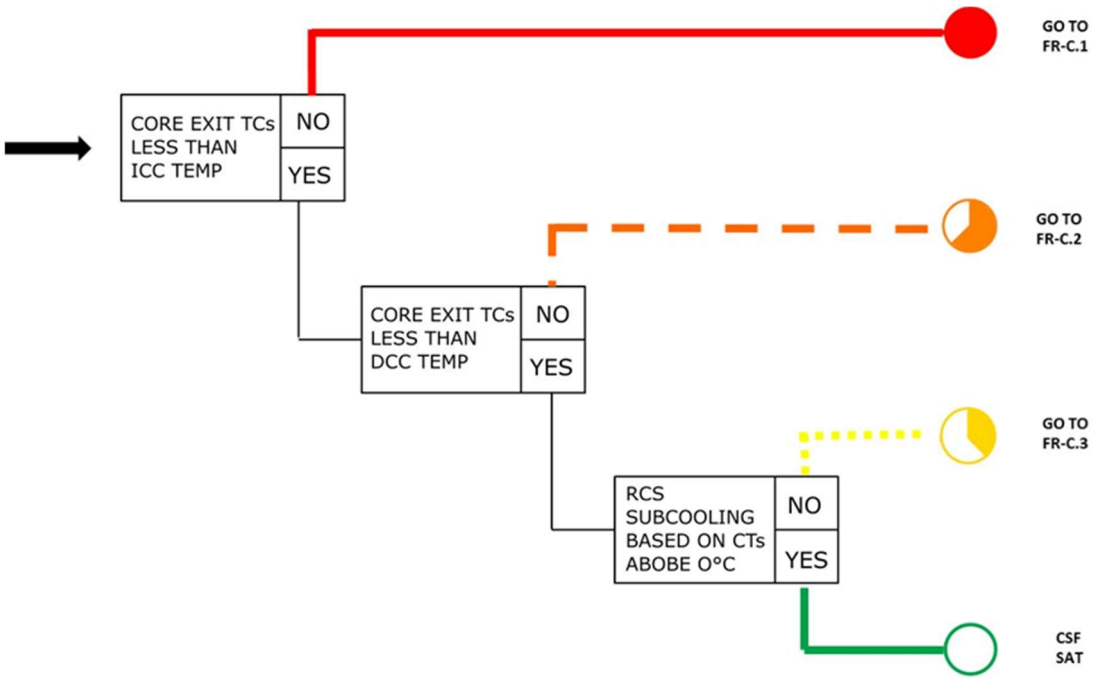

Figure 5-19 Westinghouse PWR FRG Core Cooling Status Tree (i.e., F.0.2)

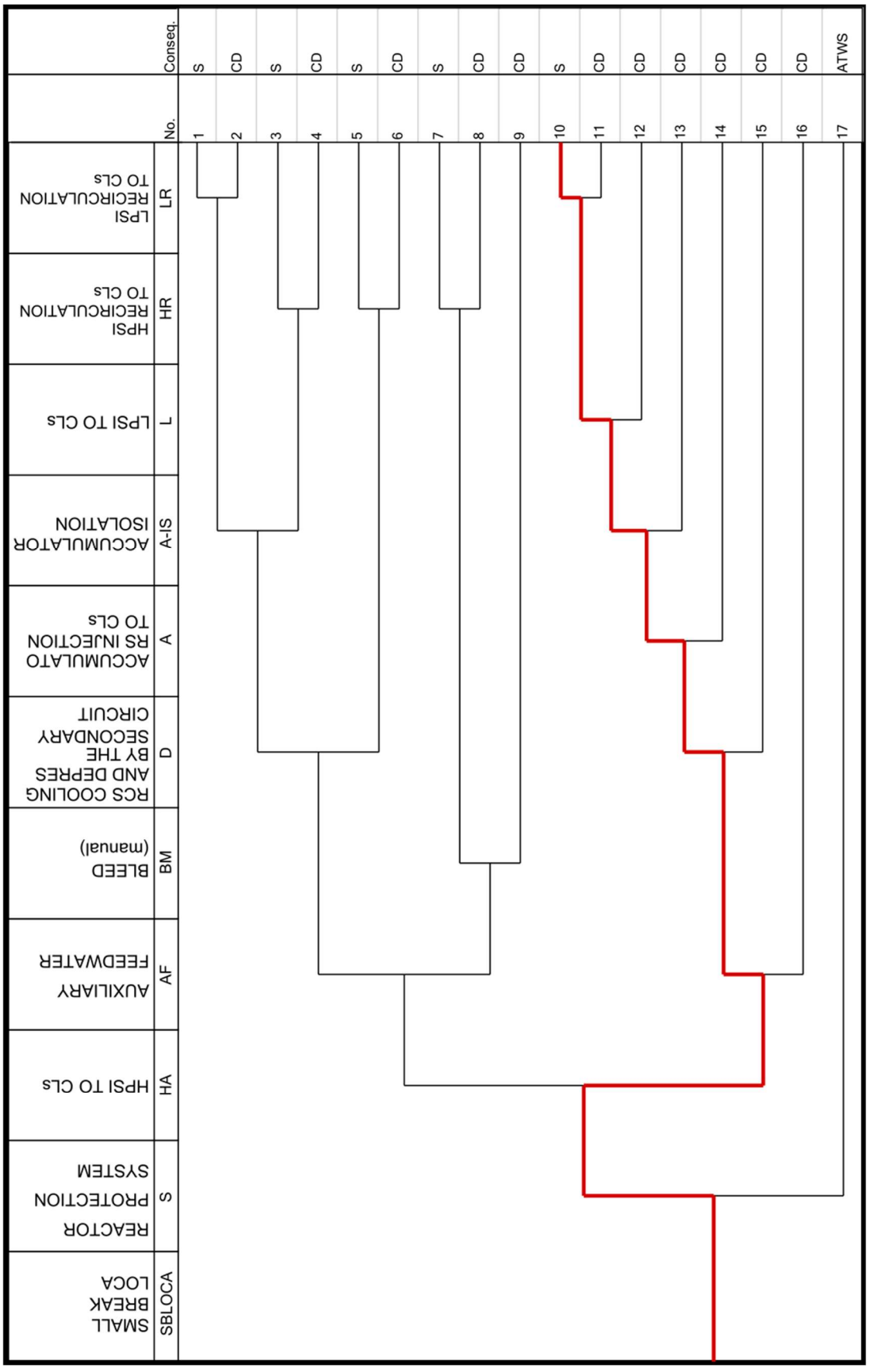

Figure 5-20 Westinghouse PWR SBLOCA ET

5.2.1.2. Management of VVER-1000/V320 SBLOCA sequences with HPIS failure

In the late 1990s, a significant number of VVER NPP decided to change their accident management approach, see (Bánáti and Ézsol, 1997; Cherubini et al., 2008; Groudev and Hadjiev, 2001; Pavlova et al., 2008, 2007). Most of the VVER-1000/V320 NPP adopted the Westinghouse EOPs-like approach, see (Bica, 1999; IAEA, 2000; Linn et al., 2002; United States General Accounting Office, 1996) and Figure 5-17. In some VVER-1000/V320 NPP, the equivalent of the PWR-W ORGs was referred to as the Accident Termination Guidelines (ATG), while the equivalent of the PWR-W FRGs were referred to as the Beyond Design Accident Management Guidance (BDBAMG), see (European commission EuropeAid Co-operation Office, 2006; Muellner, 2010). Besides, it is important to note that there is almost no public information on the EOPs of the VVER-1000/V320 reactors.

In an SBLOCA with HPIS failure sequence, before reaching ICC conditions, the management strategy carried out in VVER-1000/V320 reactors is to depressurize the SGs at a controlled RCS cooling rate. References were found indicating that the depressurization of the SGs is performed at an RCS cooling rate of 30 K/h or 60 K/h, see (Iegan et al., 2018; Muellner, 2010; Skalozubov et al., 2010). When the ICC condition is reached, the EOPs specify that it is necessary to initiate SGs depressurization at the maximum RCS cooling rate, i.e., full opening of the BRU-K or the BRU-A valves. References have been found indicating that the ICC condition is considered when the CET temperature exceeds between 350 ^{o}C (623 K) and 400 ^{o}C (673 K) (Groudev, 1998; P. P Groudev and Georgieva, 2010; Muellner, 2010).

In order to develop and qualify the new EOPs for the VVER-1000 reactors, part A of project R2.03 of the TACE-97 program "Development of software for VVER and RBMK reactor accident analysis" was launched (Del Nevo and D'Auria, 2007; European commission EuropeAid Co-operation Office, 2006; Parisi et al., 1997). Within this project, experiments were performed at the PSB-VVER experimental facility (Araneo, 2008; Del Nevo and D'Auria, 2007; Kardos et al., 2024). Among the experiments carried out in the PSB-VVER facility, four can be highlighted in which SBLOCA sequences were reproduced: tests 11 and 12, where the management action consisted in the controlled SGs depressurization at an RCS cooling rate of 30 K/h; and tests 4 and 16, where the management action consisted in the SGs depressurization at the maximum RCS cooling rate.

On the other hand, the SBLOCA ET for VVER-1000/V320 reactors (Skalozubov et al., 2010) shows that in case of HPIS failure, the remaining ET headers have to be fulfilled for the sequence to be successful, see Figure 5-21 (sequence 3). These headers are the following:

- [S] SCRAM
- [D] RCS cooling by a controlled SGs depressurization along with operation of the EFW or the AFW pumps.
- [B] Boron injection.
- [EGRS] Opening of the EGRS valve.
- [A] Effective injection of the HA-1.
- [L] Injection of the LPIS from containment sump tanks.

Therefore, the ET indicates that, in addition to the RCS cooling through the controlled SG depressurization, the EGRS actuation is also required. On the other hand, it should be noted that in the VVER-1000/V320 reactors, the RCS cooling by the SGs depressurization is performed through the BRU-K or through the BRU-A if the condenser is not available. In summary, the main strategies found in the VVER-1000/V320 reactors in the event of an SBLOCA with HPIS failure sequence are as follow:

- Controlled SGs depressurization at a RCS cooling rate of 30 K/h or 60 K/h.
- Controlled SGs depressurization along with EGRS actuation.
- Fast SGs depressurization at maximum RCS cooling rate when ICC condition is reached.

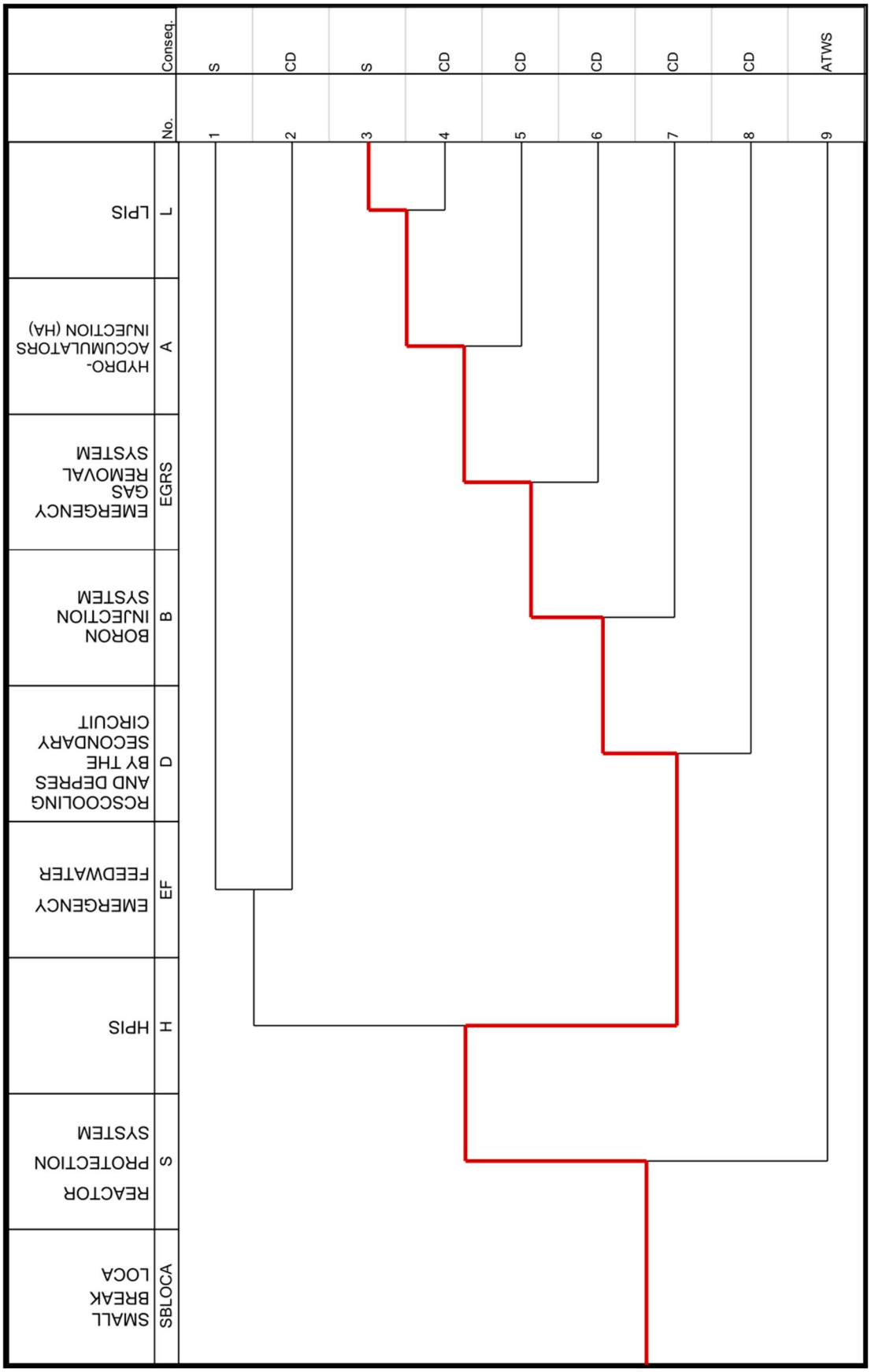

Figure 5-21 VVER-1000/V320 SBLOCA ET (Skalozubov et al., 2010)

5.2.2. VVER-1000/V320 SBLOCA sequence with HPIS failure without human actions

The SBLOCA sequence with HPIS failure is analyzed without considering the actions taken by the MCR crew. First, SBLOCA with HPIS failure and no human intervention is analyzed as a base case. Then, the impact of the break size on the sequence is analyzed and the so-called PD curve is constructed.

5.2.2.1. SBLOCA sequence with HPIS failure: Base case

A break size of 1.5 inches located in the CL 1 was chosen for the SBLOCA sequence with HPIS failure without human action. In addition, the following hypotheses were made:

- Core power at the beginning of the transient: 100%.
- The LPIS and HA-1 availability correspond to the SBLOCA SC: 2 out of 4 HA-1 trains available and 1 out of 3 LPIS trains available (Skalozubov et al., 2010).
- The HPIS is unavailable.

The accidental sequence begins 300 s after the start of the simulation. During the first few seconds of the transient, the RCS pressure drops and reaches the HPIS setpoint, see Figure 5-22, however the HPIS pumps do not inject during the sequence. The RCS pressure continues to fall, but remains just above the HA-1 pressure, preventing the HA-1 injection into the RPV. Therefore, the collapsed core water level does not recover as no safety system is refilling it, see Figure 5-23. The core starts to uncover at about 6000 s, see Figure 5-24. At 7081s, the RCS pressure becomes equal to that of the HA-1, allowing injection, but too late as the core water collapsed level is low. Finally, CD is reached when the PCT exceeds 1477 K at 8126 s. At this point, the total inventory lost due to the break is approximately 2.1 x 105 kg, see Figure 5-25. Besides, it is worth noting that CD occurs when the RCS pressure is well above the LPIS setpoint.

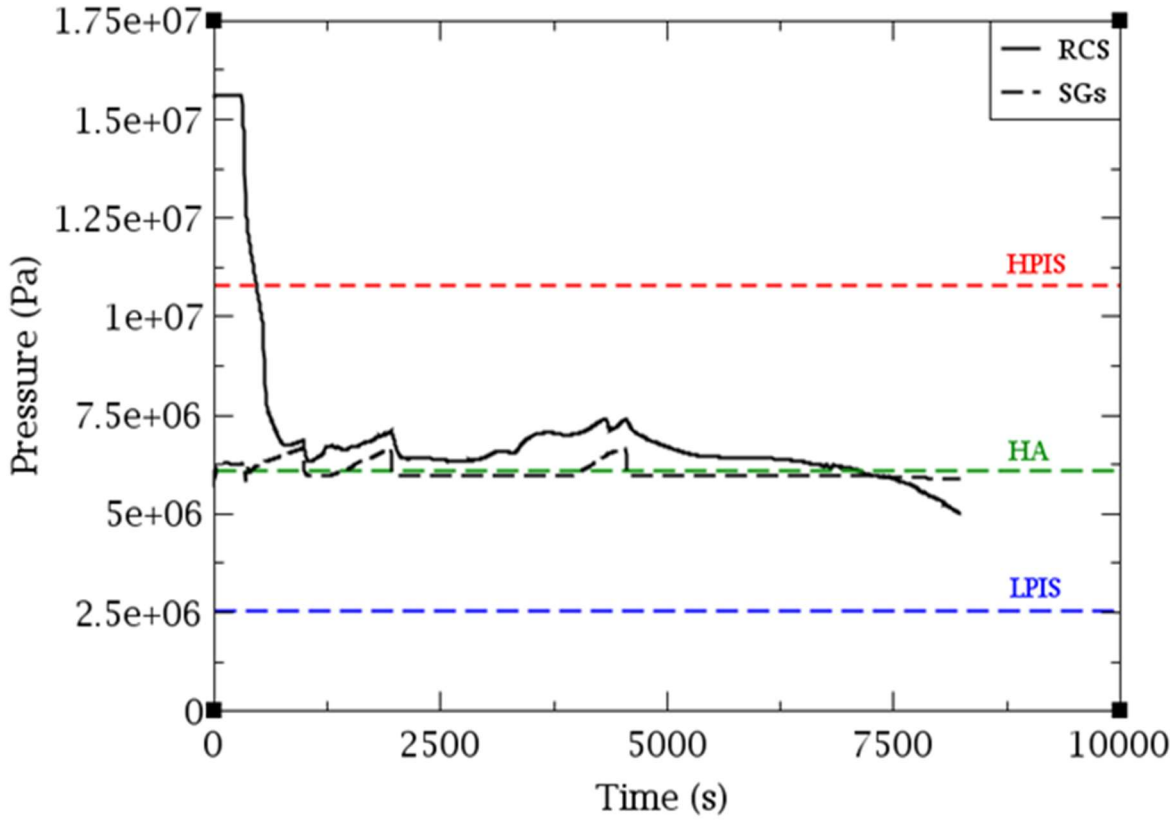

Figure 5-22 RCS and SGs pressure, SBLOCA (1.5 inches) with HPIS failure without human action

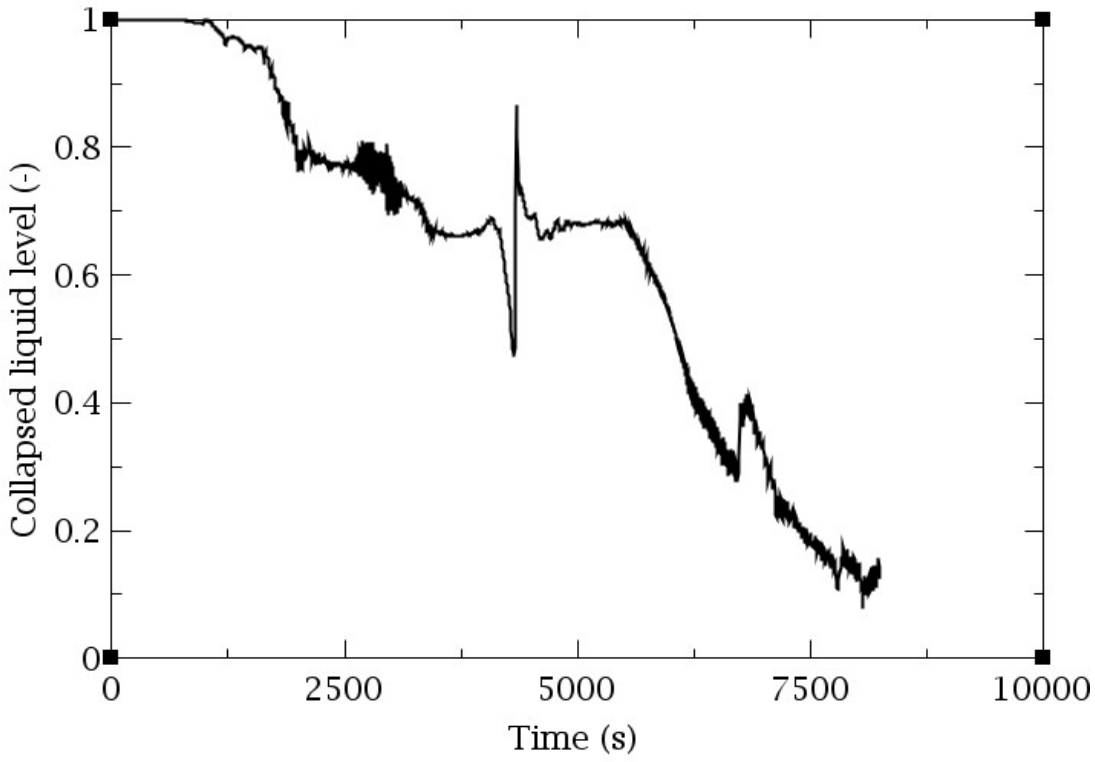

Figure 5-23 Collapsed Core Level, SBLOCA (1.5 inches) with HPIS failure without human action

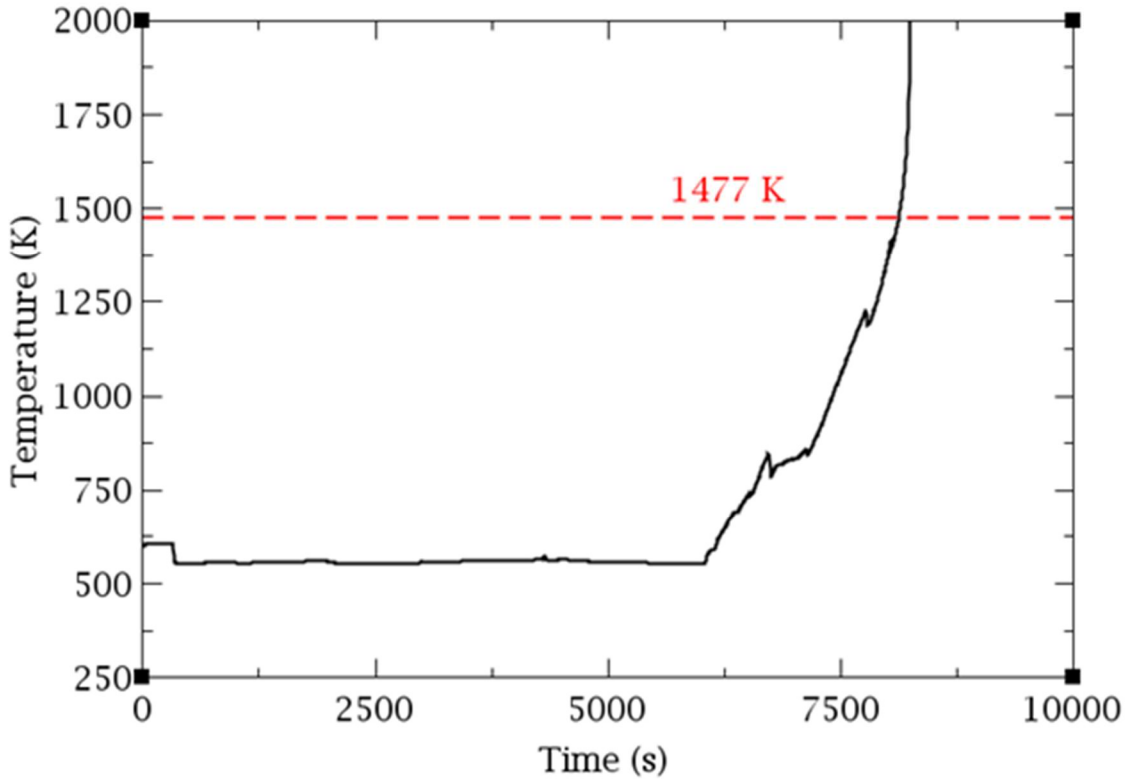

Figure 5-24 PCT, SBLOCA (1.5 inches) with HPIS failure without human action

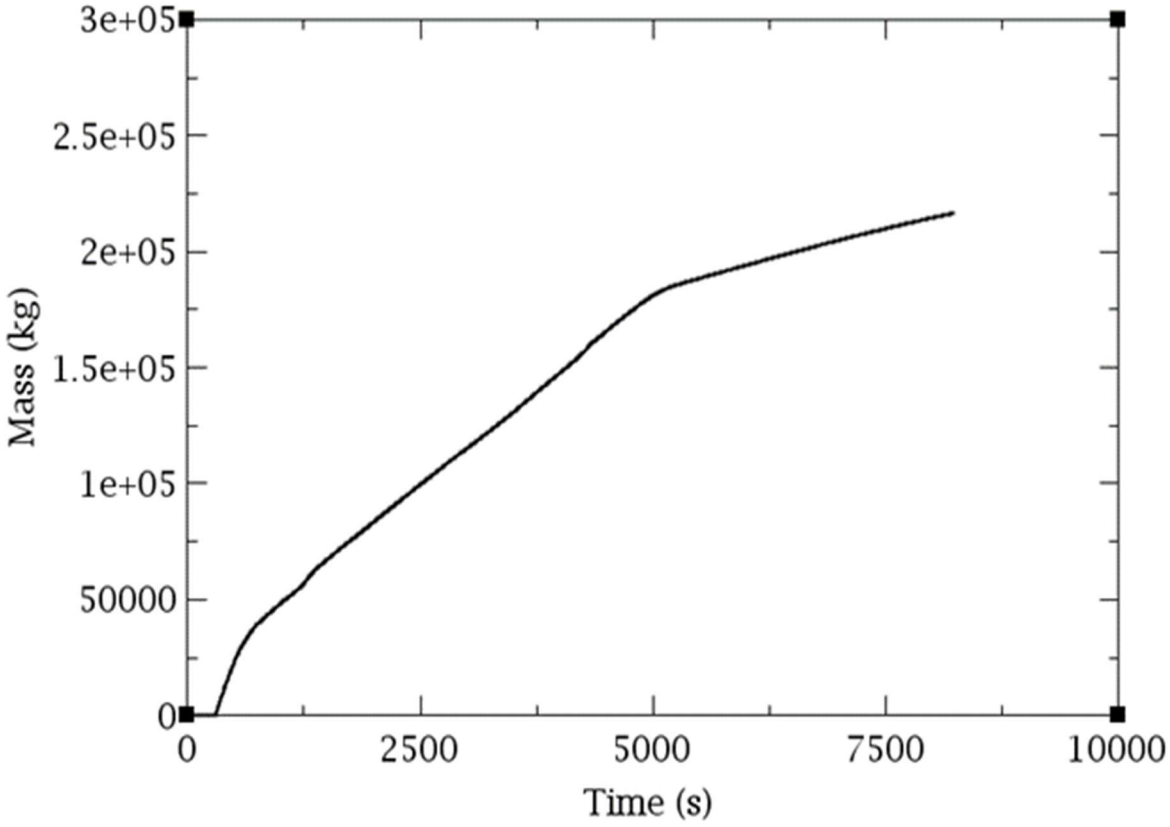

Figure 5-25 Integral of the mass flow through the break, SBLOCA (1.5 inches) with HPIS failure without human action

5.2.2.2. Previous Damage Curve. Impact of break size in SBLOCA evolution

In order to assess the effectiveness of a management strategy in an accidental sequence, it is essential to know first when CD would occur without human actions. This information is provided by the denominated PD curve. To obtain the PD curve, SBLOCA with HPIS failure sequences have been simulated for different break sizes without any management action. The range for the break sizes considered is between 1 to 6 inches with a step of 0.25 inches. Each simulated case can reach two conditions: damage, if the PCT exceeds 1477 K, or success if the PCT does not exceed this temperature, see Figure 5-26. Besides, the RCS depressurization is also analyzed, see Figure 5-27.

For the cases that CD is reached, CD times are plotted against the break sizes, see Figure 5-28. The "damage" sequences are represented by a red marker at the time CD is reached, while the "success" sequences are represented by a green marker (see electronic version). The curve that follows all the red markers is called the PD curve. A detailed analysis of the PD obtained shows:

- From 2.5 inches onwards the LOCA sequences with HPIS failure, are successful. This is because the RCS is depressurizing through the break fast enough allowing the injection of the HA-1 and LPIS on time.
- Between 1 and 2.25 inches, all the sequences exceed the damage condition. For smaller breaks sizes, CD takes longer to occur, and as the break sizes get larger, CD occurs earlier.

Along with the PD curve, the core uncovering time curve, the HA-1 time injection curve and the LPIS time injection curves have also been plotted, see Figure 5-28. The following conclusions can be drawn from these curves:

- The HA-1 inject at every break size analyzed, but at smaller break sizes, between 1 and 2.25 inches, it is too late to stop the PCT from rising.
- The LPIS injects before damage for break sizes from 2.25 inches onwards. This is because for smaller LOCA the RCS pressure remains around the HA-1 pressure, preventing it from reaching the LPIS shutoff pressure (2.55 MPa).
- The SBLOCA with HPIS failure sequences are successful when the LPIS inject water into the RCS before CD.
- There is core uncovering from 1 to 3 inches but from 2.5 inches onwards LPIS injection avoid CD.

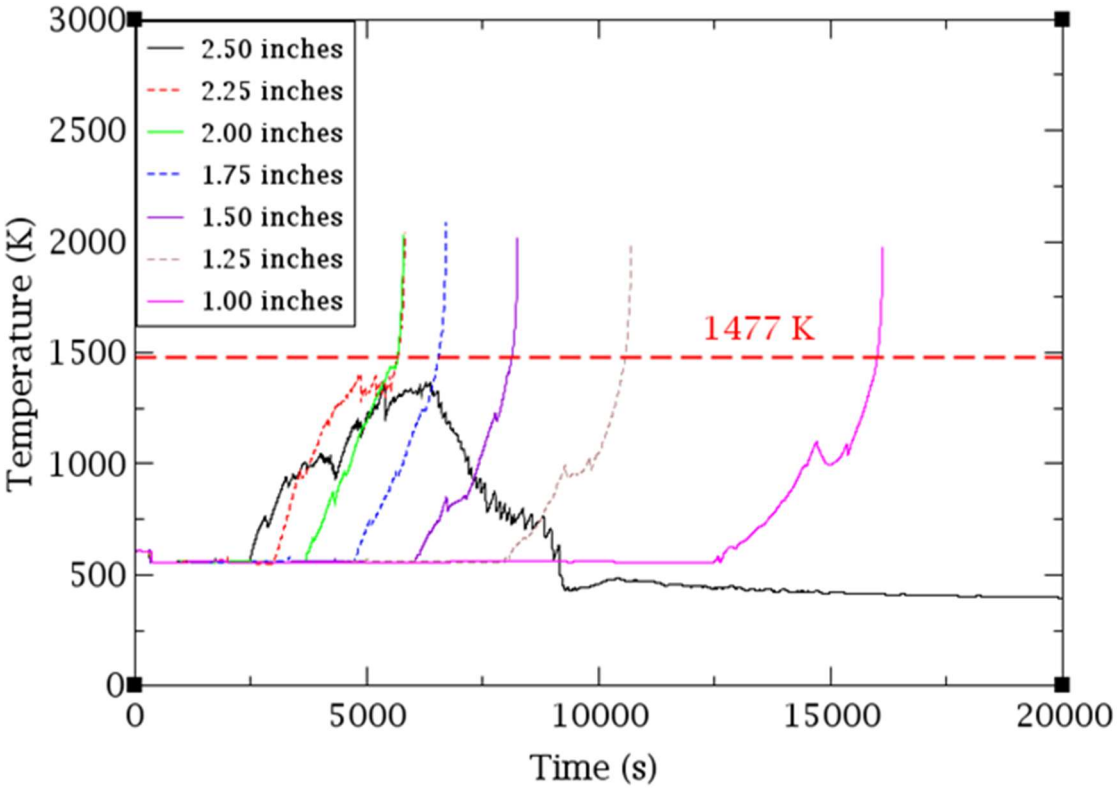

Figure 5-26 PCT, SBLOCA (1 – 2.5 inches) with HPIS failure without human action

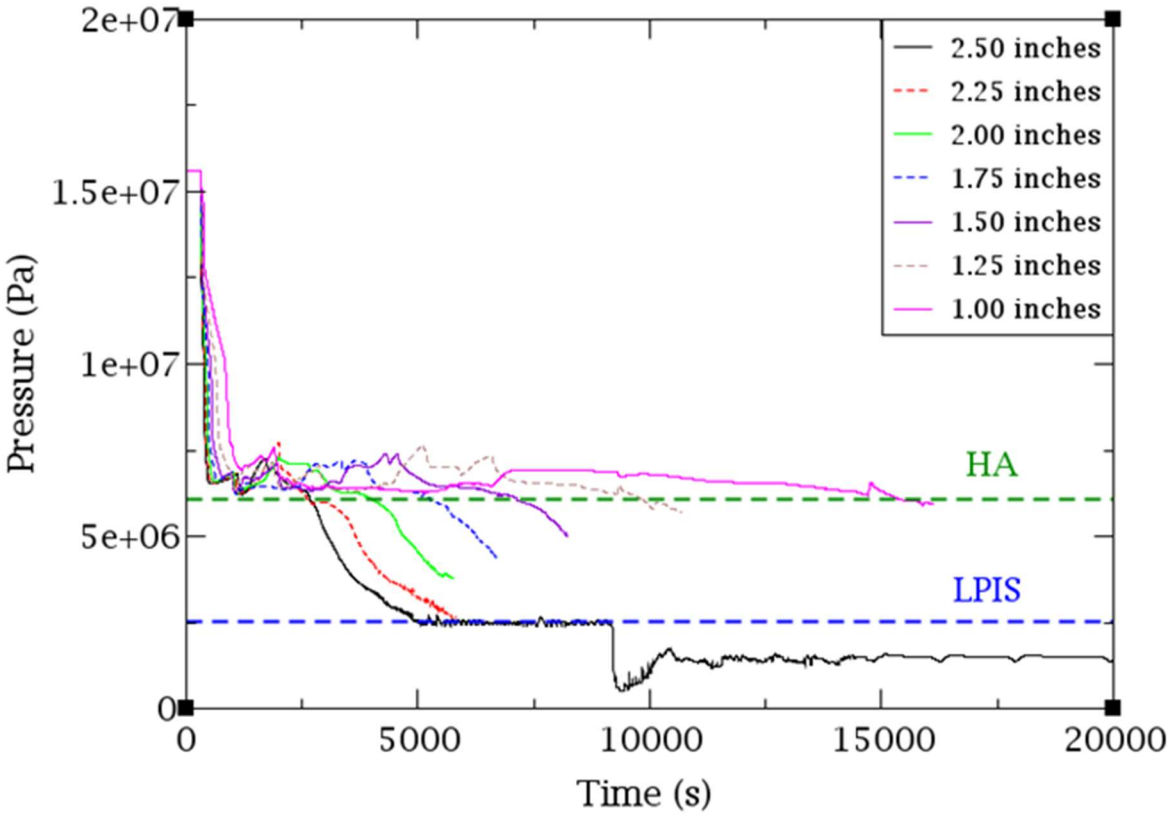

Figure 5-27 RCS pressure, SBLOCA (1 – 2.5 inches) with HPIS failure without human action

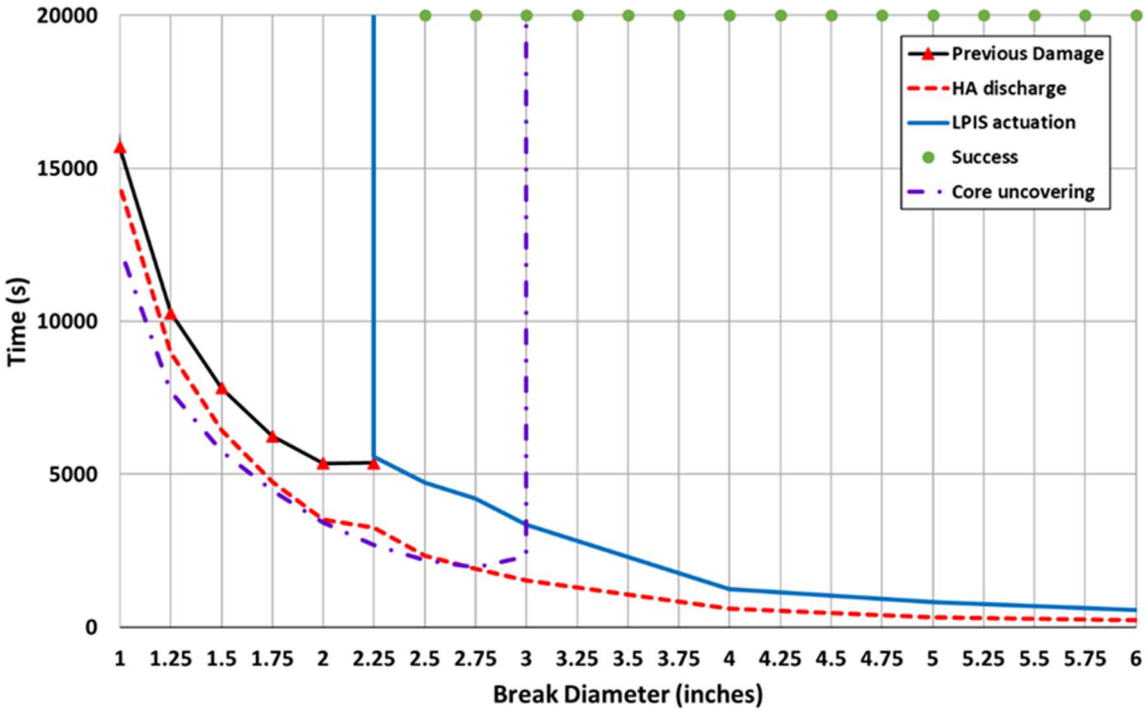

Figure 5-28 Previous Damage curve for SBLOCA with HPIS failure (VVER-1000/V320)

5.2.3. VVER-1000/V320 SBLOCA sequence with HPIS failure and controlled SGs depressurization

By obtaining the PD curve of the SBLOCA sequence with HPIS failure, it has been found that there is a range of break sizes that reach CD if no human actions are credited. Therefore, in these sequences, it is necessary that the control room crew performs a management strategy to ensure core cooling. The analysis of the controlled depressurisation action of the SGs to cool the RCS consists of the following items:

- Section 5.2.3.1: A set of four cases of the SBLOCA with HPIS failure and controlled SGs depressurization is shown for each of the RCS cooling rates under study, 30 K/h and 60 K/h.
- Section 5.2.3.2: The DDs for 30 K/h and 60 K/h are obtained.
- Section 5.2.3.3: A Sensitivity analysis of the DD on certain boundary conditions is presented.

5.2.3.1. SBLOCA sequence with HPIS failure and SGs controlled depressurization: Base Cases

The sequences in which the operators have performed the action of depressurizing the SGs in a controlled manner, is analyzed in detail below for both RCS cooling rates, 30 K/h and 60 K/h. For both cooling rates, the SBLOCA sequence has been simulated with different start times of the manual action, to assess how sensitive the success of the sequence is to this time value. The break size chosen has been the 1.5 inches located in the CL 1 with the hypotheses considered in the base case of the SBLOCA sequence with HPIS failure without human actions.

Depressurization with 30 K/h RCS cooling rate

The start time, from the beginning of the SBLOCA sequence (1.5 inches), selected for the SGs depressurization at a 30 K/h rate have been 7000 s, 6200 s, 5400 s and 3700 s. The SBLOCA sequence starts 300 s after the beginning of the simulation and the evolution of the events is that of the sequence without SGs depressurization until the manual action is initiated. From then on, each SBLOCA sequence evolves in a different way, depending on the start of the SGs depressurization:

- 7000 s: In this case the operator action starts too late, Figure 5-29, since in the PD curve shows that the previous CD occurs at 7500 s.
- 6200 s and 5400 s: In these cases, the SGs pressure starts to reduce the RCS pressure as soon as the manual action is initiated, see Figure 5-30. The RCS pressure reaches the HA-1 pressure and continues to fall, but before it reaches the LPIS cut-off pressure, CD occurs, see Figure 5-29. This is because the collapsed core level is already low when the operator action is initiated, see Figure 5-31.
- 3700 s: In this case, since the manual action is initiated earlier, the RCS pressure reaches the LPIS cut-off pressure before CD occurs, see Figure 5-30. It can be seen that the RCS cools at a rate of 30 K/h until it reaches the LPIS cut-off pressure at about 12000 s, see Figure 5-32. When this point is reached, the core is reflooded, see Figure 5-31.

For the four analyzed start times for the controlled SGs depressurization at an RCS rate of 30 K/h that have been analyzed, it can be observed that the core uncovering, which occurs once the PCT starts to increase, begins when the collapsed liquid level in the core is below 50 %, Figure 5-29 and Figure 5-31.

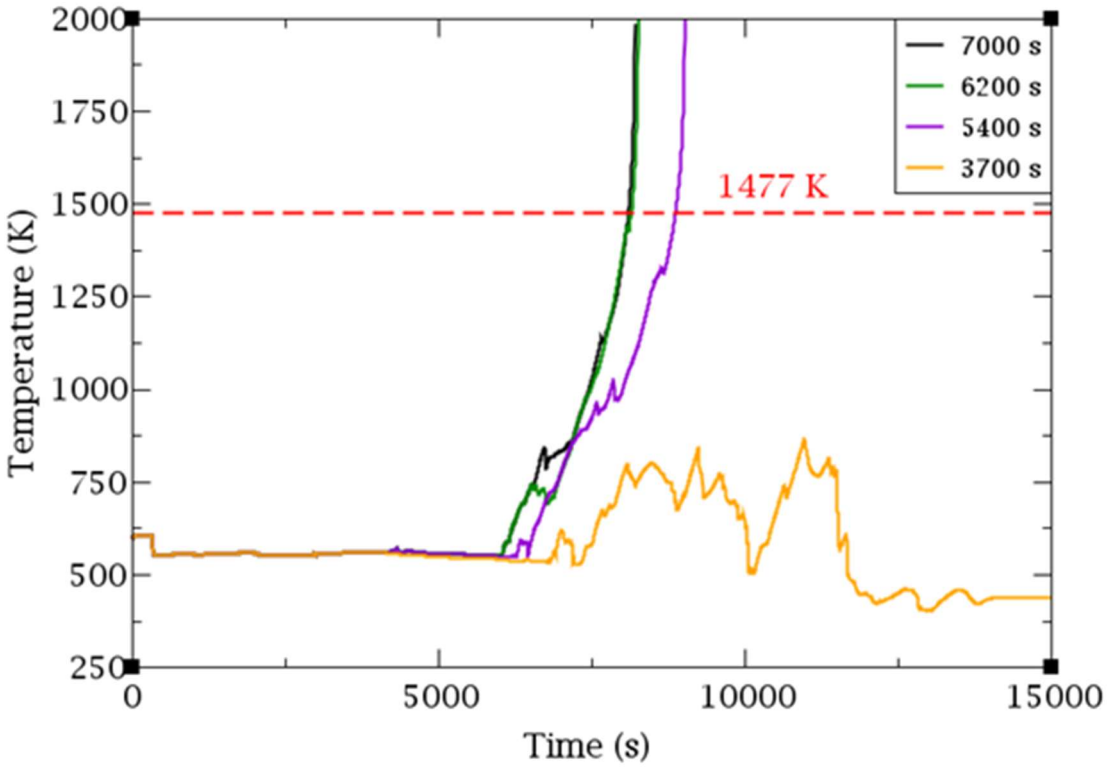

Figure 5-29 PCT, SBLOCA (1.5 inches) with HPIS failure and RCS cooling at 30 K/h

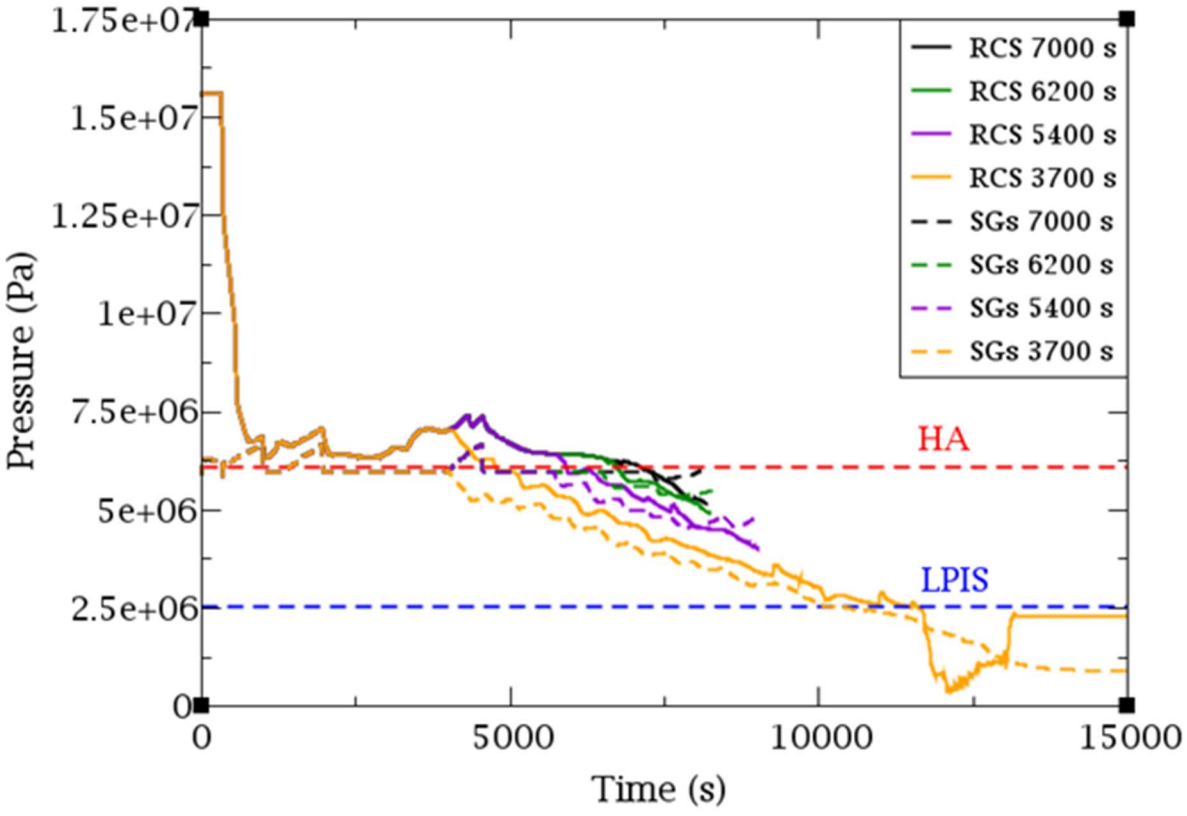

Figure 5-30 RCS and SGs pressure, SBLOCA (1.5 inches) with HPIS failure and RCS cooling at 30 K/h

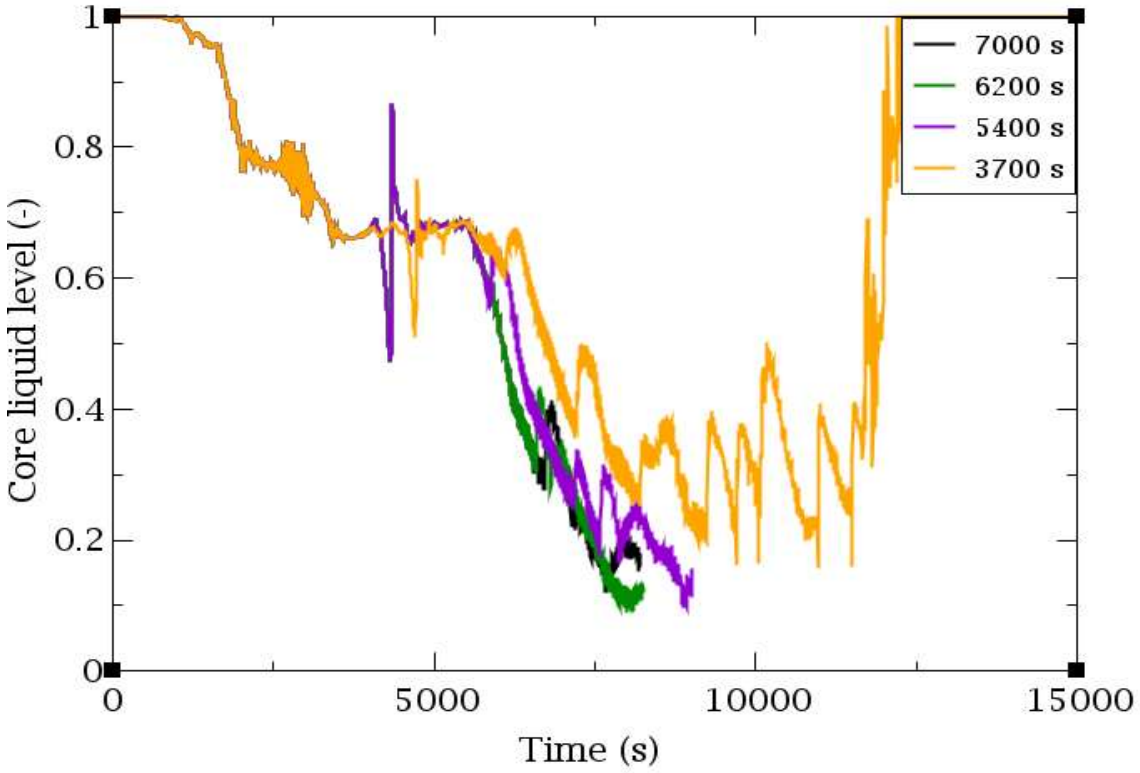

Figure 5-31 Collapsed liquid level, SBLOCA (1.5 inches) with HPIS failure and RCS cooling at 30 K/h

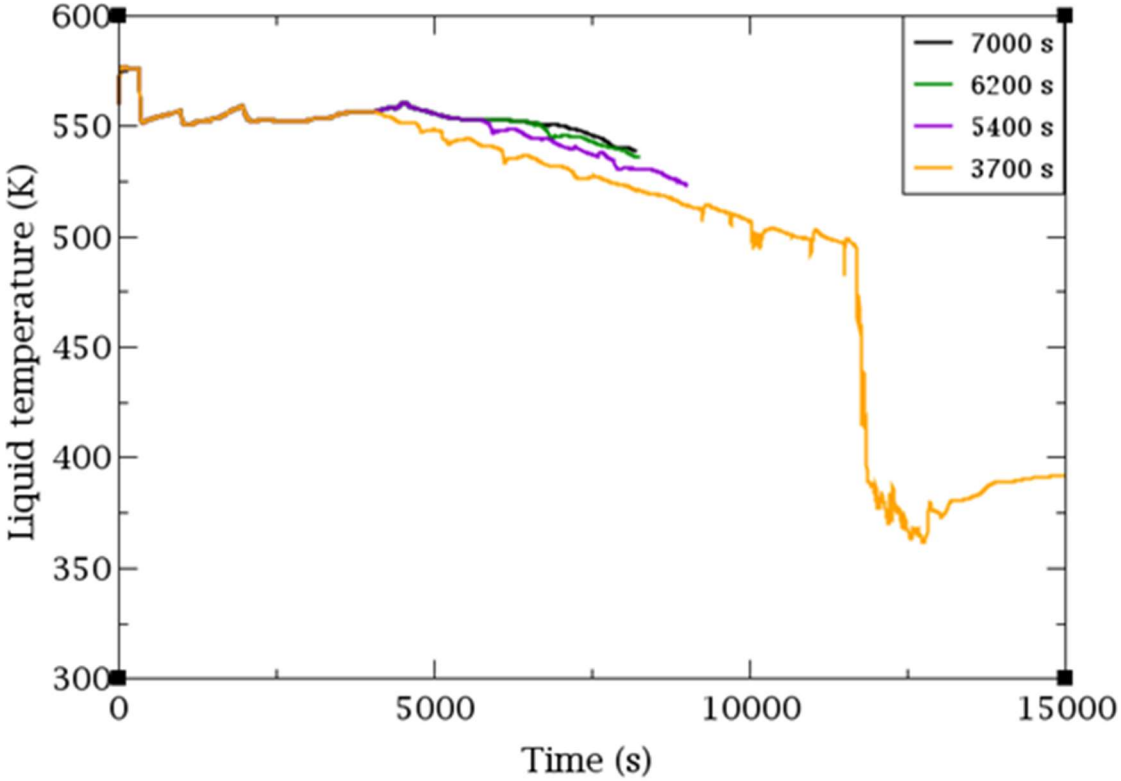

Figure 5-32 RCS average liquid temperature, SBLOCA (1.5 inches) with HPIS failure and RCS cooling at 30 K/h

Depressurization with 60 K/h RCS cooling rate

The start time, from the beginning of the SBLOCA sequence (1.5 inches), selected for the SGs depressurization at a 60 K/h rate have been between 3700 and 7000 s. The SBLOCA sequence starts 300 s after the beginning of the simulation and the evolution of the events is that of the sequence without SGs depressurization until the manual action is initiated. Thereafter, each of the four SBLOCA sequences has a different evolution:

- 7000 s: It can be observed that as soon as the depressurization of the SGs starts, the RCS pressure starts to drop rapidly, however, the core level is too low when the HA-1 discharge starts, so that finally CD cannot be avoided, see Figure 5-33.
- 6200 s: Although core uncovering occurs, see Figure 22, the RCS pressure successfully reaches the LPIS cut-off pressure in time to reflood the core, see Figure 21, before the PCT exceeds 1477 K, see Figure 20.
- 5400 s and 3700 s: The RCS pressure successfully reaches the LPIS cut-off pressure, see Figure 5-34.

As expected, the depressurization of the SGs at an RCS cooling rate of 60 K/h, Figure 5-34 and Figure 5-36 allows the RCS pressure to reach the LPIS cut-off pressure earlier than for a cooling rate of 30 K/h. This means that core reflooding starts much earlier, when the PCT is not yet high. For the four analyzed start time, it can be observed that the core uncovering, which occurs once the PCT starts to increase, begins when the collapsed liquid level in the core is below 50 %, see Figure 5-33 and Figure 5-35.

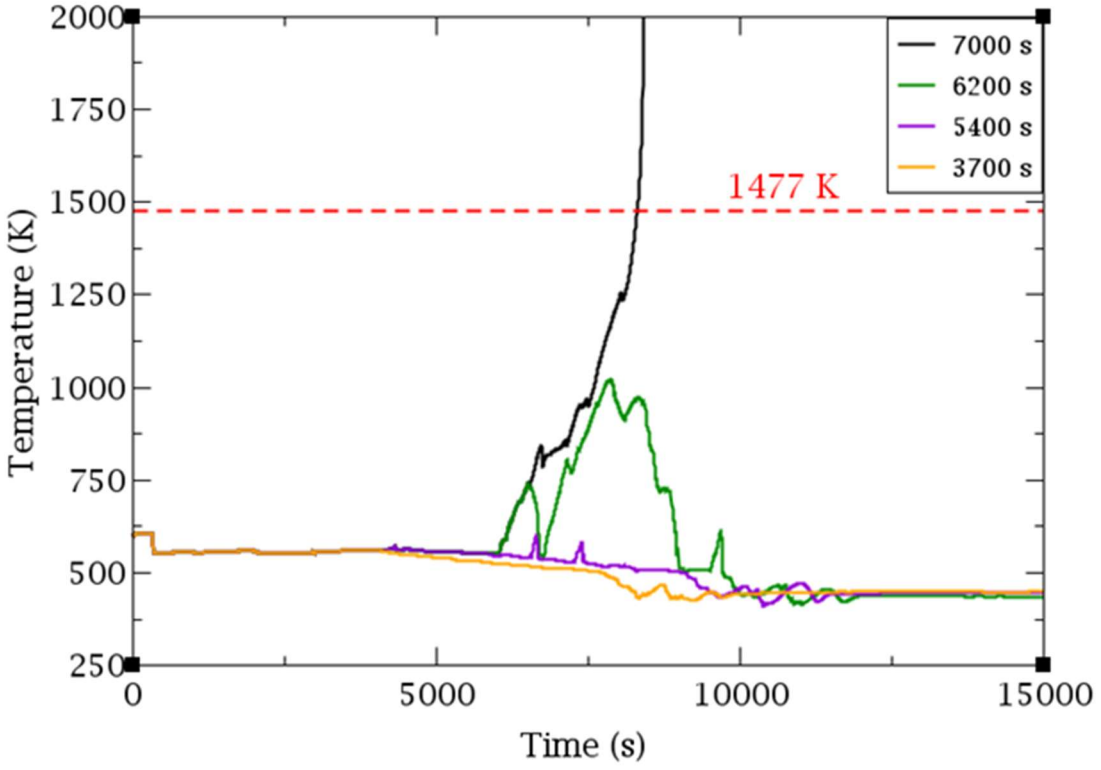

Figure 5-33 PCT, SBLOCA (1.5 inches) with HPIS failure and RCS cooling at 60 K/h

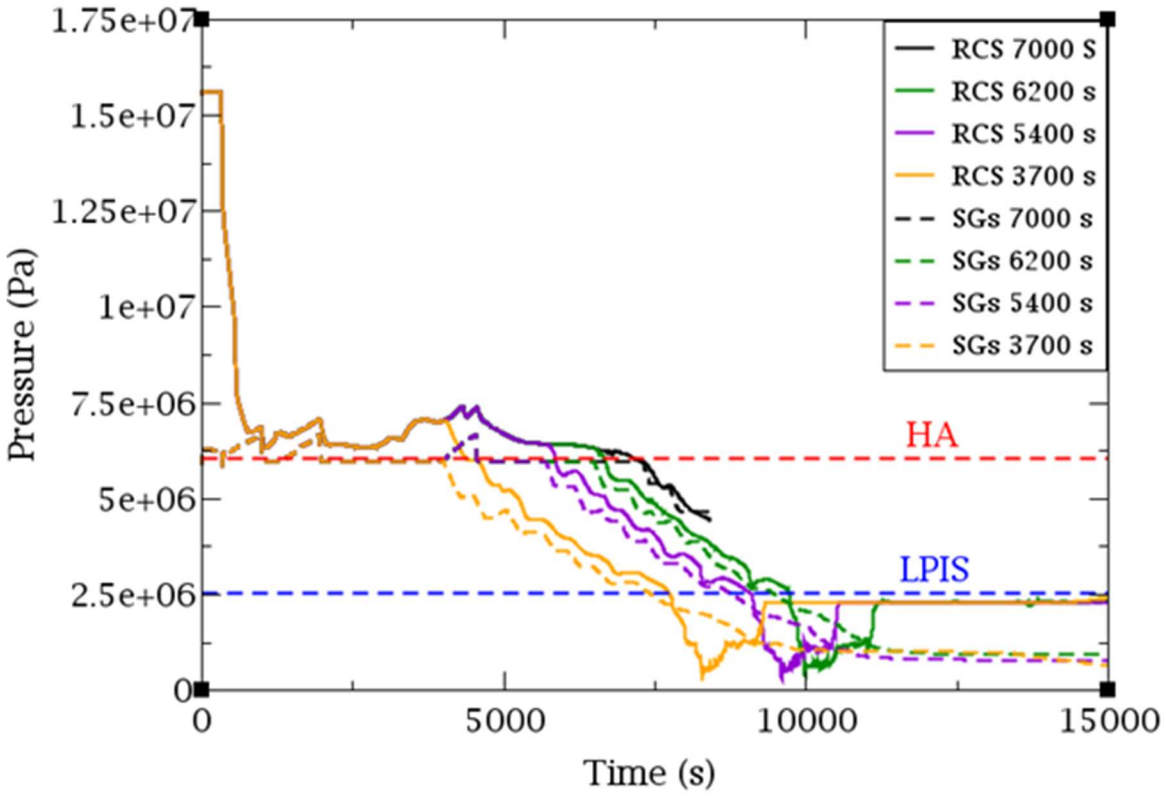

Figure 5-34 RCS and SGs pressure, SBLOCA (1.5 inches) with HPIS failure and RCS cooling at 60 K/h

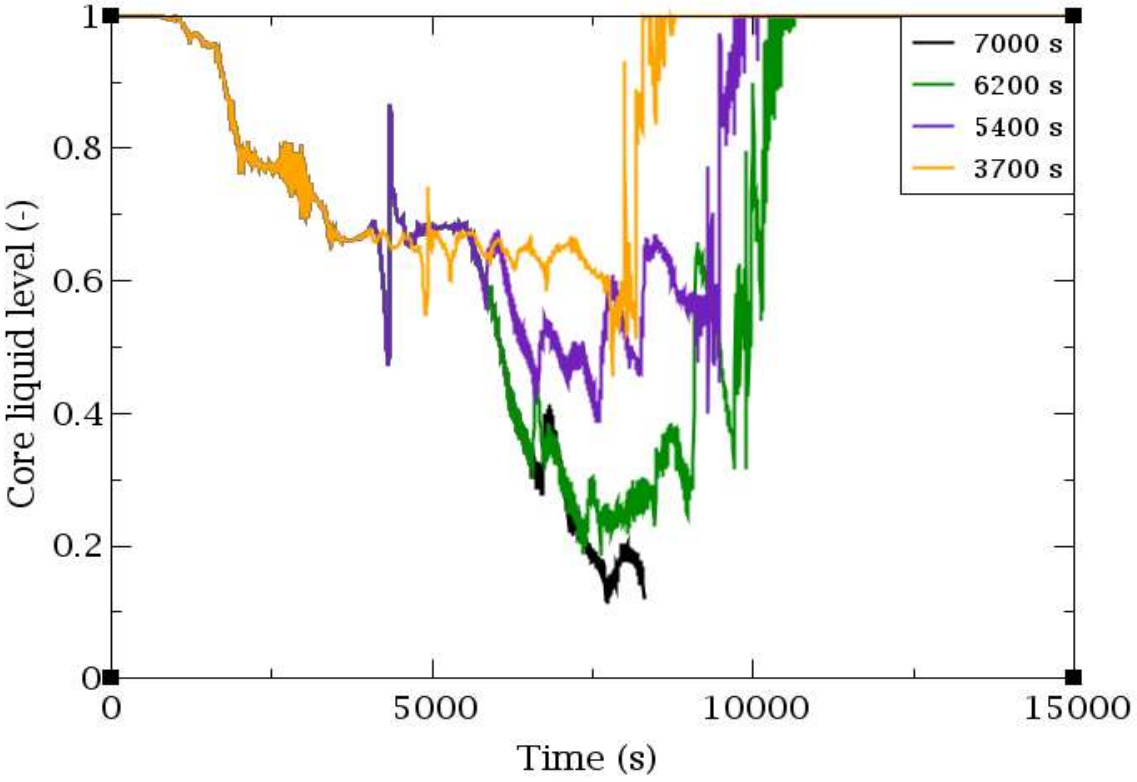

Figure 5-35 Collapsed liquid level, SBLOCA (1.5 inches) with HPIS failure and RCS cooling at 60 K/h

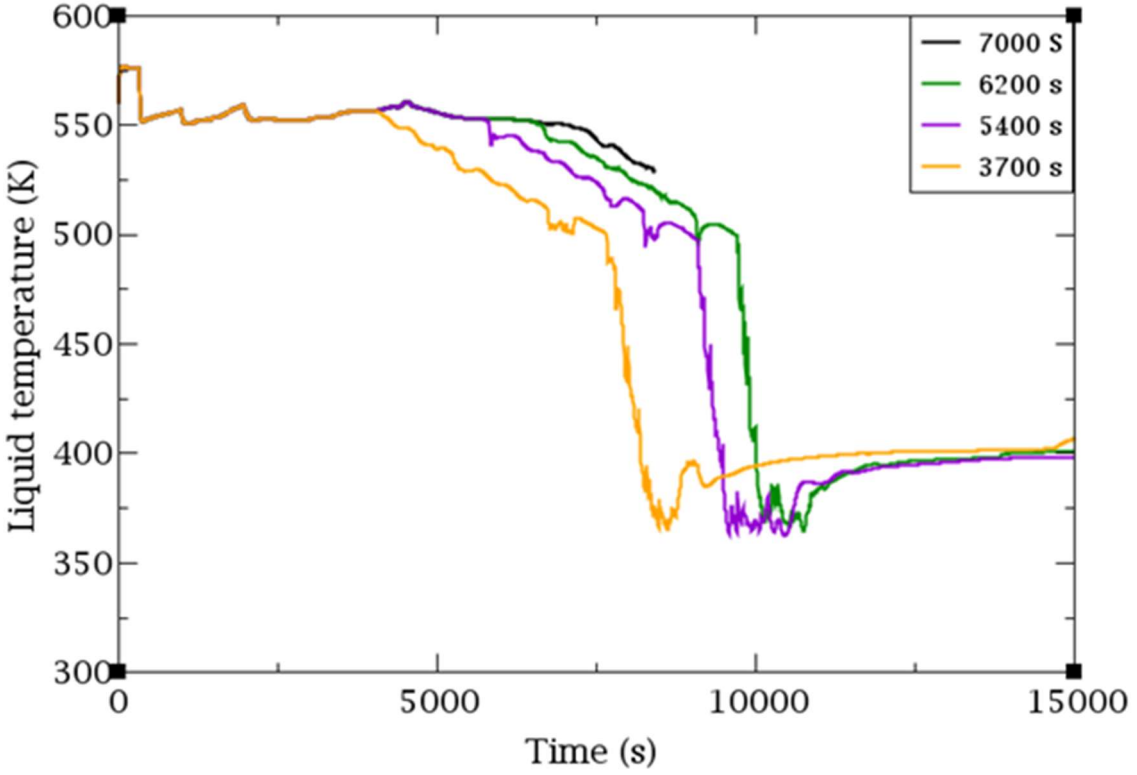

Figure 5-36 RCS average liquid temperature, SBLOCA (1.5 inches) with HPIS failure and RCS cooling at 60 K/h

5.2.3.2. Damage domains for the SGs controlled depressurization

The DD for a given action in a given sequence can be defined as the region of the space of uncertain parameters where CD (or any damage condition considered) is reached. The number of dimensions for this space region corresponds to the number of uncertain parameters involved in the analyzed sequence. The considered DD for the SBLOCA sequence with HPIS failure with controlled SGs depressurization has two dimensions, the break size and the start time of the manual action.

In order to obtain the DD, a series of TH simulations are performed by varying the parameters considered. For that purpose, it is previously established which are the limits for the seeking of the DD. The following considerations have been made in this analysis:

- Break Size: the DD in the break size dimension lies between the limits of the PD curve (1, 2.25 inches). This is because the sequences with larger break sizes that do not fall within the PD curve are successful without the need for any manual action.
- Depressurization start time: The DD enclosed the PD curve in the depressurization beginning time dimension.

In order to obtain the DD for both RCS cooling rates of 30 K/h or 60 K/h, the SBLOCA with HPIS failure sequence has been simulated for each break size between 1 and 2.25 inches, with an interval of 0.25 inches, testing different start times of the manual action from the PD curve, see Figure 5-37 (left) and Figure 5-38 (left). The DD is then obtained by drawing the line separating the damage and success regions, see Figure 5-37 (right) and Figure 5-38 (right).

The DD provides information on the time from which the manual action considered is no longer effective, but another factor has to be taken into account: the time it takes for the MCR crew to reach the EOP step where the action is indicated to be performed. The time required by the MCR crew to initiate the controlled depressurization of the SGs is around 600 s (t_{min} = 600 s). Subtracting this time from the DD lower limit gives the available time to accomplish the human action, see Figure 5-39.

$$t_{available} = t_{damage\ domain} - t_{min}$$

In this study, the available time is classified into three categories: short, if it is less than 15 minutes, medium, if it is between 15 minutes and 1 hour, or long, if it is more than 1 hour. The following conclusions can be drawn from these curves:

- 30 K/h RCS cooling rate: The break sizes around 2.25 inches have no available time to depressurize at an RCS cooling rate of 30 K/h. The available time is short for the 2 inches break size, medium between 1. 75 and 1.5 inches, and long below 1.5 inches.
- 60 K/h RCS cooling rate: The smallest available time is given for the 2 inches break size, but in this case the available time is medium, 2900 s. The available time is medium between 2.25 and 2 inches and long below 1.75 inches.

The available time obtained corresponds to a t_{min} = 600 s. It should be noted that there is some uncertainty in the time required by the MCR crew. Therefore, if a larger t_{min} value is found, the available time for the 60 K/h RCS cooling rate would be lower and the range of break sizes without available time for the 30 K/h RCS cooling rate would be greater, see Figure 5-39.

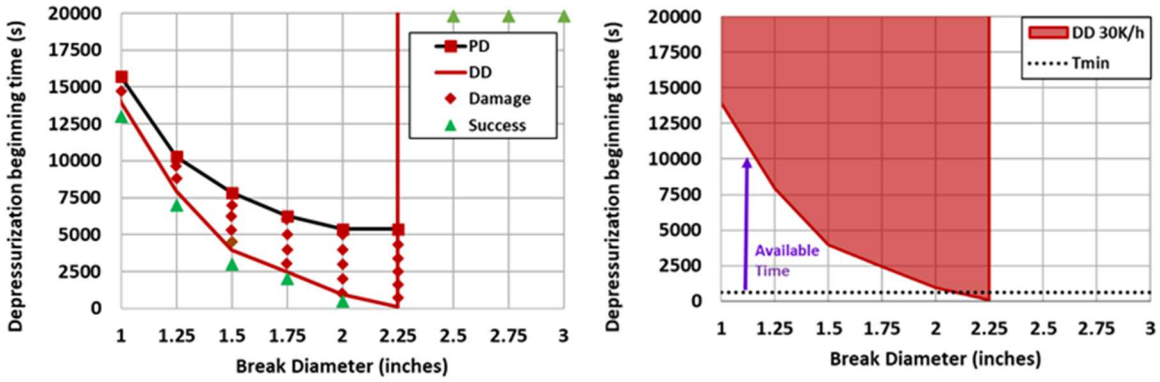

Figure 5-37 Damage Domain for SBLOCA with HPIS failure and 30 K/h RCS cooling (VVER-1000/V320)

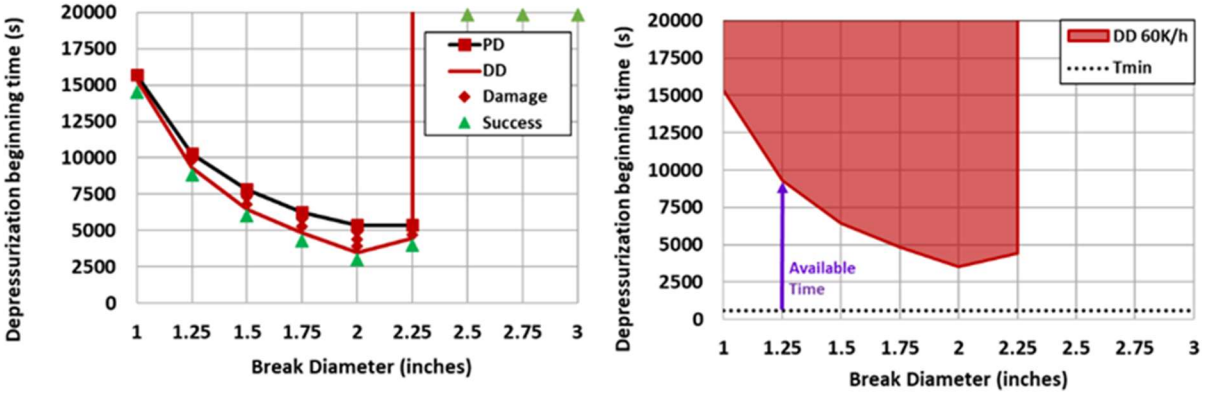

Figure 5-38 Damage Domain for SBLOCA with HPIS failure and 60 K/h RCS cooling (VVER-1000/V320)

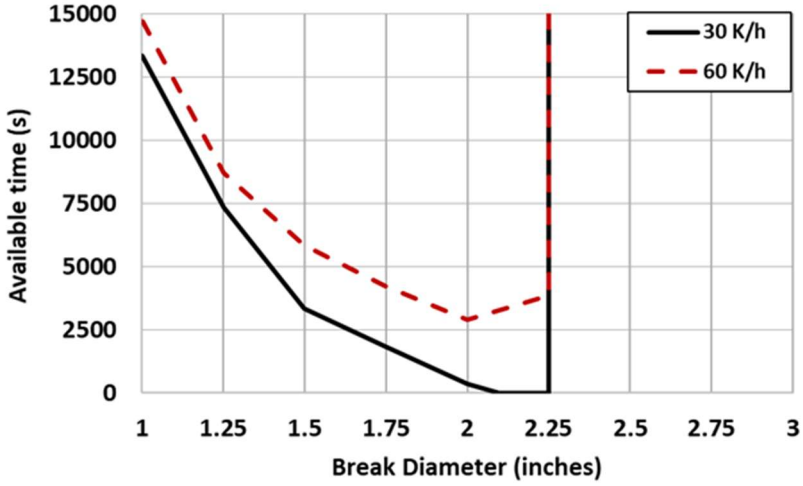

Figure 5-39 Available Times for SBLOCA with HPIS failure sequence with 30 K/h and 60 K/h RCS cooling (VVER-1000/V320)

In view of the above, it is important to make the following observation. On the one hand, the SBLOCA ET for the VVER-1000/V320 reactor, see Figure 5-21, shows that for the SBLOCA sequence in which the HPIS is not successful, it is necessary, among other things, that the B and EG headers are successful. On the other hand, the simulations in this analysis have been performed without considering the availability of EBIS and EGRS.

Based on the results of the analysis, there is enough time for the manual action related to a cooling rate of the RCS of 60 K/h for all breaks without considering the availability of EBIS and EGRS. Therefore, the ET of the SBLOCA could be simplified, see Figure 5-40.

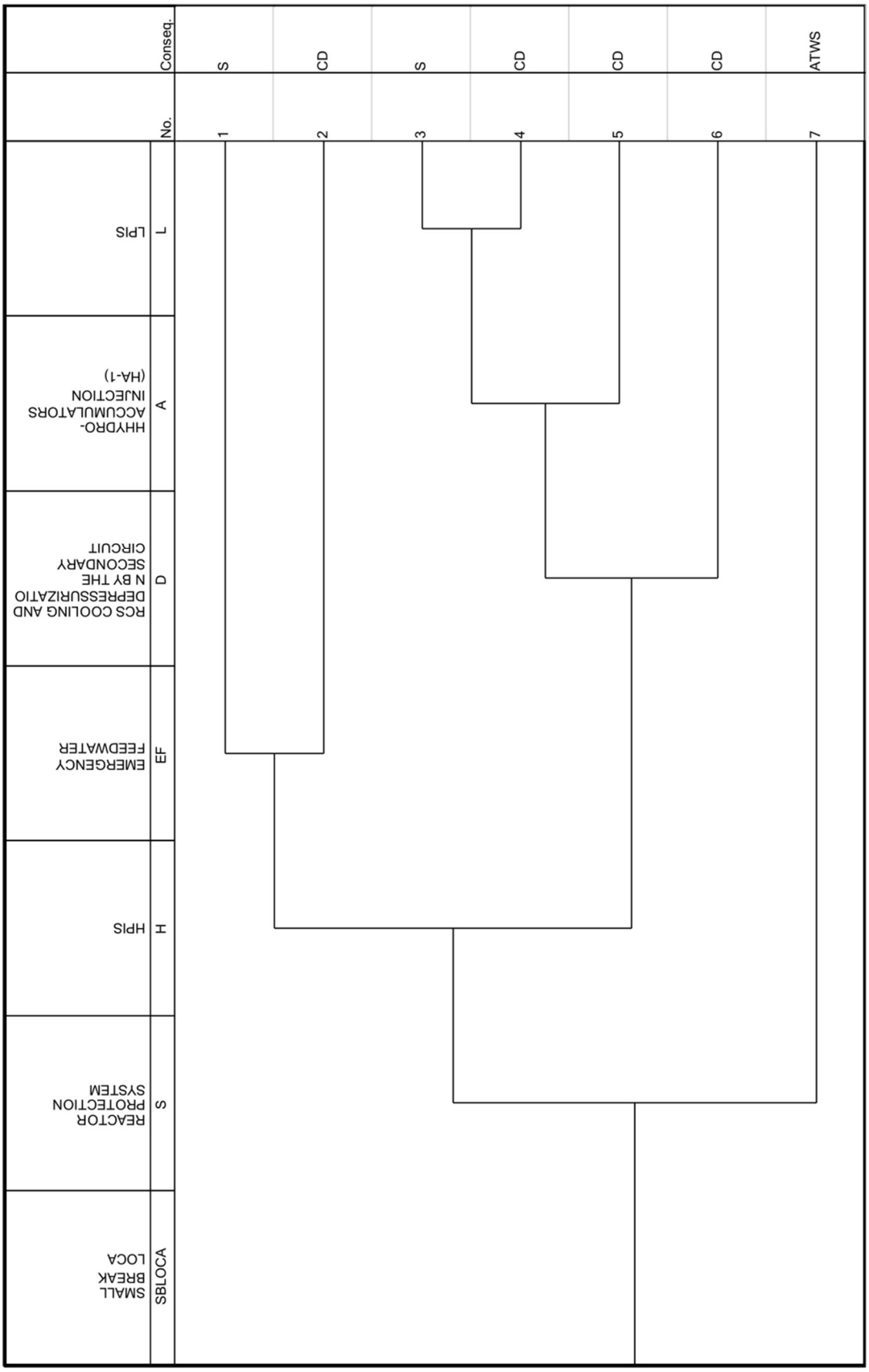

Figure 5-40 VVER-1000/V320 SBLOCA ET without considering EBIS and EGRS

5.2.3.3. SGs controlled depressurization. Damage Domain sensitivity analysis

Previously, the DDs have been obtained for the SBLOCA sequence with HPIS failure and controlled SGs depressurization by considering the following hypotheses: the accidental transient occurs with the core power is at 100 % and the available HA-1 and LPIS trains are those of the SC. In the following, a sensitivity analysis of the DDs to different boundary conditions for the core power and availability of the HA-1 and LPIS trains has been carried out:

- Original case: The ECCS available trains are 2 out of 4 HA-1 trains and 1 out of 3 LPIS trains. Core power at 100%.
- 2nd case (Power uprate): The ECCS available trains are 2 out of 4 HA-1 trains and 1 out of 3 LPIS trains. Core power at 120%.
- 3rd case (ECCS fully available): The ECCS available trains are 4 out of 4 HA-1 trains and 3 out of 3 LPIS trains. Core power at 100%.
- 4th case (Power uprate and ECCS fully available): The ECCS available trains are 4 out of 4 HA-1 trains and 3 out of 3 LPIS trains. Core power at 120%.

The sensitivity analysis has been performed for both the 30 K/h and the 60 K/h RCS cooling rates, see Figure 5-41 and Figure 5-42. The overall outcome is that the DD is much more sensitive to the available HA-1 and LPIS trains than to the core power. For each cooling rates the following can be highlighted:

- 30 K/h cooling rate: The most limiting case is the second (power uprate), as it extends to 2.75 inches and there is no available time between 2.25 and 2.75 inches. For the third case (ECCS fully available) the DD is reduced to 1.75 inches where the border reaches 4500 s, while, for the fourth case (power uprate and ECCS fully available) the DD is also reduced to 2 inches where it reaches 2200 s.

  The sensitivity analysis on the DD associated with the 30 K/h cooling rate strategy shows that if the HA-1 and the LPIS trains are fully available, the DD is smaller, both in the break size dimension and in the depressurization beginning time dimension. Therefore, the 30 K/h cooling rate could be enough to provide the MCR crew with a large available time in the case of 100% power with 4 out of 4 HA-1 and 3 out of 3 LPIS trains are available.
- 60 K/h cooling rate: it should be noted that the DDs for the 60 K/h RCS cooling rate reach the same break size limits as the DDs for the 30 K/h RCS

cooling rate, but they extend less in the time. The most limiting case is the second (power uprate) as it extends to 2.75 inches for which it reaches 850 s. For the third case (ECCS fully available) the DD reaches 7850 s for 1.75 inches, while, for the fourth case (power uprate and ECCS fully available), the DD reaches 5400 s for 2 inches.

It should be noted that if a 20 % power uprate is performed in a VVER-1000/V320 reactor, the strategy associated with the controlled SGs depressurization at an RCS cooling rate of 60 K/h may not be enough to avoid CD, considering the time required by the operator to initiate the management action. Therefore, in this case, it would be necessary to study other strategies to complement the controlled SGs depressurization or to apply higher cooling rates.

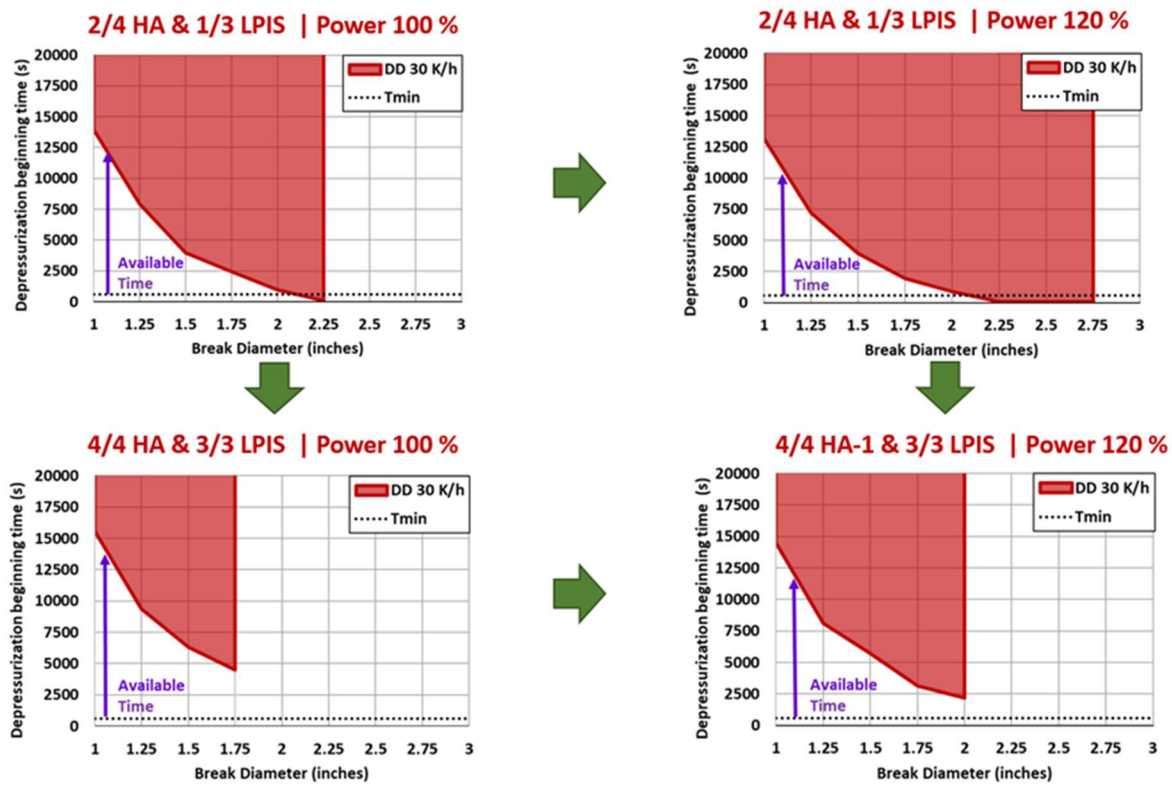

Figure 5-41 Damage Domains sensitivity analysis for SBLOCA with HPIS failure and 30 K/h RCS cooling (VVER-1000/V320)

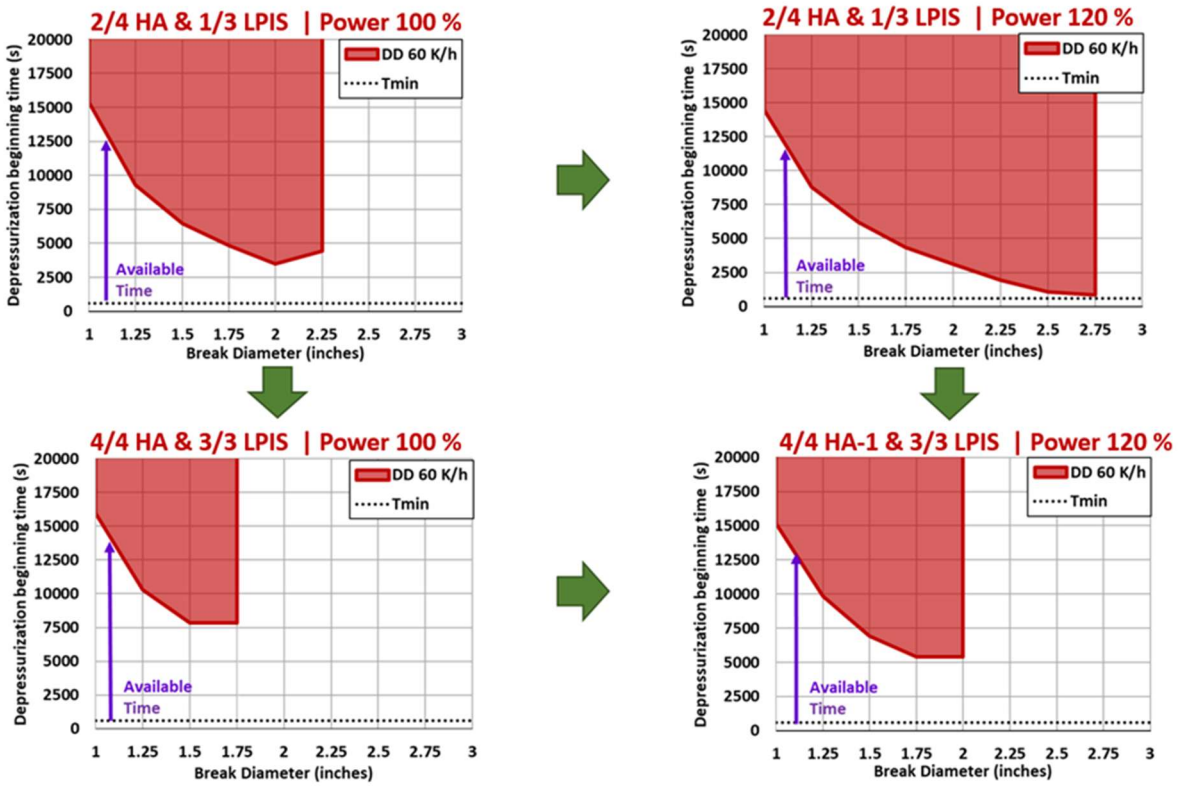

Figure 5-42 Damage Domains sensitivity analysis for SBLOCA with HPIS failure and 60 K/h RCS cooling (VVER-1000/V320)

5.2.4. VVER-1000/V320 SBLOCA sequences with HPIS failure, controlled SGs depressurization and EGRS actuation

The EGRS is a safety system developed to remove the steam-gas mixture from the upper RPV, the PZR and the primary side of the SGs, (Iegan et al., 2018). In the references, some cases have been found where the depressurization of the RCS through the EGRS is studied in SBLOCA sequences with HPIS failure (Groudev, 1998), or TLFW sequences, (Gencheva et al., 2005). Besides, the SBLOCA ET for the VVER-1000/V320 reactor, Figure 5-21 and (Skalozubov et al., 2010), shows that for the sequence in which the HPIS is not available, in addition to the RCS cooling by the controlled SGs depressurization, the EGRS opening valve is also required to avoid CD.

Based on the DDs obtained for the controlled SGs depressurization, it was verified that the EGRS actuation is not necessary when the depressurization is performed at an RCS cooling rate of 60 K/h. However, when the SGs depressurization is performed at an RCS cooling rate of 30 K/h, see Figure 5-37 (right), the DD

indicates that the opening of an EGRS valve might be useful in order to avoid CD for the whole SBLOCA spectrum.

In order to analyse the impact that the EGRS could have in the SBLOCA without HPIS sequences in VVER-1000/V320 reactors, the DD for the EGRS actuation has been obtained in Section 5.2.4.1. Then, in Section 5.2.4.2, it has been performed a sensitivity analysis on the EGRS valves diameter.

5.2.4.1. Damage domains for the EGRS actuation

The aim is to analyse the impact of the EGRS performance in SBLOCA sequences with HPIS failure where the controlled SGs depressurization at a rate of 30 K/h is applied. It has been considered that the actuation of this safety system consists in the opening of a valve located in the PZR with a diameter of 1.25 inches.

First, the DD of the EGRS actuation alone has been obtained, see Figure 5-43-B. It can be seen that the DD extends over the entire beginning depressurization time dimension from 1 to 1.75 inches, i.e., even if the EGRS valve were opened at the time the SBLOCA occurs the sequence would not be successful. However, for break sizes of 2 and 2.25 inches, the DD limit is similar to the PD curve values. This is because opening an EGRS valve is equivalent to inducing a second LOCA of 1.25 inches in the RCS. The sum of both areas, i.e. the EGRS valve are and the LOCA break, is shown in Table 5-9. Therefore, despite the EGRS, sequences from 1 to 1.75 inches are not successful, because the RCS opening areas (LOCA + EGRS valve) are still small enough to allow it to depressurize in time for the HA-1 and LPIS injection before CD.

Subsequently, the DD of both combined strategies, SGs depressurization at 30 K/h and EGRS valve opening, has been obtained, see Figure 5-43-C. It has been considered that the operator opens the EGRS valve 100 seconds after the beginning of the controlled SGs depressurization. It can be seen how the resulting DD is a combination of the DD for the controlled depressurization at 30 K/h and the DD of the EGRS performance.

Then, the available time for the strategy of controlled SGs depressurization combined with the opening of a 1.25 inches EGRS valve has been calculated. The available time obtained has been compared with that of the two strategies alone, see Figure 5-44. The following conclusions can be drawn:

- 1 to 1.75 inches: The shape of the available time curve is similar to the available time curve for the controlled SGs depressurization at 30 K/h, but

the time values are lower. The 1.75 inches break size has no available time, it is medium for 1.5 inches and long from 1 to 1.25 inches.

- 2 to 2.25 inches: The available time curve is very close to the available time curve for the EGRS strategy alone. A long available time is considered, because it is greater than 1 hour.

Table 5-9 SBLOCA area along with the EGRS valve area

Break diameter (inches)	Break area (m^2)	Break area + EGRS area (m^2)
1	5.07E-4	1.31E-3
1.25	7.92E-4	1.60E-3
1.5	1.14E-3	1.94E-3
1.75	1.55E-3	2.35E-3
2	2.03E-3	2.83E-3
2.25	2.57E-3	3.36E-3

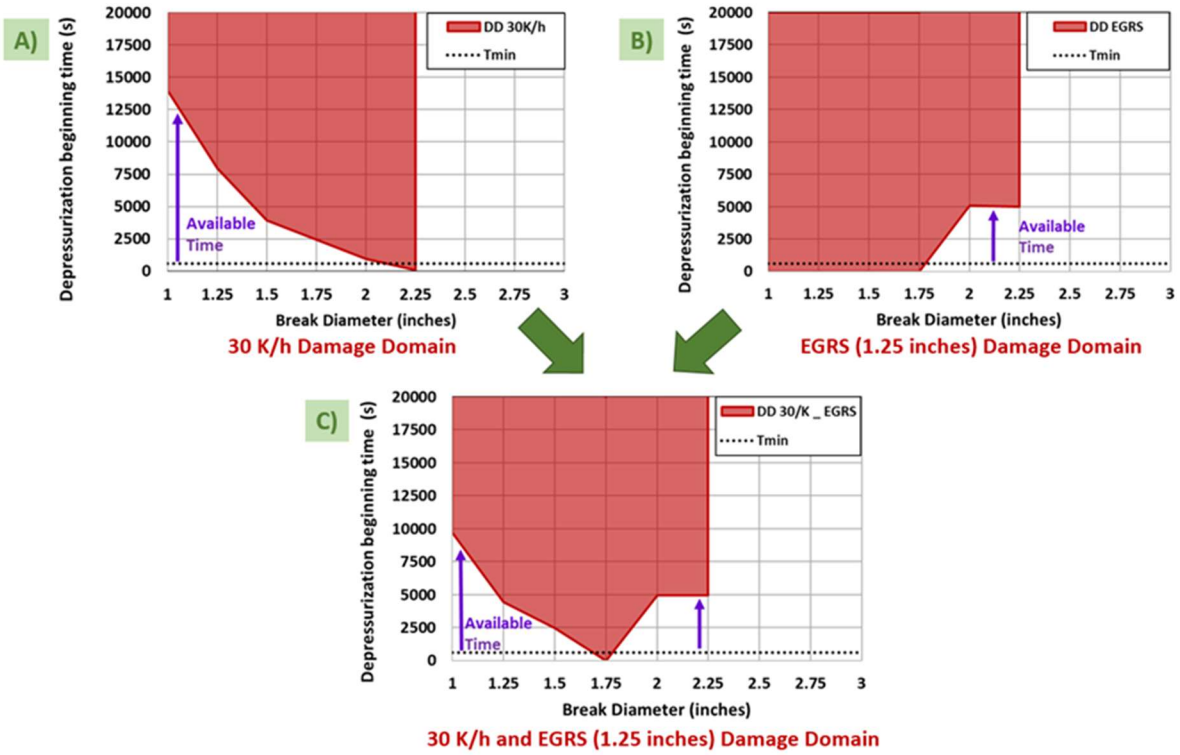

Figure 5-43 Damage Domains for SBLOCA with HPIS failure and 30 K/h RCS cooling along with EGRS actuation (VVER-1000/V320)

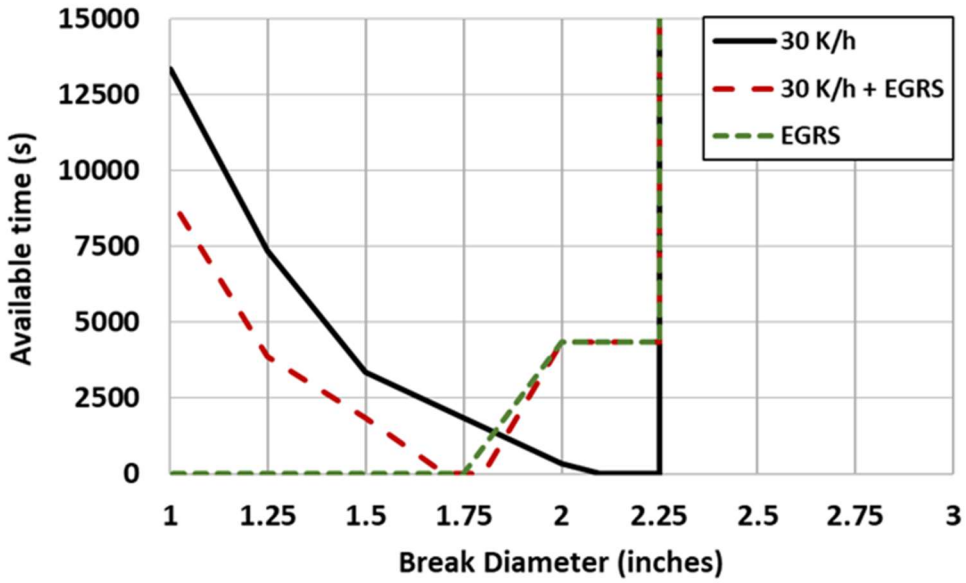

Figure 5-44 Available time for SBLOCA with HPIS failure and 30 K/h RCS cooling along with EGRS actuation (VVER-1000/V320)

5.2.4.2. EGRS valves diameter sensitivity analysis

A sensitivity analysis has been performed on the EGRS valve diameter to see its impact on the DD of the strategy consisting of controlled SGs depressurization at an RCS cooling rate of 30 K/h in combination with the opening of one of the EGRS valves, see Figure 5-45. It is important to note that the size of the EGRS valves can be different for NPPs of the same reactor design. Therefore, the DD has been obtained for the following cases:

- The opening valve has the diameter as one of the PZR relief and safety valve (diameter =2.5 inches). This option has been considered as the EOPs of some VVER-1000/V320 NPPs may consider opening the PZR relief and safety valves instead of the EGRS valves.
- The opening valve had half the area of the PZR relief and safety valve (diameter = 1.72 inches). This option has been considered as references (Muellner, 2010) indicated that the EGRS valves area can be half that of the PZR relief and safety valves area.

The lowest value obtained for the DD limit is 2000 s (diameter = 1.72 inches, half the area of the 2.5 inches diameter valve), so despite considering the minimum time needed by the operator to execute the strategy, there would be enough available time. If the opening EGRS valve has the area of one of the PZR relief and safety valves, the DD limit has values close to those of the PD curve. This is

because the opening of a valve with diameter of 2.5 inches causes high cooling rates, more than 60 K/h. In case of considering a valve with a diameter of 1.72 inches, the DD limit is close to the PD curve from 1.75 to 2.25 inches break sizes.

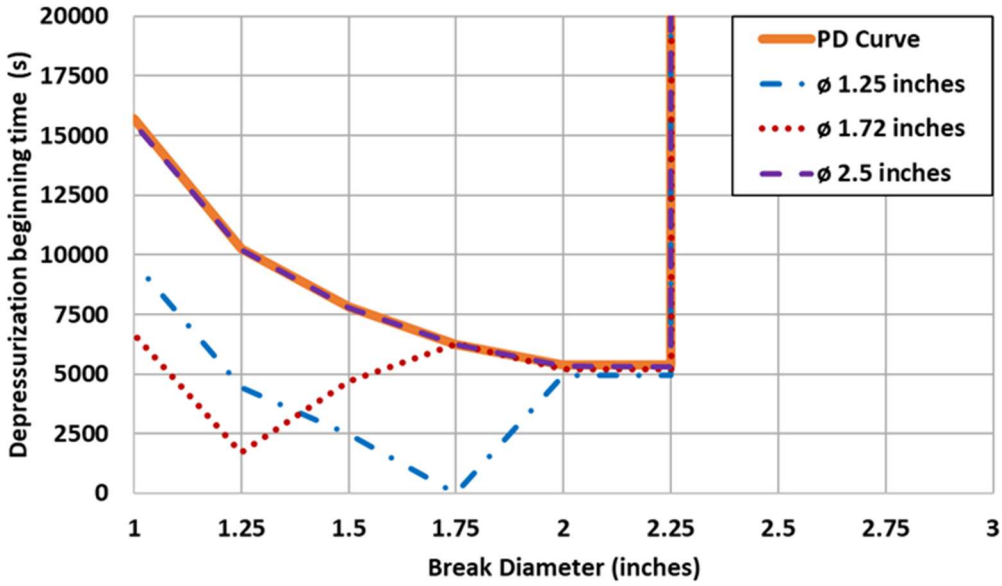

Figure 5-45 Damage Domains sensitivity analysis on the EGRS (VVER-1000/V320)

5.2.5. VVER-1000/V320 SBLOCA sequences with HPIS failure and SGs depressurization at maximum RCS cooling rate

In the management of the SBLOCA sequences with HPIS, there is an alternative manual action for those cases where the core cooling CSF is not fulfilled, i.e., when the ICC condition is reached. This consists in performing a maximum RCS cooling by means of a fast SGs depressurization, which implies the full opening of the BRU-A valves. It should be noted that the fast SG depressurization causes high RCS cooling rates, exceeding 200 K/h, which can lead to hazardous thermal shock conditions.

References have been found where the SGs fast depressurization is performed when the CET temperature exceeds 350 ºC (623 K) (Muellner, 2010). On the other hand, in the PWR-W, whose EOPs were used as a reference for the actual EOPs of the VVER-1000/V320 reactors, the ICC condition is reached when the CET temperature exceeds 650 ºC (923 K) (FR C.1). Taking this information into account, it has been decided to analyze the fast SGs depressurization in VVER-1000/V320 reactors considering both ICC temperature values, 350 ºC (623 K) and 650 ºC (923 K).

First it has been obtained when the ICC temperatures considered are reached. For this purpose, the SBLOCA with HPIS failure sequences without human action have been simulated and it has been found when the steam temperature at the core exit exceeded 350 ºC (623 K) and 650 ºC (923 K), see Figure 5-46.

Subsequently, the margin time curve, which gives the time from the occurrence of the ICC to the occurrence of the PD has been then obtained. This was done by subtracting the ICC time and the time taken by the MCR crew to initiate the action from the PD curve values. The value considered for the time required by the MCR crew is 60 s, as this is the time taken by the operators to perform this action in simulator training. The following conclusions can be drawn from the time margin curves obtained:

$$t_{margin} = t_{previous\ damage} - t_{ICC} - t_{min}$$

- ICC = 350 ºC (623 K): the margin time obtained is similar for all the break sizes. The break size with the largest margin being the 2.25 inches with 2296 s and the one with the smallest margin being the 1.75 inches with 1381 s, see Figure 5-47.
- ICC= 650 ºC (923 K): the margin time obtained is much smaller than the time margin obtained for ICC = 350 ºC (623 K). The break size with the largest margin being the 2.25 inches with 1151 s and the one with the smallest margin being the 1 inch with 265 s, see Figure 5-48.

Afterwards, the DD for the fast SGs depressurization has been obtained. For this, the steps described previously for calculating the DD for the controlled SGs depressurizations have been followed. The DD obtained has been plotted together with the two ICC curves (350 ºC and 650 ºC) for those cases without depressurization, this allow to check how closed they are to the DD border, see Figure 5-49. In addition, a surface has also been generated showing the PCT values as a function of the start time of the fast SGs depressurization and of the break sizes. On this surface, two curves have been plotted showing the PCT values reached in the case where the manual action starts just when the ICC conditions occur, see Figure 5-50.

Finally, the available time to perform the maximum RCS depressurization and cooling by a fast SGs depressurization has been calculated. This time is determined by subtracting the time in which the ICC condition occurs from the DD, minus the time required by the MCR crew to initiate the action, see Figure 5-51.

$$t_{available} = t_{damage\ domain} - t_{ICC} - t_{min}$$

The following conclusions can be drawn from the obtained curves:

- The available time to perform the action is longer when considering that the ICC condition occurs when the CET temperature exceeds 350 ºC (623 K).
- Considering that the ICC occurs when the CET temperature exceeds 350 ºC (623 K), the break size with the shortest available time is 1.75 inches at 1352 s. The available time for all the break sizes is medium, ranging from 15 minutes to 1 hour.
- Considering that the ICC occurs when the CET temperature exceeds 650 ºC (923 K), the break size with the shortest available time is 2 inches at 190 s. The available time for all break sizes, except for 2.25 inches is considered shot because it is less than 15 min.

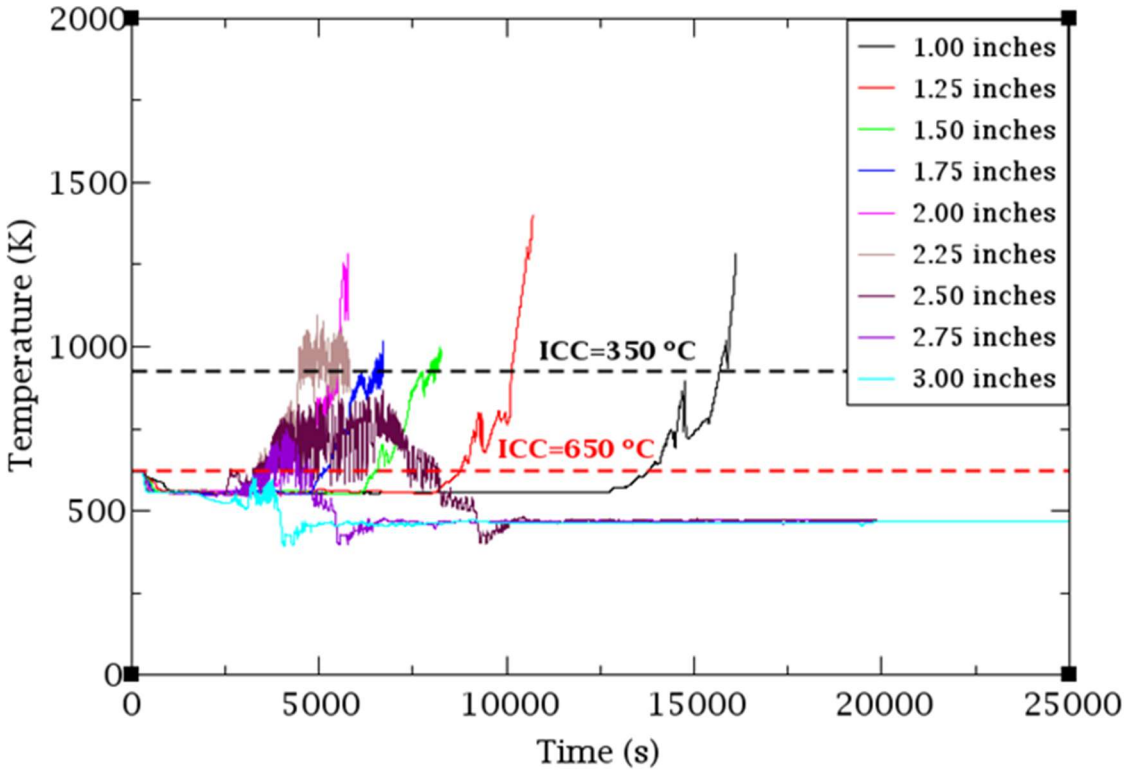

Figure 5-46 CET SBLOCA with HPIS failure without human actions (VVER-1000/V320)

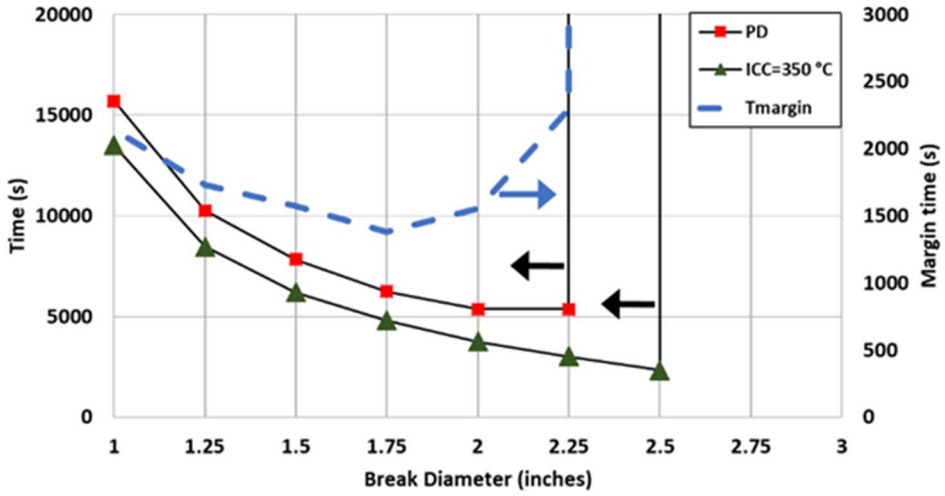

Figure 5-47 Time margin for maximum RCS cooling, ICC = 350 ^{0}C (VVER-1000/V320)

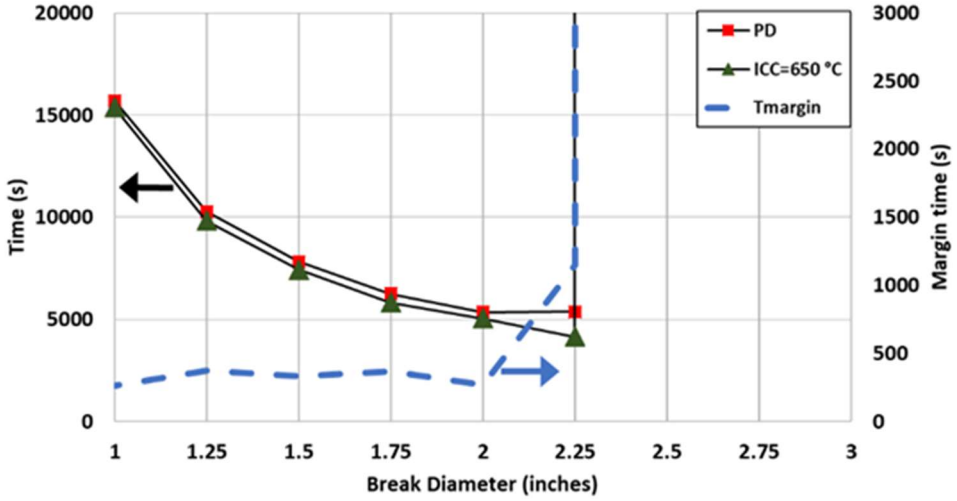

Figure 5-48 Time margin for maximum RCS cooling, ICC = 650 ^{0}C (VVER-1000/V320)

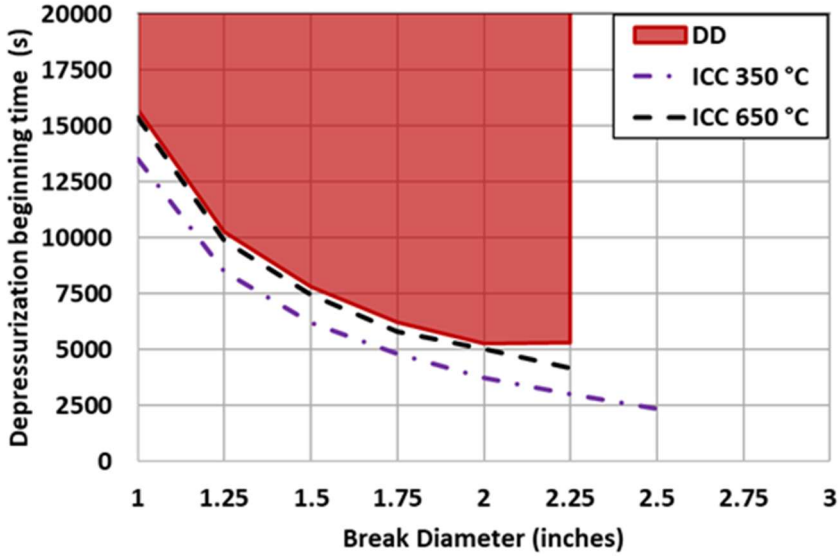

Figure 5-49 DD for RCS maximum cooling rate via the SGs (VVER-1000/V320)

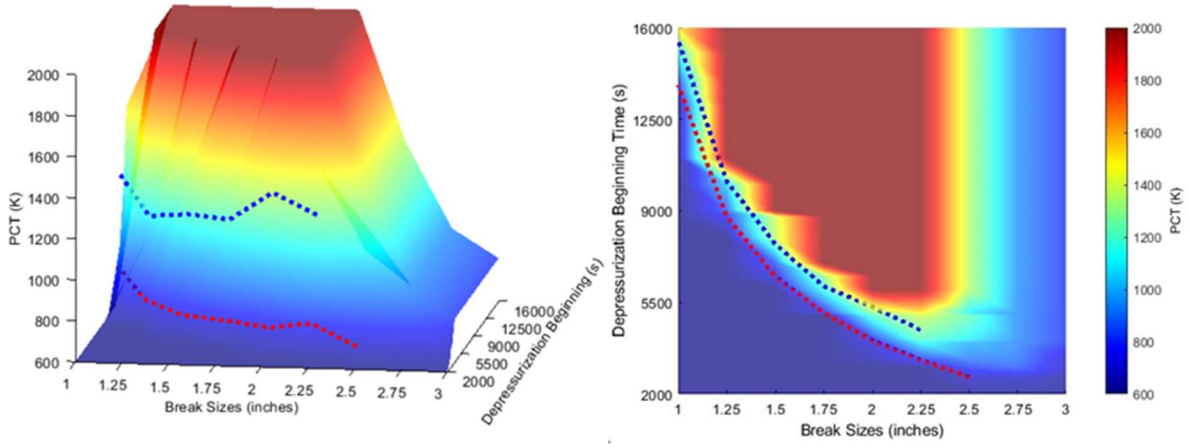

Figure 5-50 PCT in SBLOCA with HPIS failure and RCS maximum cooling rate via the SGs (VVER-1000/V320)

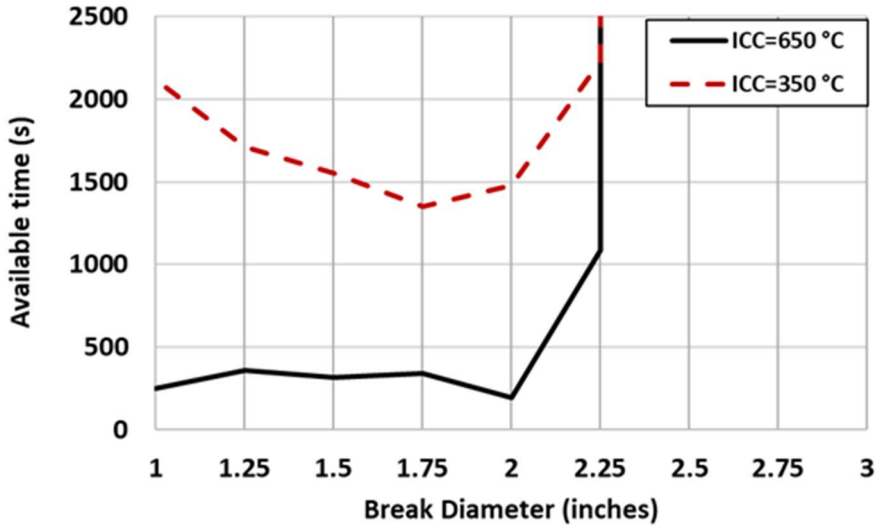

Figure 5-51 Available time for SBLOCA with HPIS failure sequence and RCS maximum cooling rate via the SGs at ICC = 350 0C and ICC = 650 0C (VVER-1000/V320)

5.2.6. Comparison of management strategies for VVER-1000/V320 SBLOCA sequences with HPIS failure

An overview is given of the different strategies that can be implemented in a VVER-1000/V320 reactor to manage an SBLOCA sequence with HPIS failure. The following have been analyzed in this work:

- The controlled SGs depressurization at an RCS cooling rate of 30 K/h and 60 K/h.
- Controlled SGs depressurization at an RCS cooling rate of 30 K/h along with the EGRS actuation.

- The SGs depressurization at maximum RCS cooling rate when ICC condition is reached.

The DDs obtained for all analyzed strategies have been compared by plotting the lines delimiting these DDs on the same graph, see Figure 5-52. Likewise, the available time curves obtained for the different strategies have been compared, see Figure 5-53 and Table 5-10. From this comparison, it can be concluded the following:

- The strategy with the highest available time for the whole range of break sizes is the controlled SGs depressurization at an RCS cooling rate of 60 K/h. The second one is the corresponding to the fast SGs depressurization.
- The other strategies cannot avoid CD in the whole range of break sizes.

As mentioned in the previously, the available times obtained are highly dependent on the time required by the MCR crew to perform the corresponding management action, i.e., the t_{min} selected. However, it should also be noted that the calculated available times are subject to other uncertainties, mainly related to the options and hypotheses assumed in the model and the system code applied in the analysis.

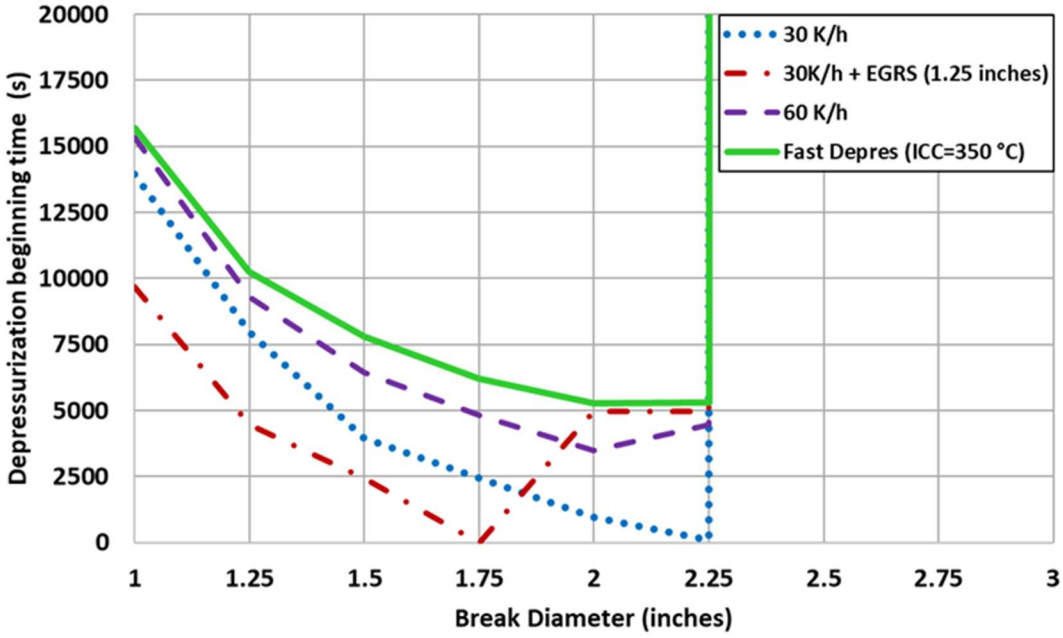

Figure 5-52 Damage Domains comparison for SBLOCA with HPIS failure management strategies (VVER-1000/V320)

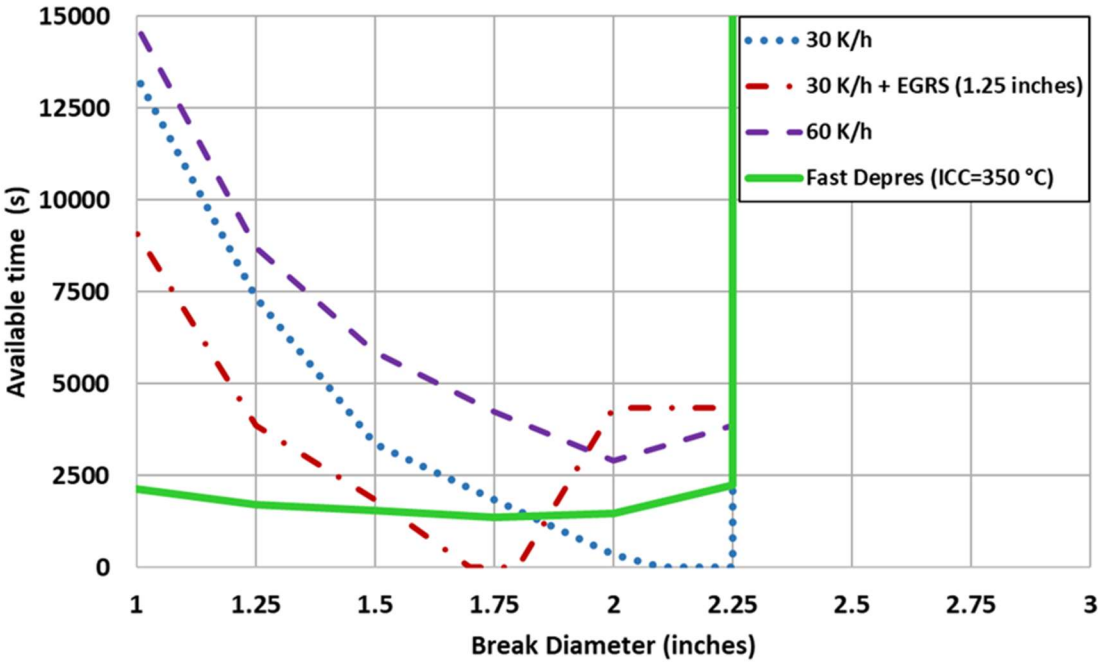

Figure 5-53 Available times comparison for SBLOCA with HPIS failure management strategies (VVER-1000/V320)

Table 5-10 Minimum available time in VVER-1000/V320 for SBLOCA with HPIS failure sequence strategies

Strategy		Min Available Time (s)
Controlled SG depressurization at 30 K/h		0
Controlled SG depressurization at 60 K/h		2900
Controlled SG depressurization at 30 K/h along with the opening of a EGRS valve	EGRS valve diameter = 1.25 inches	0
	EGRS valve diameter = 1.72 inches	1100
	EGRS valve diameter = 2.5 inches	4705
Fast SG depressurization	ICC =350 °C	1352
	ICC =650 °C	190

5.2.7. Verification of EOPs strategies in Westinghouse PWR for SBLOCA sequences with HPSI failure

This Section 5.2.7 is focused on the analysis of the different management strategies that can be found in a 3 loops PWR-W for the SBLOCA sequence with HPSI failure. In 3 loops PWR-W two strategies can be distinguished depending on whether ICC condition has been reached:

- Controlled SGs depressurization: The PWR-W EOP ES-1.2 and EOP FR-C2 indicate that this action is performed at 55 K/h.
- Fast SGs depressurization: this strategy is adopted when the ICC condition has been reached, i.e., CETs exceed 650 °C (923 K).

The hypotheses considered in the 3 loops PWR-W model are similar to those considered for the VVER-1000/V320 model: the core power at the beginning of the accidental sequence is 100 % and the available trains of the ACC (2 out of 3 trains) and the LPSI (1 out of 2 trains) are those of the SC. On the other hand, it is noteworthy that the PWR-W do not have automatic MCPs trip, unlike the VVER-1000/V320 reactors. Therefore, in order for the conditions considered in both models analyzed to be similar, it has been assumed that the RCSs in the 3 loops PWR-W are triggered at the beginning of the accidental sequence.

To analyze both strategies, the PD curve has first been obtained using the methodology applied to the VVER-1000/V320 reactor. Along with the PD curve, the core uncovered curve, the ACC injection curve and the LPSI injection curves have also been plotted, see Figure 5-54. As can be seen, the PD occurs up to 2 inches break sizes, and the break size where the PD occurs first is 1.5 inches at 7263 s. While the ACC inject prior to the PD for all sizes, only those break sizes where the LPSI injects are successful, except for the 2 inches break size, for which it does so after the PD has already occurred.

From the PD curve, the DD have been generated both for the controlled SGs depressurization at an RCS cooling rate of 55 K/h, see Figure 5-55, and for the SGs depressurization at the maximum RCS cooling rate, see Figure 5-56. The approach has been the one applied in the search for DDs in the VVER-1000/V320 reactor strategies.

Subsequently, the available time has been calculated for both strategies, see Figure 5-57. The following can be drawn from the results obtained:

- The available time for depressurization at maximum RCS cooling rate is much smaller than for controlled depressurization. This is because depressurization at maximum RCS cooling rate is initiated only if the ICC condition has been reached.
- The lowest available time in the controlled SGs depressurization strategy is 900 s, for 1.75 inches, which is considered medium as it is 15 minutes.
- The break size with the lowest available time in the fast SGs depressurization strategy is 1.25 in, which is 460 s. This is considered to be a short available time, as it is less than 15 minutes. Although the minimum available time is short, it may be reasonable as the MCR crew would be particularly attentive to the CET temperatures under these conditions.

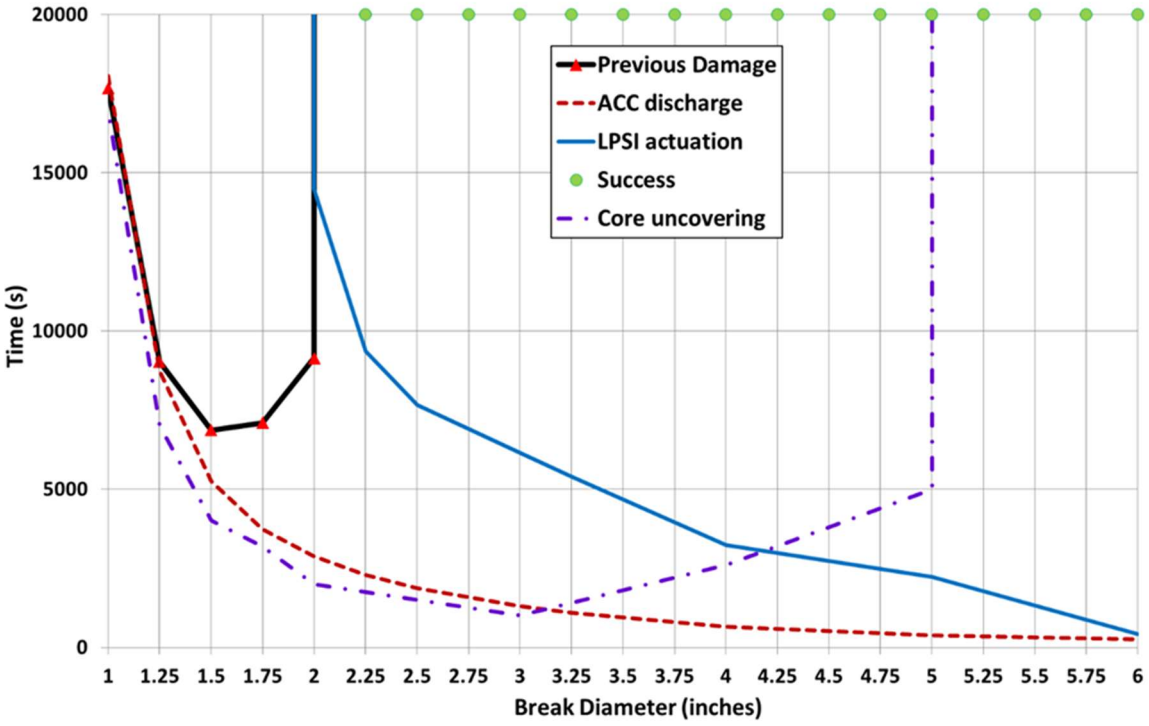

Figure 5-54 Previous Damage Curve for SBLOCA with HPIS failure (3 loops PWR-W)

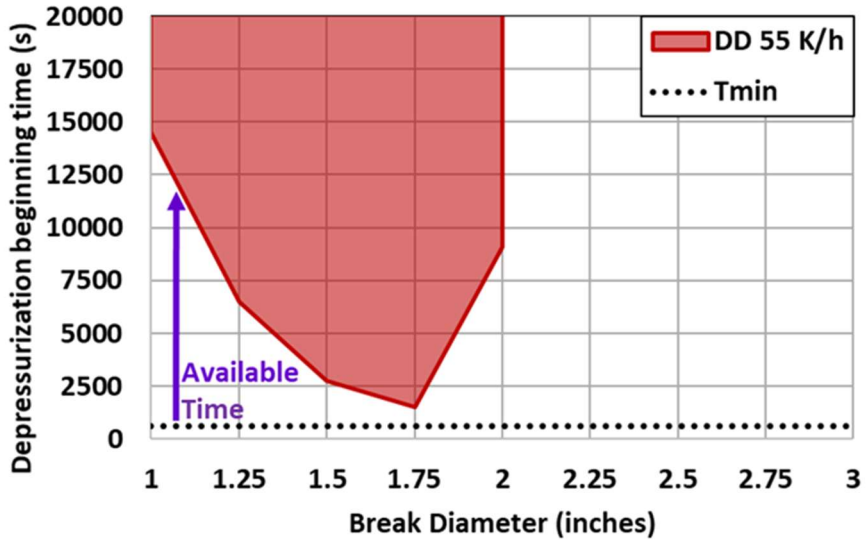

Figure 5-55 Damage Domains for SBLOCA with HPIS failure and 55 K/h RCS cooling (3 loops PWR-W)

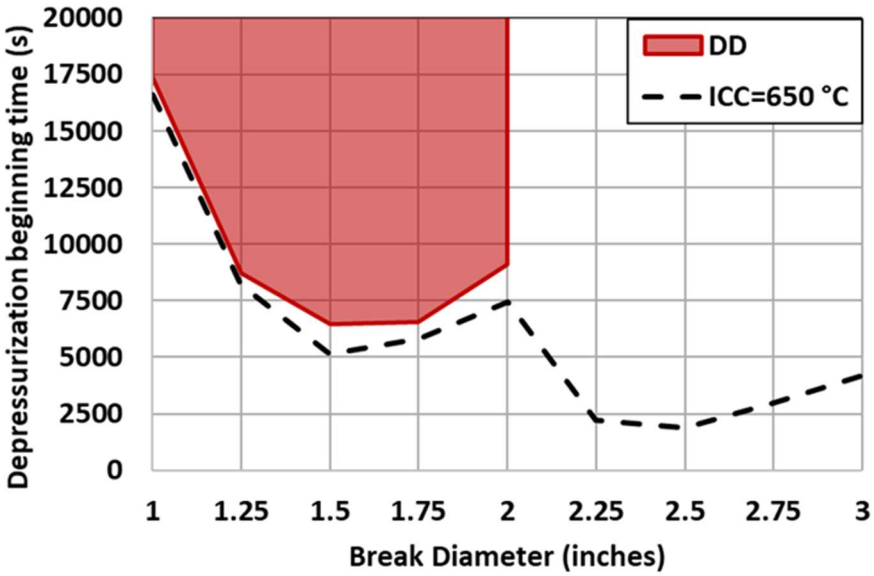

Figure 5-56 Damage Domain for SBLOCA with HPIS failure and maximum RCS cooling via the SGs (3 loops PWR-W)

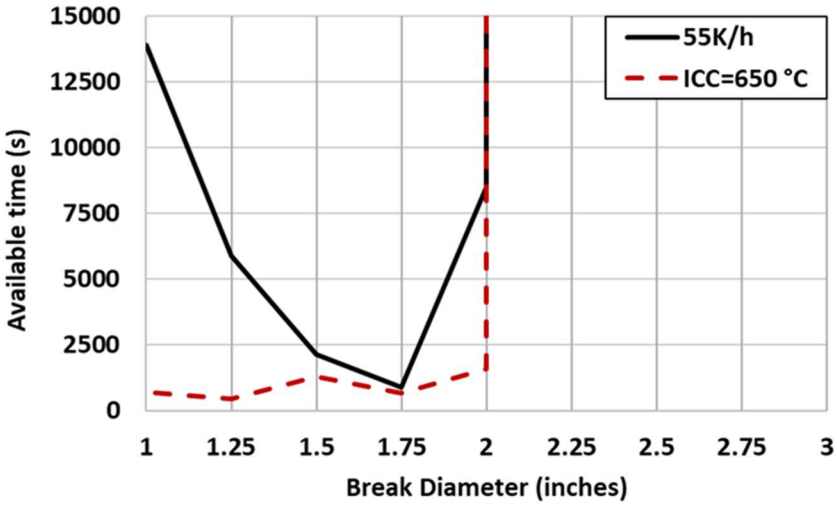

Figure 5-57 Available time for SBLOCA with HPIS failure and RCS cooling (3 loops PWR-W)

5.2.8. Comparison of VVER-1000/V320 and Westinghouse PWR strategies in SBLOCA sequences with HPIS or HPSI failure

A comparison of the results previously obtained with the model for the TRACEV5P5 code of a VVER-1000/V320 reactor with those of a model of a 3 loops PWR-W is shown below. To be consistent, the DD for the controlled SGs depressurization at a 55 K/h RCS cooling rate in 3 loops PWR-W has been compared with that for the controlled SGs depressurization at 60 K/h RCS cooling rate in VVER-1000/V320 reactor. On the other hand, the DD for the SGs depressurization at maximum RCS cooling rate for the 3 loops PWR-W has been compared with that for the VVER-1000/V320 reactor. The following can be drawn:

- Controlled SGs depressurization: While for the 3 loops PWR-W the DD limit reaches 2 inches, for the VVER-1000/V320 reactor it reaches 2.25 inches. However, the DD is larger in the 3 loops PWR-W up to 1.75 inches, see Figure 5-58.
- SGs fast depressurization: While for the 3 loops PWR-W the DD reaches 2 inches, for the VVER-1000/V320 reactor it reaches 2.25 inches. For smaller break sizes and for those larger than 1.75 inches the DD is greater for the VVER-1000/V320 reactor, but for break sizes between 1.25 and 1.75 inches the DD is greater for the 3 loops PWR-W, see Figure 5-59.

In addition to the comparison of DDs, the available times for both PWR designs have also been compared, for the controlled SGs depressurization strategy, see

Figure 5-60, and for the SGs depressurization at maximum RCS rate, see Figure 5-61. Moreover, the minimum available time for each strategy is shown in Table 5-11. The following main conclusions can be drawn from the results obtained:

- The strategy with the highest available time for the whole range of break sizes is the controlled SGs depressurization at an RCS cooling rate of 60/55 K/h for both designs.
- The second one is the corresponding to the fast SGs depressurization.

Table 5-11 Minimum available time in 3 loops PWR-W and VVER-1000/V320

PWR design	Strategy	Minimum Available Time (s)
VVER-1000/V320	Controlled SG depressurization at 60 K/h	2900
	Fast SG depressurization (ICC = 350 °C)	1352
	Fast SG depressurization (ICC = 650 °C)	190
3 loops PWR-W	Controlled SG depressurization at 55 K/h	900
	Fast SG depressurization (ICC = 650 °C)	460

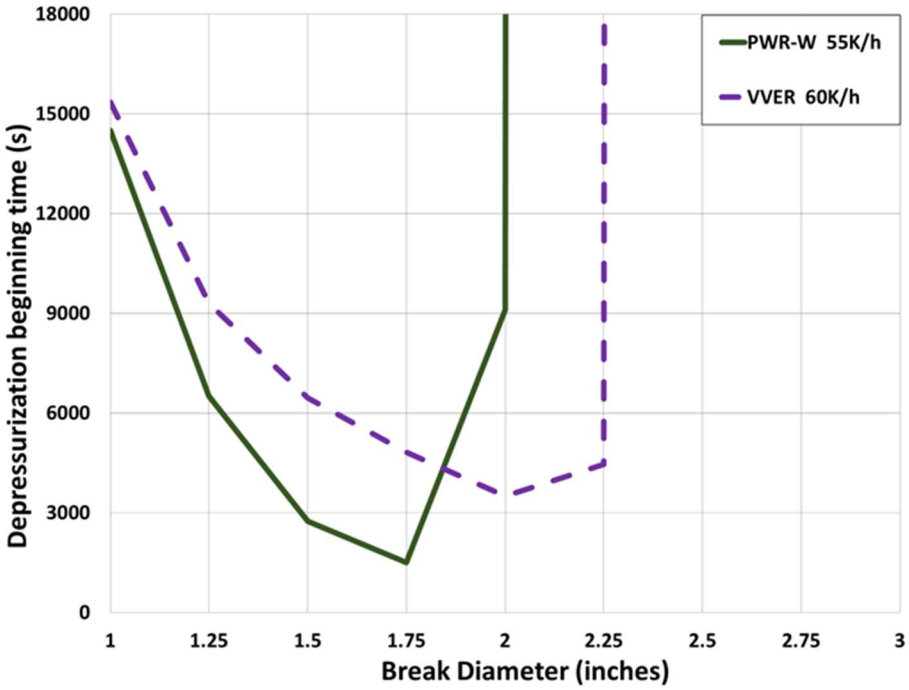

Figure 5-58 Damage Domain for SBLOCA with HPIS failure and controlled SGs depressurization in 3 loops PWR-W and VVER-1000/V320

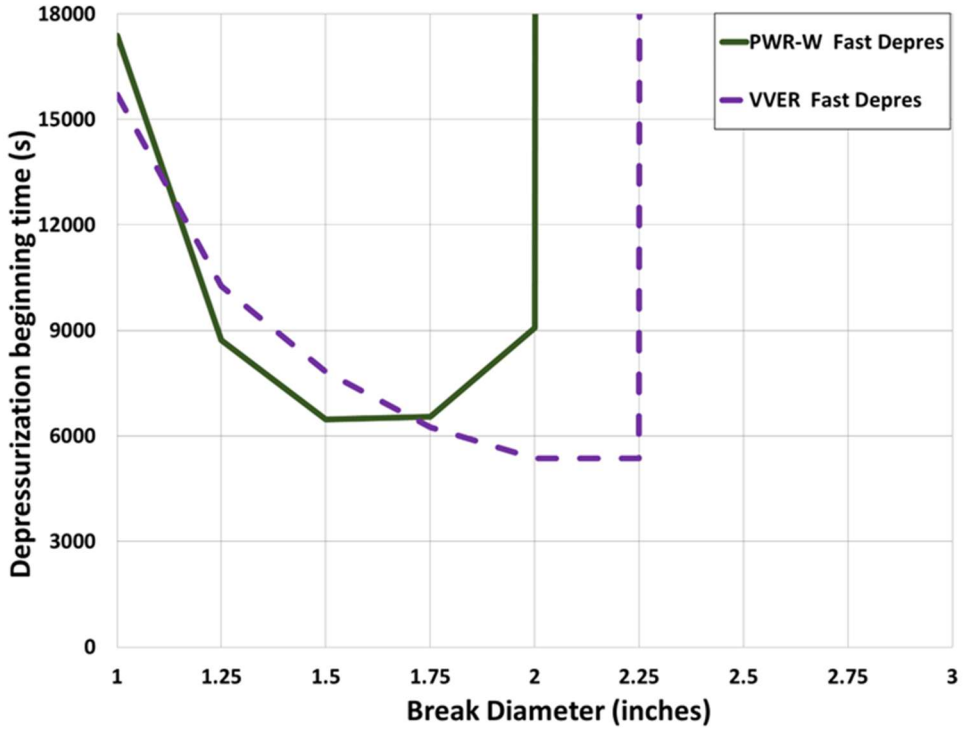

Figure 5-59 Damage Domain for SBLOCA with HPIS failure and maximum RCS cooling rate in3 loops PWR-W and VVER-1000/V320

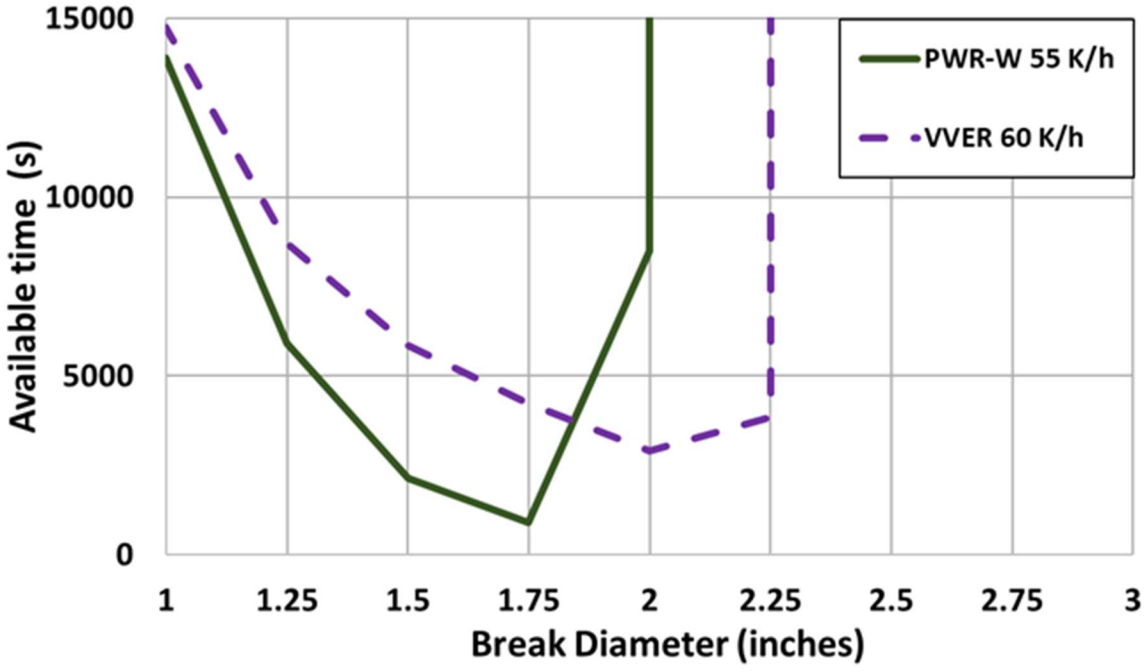

Figure 5-60 Available times for SBLOCA with HPIS failure controlled SGs depressurization in 3 loops PWR-W and VVER-1000/V320

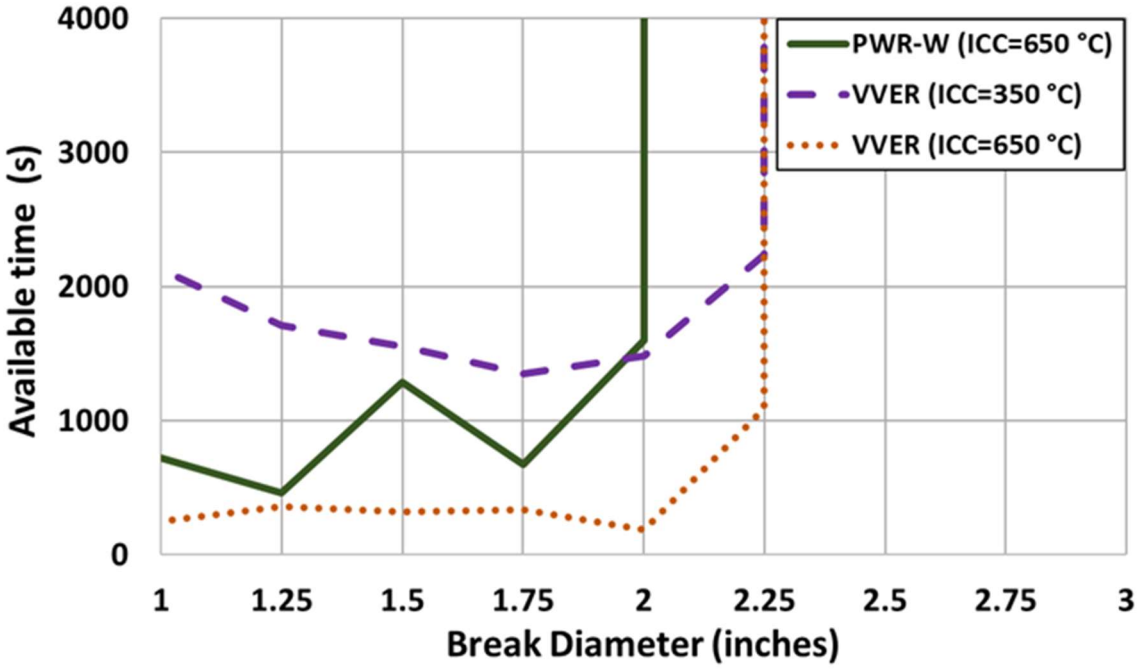

Figure 5-61 Available times for SBLOCA with HPIS failure and fast cooling in 3 loops PWR-W and VVER-1000/V320

5.2.9. Conclusions regarding the management strategies for SBLOCA sequences with HPIS failure

In Section 5.2, different management strategies to ensure core cooling in SBLOCA sequences with HPIS failure in both VVER-1000/V320 reactor and Westinghouse PWR have been reviewed and analyzed. The main conclusions obtained by means of the ISA methodology are as follows:

- In the VVER-1000/V320 reactor, if the SC are considered for the HA-1 and LPIS trains, there are break sizes with no available time for the controlled SGs depressurization at an RCS cooling rate of 30 K/h. However, the controlled SGs depressurization at an RCS cooling rate of 60 K/h strategy provides a longer available time.
- The sensitivity analysis performed on the DD of the controlled SGs depressurization at 30 K/h strategy in VVER-1000/V320 has shown that if the HA-1 and the LPIS trains are fully available, the DD limits are smaller, so that there can be enough available time over the whole range of break sizes. However, if a 20 % power uprate is performed, the DD limits are larger, so that the range of break sizes without available time increases.

- The sensitivity analysis performed on the DD of the controlled SGs depressurization at 60 K/h strategy has shown that if a 20 % power uprate is performed in a VVER-1000/V320 reactor, this management strategy may not be enough to avoid CD.
- In the VVER-1000/V320 reactor, the available time for the controlled SGs depressurization at an RCS cooling rate of 30 K/h is significantly modified if this is performed in combination with the opening of an EGRS valve. When the opening EGRS valve diameter is approximately 1.7 inches, there is enough available time for the entire range of break sizes, whereas for the smaller diameters, there is no available time for some break sizes. The success of this strategy then depends on the EGRS valve sizes of each NPP.
- The available time for controlled SGs depressurization at an RCS cooling rate of 55 K/h in the 3 loops PWR-W is large enough for the MCR crew.
- In the VVER-1000/V320 reactor, the fast SGs depressurization provides an adequate available time if it is considered that the ICC condition is reached when the CET temperature exceeds 350 ^{o}C (623 K) instead of 650 ^{o}C (923 K).
- In the PWR-W, when ICC conditions are reached, i.e., the CET temperature exceeds 650 ^{o}C (923 K), the maximum RCS cooling rate depressurization strategy allows to avoid core damage with enough available time.

It is emphasized that a thorough review of ETs, EOPs and the public references related to SBLOCA with HPIS failure sequences, has been carried out, combined with the application of the ISA methodology. This comprehensive approach has allowed the identification of the available times for the MCR crew under different management strategies for both designs VVER-1000/V320 and PWR-W.

Chapter 6. Safety analyses considering passive safety systems

Chapter 6 focuses on safety analyses assessing the performance of two PSSs: the HA-2, from the VVER-1200/V392M design, and the air-cooled PHRS, from the VVER-1000/V412 design (KKNPP). Both analyses deal with LOCA sequences under SBO conditions, with the first analysis evaluating the impact of the HA-2 system and the second the combined impact of the air-cooled PHRS and HA-2 systems.

6.1. Safety margins improvement by means of the HA-2 in VVER-1000 reactors

The aim of the Section 6.1. is to analyse the impact of the HA-2 on the events of a LOCA sequence, with and without SBO. For this purpose, the VVER-1000/V320 model for TRACEV5P5 code has been modified to include the HA-2 system, see Section 3.4.

The first motivation for the present research lies in the limited public information available on the HA-2 PSS, which is included in Gen-III/III+ VVER reactors and not present in any western design. Only a few severe accident analyses related with HA-2 PSS have been found in the literature, see (IAEA, 2017; Lityshev et al., 2013; Thi Hoa and Chi Thanh, 2015), which consider its performance during a LBLOCA along with SBO, but no detailed analyses have been performed with system codes. The second main motivation of this research is to evaluate the impact on MBLOCA and LBLOCA SC of the HA-2 PSS implementation and look for possible "relaxations" of the number of trains required to adequately cope with the transient.

The Section 6.1. is organized as follows: First, Section 6.1.1 analyses the impact of the HA-2 on LOCA along with SBO sequences. Subsequently, Section 6.1.2 discusses how the implementation of the HA-2 can relax the ECCS SC in MBLOCA/LBLOCA sequences without SBO. Finally, the conclusions drawn from this research are set out in Section 6.1.3.

6.1.1. Impact of the HA-2 system in LOCA along with SBO sequences

The Design Basis Accident (DBA) for which the HA-2 PSS has been mainly designed is the LOCA along with SBO (Asmolov et al., 2017; Turkish Atomic Energy Authority, 2018). According to (ROSATOM, 2022), the HA-2 PSS, with the availability of 3 out of 4 trains, and the operation of the PHRS are able to avoid the CD during 24 h, furthermore reference, (Agrawal et al., 2006), reports that the HA-2 PSS has the capacity to remove all the decay heat with the availability of 3 out of 4 trains for 8 h without the PHRS operation.

Considering this information, this Section 6.1.1 focuses on the analysis concerning the impact of the HA-2 PSS in LOCA sequences along with SBO for a VVER-1000 reactor. First an analytical study, verified later by TH simulations, is carried out to evaluate the HA-2 PSS capability to remove the decay heat over 24 h. The HA-1 SC to ensure core cooling during the initial phase of the accidental sequence are then analyzed.

6.1.1.1. Analysis of the HA-2 capacity to perform its safety function.

In order to verify the ability of the HA-2 PSS to perform its long-term safety function, once the HA-1 inventory has discharged and it is the only ECCS available, the maximum theoretical energy that the system would be able to remove has been calculated for the DEGB LBLOCA along with SBO sequence, since it is the most limiting break size. The calculation has been performed considering the complete vaporization of the HA-2 mass flow rate, i.e. G, for 2 out of 4 trains, 3 out of 4 trains and 4 out of 4 trains available.

$$Q_{vap} = G\ (h_{out} - h_{in}) = G\ (\ h_{v,out}^{sat} - h_{l,in})$$

Since the objective is to know the maximum capacity of the system to remove heat, the enthalpy of the water in HA-2 ($h_{l,in}$= 1.26E+05 J/kg) has been selected assuming that the tanks are at environmental temperature (303.15 K) while the steam coming out of the break has been considered to be saturated at atmospheric pressure ($h_{v,out}^{sat}$ = 2.68E+06 J/kg). The HA-2 mass flow rate for each of the four

stages has been established according to the available trains, see Table 6-1. The analytical calculations, see Figure 6-1, show that:

- If 2 out of 4 trains are considered, the HA-2 PSS alone cannot remove the decay heat from the last three stages.
- If 3 of the 4 trains are considered, the HA-2 PSS alone is only enough to cool the reactor during the first three injection stages, i.e. 8 hours. Which agrees with (Agrawal et al., 2006).
- If 4 out of 4 trains are considered, it is enough to cool the core during the four stages (24 h) since the decay heat power is lower than the power removed by the four trains in all of them. Therefore, the actuation of the PHRS is not needed in this case.

It is important to notice that a positive energy balance, between the energy that the HA-2 is able to remove and the energy released in the core, is only a necessary condition but not a sufficient condition for the success of the sequence, since other phenomena such as RCS inventory distribution must be considered, and then TH simulations are needed in order to verify these conclusions. Therefore, a large number of LOCA diameters along with SBO sequences have been simulated with the VVER-1000/V320 model for TRACEV5P5 code. The simulations have been performed considering the full availability of the HA-1, for both cases assuming the operation of 3 out of 4 trains and 4 out of 4 trains of the HA-2 PSS.

The simulation results agree with those obtained analytically and with (Agrawal et al., 2006), showing that the performance of the HA-2 PSS with four trains is enough to maintain core cooling with the PCT below 1477 K for 24 hours, see Figure 6-2 and Figure 6-3, and that if 3 out of 4 trains are available, the core cooling is assured only for the first 8 h, see Figure 6-4 and Figure 6-5.

The evolution of the events for the DEGB and 3 inches LOCA along with SBO sequence is shown in Table 6-2 (for both 3 out of 4 HA-2 and 4 out of 4 HA-2 configurations). The onset of injection for both HA-1 and HA-2 PSS is earlier for the DEGB LOCA than for the 3 inches LOCA, because the depressurization of the RCS in 3 inches LOCA is slower. However, for both break sizes with the 4 out of 4 HA-2 PSS configuration, the PCT does not exceed 1477 K, while with 3 out of 4 HA-2 it does, being about 25000 s earlier for the DEGB LOCA. Finally, it can be observed that for the successful sequences, the HA-2 fourth injection stage ends 24 hours after its start.

It is worth noting that in the simulations there are no effective interactions found between the HA-1 and the HA-2 systems, i.e. there is no mass flow rate HA-1 reduction because HA-2 injection. For medium break sizes (less than 6 inches) there is a short period when both systems are injecting simultaneously but there is no reduction in the HA-1 mass flow rate. For larger break sizes (more than 6 inches) the HA-1 are isolated before the HA-2 injection, see rows 6 and 7 in Table 6-2. The reason for this is that the HA-1 injects until its isolation valves close, when the HA-1 pressure reaches almost 0.8 MPa, and the HA-2 begins injection between 0.78 and 0.3 MPa (for 6 inches onwards), due to the delay in the HA-2 actuation signal. As a result, both systems do not overlap.

Table 6-1 HA-2 mass flow rates for different configurations

	Stage 1	Stage 2	Stage 3	Stage 4
Time (s)	100 – 4000	4001 – 10000	10001 – 30000	30001 – 86400
Total Mass Flow (kg/s) 4 out of 4 trains	40	20	13.2	7.12
Total Mass Flow (kg/s) 3 out of 4 trains	30	15	9.9	5.34
Total Mass Flow (kg/s) 2 out of 4 trains	20	10	6.6	3.56

Note that the HA-2 design considered in the doctoral thesis is from the VVER-1200 design reactors, with a thermal power of 3200 MW_{th}. However, this study has been carried out on a VVER-1000/V320 model with a thermal power of 3000 MW_{th}. To account for this difference, additional simulations have been performed in which the capacity of the HA-2 PSS has been rescaled by reducing the mass flow rate at each stage by 6.25% (VVER-1000 and VVER-1200 thermal difference). The

conclusions obtained from these simulations are the same as those obtained by considering the 100% mass flow at each stage of the HA-2 PSS.

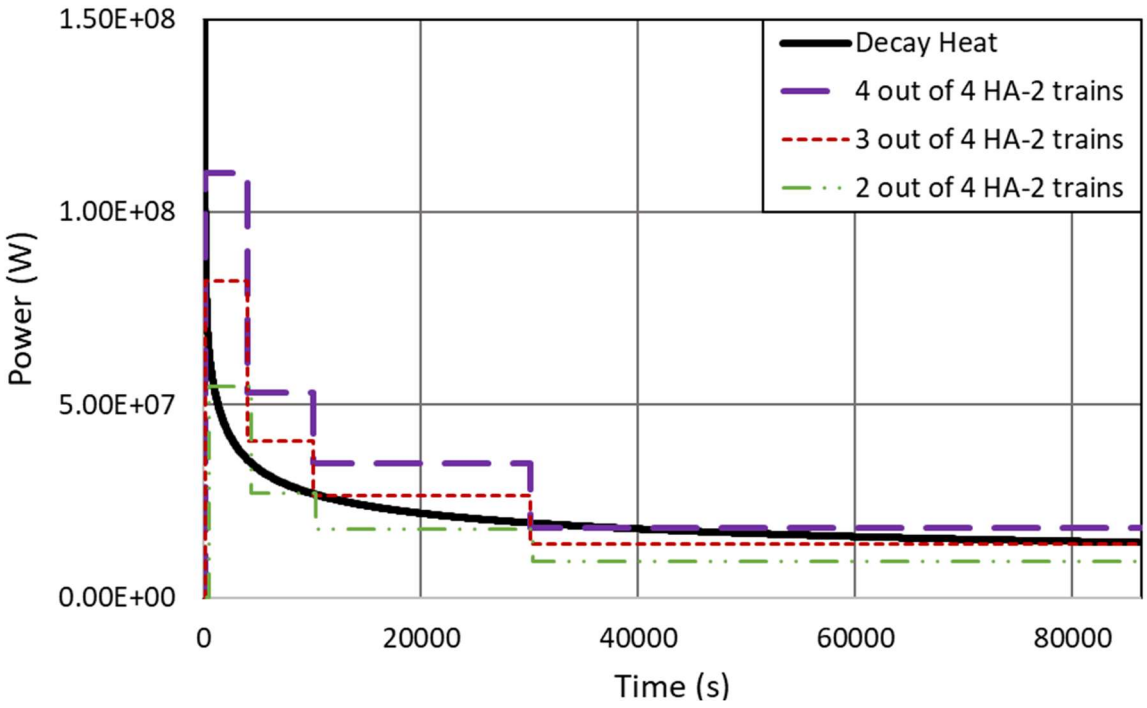

Figure 6-1 Maximum heat removal capacity of the HA-2 system vs decay heat in a DEGB LOCA along with SBO sequence

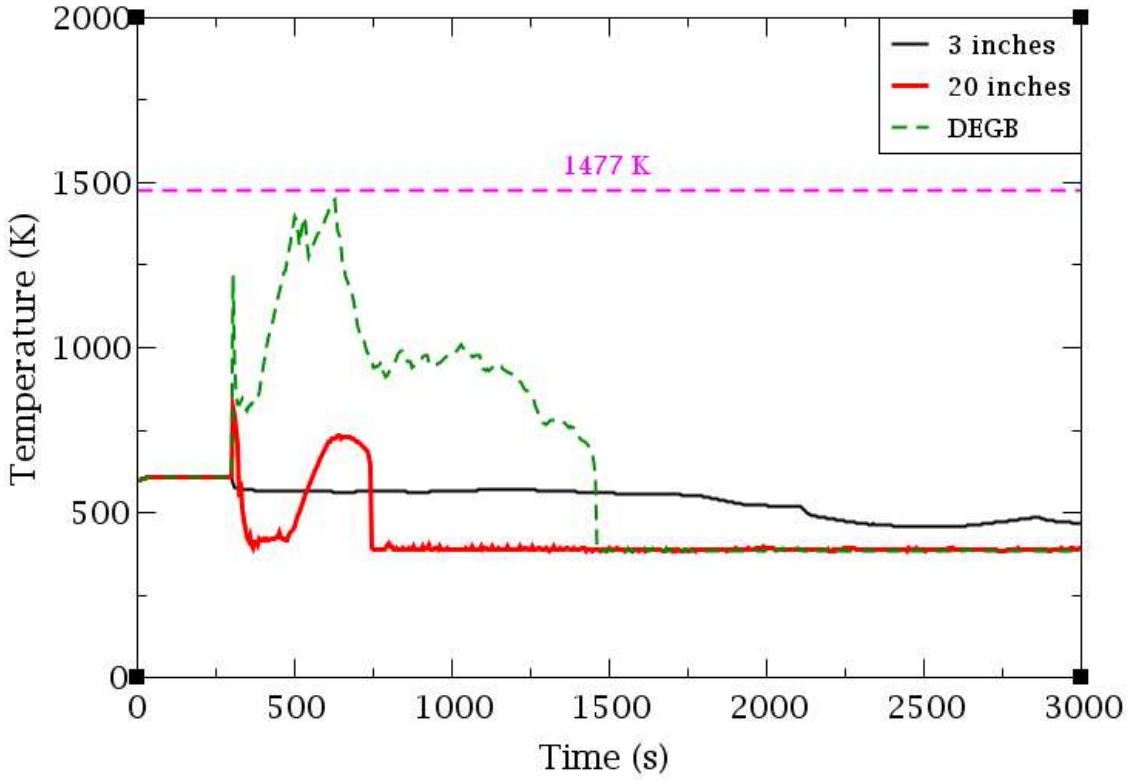

Figure 6-2 PCT, LOCA + SBO sequences in the short term (4 out of 4 HA-2 trains)

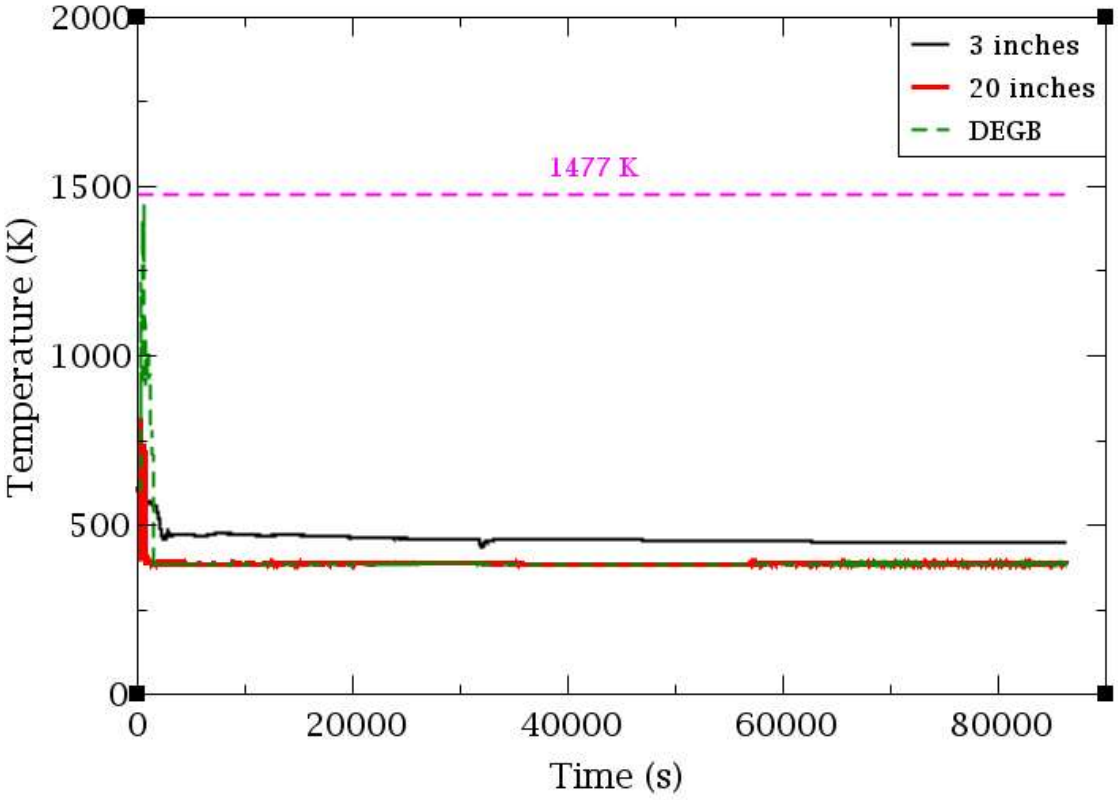

Figure 6-3 PCT, LOCA + SBO sequences in the long term (4 out of 4 HA-2 trains)

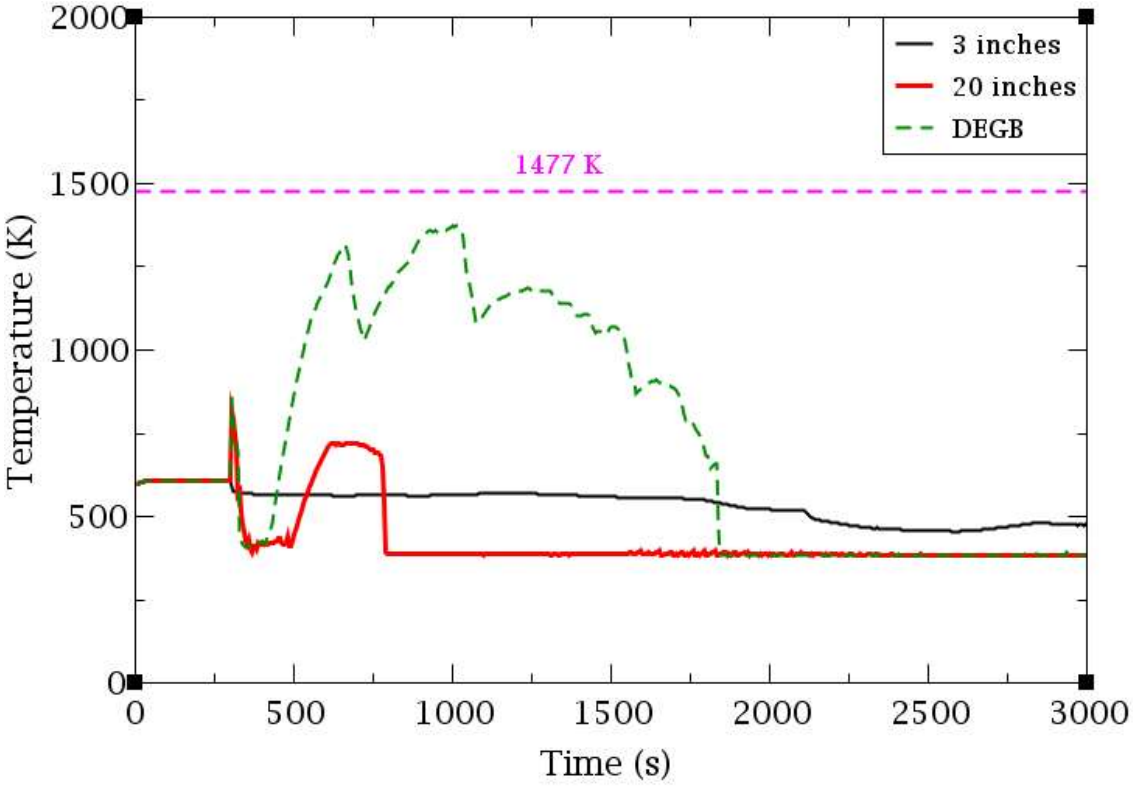

Figure 6-4 PCT, LOCA + SBO sequences in the short term (3 out of 4 HA-2 trains)

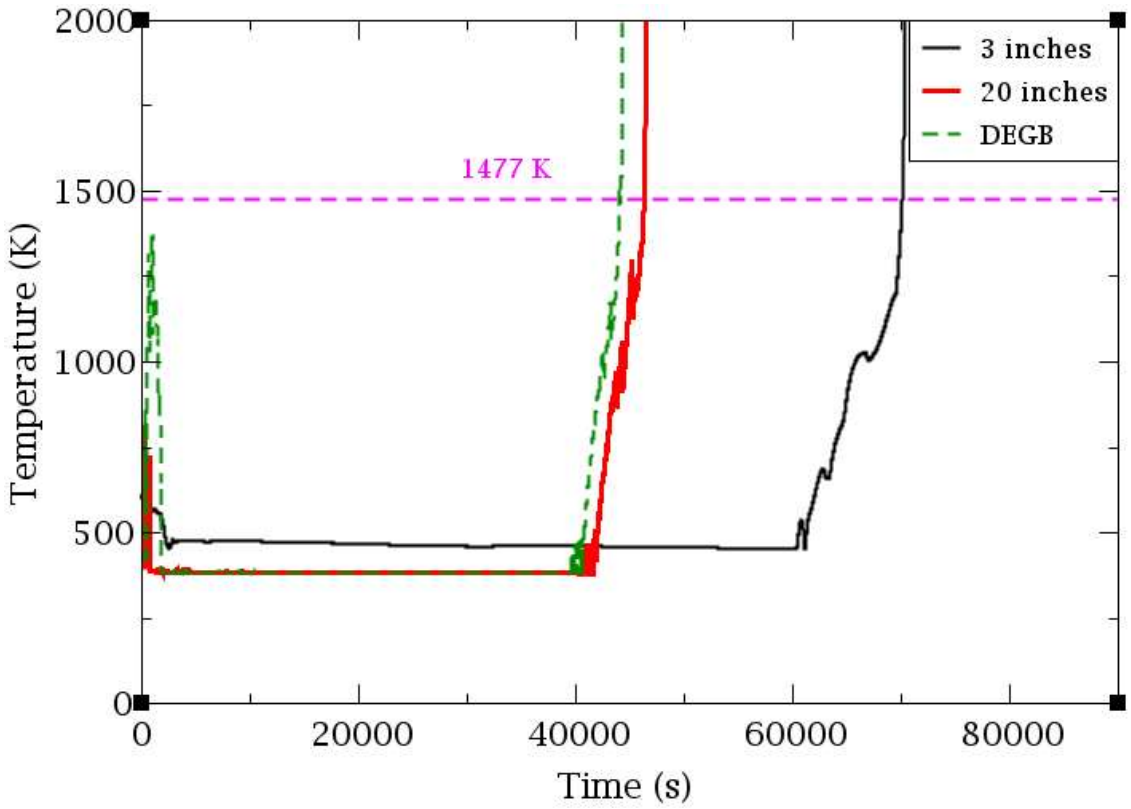

Figure 6-5 PCT, LOCA + SBO sequences in the long term (3 out of 4 HA-2 trains)

Table 6-2 DEGB LBLOCA and MBLOCA (3 inches) along with SBO sequences events

Event	3 inches 3 /4 HA-2/ 4 /4 HA-2 (s)	DEGB 3/4 HA-2/ 4/4 HA-2 (s)
DEGB LBLOCA along with SBO	0	0
CRAs fully inserted	5	4
HA-1 injection	1470	10
HA-2 setpoint (RCS Pressure < 1.5 MPa)	1935	25
1st stage HA-2 (RCS Pressure < 1.5 MPa + delay)	2035	125
HA-1 injection ends	2250/ 2295	75
2nd stage HA-2 injection begins	5935	4025
3rd stage HA-2 injection begins	11935	10325
4th stage HA-2 injection begins	31939	30325
PCT > 1477 K	69803/-	43867/-
HA-2 injection ends	-/88335	-/86525

6.1.1.2. PSA level 1 HA-1 success criteria with HA-2 fully availability

Previously analytical calculations and TH simulations lead to the conclusion, that the full availability of the HA-2 PSS is necessary to ensure the core cooling for 24 hours in LOCA along with SBO sequence, where the only available ECCS are the HA-1 and the HA-2 and there are no human actions. In the following, the HA-1 SC in these sequences has been examined. This analysis has been done in two steps:

- The break size range for which the HA-2 performance is guaranteed prior to reaching CD has been searched.
- The minimum HA-1 configuration to prevent the second core peak temperature of the LOCA sequence from exceeding 1477 K has been found for the range of break sizes previously obtained.

As mentioned in the introduction, the HA-2 setpoint is 1.5 MPa, lower than the pressure setpoint of the LPIS (2.55 MPa), which means that to come into operation it will need that the pressure in the RCS dropped considerably. Therefore, HA-2 starts injecting straight away without the need of another safety system actuation in the case of MB/LBLOCAs, however in the case of a SBLOCA, a previous depressurization of the RCS is necessary since the pressure remains stagnant well above 1.5 MPa making it impossible for HA-2 PSS to start operating on time.

Therefore, a wide range (from 2 inches to DEGB) of the LOCA along with SBO sequences, without the actuation of the HA-2 PSS, has been simulated in order to know from what break size the RCS pressure would allow the injection of HA-2 before the CD has been reached, without considering any depressurization action. The results show that from 3 inches break onwards the HA-2 is able to inject water before the CD occurs, see Table 6-3.

Next, a sensitivity analysis has been performed, by simulating the LOCA along with SBO sequence with the HA-2 full availability from 3 inches to DEGB, to find out the HA-1 SC, see Figure 6 6 and Figure 6 7. The results show that the HA-1 SC to 3 inches is 2 out of 4 trains, for larger MBLOCA breaks it relaxes, becoming unnecessary the HA-1 injection from 6 to 8 inches, however for LBLOCA the minimum HA-1 configuration increases again, becoming even 4 out of 4 from 30 inches onwards, see Figure 6 8.

Table 6-3 Times for HA-2 start operating, PCT = 1477 K and margin time, LOCA along with SBO

LOCA size (inches)	Time HA-2 can start injecting (s)	Time PCT = 1477 K (s)	Time margin (s)
2	8705	5361	Not available (<0)
3	5847	7088	1241
4	1375	5661	4286
6	650	2640	1990
8	405	2245	1840
12	230	1610	1380
20	150	705	555
25	135	245	210
30	126	196	70
DEGB (47)	120	190	70

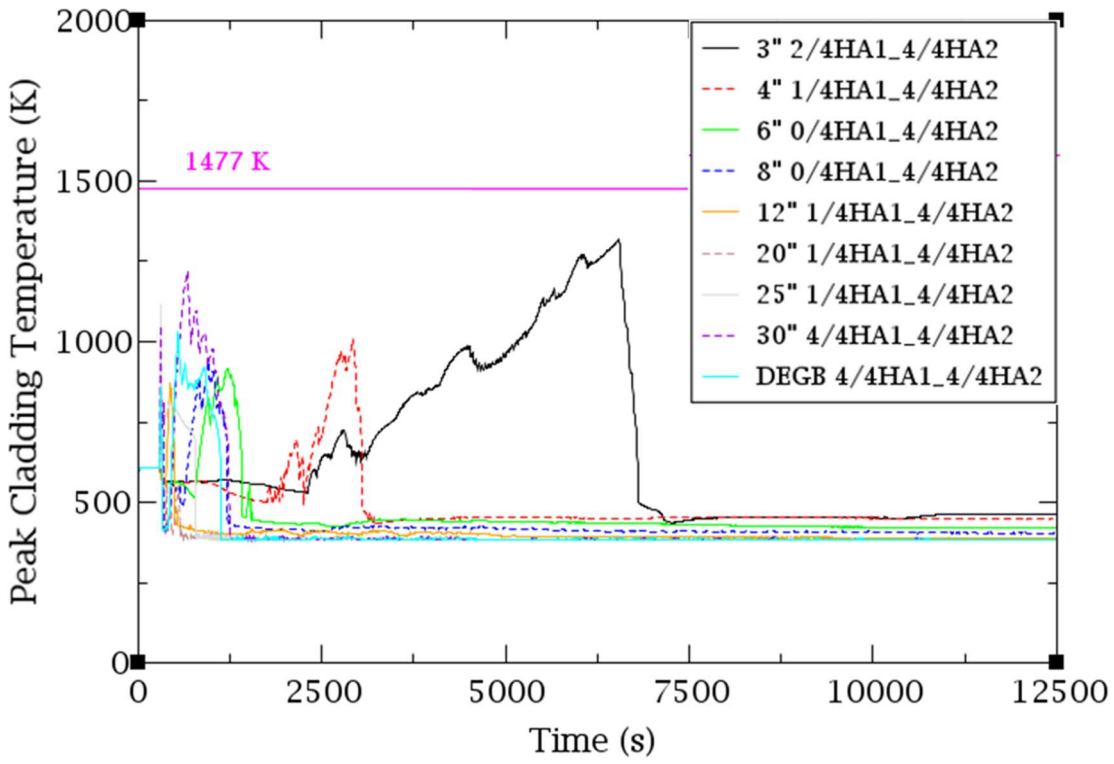

Figure 6-6 PCT, MB/LBLOCA along with SBO with the minimum HA-1 configuration required (HA-2 fully available)

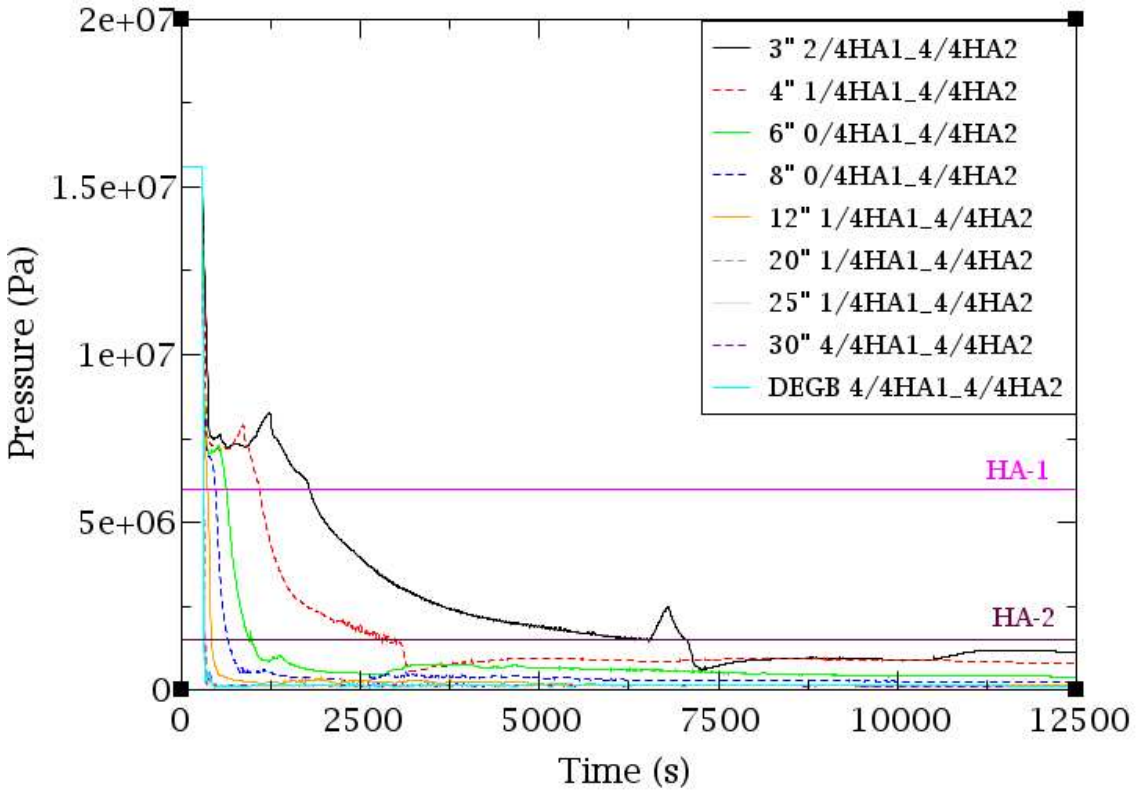

Figure 6-7 RCS pressure, MB/LBLOCA along with SBO with the minimum HA-1 configuration required (HA-2 fully available)

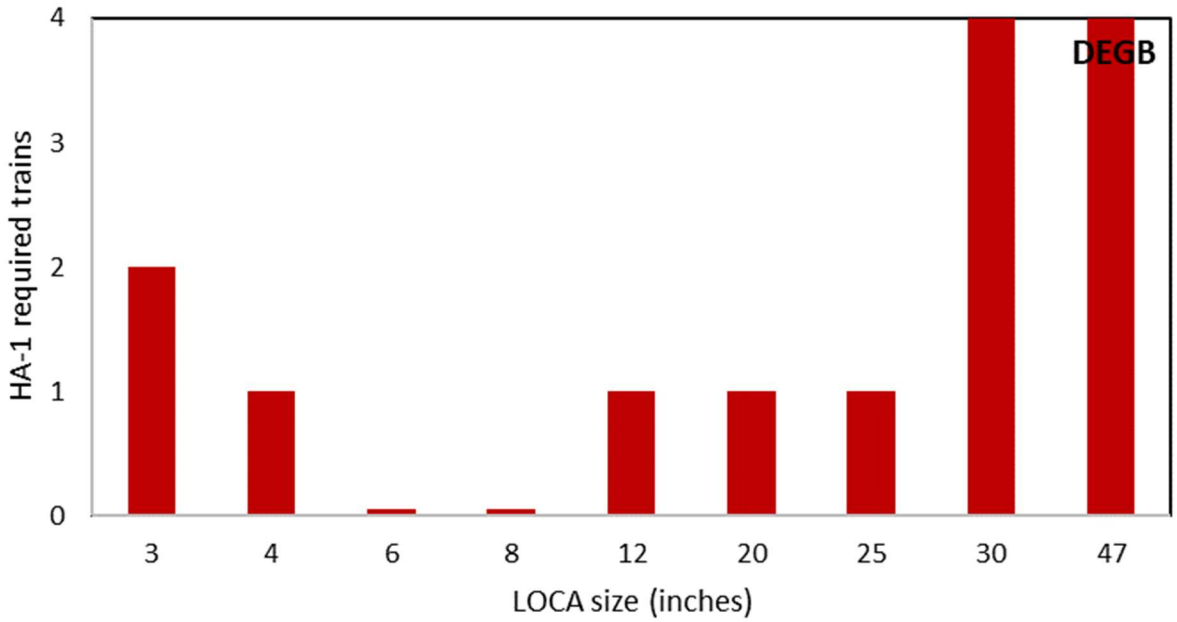

Figure 6-8 Number of HA-1 trains required to avoid core damage in LOCA along with SBO sequences with the HA-2 system performance

6.1.2. HA-2 impact in MBLOCA and LBLOCA success criteria

After the study of the impact of the HA-2 PSS in LOCA along with SBO sequences, the focus is now on the analyse how the ECCS SC in MB/LBLOCA sequences, without SBO, can be relaxed if the performance of the HA-2 system is considered. The SC analysis is performed into two steps. First the SC without considering HA-2 are presented (Section 6.1.2.1), then the new SC considering HA-2 actuation are obtained (Section 6.1.2.2).

Above all, it should be mentioned that in this analysis, a sequence is defined by concatenating the letter that identifies its headers written in upper or lower case so, if it is uppercase, it represents success while if it is in lower case it represents failure of the system. A or a represent the HA-1, H or h represent the HPIS and L or l represent the LPIS. In addition, the number of operating trains out of the total is written before the letter if the system is available. For instance, the sequence "1/3H-a-l" denotes a sequence in which one HPIS train is available and the HA-1 and the LPIS systems have failed.

6.1.2.1. MBLOCA and LBLOCA success criteria without considering HA-2

In Section 5.1, a verification of the SC of ETs for MB/LBLOCA sequences described in (Skalozubov et al., 2010) was carried out. A large number of simulations were then performed to analyse all possible ECCS configurations that allow avoiding CD for break sizes from 2 inches to DEGB, see Table 6-4.

As shown in Table 6-4, 1 out of 3 HPIS trains is enough for success over the entire MBLOCA range. However, 1 out of 3 LPIS trains is enough to succeed only between 3 to 8 inches, with all the HA-1 and the LPIS trains needed for 2 inches. In the LBLOCA range it is remarkable that from 8 to 12 inches, the availability of 1 out of 3 HPIS or LPIS trains is enough for success. However, as the size of the break increases, the need for more than one ECCS trains or even the joint performance of trains from different ECCSs becomes necessary.

Table 6-4 MBLOCA and LBLOCA success criteria with standard ECCS

<table>
<tr><th rowspan="2">Sequence</th><th colspan="2" rowspan="2">MBLOCA</th><th colspan="5">LBLOCA</th></tr>
<tr><th>8 inches</th><th>12 inches</th><th>20 inches</th><th>25 inches</th><th>30 inches</th><th>DEGB</th></tr>
<tr><td>S1: H-A-L</td><td colspan="2" rowspan="4">1/3 H</td><td colspan="3" rowspan="3">1/3 H</td><td>1/3 H + 1/4 A</td><td>2/3 H + 1/4 A
1/3H + 2/4 A</td><td>1/3H + 1/4 A</td><td>1/3 H+ 1/4 A + 1/3 L</td></tr>
<tr><td>S2: H-A-l</td><td>2/3 H + 1/4 A</td><td>2/3 H + 1/3 L</td></tr>
<tr><td>S3: H-a-L</td><td colspan="2" rowspan="2">2/3 H</td><td>3/3 H</td><td>1/3 H + 1/3 L</td><td rowspan="2">CD</td></tr>
<tr><td>S4: H-a-l</td><td>4/4 A + 3/3 L</td><td>1/3 L</td><td colspan="2">1/3 L</td><td>1/4 A + 1/3 L</td><td>2/4 A + 1/3 L</td></tr>
<tr><td>S5: h-A-L</td><td>4/4 A + 3/3 L</td><td>1/3 L</td><td colspan="3" rowspan="2">1/3 L</td><td colspan="2" rowspan="2">CD</td><td>2/3 L</td></tr>
<tr><td>S6: h-A-l</td><td colspan="2">CD</td><td>CD</td><td colspan="2">1/3 L</td></tr>
<tr><td>S7: h-a-L</td><td colspan="2">CD</td><td colspan="2">1/3 L</td><td colspan="3">1/3 L</td><td>2/3 L</td></tr>
</table>

6.1.2.2. MBLOCA and LBLOCA success criteria considering HA-2 actuation

In order to simplify this analysis, it has been reviewed in which sequences the actuation of the HA-2 allows to relax the SC for any of the other ECCSs. Therefore, only those sequences in Table 6-4 that require more than one train of the LPIS, HPIS or/and HA-1 have been selected, see second column of the Table 6-5. Having identified the sequences that have the potential to relax some SC, the time at which the HA-2 setpoint is reached, i.e. 100 s after the RCS pressure drops below 1.5 MPa, was obtained. The time margin to avoid CD was then calculated by subtracting the HA-2 start operating time from the time at which the PCT exceeded 1477 K, see Table 6-5.

Following this analysis, it has been obtained that the sequences in which HA-2 PSS can avoid CD are 20 inches LBLOCA (1/3H-a-l), 25 inches LBLOCA (1/3H-1/4A-l), DEGB LBLOCA (1/3H-1/4A-l) and DEGB LBLOCA (h-1/4A-1/3L). Two sequences have been identified in which the time at which the HA-2 PSS can actuate and the time when the CD is reached differed only by 1 s. Therefore, it is considered that in them the HA-2 PSS would not actuate in time to prevent the core temperature from exceeding 1477 K, these sequences are 30 inches LBLOCA (h-a-1/3L) and DEGB LBLOCA (h-a-1/3L), see fifth column of Table 6-5.

In order to verify that the four sequences, with the possibility of the HA-2 PSS having an impact on their SC, are successful, they have been simulated with the model. The results of the simulations show that three of the four sequences are indeed successful.

- In 25 inches LBLOCA (1/3H-1/4A-l) sequence, it can be observed as the HA-2 system is able to reduce the maximum PCT from 1787 K to 1074, see Figure 6-9.
- In DEGB LBLOCA (1/3H-1/4A-l) sequence without the HA-2 actuation the PCT exceeds 1477 K, on the other hand the code stops the simulation when the PCT reaches 2018 K and then the long term evolution cannot be analyzed. The actuation of the HA-2 PSS allows to reduce the PCT to a maximum value of 1350 K, see Figure 6-10.
- In the DEGB LBLOCA (h-a-1/3L) sequence HA-2 system is able to reduce the PCT from 1594 K to 1149 K see Figure 6-11.

As some of the cases have a low time margin of a few seconds, it would be possible to perform a BEPU analysis to confirm the probability of success. However, this

quantification time is not a requirement for PSA; hence is not performed in this analysis. On the other hand, increasing the HA-2 PSS setpoint could potentially allow an earlier injection of the HA-2 PSS and prevent the CD in a few more LOCA sequences. Nevertheless, it appears that this modification could not have a significant impact on the CD frequency. Consequently, no setpoint modification is proposed.

Finally, Table 6-6 shows the final MB/LBLOCA SC when the performance of the HA-2 PSS is considered. In white background are those sequences in which the SC has not been change, i.e. they are the ones in Table 6-4. In colour background (see electronic version) are those in which the SC have changed, in green the new SC in sequences with an active ECCS, either HPIS or LPIS, and in yellow are the SC for the sequences without active ECCS.

Table 6-5 Times for HA-2 start operating, PCT = 1477 K and margin time, LOCA sequences

LOCA (inches)	Sequence	Time HA-2 injection (s)	Time PCT = 1477 K (s)	Time margin (s)
2	h-4/4A-2/3L	~ 15000	10368	Not available
	h-3/4A-3/3L	~ 13000	7176	Not available
20	1/3H-a-l	490	495	5
25	2/3H-a-l	435	430	Not available
	1/3H-1/4A-l	445	465	10
30	3/3H-a-l	426	405	Not available
	h-a-1/3L	426	427	1 (not enough time)
DEGB (47)	3/3H-a-l	421	389	Not available
	1/3H-1/4A-l	420	459	39
	1/3H-a-1/3L	421	403	Not available
	h-1/4A-1/3L	462	470	8
	h-a-1/3L	434	435	1 (not enough time)

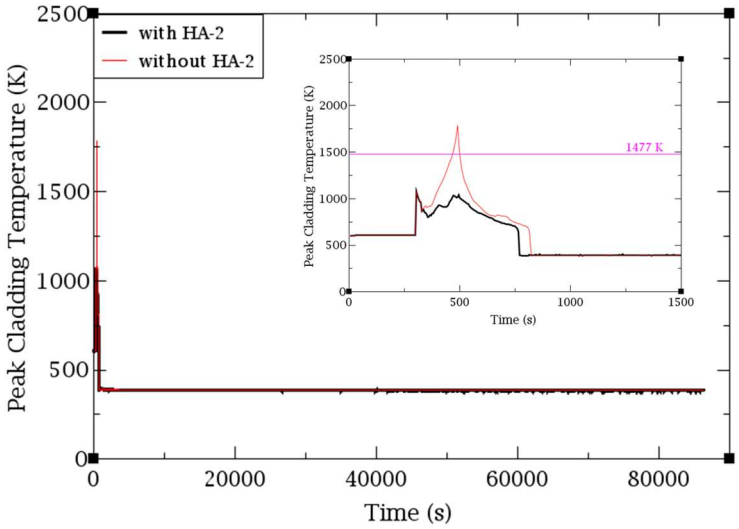

Figure 6-9 PCT, 1/3H-1/4A-l LBLOCA (25 inches)

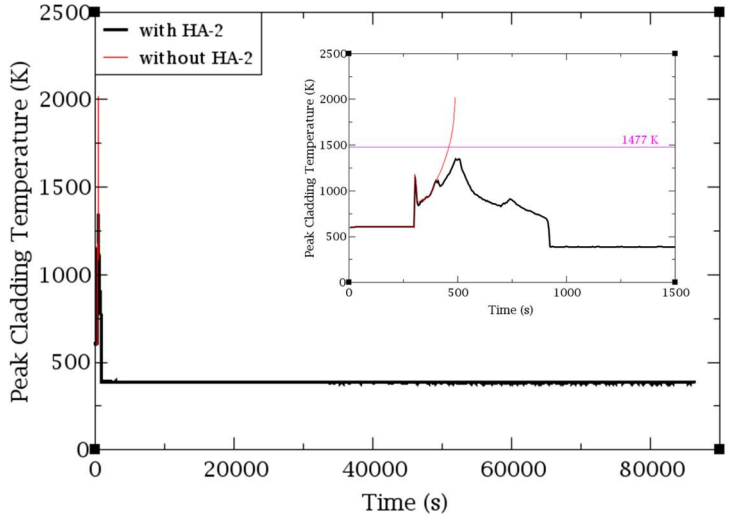

Figure 6-10 PCT, 1/3H-1/4A-l DEGB LBLOCA

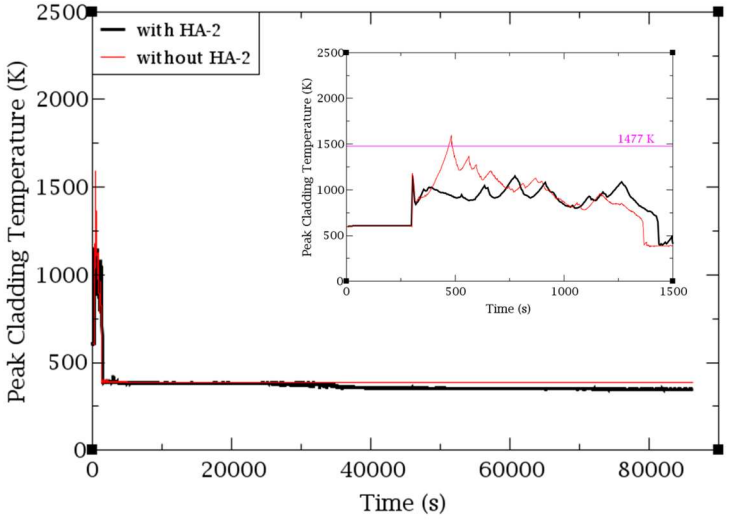

Figure 6-11 PCT, h-1/4A-1/3L DEGB LBLOCA

Table 6-6 New success criteria for MB/LBLOCA sequences considering the HA-2

Sequence	MBLOCA				LBLOCA					
	2 inches	3 inches	4 inches	6 inches	8 inches	12 inches	20 inches	25 inches	30 inches	DEGB
S1: H-A-L S2: H-A-I	1/3 H (607 K)	1/3 H (607 K)	1/3 H (607 K)	1/3 H (607 K)	1/3 H (607 K)	1/3 H (723 K)	1/3 H + 1/4 A (849 K)	1/3 H + 1/4 A (1074 K)	1/3H + 1/4 A (1119 K)	1/3H + 1/4 A (1350 K)
S3: H-a-L							2/3 H (1266 K)	3/3 H (1309 K)	1/3 H + 1/3 L (1338 K)	2/3 H + 1/3 L (1349 K)
S4: H-a-I									CD (>1477 K)	CD (>1477 K)
S5: h-A-L	4/4 A + 3/3 L (1374 K)	1/3 L (1169 K)	1/3 L (923 K)	1/3 L (656 K)	1/3 L (655 K)	1/3 L (1067 K)	1/3 L (1314 K)	1/3 L (1392 K)	1/4 A + 1/3 L (1169 K)	1/4 A + 1/3 L (1149 K)
S6: h-A-I (24 hours)	CD (>1477 K)	2/4 A (1314 K)	1/4 A (1009 K)	0/4 A (916 K)	0/4 A (939 K)	1/4 A (872 K)	1/4 A (818 K)	1/4 A (1117 K)	4/4 A (1219 K)	4/4 A (1030 K)
S7: h-a-L		1/3 L (1169 K)	1/3 L (923 K)	1/3 L (656 K)	1/3 L (655 K)	1/3 L (1067 K)	1/3 L (1314 K)	1/3 L (1392 K)	2/3 L (1251 K)	2/3 L (1275 K)

6.1.3. Conclusions regarding the impact of the HA-2

A large number of TRACEV5P5 simulations of different LOCA sequences for the VVER-1000/V320 reactor have been carried out to study the impact on the accident progression of the HA-2. Based on the performed investigations, following conclusions can be drawn:

- The TRACEV5P5 code is robust for a wide range of VVER LOCAs with various combinations of the availability of safety systems.
- In LOCA along with SBO sequences, from 3 inches to DEGB, with the full availability of the HA-1 PSS, 4 out of 4 HA-2 trains are enough to avoid CD for 24 h without the need for any other safety system.
- In LOCA along with SBO sequences, from 3 inches to DEGB, with the full availability of the HA-1 PSS, 3 out of 4 HA-2 trains are able to cool the core for 8 h, thereafter PHRS intervention or active ECCS recovery would be required.
- The HA-1 SC in case of LOCAs ranging from 3 inches to DEGB along with SBO sequences were identified thanks to the systematic studies performed with TRACEV5P5 assuming full availability of the HA-2 PSS.
- If the actuation of the HA-2 is considered, the TRACEV5P5 analysis of some MB/LBLOCA sequences have shown that it is possible to relax the combined SC of the LPIS, HPIS and HA-1.
- In the sequences analyzed, no negative interactions were found between HA-2 and the other injection systems.
- The main uncertainties in this kind of analysis are related to flow resistance and RCS liquid levels. BEPU analyses should be considered if they want to be taken into account.

6.2. Safety margins improvement by means of the air-cooled PHRS and the HA-2 in VVER-1000 reactors

Section 6.2 presents a detailed discussion of the safety margin provided by the air-cooled PHRS together with the HA-2 in the full plant model of the VVER-1000/V320 reactor developed through the PhD thesis. The selected air-cooled PHRS design to be studied has been the air-cooled PHRS present in the VVER-1000/V412, which has been described in detail in Section 2.2.4.

Previous studies have developed isolated models of this air-cooled PHRS, see (Ayhan and Sokmen, 2016a, 2016b; Khubchandani et al., 2013a). However, only a few references analyse in detail the effect of the air-cooled PHRS in SBO sequences, both with and without LOCA, see (IAEA, 2012; ROSATOM, 2022). In the present analysis, a SBO, an SBLOCA and an LBLOCA along with SBO sequences have been analyzed with the PHRS operating in the SGs.

Section 6.2 is organized as follows: Sections 6.2.1, 6.2.2, and 6.2.3 present simulations of the SBO sequence and the SBLOCA/LBLOCA along with SBO sequences, respectively, using the VVER-1000/V320 plant model with the PHRS integrated. Lastly, Section 6.2.4 provides the main conclusion related the impact of the PHRS along with the HA-2.

6.2.1. Performance of the PHRS during an SBO sequence

The aim is to analyze the behavior of the air-cooled PHRS when operating in SG pressure maintenance mode during an SBO sequence. It should be noted that this sequence is analyzed only for the VVER-1000/V392 design in (IAEA, 2012), both considering and not considering the air-cooled PHRS performance, and for the VVER-1200 in (ROSATOM, 2022).

In the present work, the sequence has been analyzed taking into account the air-cooled PHRS SC of 3 out of 4 trains, i.e., the trains connected to SGs 1, 3, and 4 are available, while SG 2 is unavailable. In addition, this analysis does not consider the potential leakages of the RCS inventory through the MCPs. It is important to note that a large number of operating NPPs, both Gen-II and Gen-III/III+, have passive thermal shutdown seals (or hydrodynamic seals) on the MCPs to prevent leakage of the RCS inventory through the MCPs in the SBO sequence. Furthermore, the SBO sequence with MCPs leakages is covered by the SBLOCA with SBO analysis.

Following, the SBO sequence is first analyzed considering the availability of the air-cooled PHRS. Subsequently, it is analyzed how long it would take for the sequence to reach CD if the PHRS operation is not considered.

6.2.1.1. SBO sequence with PHRS available

The SBO sequence starts after 300 seconds of SS. At that instant there is a total loss of AC power, failure to start of the EDGs, reactor SCRAM, MCPs trip, loss of the CVCS, MFW pumps trip, TT and loss of the condenser. The evolution of the main events during this sequence is shown in Table 6-7.

At the beginning of the sequence, the SGs pressure starts to rise, but the condenser relief valves, BRU-K, do not open as the condenser is lost. Therefore, the SGs pressure continues to rise until it reaches the setpoint of the steam line relief valves, BRU-A, see Figure 6-12 and Figure 6-13. Within 30 seconds of the AC power loss signal, the air gates begin to open, both upstream and downstream of the PHRS HXs. The three available PHRS trains are at 100% capacity 90 seconds later. Due to the action of the PHRS, the pressure in the SGs starts to decrease, which causes the BRU-A valves to close. At 1465 s, the pressure in the SGs drops below 6.05 MPa, causing the air-cooled PHRS regulator to begin closing (by means of the passive actuator), see Figure 6-15.

By gradually closing the regulators, the air flow in the air ducts is passively regulated. It is observed that the air flow per air-cooled PHRS train is about 200 kg/s at the beginning of the sequence, decreasing to around 30 kg/s after 24 hours, as shown in Figure 6-16. This air flow at 303.15 K allows the extraction of a power between 25 MW at the beginning of the sequence and 5 MW after 24 hours per train of the air-cooled PHRS, see Figure 6-14. Note also that the heat removed from the RCS by the SGs is less than that removed by the PHRS tubes at the beginning of the sequence, but in the long term both become equal.

In the steam and the condensate lines of the air-cooled PHRS, it is possible to observe how the heat transfer between the secondary side of the SGs and the air establishes a natural circulation of about 4 kg/s after 24 hours of the sequence, Figure 6-17.Futhermore, it can also be observed that the void fraction at the outlet of the PHRS tubes is 90%, see Figure 6-18, causing a mixture of steam and saturated liquid at a temperature of 540 K to return to the SGs, see Figure 6-19.

Moreover, SGs inventory, which is at saturation, has a lower temperature than the liquid in the HLs, see Figure 6-20. This cooling leads natural circulation in the

RCS of about 125 kg/s for each of the three loops with the available PHRS. In loop 2, where the PHRS is not operational, there is a gradual loss of natural circulation, see Figure 6-21. The integral of the mass flow rate of the four CLs is shown in Figure 6-22.

It can thus be concluded that the performance of 3 out of 4 air-cooled PHRS trains enables the control of pressure in both the RCS and the SGs without the need for human actions or the intervention of any other safety system. It is noteworthy that the decay heat removal by the SGs, due to the air-cooled PHRS performance, becomes equivalent to the core thermal power, see Figure 6-24. This ensures that the PCT in the core does not increase during the first 24 hours of the sequence, see Figure 6-23.

Table 6-7 Main events in the SBO sequence [with PHRS]

Time (s)	Event
300	SBO (SCRAM, MFW and MCPs trip, TT, loss of the condenser, CVCS)
310	BRU-A opening (SL pressure > 7.25 MPa)
330	Air gates opening (SBO + 30 s delay)
420	PHRS full capacity (90 s opening)
499	BRU-A closed (SL pressure < 6.67 MPa)
1465	PHRS regulators start to close (P_{SG} = 6.05 MPa)
86400	End simulation (24 hours)

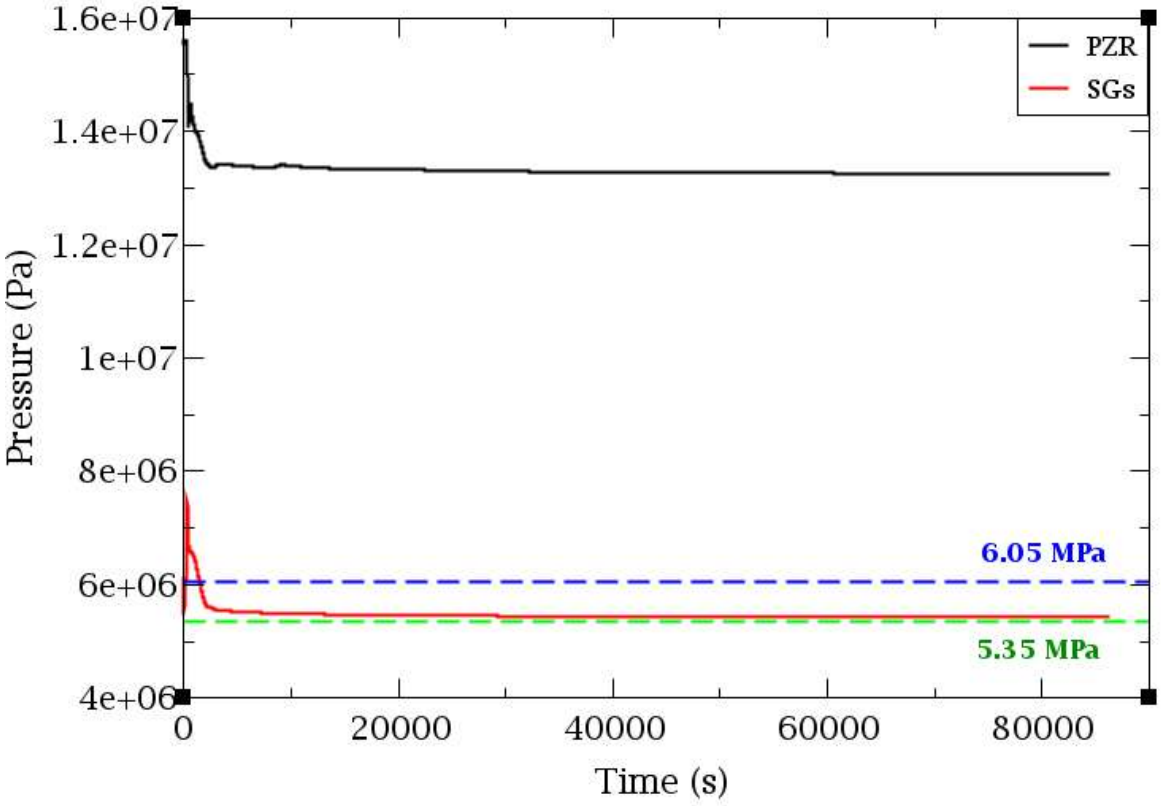

Figure 6-12 RCS and SGs pressure, SBO sequence

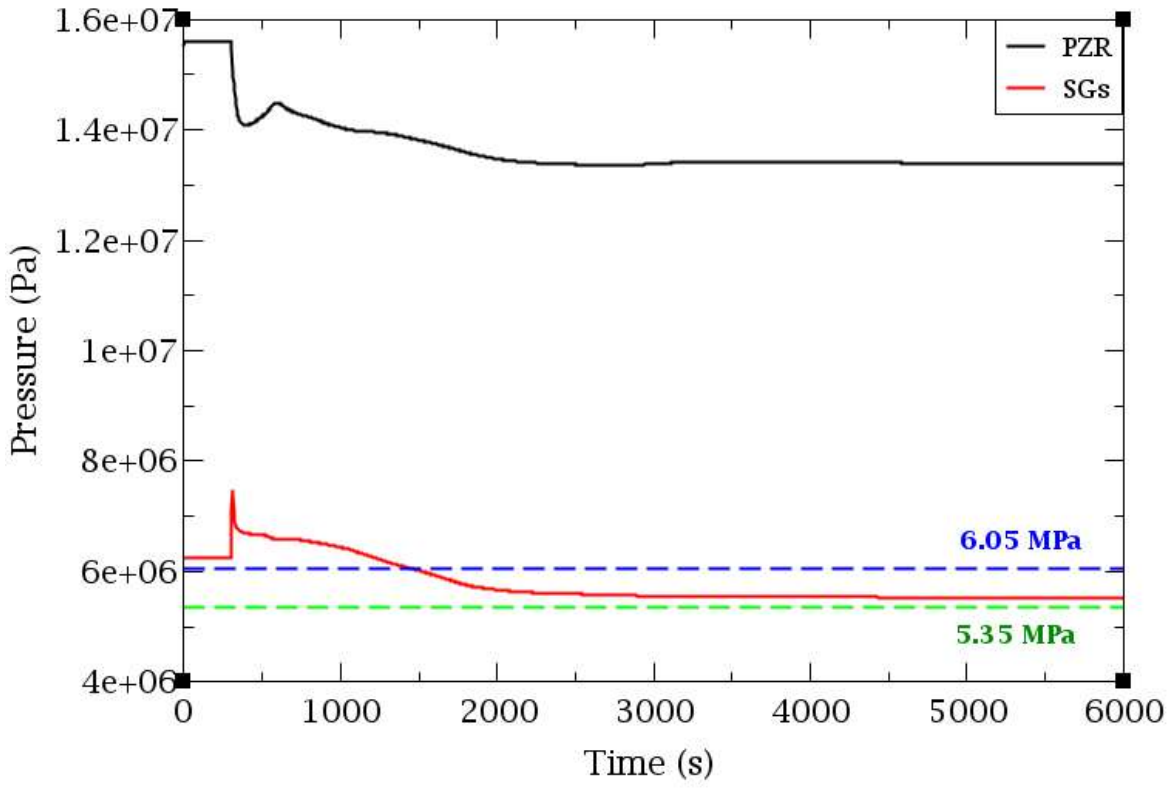

Figure 6-13 RCS and SGs pressure, SBO sequence (from 0 s to 6000 s)

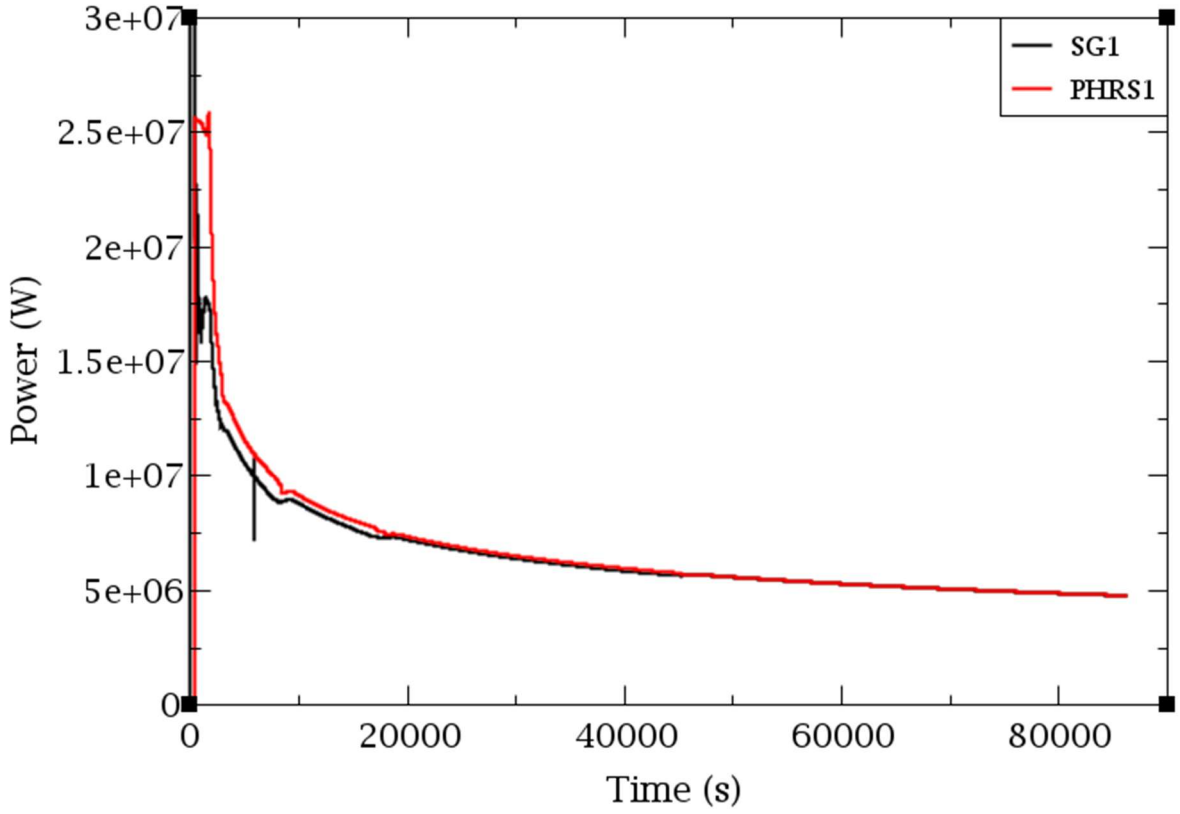

Figure 6-14 PHRS 1 vs. SG1 power, SBO sequence

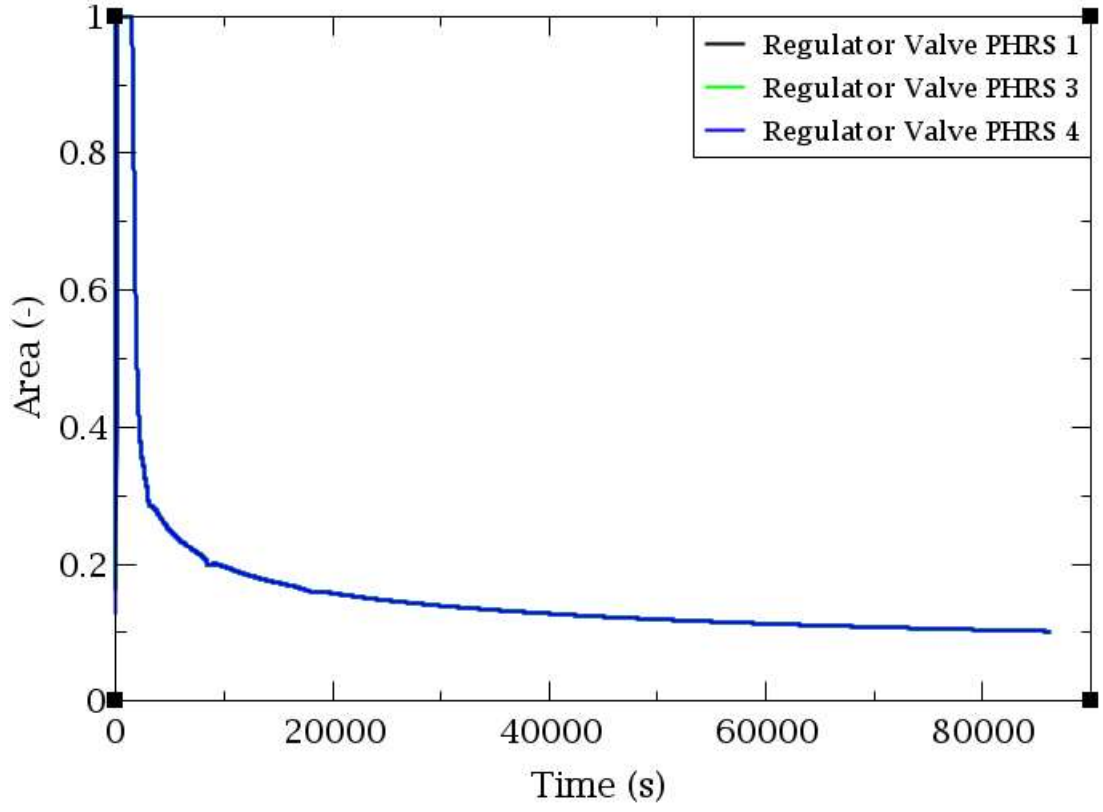

Figure 6-15 PHRS regulators are fraction, SBO sequence

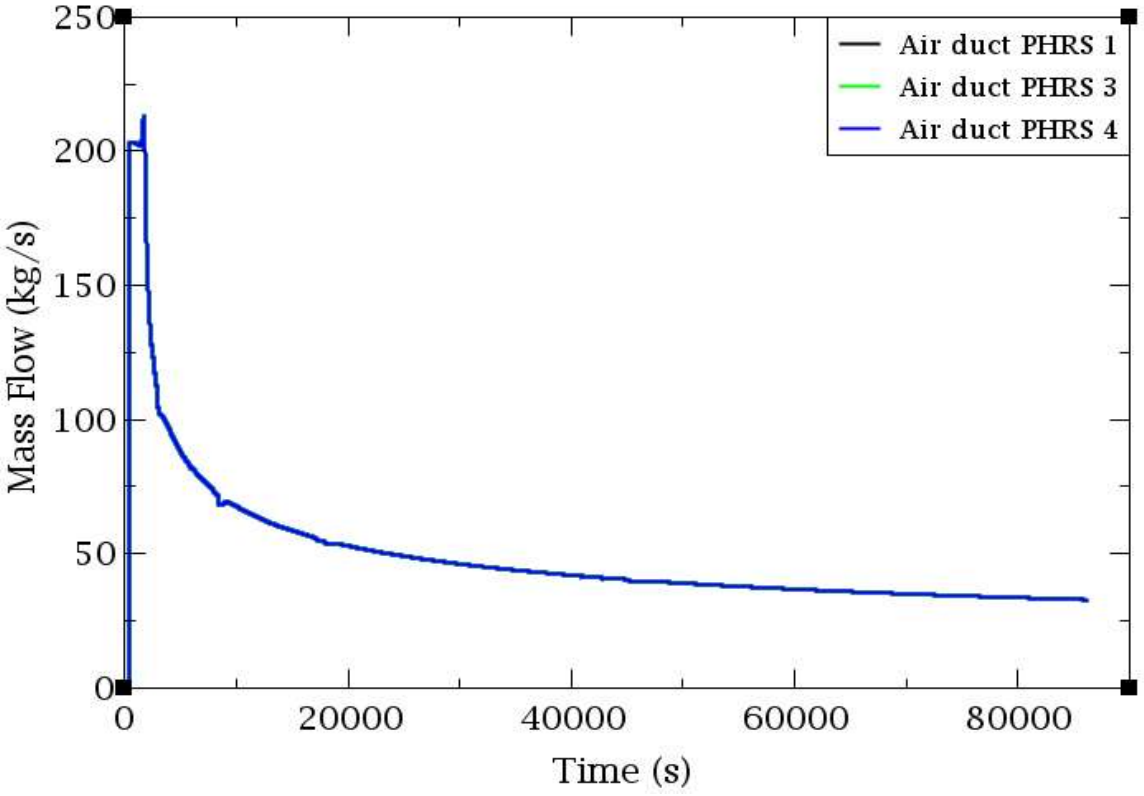

Figure 6-16 PHRS air duct mass flow rate per train, SBO sequence

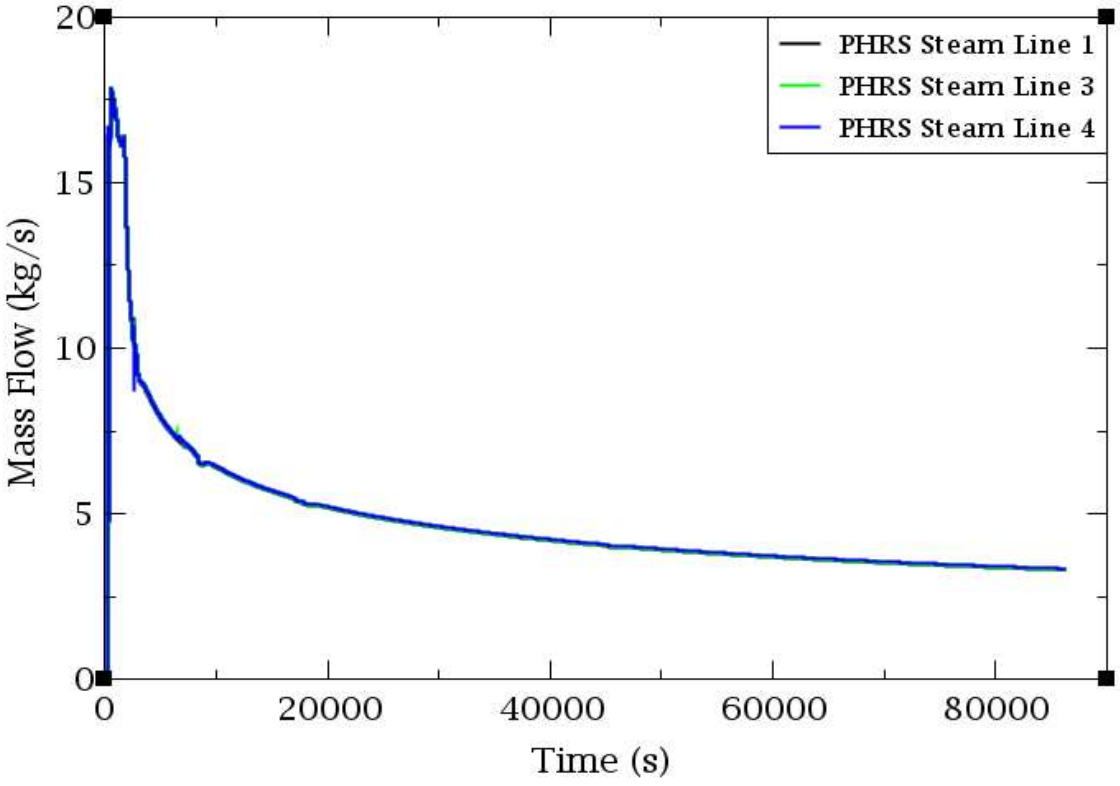

Figure 6-17 PHRS steam lines mass flow rate, SBO sequence

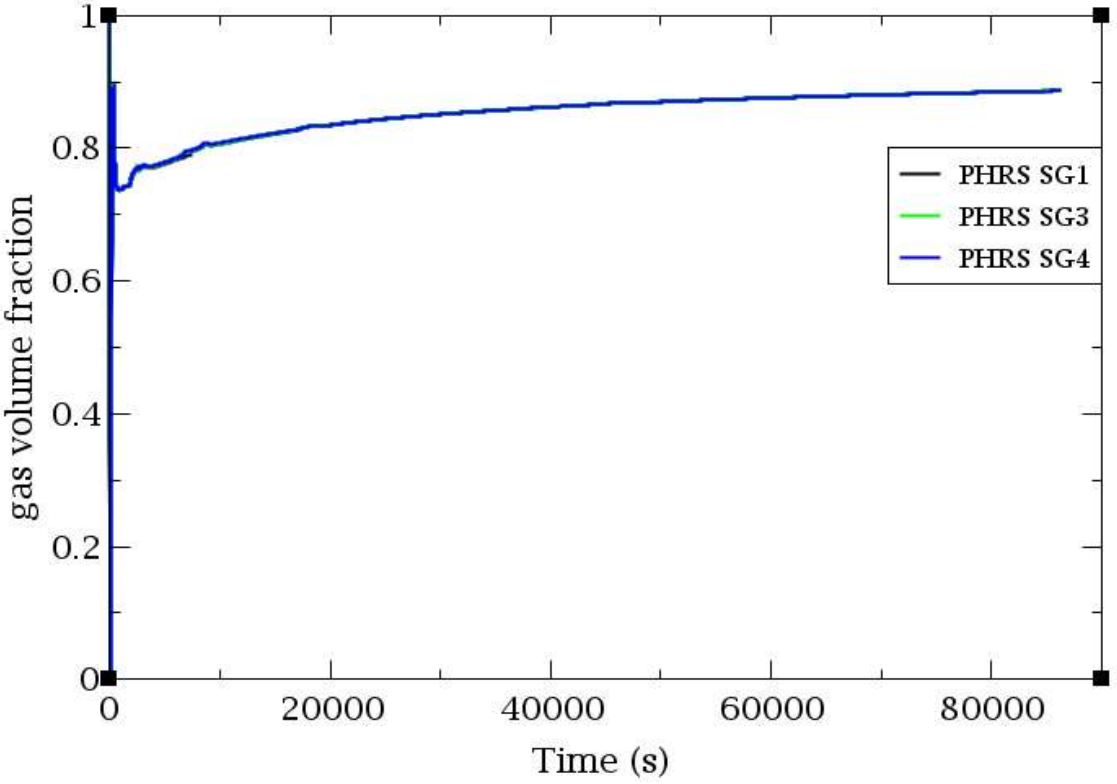

Figure 6-18 PHRS outlet bundle tubes void fraction, SBO sequence

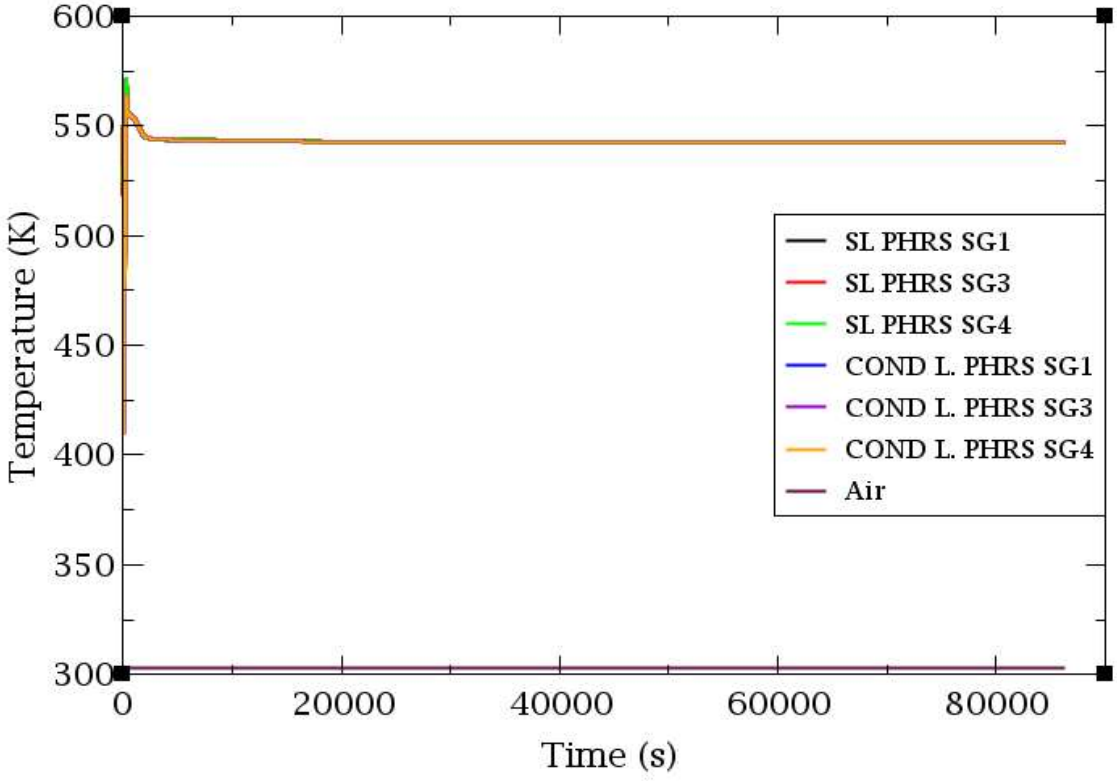

Figure 6-19 PHRS steam lines and condensate lines temperature, SBO sequence

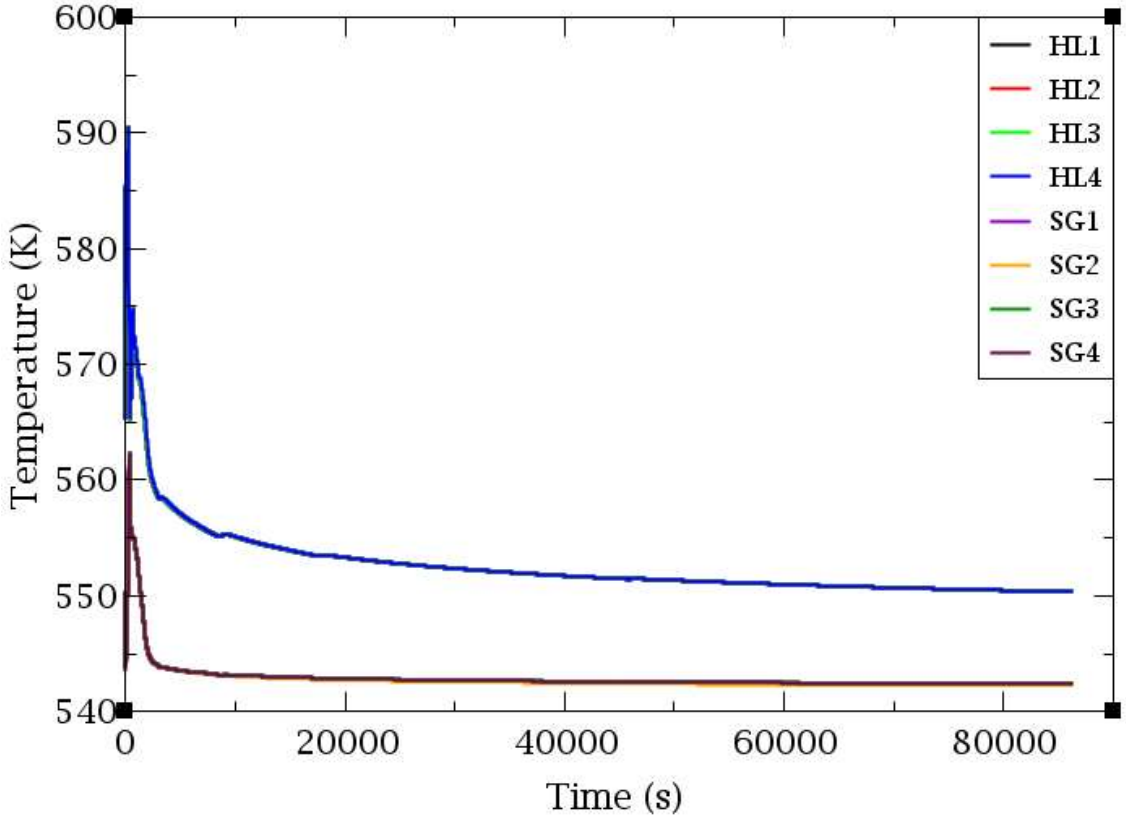

Figure 6-20 HLs and outlet SGs temperature, SBO sequence

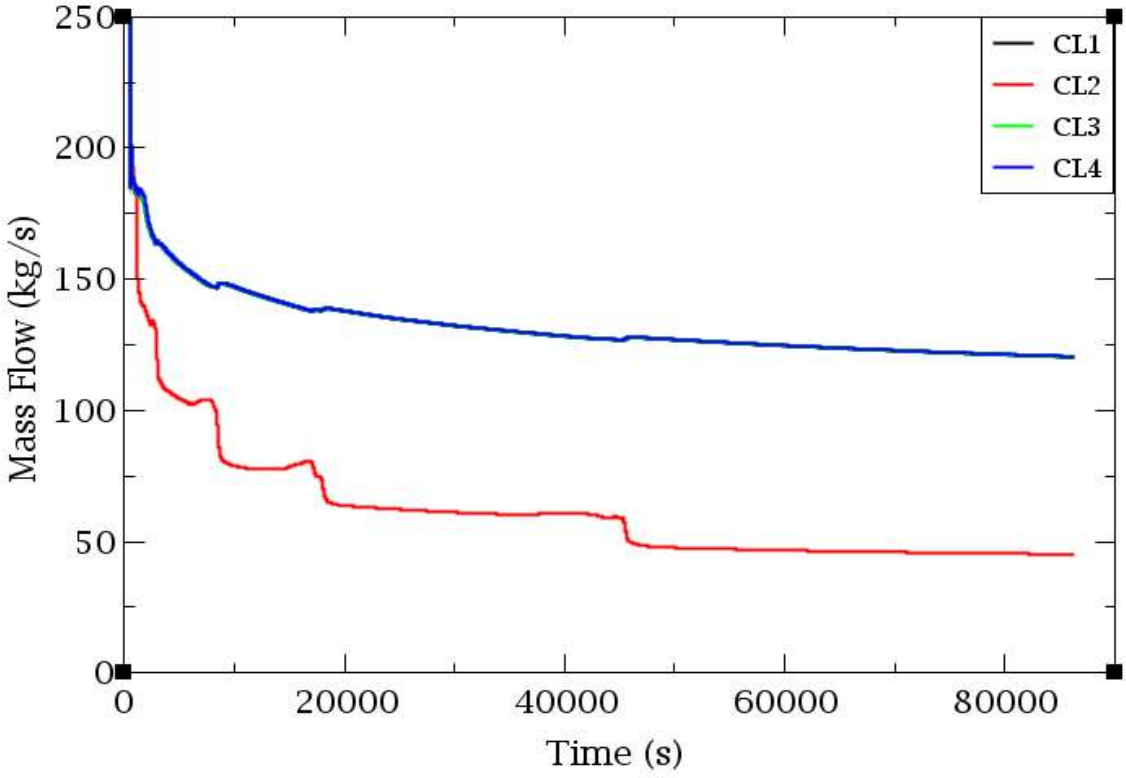

Figure 6-21 RCS mass flow rate, SBO sequence (enlarged)

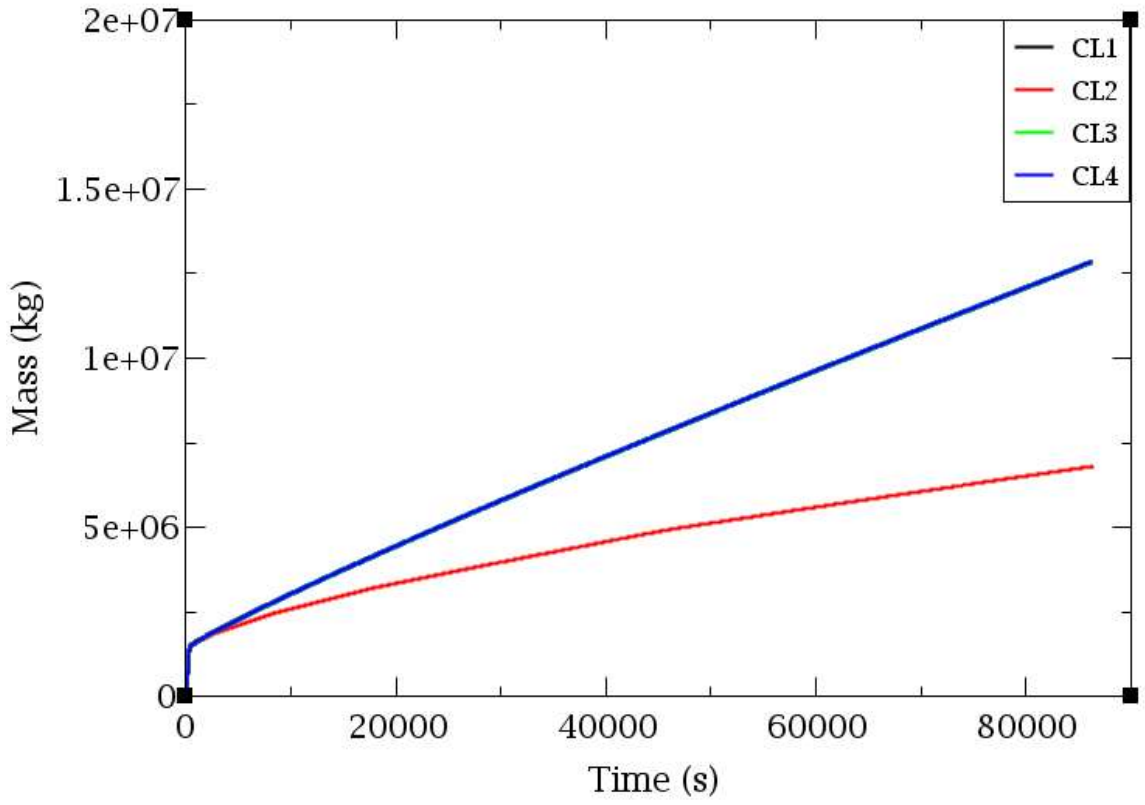

Figure 6-22 RCS mass flow rate integral, SBO sequence

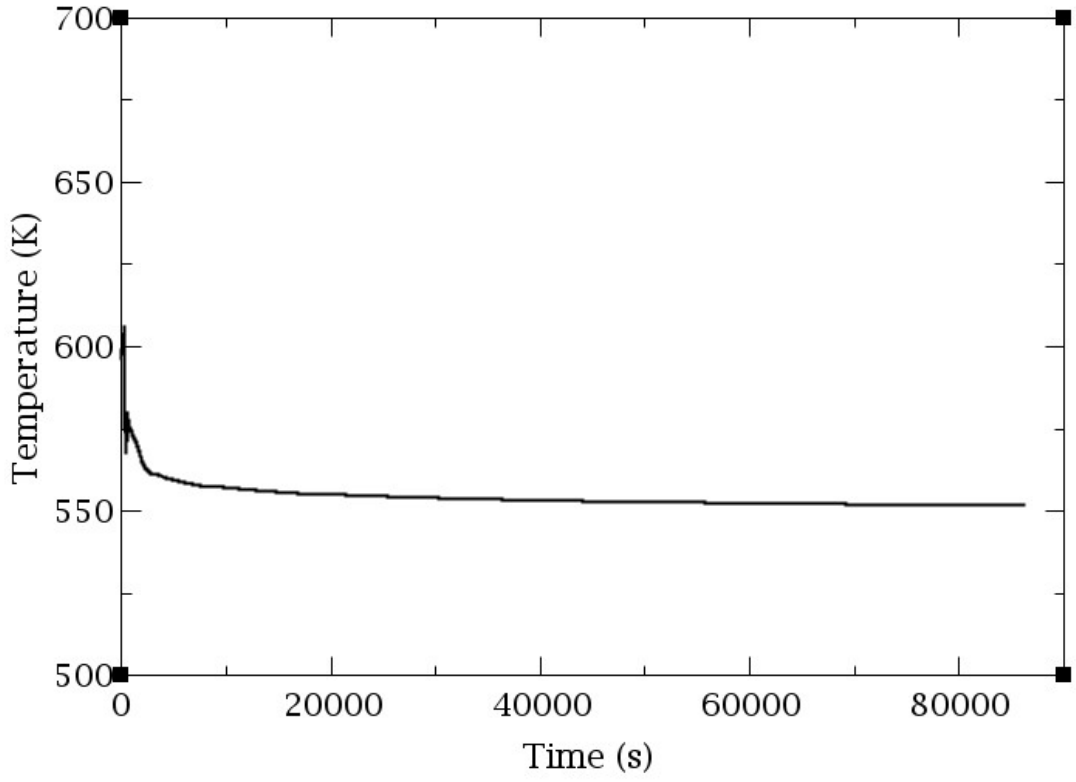

Figure 6-23 PCT, SBO sequence

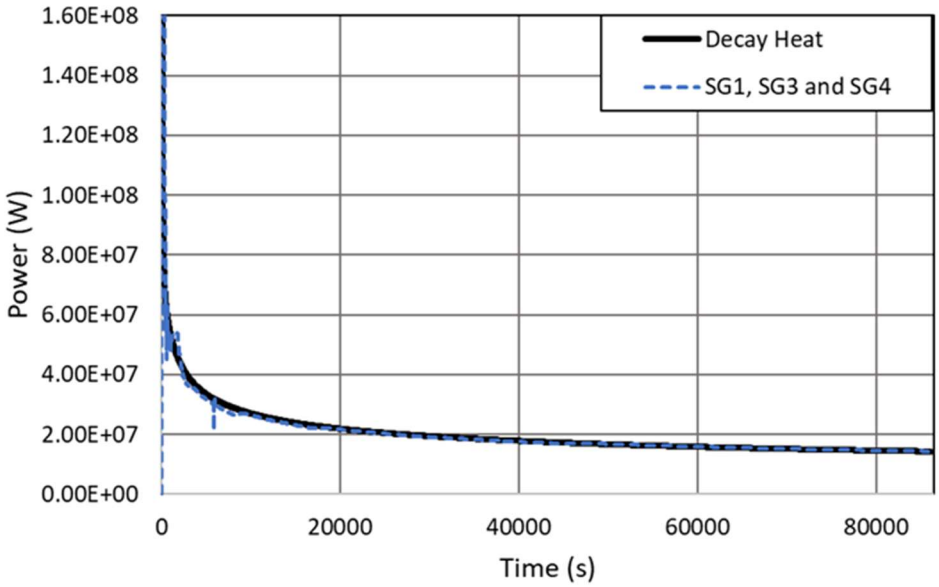

Figure 6-24 Heat removal capacity of the PHRS vs decay heat in the SBLOCA along with SBO sequence

6.2.1.2. SBO sequence with PHRS unavailability

The aim of this section is to analize how the SBO sequence evolves without the air-cooled PHRS performance, in order to know how long it would take for the sequence to find the CD if the PSS is not taken into account.

The results show that when the PHRS is not available, the SGs act as a cold source as long as they have some inventory. Once they are empty, the capacity to remove the decay heat through the SGs is lost, so the RCS pressure increases until it reaches the setpoint of the PZR relief valves, Figure 6-26. From this point on, the RCS inventory starts to be lost, leading to core uncovering at around 15000 s and finally to the CD a few minutes later, Figure 6-25.

In summary, it can be observed that without the PHRS performance, the inventory of the SGs and subsequently the PZR relief capacity are able to maintain the core temperature below 1477 K for at least 4 hours. After this time, if air-cooled PHRS is not available, the SBO sequence reaches CD.

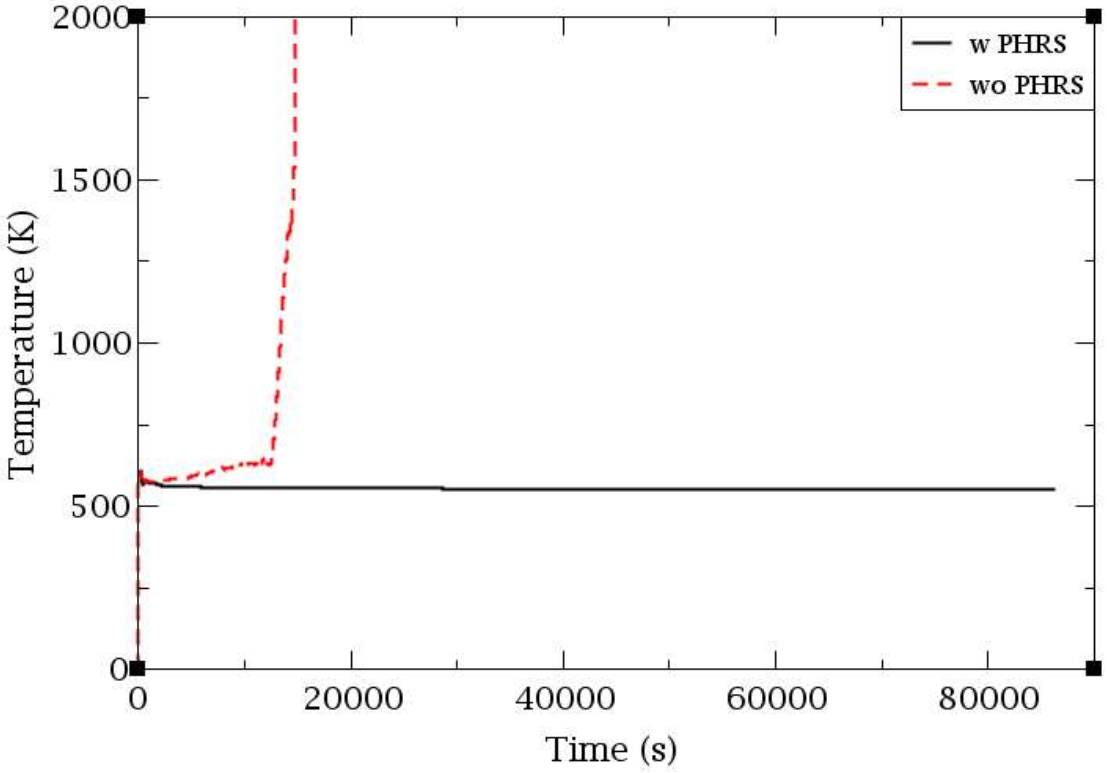

Figure 6-25 PCT, SBO sequence with HA-2 and PHRS, with HA-2 and without PHRS, without PHRS and with HA-2

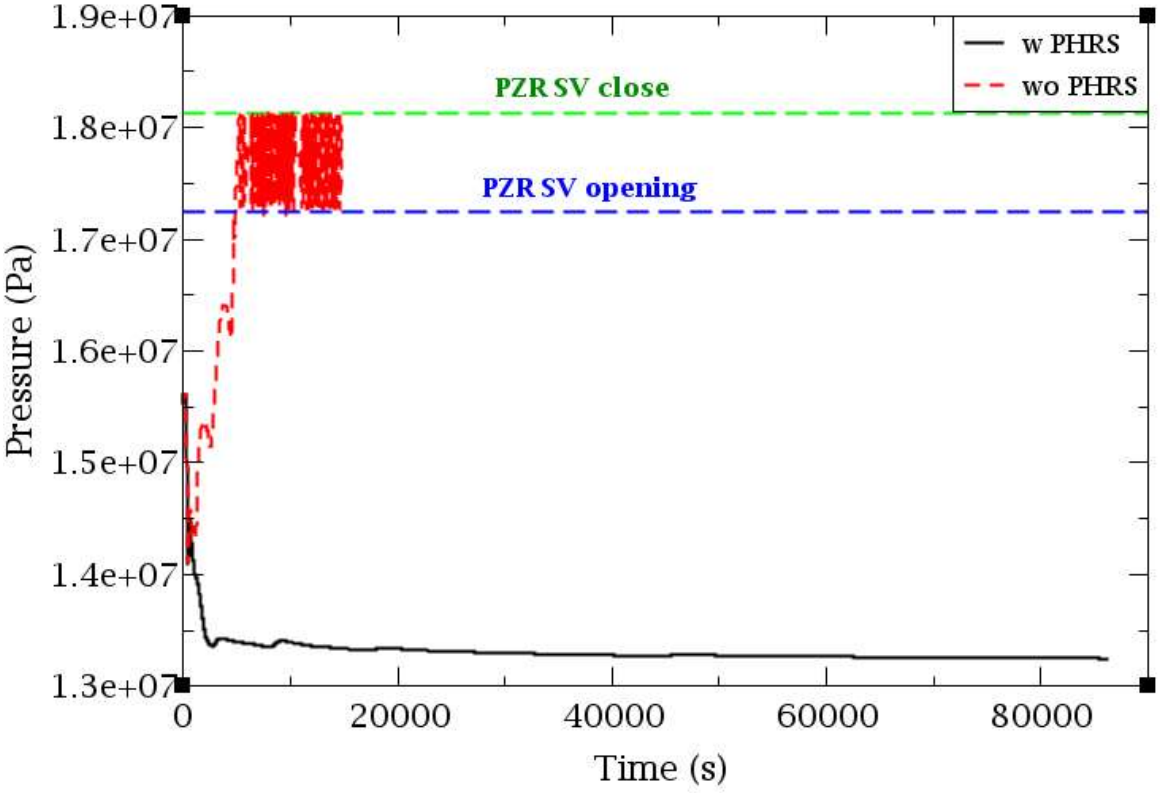

Figure 6-26 RCS pressure, SBO sequence with HA-2 and PHRS, with HA-2 and without PHRS, without PHRS and with HA-2

6.2.2. Performance of the PHRS and HA-2 in SBLOCA along with SBO sequence

The aim of this section is to determine the performance of the air-cooled PHRS in RCS cool-down mode during an SBLOCA sequence under SBO conditions. Similar sequences have been analyzed for the VVER-1200 designs, (ROSATOM, 2022). In addition, three SBLOCA experiments with SBO were performed in the PSB experimental facility with a VVER-TOI configuration, see (Elkin et al., 2018).

In order to determine the containment pressure in this sequence, the available literature was consulted and only one reference was found where the containment pressure in a LOCA due to a PZR surge line break under SBO conditions (no containment sprays available) stabilizes at around 0.14 MPa (ROSATOM, 2022). Therefore, in the present analysis, for a significantly smaller break, the selected boundary condition for the containment pressure was 0.1 MPa. Subsequently, to verify the impact of a higher pressure in the containment, a second case was simulated with a containment pressure of 0.2 MPa, finding that the impact of this difference was negligible.

The SBLOCA break diameter is 2 inches and it is located in the CL1. The external atmospheric temperature chosen for this analysis is 303.15 K (30 ^{o}C). In addition, the SC considered for the PSS involved in the SBLOCA sequence are as follows:

- HA-1: 2 out of 4 trains
- HA-2: 3 out of 4 trains
- PHRS: 3 out of 4 trains

Therefore, the SBLOCA sequence under SBO conditions is first analyzed, considering the performance of the air-cooled PHRS in addition to the HA-2 PSS. Then the SBLOCA along with SBO sequence is analyzed without considering the actuation of one PSS (HA-2 or PHRS), in order to confirm the necessity of their actuation for the success of the sequence.

6.2.2.1. SBLOCA along with SBO sequence with PHRS and HA-2 available

In this analysis, the SBLOCA is coincident with the SBO at 300 s, see Figure 6-27 and Figure 6-28. At that instant there is a total loss of AC power, with no availability of the EDGs, which causes the SCRAM, the loss of the CVCS, MCPs trip, MFW pumps trip, TT and loss of the condenser. The evolution of the main events is shown in Table 6-8.

At the beginning of the transient the PHRS air gates begins to open 30 s after the SBO, and they take about 90 s to fully open. Moreover, simultaneously with SBO the SGs pressure starts to increase until it reaches the setpoint of the BRU-A valves at 310 s. At 485 s the subcooling signal ($T_{sat} - T_{HL} < 8$ °C) occurs, causing the air-cooled PHRS to switch from the SG pressure maintenance mode to the RCS cool-down mode. The total opening of the air duct regulators causes a gradual decrease in the SGs pressure, see Figure 6-29 and Figure 6-30. When the pressure in the SL reaches 4.69 MPa, the MSIV isolation signal is generated.

In the RCS side, the PHRS operation allows it to cool-down through the SGs, see Figure 6-31, resulting in an RCS pressure drop that reaches the HA-1 setpoint at 2275 s, see Figure 6-32 and Figure 6-33. The injection of the HA-1, which empties at 7211 s, causes an increase in the core collapsed liquid level, see Figure 6-34 and Figure 6-35. The HA-2 pressure setpoint is reached at 5640 s, but they do not start injecting until 100 s later due to a delay in the signal. The second stage of the HA-2 injection starts at 9640 s, the third stage at 15640 s and finally the fourth stage at 35640 s, see Figure 6-36. On the other hand, due to the emptying of the HA-2, there is inventory from the CLs sucked up by the HA-2 upstream, see Figure 6-37.

In the air ducts, it is observed that the air flow is about 200 kg/s per train at the beginning of the sequence and decreases to about 125 kg/s after 24 hours, as shown in Figure 6-38. This decrease in the air flow is due to a cooling of the inventory passing through the PHRS tubes, see Figure 6-39. The temperature difference between the air which is at 303.15 K and the SG secondary side inventory which is in saturation at 374.15 K results in a natural circulation in the SLs and the condensate lines of the PHRS of 1.92 kg/s after 24 hours of the sequence, see Figure 6-40. It can also be observed that the void fraction at the outlet of the PHRS tubes is about 93 %, see Figure 6-41, causing a mixture of steam and saturated liquid to return to the SGs.

Moreover, in the 3 loops with PHRS available, the saturated SG inventory is at a lower pressure than the RCS, which is also in saturation conditions, so there is a temperature difference of approximately 10 K between the two, see Figure 6-42, which leads to 25 kg/s of natural circulation induced mass flow rate in the RCS, see Figure 6-43. The integral of the mass flow rate from the CL 1, CL 3 and CL 4 is show in Figure 6-44. It can be noted that there is no natural circulation in the loop 2 because the PHRS is not available. Finally, no CD occurs during the first 24 hours of the SBLOCA along with SBO sequence, see Figure 6-45.

During LOCA sequences, two CSF have to be fulfilled, the decay heat removal and the RCS coolant supply. In this analysis, the performance of the PHRS together with that of the HA-2 has been verified to provide both CSF. On the one hand, the PHRS removes the residual heat from the RCS and simultaneously cools and depressurizes it. On the other hand, the HA-2 ensures the replenishment of the inventory lost through the break, which also involves a certain power removal capacity.

This can be seen as the combined power removed by the SGs due to the PHRS performance and the HA-2, exceeds the core decay heat for most of the transient duration expect for a period around 5000 s, see Figure 6-46 (blue line). However, simulations have shown that the RCS has enough inventory that the PCT is not affected.

The HA-2 power has been obtained by assuming that the mass flow rate (G) from the HA-2 tanks which enters the RCS at ambient temperature is completely evaporated, in a form similar to that calculated in Section 6.1.1.1. In addition, it has been considered the reduction in the mass flow rate by 6.25% (thermal power difference between VVER-1200 and VVER-1000 reactors).

$$Q_{vap} = G\ (h_{out} - h_{in}) = G\ (\ h_{v,out}^{sat} - h_{l,in})$$

Despite these conservative restrictions, it can be observed that the power removal potential by the HA-2 and the air-cooled PHRS exceeds the decay heat. This explains why the sequence does not reach the CD within the first 24 hours after the accidental sequence.

Identical sequences have been simulated (2 inches SBLOCA along with SBO) considering that the containment remains slightly pressurized at values between 0.1 MPa and 0.2 MPa. It has been found that both the PHRS and the HA-2 continue to perform their functions in a similar manner, ensuring that core uncovering does not occurs and therefore the PCT does not increases over 24 hours.

Table 6-8 Main events in the SBLOCA (2 inches) under SBO conditions [with PHRS and HA-2]

Time (s)	Event
300	SBLOCA along with SBO (SCRAM, MFW pumps and MCPs trip, TT, loss of the condenser, CVCS off)
310	BRU-A opening (SL pressure > 7.25 MPa)
330	Air gates opening (SBO + 30 s delay)
420	PHRS full capacity (90 s opening)
485	Signal for PHRS in cool-down mode ($T_{sat} - T_{HL} < 8$ oC)
540	BRU-A closed (SL pressure < 6.67 MPa)
2275	HA-1 injection begins (RCS pressure < 6 MPa)
2460	MSIV close (SG pressure < 4.69 MPa)
5640	HA-2 injection setpoint (RCS pressure < 1.5 MPa)
5740	First stage HA-2 injection begins (HA-2 setpoint + 100 s)
7211	HA-1 injection ends (HA-1 empty)
9640	Second stage HA-2 injection begins (HA-2 setpoint + 4000 s)
15640	Third stage HA-2 injection begins (HA-2 setpoint + 10000 s)
35640	Fourth stage HA-2 injection begins (HA-2 setpoint + 30000 s)
86700	End simulation (24 hours)

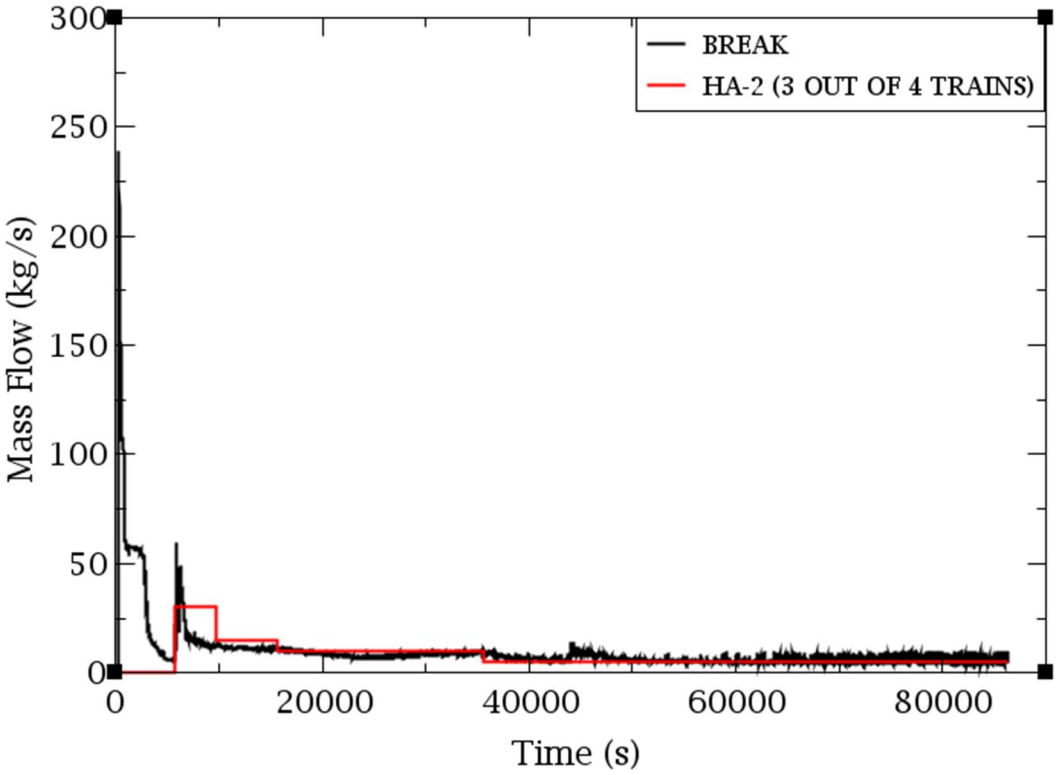

Figure 6-27 Break vs. HA-2 mass flow rate, SBLOCA (2 inches) along with SBO sequence

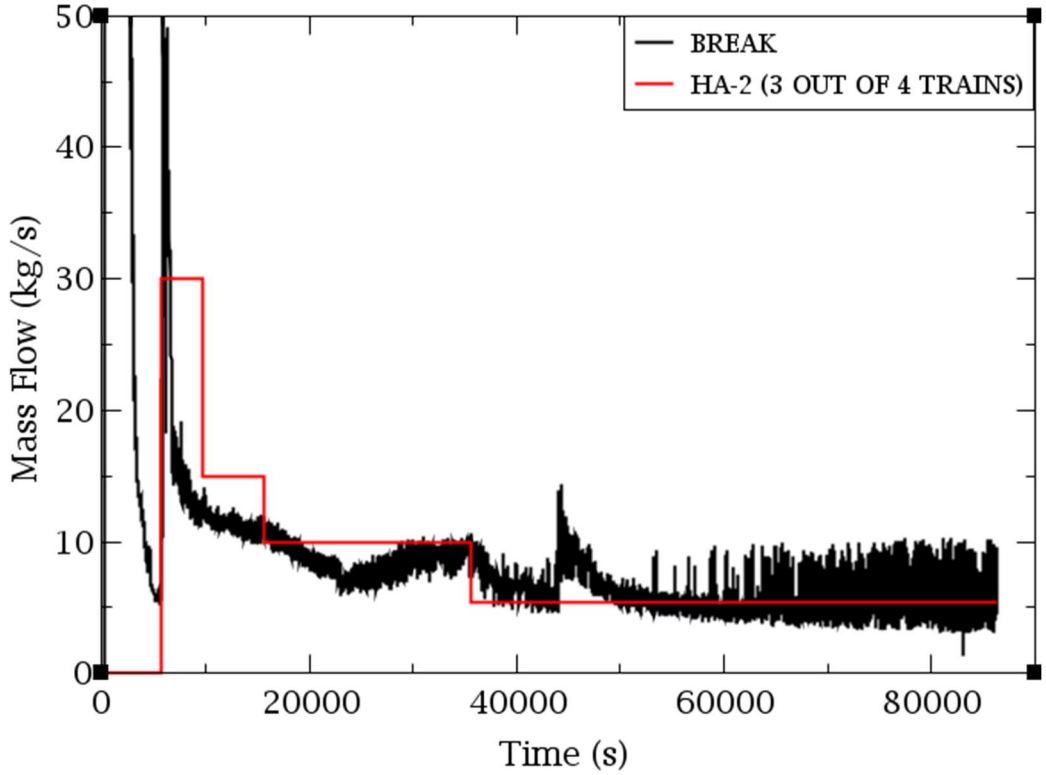

Figure 6-28 Break vs. HA-2 mass flow rate, SBLOCA (2 inches) along with SBO sequence (enlarged)

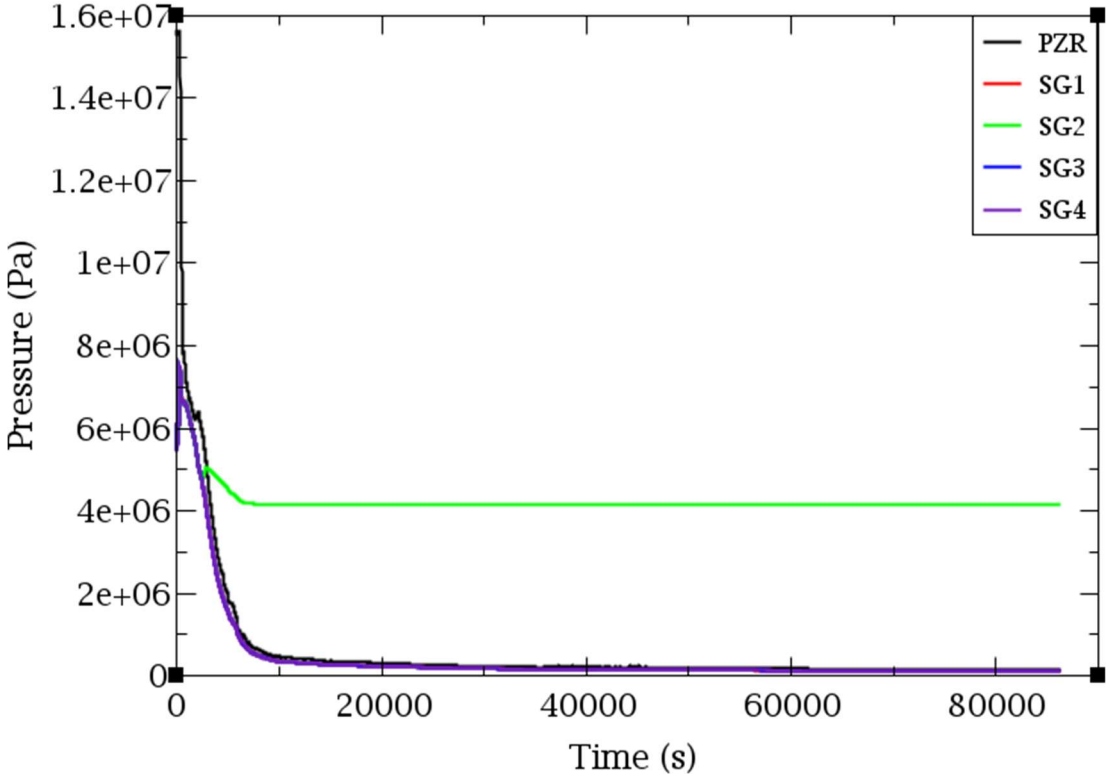

Figure 6-29 RCS and SGs pressure, SBLOCA (2 inches) along with SBO sequence

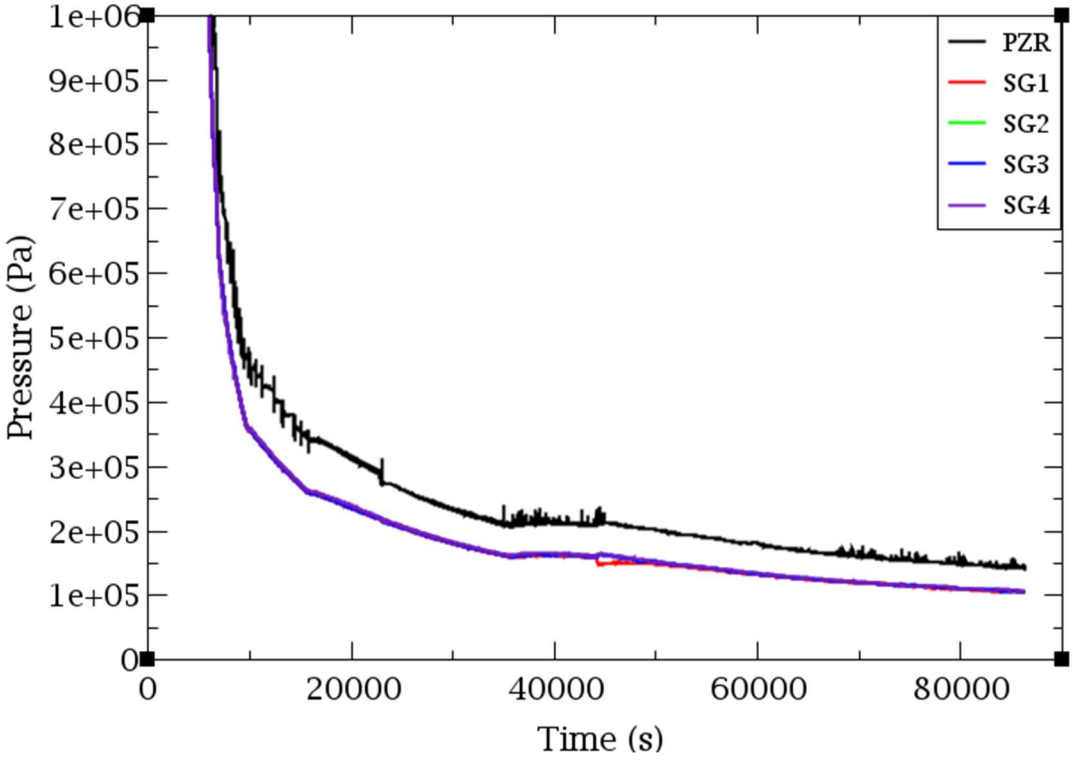

Figure 6-30 RCS and SGs pressure, SBLOCA (2 inches) along with SBO sequence (enlarged)

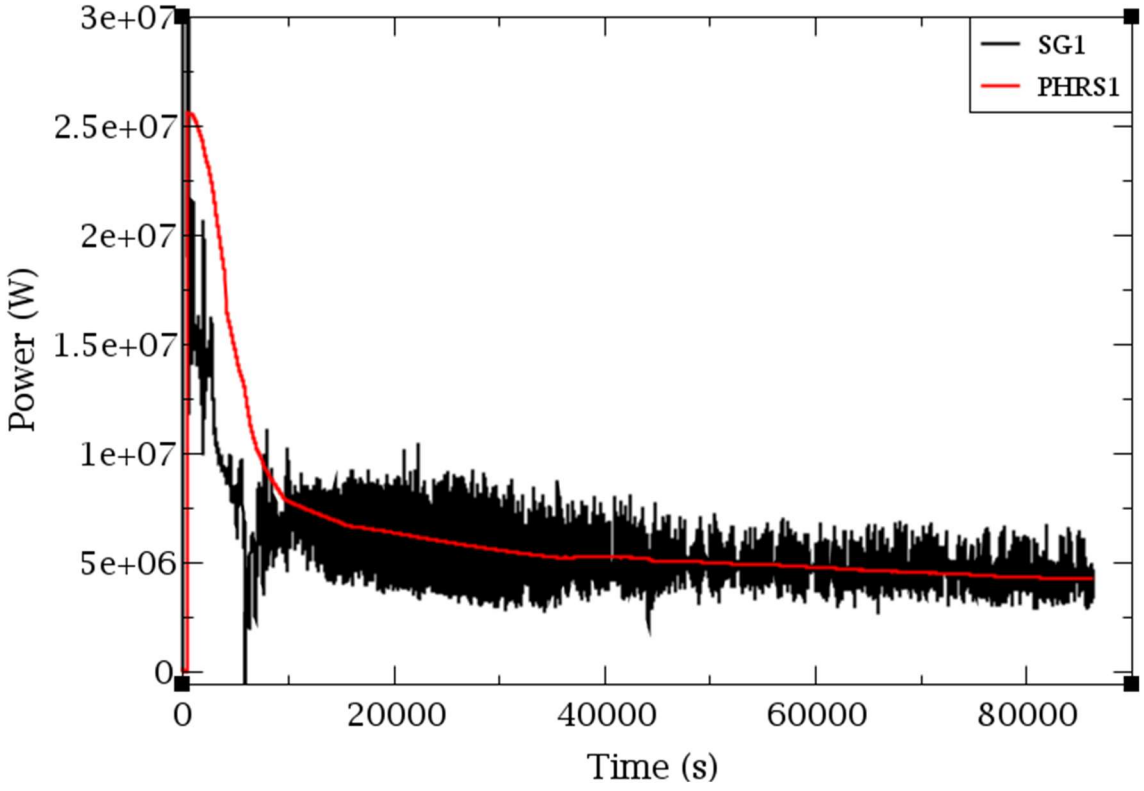

Figure 6-31 PHRS 1 vs. SG1 power, SBLOCA (2 inches) along with SBO sequence

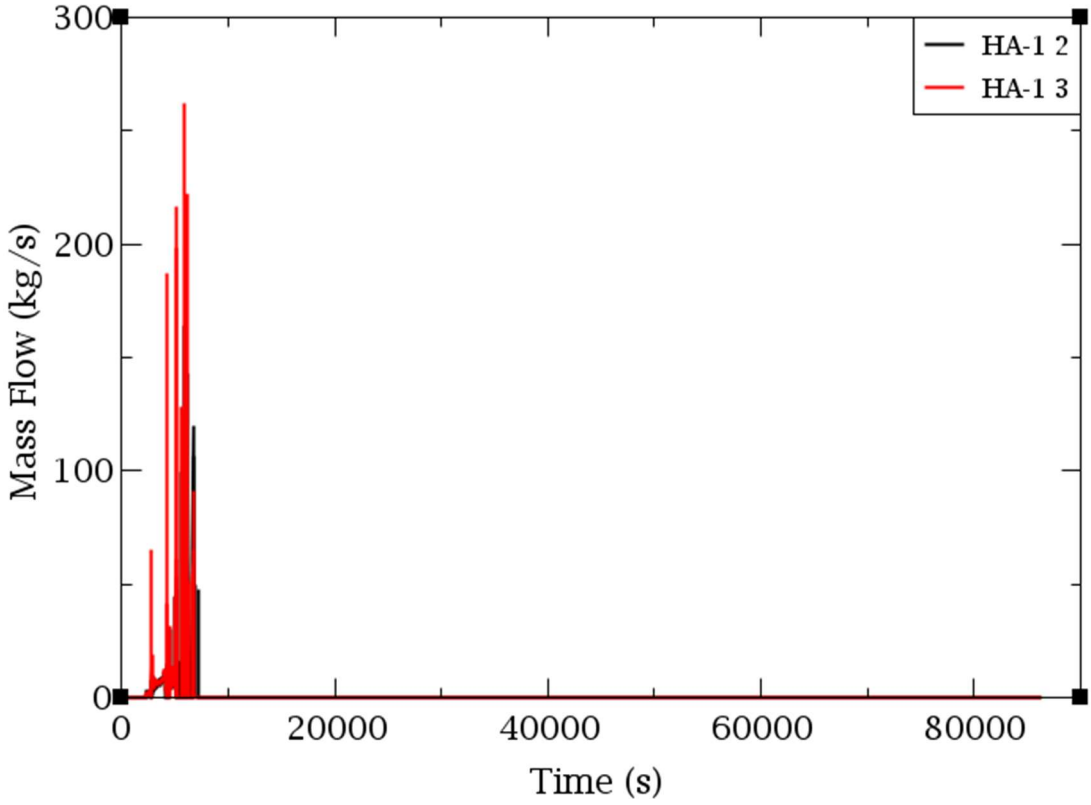

Figure 6-32 HA-1 mass flow rate, SBLOCA (2 inches) along with SBO sequence

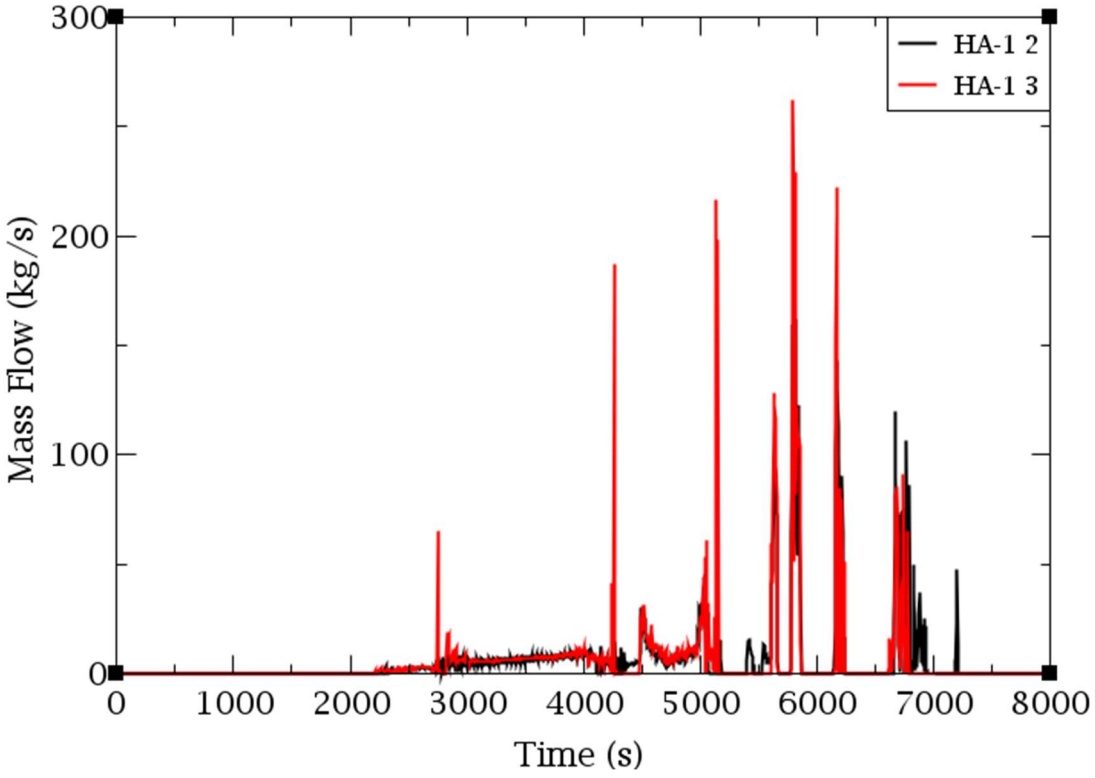

Figure 6-33 HA-1 mass flow rate, SBLOCA (2 inches) along with SBO sequence (from 0 s to 8000 s)

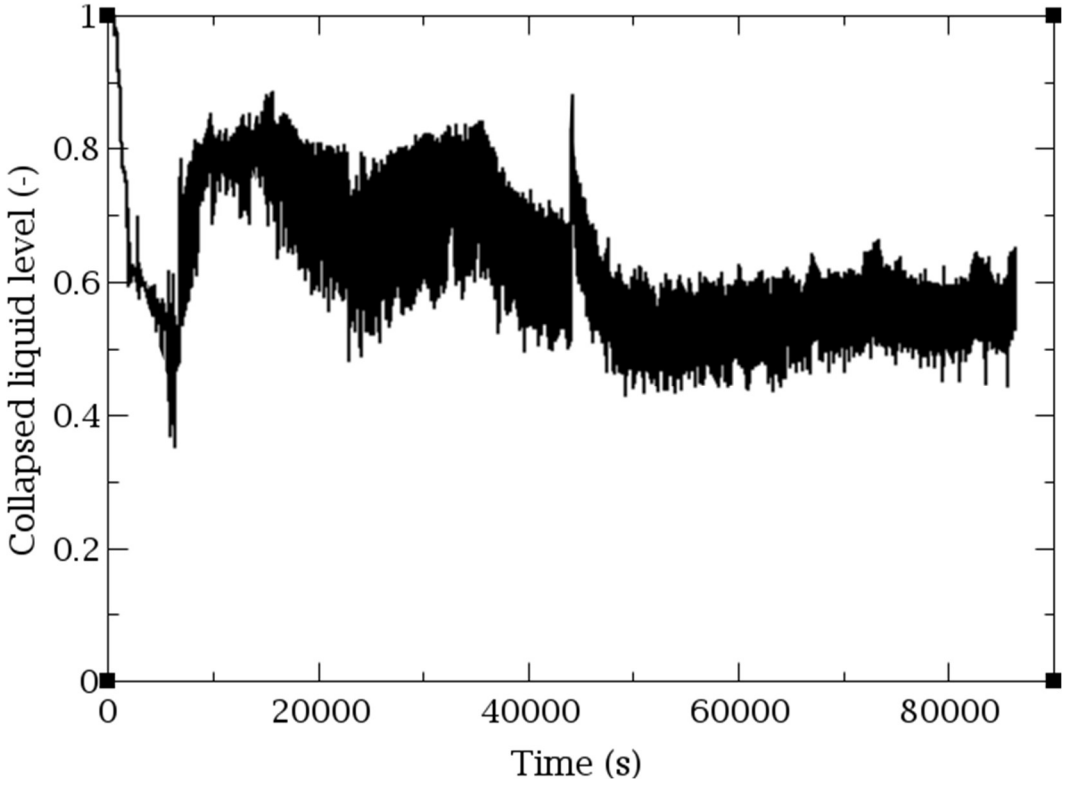

Figure 6-34 Collapsed liquid level, SBLOCA (2 inches) along with SBO sequence

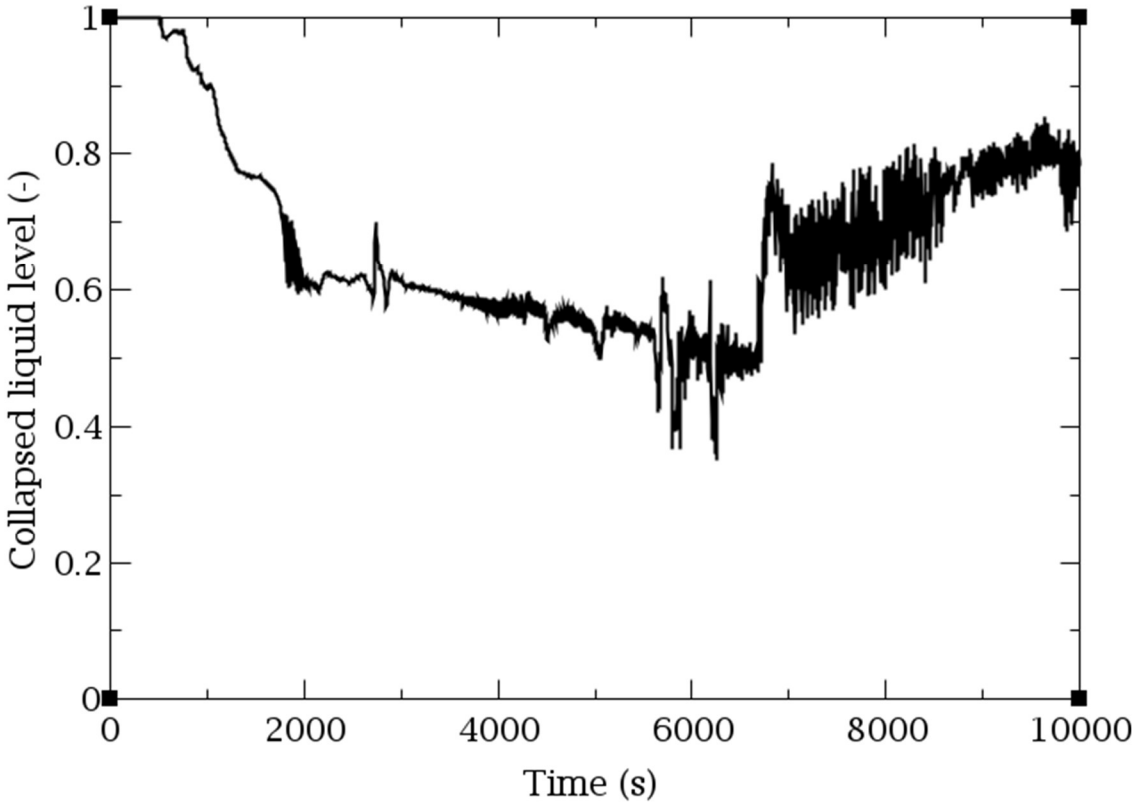

Figure 6-35 Collapsed liquid level, SBLOCA (2 inches) along with SBO sequence (from 0 s to 10000 s)

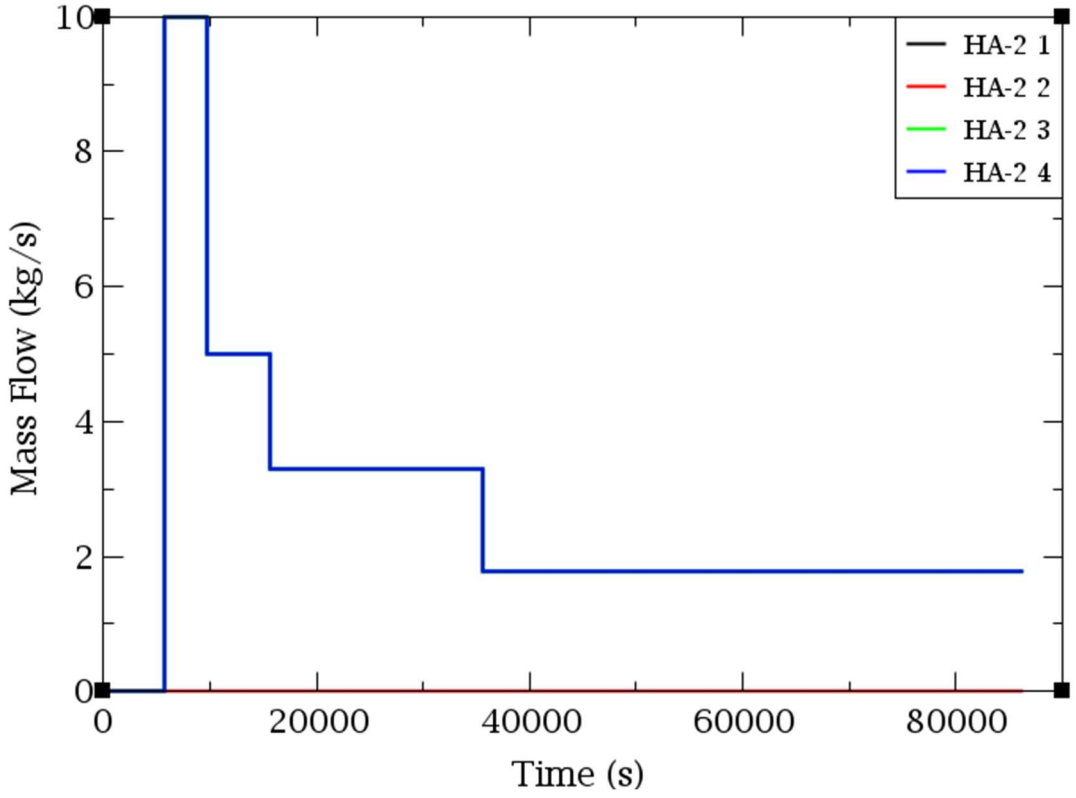

Figure 6-36 HA-2 mass flow rate per train, SBLOCA (2 inches) along with SBO sequence

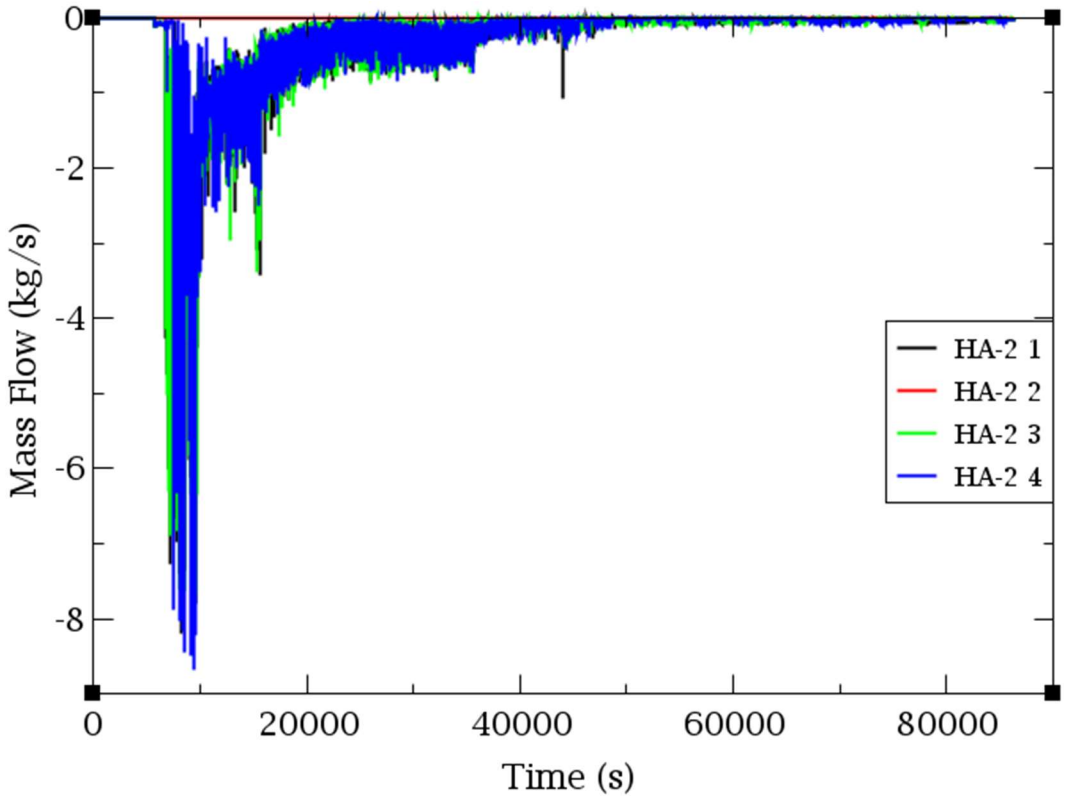

Figure 6-37 HA-2-CLs line mass flow rate per loop, SBLOCA (2 inches) along with SBO sequence

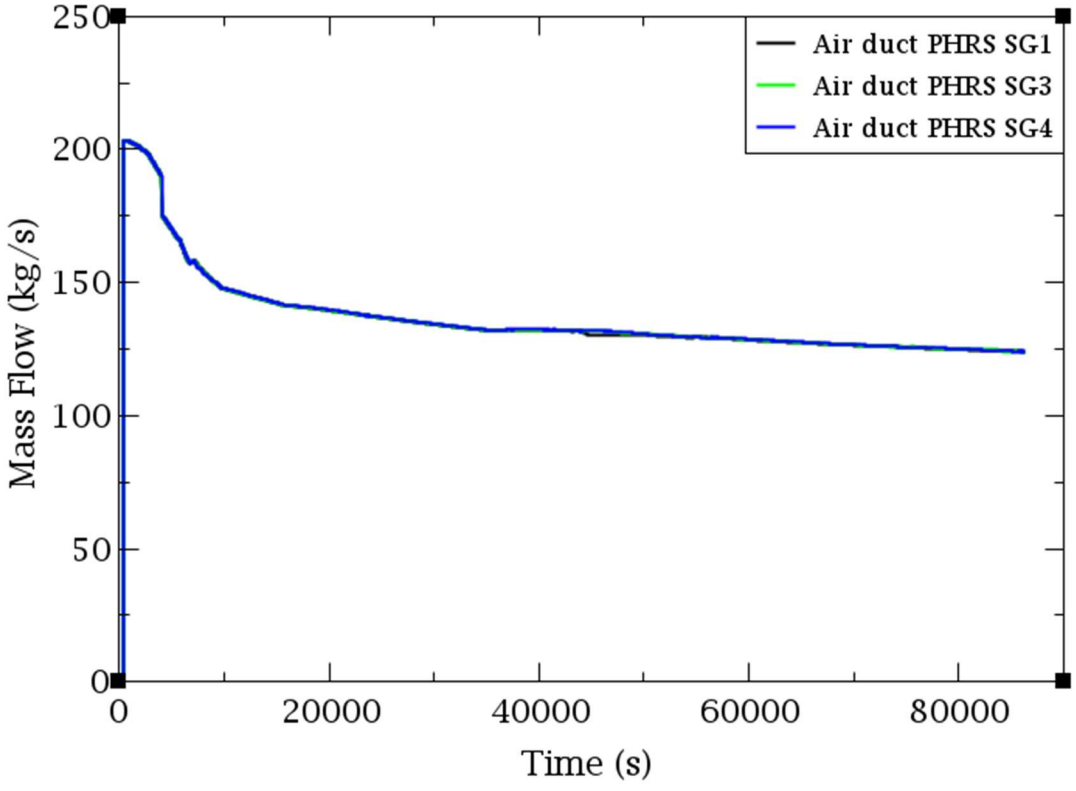

Figure 6-38 PHRS air duct mass flow rate, SBLOCA (2 inches) along with SBO sequence

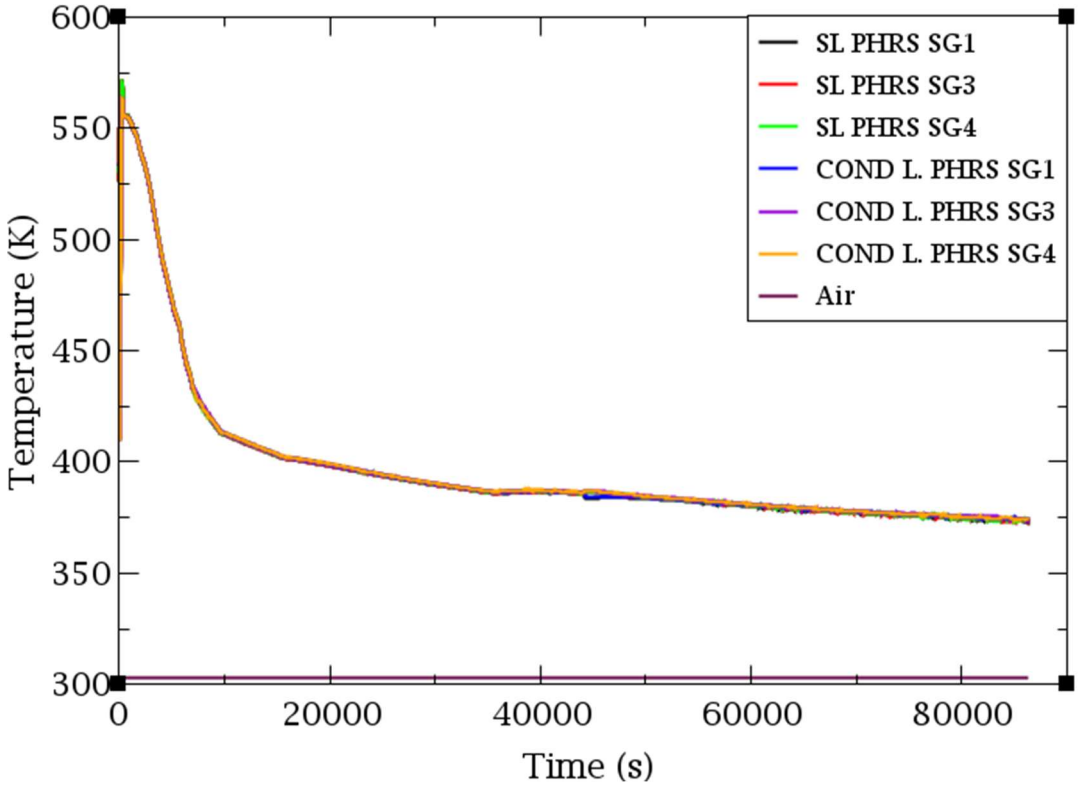

Figure 6-39 PHRS steam lines and condensate lines temperature, SBLOCA (2 inches) along with SBO sequence

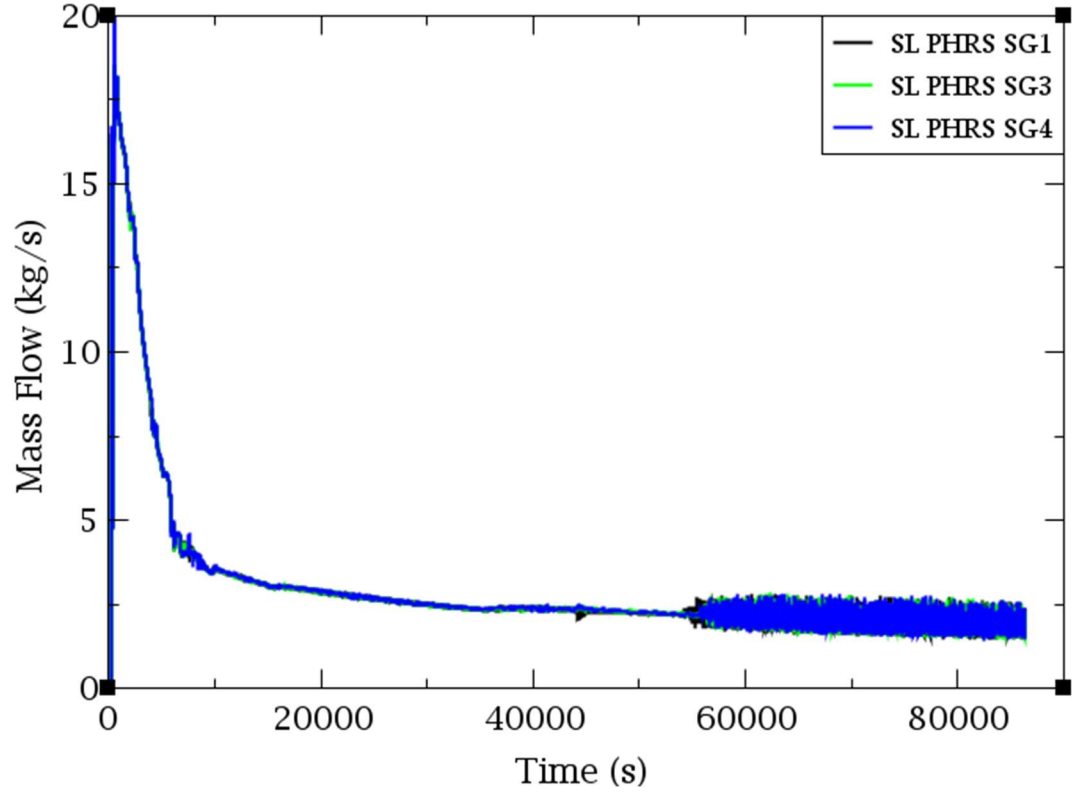

Figure 6-40 PHRS steam lines mass flow rate, SBLOCA (2 inches) along with SBO sequence

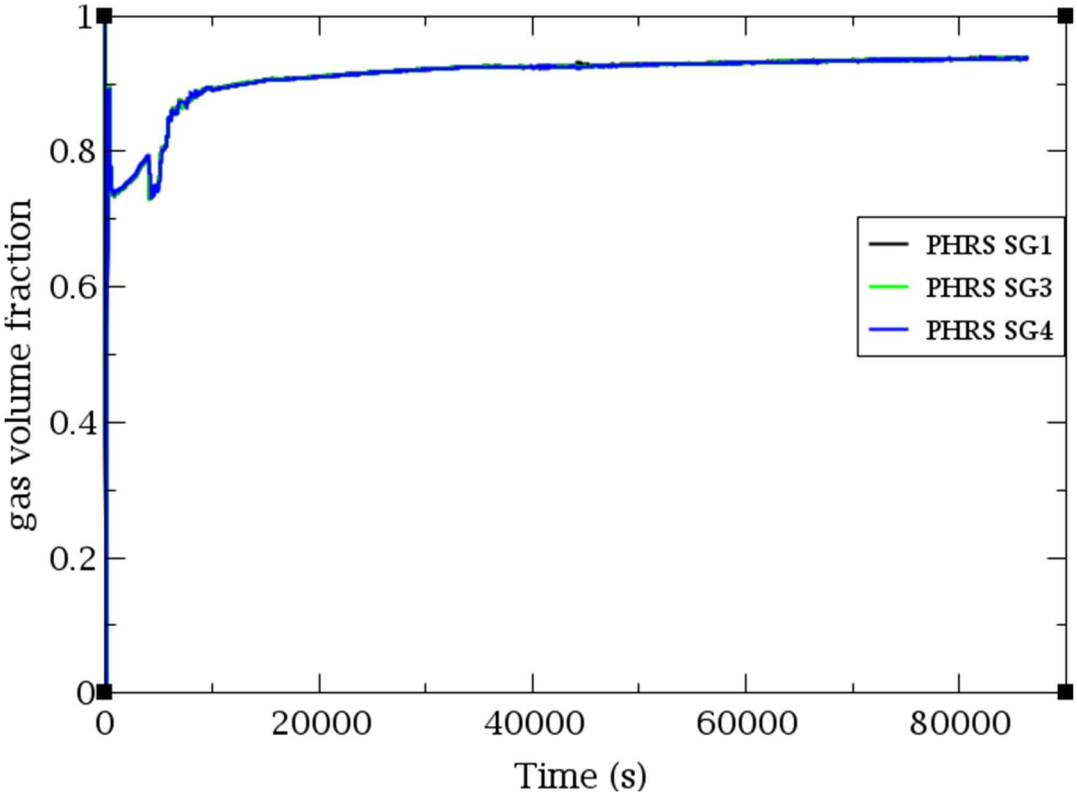

Figure 6-41 PHRS outlet bundle tubes void fractions, SBLOCA (2 inches) along with SBO sequence

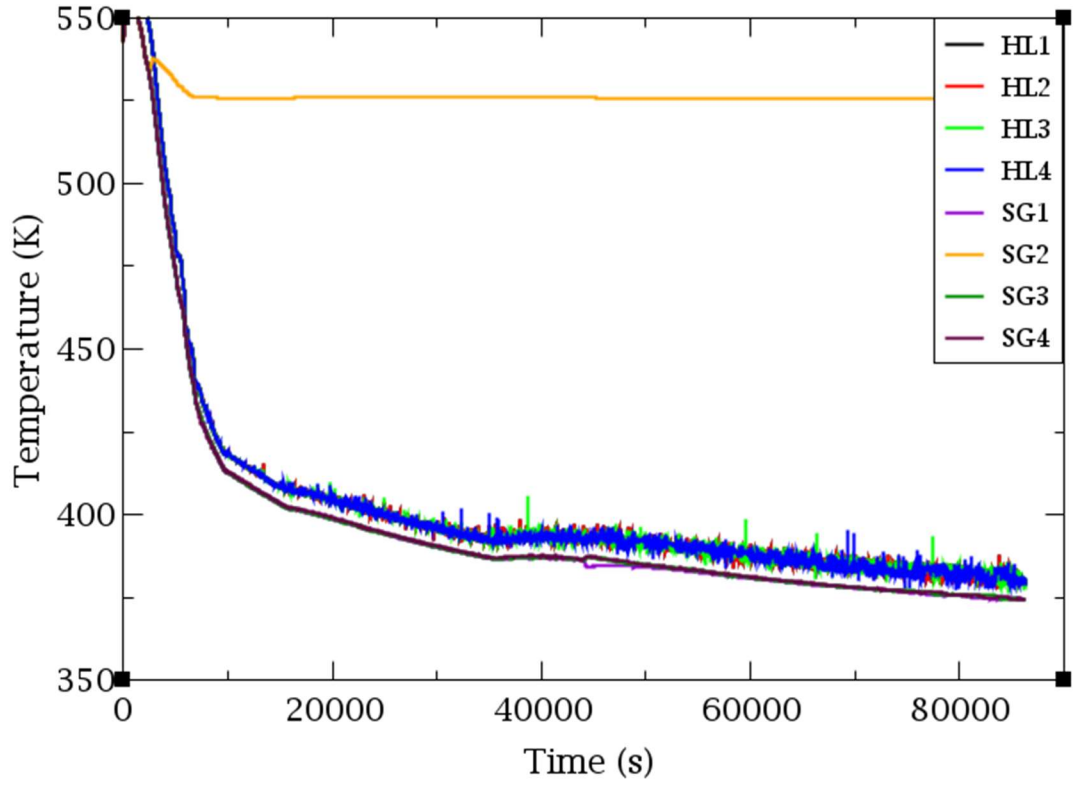

Figure 6-42 HLs and outlet SGs temperatures, SBLOCA (2 inches) along with SBO sequence

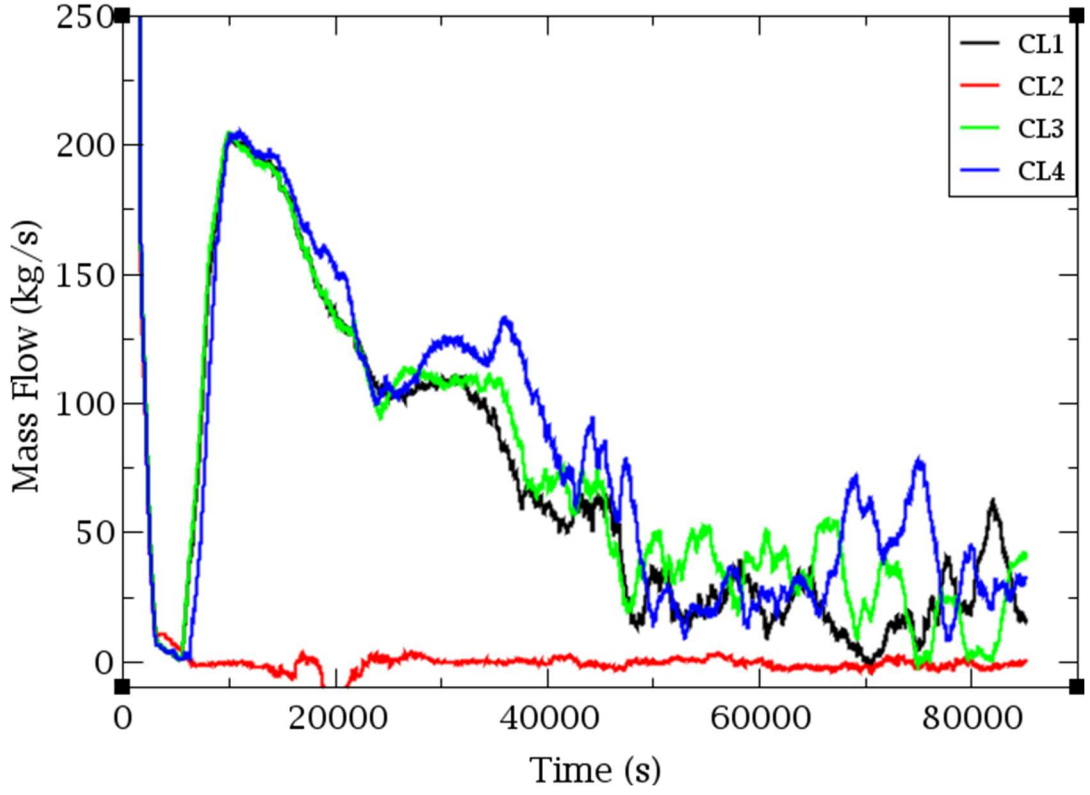

Figure 6-43 RCS mass flow rate, SBLOCA (2 inches) along with SBO sequence (enlarged)

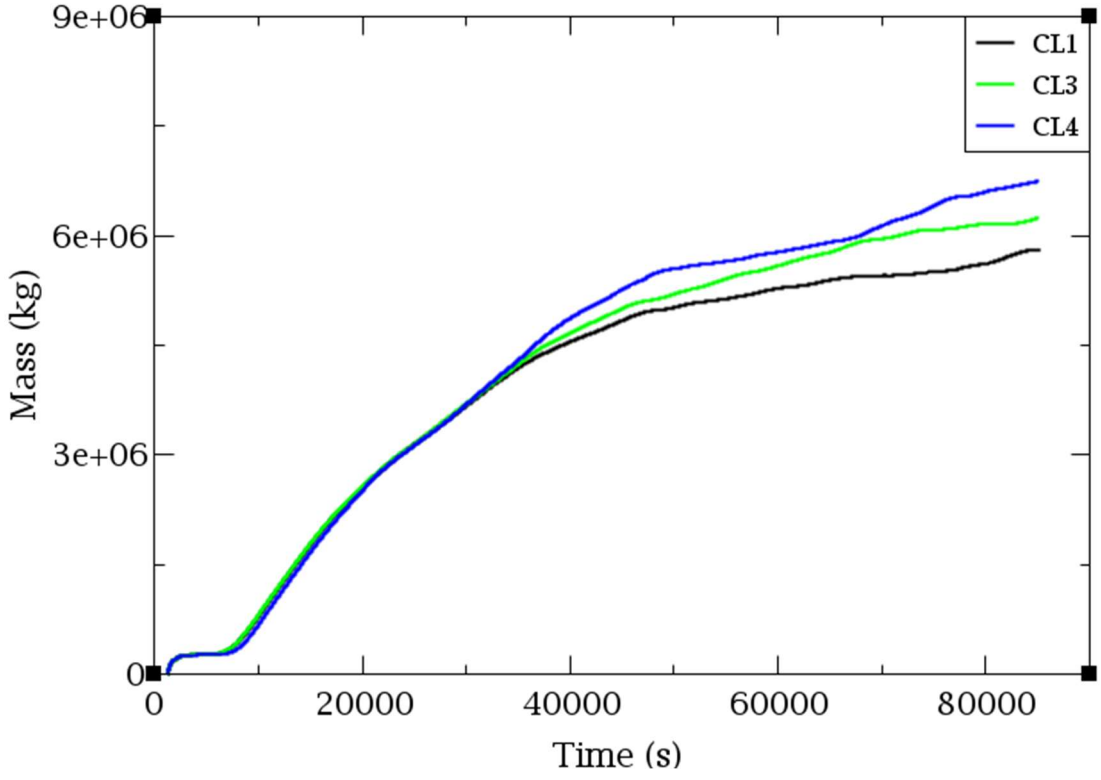

Figure 6-44 CL1, CL3 and CL4 mass flow rate integral, SBLOCA (2 inches) along with SBO sequence

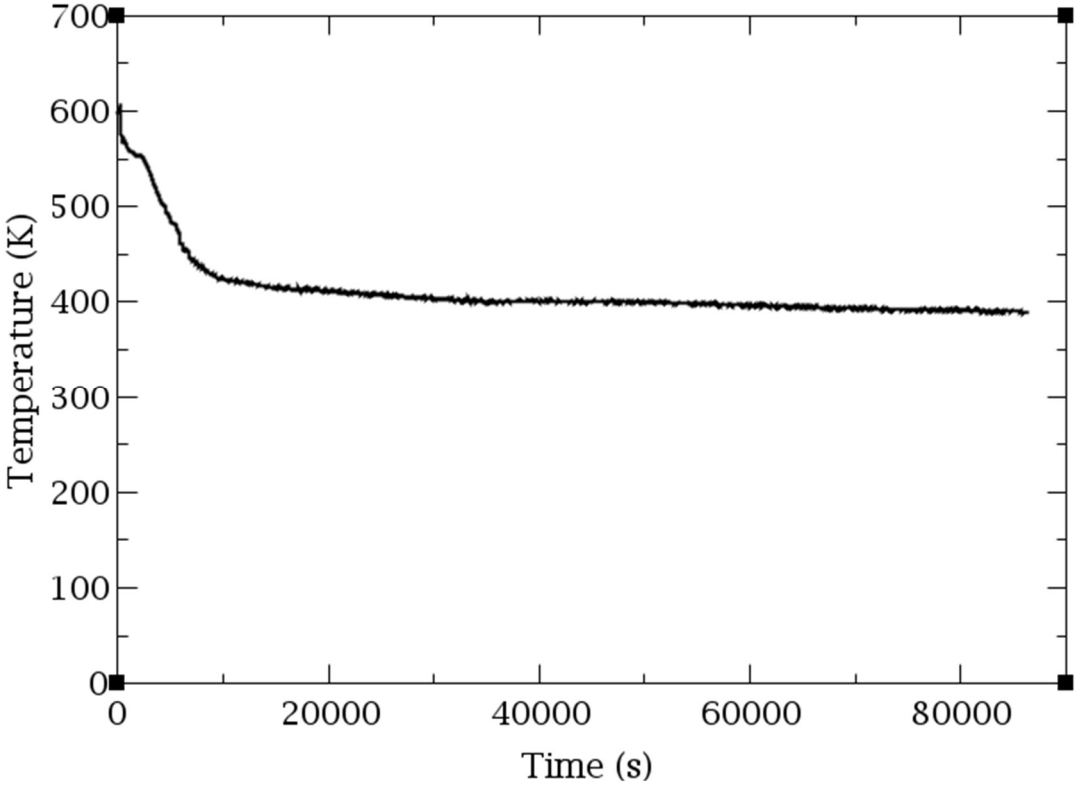

Figure 6-45 PCT, SBLOCA (2 inches) along with SBO sequence

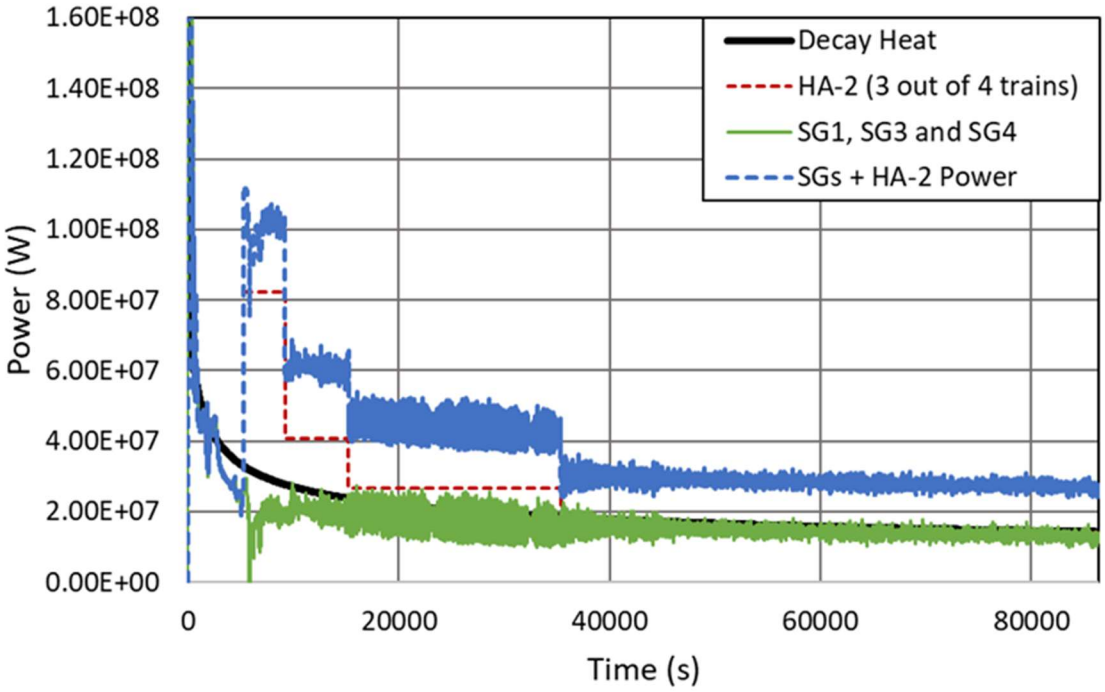

Figure 6-46 Heat removal capacity of the HA-2 and PHRS vs. decay heat in the SBLOCA (2 inches) along with SBO sequence

The video mask of the VVER-1000/V320 model for the TRACEv5p5 system code, presented in Section 3.4, has been used to generate a video showing the evolution of the void fraction during the SBLOCA sequence with SBO. The Figure 6-47 shows the void fraction at three transient times:

- The initial void fraction at the beginning of the sequence (t = 0s).
- The void fraction at the moment when the core collapsed liquid level reaches its lowest point (t = 6250 s) It can be seen that at this point the core begins to refill from both the bottom and the top. This is due to the fact that HA-2 and HA-1 are connected to both DC and UP. At this stage of the sequence, it can also be observed that the axial core temperature remains well below the CD temperature.
- The void fractions at the end of the sequence (t = 86400 s), where it can be seen that the core is completely covered.

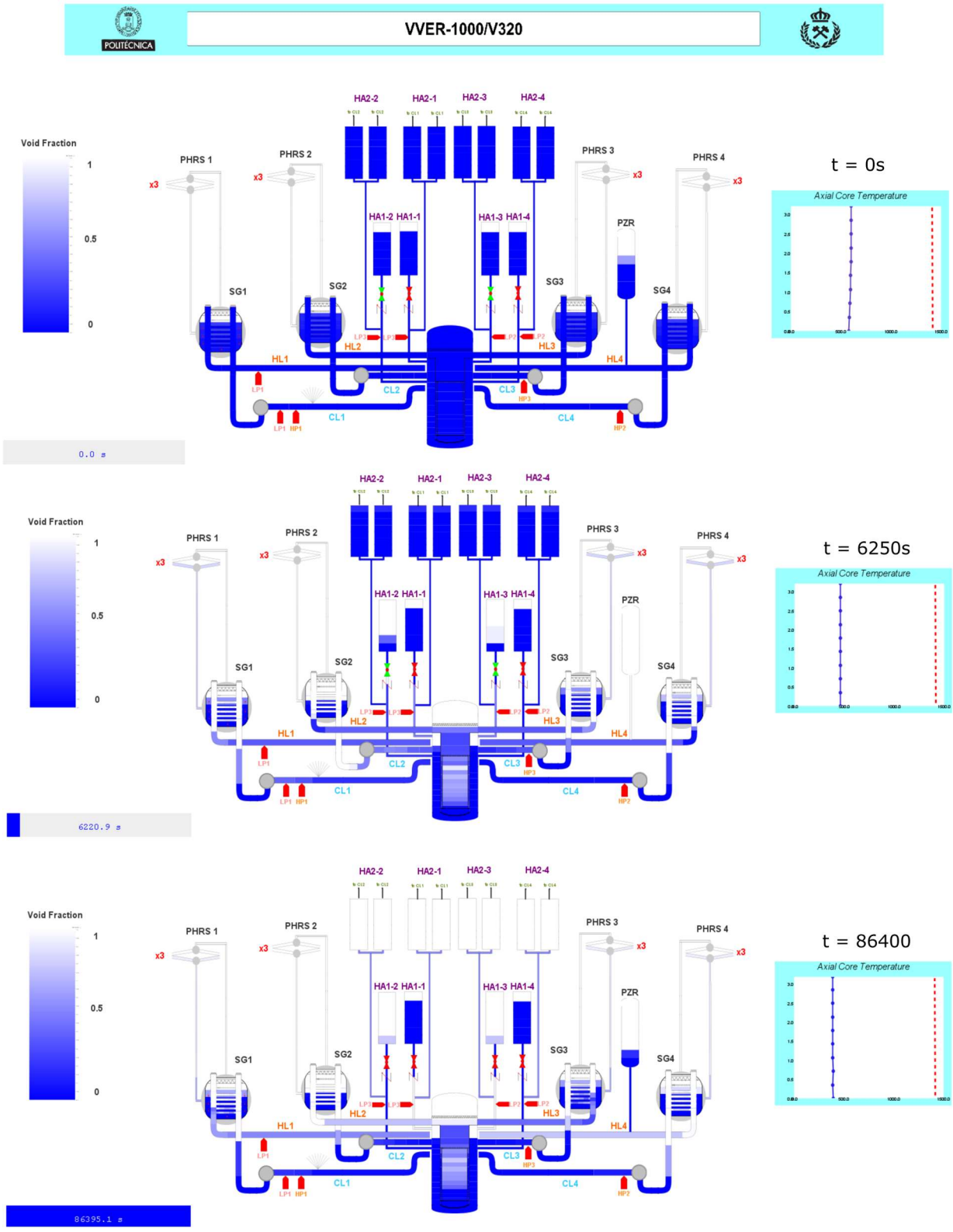

Figure 6-47 SNAP video for VVER-1000/V320 TRACEV5P5 model. SBLOCA (2 inches) along with SBO, 24-hour sequence

6.2.2.2. SBLOCA along with SBO sequence; without PHRS or HA-2 availability

The aim is to find out how the SBLOCA sequence evolves without the performance of the PSSs in order to determine whether any CSF are not fulfilled. Therefore, both cases are studied, the sequence without consider the air-cooled PHRS actuation and the sequence without consider the HA-2 actuation.

If only the HA-2 is available and not the air-cooled PHRS, the CD occurs at about 5000 s, see Figure 6-48. This is because the air-cooled PHRS is needed to cool the RCS and thus depressurize it to reach the HA-2 pressure setpoint, see Figure 6-49. Therefore, no PSS are fulfilling the heat removal and the RCS coolant replenishment CSF. This was found in a previous Section 6.1. When considering the availability of the PHRS and not the HA-2, the CD also occurs. The reason for this is that although the PHRS is able to remove much of the decay heat, there is no PSS to replenish the RCS inventory, so that the core uncovering takes place at around 40000 s, see Figure 6-48.

In summary, it has been shown that for the SBLOCA sequence with SBO to be successful, it is necessary for the HA-2 and the PHRS to operate together, since if they perform separately, the two CSF in this sequence are not fully achieved.

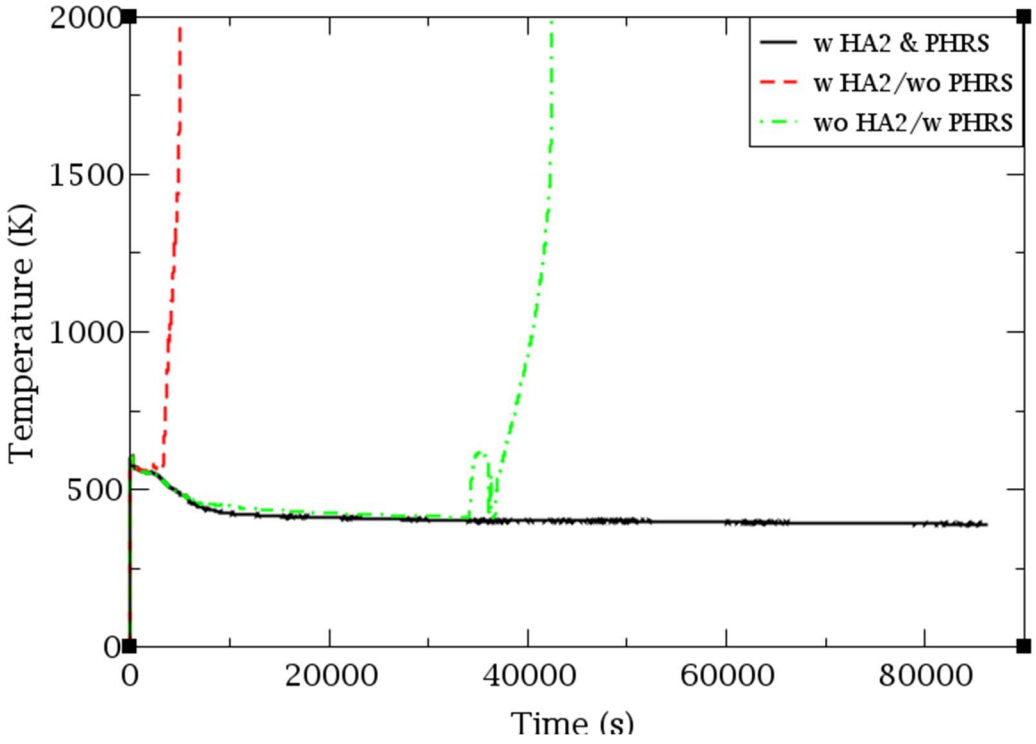

Figure 6-48 PCT, SBLOCA (2 inches) sequence with HA-2 and PHRS, with HA-2 and without PHRS, without HA-2 and with PHRS

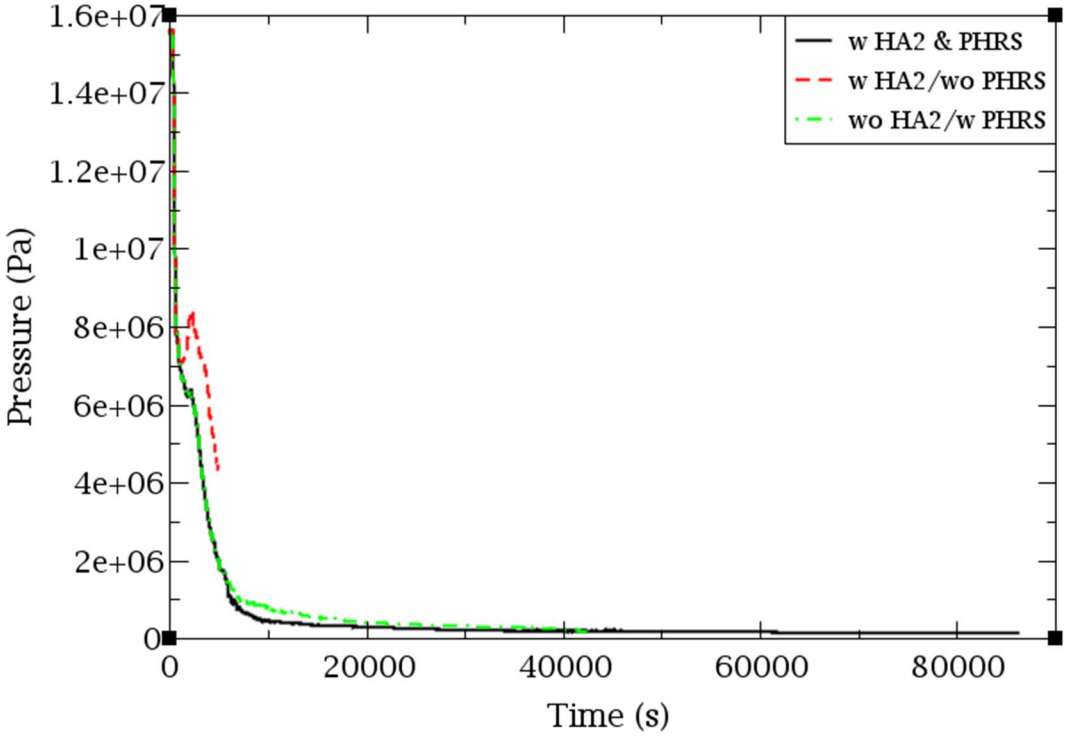

Figure 6-49 RCS pressure, SBLOCA (2 inches) sequence with HA-2 and PHRS, with HA-2 and without PHRS, without HA-2 and with PHRS

6.2.3. Performance of the PHRS and HA-2 in LBLOCA along with SBO sequences

The aim is to determine the performance of the PHRS in RCS cool-down mode in a DEGB LBLOCA sequence under SBO conditions. It is noteworthy that there is a high interest in this sequence, as it has been analyzed in (IAEA, 2012; ROSATOM, 2022) for Gen-III/III+ VVER designs.

In order to determine the containment pressure in this sequence, the available literature was consulted and was found that the containment in a LBLOCA remains pressurized in the long term, with values between 0.15 and 0.25 MPa (Lebezov et al., 2024; ROSATOM, 2022), due to the large RCS inventory discharged through the break. Therefore, in the present analysis, the containment is considered to be pressurized at 0.2 MPa.

The LBLOCA chosen corresponds to a DEGB, with an equivalent break diameter of 47 inches, located in the CL 1. The atmospheric temperature chosen for this analysis is 303.15 K (30 ^{o}C). In addition, the SC considered for the PSS involved in the LBLOCA sequence are those of the design criteria:

- HA-1: 2 out of 4 trains
- HA-2: 3 out of 4 trains
- PHRS: 3 out of 4 trains

To this end, this sequence is first analyses considering the performance of the air-cooled PHRS in addition to the HA-2. It is then analyzed in without considering the actuation of the PSS.

6.2.3.1. LBLOCA along with SBO sequence with PHRS and HA-2 available

The LBLOCA starts 300 seconds from the beginning of the simulation, see Figure 6-50 and Figure 6-51. At that instant there is a total loss of AC power, without starting the EDGs, which causes SCRAM, MCPs trip, loss of the CVCS, MFW pumps trip, TT and loss of the condenser. The evolution of the main events is shown in Table 6-9.

Due to the large size of the break, the RCS depressurizes rapidly and reaches atmospheric pressure within a few seconds, see Figure 6-53 and Figure 6-54. The HA-1 therefore injects within 15 s of the beginning of the sequence, Figure 6-56 and Figure 6-57, and the HA-2 setpoint is reached 10 s later, which causes the increase in the core collapsed liquid level, see Figure 6-58 and Figure 6-59. The second stage of the HA-2 injection starts at 4325 s, the third stage at 10325 s and finally the fourth stage at 30325 s, see Figure 6-60. On the other hand, due to the emptying of the HA-2, there is a small inventory from the CLs sucked up by the HA-2 upstream, see Figure 6-61.

The air-cooled PHRS actuation is generated by the SBO conditions. Although the air gates take 30 s to open, the SG pressure drops from the beginning of the sequence because the RCS cools the SGs by its abrupt pressure decrease. The subcooling signal ($T_{sat} - T_{HL} < 8\ ^{o}C$) is reached within 5 seconds, which means that the air duct dampers do not close at any time during the sequence. The signal for the MSIV closure occurs at 495 seconds. Subsequently, as a result of the PHRS performance, the SGs pressure drops below the RCS pressure at 3500 s. From this moment, the SGs start to cool-down the RCS, see Figure 6-55.

In the air ducts, it is observed that the air flow is about 200 kg/s per train at the beginning of the sequence and decreases to about 125 kg/s after 24 hours, as shown in Figure 6-62. This decrease in the air flow is due to a cooling of the inventory passing through the PHRS tubes, Figure 6-63. The temperature difference between

the air which is at 303.15 K and the SG inventory which is in saturation results in a natural circulation in the PHRS SLs of about 2.26 kg/s after 24 hours of the sequence, see Figure 6-64. It can also be observed that a void fraction of 92.8 % at the outlet of the PHRS tubes, see Figure 6-65, causing a mixture of steam and saturated liquid to return to the SGs.

Besides, the saturated SG inventory is at a lower pressure than the RCS, which is also in saturation conditions, so there is a temperature difference between the two, see Figure 6-66, which leads to a slight natural circulation in the RCS loops 3 and 4, see Figure 6-67. The integral of the mass flow rate for the CL 3 and CL 4 is shown in Figure 6-68. Note that the no mass flow rate from the CL1 enters into the RPV as it is loosed through the break.

As shown in Figure 6-52, at approximately 700 seconds, the mass flow rate due to the break becomes less than the injected mass flow rate from the three HA-2 trains available. From this point the second peak of the PCT begins to decrease, without reaching 1477 K, which marks the start of the reflooding phase. Finally, it can be concluded that no CD occurs during the first 24 hours of the SBLOCA along with SBO sequence, see Figure 6-69 and Figure 6-70.

The need to fulfil two CSFs in LOCA sequences has already been mentioned: decay heat removal and RCS coolant supply. As in the SBLOCA sequence, it has been verified that in the LBLOCA sequence with SBO conditions, the combined performance of the HA-2 and the PHRS ensures both CSFs for at least 24 hours.

The joined power removal potential by the SG3 and SG4 (SG1 is not considered because of the DEGB), due to the PHRS performance, and the HA-2 is shown together with the core decay heat in Figure 6-71 (blue line). As for the SBLOCA under SBO conditions sequence, it has considered a reduction in the mass flow rate in the four stages of the HA-2 by 6.25%.

Again, it has been obtained that the power removal potential of the HA-2 and the air-cooled PHRS exceeds the decay heat. This explains why the sequence does not reach the CD within the first 24 hours after the accidental sequence.

The HA-2 power has been obtained by assuming that the mass flow rate (G) from the HA-2 tanks which enters the RCS at ambient temperature is completely evaporated, in a form similar to that calculated in previous Section and in Section 6.1.1.1.

$$Q_{vap} = G\ (h_{out} - h_{in}) = G\ (\ h_{v,out}^{sat} - h_{l,in})$$

Table 6-9 Main events in the DEGB LBLOCA under SBO conditions [with PHRS and HA-2]

Time (s)	Event
300	LBLOCA along with SBO (SCRAM, MFW pumps trip, MCPs trip, TT, loss of the condenser, CVCS off)
305	Signal for PHRS in cool-down mode ($T_{sat} - T_{HL} < 8$ °C)
315	HA-1 injection begins (RCS pressure < 6 MPa)
325	HA-2 injection setpoint (RCS pressure < 1.5 MPa)
330	Air gates opening (SBO + 30 s delay)
365	HA-1 injection ends (HA-1 empty)
420	PHRS full capacity (90 s opening)
425	First stage HA-2 injection begins (HA-2 setpoint + 100 s)
495	MSIV close (SG pressure < 4.69 MPa)
4325	Second stage HA-2 injection begins (HA-2 setpoint + 4000 s)
10325	Third stage HA-2 injection begins (HA-2 setpoint + 10000 s)
30325	Fourth stage HA-2 injection begins (HA-2 setpoint + 30000 s)
86400	End simulation (24 hours)

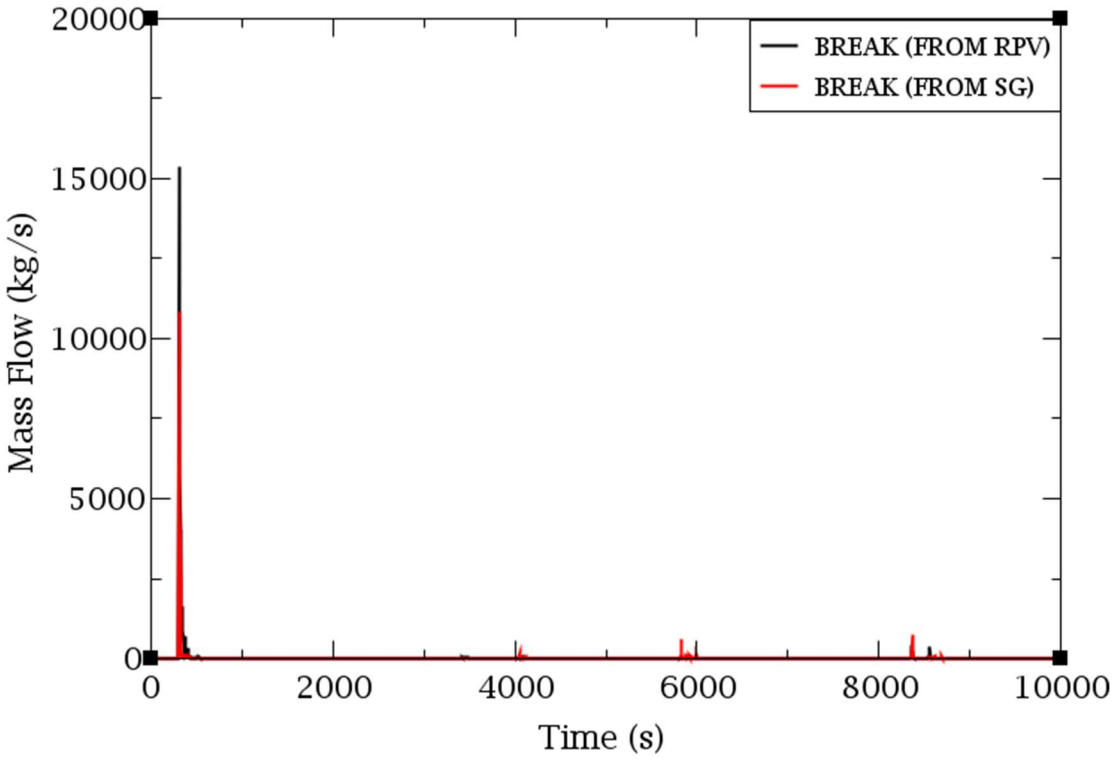

Figure 6-50 Break mass flow rate, DEGB LBLOCA along with SBO sequence (from 0 s to 10000)

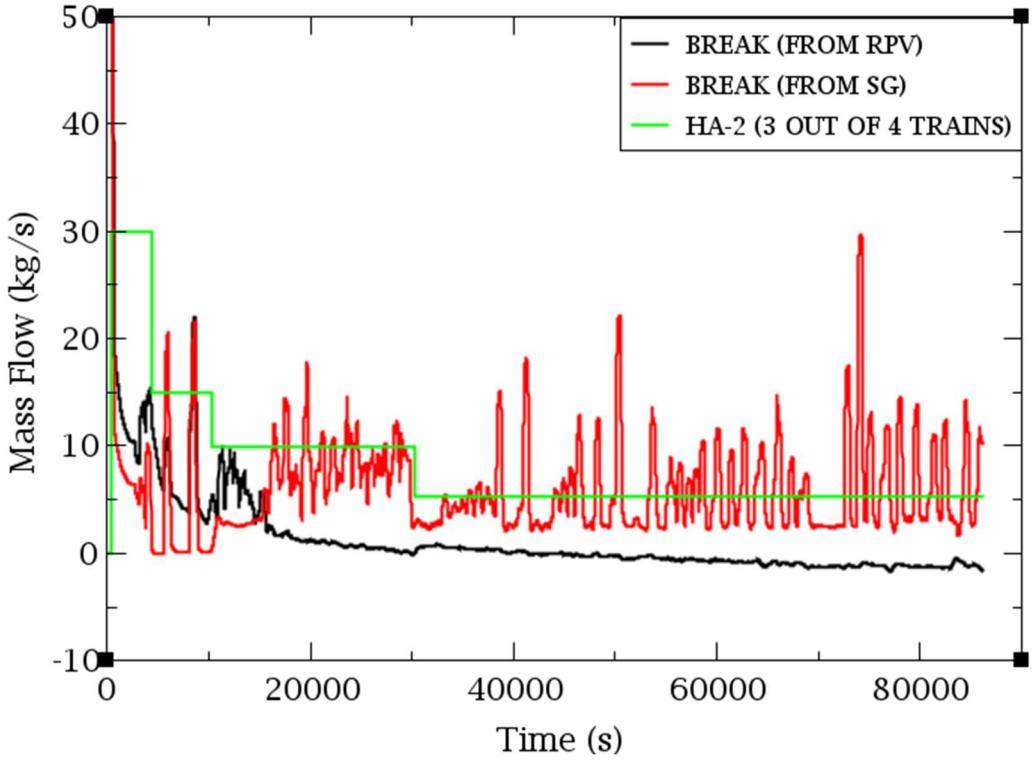

Figure 6-51 Break vs. HA-2 mass flow rate, DEGB LBLOCA along with SBO sequence (enlarged)

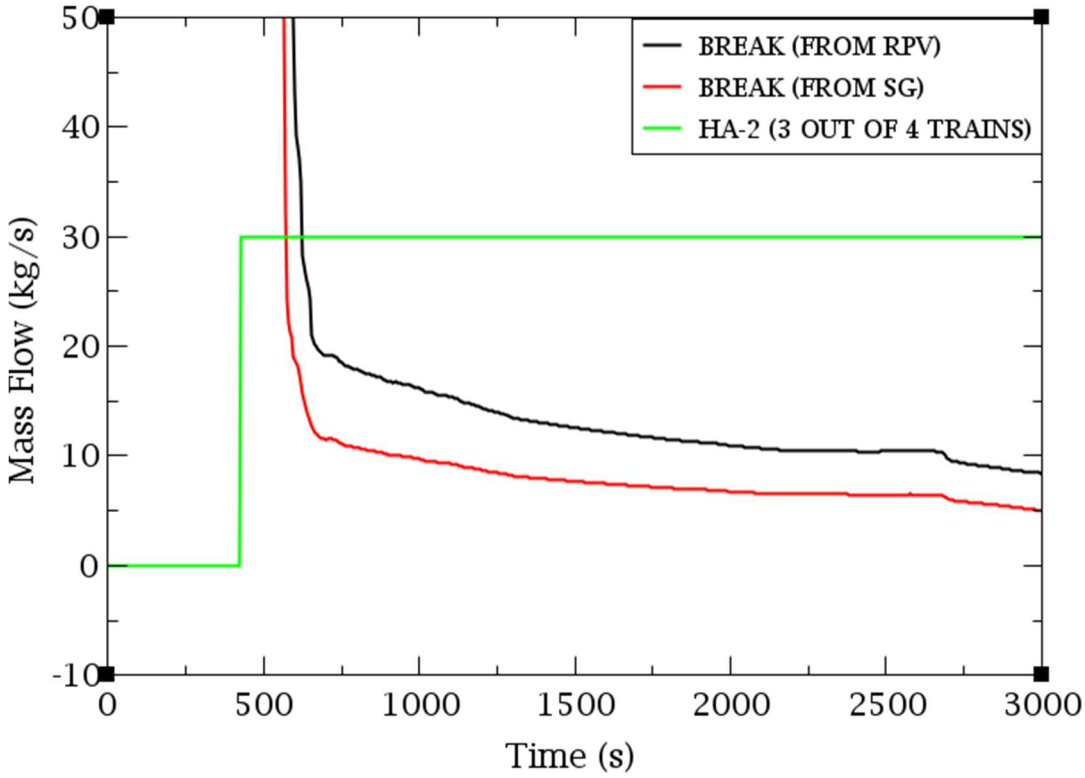

Figure 6-52 Break vs. HA-2 mass flow rate, DEGB LBLOCA along with SBO sequence (from 0 s to 3000 s) (enlarged)

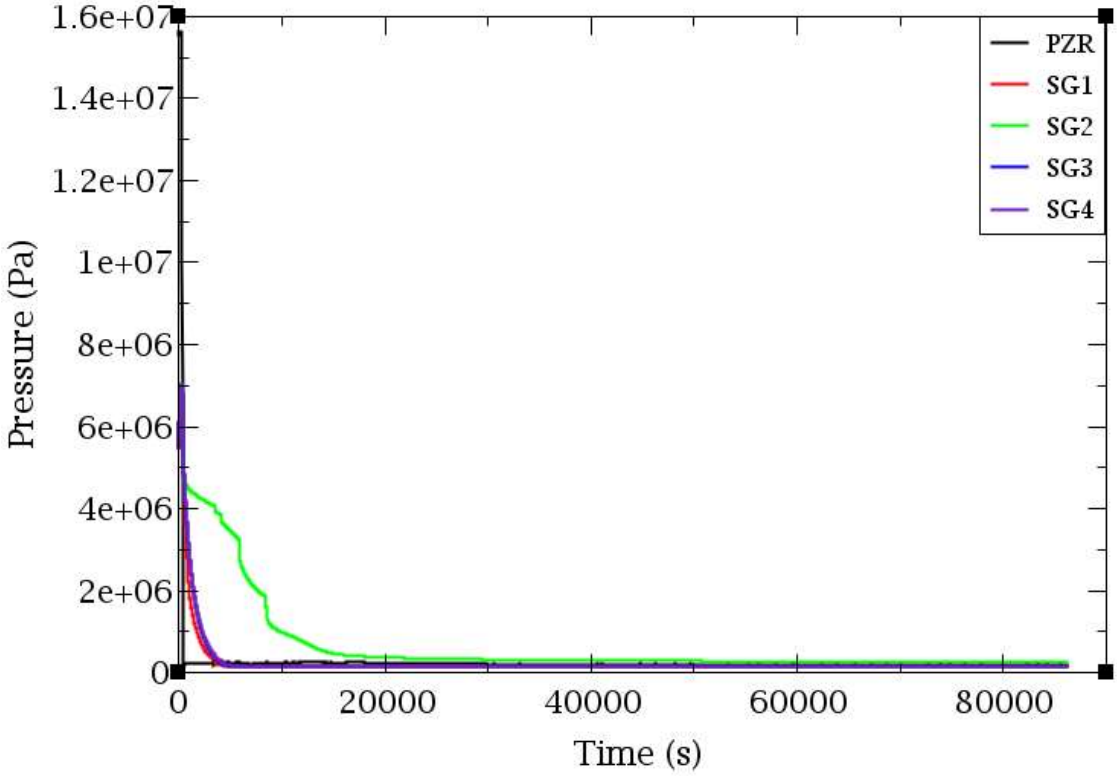

Figure 6-53 RCS and SGs pressure, DEGB LBLOCA along with SBO sequence

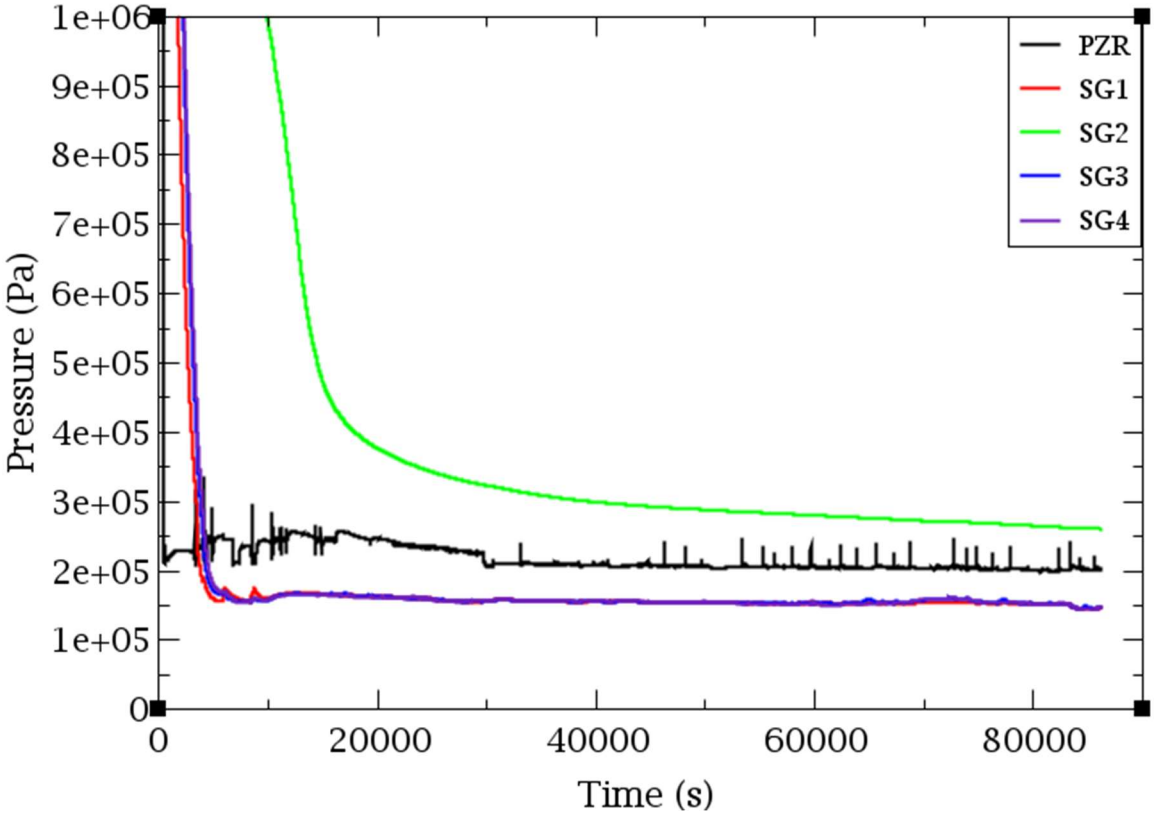

Figure 6-54 RCS and SGs pressure, DEGB LBLOCA along with SBO sequence (enlarged)

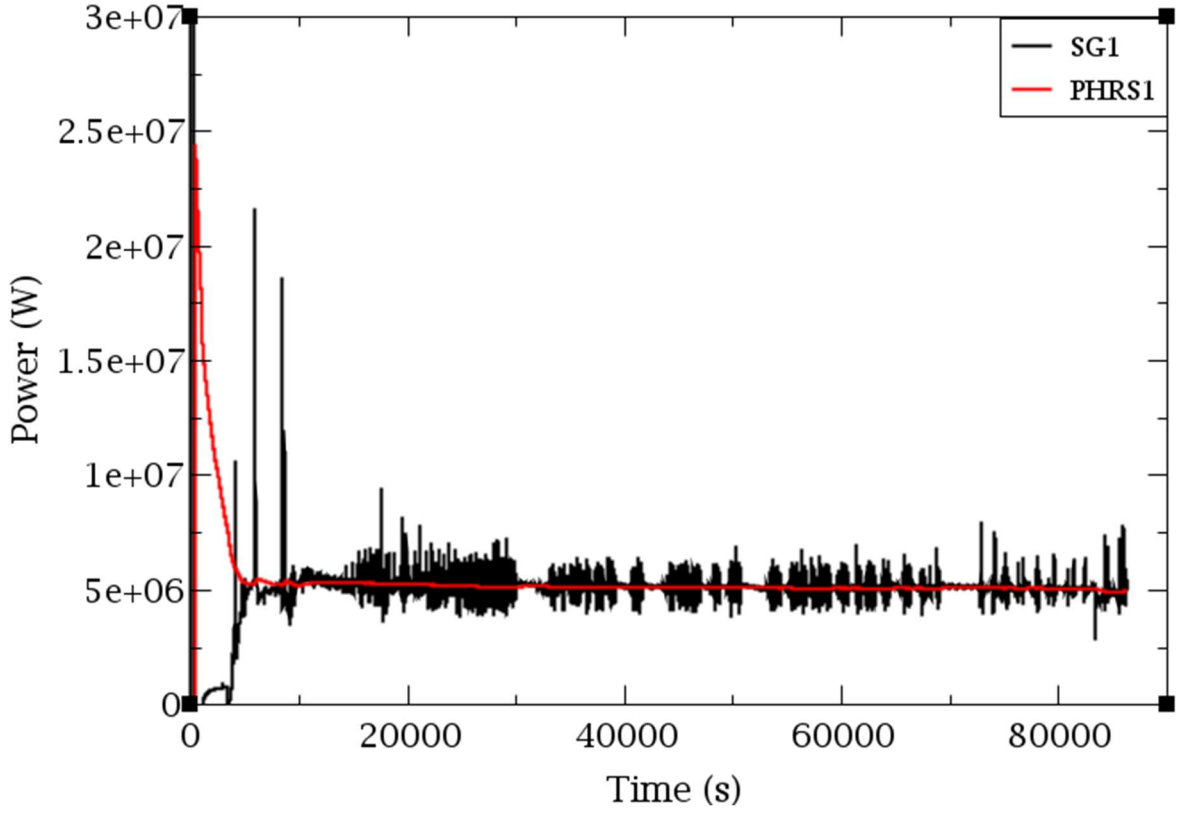

Figure 6-55 PHRS 1 vs. SG1 power, DEGB LBLOCA along with SBO sequence

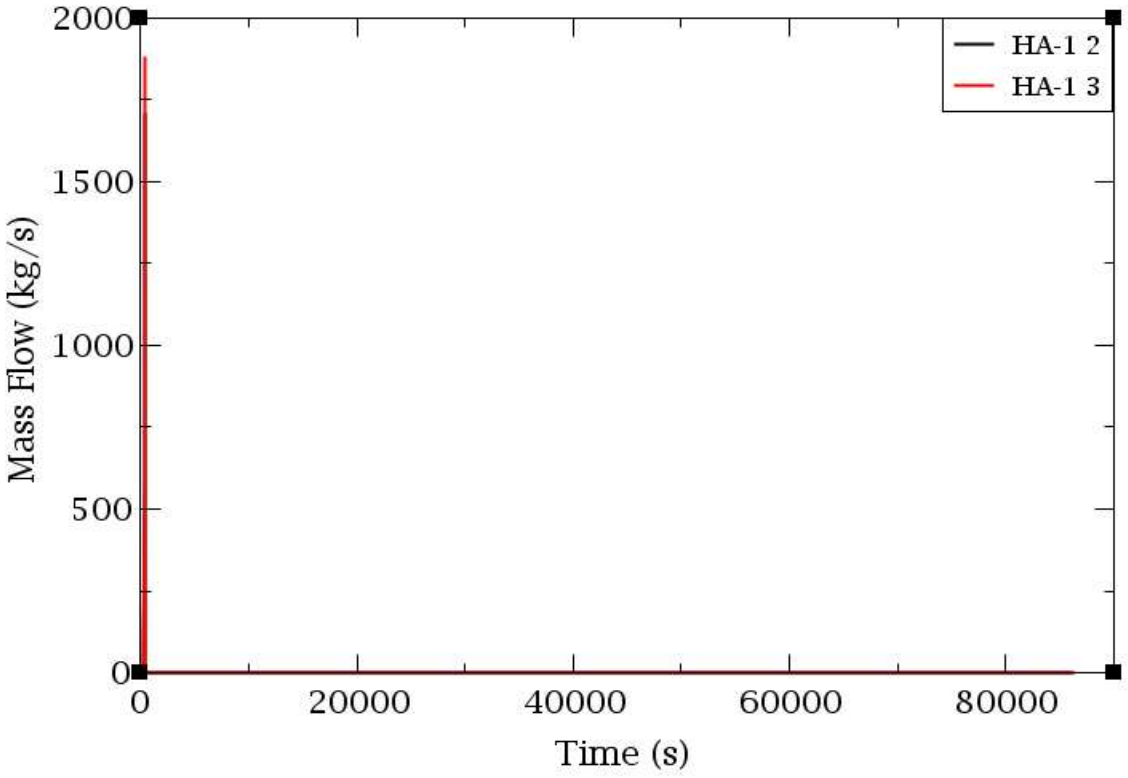

Figure 6-56 HA-1 mass flow rate, DEGB LBLOCA along with SBO sequence

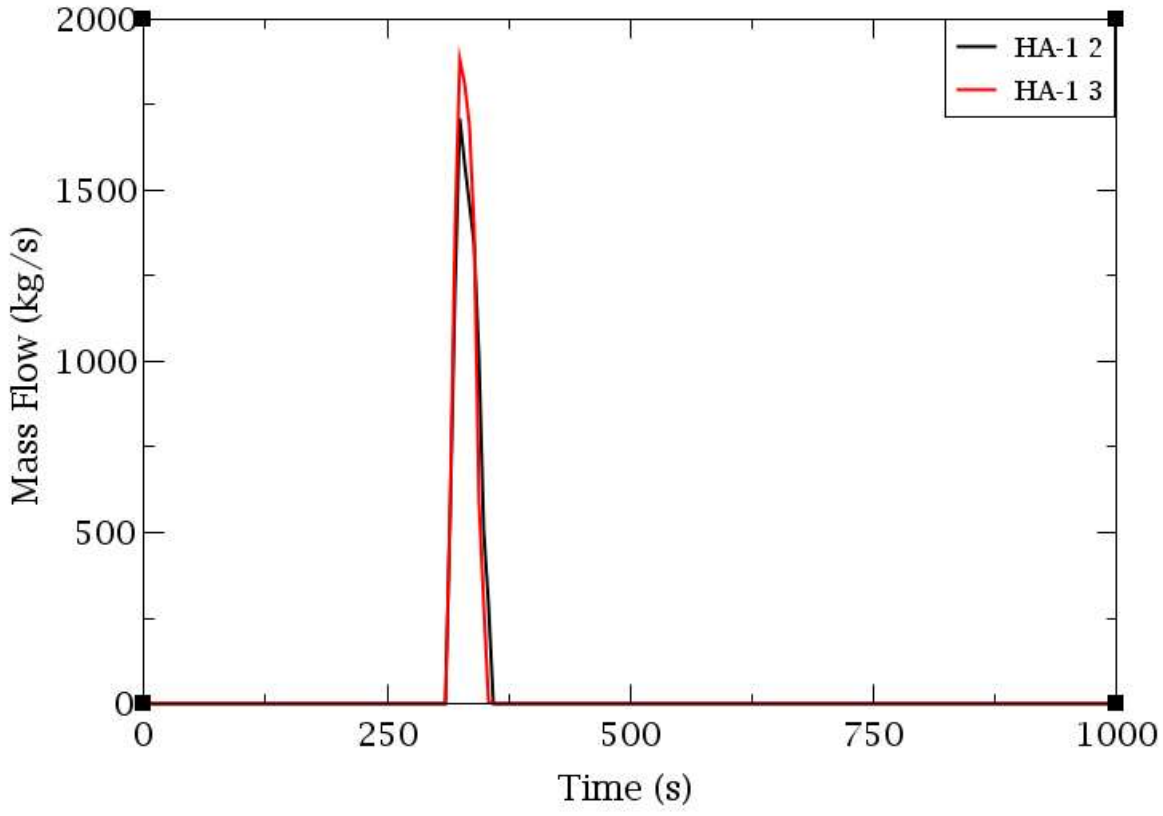

Figure 6-57 HA-1 mass flow rate, DEGB LBLOCA along with SBO sequence (from 0 s to 1000 s)

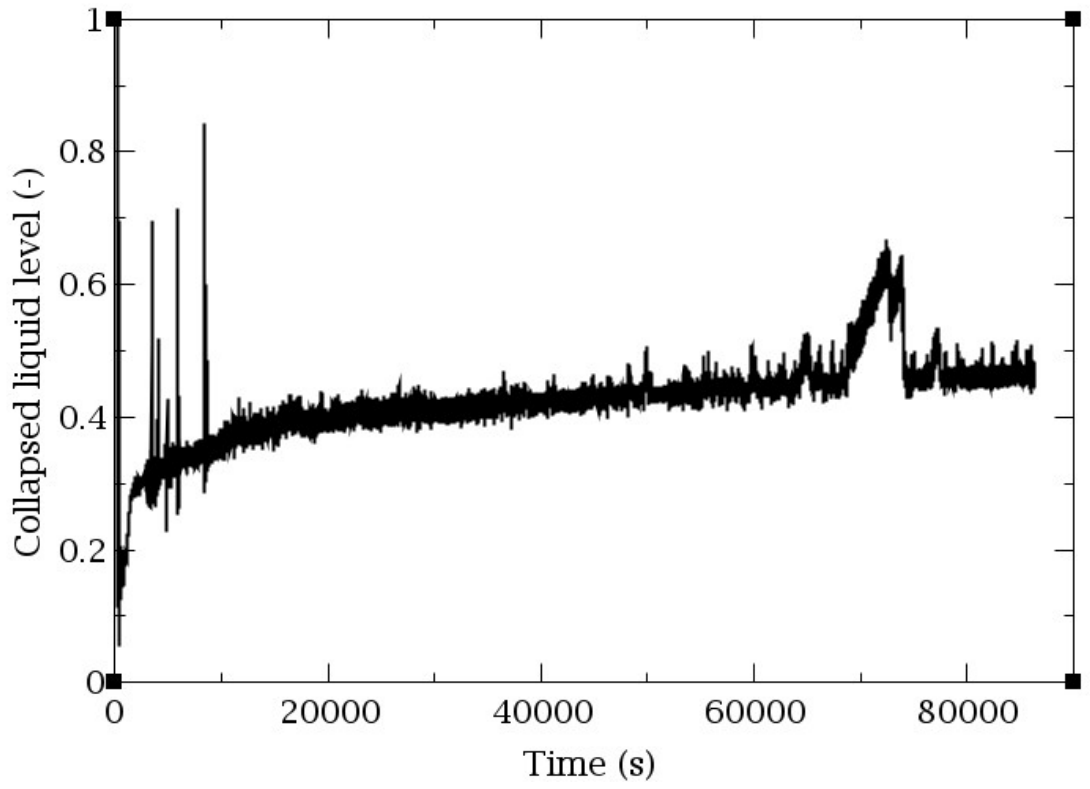

Figure 6-58 Collapsed liquid level, DEGB LBLOCA along with SBO sequence

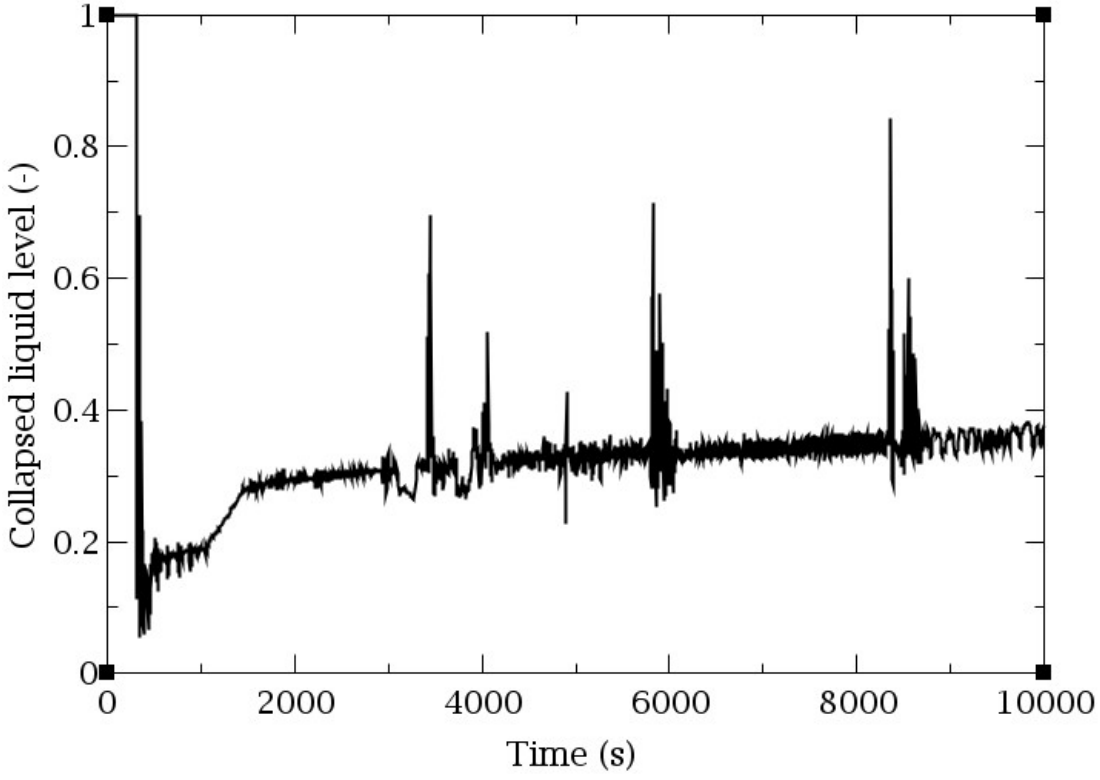

Figure 6-59 Collapsed liquid level, DEGB LBLOCA along with SBO sequence (from 0 s to 10000 s)

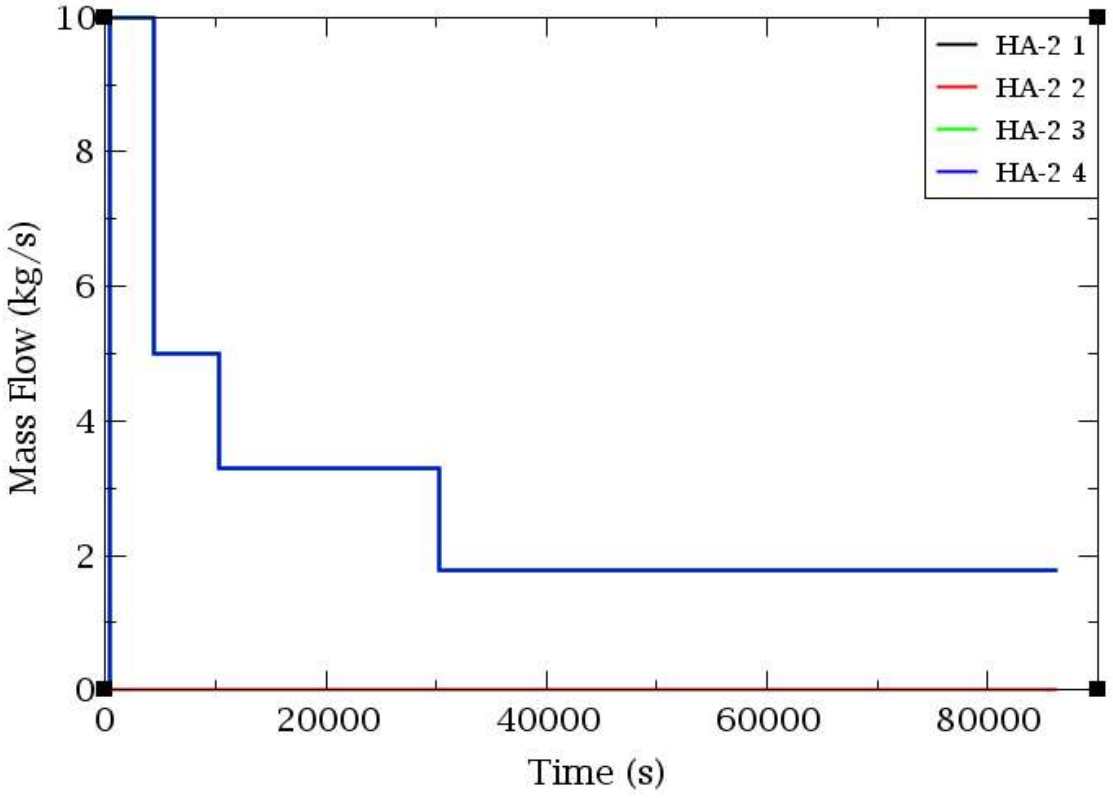

Figure 6-60 HA-2 mass flow rate per train, DEGB LBLOCA along with SBO sequence

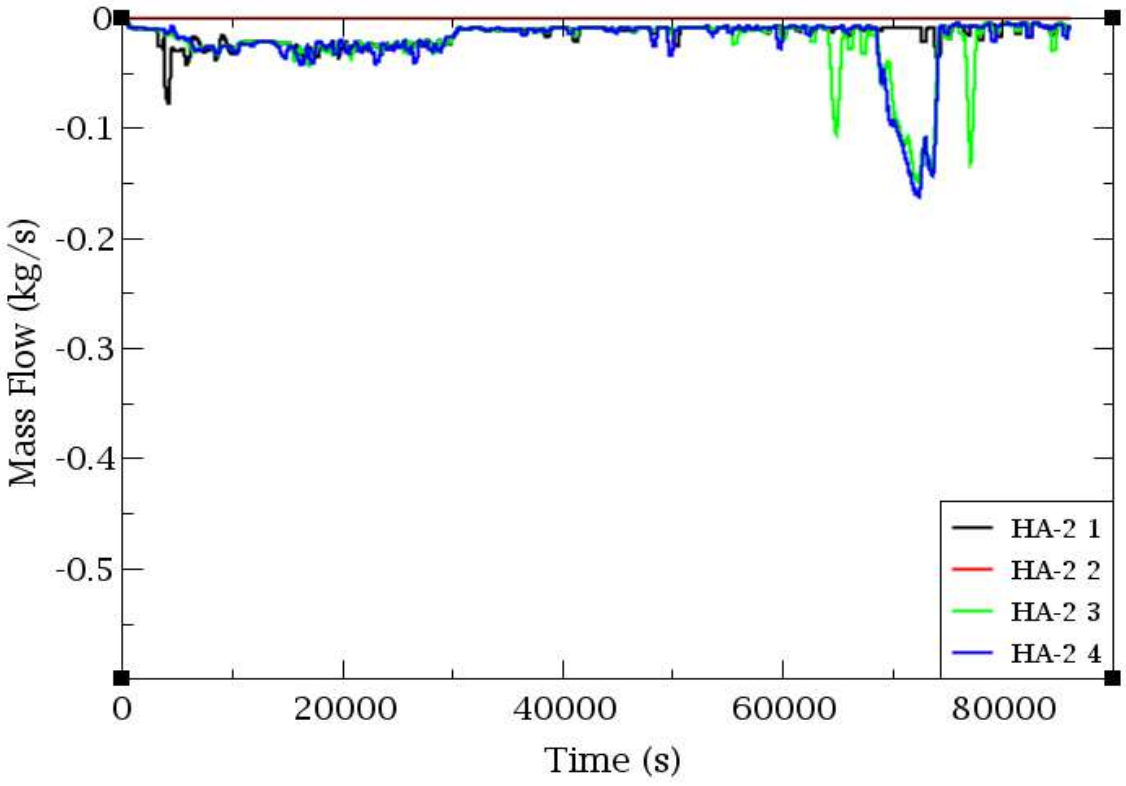

Figure 6-61 HA-2-CLs line mass flow rate per loop, DEGB LBLOCA along with SBO sequence

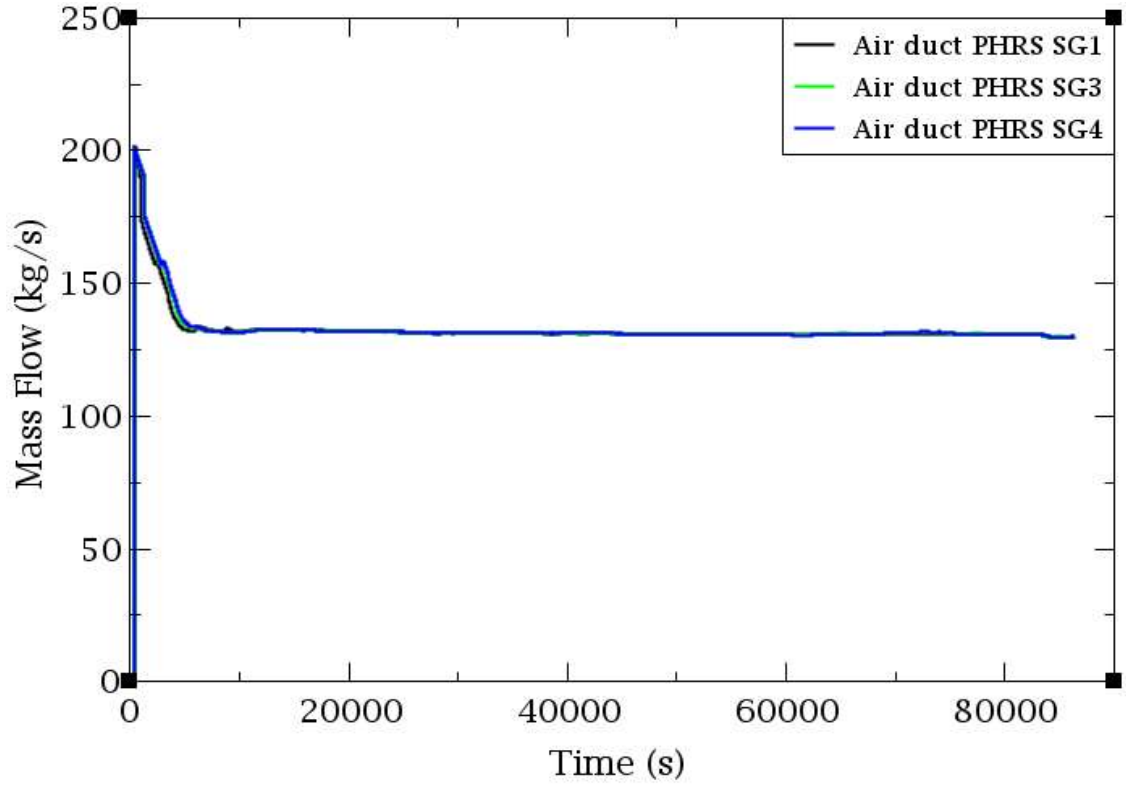

Figure 6-62 PHRS air duct mass flow rate per train, DEGB LBLOCA along with SBO sequence

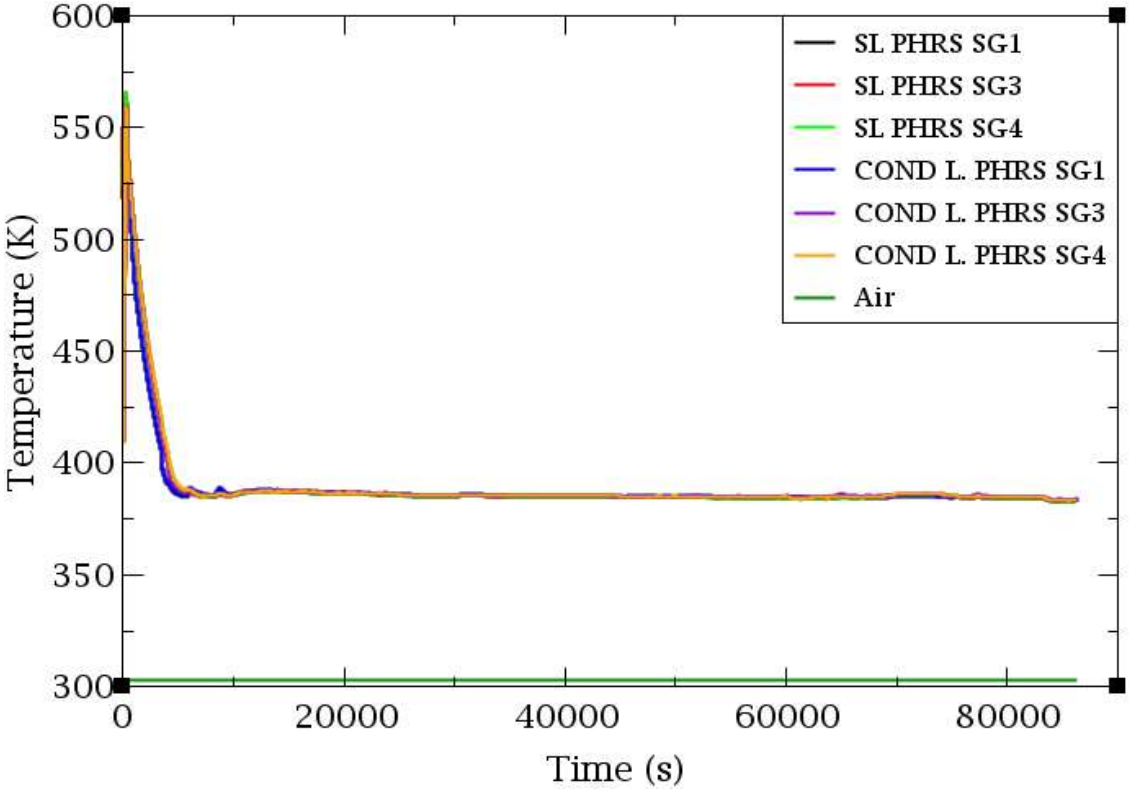

Figure 6-63 PHRS steam lines and condensate lines temperature, DEGB LBLOCA along with SBO sequence

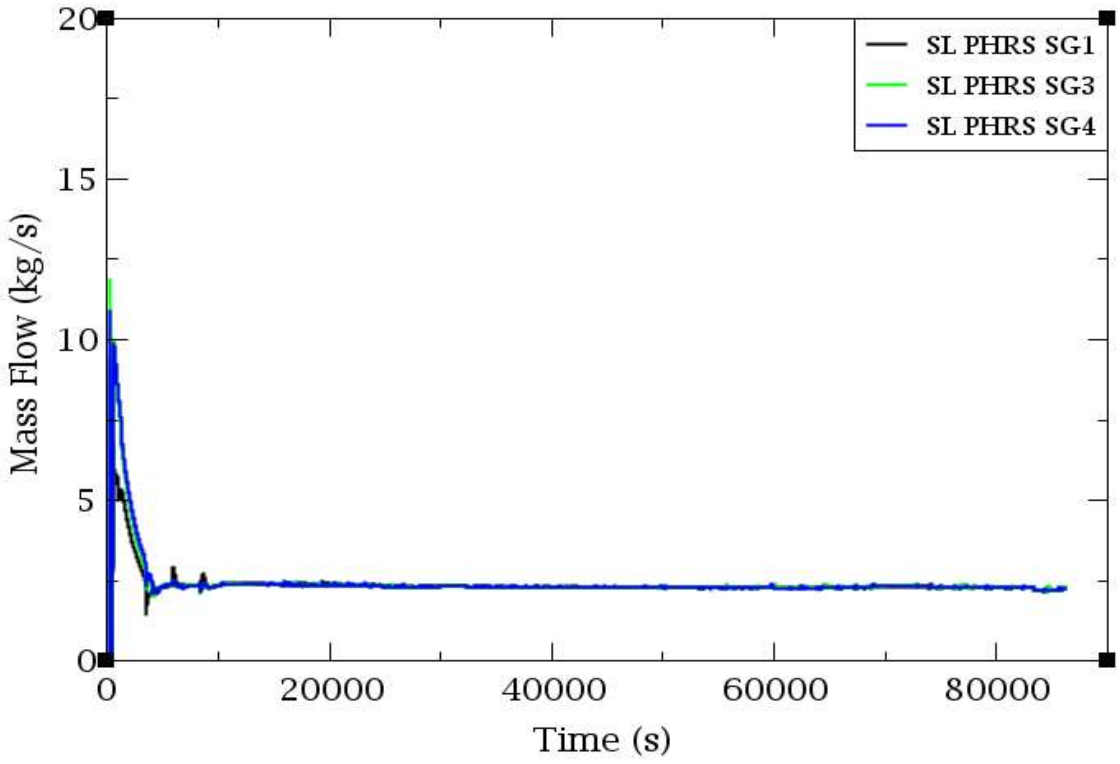

Figure 6-64 PHRS steam lines mass flow rate, DEGB LBLOCA along with SBO sequence

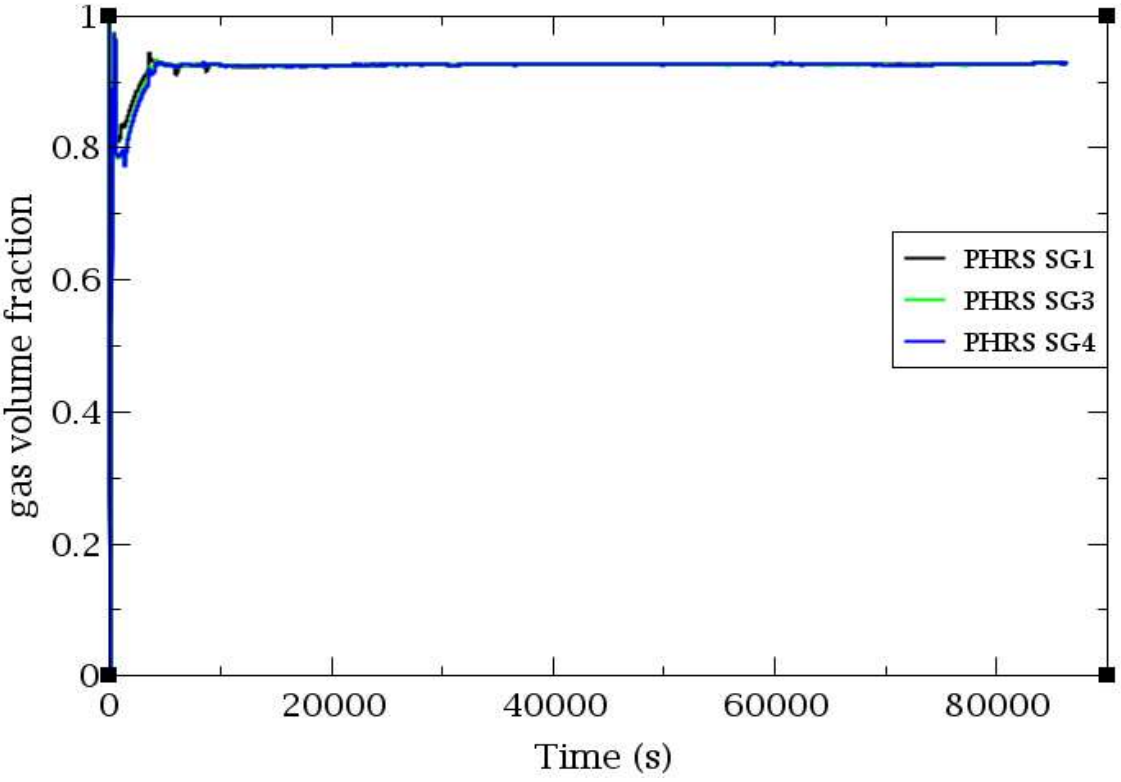

Figure 6-65 PHRS outlet bundle tubes void fraction, DEGB LBLOCA along with SBO sequence

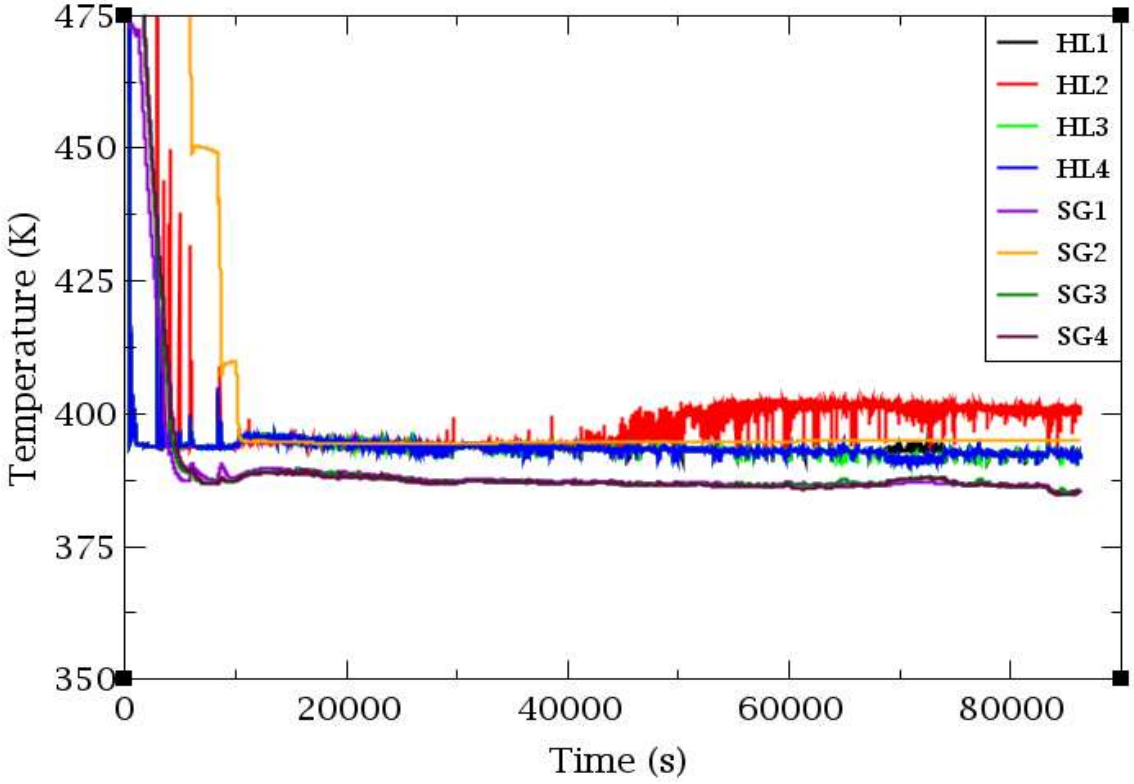

Figure 6-66 HLs and outlet SGs temperature, DEGB LBLOCA along with SBO sequence

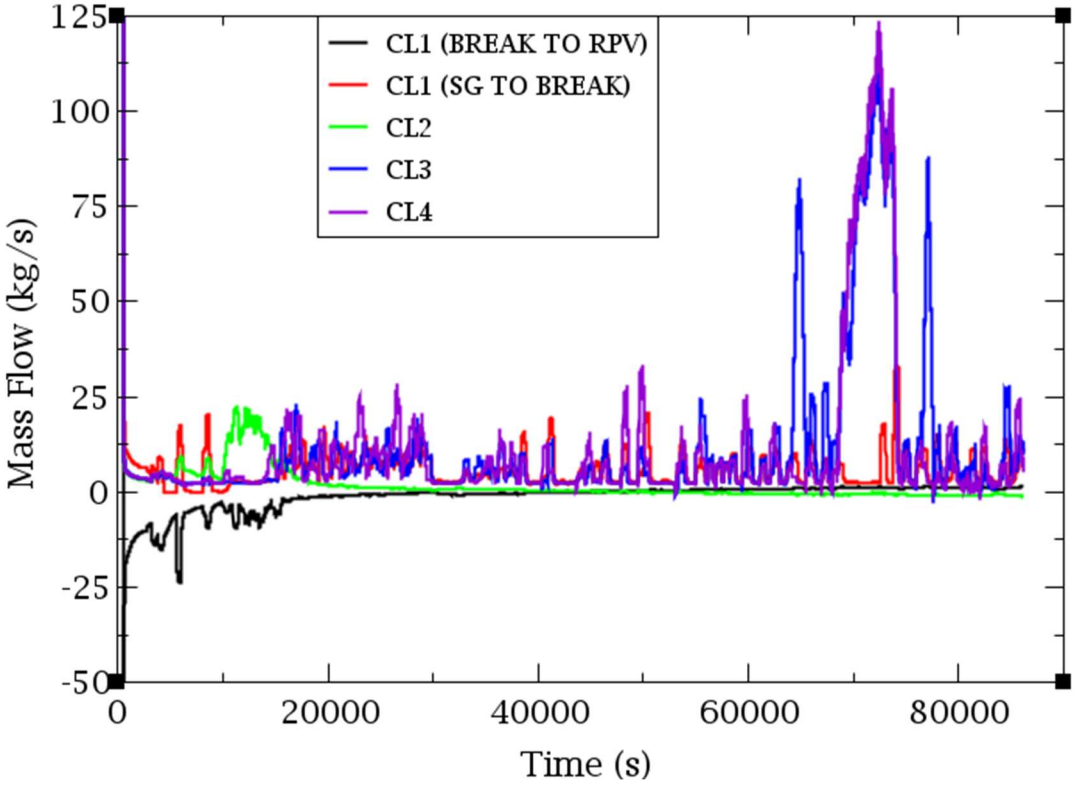

Figure 6-67 RCS mass flow rate, DEGB LBLOCA along with SBO sequence (enlarged)

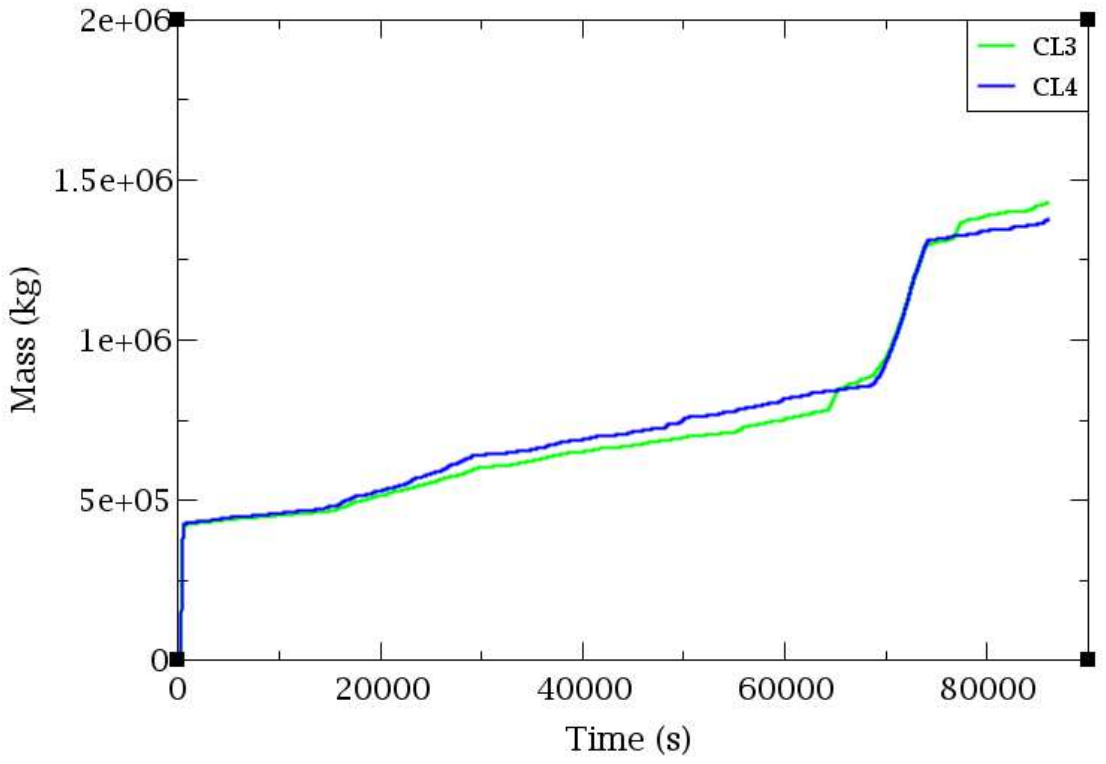

Figure 6-68 CL3 and CL4 mass flow rate integral, DEGB LBLOCA along with SBO sequence

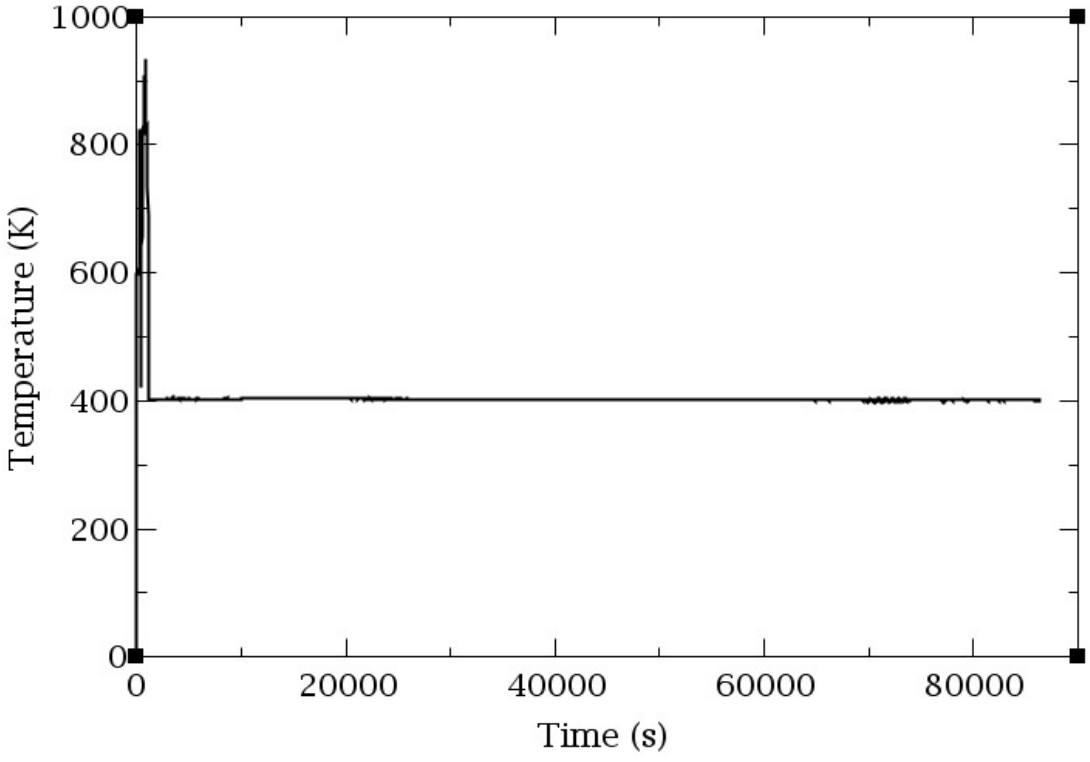

Figure 6-69 PCT, DEGB LBLOCA along with SBO sequence

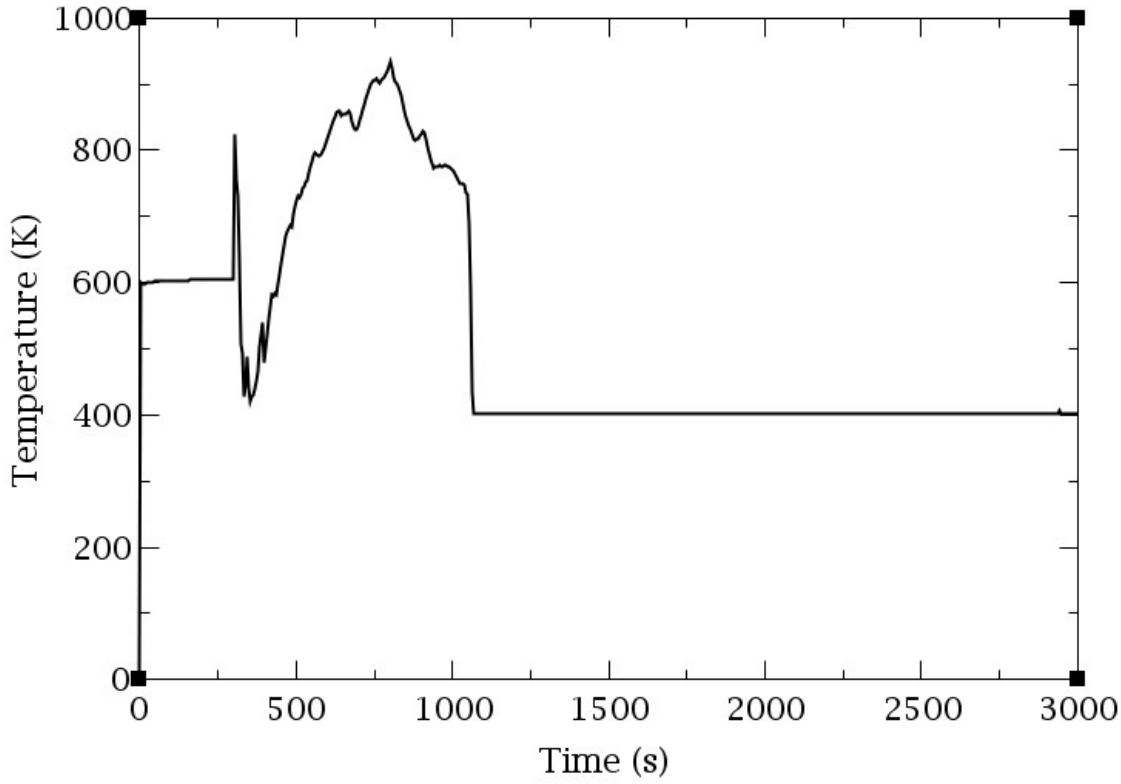

Figure 6-70 PCT, DEGB LBLOCA along with SBO sequence (from 0 s to 3000 s)

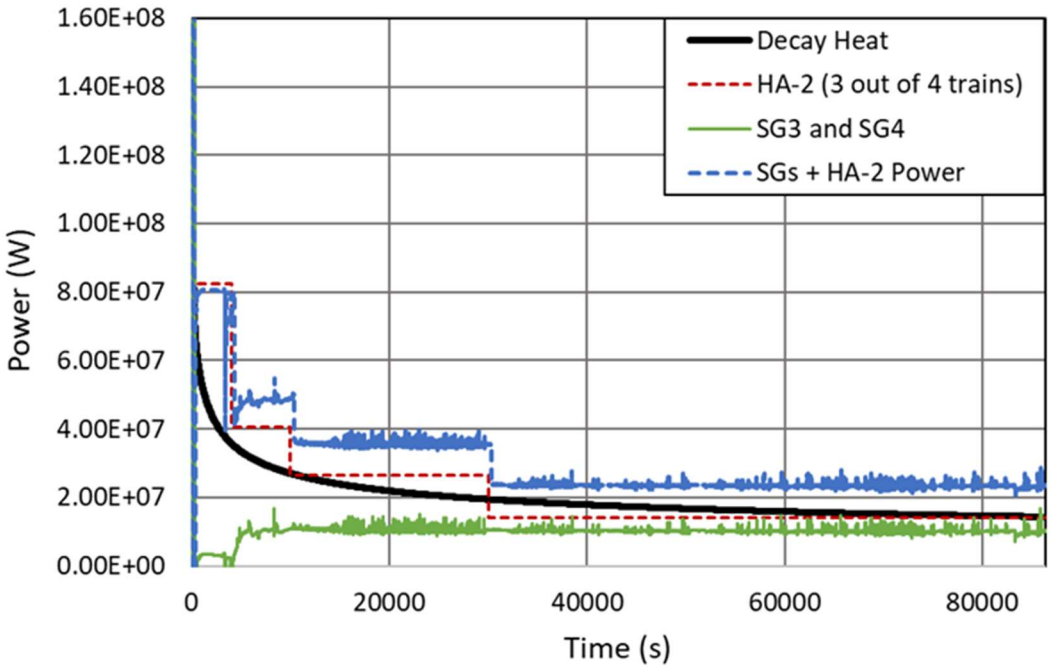

Figure 6-71 Heat removal capacity of the HA-2 and PHRS vs decay heat in the DEGB LBLOCA along with SBO sequence

Similar to the SBLOCA sequence with SBO, a video has also been generated using the SNAP tools for the LBLOCA sequence with SBO to examine the evolution of the void fraction. The void fraction at four different times of the transient is shown in the Figure 6-72:

- The void fraction at the beginning of the sequence (t = 0s).
- The void fraction at the end of the refill phase, when the DC is already filled with water from the passive ECCS (t = 805 s). At this point the core is uncovered as the axial core temperature is high, note that the void fraction is very high.
- The void fraction in the reflood phase (t = 1080 s). At this point the core void fraction is smaller, particularly in the lower part. In addition, the axial temperature of the core has decreased and is now well below the CD temperature.
- The void fraction at 24 hours into the sequence (t = 86400 s). It can be seen that the HA-2 inventory continues to enter the core through both the DC and the UP, resulting in a further reduction in the void fraction.

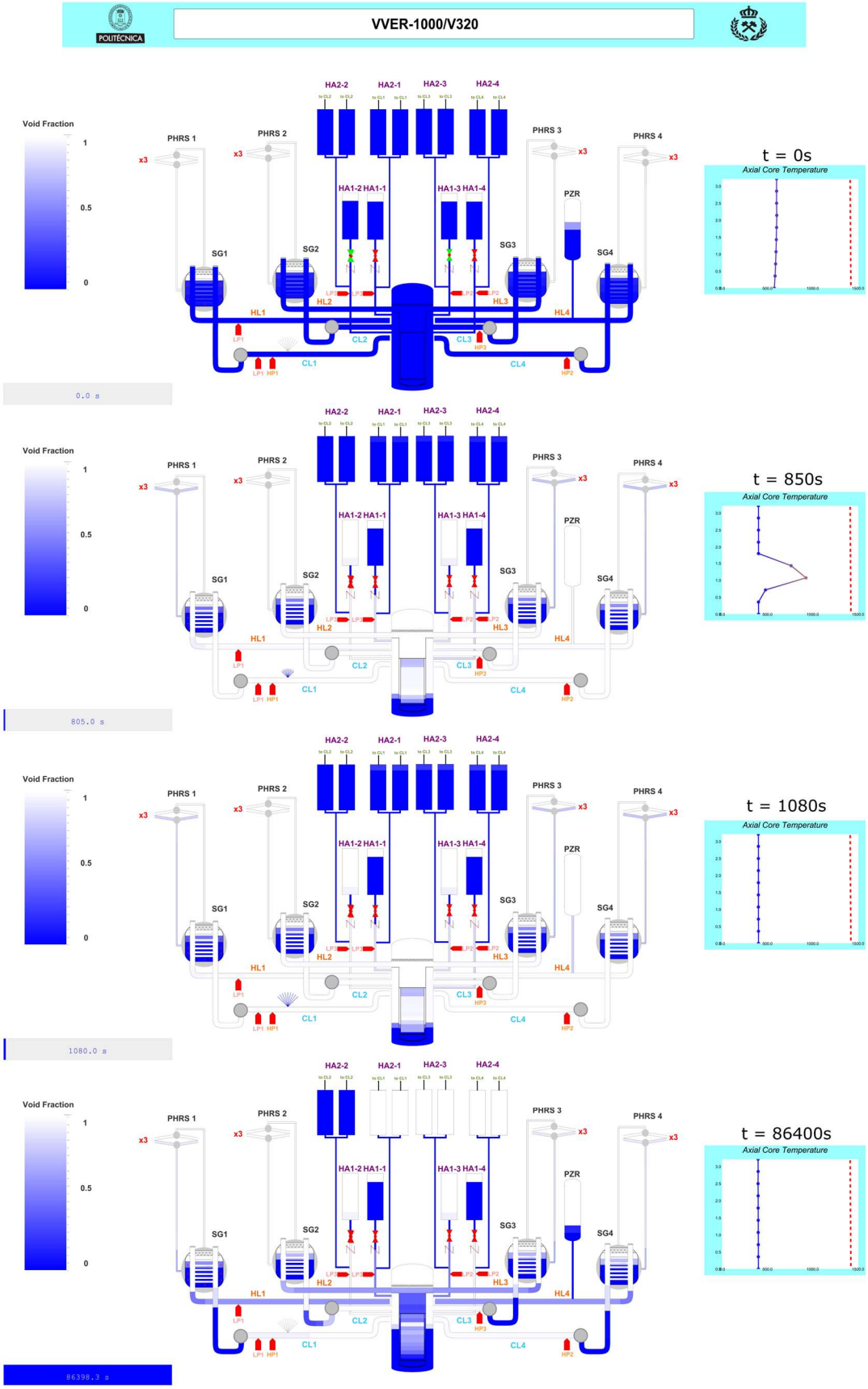

Figure 6-72 SNAP video for VVER-1000/V320 TRACEV5P5 model. DEGB LBLOCA along with SBO, 24-hour sequence

6.2.3.2. LBLOCA along with SBO sequence; without PHRS or HA-2 availability

In this section, both cases are studied, the LBLOCA with SBO sequence without considering the air-cooled PHRS actuation and without considering the HA-2 actuation. The aim is to know when the CD is reached if one of the two CSFs, the heat removal and the RCS coolant supply, is not fulfilled.

If only 3 out of 4 HA-2 trains (HA-2 SC) are considered, and not the air-cooled PHRS, it is found that the air-cooled PHRS is not necessary for the HA-2 to start injecting water into the RCS, as the break is sufficient to allow the RCS pressure to reaches atmospheric values in a few minutes, see Figure 6-74. During the first three stages of HA-2 injection, the heat removed by this PSS is greater than the core decay heat, see Figure 6-71 (red line), but in the fourth stage of injection, the thermal power of the core becomes greater. The result is that from 40000 s onwards, the core is uncovered and subsequently the CD is reached, see Figure 6-73. This was found in a previous Section 6.1, where it was also obtained that if 4 out of 4 HA-2 trains are considered instead of the SC number of trains, the HA-2 removal power is enough to avoid the CD for 24 hours.

On the other hand, if only 3 out of 4 trains (PHRS SC) of the PHRS are available, CD is reached within a few seconds after the beginning of the accidental sequence, see Figure 6-73, since the inventory of the HA-1 is not sufficient to prevent the core uncovering.

To conclude, it has been shown that for the LBLOCA sequence under SBO conditions the combined actuation of the HA-2 and the PHRS, considering the design criteria of both, is necessary to ensure core cooling for at least 24 hours.

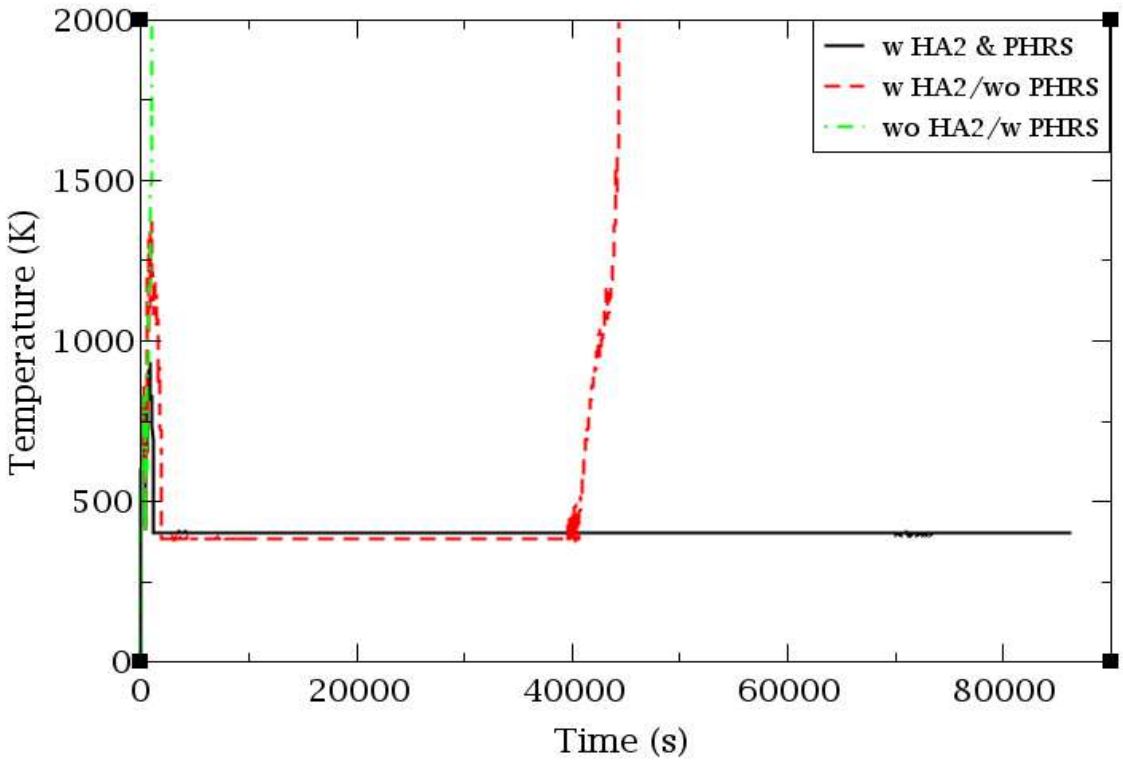

Figure 6-73 PCT, DEGB LBLOCA sequence with HA-2 and PHRS, with HA-2 and without PHRS, without HA-2 and with PHRS

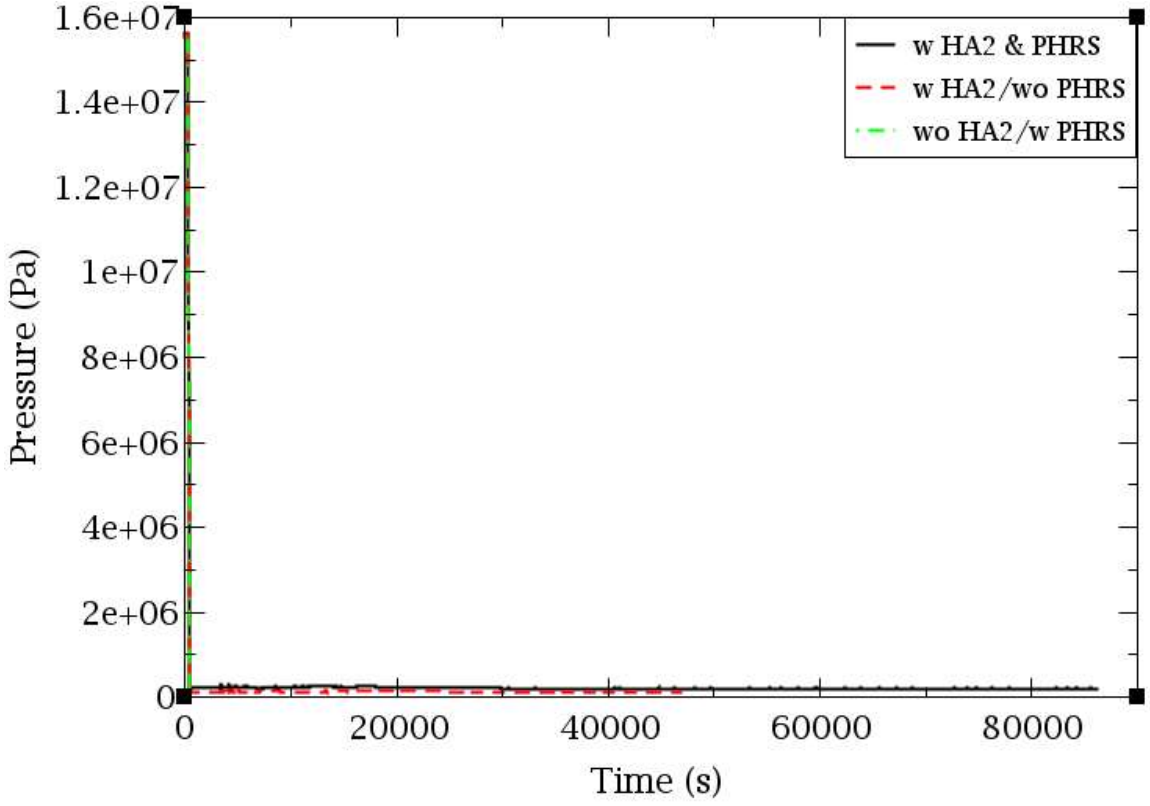

Figure 6-74 RCS pressure, DEGB LBLOCA sequence with HA-2 and PHRS, with HA-2 and without PHRS, without HA-2 and with PHRS

6.2.4. Verification of the PHRS operating modes in the sequences analyzed

The purpose of Section 6.2.4 is to confirm that the characteristic curves of the air-cooled PHRS operating modes (SG pressure maintenance mode and RCS cool-down mode), as shown in Figure 2-73 of Section 2.2.4, are met in the three scenarios analyzed in Section 6.2: an SBO, an SBLOCA and an LBLOCA under SBO conditions. To do this, the power removed by the air-cooled PHRS has been plotted against the SGs pressure, see Figure 6-75.

In the LOCA sequences, the air-cooled PHRS power vs. SG pressure curve follows a very similar behaviour to that of the curve calculated for the isolated PHRS model in Section 3.5, see Figure 3-19. This is because in the LOCA scenarios the air-cooled PHRS operates in RCS cool-down mode, so the regulators flaps are open throughout the sequence, and therefore the HXs remove the maximum power which they can for each pressure value.

On the other hand, in the SBO sequence, it is observed that once the SGs pressure reaches 6.08 MPa, without having reached the set point of the 8 ^{o}C subcooling signal in the HLs, there is a change in the trend of the air-cooled PHRS power vs. SGs pressure curve. This is because the regulators start to gradually close in order to reduce the air mass flow through the HXs. As a result, the power that the HXs are able to remove at different pressure points in the SGs starts to decrease.

Thus, when the SGs pressure reaches values close to 5.35 MPa in the SBO sequence, the power removed by the air-cooled PHRS is similar to the power removed in the LOCA sequences when the pressure is close to atmospheric values.

Finally, it is important to note that the air-cooled PHRS power vs. SGs pressure curves from the isolated PHRS, see Figure 3-19 model, were obtained through steady states, i.e. the PHRS power values were obtained for eight different pressure values, which were then plotted together to form the curves. However, the curves in Figure 6-75 are from the simulation of the three transients analyzed. This explains why irregular behaviour is observed for some pressure values in the three curves.

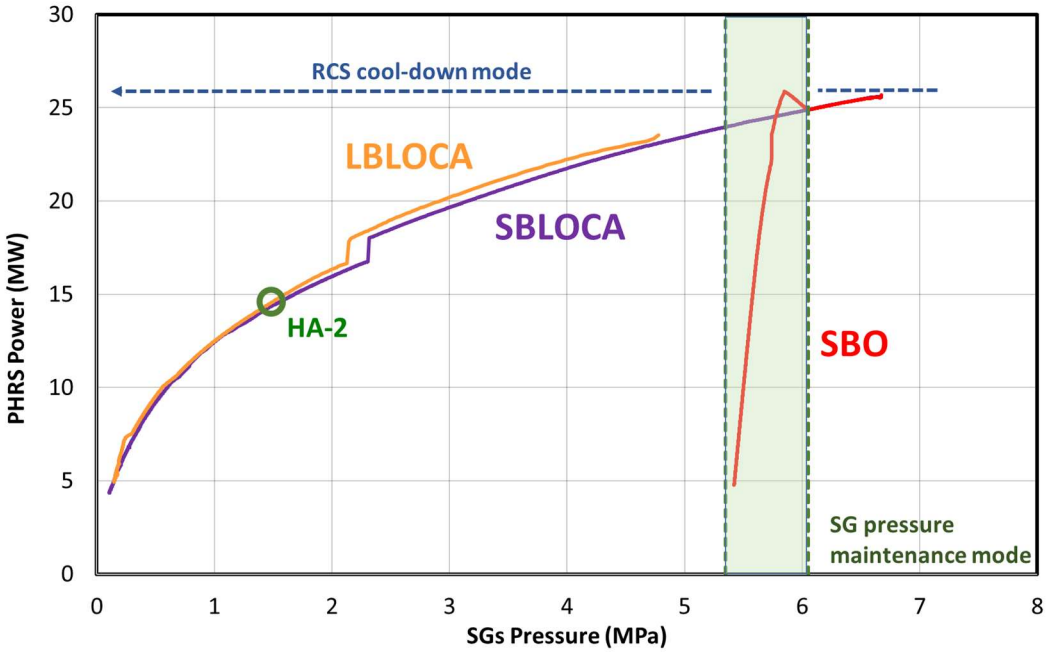

Figure 6-75 PHRS power vs. SGs pressure curves in the analyzed SBO and SB/LBLOCA under SBO conditions sequences

6.2.5. Conclusions regarding the impact of the air-cooled PHRS

A detailed analysis of the impact of the air-cooled PHRS and the HA-2 PSSs performance on SBO sequences, with and without a simultaneous LOCA has been performed. The following conclusions have been reached:

- The simulations of the SBO sequence show that the performance of the air-cooled PHRS, considering its design criteria, in SGs pressure maintenance mode, allows cooling the core for 24 hours, preventing the RCS from boiling.
- The simulation of the SBLOCA sequence show that the performance of air-cooled PHRS, considering its design criteria, in RCS cool-down mode allows the RCS pressure to decrease, reaching the HA-2 setpoint in time to avoid core uncovering.
- The simulation of the LBLOCA sequence show that the performance of the air-cooled PHRS, considering its design criteria, in RCS cool-down mode, allows to keep the RCS cooled for 24 hours, while operating the HA-2 with its design criteria.

In summary, the results show that the safety margins are significantly increased as the alternatives to prevent CD in the analyzed sequence, are diversified, thus reducing the conditional probability of damage.

6.3. Proposal of new Event Trees considering the HA-2 and the air-cooled PHRS

The LBLOCA ET has been reviewed in detail, the SC have been verified, and new ETs have been proposed in Section 5.1. Subsequently, in Section 5.2, the SBLOCA ETs have been considered, with particular interest in the sequences where there is no HPIS and the SGs have to be depressurised. On the other hand, in Section 6.1, a detailed study has been carried out on the influence of the HA-2 in LOCA sequences with SBO conditions, in order to determine the safety margin obtained with its performance. Finally, Section 6.2 has provided a comprehensive understanding of the PHRS impact on SBO sequences and LOCA sequences considering the HA-2 performance.

On the basis of all these analyses, the aim of the Section 6.3 is to determine how LOOP, SBLOCA and LBLOCA ETs, which were presented in Section 2.3, see Figure 2-77, Figure 2-78 and Figure 2-80, would be if new headers incorporating the HA-2 and the air-cooled PHRS performance are introduced.

Two new headers, HA-2 and PHRS, have been included in the proposed new ET. The former refers to the injection of the HA-2 and the latter refers to the availability of the air-cooled PHRS. Note that in the LOOP ET the PHRS header is related to the performance of this system in pressure maintenance mode, whereas in the SBLOCA and LBLOCA ETs it is related to the performance of the system in RCS cool-down mode. The SC for both the HA-2 and the PHRS headers is 3 out of 4 trains for the three proposed ETs. The remaining headers are described in Section 2.3., see Table 2-22. In addition, Table 6-10 provides a summary of the SC for all headers included in the proposed ETs.

Table 6-10 Success Criteria for the new Event Trees proposed

Header	LOOP ET	SBLOCA ET	LBLOCA ET
S	Forming a signal of SCRAM and the activation of the reactor control and protection system		-
EDG	1 out of 3 EDG	-	-
H	-	1 out of 3 trains	2 out of 3 trains
EF	1 out of 3 EFW pumps + 1 out of 4 BRU-A or BRU-K valves (SG pressure maintenance mode)	1 out of 3 EFW pumps or 1 out of 2 AFW pumps + 1 out of 4 BRU-A or BRU-K valves (SG pressure maintenance mode)	-
D	-	1 out of 3 EFW pumps or 1 out of 2 AFW pumps + 1 out of 4 BRU-A or BRU-K valves (human action) (RCS cool-down mode)	-
PHRS	3 out of 4 trains (SGs pressure maintenance mode)	3 out of 4 trains (RCS cool-down mode)	3 out of 4 trains (RCS cool-down mode)
A	-	2 out of 4 trains	2 out of 4 trains
L	-	1 out of 3 trains	1 out of 3 trains
HA-2	-	3 out of 4 trains	3 out of 4 trains
R-EX	Recovery of 1 safety but	-	-

For the LOOP sequence to be successful, it is necessary to cool the RCS through the SGs. This can be achieved in two ways: either by using the EDGs to start the EFW pumps or by having the air-cooled PHRS available in SG pressure maintenance mode. If the EFW pumps or the PHRS are not available, it is imperative that the external power is restored to avoid the CD.

Based on this and the various simulations and analyses carried out during the PhD thesis, a new LOOP ET has been proposed. The new proposed ET for the LOOP accident is shown in Figure 6-76, the headers included in the new proposed ET and their SC are shown in Table 6-10.

In the LOOP ET, sequence 1 involves the successful of the S, the EDG and the EF headers. This sequence is similar to the SCRAM sequence analyzed in Section 4.1, where it has been confirmed that a success end state is reached. In sequences 2 and 4, instead of the EF header being successful, the PHRS header is successful, with or without the EDG header also being successful. As analyzed in Section 6.2, these sequences also reach a success end state.

On the other hand, sequences 3 and 6 lead to the CD end state, as they both involve the failure of headers related to the cooling of the SGs. In sequence 3, neither the EF nor the PHRS headers are successful. In sequence 6, both the EDG and R-EX headers fail, resulting in no EFW/AFW pumps injection to the SGs, and the PHRS header also fails. Scenarios without EFW/AFW and PHRS have been analyzed in Section 4.3 and confirmed to result in a CD end state.

In contrast, sequence 5 includes the failure of the EDG, EF and PHRS headers, but with a successful R-EX header. This sequence leads to a GT sequence, see Figure 2-76. Finally, if the S header fails, there is an immediate transition to the ATWS ET, which was not analyzed in this PhD thesis.

Furthermore, this work does not consider MCPs leakages during the SBO conditions. However, if they were to be considered, it should be noted that in sequence 4 of the LOOP ET there would be a transfer to the SBLOCA ET as the EDG header is not successful and therefore there are no CVCS pumps injection water to the RCPs seals.

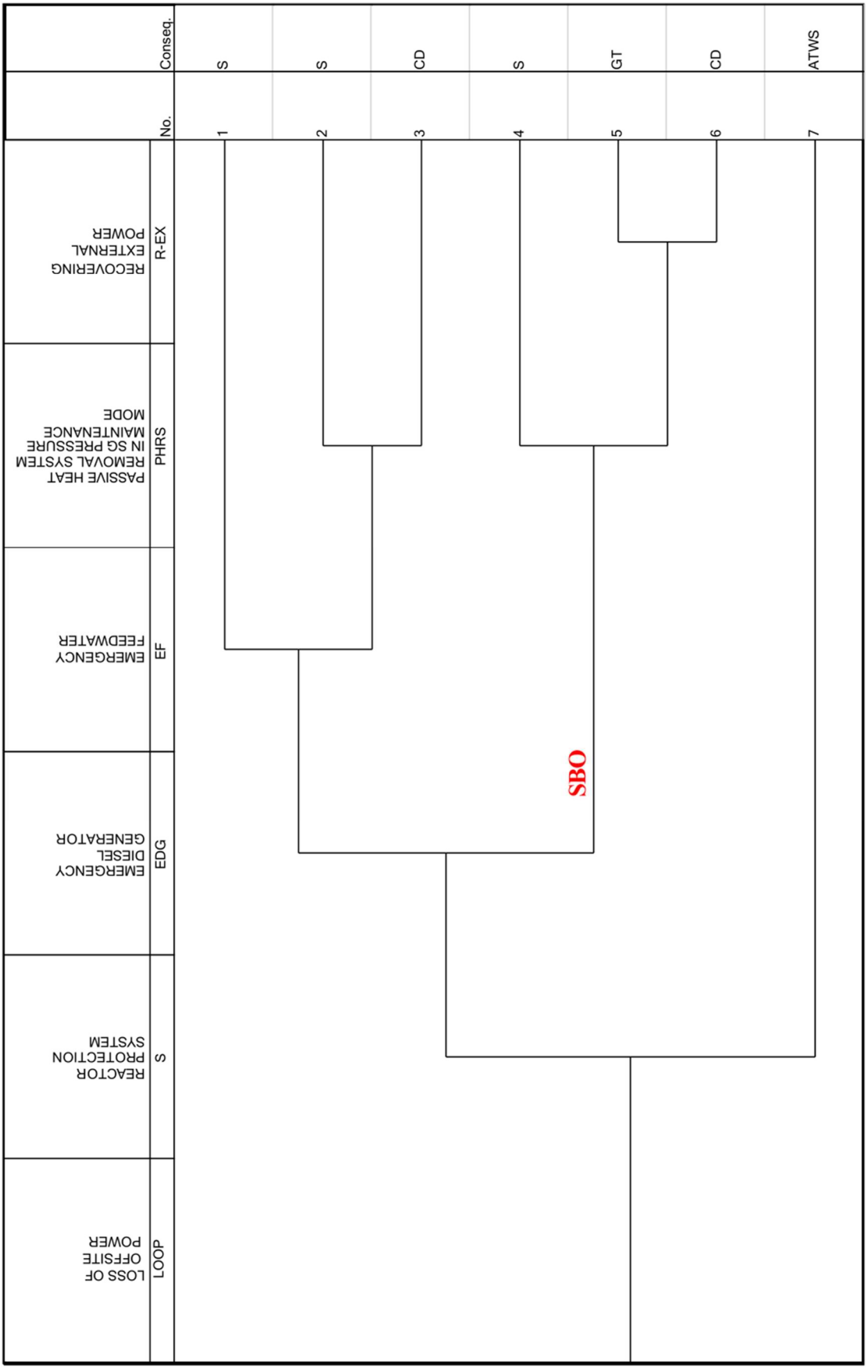

Figure 6-76 LOOP ET including the PHRS

In SBLOCA sequences without HPIS actuation, it is necessary to cool and depressurize the RCS, in order to reach the setpoint of the low pressure ECCS. In VVER-1000/V320 reactors, the cooling and depressurization of the RCS is achieved by the joint actuation of the EFW/AFW and the BRU-A valves, with the drawback that AC power is required. In some Gen-III/III+ VVERs, in a scenario where AC power is not available, this action of cooling and depressurizing the SGs is performed by the air-cooled PHRS. Once the RCS has been depressurized, the action of replenishing the inventory in the RCS is carried out by the LPIS if AC power is available. In the Gen-III/III+ VVER reactors with air-cooled PHRS, the low pressure inventory replenishment action is performed by the HA-2 if the LPIS is not available.

Based on these findings from the simulations and analyses carried out in the PhD thesis, a new ET for SBLOCA is proposed, see Figure 6-77. The headers included in the proposed ET and their SC are shown in Table 6-10. It should be noted that the headers related to the EBIS and with the EGRS, which are included in the ET of (Skalozubov et al., 2010), have not been considered, as it has been seen in Section 5.2. that these headers have not a relevant interest for the SBLOCA if the SGs depressurization is performed at an RCS cooling rate of 60 K/h, see Figure 5-40.

In the SBLOCA ET, the success end state is reached when the H header is successfully combined with either the EF header, sequence 1, or the PHRS header, sequence 2. The SBLOCA sequence with both HPIS and EFW systems available has been analyzed in Section 4.5, where it has been confirmed that this combination leads to a successful end state. Conversely, if neither the EFW nor the PHRS headers are successful, CD occurs. As assumed in (Skalozubov et al., 2010), the activation of the EFW system is required for the sequence to be successful.

If the H header fails, the sequence may still succeed if either the D header or the PHRS header succeeds. In these cases, successful of the A header is also required along with either the L header, sequences 4 and 8, or the HA-2 header, sequences 5 and 9. Sequence 4 has been analyzed in Section 5.2 and sequence 9 in Section 6.2, both of which have been confirmed to reach a success end state. On the other hand, sequence 12, where neither the D nor the PHRS header is successful, results in a CD end state, as has been verified in Section 5.2 and 6.2. It is also assumed that any sequence in which the A header fails does not lead to a successful end state, see (Skalozubov et al., 2010). Finally, in the SBLOCA ET, sequence 13 includes the failure of the S header, which results in a transition to the ATWS ET.

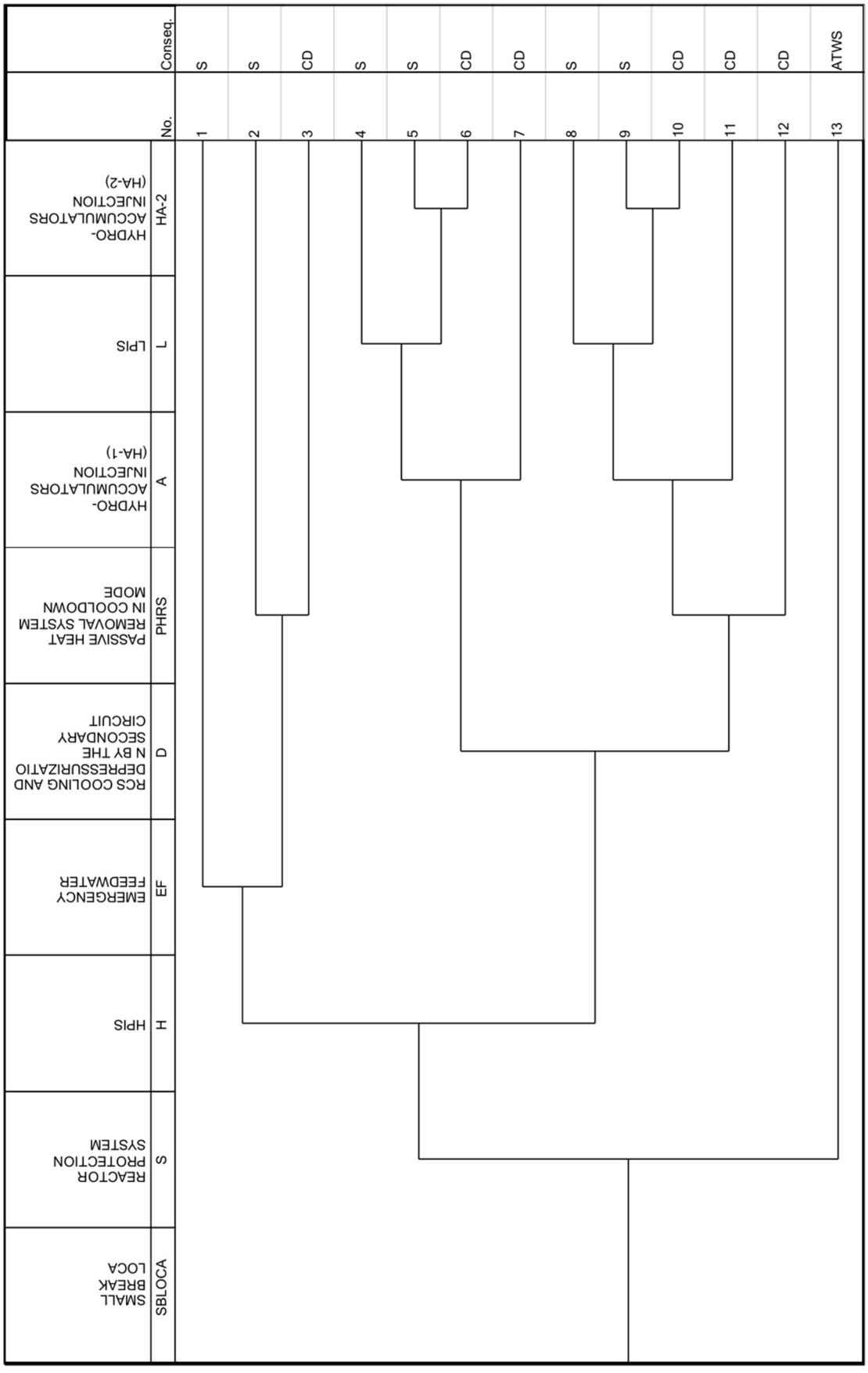

Figure 6-77 SBLOCA ET including the HA-2 and the PHRS

In LBLOCA sequences, the action of cooling and depressurizing the RCS through the SGs is not necessary, even when the HPIS is not available. Therefore, the classical LBLOCA ET of the VVER-1000/V320 does not include the headers corresponding to EFW (or the AFW) with the BRU-A in RCS cool-down mode (D), see Figure 2-80. Besides, in Gen-III/III+ VVER reactors with air-cooled PHRS and HA-2 PSSs, they do not require PHRS operation to depressurize the RCS and allow HA-2 operation in LBLOCA sequences without HPIS or/and LPIS unavailability. However, in the long term, the HA-2 are capable of removing decay heat for 24 hours if all four trains are available, as has been observed in the analysis of the Section 6.1. But, when 3 out of 4 trains or less are available, the power removed by the HA-2 is less than the core power, so PHRS operation is required for the fourth injection stages.

Based on these findings from the simulations and analyses carried out in the PhD thesis, a new ET for LBLOCA is proposed, see in Figure 6-78. The headers included in the new proposed ET and their SC are shown in Table 6-10.

In Section 5.1, sequence 1 of the LBLOCA ET, where both the H and A headers are successful, has been analyzed and found to achieve a successful end state. Conversely, in Section 5.1 it has also been observed that the sequences where the A header fails, specifically sequences 2 and 9, do not achieve a successful end state when a 1 out of 3 SC is applied to the LPIS. In addition, this study also showed that when the only successful ECCS is the HA-1, as in sequence 8, the sequence reaches the CD end state.

The failure of the H header can still result in a success end state if the L and A headers are successful, regardless of the availability of the PHRS, sequences 3, or not, sequence 6. It is important to note that sequence 6 has been analyzed in Section 5.1, where it was found that the sequence did not reach the CD. Therefore, it is assumed that sequence 3, which also takes into account the availability of the PHRS, reaches a successful end state.

Furthermore, in Section 6.1 it has been found that sequence 7, where both HA-1 and HA-2 are available, can only succeed if all 4 HA-2 trains are operational. However, sequence 4, where the PHRS is available, reaches a successful end state with a SC for HA-2 of 3 out of 4 trains. Also, the results performed in Section 6.2 show that if the PHRS is available, but neither the HPIS, the LPIS nor the HA-2 are available, as in sequence 5, the CD is reached.

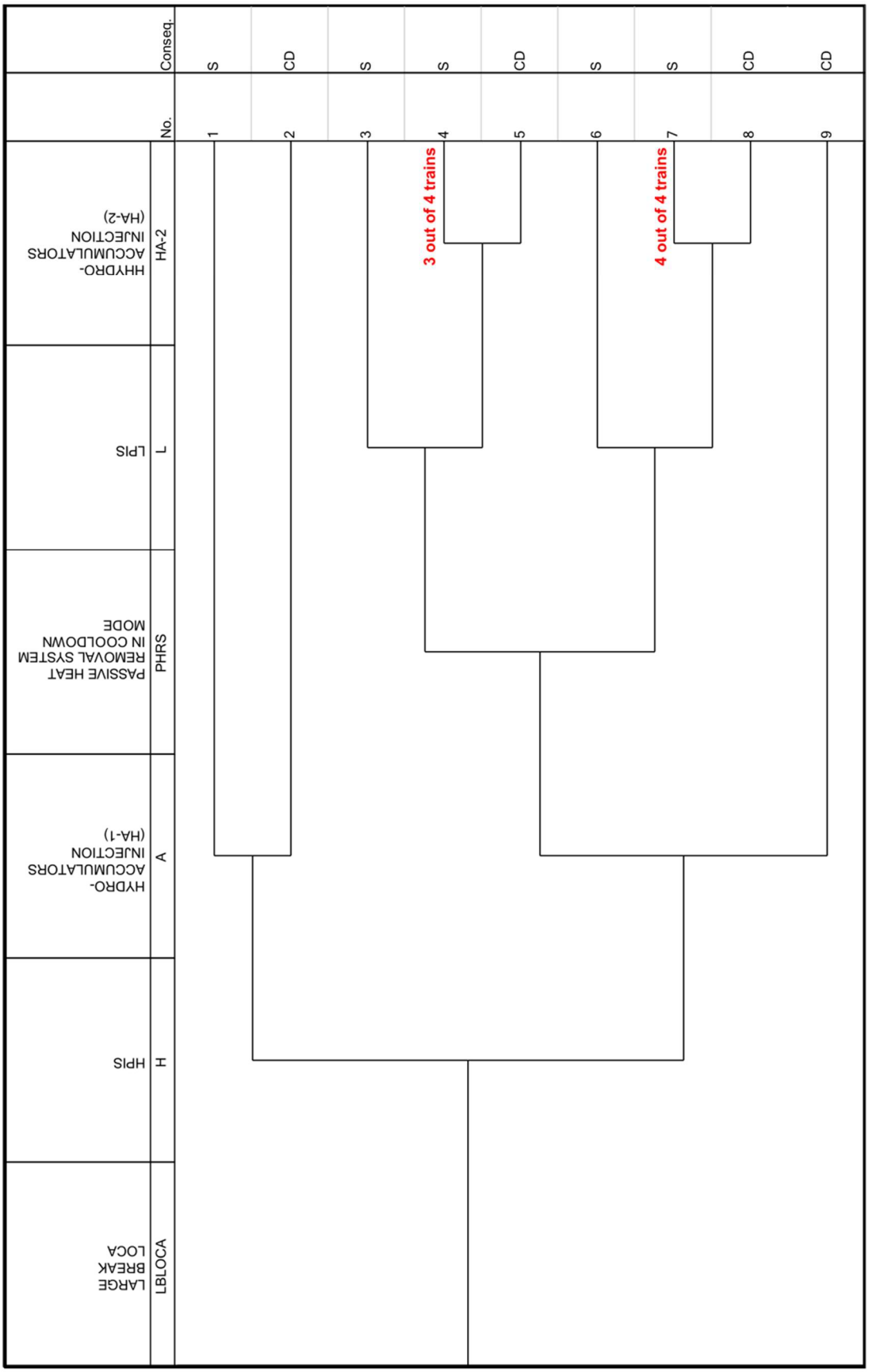

Figure 6-78 LBLOCA ET including the HA-2 and the PHRS

It is noteworthy that in the three proposed ETs with the HA-2 and PHRS headers, there are sequences in which only the headers corresponding to the PSSs are successfully. However, in the standard ETs, the success of some headers related to the active safety systems is mandatory for the sequence to be successful.

Chapter 7.
Summary and final remarks

During the course of this doctoral thesis, a VVER-1000/V320 model has been developed, for the TRACEV5P5 system code, including human actions and two PSSs found in Gen-III/III+ VVER reactors, the HA-2 and the air-cooled PHRS.

Using the developed TRACEV5P5 model, LBLOCA, MBLOCA and SBLOCA sequences have been analyzed first. These analyses have provided an in-depth understanding of the configurations, actuation signals and capabilities the conventional safety systems incorporated in VVER-1000/V320 reactors. In addition, they provided insights into the human actions implemented in these reactors to manage sequences where the automatic safety systems on their own are not enough to prevent CD. The main conclusions of this part of the study are as follows:

- The SCs of the MBLOCA and LBLOCA ETs found in the references contain some conservatism. The simulations carried out have made it possible to verify that it is possible to carry out a re-evaluation of the SCs.
- It is possible to consider a re-grouping of the MBLOCA and LBLOCA ETs, proposing other break sizes ranges and SCs that allow for a best-estimated approach.
- EETs have been applied to LBLOCA sequences over 20 inches to DEGB, allowing different SCs to be considered for a single header of ETs.
- The SBLOCA sequences, in case the HPIS is not available, require human actions in order to cool and depressurise the RCS to allow the injection of the HA-1 and LPIS. These management strategies consist of depressurising the RCS through the SGs at maximum RCS cooling or at a controlled RCS cooling rate (30 K/h and 60 K/h); or depressurising the RCS through the EGRS valves in the PZR.
- Depending on the break size, there are management strategies with more available time to perform them than others, and there are even some break sizes in which certain strategies have no available time. Despite this, the

strategy that yields the best results is to depressurise the SGs at an RCS cooling rate of 60 K/h.

- The available times for different management strategies considered for the VVER-1000/V320 reactors are very similar to those for Westinghouse PWR reactors. This is related to the fact that in the 1990s, VVER reactors adopted a Westinghouse EOPs-like approach.

After understanding the response of the developed model for the TRACEV5P5 code, including the safety systems and human actions considered in the Gen-II VVER-1000/V320 reactors, the impact of the PSSs has been studied. This study has mainly focused on sequences under SBO conditions. The following main conclusions are drawn from these studies:

- In LOCA sequences from 3 inches to DEGB, the RCS pressure decreases fast enough to reach the HA-2 pressure setpoint before CD occurs. However, for break sizes smaller than 2 inches, human actions or the actuation of a safety system is necessary to reduce the RCS pressure to reach the HA-2 pressure setpoint.
- In LOCA sequences from 3 inches to DEGB, under SBO conditions, 4 out of 4 available HA-2 trains are able to avoid the CD. However, 3 out of 4 HA-2 trains are only able to cool the core for 8 hours, after that air-cooled PHRS intervention or active ECCS recovery would be required. This is due to the fact that, from this time onwards, the HA-2 power removal potential is less than the decay heat of the core.
- If the actuation of the HA-2 is considered, the TRACEV5P5 analysis of some MB/LBLOCA sequences without SBO have shown that it is possible to relax the combined SCs of the LPIS, HPIS and HA-1
- The air-cooled PHRS in the SG pressure maintenance mode during SBO sequences is capable of cooling the core for at least 24 hours, preventing the RCS from boiling.
- On the one hand, 3 out of 4 air-cooled PHRS trains in RCS cool-down mode during the SBLOCA sequence under SBO conditions, allows the RCS pressure to decrease, reaching the HA-2 setpoint in time to replenish the core before CD is reached. On the other hand, the simulation of the LBLOCA sequence shows that the performance of the design criteria PHRS number

of trains, in RCS cool-down mode, allows to keep the RCS cooled for 24 hours, while the HA-2 is operated with its design criteria (3 out of 4 trains).

- In the sequences analyzed, no negative interactions have found between the HA-2 and the air-cooled PHRS with the conventional safety systems.

The knowledge gained from all these safety analyses, covering both the conventional and passive safety systems of the Gen-III/III+ VVER, has led to the proposal of new ETs for the SBLOCA, LBLOCA and LOOP sequences to be used in a hypothetical VVER-1000/V320 reactor incorporating the HA-2 and the air-cooled PHRS systems.

As a final conclusion of this doctoral thesis, it can be stated that this work has significantly contributed to the open literature, not only by providing safety analysis on the design of the VVER-1000/V320 reactor, but also by addressing the passive safety systems integrated in Gen-III/III+ VVER reactors. This is particularly important as there are very few public studies on Gen-II or Gen-III/Gen-III+ VVER reactors.

This study has enhanced the understanding of the VVER-1000/V320 reactors, one of the most built nuclear reactors in the world, with 25 units currently in operation. It is an important contribution to improving the nuclear safety assessment of new VVER reactors based on the well-established VVER-1000/V320 technology.

Numerous countries, including Russia, China, India, Hungary, Slovakia, the Czech Republic, Bulgaria, Turkey, and Bangladesh, either operate VVER reactors or are integrating them into their energy strategies. The impact of this research extends beyond technical insights, highlighting the global significance of the VVER reactor designs.

References

Agrawal, S., Chauhan, A., Mishra, A., 2006. The VVERs at KudanKulam. Nuclear Engineering and Design 236, 812–835. https://doi.org/https://doi.org/10.1016/j.nucengdes.2005.09.030

Ahmed Pirouzmand, R., Shahabinejad, A., 2021. Thermo-hydraulic analysis of the safety system of the passive heat recovery reactor VVER1000 with use code RELAP5 (in Persian). Technology and nuclear energy 4, 32–42.

Andruschenko, S.A., Afrov, A.M., Vasiliev, B.Y., Generalov, V.N., Kosourov, K.B., Semchenkov, Y.M., Ukrainets, V.F., 2010. VVER-1000 Nuclear Power Plants. From the physical principles of operation to the evolution of the design (in Russian).

Araneo, D.A., 2008. Realization of a Methodology for the assessment of "Best Estimate" codes for the analysis of nuclear systems and application to Cathare2 V2.5 code. Università di Pisa PhD Thesis.

AREVA, 2007. Fundamental safety overview. Volume 1: Head document. Chapter A: EPR design description.

AREVA, n.d. AREVA Design Control Document Rev. 1 - Tier 2 Chapter 06 - Engineered Safety Features - Section 6.3 Emergency Core Cooling System.

Asmolov, G., Gusev, I.N., Kazanskiy, V.R., Povarov, V.P., Statsura, D.B., 2017. New generation first-of-the kind unit – VVER-1200 design features. Nuclear Energy and Technology 3, 260–259. https://doi.org/https://doi.org/10.1016/j.nucet.2017.10.003

Asmolov, V.G., 2009. Development of the NPP designs based on the VVER technology, in: Https://Www.Oecd-Nea.Org/Mdep/Events/Conf_sept_2009/Conference-Presentations/Session%204%20-1-4%20-%20ROSATOM.Pdf. Paris, France.

Asmolov, V.G., 2011. Passive safety in VVERs. https://www.neimagazine.com/analysis/passive-safety-in-vvers/ [WWW Document]. Nuclear Engineering International.

Atomenergoproekt, 2021. VVER-TOI Design. Available: https://www.rosatom.ru/upload/ iblock/4c2/ 4c287b01028620e7f17ee1b50f8c93af.pdf. [Accessed 2021] [WWW Document].

Ayhan, H., Sokmen, C.N., 2016a. Design and modeling of the passive residual hear removal system for VVERs. Ann Nucl Energy 95, 109–115. https://doi.org/https://doi.org/10.1016/j.anucene.2016.05.003

Ayhan, H., Sokmen, C.N., 2016b. Investigation of passive residual hear removal system for VVERs: effect of finned type heat exchanger tubes. Appl Therm Eng 108, 466–474.

Ayhan, H., Sokmen, C.V., 2015. Determination of geometrical and operating parameters of PRHRS for VVER reactors: cooling by natural circulation of atmospheric air, in: 24th International Conference Nuclear Energy for New Europe (NENE). Portoroz, Slovenia.

Bajorek, S., 2007. AP1000 Passive Safety Systems. AP1000 Design Workshop. AP1000 Design Workshop.

Bánáti, J., Ézsol, G., 1997. Simulation of some emergency operating procedures for VVER-440 reactors. NE-Vol.21, Proceedings of the ASME Nuclear Engineering Division.

Begun, B. V, Gorbunov, O. V, Kadenko, I.N., Pismenny, E.N., Zenyuk, A.Y., Litvinsky, L.L., 2000. Probabilistic safety analysis of a nuclear power plant (PSA). Ministry of education and science of Ukraine.

Belarus nuclear regulatory authority, 2017. National report of the republic of Belarus on the Belarusian NPP (Stress test). Minsk.

Belozerov, V.I., Zhuk, M.M., Terekhova, A.M., 2019. Investigation of the small break conditions in the primary circuit of a VVER-1000 reactor. Nuclear Energy and Technology 5(1): 47–52.

Berkovich, V.M., Korshunov, A.S., Taranov, G.S., Kalyakin, S.G., Morozov, A. V., Remizov, O. V, 2006. Development and Validation of a technology for removal of noncondensing gases to ensure the operability of a passive heat removal system. Atomic Energy 100.

Bezlepkin, V., Semashko, S., Alekseev, S., Ivanova, M., Vardanidze, T., Petrov, Y., 2014. Improvement of the system for passive heat removal through steam generators (SG PHRS) in NPP VVER-1200 in the light of “Fukushima”

accident), in: Proceedings of the 2014 22nd International Conference on Nuclear Engineering (ICONE22). Prague, Czech Republic.

Bharat Heavy Electricals Limited, n.d. Technical Conditions of Contract (TCC). Volume-ia, Part-II, Chapter-2. Technical specifications and scope of work detailed. https://bhel.com/sites/default/files/tcc_2-1605099120.pdf.

Bica, M., 1999. EOPs at NPP Temelin analytical support for EOPs verification, in: RER/9/046 Workshop on Development and Validation of EOP/AMG. Bratislava, Slovakia.

Blaha, M., 2014. Validation of the TRACE code using PSB-VVER experiments, in: Proceedings of the 2014 15th International Scientific Conference on Electric Power Engineering (EPE).

Bryk, R., Mull, T., Schmidt, H., 2019. Experimental investigation of LWR passive safety systems performance at the INKA test facility. E3S Web of Conferences. Research & development in power engineering, Research & development in power engineering 137, 01035.

Buchholz, S., Krussenberg, A., Schaffrath, A., 2015. Safety and International Develpment of Small Modular Reactors (SMR) - A Study of GRS. Atw. Internationale Zeitschrift fuer Kernenergie 60, 645–653.

Buchholz, S., Ricotti, M., Martin, O., Thuy, N., Lombardo, A., Kornytskyi, N., Kaliatka, A., 2020. Improved safety features of LWR-SMR. WP 1: Identification of improved safety features of LW-SMRs (ELSMOR), WP 1: Identification of improved safety features of LW-SMRs (ELSMOR). Ref. Ares (2020)2308093.

Bui, T.H., Tran, C.T., 2015. Evaluation of VVER-1200/V491 reactor pressure vessel integrity during large break LOCA along with SBO using MELCOR 1.8.6. ISSN 1810-5408. Nuclear Science and Technology 5, 54–63. https://doi.org/https://doi.org/10.53747/jnst.v5i4.207

Burgazzi, L., 2012. Chapter 2 Reliability of Passive Systems in Nuclear Power Plants, in: NUCLEAR POWER – PRACTICAL ASPECTS. Wael Ahmed.

Bykov, M., 2013. Safety System of Reactor Plant V-491 and Safety Analyses Resuts, in: 7th INPRO Dialogue Forum on Sustainability of Nuclear Energy Systems Based on Evolutionary Reactors.

ČEZ, 2012. Stress tests of nuclear power plants – ČEZ, a.s. Evaluation of nuclear safety and safety margins of Temelin NPP (on the background of events at the Fukushima NPP).

Chatterjee, B., Kumar, R., Mukhopadhyay, D., Lele, H.G., Ghosh, A.K., Kushwaha, H.S., 2008a. Inter code comparision of severe accident analysis for VVER-1000, in: The 7th International Topical Meeting on Nuclear Reactor Thermal Hydraulics, Operation and Safety (NUTHOS-7). Seoul, Korea.

Chatterjee, B., Mukhopadhyay, D., Lele, H.G., Ghosh, A.K., 2008b. Effect of break size on severe core damage behaviour for VVER 1000 reactor with the ASTEC V1 code. Paper 8295, in: International Congress on Advances in Nuclear Power Plants (ICAPP 08). Anaheim, CA USA.

Chatterjee, B., Mukhopadhyay, D., Lele, H.G., Ghosh, A.K., Groudev, P., Atanasova, B., 2009. Influence on steam generator inventory on severe core damage behaviour during SBO for VVER 1000 reactors, in: Proceedings of Bulgarian Nuclear Society Nuclear Power for the People Conference. Veliko Tarnovo, Bulgaria.

Chatterjee, B., Mukhopadhyay, D., Lele, H.G., Ghosh, A.K., Kushwaha, H.S., Groudev, P., Atanasova, B., 2010. Analyses for VVER-1000/320 reactor for spectrum of break sizes along with SBO. Ann Nucl Energy 37, 359–370.

Chaudhary, S., Krishna Kumar, P., Rammohan, H.P., 2017. Study of performance of passive air cooled heat exchangers as a safety system for nuclear power plants, in: Proceedings of the 24th National and 2nd International ISHMT-ASTFE. Heat and Mass Transfer Conference (IHMTC-2017). BITS Pilani, Hyderabad, India.

Cherubini, M., Muellner, N., D'auria, F., Petrangeli, G., 2008. Application of an optimized AM procedure following a SBO in a VVER-1000. Nuclear Engineering and Design 238, 74–80. https://doi.org/https://doi.org/10.1016/j.nucengdes.2007.04.016.

Chetal, S.C., 2011. 500 MWe PFBR: Concept to Realisation and Approach for Future 500 MWe FBRs. Vienna, Austria.

China Nuclear Engineering Group Corporation (CNEC), 2019. HTR PM Technology (Pebble Bed Reactor). https://www.youtube.com/watch?v=op_Zzscs73U [WWW Document].

Choi, J.-B., 2009. Status of Fast Reactor and Pyroprocess Technology Development in Korea, in: International Conference on Fast Reactors and Related Fuel Cycles (FR09). Kyoto, Japan.

Chul-Hwa, S., Jong-Kyun, P., 2004. Thermal-hydraulic Experiments and the Evaluation of the New Safety Features in the APR1400. IAEA-CN-114/E-8.

D. C. Cacuci (ed.), 2010. VVER Type reactors of Russian design. Handbook of Nuclear Engineering (Chapter 20), Springer. ed.

De Grandis, S., Apostol, M., Saverio Nitt, F., 2019. D1: Project Presentation. Passive Isolation Condenser. PIACE project, Passive Isolation Condenser. PIACE project.

Del Nevo, A., D'Auria, F., 2007. Comparative study of the thermal-hydraulic system codes performances in predicting experiments performed in VVER-1000 simulator, in: The 5th International Conference "Safety Assurance of NPP with WWER" FSUE OKB "GIDROPRESS." Podolsk, Russia.

Deng, J., Dang, G., Ding, S., Qiu, Z., 2020. Analysis of post-LOCA long-term core safety characteristics for the Small Modular Reactor ACP100. Ann Nucl Energy 142, 107349. https://doi.org/https://doi.org/10.1016/j.anucene.2020.107349

Dina, A., Nikonov, S., Travleev, A., 2019. The first circuit of VVER-1000 and the most dangerous places of LBLOCA as a source of dynamic load on the equipment, in: 11th International Scientific and Technical Conference Safety Assurance of NPP with VVER. Podolsk, Russia.

Dolganov, K.S., 2024. Integral simulation of the first 3 weeks of severe accident at Fukushima Daiichi Unit 1 with SOCRAT code. Part I – Qualification of model and simulation of the initial phase. Nuclear Engineering and Design 416. https://doi.org/https://doi.org/10.1016/j.nucengdes.2023.112771

Ebrahimgol, H., Aghaie, M., Zolfaghari, A., 2021. Evaluation of ATFs in core degradation of a PWR in unmitigated SBLOCA. Ann Nucl Energy 152, 107961. https://doi.org/https://doi.org/10.1016/j.anucene.2020.107961

Egorov, M., Kasatkin, I., Kovalenko, I., Krectunova, I., Lavrovskaya, N., Litvinova, N., 2020. Russian and foreign steam generators for NPP power units with wet steam turbines. E3S Web of Conferences 178, 01007 (2020). https://doi.org/10.1051/e3sconf/202017801007.

Eisenhut, D.G., 1982. Inadequate Core Cooling Instrumentation System. Generic Letter 82-28. USNRC.

Ekariansyah, A.S., Widodo, S., Susyadi, Tjahjono, H., 2021. Preliminary assessment of engineered safety features against station blackout in selected PWR models. Tri Dasa Mega 23, 47–56.

Elkin, I.V., Melikhov, O.I., Melikhov, V.I., Nikonov, S.M., Kapustin, A.V., Selkin, S.S., 2018. Experimental studies in the PSB-VVER bench of thermal hydraulics of emergency modes at NPPs with VVER-TOI (in Russian). Technologies for supporting the life cycle of NPP 4.

Environment Agency Austria, 2019. Technical data of the nuclear power plant (in German). 43-814.203.004.OE.13.03. https://www.umweltbundesamt.at/fileadmin/site/themen/energie/kernenergie/verfahren/ukraine/uvp_k3_4/2019/uebersetzungen2019/13_03_2_technische_daten_des_kraftwerksblocks.pdf.

EPRI, 2011. Education of Risk Professionals Module 3: Initiating Events, Accident Sequences and Success Criteria. 1022996 final Report.

European commission EuropeAid Co-operation Office, 2006. TACIS PROJECT R2.03/97. Software development for accident analysis of VVER and RBMK reactors in Russia. Part A (VVER-1000). Final technical report. EC Contract 30303.

Fadaei, A.H., Setayeshi, S., 2009. Control rod worth calculation for VVER-1000 nuclear reactor using WIMS and CITATION codes. Progress in Nuclear Energy 51, 184–191.

Federal Environmental, 2005. Industrial and Nuclear Supervision Service of Russia (Rostechnadzor) with support from the U.S. Nuclear Regulatory Commission, Kalinin VVER-1000 nuclear power station unit 1 PRA (beta project), NUREG/ IA-0212 1.

Fennovioma, 2015. FH1 Program Preliminary Safety Analysis Report Chapter 1: General Plant. Helsinki, Finland.

Fil, N., Allen, P., Kirmse, R., Kurihara, M., Oh, S., Sinha, R., 1999. Balancing passive and active systems for evolutionary water cooled reactors. IAEA-SM-353/18.

Fortava, A., 2018. VVER-1000 pressurizer system and control modelling in DYMOLA. Master Thesis in Czech Technical University in Prague.

Freixa, J., Laborda, A., Martinez-Quiroga, V., 2021. Effectiveness of the ASVAD valve in a reactor vessel bottom leak scenario. Ann Nucl Energy 160, 108387. https://doi.org/https://doi.org/10.1016/j.anucene.2021.108387

GadEl-karim, K., Badawi, A., EmadEl-Din, A., Abo Elnour, A.G., 2025. Investigation of Thermal Hydraulics Parameters of VVER-1000/V-320 during LOCA Accident. Arab Journal of Nuclear Sciences and Applications 58, 65–73. 10.21608/ajnsa.2024.321389.1853.

Galiev, K.F., Yaurov, S. V, Goncharov, Ye. V, Volnov, A.S., 2017. Experience of commissioning of the V-392M reactor plant passive heat removal system. Nuclear Energy and Technology 3, 291–196. https://doi.org/https://doi.org/10.1016/j.nucet.2017.11.003

Gavrilas, M., Hejzlar, P., Todreas, N.E., Shatilla, Y., 1995. Safety Features of Operating Light Water Reactors of Western Design, CRC. ed.

GE Hitachi Nuclear Energy, 2014. ESBWR Design Control Document. Engineered Safety Features. Chapter 6. 26A6642AT. Revision 10.

Gencheva, R., Groudev, P.P., 2000. Investigation of Steam Generator tube rupture accident for VVER-1000. Institute for nuclear research and nuclear energy. Annual report 2001.

Gencheva, R. V, Stefanova, A.E., Groudev, P.P., 2005. RELAP5/MOD3.2 investigation of reactor vessel YR line capabilities for primary side depressurization during the TLFW in VVER1000/V320. Ann Nucl Energy 32, 1407–1434. https://doi.org/https://doi.org/10.1016/j.anucene.2004.12.003.

General Nuclear System, 2021. Pre-Construcion Safety Report. Chapter 7. Safety Systems. HPR/GDA/PCSR/0007.

Georgieva, E., Ivanov, K., Stieglitz, R., 2015. Explicit modeling of a VVER-1000 radial reflector by a ring of assembly-size nodes. Paper 15075, in: Proceedings of ICAPP 2015. Nice, France.

Ghazanfari, V., Ansarifar, G.R., Esteki, M.H., 2014. Drift flux modeling of the VVER-1000 horizontal nuclear steam generator. Progress in Nuclear Energy 76, 36–43. https://doi.org/https://doi.org/10.1016/j.pnucene.2014.04.021

Gibson-Daud-Thulu, F., Elshahat, A., Hassan, M.H.M., 2021. Simulation of VVER-1000 guillotine large break Loss of coolant accident using RELAP5/SCDAPSIM/ MOD3.5. Journal of Nuclear Engineering 2, 516–532. https://doi.org/https://doi.org/10.3390/jne2040035

Gluekler, E.L., 1997. U.S. ADVANCED LIQUID METAL REACTOR (ALMR). Progress in Nuclear Energy 31, 43–61. https://doi.org/https://doi.org/10.1016/0149-1970(96)00003-0

Grant, G.M., Poloski, J.P., Gentillon, C.D., Galyean, W.J., 1996. Isolation Condenser System Reliability. INEL-95/0478. NUREG/CR-5500, Volume 6.

Groudev, P., Andreeva, M., 2016. Study of Accident Progression in Unsealed WWER-1000/V320 Reactor during Maintenance. Journal of Power and Energy Engineering 4, 68–78.

Groudev, P., Hadjiev, V., 2001. Analytical validation of EOPs for Kozloduy NPP VVER 1000, in: WANO-MC Workshop "Emergency Operating Instructions: Validation, Inculcation of EOI and Personnel Training." Paks NPP, Hungary.

Groudev, P., Kitchev, E., 1998. Station Blackout with reduction of pressure in primary circuit, in: Information Exchange Forum on Analytical Methods and Computational Tools for NPP Safety Assessment. Obninsk, Russia.

Groudev, P., Kitchev, E., Slovik, G., 1997. Opening and Stuck Open of Pressurizer Safety Valve, in: International Information Exchange Forum on ANALYTICAL METHODS AND COMPUTATIONAL TOOLS FOR NPP SAFETY ASSESSMENT. Proceedings of ANL/USA. Obninsk, Kaluga Region, Russia.

Groudev, P., Pavlova, M., 2004. Simulation of Loss-Of-Flow transient in a VVER-1000 nuclear power plant with RELAP5/MOD3.2. Progress in Nuclear Energy 45, 1–10.

Groudev, P., Pavlova, M., 2002. RELAP5/MOD3.2 investigation of a VVER-1000 MCP switching on problem, in: The Tenth International Conference on Nuclear Engineering (ICONE 10). Arlington, Virginia, USA.

Groudev, P.P., 1998. Analyzing SBLOCA in Support of EOP Development, in: Bulgarian Nuclear Society. Sofia, Bulgaria, pp. 18–19.

Groudev, P.P, Georgieva, E.L., 2010. Loss of 'Core cooling' at low power and cold condition of VVER-1000/V320. Progress in Nuclear Energy 52, 229–235.

Groudev, P. P, Georgieva, E.L., 2010. Loss of 'Core cooling' at low power and cold condition of VVER-1000/V320. Progress in Nuclear Energy 52, 229–235. https://doi.org/https://doi.org/10.1016/j.pnucene.2009.06.017.

Heung Chang, S., Ho Kim, S., Young Choi, J., 2013. Design of integrated passive safety system (IPSS) for ultimate passive safety of nuclear power plants. Nuclear Engineering and Design 260, 104– 120. https://doi.org/https://doi.org/10.1016/j.nucengdes.2013.03.018

Hossain-Khan, A., Al-Imran, M.I., Fyza, N., Sarkar, M., 2019. A numerical study on the transient response of VVER-1200 plant Parameters during a large-break Loss of coolant accident. Indian J Sci Technol 12. https://doi.org/10.17485/ijst/2019/v12i27/145294

Hosseini, S.A., Najafi, A., Shirani, A.S., Queral, C., D'Auria, F., 2024. Prolonged operation of hydro-accumulators in VVER-1000/V446 considering flow restriction components. Nuclear Technology. https://doi.org/10.1080/00295450.2024.2337313. https://doi.org/https://doi.org/10.1080/00295450.2024.2337313

Hosseini, S.A., Shirani, A.S., Zangian, M., Najafi, A., 2020. Re-assessment of accumulators performance to identify VVER-1000 vulnerabilities against various break sizes of SB-LOCA along with SBO. Progress in Nuclear Energy 119. https://doi.org/https://doi.org/10.1016/j.pnucene.2019.103145

Huang, X., Zong, W., Wang, T., Lin, Z., Ren, Z., Lin, C., Yin, Y., 2020. Study on typical design basis conditions of HPR1000 with nuclear safety analysis code ATHLET. Frontiers in Energy Research. https://doi.org/10.3389/ fenrg.2020.00127. https://doi.org/https://doi.org/10.3389/fenrg.2020.00127

IAEA, 2019. Passive Safety Systems in Water Cooled Reactors: An Overview and Demostration with Basic Principle Simulators.

IAEA, 2017. Technical meeting on the status and evaluation of severe accident simulation codes for water cooled reactos. Vienna, Austria.

IAEA, 2016. Design Safety Considerations for Water Cooled Small Modular Reactors Incorporating Lessons Learned from the Fukushima Daiichi Accident.

IAEA, 2013. Defence in Depth — Advances and Challenges for Nuclear Installation Safety," in International Conference on Topical Issues in Nuclear Installation Safety. Vienna, Austria.

IAEA, 2012. Natural circulation phenomena and modelling for advanced water cooled reactors. IAEA-TECDOC-1677.

IAEA, 2011a. Status report 82 - KERENATM (KERENATM).

IAEA, 2011b. WWER-1000 reactor simulator. Material for Training Courses and Workshops. Third Edition.

IAEA, 2009. Passive safety systems and natural circulation in water cooled nuclear power plants. IAEA-TECDOC-1624.

IAEA, 2001. Fuel behaviour under transient and LOCA conditions, in: Proceedings of a Technical Committee Meeting. Halden, Norway.

IAEA, 2000. Performance of operating and advanced light water reactor designs. IAEA-TECDOC-1245, in: Technical Committee Meeting. Munich, Germany.

IAEA, 1999. Status of liquid metal cooled fast reactor technology. IAEA-TECDOC-1083.

IAEA, 1994. Technical feasibility and reliability of passive safety systems for nuclear power plants, in: Proceedings of an Advisory Group Meeting. IAEA-TECDOC-920, Germany.

IAEA, 1991. Safety related terms for advanced nuclear plants. IAEA-TEDOC-626.

Ibánez, L., Hortal, J., Queral, C., Gómez-Magán, J., Sánchez-Perea, M., Fernández, I., Meléndez, E., Expósito, A., Izquierdo, J.M., Gil, J., Marrao, H., Villalba-Jabonero, E., 2016. Application of the Integrated Safety Assessment methodology to safety margins. Dynamic Event Trees, Damage Domains and Risk Assessment. Reliab Eng Syst Saf 147, 170–193. https://doi.org/https://doi.org/10.1016/j.ress.2015.05.016.

IEEE, 2002. IEEE Standard Criteria for Accident Monitoring Instrumentation for Nuclear Power Generating Stations Std. 497-2002. Institute of Electrical and Electronics Engineers.

Iegan, S., Mazur, A., Vorobyov, Y., Zhabin, O., Yanovskiy, S., 2018. TRACE VVER-1000/V-320 Model Validation. NUREG/IA-0490.

Ivanov, B., Ivanov, K., Groudev, P., Pavlova, M., Hadjiev, V., 2004. VVER-1000 COOLANT TRANSIENT BENCHMARK – PHASE 1. Volume 1 Final specifications. Paris, France.

Jensen, S.E., Ølgaard, P.L., 1995. Description of the Prototype Fast Reactor at Dounreay. Riso National Laboratory. DK-4000 Roskilde, Denmark.

Kaliatka, A., 2017. Issues related to the safety assessment of the SMR concepts, in: Technical Meeting on Challenges in the Application of the Design Safety Requirements for Nuclear Power Plants to Small and Medium Sized Reactors. Vienna, Austria. .

Kardos, T., Orosz, R., Kardos, B., Biró, B., Aszódi, A., 2024. Analysis of a PSB-VVER small break LOCA experiment with APROS and TRACE system codes. Ann Nucl Energy 206. https://doi.org/https://doi.org/10.1016/j.anucene.2024.110662

Kasapoglu, B., Sezen, H., Aldemir, T., Denning, R., 2024. Dynamic seismic probabilistic risk assessment of nuclear power plants using advanced structural methodologies. Nuclear Engineering and Design 427, 113416.

Khalil Mousavian, S., D'Auria, F., Galassi, G.M., Petruzzi, A., Salehi, M.A., 2003. Uncertainty Analysis of LB-LOCA in VVER-1000 Geometry, in: International Conference Nuclear Energy for New Europe (NENE 2003). Portorož, Slovenia.

Khubchandani, P., Srivastava, A., Lele, H.G., 2013a. Reliability assessment of passive heat removal system of VVER-1000 at Kudankulam NPP, in: The 15th International Topical Meeting on Nuclear Reactor Thermal - Hydraulics, NURETH-15. Pisa, Italy.

Khubchandani, P., Srivastava, A., Lele, H.G., 2013b. Reliability assessment of the passive heat removal system of the VVER-1000 reactor at Kudankulam NPP. Kerntechnik 78, 489–495. https://doi.org/10.3139/124.110362

Kim, Y.-S., Kang, K.-H., Park, H.-S., 2020. Investigation of CMT behavior between the ATLAS and SMART-ITL tests. Ann Nucl Energy 135, 106979. https://doi.org/https://doi.org/10.1016/j.anucene.2019.106979

Kolev, N., Petrov, N., Donov, J., Angelova, D., Aniel, S., Royer, E., Nikonov, S., 2006. VVER-1000 Coolant Transient Benchmark - Phase 2 (V1000CT-2). Vol. 11: MSLB Problem - Final Specifications. NEA/NSC/DOC(2006)6, Phase. MSLB Problem - Final Specifications.

Komolov, V.M., Evdokimenko, V.V., Piminov, V.A., Tregubov, I.O., Tsofin, V.I., Margolin, B.Z., Sorokin, A.A., Minkin, A.I., Zhemkov, I.Y., Neustroev, V.S., Shamardin, V.K., 2019. Role of JSC OKB "GIDROPRESS", JCS "GNC NIIAR" and CNII KM "PROMETEY" in international project TACIS 2002 (R2/01.02),

in: The 11th Conference on Reactor Materials Science Dedicated to the 55th Anniversary of the RIARs Reactor Materials Testing Complex.

Kopytov, I.I., Kalyakin, S.G., Berkovich, V.M., Morozov, A. V, Remizov, O. V, 2009. Experimental investigation of non-condensable gases effect on Novovoronezh NPP-2 steam generator condensation power under the condition of passive safety systems operation, in: Proceedings of the 17th International Conference on Nuclear Engineering (ICONE17). Brussels, Belgium.

Kopytov, I.I., Maltsev, M.B., Taranov, G.S., Kalyakin, S.G., Remizov, O. V, Morozov, A. V, 2011. Experimental study of NV NPP-2 steam generator model operation in condensation mode by steady states technique, in: 19th International Conference on Nuclear Engineering (ICONE19). Chiba, Japan.

Korea Hydro & Nuclear Power Co., 2012. Fluidic Device Design for the APR1400. APR1400-Z-M-TR-12003-NP Rev.0.

Kovacs, Z., 2014. Probabilistic Safety Assessment of WWER440 Reactors: Prediction, Quantification and Management of the Risk, Springer. ed. Bratislava, Slovakia.

Kral, P., Macek, J., Hofmann, E., Trnka, M., 2011. Thermal hydraulic analyses for optimization of hydroaccumulator parameters in VVER-440, in: The 14th International Topical Meeting on Nuclear Reactor Thermalhydraulics, NURETH-14. Toronto, Canada.

Kurisaka, K., 2012. Study on Preliminary Level-1 PSA for Japan Sodium-Cooled Fast Reactor. NEA/CSNI/R(2012)2, in: Workshop on PSA for New and Advanced Reactors OECD Conference Centre. Paris, France.

Kuzmanov, B., 2021. 3D Computer Simulator of VVER-1000/V-320 Systems, Equipment and Plant Layout. https://www.youtube.com/watch?v=v9T1LsqNv0o [WWW Document].

Laaksonen, L., 2015. Advanced safety features of 3rd generation VVER plants, in: OECD/NEA Workshop on Innovations in Water-Cooled Reactor Technologies. Paris, France.

Lebezov, A.A., Morozov, A. V, Shlepkin, A.S., Sakhipgareev, A.R., Soshkina, A.S., 2024. Experimental study of heat and mass transfer processes affecting the duration of operation of VVER passive core cooling systems. Nuclear Engineering and Desing 419. https://doi.org/https://doi.org/10.1016/j.nucengdes.2024.112963

Lee, J., Cho, N.Z., 2006. AFEN method and its solutions of the hexagonal three-dimensional VVER-1000 benchmark problem. Progress in Nuclear Energy 48, 880–890. https://doi.org/https://doi.org/10.1016/j.pnucene.2006.06.009

Li, Y., Zhang, D., Sun, D., Zan, Y., Xi, Z., Zhuo, W., Li, P., 2021. Experimental investigation on steam contact condensation in emergency makeup tank. Nuclear Engineering and Design 384, 111470. https://doi.org/https://doi.org/10.1016/j.nucengdes.2021.111470

Linn, P.A., Julian, H. V, Chapman, J.R., Trifanov, A., Zhabin, O., Fedorchenko, S., Rybchuk, A., 2002. Applying U.S. EOP analytical justification experience for VVER plants in the Ukraine, in: 10th International Conference on Nuclear Engineering, ICONE10-22640. Arlington, VA.

Lityshev, A., Hvostov, M., Pantyushin, S., Shchekoldin, V., Bukin, N., Bykov, M., Dolganov, K., Kapustin, A., Tomashchik, D., Kiselev, A., 2013. Analysis of AES-2006 VVER severe accidents with SOCRAT code and cross-verification with thermal-hydraulic codes TECH-M-97 and KORSAR/GP for the initial accident phase., in: The 15th International Topical Meeting on Nuclear Reactor Thermal - Hydraulics (NURETH-15). Pisa, Italy.

Luciano, N.P., Collins, P.E., Maldonado, G.I., Gauld, I., 2016. Modeling and simulation of an operational VVER-1000 benchmark with NESTLE, in: 2016 International Congress on Advances in Nuclear Power Plants (ICAPP 2016). San Francisco, CA, USA.

Lutz, R.J., 2004. Post-Accident Monitoring Instrumentation Re-Definition for Westinghouse NSSS Plants. Technical Report WCAP-15981-NP. WestinghouseElectric Company.

Ma, Y., Zhang, J., Wang, M., Tian, W., Chen, R., Wu, Y., Su, G.H., Qiu, S., 2021. Performance analysis of PRHRS in primary and secondary circuit for offshore floating nuclear plant. Ann Nucl Energy 164. https://doi.org/https://doi.org/10.1016/j.anucene.2021.108580

Macek, J., Vyskocil, L., 2013. Simulation of SDA opening test at VVER-1000 NPP by coupled system of ATHLET, DYN3D and FLUENT codes, in: The 15th International Topical Meeting on Nuclear Reactor Thermal - Hydraulics (NURETH-15). Pisa, Italy.

Malakhov, A.A., du Toit, M.H., Avdeenkov, A.V., Bessarabov, G. d, 2024. Numerical modelling of catalytic hydrogen combustion in passive autocatalytic recombiners: A review. Progress in Nuclear Energy 171.

Maltsev, M., 2015. Additional information on modern VVER GEN III Technology. Paris, France.

Mascari, F., Bersano, A., Alcaro, F., Stempniewicz, M., Albright, L., Jevremovic, T., Andrews, N., Gauntt, R., Austregesilo, H., Buchholz, S., Bellomo, A., D'Auria, F., Di Palma, G., Lanfredini, M., Spina, G., Bertani, C., De Salve, M., Falcone, N., Caruso, G., Giannetti, F., Narcisi, v, Choi, C., Ha, K., Jeon, B.G., Kang, K.H., Kim, K., Park, H.S., Karppinen, I., Lahovský, L.F., Meca, R., Parduba, Z., Lien, P.H., Tomashchik, D.Y., Burgazzi, L., Lombardo, C., Meloni, P., Ferri, R., 2023. OECD/NEA/CSNI/WGAMA PERSEO benchmark: Main outcomes and conclusions. Nuclear Engineering and Design 405, 112220. https://doi.org/https://doi.org/10.1016/j.nucengdes.2023.112220

Mazzini, G., Kyncl, M., Miglierini, B., Kopecek, V., 2015. Analyses of SBO Sequence of VVER1000 Reactor using TRACE and MELCOR Codes, in: 23th International Conference on Nuclear Engineering (ICONE-23). Chiba, Japan.

Melikhov, O.I., Elkin, I.V., Nikonov, S.M., Basov, A.V., Kapustin, A.V., 2008. Final Report OECD PSB-VVER Project (Version 4).

Misak, J., 2024. Chapter 4 - History, specific design features, and evolution of VVER reactors. Nuclear Power Reactor Designs.

Mokhov, V.A., 2010. Advanced designs of VVER reactor plant, in: VVER-2010. Experience & Perspectives. Prague. Czech Republic.

Montero-Mayorga, J., Queral, C., Rivas-Lewicky, J., González-Cadelo, J., 2014. Effects of RCP trip when recovering HPSI during LOCA in a Westinghouse PWR. Nuclear Engineering and Design 280, 389–403. https://doi.org/10.1016/J.NUCENGDES.2014.09.005

Montotut, M., 2021. Progress towards simulation of passive safety systems., in: SNETP FORUM 2021 – Towards Innovative R&D in Civil Nuclear Fission. Virtually.

Morozov, A. V, Remizov, O. V, Kalyakin, D.S., 2014. Experimental investigations of thermal–hydraulic processes arising during Operation of the passive safety systems used in new projects of nuclear power plants equipped with VVER reactors. ISSN 00406015, Thermal Engineering 61, 357–363.

Morozov, A. V, Sakhipgareev, A.R., 2017. Experimental estimation of the effect of contact condensation of steam–gas mixture on VVER passive safety systems operation. Nuclear Energy and Technology 3, 98–104. https://doi.org/https://doi.org/10.1016/j.nucet.2017.05.002

Mousavian, S.K., D'Auria, F., Galassi, G., Petruzzi, A., Salehi, M., 2003. Uncertainty analysis of LB-LOCA in VVER-1000 geometry, in: International Conference Nuclear Energy for New Europe (NENE). Portoroz, Slovenia.

Muellner, N., Giannotti, W., D'Auria, F., 2005. RELAP5 analysis of an EOP based on mobile pumps, at a generic VVER-1000 NPP in case of a total loss of the primary heat sink (for BDBA conditions), in: The 11th International Topical Meeting on Nuclear Thermal-Hydraulics (NURETH-11). Avignon, France.

Muellner, N., 2010. Simulation of Beyond Design Basis Accidents – a Contribution to Risk Analysis of Nuclear Power Plants. Universität Wien PhD thesis.

Najafi, A., Shahsavand, A., Hosseini, S.A., Shirani, A.S., Yousefpour, F., Karimi, K., 2022. Transformation of classical PSA and DSA into the form of conditional event tree: an approach of human action in time dependent core damage risk. Ann Nucl Energy 165. https://doi.org/https://doi.org/10.1016/j.anucene.2021.108662

NEA, 2022. Summary Report of the NEA ATLAS-2 Joint Project.

NEA, 2020. URL. https://www.oecd-nea.org/jcms/pl_23462/working-group-on-analysis-and-management-of-accidents-wgama [WWW Document].

NEA, 2004. URL. https://www.oecd-nea.org/jcms/pl_59465/experimental-thermal-hydraulics-for-analysis-research-and-innovations-in-nuclear-safety-etharinus-project [WWW Document].

Noori-Kalkhoran, O., Minuchehr, A., Rahgoshay, M., Shirani, A.S., 2014. Short-term and long-term analysis of WWER-1000 containment parameters in a large break LOCA. Progress in Nuclear Energy 74, 201–212. https://doi.org/https://doi.org/10.1016/j.pnucene.2014.03.007

NRC, 2017. TRACE V5.840 User Manual: Input Specification. Input Specification, User's Manual.

NRC, 2006. Criteria for Accident Monitoring Instrumentation for Nuclear Power Plants. Regulatory Guide 1.97, Rev. 4.

NRC, 1983. Instrumentation for Light-Water-Cooled Nuclear Power Plants to Assess Plant and Environs Conditions During and Following an Accident. Regulatory Guide 1.97, Rev. 3.

Nuclear Regulatory Agency, 2011. European "stress tests" for nuclear power plants. National report of Bulgaria.

Nu-Power, 2015. Kudankulam-1 in the service of the nation. International Journal of Nuclear Power, ISSN 0971-9911. LC No.:99936677. Vol.27 (1-2).

NuScale Power LLC, 2020. Final Safety Analysis Report (Rev. 5) Chapter 01: Introduction and General Description of the Plant, ADAMS Accession Number: ML20224A481.

NuScale Power LLC, 2019. NuScale Standard Plant Design Certification Application. Introduction and General Description of the plant. Chapter one. Revision 5.

OECD, 2001. Validation matrix for the assessment of thermal-hydraulic codes for LOCA and transients. A report by the OECD support group on the VVER thermal-hydraulic code validation matrix. JT00108841. NEA/CSNI/R(2001) 4.

Parisi, C., D'Auria, F., Mazzini, M., Jankowski, M., 1997. An overview of the TACIS project (R2.03/97) dealing with WWER-1000 and RBMK technologies. IAEA-CN-114/44p.

Pavlova, M., Stefanova, A., Gencheva, R., Groudev, P., 2004. RELAP5/MOD3.2 Preliminary Investigation of a VVER 1000 Loss of Feed Water (LOFW) transient at KNPP, Unit 6, in: Science and Technology Journal of the BgNS, Vol. 9, No 1 Pp 269-275. , ISSN 1310-8727. Plovdiv, Bulgaria.

Pavlova, M.P., Andreeva, M., Groudev, P.P., 2007. RELAP5/MOD3.2 blackout investigation for validation of EOPs for KNPP VVER-1000/V320. Progress in Nuclear Energy 49, 409–427. https://doi.org/https://doi.org/10.1016/j.pnucene.2007.06.001.

Pavlova, M.P., Groudev, P.P., Hadjiev, V., 2008. Systematic approach for the analytical validation of Kozloduy NPP, VVER-1000/V320 symptom-based emergency operating procedures. Progress in Nuclear Energy 50, 27–32. https://doi.org/https://doi.org/10.1016/j.pnucene.2007.10.002.

Petkevich, I.G., Alekhin, G.V., Bykov, M.A., 2011. Solution of the international benchmark with trip of one of the four reactor coolant pumps for VVER-1000

reactor plants using the computer code package KORSAR/GP and COMPLEX reactor nodalization, in: The 14th International Topical Meeting on Nuclear Reactor Thermalhydraulics (NURETH-14). Toronto, Ontario, Canada.

Polunichev, V.I., Shumailov, G.P., Gorbunov, P.A., Grigor'ev, M.M., Plakseev, A.A., Taranov, G.S., 2007. Development and investigation of the regulator of the passive heat-removal system for the Kudankulam nuclear power plant (India). UDC 621.039.562. Atomic Energy 102.

Pouresgandar, M., Safarzadeh, O., Talebi, S., 2022. Evaluation of advanced accumulator in a VVER-1000 reactor in loss of coolant accident. Annals of Nuclear Energy 170, 108988. https://doi.org/https://doi.org/10.1016/j.anucene.2022.108988

Prosek, A., Cizelj, L., Kljenak, I., Tiselj, I., 2022. Deliverable 3.1. Report on identification of the regulatory elements for design of components and systems. CO2-4-NPP project: Innovative sCO2-based heat removal technology for an increased level of safety of nuclear power plants (sCO2-4-NPP - 847606).

Qiu, Z., Yu, H., Xiong, Q., Cao, X., Tong, L., 2023. Uncertainty and sensitivity analysis of the DVI line break loss of coolant accident for small modular reactor. Progress in Nuclear Energy 157, 1104575. https://doi.org/https://doi.org/10.1016/j.pnucene.2023.104575

Queral. C, Fernandez-Cosials, K., Zugazagoitia, E., Paris, C., Magan, J., Mendizabal, R., Posada, J., 2021. Application of Expanded Event Trees combined with uncertainty analysis methodologies, Reliability Engineering & System Safety. Reliab Eng Syst Saf 205. https://doi.org/https://doi.org/10.1016/j.ress.2020.107246

Queral, C., Gómez-Magán, J., París, C., Rivas-Lewicky, J., Sánchez-Perea, M., Gil, J., Mula, J., Meléndez, E., Hortal, J., Izquierdo, J.M., Fernández, I., 2018. Dynamic event trees without success criteria for full spectrum LOCA sequences applying the integrated safety assessment (ISA) methodology. Reliab Eng Syst Saf 171, 152–168. https://doi.org/10.1016/J.RESS.2017.11.004

Queral, C., Montero-Mayorga, J., Gonzalez-Cadelo, J., Jimenez, G., 2015. AP1000® Large-Break LOCA BEPU analysis with TRACE code. Ann Nucl Energy 85, 576–589. https://doi.org/https://doi.org/10.1016/j.anucene.2015.06.011

Queral, C., Montero-Mayorga, J., Rivas-Lewicky, J., Rebollo, M., 2017. Verification of AP1000 low-margin PRA sequences based on best-estimate calculations.

Ann Nucl Energy 104, 9–27. https://doi.org/https://doi.org/10.1016/j.anucene.2017.02.001

Queral, C., Sánchez-Espinoza, V., Egelkraut, D., Fernández-Cosials, K., Redondo-Valero, E., García-Morillo, A., 2021. Safety Systems of Gen-III/Gen-III+ VVER reactors. Nuclear España. https://doi.org/https://www.revistanuclear.es/wp-content/uploads/2021/10/Art.seguridad-reactores.pdf

Rabiee, A., Kamalinia, A.H., Haddad, K., 2016. Horizontal steam generator thermal hydraulic simulation in typical steady and transient conditions. Nuclear Engineering and Design 305, 465–475. https://doi.org/https://doi.org/10.1016/j.nucengdes.2016.06.004

Rassame, S., Hibiki, T., Ishii, M., 2017. ESBWR passive safety system performance under loss of coolant accident. Progress in Nuclear Energy 96, 1–17. https://doi.org/https://doi.org/10.1016/j.pnucene.2016.12.005

Rijova, N., Steinborn, J., 2008. Analysis Simulator for Kozloduy NPP Units 5 and 6, in: International Nuclear Forum. Bulgarian Nuclear Energy - National, Regional and World Safety. Varna, Bulgaria.

ROSATOM, 2023. Eight heat exchangers of passive heat removal system have been installed at Rooppur NPP Unit 1 [WWW Document]. https://www.rosatom.ru/en/press-centre/news/eight-heat-exchangers-of-passive-heat-removal-system-have-been-installed-at-rooppur-npp-unit-1/#:~:text=PHRS%20is%20a%20passive%20safety,of%20all%20power%20supply%20sources.

ROSATOM, 2022. Course on technological aspects of AES-2006 (VVER-1200) development of nuclear curricula on VVER technology".

ROSATOM, 2021. Historical Overview of Nuclear Engineering in Russia (in Russian). https://ase-ec.ru/en/about/history/ [WWW Document].

ROSATOM, 2019a. Rosatom SMR solutions RITM series [WWW Document]. https://fnpp.info/files/rosatom-smr-solutions-brochure.pdf.

ROSATOM, 2019b. Double-core water-water (in Russian). https://atomicexpert.com/review_vver?ysclid=lv8b424llc317238857 [WWW Document].

Rosenergoatom, 2017. URL. https://www.youtube.com/watch?v=_4iftW-b9PE [WWW Document].

Ryzhov, S.B., Mokhov, V.A., Nikitenko, M.P., Bessalov, G.G., Podshibyakin, A.K., Anufriev, D.A., Gadó, J., Rohde, U., 2010. VVER-Type Reactors of Russian Design. Handbook of Nuclear Engineering. Springer US.

Sabotinov, L., Lutsanych, S., Kadenko, I., 2013. Primary LOCA in VVER-1000 by pressurizer PORV failure, in: Bulgarian Nuclear Society International Conference "Nuclear Energy in Europe - Present and Future." Bulgaria.

Sabotinov, L., Srivastava, A., 2008. Large break Loss of coolant accident analysis of VVER-1000 reactor using CATHARE code, in: Congress on Advances in Nuclear Power Plants (ICAPP '08). Anaheim, CA, USA.

Sanchez-Espinoza, V., Bottcher, M., 2006. Investigations of the VVER-1000 coolant transient benchmark phase with the coupled system code RELAP5/PARCS. Progress in Nuclear Energy, Progress in Nuclear Energy 48, 865–879. https://doi.org/https://doi.org/10.1016/j.pnucene.2006.06.004

Sanchez-Espinoza, V., Gabriel, S., Suikkanen, H., Telkkä, J., Valtavirta, V., Bencik, M., Lestani, H., 2021. The H2020 McSAFER Project: Main Goals, Technical Work Program, and Status. Energies (Basel) 14, 6348. https://doi.org/https://doi.org/10.3390/en14196348

Sanchez-Torrijos, J., Queral, C., París, C., Rebollo, M.J., Sanchez-Perea, M., Posada, J.M., 2022. On the use of time-dependent success criteria within risk-informed analyses. Application to LONF-ATWS sequences in PWR reactors. Nuclear Engineering and Technology. https://doi.org/10.1016/j.net.2022.08.019. https://doi.org/https://doi.org/10.1016/j.net.2022.08.019

Sang-Won, L., Tae-Hyub, H., Mi-Ro, S., Young-Seung, L., Hyeong-Taek, K., 2014. Extended Station Blackout Coping Capabilities of APR1400. Science and Technology of Nuclear Installations ID 980418, 10. https://doi.org/https://doi.org/10.1155/2014/980418

Science Applications International Corporation (SAIC), 1987. Definition of baseline VVER-1000, V320 systems and evaluation of plant response to postulated accidents.

Shahedi, S., Jafari, J., Boroushaki, M., D'Auria, F., 2010. Development of a qualified nodalization for small-break LOCA transient analysis in PSB-VVER integral test facility by RELAP5 system code. Nuclear Engineering and Design 240.

Shi, G., Xu, C., Yan, J., Fan, P., Yang, Z., Cai, X., Zhu, S., 2021. CAP1400 passive core cooling integral testing and application in code validation. Ann Nucl Energy 154, 107997. https://doi.org/https://doi.org/10.1016/j.anucene.2020.107997

Shlepkin, A.S., Morozov, A. V, Sakhipgareev, A.R., 2020. Experimental study of heat transfer processes during the operation of WWER steam generator in emergency mode on a single-tube model. Journal of Physics: Conference Series. XXXVI Siberian Thermophysical Seminar (STS 36).

Shoushtari, M., Jafari, J., Aghaie, M., Vosoughi, N., Nemati, M., 2016. Analysis of accumulators configuration in LB-LOCA for Bushehr NPP. Ann Nucl Energy 92, 96–106. https://doi.org/https://doi.org/10.1016/j.anucene.2016.01.018

Skalozubov, B., Klyuchnikov, A., Kolykhanov, B., 2010. Fundamentals of management of design accidents with loss of coolant at the power plant (in Russian). National Academy of Sciences of Ukraine, Institute of NPP Safety Problems. - Chernobyl (Kiev region): Institute of NPP Safety Issues, 2010. lSBN 978-966-02-5203-5.

Slugen, V., 2011. Safety of VVER-440 Reactors. Barriers Against Fission Products Release, Springer. ed.

Sri Krishna College of Engineering and Technology (SKCET), 2019. KKNN 1.3.4 Field Projects Report. Kudankulam nuclear power plant.

State nuclear regulatory inspectorate of Ukraine, 2011. Stress test results. National report of Ukraine.

Statsura, D.B., Volnov, A.G., Shkalenkov, V.N., Zhirnov, K.V., Topchian, R.M., 2017. Key results of commissioning activities for the emergency and scheduled cooldown system of the AES-2006 unit with the V-392M reactor plant. Nuclear Energy and Technology 3, 278–284. https://doi.org/https://doi.org/10.1016/j.nucet.2017.11.001

Stefanova, A., Gencheva, R., Groudev, P., 2002. Investigation of critial safety function “integrity” in case of steam line break accient for VVER-1000/V320, in: International Conference “12th Symposium of AER.” Sunny Beach.

Sun, D., Xi, Z., Li, Y., Zan, Y., Xiong, W., Li, P., Zhuo, W., 2018. Experimental investigation on natural circulation characteristics of emergency passive residual heat removal system in HPR1000. Progress in Nuclear Energy 103, 1–7. https://doi.org/https://doi.org/10.1016/j.pnucene.2017.11.001

Surip, W., Putra, N., Antariksawan, A.R., 2022. Design of passive residual heat removal systems and application of two-phase thermosyphons: A review. Progress in Nuclear Energy 154, 104473. https://doi.org/https://doi.org/10.1016/j.pnucene.2022.104473

Svetlov, S., 2017. New VVERs in Russia and abroad, in: 4th MDEP Conference on New Reactor Design Activities. London, UK.

Tabadar, Z., Ansarifar, G., Pirozumand, A., 2019. Thermal- hydraulic modeling for deterministic safety analysis of portable equipment application in the VVER-1000 nuclear reactor during loss of ultimate heat sink accident using RELAP5/MOD3.2 code. Ann Nucl Energy 127, 53–67. https://doi.org/https://doi.org/10.1016/j.anucene.2018.11.046

Takeda, T., Inagaki, Y., 2021. High Temperature Gas-cooled Reactors. JSME Series in Thermal and Nuclear Power Generation. ISBN: 978-0-12-821031-4. Elsevier.

Tarantino, M., D'Auria, F., Galassi, G., 2001. Simulation of a large break LOCA on VVER- 1000 NPP by RELAP5/MOD3.2 code, in: ANS/HPS Student Conference. Texas, US.

Tarasov, O.V., Kiselev, A.E., Filippovm, A.S., Yudina, T.A., Grigoruk, D.G., Koshmanov, D.E., Keller, V.D., Khristenko, E.B., 2017. Development and verification of a model of RVK-500, -1000 recombiners for modelling the containment shells of NPP with VVER by computatitonal hydrodynamics. Atomic Energy 121.

TECNATOM, 1999. Introduction to Accident Analysis, TECNATOM Operating Practices Course, PF3T-LA-M12 (in Spanish).

Thi Hoa, B., Chi Thanh, T., 2015. Evaluation of VVER-1200/V-491 Reactor Pressure Vessel integrity during large break LOCA along with SBO using MELCOR 1.8.6. J Nucl Sci Technol 5, 54–63. https://doi.org/https://doi.org/10.53747/jnst.v5i4.207

Turkish Atomic Energy Authority, 2018. European "Stress test" for nuclear power plants. National report of Turkey. Revision 2, National report of Turkey. Revision.

Tusheva, P., 2012. Modelling and analysis of severe accidents for VVER-1000 reactors. Doctoral Thesis in Technische Universität Dresden.

Tusheva, P., Reinke, N., Altstadt, E., Schaefer, F., Weiss, F.P., Hurtado, A., 2009. Analysis of severe accidents in VVER-1000 reactors using the integral code ASTEC. ICONE17-75563, in: Proceedings of the 17th International Conference on Nuclear Engineering (ICONE17). Brussels, Belgium.

Tusheva, P., Schaefer, F., Reinke, N., Weiss, F.-P., 2010. Assessment of early-phase accident management strategies in a Station Blackout scenario for VVER-1000 reactors, in: Proceedings of the 18th International Conference on Nuclear Engineering (ICONE 18). Xi'an, China.

Udalov, Yu.P., Poznyak, I., Srank, J., Sázávaský, P., Kiselova, M., Strejc, M., Votava, P., 2014. Modifications in the Structure of Oxide Corium Melt and Phase Formation During Its Crystallization Caused by Interaction With Sacrificial Concretes of Core Catcher, in: International Conference on Nuclear Engineering. Prague, Czech Republic.

United States General Accounting Office, 1996. Status of U.S. assistance to improve the safety of Soviet-Designed reactors. GAO/RCED-97-5.

U.S. Nuclear Regulatory Commission, 2021. Technical Letter Report: An overview of Non-LWR Vessel Cooling Systems for Passive Decay Heat Removal. ANL/NSE-21/3.

USNRC HRTD, 2011. Pressurized Water Reactor B&W Technology Cross training Course Manual. Chapter 4.0. Emergency Core Cooling System and Nuclear Service Water System.

Varju, T., Orosz, R., Kardos, B., Biró, B., Aszódi, Á., 2024. Analysis of a PSB-VVER small break LOCA experiment with APROS and TRACE system codes. Ann Nucl Energy 206.

Velkov, K., Langenbuch, S., Nikonov, S., 2009. Impact of Modeling Effects, Initial and Boundary Conditions on Performing ATWS Analysis with the Coupled System Code ATHLET/BIPR-VVER, in: The 13th International Topical Meeting on Nuclear Reactor Thermal Hydraulics (NURETH-13). Kanazawa City, Ishikawa Prefecture, Japan.

Veselov, D.O., Tishin, R.E., 2017. WWER reactor plants for AES-92 AND AES-2006. Nuclear España.

VVER working group, 2019. Multinational Design Evaluation Programme (MDEP). Technical Report. TR-VVERWG-06. Preliminary analyses and comparison of design differences between VVER-1000 reactors.

Westinghouse, 2011. Westighouse AP1000 Design Control Document. Engineered Safety Features. Chapter 6, Section 6.3.

Westinghouse owners group, 1983. Emergency response guidelines revision1. Validation program plant.

World Nuclear Association, 2024. URL. https://world-nuclear.org/ [WWW Document].

WWER-1200 Nucleopedia, 2021. URL. https://de.nucleopedia. org/wiki/WWER-1200. Distributed under a CC BY-SA 4.0 license. (Accessed 2021) [WWW Document].

Xing, J., Song, D., Wu, Y., 2016. HPR1000: Advanced pressurized water reactor with active and passive safety. Engineering 2, 79–87. https://doi.org/https://doi.org/10.1016/J.ENG.2016.01.017

Yamada, K., Tuniz, C., 2011. Joint ICTP-IAEA Course on Science and Technology of Supercritical Water Cooled Reactors.

Yang, H., Gao, P., Zhang, B., Cao, S., Li, J., Miao, F., Tang, S., Shan, J., 2024. Study on the lower head failure in severe accidents Part II: Thermal-mechanical coupling behavior analysis on CAP1400 reactor lower head. Ann Nucl Energy 207.

Yeh, S.-E., Xie, H., 2024. CMT and PBL study in the high-pressure phase on the advance core-cooling mechanism experiment with RELAP 5. Ann Nucl Energy 198.

Yücehan-Kutlu, O., 2019. Analysis of VVER-1200 Passive Heat Removal Systems: Steam Generator PHRS and Containment PHRS. Master's Thesis. Lappeenranta University of Technology (LUT).

Yusheng, L., Li, D., Tan, S., Jianping, J., Jilin, T., Shuguang, W., Jiahao, S., Ruifeng, T., 2024. Review and identification on thermal hydraulic phenomena related to core make-up tank in PWR. Nuclear Engineering and Design 425.

Zeliang, C., Mi, Y., Tokuhiro, A., Lu, L., Rezvoi, A., 2020. Integral PWR-Type Small Modular Reactor Developmental Status, Design Characteristics and Passive Features: A Review. Energies (Basel) 2898, 13 (11). https://doi.org/https://doi.org/10.3390/en13112898

Zhang, Y., Qiu, S., Su, G., Tian, W., 2011. Design and transient analyses of emergency passive residual heat removal system of CPR1000. Part I: Air

cooling condition. Progress in Nuclear Energy. Progress in Nuclear Energy 53, 471–479. https://doi.org/https://doi.org/10.1016/j.pnucene.2011.03.001